JOURNAL OF ATMOSPHERIC AND TERRESTRIAL PHYSICS

EDITORIAL ADVISORY BOARD

H. O. G. ALFVÉN-STOCKHOLM · J. BARTELS-GÖTTINGEN · P. M. S. BLACKETT-LONDON · E. G. BOWEN-SYDNEY · SIR DAVID BRUNT-LONDON R. BUREAU-BAGNEUX S. CHAPMAN-ALASKA · J. EGEDAL-COPENHAGEN · H. FICKER-VIENNA V. F. HESS-NEW YORK · E. O. HULBURT-WASHINGTON, D.C. · H. ISRAEL-TÜBINGEN D. H. MENZEL-CAMBRIDGE, MASS. · S. K. MITRA-CALCUTTA · M. NICOLET-UCCLE E. H. NORINDER-UPSALA · B. van der POL-GENEVA · J. A. RATCLIFFE-CAMBRIDGE E. REGENER✤-WEISSENAU (BODENSEE) · O. E. H. RYDBECK-GOTHENBURG · SIR GEORGE SIMPSON-LONDON · H. SOLBERG-OSLO · C. STØRMER-OSLO VELDKAMP-DE BILT · M. WALDMEIER-ZÜRICH · R. v. d. R. WOOLLEY-CANBERRA J. ZENNECK-ALTHEGNENBERG

EDITOR IN CHIEF

SIR EDWARD APPLETON, F.R.S.
EDINBURGH

VOLUME 6
JANUARY—JUNE
1955

PERGAMON PRESS · LONDON & NEW YORK

J. Atmosph. Terr. Phys.

VOL.
6
1955

CONTENTS

No. 1

ROBERT E. JONES: The development of an *E*-region model consistent with long wave phase path measurements 1

KENNETH DAVIES and E. L. HAGG: Ionospheric absorption measurements at Prince Rupert 18

J. G. SCHOLTE and J. VELDKAMP: Geomagnetic and geoelectric variations 33

S. H. H. LARSEN: Vertical distribution of atmospheric ozone at Longyearbyen, Spitzbergen (78°N) 46

R. B. BANERJI: The autocorrelogram of randomly fading waves 50

EDWARD V. ASHBURN: Measurements of the specific intensities of the auroral green line at College, Alaska 57

Research Notes:

O. OMHOLT: Intensity measurements of the second positive band system of nitrogen in high-latitude aurorae 61

D. M. HUNTEN and G. G. SHEPHERD: Vibrational temperatures from second positive bands 64

EDWARD V. ASHBURN: The altitudes of the luminous layers in the Earth's atmosphere . 67

Book Review:

"Thunderstorm Electricity" Ed. by HORACE R. BYERS (reviewed by J. A. CHALMERS) . 68

Nos. 2/3

K. BIBL, R. BUSCH, K. RAWER et K. SUCHY: La nomenclature ionospherique et les conventions pour le depouillement 69

J. W. DUNGEY: Solar electrodynamics 88

C. M. MINNIS: Ionospheric behaviour at Khartoum during the eclipse of 25th February, 1952 91

N. C. GERSON: Sporadic *E* propagation 113

B. W. OSBORNE: Horizontal movements of ionization in the equatorial *F*-region . . 117

G. J. PHILLIPS: An apparatus for recording time-delays between radio fading characteristics 124

R. P. WALDO LEWIS: The geomagnetic post-perturbation effect 129

J. S. GREENHOW and E. L. NEUFELD: The diffusion of ionized meteor trails in the upper atmosphere 133

SIR EDWARD APPLETON and W. J. B. BEYNON: An ionospheric attenuation equivalence theorem 141

J. ALAN CHALMERS and W. W. MAPLESON: Point discharge currents from a captive balloon 149

S. S. BARAL: Studies on the sunrise effect in regions *E* and *F* 160

Research Note:

D. R. BATES: Collisional deactivation and the night airglow 171

K-indices of geomagnetic activity from the observatories at Abinger, Eskdalemuir and Lerwick, from September to December, 1954 173

Book Review:

"High Altitude Rocket Research" by HOMER E. NEWELL, JR. (reviewed by H. S. W. MASSEY) 176

No. 4

N. J. SKINNER and R. W. WRIGHT: Some geomagnetic effects in the equatorial F_2 region 177

PIERRE ST. AMAND, HELEN B. PETTIT, F. E. ROACH and D. R. WILLIAMS: On a new method of determining the height of the nightglow 189

K. BULLOUGH and T. R. KAISER: Radio reflections from aurorae—II 198

B. C. LANDSEER-JONES: The significance of a nonterrestrial magnetic field in neutral stream theories of the aurora 215

Book Reviews:

"Astronomical Photoelectric Photometry" Ed. by FRANK BRADSHAW WOOD (reviewed by S. C. CURRAN) 227

"Rocket Exploration of the Upper Atmosphere" Ed. by R. L. F. BOYD and M. J. SEATON (reviewed by L. R. SHEPHERD) 227

"The Sun" (Volume 1 of The Solar System) (reviewed by W. M. H. GREAVES) 229

"An Atlas of Typical Expansion Chamber Photographs" by W. GENTNER, H. MAIER LEIBNITZ and W. BOTHE (reviewed by N. FEATHER) 231

No. 5

C. G. STERGIS, S. C. CORONITI, A. NAZAREK, D. E. KOTAS, D. W. SEYMOUR and J. V. WERME: Conductivity measurements in the stratosphere 233

E. THEISSEN: L'influence du cycle solaire sur le facteur de transmission $(M3000)F_2$. 243

W. GALBRAITH and J. V. JELLEY: Light-pulses from the night sky and Cerenkov radiation. Part I 250

N. C. GERSON: Radio observations of the aurora 263

F. H. HIBBERD: Ionospheric self-interaction of radio waves 268

Research Notes:
C. A. Shain and F. J. Kerr: A note on factors affecting the interpretation of observations of transient echoes from the ionosphere 280
Walter Orr Roberts and Dorothy E. Trotter: Solar prominences and geomagnetic disturbance 282
Björn Landmark: Measurements of limiting polarization of radio waves reflected from the *F*-layer 284
K-indices of geomagnetic activity from the observatories at Abinger, Eskdalemuir and Lerwick, from January to March, 1955 287
Book Review:
"Four-Place Tables of Transcendental Functions" by W. Flügge and "Siebenstellige Tafeln der elementaren transendenten Funktionen" by Friedrich Lösch (reviewed by Balth. van der Pol) 290

No. 6

H. R. Peiffer and A. P. Mitra: The effect of vertical ion transport on the night-time *E*-region 291
J. V. Jelley and W. Galbraith: Light pulses from the night sky and Čerenkov radiation. Part II 304
J. H. Meek: The location and shape of the auroral zone 313
H. Israël: An experimental problem in the atmospheric-electrical synopsis 322
G. G. Shepherd and D. M. Hunten: On the measurement of rotational temperature from unresolved auroral nitrogen bands 328
A. Vallance Jones and A. W. Harrison: Rotational temperatures of the auroral N_2^+ bands 336
Research Note:
J. F. Clark and J. H. Kraakevik: The charge on the earth 344
K-indices of geomagnetic activity from the observatories at Abinger, Eskdalemuir and Lerwick, for April, 1955 346

AUTHOR INDEX TO VOLUME 6

(B) denotes a book review

Appleton, Sir Edward p. 141
Ashburn, E. V. pp. 57, 67
Banerji, R. B. p. 50
Baral, S. S. p. 160
Bates, D. R. p. 171
Beynon, W. J. B. p. 141
Bibl, K. p. 69
Bullough, K. p. 198
Busch, R. p. 69
Chalmers, J. A. pp. 68 (B), 149
Clark, J. F. p. 344
Coroniti, S. C. p. 233
Curran, S. C. p. 227 (B)
Davies, K. p. 18
Dungey, J. W. p. 88
Feather, N. p. 231 (B)
Galbraith, W. pp. 250, 304
Gerson, N. C. pp. 113, 263
Greaves, W. M. H. p. 229 (B)
Greenhow, J. S. p. 133
Hagg, E. L. p. 18
Harrison, A. W. p. 336
Hibberd, F. H. p. 268
Hunten, D. M. pp. 64, 328
Israël, H. p. 322
Jelley, J. V. pp. 250, 304
Jones, R. E. p. 1
Kaiser, T. R. p. 198
Kerr, F. J. p. 280
Kotas, D. E. p. 233
Kraakevik, J. H. p. 344
Landmark, B. p. 284
Landseer-Jones, B. C. p. 215
Larsen, S. H. H. p. 46
Lewis, R. P. W. p. 129
Mapleson, W. W. p. 149
Massey, H. S. W. p. 176 (B)
Meek, J. H. p. 313
Minnis, C. M. p. 91
Mitra, A. P. p. 291
Nazarek, A. p. 233
Neufeld, E. L. p. 133
Omholt, A. p. 61
Osborne, B. W. p. 117
Pettit, H. B. p. 189
Peiffer, H. R. p. 291
Phillips, G. J. p. 124
Rawer, K. p. 69
Roach, F. E. p. 189
Roberts, W. O. p. 282
Scholte, J. G. p. 33
Seymour, D. W. p. 233
Shain, C. A. p. 280
Shepherd, G. G. pp. 64, 328
Shepherd, L. R. p. 227 (B)
Skinner, N. J. p. 177
St. Amand, P. p. 189
Stergis, C. G. p. 233
Suchy, K. p. 69
Theissen, E. p. 243
Trotter, D. E. p. 282
Vallance Jones, A. p. 336
Van der Pol, Balth. p. 290 (B)
Veldkamp, J. p. 33
Werme, J. V. p. 233
Williams, D. R. p. 189
Wright, R. W. p. 177

VOL. 6 1955

Journal of Atmospheric and Terrestrial Physics, 1955, Vol. 6, pp. 1 to 17. Pergamon Press Ltd., London

The development of an *E*-region model consistent with long wave phase path measurements*

ROBERT E. JONES
Ionosphere Research Laboratory, The Pennyslvania State University, State College, Pennsylvania

(*Received* 18 *March* 1954)

ABSTRACT

The diurnal and seasonal variations in phase height of the main *E*-region reflection level at 150 kc at State College are summarized for a period of 15 months.

An electron density model, moderately "sharp" on the lower side, is evolved by modification of the Chapman theory to include the effects of variable scale height, dissociation of molecular oxygen, and variable recombination. The model is checked, primarily, against 150-kc phase height data, but also against 2·4-mc phase heights and *E*-region critical frequency.

1. INTRODUCTION

The changes in phase path of long-wave pulsed radio signals reflected from the lower *E*-region of the ionosphere have been studied at The Pennsylvania State University for a period of more than a year. The instrumentation for this investigation has already been described (JONES, 1953*b*) and certain of the data obtained have been used in a study of ionospheric winds (JONES, MILLMAN, and NERTNEY, 1953). In this paper some additional data analysis is reported whose results are then incorporated in the development of an electron density model of the *E*-region.

The phase path of the RF under the echo envelope of a pulsed signal propagated through the ionosphere may be defined as

$$P = c \int \frac{ds}{v}$$

where c is the velocity of electromagnetic radiation *in vacuo*, v is the phase velocity in the medium, and s is the variable of path. The integration is carried over the actual path traversed by the signal. If the ionosphere is homogeneous in the horizontal plane, and if the signal is vertically incident, then the phase path is just twice the phase height, which is the apparent or virtual height of reflection for the individual wave crests. Since these conditions are assumed for this experiment, we shall use the phase height, $h = P/2$, where the integration is over one-half the total path.

The phase height of a reflecting region (or the phase path of a radio sounding signal) cannot be measured by radio sounding methods as an absolute quantity. The quantity observed is the phase of the RF signal which is indeterminate by a multiple of 2π. Therefore, only *changes* in phase and, hence, changes in phase height are observed. The relationship between the two variations is

$$\Delta h = -\frac{\lambda}{2}\frac{\Delta\phi}{2} \qquad (1)$$

* The research reported in this paper has been sponsored by the Geophysics Research Division of the Air Force Cambridge Research Center, Air Research and Development Command, under Contract AF19(122)-44.

where λ is the wave length of the radiation *in vacuo* and ϕ is the RF phase of the signal.

The radio frequency used in this experiment is 150 kc for which the principal critical electron density of 3060 cm^{-3} is first met in the *E*-region at a height of about 90–110 km. This "main" *E*-region reflection is normally obtained continuously at State College, Pa., although there is a high absorption of the incident wave during the day in the summer season, resulting in a frequent loss of daytime data (LINDQUIST, 1953).

The use of a critical electron density as the reflection condition may imply that the signals are reflected at a definite height, the "true height" of reflection, as from a metallic surface. This is not the true situation, of course, as reflection takes place in depth. It is convenient, however, to use the height at which this ray theory condition obtains as a reflection height parameter and the term will be used in this way. Other ray theory ideas will be used here with the understanding that, while they often do not describe the true condition correctly, they do represent parallel ideas in the wave theory, actually used, which may be much more difficult to describe or identify.

2. EXPERIMENTAL DATA

The diurnal and seasonal variations in the phase height of the main *E*-region reflection condition constitute the principal experimental data to be discussed here. In Fig. 1 seasonal averages of the diurnal curves are presented for a period of 15 months from November 1951 through January 1953. The seasons are defined as Winter, November through February; Equinox, March, April, September, and October; and Summer, May through August.

The mean curves (dashed) were obtained by visual averaging of sets of daily curves. The solid lines indicate an approximate spread of the curves during the period. Uncertainties in the reduction of data and day-by-day variations both contribute to this spread. The earliest and latest times of ground sunrise and sunset for the season are indicated on each graph. Table 1 summarizes the total diurnal variation of the average curves and also tells how many days data are represented by each.

Table 1. *Total diurnal variation of phase height*

Season	*Number of days*	*Total* Δh *— km*
Summer	36	15
Equinox	47	15·5
Winter	135	11·5

The variation in 150-kc phase height shown in Fig. 1 has two particular features whose appearance prompted the main theoretical work of this paper. These are the observed total change in phase height from day to night and the distinct flatness of the curves during the midday period. Because of the inadequacy of the simple Chapman theory to explain these two results, as discussed

VOL. 6 1955

below, it was decided to seek modifications of that theory, on a sound physical basis, with the hope of developing a model of the E-region whose phase height variations would fit the observations.

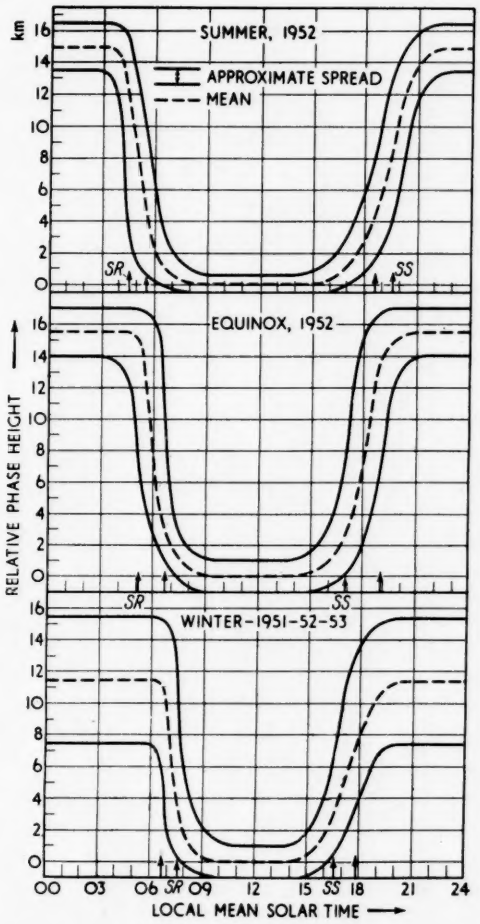

Fig. 1. Experimental diurnal variation of phase height at 150 kc.

3. E-Region Models

The theory of Chapman (1931a) developed to describe the photoionization or dissociation of atmospheric constituents is generally taken as the starting point for the theoretical formulation of ionospheric layers by the action of solar radiation. As an introduction to the following work, the formulas resulting from his treatment are reviewed briefly below (the notation differs from Chapman's), along with a few other introductory ideas.

The ionization production function resulting from CHAPMAN's theory may be expressed:

$$q(z, \chi) = q_0 \exp(1 - y - \sec \chi \, e^{-y}) \tag{2}$$

where χ is the solar zenith angle or the radiation angle of incidence,

z is the height above the ground,

q_0 is the maximum value of q, $q_0 = q(z_0, 0)$,

$y = (z - z_0)/H$

z_0 is the height of maximum ion production at $\chi = 0$,

H is the scale height, $H = kT/Mg$,

k is the Boltzmann constant,

T is the absolute temperature,

M is the mean molecular mass,

g is the mean acceleration due to gravity.

In the derivation it is assumed that:

(a) the ionizing radiation is monochromatic,

(b) the scale height is constant over the region in question,

(c) the atmosphere may be considered to be stratified in horizontal planes.

Given this production function, we can now consider how the ionization density at a point changes with time. If we assume that the ions effective in producing ionospheric effects are electrons (because of their greater mobility), we may write for a particular localized region in the atmosphere

$$\frac{dN_e}{dt} = q(t) - \alpha N_e^2(t) \tag{3}$$

where

N_e is the number density of electrons

α is the coefficient of the effective recombination (or disappearance) of electrons.

Under certain conditions, this equation may be simplified, which must be done if analytic solutions are to be obtained. In the E-region the electron density changes slowly with time, during daytime, so that for such an approximation we may write

$$q = \alpha N_e^2 \tag{4}$$

or

$$N_e(z, \chi) = \sqrt{\frac{q_0}{\alpha}} \exp\{\tfrac{1}{2}[1 - y - \sec \chi \, e^{-y}]\} \tag{5}$$

In the simple Chapman theory, the effective recombination coefficient is considered to be independent of height in a particular ionospheric region, a conclusion that is deduced from experimental observation (MITRA, S. K., 1952).

VOL. 6 1955

These additional assumptions, to those mentioned above, in obtaining equation (5) from equation (2) may now be summarized:

(d) electrons are the only ions contributing to the electrical properties of the ionosphere affecting radio waves.
(e) a quasi-equilibrium exists; that is, $dN_e/dt \cong 0$.
(f) the effective recombination coefficient is independent of height for a given region.

It should be noted that while CHAPMAN did not make the assumption (d) and (e), nor state (f) as an established fact, the usual treatment of a "Chapman region" involves them substantially as stated.

So far the development has not specified a particular ionospheric layer. However, certain of the latter assumptions are more nearly valid for the lower regions than for the F-regions. The assumption of a quasi-equilibrium, while valid around noon at almost all heights, is probably good during most of the day only in the lower regions. Similarly, constant recombination is certainly not valid in F_2, although for E and F_1 it is a reasonable zero-order approximation. In general, E-region is more nearly "Chapman" than F.

Assumption (c) is valid for values of χ less than about 85°. Near sunrise and sunset, however, the curvature of the earth and its concentric stratified atmosphere must be taken into account. CHAPMAN (1931b, 1953) has studied this case in detail also and has derived a function $f(R, \chi)$ which replaces sec χ in equations (2) and (5) and in other formulas that were derived for a plane earth. The parameter R is

$$R = \frac{a + z_0}{H}$$

where a is the earth's radius.

For a given region R may be considered constant for $\chi \leq 90°$ and so we shall consider f as a function of χ alone. The value of R for E-region is about 650. Equation (5) may now be revised as

$$N_e(z, \chi) = N_0 \exp\{\tfrac{1}{2}[1 - y - f(\chi)e^{-y}]\} \tag{6}$$

where $N_0 = \sqrt{q_0/\alpha}$, the maximum value of N_e.

For some special analyses a simplified layer obtained from this for $\chi \cong 0$ and for y small, that is for regions not far from the layer maximum, a parabolic approximation, may be used (MITRA, S. K., 1952) but in the present work this is not sufficiently rigorous and will not be considered. Such an approximation is sometimes referred to as a "simple Chapman region" but that name will be used here to describe rather a region represented by equations (5) or (6), that is under the assumptions enumerated above with the possible exception of (c).

3.1. *A simple Chapman model*

In calculating a Chapman model, as from equation (6), three parameters must first be evaluated: the scale height, H; the height of the $\chi = 0$ maximum electron density, z_0; and either N_0 or some other value of N_e at a specified height. On the assumption of constant scale height we may choose, for E-region, $H = 10$ km, as

suggested by MITRA, S. K. (1952). For the height of the maximum, we may choose 100 km. The absolute evaluation of N_e can be avoided by calculating N_e/N_0, but can be effected from critical frequency data.

Fig. 2 shows such a height distribution, calculated by means of a generalized Chapman function due to HACKE (1948). The broken vertical line indicates the electron density of 3060 cm^{-3}, the main E-region reflection condition for 150-kc waves. The position of this line was obtained by assigning a value $N_e = 1{\cdot}2 \times 10^5$ cm^{-3} at State College at noon of the winter solstice when $\chi = 64{\cdot}2°$.

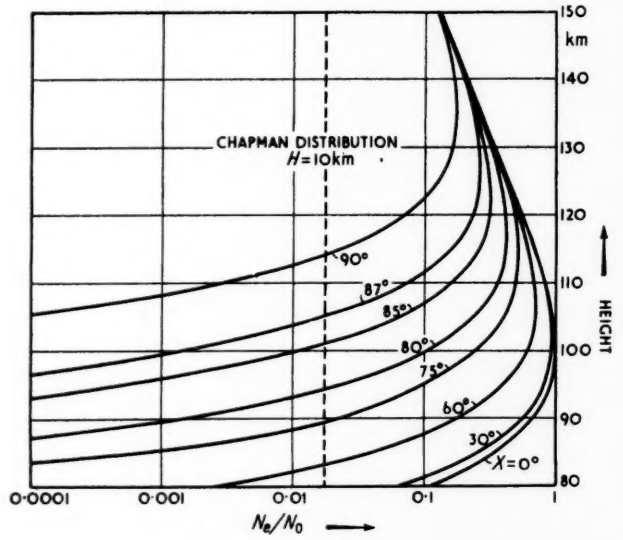

Fig. 2.

By following the height of the model along the 3060-line as χ varies, we obtain the diurnal variation of the 150–kc reflection height. From Fig. 2 we see that the total variation for the winter solstice is 29 km. GIBBONS and NERTNEY (1951) have calculated wave theory phase heights for a model having Chapman shape and from their variation of h with layer critical frequency, f_0, it can be shown that the difference between h and height of reflection is not large during most of the day and does not exceed 2 km for the lowest critical frequency, at $\chi = 90°$. Taking account of the maximum error, we can still expect a diurnal variation of 27 km which, in view of the observed Δh of 11·5 km in Table 1 or even the maximum spread of 16·5 km, is too large by a considerable factor.

Another failure of the model of Fig. 2 is the shape of the diurnal variation of h at 150 kc. The observed phase heights show a characteristic flatness during most of the daytime. As seen in Fig. 3, the Chapman phase heights have a distinct smooth curvature showing no tendency to flatten out at noon.

The first objection to the Chapman model might easily be removed by using a smaller scale height, about half of the chosen value. This is not realistic in view of the values given by NICOLET and MANGE (1954) and others (MITRA, S. K., 1952). The

VOL. 6 1955

former give 5·5 km for the lowest H in E- or D-regions, the median between 80 and 120 km being nearer 7·5 km. In addition, the lower value of H, if admissible, still would not change the shape of the h-t variation.

3.2. *A fixed-maximum-height Chapman model*

The first attempt in this Laboratory to modify the simple Chapman model to fit experimental data followed the observation, similar to that described above, that the total diurnal height variation was too great. Thus BENNER (1950) attacked

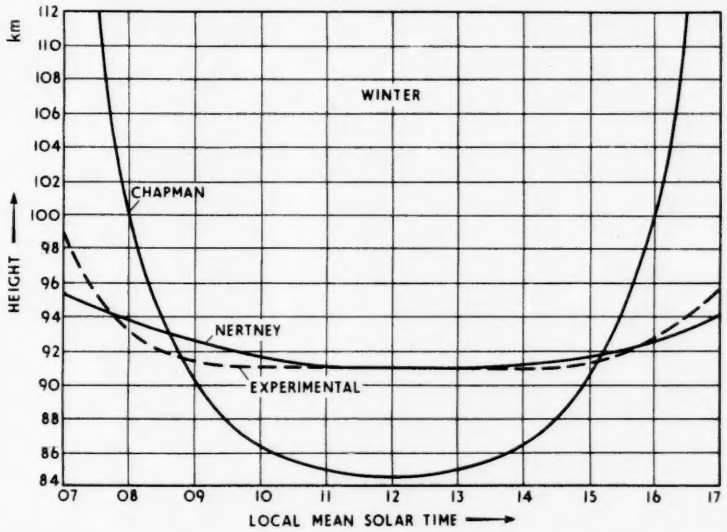

Fig. 3. Chapman, Nertney, and experimental phase heights.

the problem by fixing the height of maximum ionization. At any time the model had a Chapman shape but the large height variation was removed. GIBBONS and NERTNEY (1951) used a similar function, fixing the height at 115 km, a figure obtained from later, unpublished work of GRACE. The latter's experimental data (see, for example, GRACE, 1951) supported the constant-height thesis, at least for the middle half of the daylight hours. This, plus the use of observed critical frequencies, placed the model on an experimental foundation which was strengthened by the general correspondence of the theoretical to the experimental height variations. In Fig. 3, the 150-kc phase height variation for the winter solstice at State College is shown as the "Nertney" curve.

While the Gibbons-Nertney model is grounded on experimental data, it lacks the internal consistency of the Chapman theory. The "Chapman" shape loses its significance if it is not allowed to move vertically with $\chi(t)$. It was with this physical limitation in mind that the decision was made to approach the problem of improving the E-region model through physically reasonable modifications of the Chapman theory. In this way it is still possible to make the model fit the observed data without resorting to arbitrary constraints.

4. DEVELOPMENT OF A NEW *E*-REGION MODEL

The procedure to be followed in this development is to examine the assumptions on which the simple Chapman-type model, described above, is constructed and to remove or modify them as dictated by information obtained from recent researches.

4.1. *The scale height*

The assumption of a constant scale height is largely a convenience for calculations which has been tolerated because of the very uncertain knowledge about its true

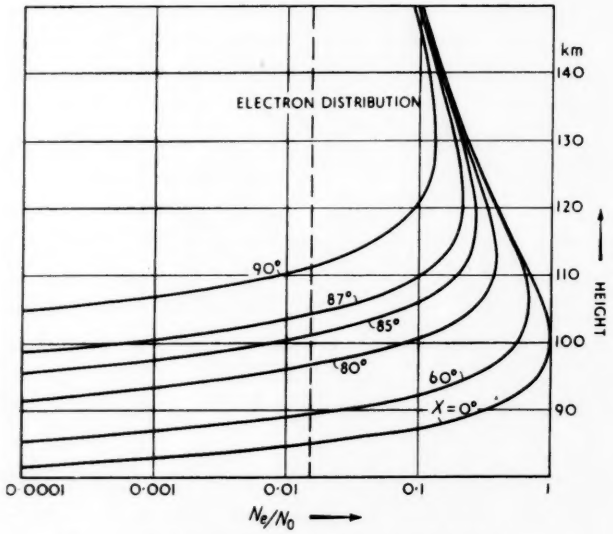

Fig. 4. Model using Nicolet-Mange scale height.

height variations. NICOLET and MANGE (1954) have recently derived a scale height model based on pressure information from rocket flights. From their height distribution it is easy to see that the constant-H assumption is quite approximate.

In 1949 NICOLET and BOSSY (1949) worked out the mathematics for a layer formation theory based on a linear scale height distribution. This may be applied to the Nicolet-Mange model by breaking the latter into linear segments. The extension of the Nicolet-Bossy treatment to a multilinear scale height is too lengthy to be derived here but has been worked out (JONES, 1953a) for a scale-height model having its minimum in the lower *E*-region. The resulting electron distribution with the maximum for $\chi = 0$ at 100 km, and constant recombination, is shown in Fig. 4 which may be compared with Fig. 2. An improvement in the total diurnal swing is seen in the 21-km change in reflection height from $\chi = 64°$ to 90°. (The dashed line is again the reflection condition for 150 kc). A general flattening of the noontime height curve is also to be expected because H is now smaller at noon than at sunrise or sunset at the reflection height; scale height is still primarily a parameter of layer thickness. Here is the first realization

, VOL. 6 1955

of the hope that logical extensions of the Chapman theory will yield reasonable phase height variations to fit the data. Assumption (b) of the simple Chapman theory is removed.

4.2. *The dissociation of* O_2

In 1938 WULF and DEMING (1938) suggested ionization of O_2 at the first ionization potential as a possible origin of *E*-region. NICOLET (1945) proposed a pre-ionization process somewhat above the first ionization energy. These two theories are still strongly supported and have recently been strengthened by new absorption data (WEISSLER and LEE, 1952; WATANABE *et al.*, 1953) and by LINDQUIST'S (1952) sunrise study. In short, there is considerable reason to believe that *E*-region is formed by the ionization of O_2 in the wavelength range of 910 to 1016Å, whether by direct first-ionization or by pre-ionization.

CHAPMAN (1930) reported that oxygen is primarily atomic above the lower *E*-region and molecular below. It was partly because of this fact that WULF and DEMING considered O_2 for *E*-region formation since this would explain the relative sharpness of the *E*-region in contrast, presumably, to a simple Chapman model. Since their 1938 paper, the problem of the distribution of O_2 in *E*-region and the nature of the "transition region," in which the dominant form changes from O_2 to O, have been the subject of several studies including their own (see NICOLET and MANGE, 1954). Among these PENNDORF (1949) and MOSES and WU (1951, 1952, 1953) have calculated O_2 distributions in lower *E*. BATES and NICOLET (1950) made a study of the reactions among oxygen, hydrogen, and their compounds from which was derived the O_2 distribution used by BATES and WITHERSPOON (1952) in their study of the minor atmospheric constituents. NICOLET and MANGE'S work (1954) is the latest and utilizes the most recent available rocket data on scale height, temperature and pressure. Although they do not propose a specific distribution of O_2 in the transition region, limits are suggested. These are roughly as follows: O_2 is not dissociated below 80 km and follows the main atmospheric distribution at about 20 per cent of the total; above 100 km $N(O)$ is greater than $N(O_2)$; above 115 km O_2 is almost completely dissociated and follows the main atmosphere with 0·2 per cent to 1·0 per cent of the total density under conditions of mixing. With these conclusions as guides, we have constructed O_2 distributions in an effort to find an acceptable electron model for *E*-region.

4.2.1. *Mitra's dissociation parameter.* In 1952 A. P. MITRA (1952) proposed a means of introducing into the non-isothermal theory of GLEDHILL and SZENDREI (1950) a parameter to take account of the variation of the O_2 density from the atmospheric distribution in the dissociation region. In the terminology used here, the parameter, b, appears in the exponent on H:

$$N = N_0 \left[\frac{H}{H_0}\right]^{-\frac{b+\beta}{\beta}} \tag{7}$$

where N is now for O_2, N_0 and H_0 are evaluated at a reference height, and β is the scale height gradient. MITRA calculated three sample layers for $\chi = 0$, for values of $b = 0{\cdot}5$, $1{\cdot}0$ and $2{\cdot}0$ illustrating that the larger values of b tended to

flatten the layers. Certain relationships derived by NICOLET and BOSSY are modified when this parameter is introduced (JONES 1953a). The model of Fig. 4 is squeezed into a narrower height range, as was indicated by MITRA. The total height variation for the $N_e = 3060$ level (the dashed line of Fig. 4) is cut by almost 50 per cent for $b = 2{\cdot}0$.

Of course, both above and below the O_2-O transition region the value of b is unity since we believe the O_2 distribution to follow the main atmosphere in those regions. Therefore, b differs from unity only in a finite region and the reduction of the height variation mentioned above is an upper limit. From the NICOLET-MANGE deduction it seems that a reasonable range of the transition region is 80–100 km.

Because of matching problems at the boundaries of the transition region, it is found that a continuous variation of b over the whole E-region is desirable. The form of this variation should ultimately be determined by experimental data, which are not now available. The several complex processes taking place in the transition area (see NICOLET and MANGE, 1954) make it extremely difficult to construct a model in that region with any degree of certainty. Because of this lack of any sound prediction it was decided to use a very simple variation of b, one which causes $N(O_2)$ to fit smoothly at the boundaries and describes a gradual transition between. A simple continuous function is a triangular variation in which $b = 1$ up to 80 km, then rises linearly to a maximum value at 90 km, decreases at the same rate to 1 at 100 km and remains unity from there upward. The expression for the particle density of O_2 is now

$$N(z) = N_0 \left[\frac{H_0 + \beta(z - z_0)}{H_0}\right]^{-\frac{\beta + b_0 + \gamma(z - z_0)}{\beta}} \tag{8}$$

where N_0, H_0, and b_0 are evaluated at the reference height z_0, and β and γ are constant over finite sub-regions. This function is presented in analytic form in the hope that the whole development of the production function may be kept analytic. For the purpose of calculation of the models described below, this was not done; the production function,

$$q(z, \chi) = Q_\infty K N(z) \exp[-N(z) K H(z) f(\chi)] \tag{9}$$

was used, for which an analytic form of $N(z)$ is not necessary. In later extensions of this work, variations of b will be generated that tend to make the analytic treatment more feasible.

In Table 2 five models of O_2 distribution are listed with the values of the parameters which distinguish them. This information, along with a model of the main atmosphere and the scale height distribution (NICOLET and MANGE 1954), completely describes the O_2 distribution. In Fig. 5 these five models are plotted between 80 and 110 km. In model N-1 the consequences of a discontinuous b are seen. Models N-2 through N-4 employ symmetric triangular functions for b while in N-5 an asymmetric variation is used.

In addition to the five distributions shown in Table 2, two others of interest were used: models adopted from MOSES and WU (1952) and BATES and WITHERSPOON (1952) designated N-6 and N-7, respectively. Both have been altered

VOL. 6 1955

Table 2. Parameters used in O_2 distributions

Model	*Transition region*	γ	b_{max}	M/N_T *(upper)*
N-1	80–100 km	0	1·865	1/100
N-2	80–100 km	±0·0856	1·856	1/100
N-3	80–100 km	±0·0979	1·979	1/150
N-4	80–90 km	±0.3795	1·897	1/150
N-5	80–100 km	$\begin{cases}+0·2324\\-0·0775\end{cases}$	2·162	1/150

somewhat from their originals for comparison with those derived from NICOLET and MANGE's physical reasoning but the essential features within the transition region are retained as that is our main interest. They are introduced here only because they represent probable outer limits of the transition region and so will

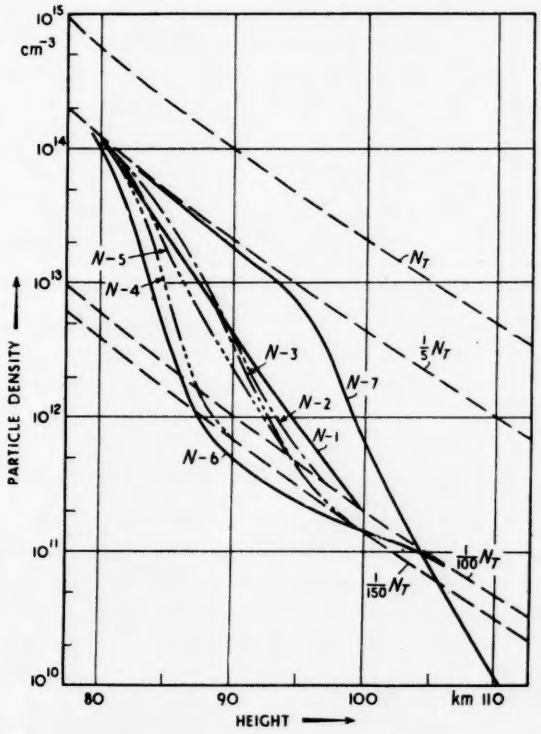

Fig. 5. Calculated O_2 distributions.

aid in pointing out what may be expected from alterations in the intermediate models. All of these distributions follow some fraction of the main atmosphere (N_T) above 110 km.

4.3. *Variable recombination*

The last important extension of the simple Chapman theory to be taken up here is the height variation of the coefficient of effective recombination. This has been studied for D- and E-regions from both the experimental and theoretical points of view (MITRA and JONES, 1954). The resulting mean experimental model is used in the subsequent calculations of electron density distribution.

4.4. *The E-region electron model*

In the process of developing the final electron model, the distributions of O_2 shown in Fig. 5 were used. Because the choice of N_e is now reduced to the choice of $N(O_2)$ the same designations (N-1, N-2, etc.) will be used to describe the electron models.

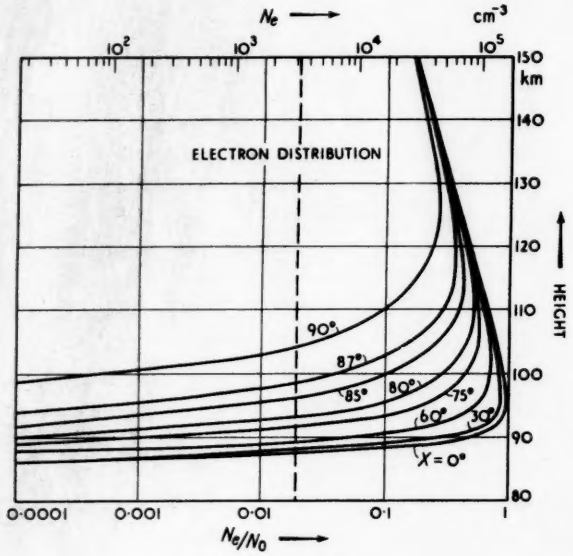

Fig. 6. Model N-3.

As mentioned above, and as seen in Fig. 5, N-6 and N-7 are representative of the outer limits on the other distributions. In choosing among all of these models, many factors must be considered and the arguments may best be summarized by comparing the relative merits of the two extreme cases and one intermediate one. Model N-3 was found to have some advantages over the others of Table 2 and was chosen to represent them.

The electron distribution derived from N-3 is shown in Fig. 6. The normalized curves were calculated from equation (9) using an absorption coefficient of $K = 5 \times 10^{-18}$ cm^2, interpolated from the data of WEISSLER and LEE (1952) and of WATANABE *et al.* (1953).

The diurnal variation of the 150-kc reflection height for December at State College is shown in Fig. 7 along with the observed phase height variation (from Fig. 1) and the reflection heights of N-6 and N-7. The outer limits of Δh as well

VOL. 6 1955

as the average curve are shown because the model calculations are done for the winter solstice rather than for an average winter day. The location in height of the experimental curve is arbitrary. While the N-3 height variation does not fit the average curve perfectly, it does generally fit within the envelope and its total diurnal swing of 14·3 km is of the order of the 11·5 km observed by experiment. The steepness in the theoretical curves around sunrise and sunset is due largely to the neglect of the dN_e/dt term and the nighttime E-layer. Certainly, it is a considerable improvement over the simple Chapman model.

The electron distributions (not shown) for N-6 and N-7 were calculated and illustrated that the former is a "broader" and the latter a "sharper" model than N-3, as would be expected. The shape of the N-7 reflection height curve in Fig. 7 seems to make it a better fit to the experimental average curve than N-3 but the total diurnal Δh is only 6·8 km, or about 60 per cent of the observed average and an even smaller fraction of the solstice variation. This value of 6·8 km seems to be in better agreement with the sunrise drop observed on long-wave oblique incidence

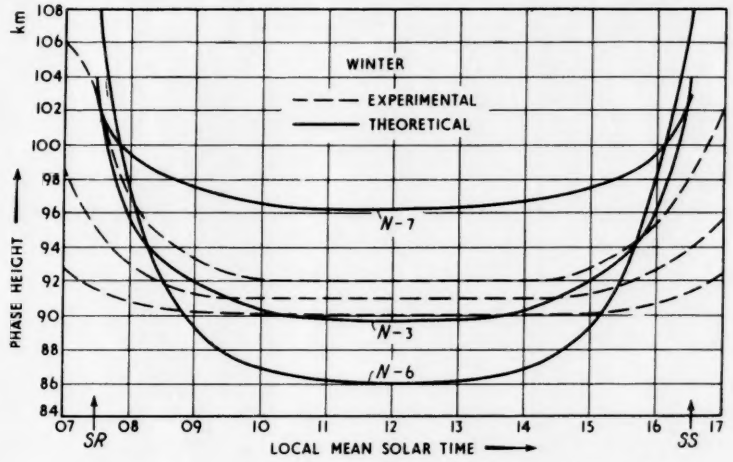

Fig. 7. Diurnal variation of reflection height for various models.

by WEEKES and STUART (1952). However, we are considering here the total drop from $\chi = 90°$ to noon, rather than the more sudden initial effect, so that their estimated 7–8 km would probably have to be increased somewhat for comparison with the "total diurnal variation."

Another E-region variable that can now be checked against the models is the critical frequency. In Fig. 8 the diurnal variation of the normalized critical frequency for December at State College is plotted. It is difficult to choose the best fit for the parameter although N-7 is closest point by point. If the experimental curve (plotted from CRPL-F bulletin data) were extrapolated to sunrise and sunset, it would fall about equidistant from all three.

In the case of the height of maximum ionization, the three models have similar shapes but differ considerably in total diurnal variation. Since there are very little experimental data with which to compare these, they are not shown here.

In his study of the middle E-region by phase heights at 2·4 mc, FINDLAY (1949, 1951) indicated that, at least qualitatively, he found E-region to behave like a simple Chapman layer. If this be so then the choice among N-3, N-6 and N-7 becomes

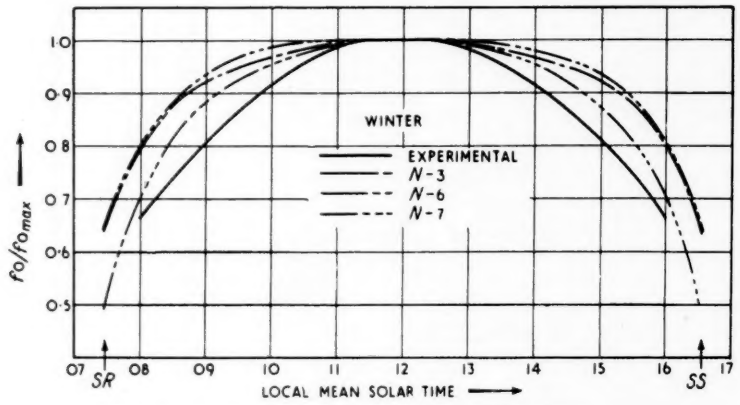

Fig. 8. Experimental and theoretical critical frequency.

more difficult, since N-6 is the most nearly Chapmanish of the three while the weight of other experimental evidence seems so far to be on the side of N-7. FINDLAY gives one complete day's record of Δh against which we may check the models. (He states that it is typical of the bulk of his results.) Fig. 9 shows the

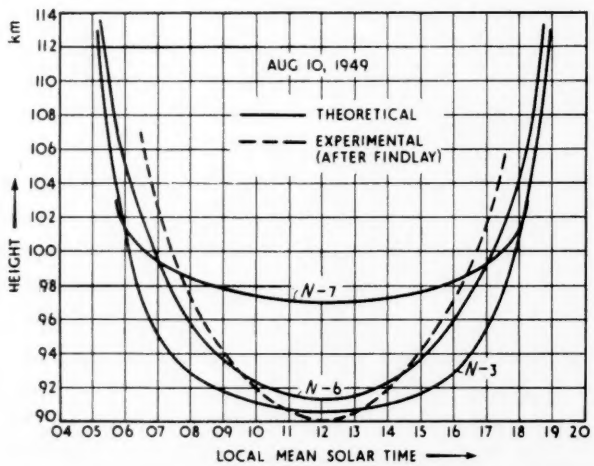

Fig. 9. Phase heights at 2·4 mc at Cambridge and theoretical reflection heights.

Cambridge $h(t)$ variation along with the calculated 2·4 mc reflection height of the three models. From this it would appear that of the three, N-6 is the best fit. N-3 is quite flat, but N-7 is almost out of the question.

We now have two groups of conflicting evidence. On the one hand, the 150-kc phase heights indicate a sharp layer while, on the other, FINDLAY's results show a

VOL. 6 1955

Chapman-like region. In between, f_0E (and possibly hE_{max}) are rather uncertain but seem to favour the sharp layer. In view of these unresolved differences, a compromise seems in order and for the moment we choose N-3 as the more likely E-region distribution.

4.5. *The phase height variation of N-3*

For the final calculation at 150 kc we must, of course, calculate the theoretical phase height variation to replace the reflection heights thus far used. In calculating

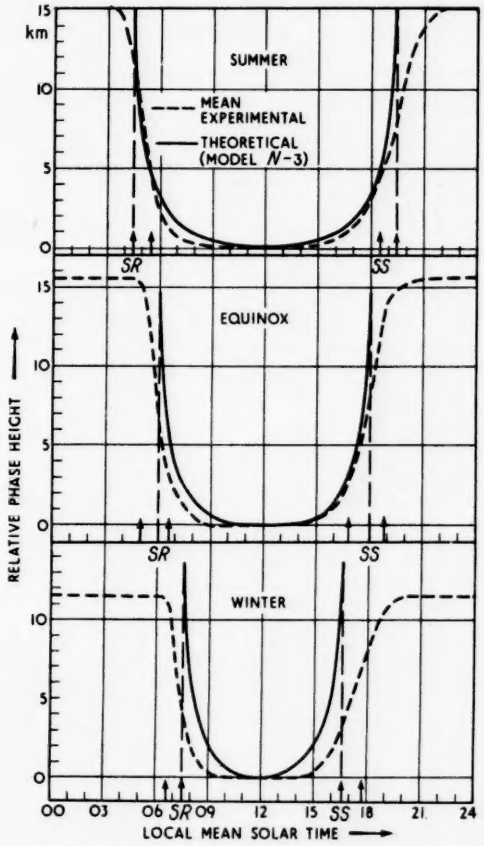

Fig. 10. Diurnal variation of 150-kc phase height, experimental and theoretical.

this quantity, the most rigorous procedure would be a wave solution such as that outlined by GIBBONS and NERTNEY (1951). However, they have shown that their wave solution phase integrals are very nearly the same as the ray theory phase integral, $\int \mu dz$. Therefore, the 150-kc phase height variation was calculated from $\int \mu dz$. It was found (JONES 1953a) to differ from the reflection heights used heretofore by less than 1 km for $\chi < 90°$. Another, though small, correction that can be made is the contribution to $h(t)$ due to transmission through the D-region.

This was also calculated (JONES 1953a) and found not to exceed one-half km at any time, and to be usually much less; certainly negligible in comparison with the several other uncertainties involved.

The calculated phase height variation of N-3 for the three seasons is superposed on the mean experimental curves of Fig. 1 in Fig. 10. With the equinox and summer variations computed, we see that the choice of model was even better than might have been expected from the winter results. Apparently, then, N-3 is a good model for 150-kc phase heights and a fair one for the other experimental data considered.

5. DISCUSSION

It is clear from the preceding work that the "compromise" model finally chosen, N-3, does not satisfy each of the experimental observations used as well as might be hoped. However, it does not seem obvious that any one modification will satisfy all of them much better than this. It is also clear that, while the boundary conditions on the transition region suggested by NICOLET and MANGE are roughly met by the model, the structure within that region is still quite arbitrary, a condition which is tolerated because of the great uncertainties involved.

A large realm of uncertainty exists also in the employment of the scale height and O_2 distributions as though they were independent of time and geographical location, or even as mean distributions. Again, we can only plead ignorance of the complex variations that must occur in these quantities, and plan to include new information as it becomes available.

Extensions of this work contemplated include recalculation of the electron densities by numerical integration of the differential equation (3) and trial of other distributions of O_2; in particular, distributions which can be expressed in analytic form, lending themselves to exact integrations.

6. ACKNOWLEDGMENTS

The material presented in this paper has been submitted in partial fulfilment of the requirements for the degree of Doctor of Philosophy in physics at The Pennsylvania State University. The author wishes to express his appreciation to Drs. A. H. WAYNICK, J. J. GIBBONS and A. P. MITRA for their advice and assistance in this work, and to Dr. M. NICOLET and Dr. P. MANGE for the use of the manuscript of their paper (1954) prior to its publication.

REFERENCES

BATES, D. R., and NICOLET, M.	1950	J. Geophys. Res. **55**, 301
BATES, D. R., and WITHERSPOON, A. E.	1952	Mon. Not. Roy. Astron. Soc. **112**, 101
BENNER, A. H.	1950	Technical Report No. 10, Radio Propagation Laboratory (now Ionosphere Research Laboratory), State College, Pa., Jan. 20.
CHAPMAN, S.	1930	Phil. Mag. **10**, 369
	1931a	Proc. Phys. Soc. **43**, 26
	1931b	Proc. Phys. Soc. **43**, 484
	1953	Proc. Phys. Soc. **66B**, 710

VOL. 6 1955

FINDLAY, J. W.	1949	The phase path of radio waves reflected from the ionosphere (doctoral thesis), Cambridge University
	1951	J. Atmosph. Terr. Phys. **1,** 353
GIBBONS, J. J., and NERTNEY, R. J.	1951	J. Geophys. Res. **56,** 355–371
GLEDHILL, J. A., and SZENDREI, M. E.	1950	Proc. Phys. Soc. **63B,** 427
GRACE, C. H.	1951	J. Geophys. Res. **56,** 452
HACKE, J. E., Jr.	1948	Proc. Inst. Radio Eng. **36,** 724
JONES, R. E.	1953a	Scientific Report No. 48, Ionosphere Research Laboratory, State College, Pa., August 25
	1953b	Rev. Sci. Instr. **24,** 433–436
JONES, R. E., MILLMAN, G. H., and NERTNEY, R. J.	1953	J. Atmosph. Terr. Phys. **3,** 79–91
LINDQUIST, R.	1952	J. Geophys. Res. **57,** 439
	1953	J. Atmosph. Terr. Phys. **4,** 10–27
MITRA, A. P.	1952	Ind. J. Phys. **26,** 79
MITRA, A. P., and JONES, R. E.	1954	J. Geophys. Res. **59,** No. 3
MITRA, S. K.	1952	The Upper Atmosphere, 2nd Edition, The Asiatic Soc., Calcutta
MOSES, H. E., and TA-YOU WU	1951	Phys. Rev. **83,** 109
	1952	Phys. Rev. **87,** 628
	1953	Phys. Rev. **91,** 1408
NICOLET, M.	1945	Mémoires de l'institut Royal Météorologique de Belgique **19**
NICOLET, M., and BOSSY, L.	1949	Ann. Géophys. **5,** 275
NICOLET, M., and MANGE, P.	1954	J. Geophys. Res. **59,** 15–46
PENNDORF, R.	1949	J. Geophys. Res. **54,** 7
WATANABE, K., INN, E. C. Y., and ZELIKOFF, M.	1953	J. Chem. Phys. **21,** 1026
WEEKES, K., and STUART, R. D.	1952	Proc. Inst. Elec. Eng. **99,** Part IV. Preprinted as Monograph No. 15 (Nov. 15, 1951)
WEISSLER, G. L., and PO LEE	1952	J. Opt. Soc. Amer. **42,** 200
WULF, O. R., and DEMING, L. S.	1938	Terr. Mag. **43,** 283

Journal of Atmospheric and Terrestrial Physics, 1955, Vol. 6, pp. 18 to 32. Pergamon Press Ltd., London

Ionospheric absorption measurements at Prince Rupert

KENNETH DAVIES and E. L. HAGG
Radio Physics Laboratory, Shirley Bay, Ottawa

Work carried out under DRB Project No. D48-95-11-02

(*Received* 18 *May* 1954)

ABSTRACT

Measurements of the ionospheric absorption of high frequency radio waves made at Prince Rupert, British Columbia, are described. The dependence of the total local noon absorption, $-\log \rho$ on wave frequency, does not appear to obey the inverse square law, i.e.,

$$-\log \rho \propto \frac{1}{(f+f_L)^2}$$

Studies of the seasonal variation of noon absorption show little dependence on solar zenith angle χ but indicate that abnormally high absorption is present during the winter months. The diurnal variation can be represented very approximately by the expression $-\log \rho \propto (\cos \chi)^n$ where n is about 0·5 on the average.

There is a pronounced correlation between night time ionospheric absorption on 2·0 Mc and the three hour range magnetic K index for values of K greater than 4. It is also found that high night time absorption is often associated with occurrence of intense sporadic E.

VOL. 6 1955

1. INTRODUCTION

Most previous measurements of the ionospheric absorption of high frequency radio waves have been made at sites well removed from the zone of maximum auroral occurrence. Studies of the E- and F-regions in and near the auroral zone (HANSON, HAGG, and FOWLE, 1953) show that the ionosphere differs profoundly there from non-auroral zone regions.

Studies of the seasonal and diurnal variations of ionospheric absorption at places outside the auroral zone (e.g., APPLETON, 1937; BEST and RATCLIFFE, 1938; WHITE and STRAKER, 1939) have revealed dependence on solar zenith angle, season, sunspot activity, and on ionospheric storms. It is of considerable interest, therefore, to see whether ionospheric absorption near the Northern auroral zone behaves differently from that observed at sites far from this zone (particularly in its relationship with magnetic disturbances) and it is believed that the present results will be of interest from this point of view. These measurements were made between April 1949 and March 1950, at Prince Rupert, B.C. (54·3°N, 130·3°W), which is situated about 1000 km from the region of maximum occurrence of the aurora.

2. THEORETICAL CONSIDERATIONS

It has been shown that, in general, the total ionospheric absorption can be divided conveniently into two parts, namely:

(i) deviative absorption, which is associated with marked group retardation and refraction of the wave, and,

(ii) non-deviative absorption, which is caused by "frictional" losses in the lower (D) region of the ionosphere where the electron collisional frequency is high.

According to the magneto-ionic theory of radio wave propagation, the

absorption (k) of a wave of angular frequency p, per unit path length, in a medium containing N electrons per unit volume, is given by

$$k = \frac{2\pi e^2}{\mu mc} \cdot \frac{N\nu}{\nu^2 + (p \pm p_L)^2} \tag{1}$$

where μ is the refractive index,

e,m, are the charge and mass of the electron,

ν is the electron collisional frequency,

p_L is the angular gyro-frequency component in the direction of propagation.

The positive sign in the denominator refers to the ordinary wave and the negative sign refers to the extraordinary wave.

k is large when:

(i) μ is small (deviative absorption) and

(ii) $N\nu$ is large (non-deviative absorption).

APPLETON (1937) has shown that for a Chapman layer the non-deviative absorption varies with solar zenith angle χ according to the relationship

$$\int k \,.\, ds \propto (\cos \chi)^{3/2} \tag{2}$$

Although (2) has been verified, for selected days, by BEST and RATCLIFFE (1938) and by WHITE and STRAKER (1939), most workers prefer the relationship,

$$\int k \,.\, ds \propto (\cos \chi)^n \tag{3}$$

where n is approximately 3/4.

3. METHOD OF MEASUREMENT

The total ionospheric absorption $\int k \,.\, ds$ in decibels, integrated over the whole of the path S, was calculated from measurements of the effective reflection coefficient ρ.

Now
$$\rho = \frac{2A_2}{A_1} = \frac{3A_3}{2A_2} = \text{etc.} \tag{4}$$

A_1, A_2, A_3, are the relative amplitudes of the first, second, third . . . order echoes.

And from the definition of absorption:

$$\int k \,.\, ds = -20 \log \rho \text{ decibels} \tag{5}$$

To determine A_1, A_2, A_3, . . . , pulses of 50 microseconds duration were emitted from a conventional pulsed oscillator of approximately 500 watts peak output power. The echoes were received on a communications receiver suitably modified for pulse reception. A calibrated attenuator in the intermediate frequency amplifier was used to measure the relative amplitudes. The latter were obtained by noting visually the attenuation required to keep the output of the receiver constant. Measurements were made every hour. The average of nine measurements was used to calculate the absorption.

Since in these experiments the antennas used did not discriminate between the ordinary and the extraordinary waves, both were superimposed in the measurements. However, it has been shown, both from theoretical and experimental considerations, that on the frequency of 2·0 Mc, with which most of the work described in this paper is concerned, the extraordinary wave is almost completely absorbed.

4. DEPENDENCE OF ABSORPTION ON WAVE FREQUENCY

According to the magneto-ionic theory of wave propagation the non-deviative absorption of the ordinary wave of frequency f should be proportional to

$$\frac{1}{(f+f_L)^2} \qquad \text{(see equation (1))}$$

where

$$f_L = \frac{eH}{2\pi mc} \cdot \cos\theta$$

H is the magnetic field and θ is the angle between the direction of wave propagation and the magnetic field.

This law (i.e., $-\log \rho \propto (f+f_L)^{-2}$) has been verified under certain specific conditions by APPLETON and PIGGOTT (1948). To see whether it is valid generally we have taken the monthly median noon values of $-\log \rho$ for the following frequencies 2·0, 2·6, 3·2, 3·8, 4·4, and 5·2 Mc and plotted the quantity $(-\log \rho)^{-\frac{1}{2}}$ against frequency.

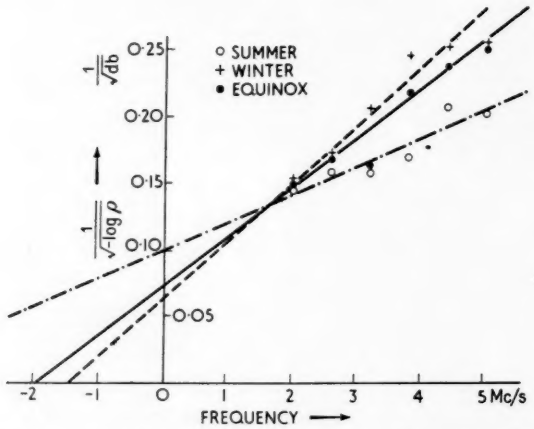

Fig. 1. Dependence of noon ionospheric absorption on wave frequency (Prince Rupert, B.C.)

For the sake of clarity the data have been grouped into seasons as follows:

Summer	May, June, July, August,
Winter	November, December, January, February,
Equinox	March, April, September, October.

The values thus obtained are plotted in Fig. 1. It can be seen that the points lie only approximately on straight lines and that the slopes and intercepts vary with the seasons.

VOL. 6 1955

5. Ionospheric Absorption and Magnetic Activity

Several workers (e.g., Wells, 1947) have directed attention to the fact that intense magnetic disturbances are accompanied by radio "blackouts." However, few quantitative correlations have been established between magnetic activity and ionospheric absorption.

Owing to the localized nature of ionospheric absorption and, although to a lesser extent, of magnetic disturbance it is advisable that both quantities be measured at the same place. Unfortunately, no magnetic data are available for

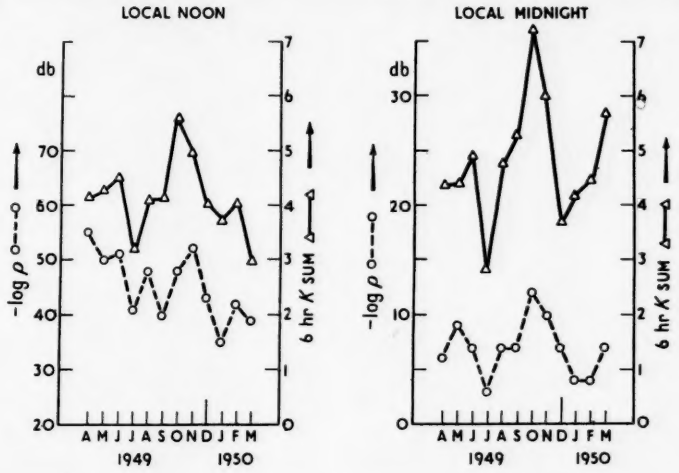

Fig. 2. Monthly median values of ionospheric absorption on 2 Mc at Prince Rupert and the monthly mean values of K for 6-hour periods centred on local noon and local midnight at Sitka.

Prince Rupert and so the magnetic three-hour range K-indices for Sitka, Alaska, have been used for the present correlation studies. (The distance between Prince Rupert and Sitka is about 420 km.)

As a first step towards establishing a quantitative correlation between ionospheric absorption and magnetic activity, the monthly median noon values and the monthly median midnight values of ionospheric absorption on a frequency of 2·0 Mc have been plotted in Fig. 2 together with the monthly mean noon and midnight values of the magnetic K indices for Sitka. The noon value of K is the average of the two 3-hour periods, 0900 hours to 1200 hours and 1200 hours to 1500 hours, 120°W mean time. Similarly, the midnight value of K is the mean of the two 3-hour periods: 2100 hours to 0000 hours and 0000 hours to 0300 hours. The lowest frequency (2·0 Mc) was chosen so as to minimize the influence of deviative absorption. Periods during which deviative absorption obviously predominated (during dark hours of January and February 1950. See Fig. 8) were excluded from this study.

From Fig. 2 it is seen that the correlation between the noon values of $-\log \rho$ and the noon values of magnetic K is not very good (correlation coefficient = $+0{\cdot}18$). On the other hand, the correlation coefficient between the two sets of

midnight values is +0·77 and, if the month of December 1949 is excluded, the correlation coefficient is raised to +0·81. Since the correlation between the night-time absorption and magnetic K is so much greater than the correlation between the noon data most attention will be confined to the night-time data.

The data plotted in Fig. 2 show that the night-time ionospheric absorption increases when the magnetic K-index increases. Hence, it is of interest to see whether there is any relationship between these two quantities. For this purpose the data have been grouped in the following way:

The mean value of the absorption has been found for all nights when the mean magnetic K-index, for the two periods 2100 to 0000 hours and 0000 to 0300 hours,

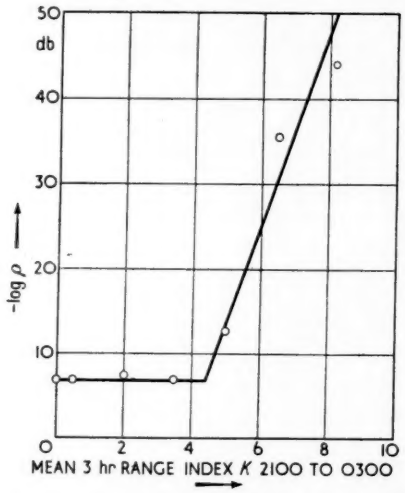

Fig. 3. Correlation between 2 Mc/s absorption at Prince Rupert (midnight) and the 3-hour range index K observed at Sitka.

lay in the range 0 to 1·0. Similarly all nights when K lay in the range 1·5 to 2·5 have been grouped together and the mean midnight absorption for these nights has been determined. This procedure has been repeated for nights when K lay in the ranges, 3·0 to 4·0, 4·5 to 5·5, 6·0 to 7·0, and 7·5 to 9·0. The six mean values of absorption thus obtained are plotted in Fig. 3. An interesting fact which emerges from this grouping of the data is that, for values of K less than 5, the ionospheric absorption is practically independent of changes in magnetic activity whereas, for values of K equal to and greater than 5, there is a direct quantitative correlation between the two phenomena. It should be noted that the value of the absorption for $K = 8{\cdot}2$ is almost certain to be too low because, in computing the midnight absorption, the absorption during a blackout has been taken to be equal to the maximum measurable absorption of 55 decibels. This maximum is set by technical limitations.

It is convenient at this point to study the correlation between the individual nightly values of $-\log \rho$ and the magnetic K-index. During the plotting of the individual midnight values of $-\log \rho$ and K (not shown), it was noticed that

, VOL. 6 1955

scatter of the data was very large and consequently the correlation was obscured. There are two reasons for this high dispersion of the data; these are:

(i) The absorption was calculated from 9 amplitude measurements only so that the errors caused by fading may be appreciable. A statistical sampling of amplitude measurements has been carried out by one of the authors (BEYNON and DAVIES, 1954) and this showed that a mean of only nine amplitude measurements may be in error by 35 per cent.

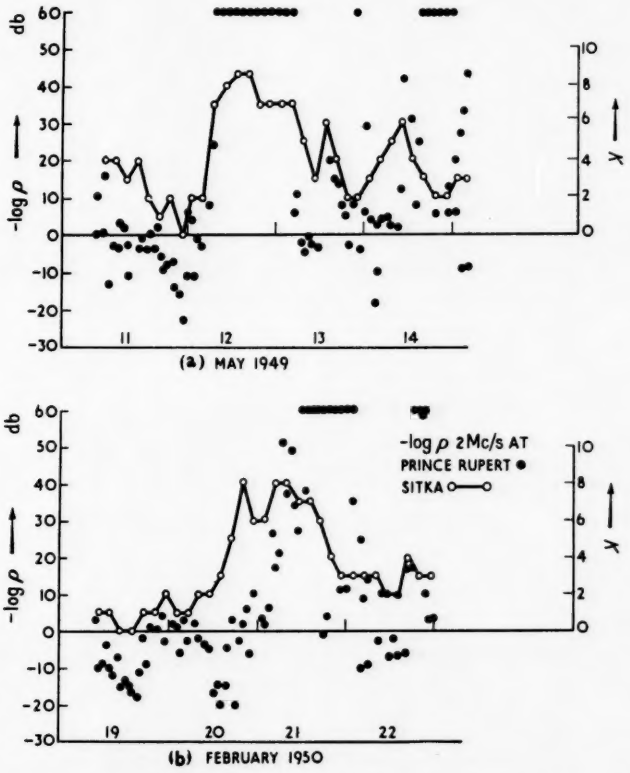

Fig. 4. Departures of hourly absorption values from the monthly median values and the 3-hour range indices K.

(ii) During ionospheric and magnetic storms the time of maximum ionospheric absorption does not, in general, coincide with the time of maximum K. One may lag or lead the other. To illustrate this point two occasions have been selected during which magnetic and ionospheric disturbances occurred during hours of darkness. In Figs. 4a and 4b the departures of the hourly absorption values from the monthly median values (thus removing the diurnal variation) are plotted together with the 3-hour range K-indices for Sitka. Fig. 4a shows that during the period 11, 12, 13, and 14 May, 1949, the magnetic and ionospheric disturbances are practically in phase. It is relevant to note that on 14 May high ionospheric

absorption persisted after the magnetic activity has subsided and that this is a common occurrence. Fig. 4b on the other hand shows a period when the magnetic storm reached an advanced stage (2000 hours GMT, 20 February) several hours before the ionospheric absorption reached a maximum (0700 hours GMT, 21 February). Here again high absorption tended to persist after the magnetic K figure had returned to normal. From (i) and (ii) above it can be seen that to obtain a reasonable correlation it is necessary to take average values of $-\log \rho$ and K for periods sufficiently long to minimize the errors due to these factors. The night-time absorption on 2·0 Mc has, therefore, been taken as the mean for the 12-hour period 1900 hours to 0600 hours inclusive 120° west meridian time. This has been done

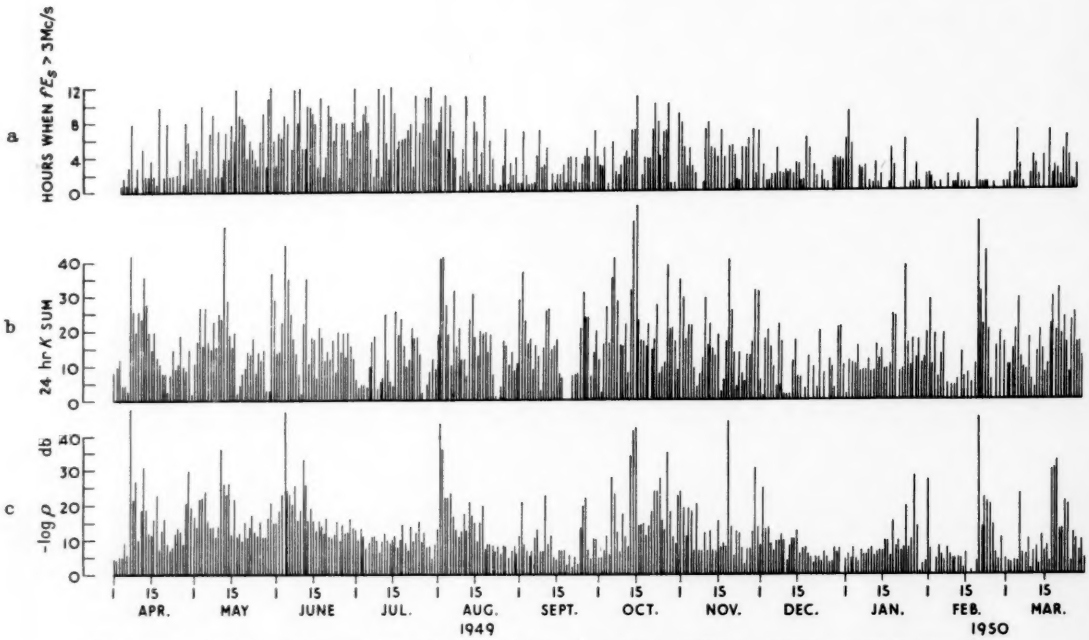

Fig. 5. Correlation between (a) 2 Mc ionospheric absorption (1900 to 0600 hrs 120° W.M.T.) at Prince Rupert; (b) 24-hour sums of Sitka 3-hour range index (1300 to 1200 hrs 120° W.M.T.); (c) number of hours for which fE_s exceeded 3 Mc in period 1900 to 0600 hrs 120° W.M.T. at Prince Rupert.

for each night of the year from April 1949 to March 1950, inclusive, and the values thus obtained are plotted in Fig. 5, together with the 24-hour sums of the 3-hour range under K centred on 120° west, midnight (i.e., 1300 hours to 1200 hours). The correlation coefficient between these two sets of data is +0·7. The correlation is particularly striking for values of the K sum greater than about 30. The monthly correlation coefficients are given in Table 1, from which it is seen that the correlation is reasonably steady throughout the year except for the months of July 1949 and December 1949, when the general levels of magnetic activity were low.

, VOL. 6 1955

Table 1

1. Correlation between night ionospheric absorption (2·0 Mc), magnetic activity, and sporadic E.

2. Values of the parameters n and B in the expression

$$-\log \rho = B \,.\, (\cos \chi)^n$$

Correlation coefficients

Month	$-\log \rho$ and K	$-\log \rho$ and E_s	n	B
April 1949	0·70	0·21	0·82	11
May	0·60	−0·02	0·80	9
June	0·73	0·02	0·64	13
July	0·26	−0·11	0·67	10
August	0·76	0·66	0·60	14
September	0·71	0·52	0·52	18
October	0·74	0·68	0·30	31
November	0·75	0·15	0·33*	35
December 1949	0·00	0·07	0·39	31
January 1950	0·55	0·31	0·29	27
February	0·72	0·67	0·45	25
March	0·62	0·59	0·39	20
Mean	0·59	0·31	0·51	20

* Doubtful value.

6. Ionospheric Absorption and Sporadic E

There is some evidence to show that during ionospheric storms sporadic E ionization is considerably enhanced (Mitra, 1952, p. 332). Considerable difficulties are encountered in attempting a quantitative correlation between ionospheric absorption and sporadic E. For instance, it is difficult to define fE_s; since this depends to some extent on the equipment characteristics. In addition to this, there is the problem of grouping the data in such a way as to bring out the desired correlation.

For the present purpose attention has been confined as far as possible to the night-time data. Taking the hours of 1900 to 0600, 120° W.M.T., the percentages of time each night for which fE_s exceeded 3·0 Mc have been calculated.

The results thus obtained are shown in Fig. 5 from which it appears that peak values of absorption are generally associated with enhanced sporadic E. The converse is not necessarily true particularly during the summer months of June and July, when strong sporadic E ionization is present but ionospheric absorption is low and steady. The monthly correlation coefficients are given in Table 1. During the months May, June, and July the correlation coefficients are very close to zero. The low correlation coefficient for December is to be expected as there was very little variation in absorption throughout the month.

7. TEMPORAL VARIATIONS IN IONOSPHERIC ABSORPTION

(a) *Seasonal variation*

The seasonal variation in the ionospheric absorption of 2 Mc radio waves is shown in Fig. 6, in which the monthly median values of the noon ionospheric absorption have been plotted. The monthly values indicate a general decrease in absorption throughout the period, which may be associated with the 11-year sunspot cycle,

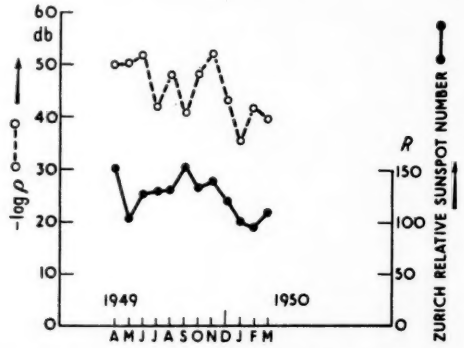

Fig. 6. Seasonal variation of 2 Mc ionospheric absorption noon at Prince Rupert (monthly median values) and monthly mean values of the Zurich relative sunspot number.

although the individual monthly median values of absorption show little or no correlation with the monthly mean relative sunspot numbers plotted in Fig. 6. It is interesting to note that the monthly median noon values of absorption show practically no dependence on solar position, which is surprising in view of the

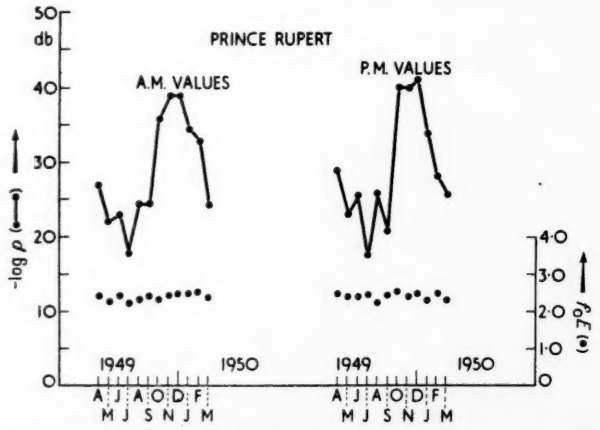

Fig. 7. Seasonal variation in 2 Mc ionospheric absorption at a constant value of solar zenith angle ($\cos \chi = 0{\cdot}2$).

general solar control of the ionosphere. There is a maximum of noon absorption in November, but this is due partly to the large number of disturbed days during the months of October and November together with the effect of the so called "winter anomaly."

VOL. 6 1955

The winter anomaly, which was first detected by APPLETON in 1937, is illustrated very clearly in Fig. 7 in which are plotted the monthly median values of 2 Mc ionospheric absorption measured at a constant value of the solar zenith angle. Whereas, according to theory, we should expect the absorption at constant solar angle to be fixed, in fact it can be seen that for the five winter months October, November, December, January, and February the ionospheric absorption is abnormally high when compared with the remaining summer months. The corresponding values of the normal E-region critical frequency which are also included in Fig. 7 show that the high winter absorption cannot be attributed to increased deviative absorption in the E-region.

(*b*) *The diurnal variation*

To study the diurnal variation, plots of the monthly median hourly values of $-\log \rho$ are shown in Fig. 8. The time scale refers to the 120° west meridian so that the mean local noon at Prince Rupert is nearly 1240 hours. In calculating the monthly median values no special selection of days has been made as it was thought desirable to study an average day rather than say a "quiet" day.

In general, these diurnal curves confirm the results of previous workers. Thus the absorption increases rapidly after sunrise, attains a maximum in the early afternoon, and decreases again, as would be expected from normal solar control.

It will be noted that during the winter months January and February the night-time absorption is apparently very high. Examination of ionospheric data shows that the mean F_2 region critical frequency was near 2 Mc, so that the high absorption is due to deviative absorption and penetration effects which give rise to very low apparent reflection coefficients.

(*c*) *Time of maximum ionospheric absorption*

It has been pointed out already that the daily maximum of ionospheric absorption takes place, usually, not at noon, when $\cos \chi$ is a maximum, but shortly afterwards. In Fig. 9 a histogram has been constructed to show the frequency distribution of the times of maximum of ionospheric absorption over the period under consideration. Days during which blackout lasted more than 3 hours were excluded from this count as it was felt that these were not due to the normal variation in D-region absorption. The mean time of maximum absorption is 1300 hours, which is about 1220 hours local mean time. This "relaxation time" of 20 minutes is in reasonably good agreement with various estimates, usually of the order of 30 minutes, made by previous workers.

8. DEPENDENCE OF ABSORPTION ON COS χ

APPLETON (1937) has shown that non-deviative absorption in a Chapman region varies as $(\cos \chi)^{3/4}$ where χ is the solar zenith angle. Although this law has been verified for F-layer reflections on magnetically quiet days (see Refs. 3 and 12) most workers have found that the diurnal variation of ionospheric absorption, particularly at frequencies reflected from the E-layer, is more closely represented by the expression:

$$-\log \rho \propto (\cos \chi)^n \qquad (3)$$

where n varies over a wide range from day to day and from month to month but has an average value of about 0·75.

To see whether the above law is valid for the present measurements, $-\log \rho$ has been plotted against $\cos \chi$ on logarithmic graph paper. Data for twelve months

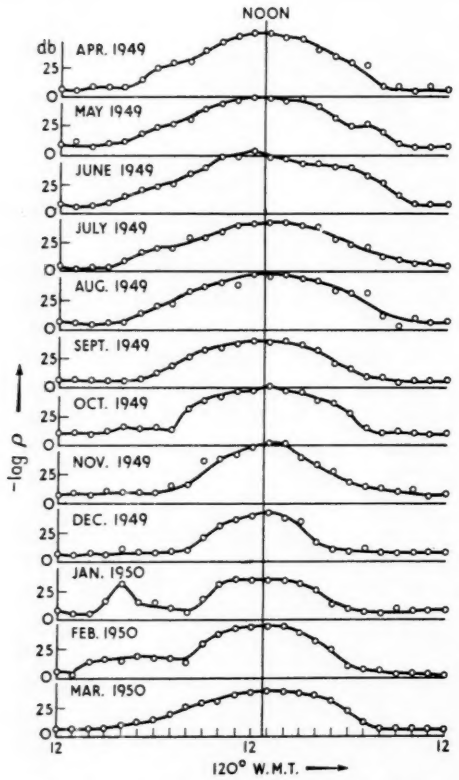

Fig. 8. The diurnal variation of 2 Mc ionospheric absorption at Prince Rupert. Monthly median hourly values.

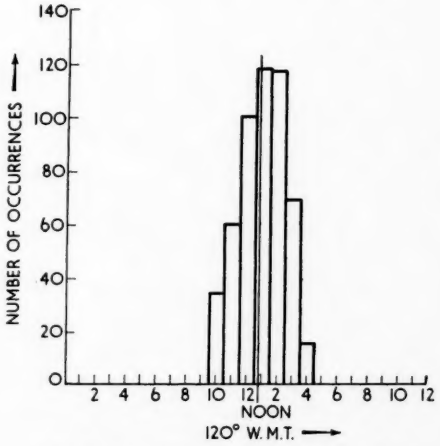

Fig. 9. Distribution of times of daily maximum of 2·0 Mc/s ionospheric absorption at Prince Rupert.

are shown in Fig. 10. The relationship is only very approximately linear and so the closest straight lines have been fitted visually and the values of n taken from the slopes.

The values of n so obtained are shown in Table 1. It is seen that there is a wide variation throughout the year, the tendency being towards high values in summer and low values in winter. The points for the month of November were so scattered that a very rough relationship only could be established. The mean value for the whole year of 0·51 is somewhat lower than the values obtained by other workers for regions well removed from the auroral zone, and this may be due to the closer proximity of the auroral zone.

VOL. 6 1955

9. Discussion

The main points which have emerged from the foregoing studies of ionospheric absorption may be stated as follows:—

(i) Monthly median noon values of ionospheric absorption do not, in general, vary with frequency as predicted by the magneto-ionic theory (i.e., $-\log \rho \propto (f + f_L)^{-2}$).

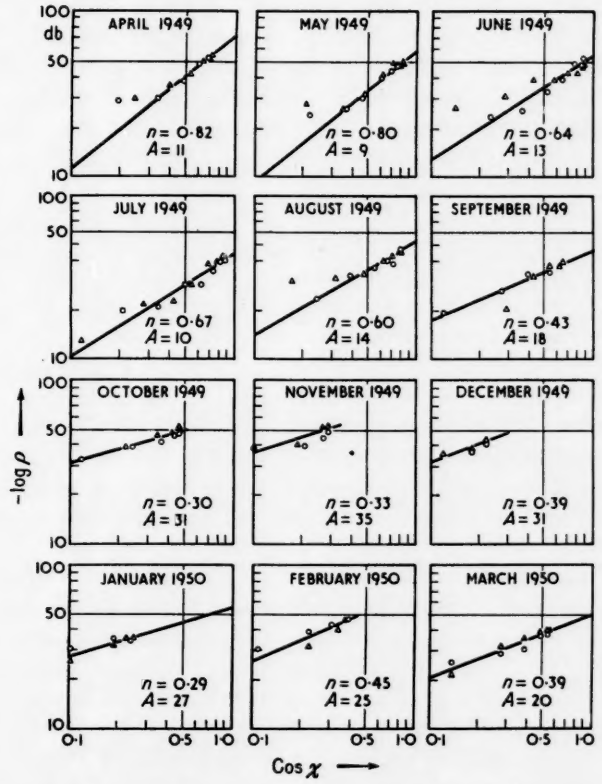

Fig. 10. Diurnal variation of 2 Mc ionospheric absorption at Prince Rupert. Dependence of monthly median hourly values of $-\log \rho$ on $\cos \chi$.
n = slope (Δ—P.M. values)
A = intercept (○—A.M. values)

(ii) The correlation between ionospheric absorption and magnetic activity is better at night than during the day. The night-time correlation between absorption and magnetic activity is very low for values of the magnetic K-index less than 5 and the correlation is high for values of K equal to and greater than 5.

(iii) Night-time absorption is often associated with a marked enhancement of sporadic E ionization. However, the converse is not necessarily true, particularly during the summer months.

(iv) Although there is some evidence to show that ionospheric absorption follows the 11-year sunspot cycle the individual monthly values show very little dependence on sunspot number.

(v) The diurnal variation of ionospheric absorption on 2 Mc does not follow the three-halves power law (i.e., $-\log \rho \propto (\cos \chi)^{3/2}$) as required by the theory of absorption in a Chapman region, but the dependence on solar angle is approximately $-\log \rho \propto (\cos \chi)^{1/2}$. The ionospheric absorption does not, in general, attain a maximum at local noon but at about 20 minutes later.

The above points shall now be considered in greater detail.

(i) It appears from these studies of the seasonal variations of the noon ionospheric absorption that the relative changes in absorption from summer to winter increase as the frequency increases. This means that the dependence of $-\log \rho$ on frequency is not the same in summer as it is in winter. Since the noon absorption on 2 Mc shows little or no change from summer to winter (except that caused by magnetic disturbances) it may be presumed that the true D-region absorption undergoes very little systematic seasonal change. However, on the higher frequencies there are more appreciable changes in absorption. It may be concluded, therefore, that the absorption in regions above the D-region is responsible for the variations on the higher frequencies.

It is of some importance to consider what effect this has on the calculation of the so called absorption index "A." This quantity is defined as the absorption suffered on an "effective" frequency of 1 Mc. By definition, this index assumes the validity of the inverse square law (i.e., $A = -\log \rho \,.\, (f + f_L)^2$). Hence, if the law is not valid, there is some doubt as to the value of this absorption index.

VOL. 6 1955

(ii) The first point of importance which has emerged from this investigation into the correlation between ionospheric absorption and magnetic activity is that the correlation is higher for the night-time absorption than for the daytime absorption. This suggests immediately that the ionization produced in the D-region by solar ultra-violet radiation is not the agent responsible for magnetic disturbances. This would be expected if the ionization produced by the ultra-violet radiation remained stationary with respect to the earth. The night-time absorption on the other hand is almost certainly produced by the bombardment of the atmosphere by corpuscular radiation. It is reasonable to suppose that such a process would give rise to the movement of ionization, and hence the production of large electric currents. This is supported by the wind experiments of CHAPMAN (1953) discussed below.

These studies of the relationship between midnight absorption and the magnetic K-index appear to offer a possible criterion for distinguishing between magnetically disturbed and magnetically quiet periods in so far as the ionosphere is concerned. Periods when K ranges from 0 to 4 may be classified as "quiet" and periods during which K ranges from 5 to 9 may be classified as "disturbed." This possibility is supported by the wind experiments of CHAPMAN (1953). He found that the mean wind velocity is sensibly independent of the K-index until the value of K exceeds four. CHAPMAN also observed that "when the K-index was five or greater, higher absorption commonly made echoes too weak for recording."

In studying the correlation between the present nightly absorption data and magnetic data it should be borne in mind that the two observing sites, Prince Rupert, B.C., and Sitka, Alaska, are separated by some 420 kilometres. The mean monthly correlation coefficient of +0·59 compares favourably with the value of about +0·3 obtained by RAWER (1952) for the correlation between simultaneous absorption values at stations separated by about the same distance.

(iii) The present work on the correlation between absorption and the occurrence of sporadic *E* confirms the observations of other workers. One of the difficulties encountered here was the problem of arranging the data is such a way that the desired effect might be brought out. However, by treating the data as in Section 6, the conclusion that high absorption is generally associated with enhanced sporadic *E* ionization is confirmed.

But here again, there are two types of sporadic *E*, namely,

(*a*) The type which increases from winter to summer and which may be present even when the ionospheric absorption is small, and

(*b*) the type which is associated with high ionospheric absorption.

As far as is known the latter type of sporadic *E* occurs only in polar regions.

(iv) Although the long term variations in ionospheric absorption tend to follow the sunspot cycles (RAWER, 1952) the individual monthly median values of the two quantities show little interdependence. It may be that the changes in visible solar activity are not connected directly with the ionizing radiation responsible for the production of the absorbing layer.

(v) One of the striking features which emerges from the present work is the large increase in ionospheric absorption during the winter months, October, November, December, 1949 and January 1950. This manifests itself in three ways:

1. The winter noon absorption values show no tendency to fall below the summer noon values, and

2. For a constant value of $\cos \chi$ the absorption shows a marked increase during the winter months.

3. The monthly values of the parameter *B*, defined in equation (6) below, show a marked increase during these winter months. These values of *B* are tabulated in Table 1.

This cannot be attributed to magnetic disturbances, since December 1949 was a comparatively quiet month whereas February 1950 was relatively disturbed. Neither does it appear likely to be due to increased deviative absorption in the *E*-region, since, for a constant value of $\cos \chi$, there is no appreciable seasonal change in f_0E. It is concluded, therefore, that the winter anomaly is due to increased absorption in the *D*-region.

(vi) PIGGOTT (1950) has shown that the diurnal variation of non-deviative absorption at Slough can be represented approximately by the relation,

$$-\log \rho = B \,.\, (\cos \chi)^{0.75} \qquad (6)$$

where *B* is a parameter which may vary from one month to another. The above value of the power of $\cos \chi$ compares with a value of 0·5 for the Prince Rupert data.

Thus it appears that as the auroral zone is approached the value of the power decreases. A similar phenomenon in the E-region has been pointed out by SCOTT (1952), who showed that the value of n in the relation

$$f_0E \propto (\cos \chi)^n \tag{7}$$

decreased from about 0·25 outside the auroral zone to about 0·1 inside the zone. It is interesting also to note that this similarity between the value of n for the D and E regions extends to the seasonal variation of the indices, namely that n tends to be higher in summer than in winter.

It is concluded that, near the auroral zone, ionization by solar ultra-violet radiation is modified by the influence of charged corpuscles.

10. CONCLUSIONS

As there is very little published work on the subject of ionospheric absorption near the auroral zone it is hoped that the present study will be of some help in extending our knowledge of a region of great importance in ionospheric research. The data were collected more or less on a routine basis without a definite objective in view and hence their value is somewhat restricted. However, the results may be of some importance from a statistical point of view.

11. ACKNOWLEDGMENTS

The absorption measurements described above were made at the suggestion of Mr. J. H. MEEK and were carried out by the Royal Canadian Corps of Signals under the supervision of Sgt. E. G. LUSHINGTON.

, VOL. 6 1955

REFERENCES

APPLETON, E. V.	1937	Proc. Roy. Soc. A **162**, 451
APPLETON, E. V., and PIGGOTT, W. R.	1948	U.R.S.I. Proceedings, p. 330
BEST, J. E., and RATCLIFFE, J. A.	1938	Proc. Phys. Soc. **50**, 233
BEYNON, W. J. G., and DAVIES, K.	1954	J. Atmosph. Terr. Phys. **5**, 273
CHAPMAN, J. H.	1953	Canad. J. Phys. **31**, 120
HANSON, HAGG, L., and FOWLE,	1953	The interpretation of ionospheric records, DRTE Report R2
MITRA, S. K.	1952	The Upper Atmosphere, p. 332
PIGGOTT, W. R.	1951	Radio Research 1950 (H.M.S.O.)
RAWER, K.	1951	J. Atmosph. Terr. Phys. **2**, 38
SCOTT, J. C. W.	1952	J. Geophys. Res. **57**, 369
WELLS, H. W.	1947	Terr. Mag. and Atmosph. Elec. **52**, 315
WHITE, F. W. G., and STRAKER, T. W.	1939	Proc. Phys. Soc. **51**, 865

Journal of Atmospheric and Terrestrial Physics, 1955, Vol. 6, pp. 33 to 45. Pergamon Press Ltd., London

Geomagnetic and geoelectric variations

J. G. SCHOLTE and J. VELDKAMP
Royal Netherlands Meteorological Institute, De Bilt

(*Received* 3 *June* 1954)

ABSTRACT

The geomagnetic variations and their relation to earth-currents have been investigated, especially the pulsations with periods of 10 to 10^2 seconds.

A worldwide survey of a few examples of pulsations (selected from the IATME Bulletins and the quarterly De Bilt reports) indicates that the source of the phenomenon may be the ionospheric vibrations caused by a disturbance of the ionization equilibrium.

The connection with the electric field induced in the earth was studied by measuring the ratio of amplitudes of the N–S component H_y of the magnetic field and the E–W component E_x of the electric field; the phase-difference between these quantities has been determined for a great number of pulsations.

As it was doubted if the theory of plane waves reflected by a plane earth was valid in this case, the earth's radius being small compared with the wavelength of these vibrations, the reflection by a sphere has been investigated theoretically. The results are very similar to those of the plane-earth theory, with the exception of the ratio between horizontal and vertical magnetic components.

The values of E/H and of the phase-difference between electric and magnetic variations depend on the structure of the earth; it is therefore possible to derive some knowledge of the upper layers from the measurements. In this way some information with respect to the distribution of the conductivity in the ground at the observatory Witteveen has been obtained.

It is a well-known fact that geomagnetic variations are accompanied by variations of the electric field, as measured between two electrodes in the earth. The geomagnetic variations in the N–S direction are paralleled by geoelectric fluctuations in the E–W direction, and vice versa.* This is not only true for magnetic bays with very large periods, but also for pulsations with periods between 10 and 150 seconds (SCHLUMBERGER and KUNETZ, 1948).

For a detailed investigation the irregular bays are not very suitable, but pulsations are often recorded as long series of nearly harmonic waves, so that they can better be compared with theory. Two types of pulsations can be distinguished. The first type is found during the day, and is at Wi characterized by periods between 10 and 60 seconds, with a most frequent value of about 45 seconds, and with amplitudes of a few gammas. Especially on disturbed days these pulsations can last for hours. The second type is recorded in the evening and night hours, very often at the beginning of a bay-like disturbance. These evening pulsations have a greater period (about 110 seconds) and often a greater amplitude (about 10 gammas).

A few strong pulsations of the second type were selected from the p.s.c.'s published in the IATME Bulletins No. 12a–12g, and in the three monthly reports from the C + K—Centre De Bilt. Magnetograms were kindly supplied by a great number of observatories. A few observatories (Le, Lo, Es, Rs, Ab, Wi, CF, and Hr) sent quick-run records as well. Figs. 1 and 2 show the magnetograms of a small number of the observatories for two of the selected cases. The stations are

* See S. CHAPMAN and J. BARTELS, *Geomagnetism*, Vol. I, Chap. 13.

indicated by the international two-letter symbol (see IATME Bulletins No. 12a–12g). The observatories are chosen along three meridians, viz. 0°, 90°, and 180° W.L. A scale of 50 γ is drawn near to each curve to give some idea of the amplitudes

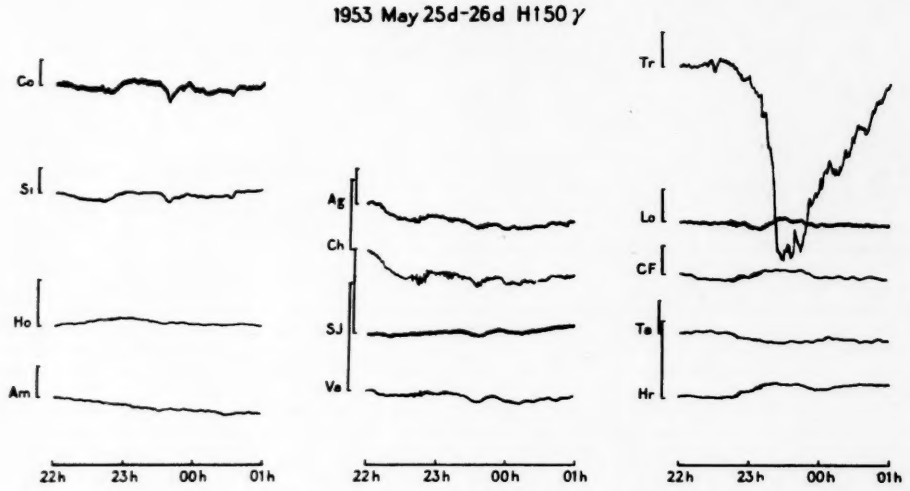

Fig. 1. Magnetograms (horizontal component) of a polar disturbance near the observatory Tromsö, accompanied by a pulsation. The vertical scales indicate 50 gammas.

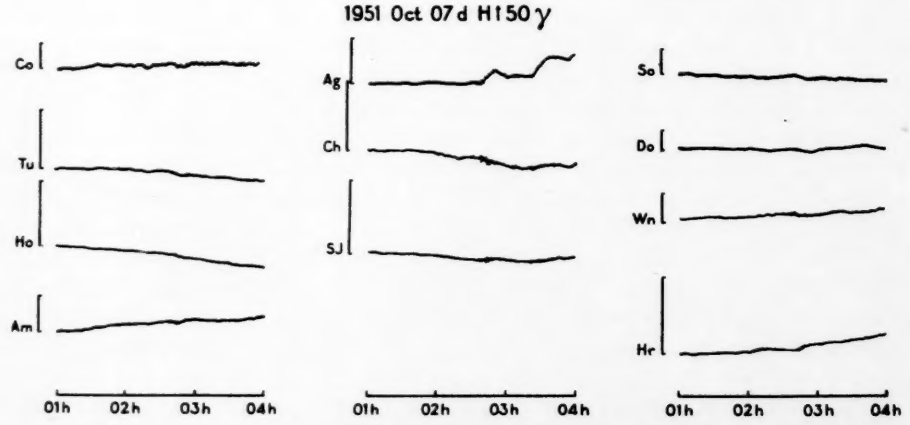

Fig. 2. Magnetograms of a polar disturbance near the observatory Agincourt, accompanied by a pulsation. Vertical scales of 50 gammas.

involved. The reproduced magnetograms are more or less arbitrarily chosen out of the great number received from thirty-eight observatories; other magnetograms show essentially the same features. In Figs. 3 and 4 are drawn the disturbance vectors of the recorded pulsations, calculated from the quick-run records.

VOL. 6 1955

In these figures the observatories are arranged roughly according to their geographical situation; the total length of each N–S and E–W axis is 10 γ.

The vertical amplitude of the disturbance vector is indicated at the northerly end; $Z = -2$ means that this end dips 2 γ below the horizontal plane.

In the first case reproduced (Figs. 1 and 3) the pulsation is connected with the beginning of a local disturbance near the auroral zone, which is recorded as a very large bay at Tr. With increasing distance from Tr the amplitude of the bay disturbance falls off very fast, so that at a distance of, say, 1000 km only a small bay can be perceived. The cause of this bay disturbance must be a quite local

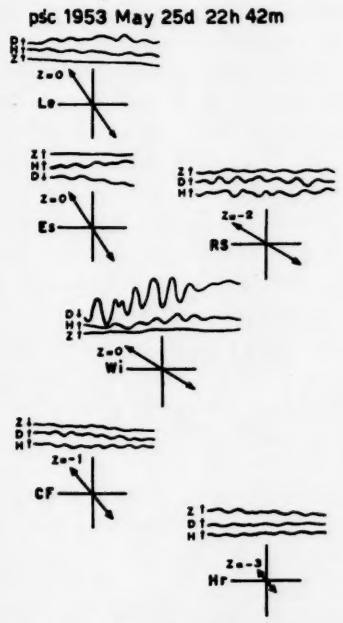

Fig. 3. Quick-run records and vector diagrams of the pulsation accompanying the beginning of the bay disturbance of Fig. 1.

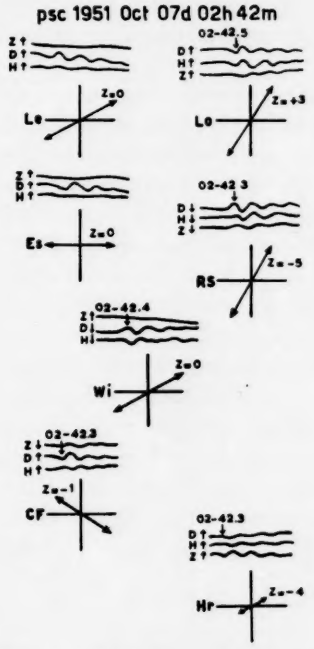

Fig. 4. Quick-run records and vector diagrams of the pulsation at the beginning of the polar disturbance of Fig. 2.

current-system near Tr. The amplitude of the pulsation, connected with the beginning of the bay, diminishes more slowly; the pulsation is recorded over more than half of the earth's surface, in stations as far apart as Ho and Hr.

Apparently the cause of the pulsation, if near the earth, must have very large horizontal dimensions (BEAUFILS, 1950), or it must be situated at a very large distance from the earth. During the pulsation the disturbance vector describes a straight line or a very flat ellipse moving from SE to NW and dipping to the north.

The second case reproduced (Figs. 2 and 4) is an example of a pulsation which was recorded in Europe in the absence of a bay disturbance. In Canada, however, this pulsation was accompanied by the beginning of a local storm, recorded at the observatory Ag. Even in this case the pulsation was recorded over more than

a hemisphere, as far as in Am and Hr. The beginning of the pulsation occurred at nearly the same time in Europe as in South Africa, and the amplitudes of the disturbance-vectors at the widely separated stations Le and Hr are not very different.

So we are led to the conclusion that in these investigated cases the pulsation was connected with the sudden commencement of a magnetic disturbance. We may suppose that a vibration is set up in the ionosphere by the incidence of solar corpuscula and that this perhaps is the cause of all pulsations. One might think of an eigen-vibration of the ionosphere, set up by a disturbance of the normal ionization. A similar idea was put forward by HOLMBERG (1953), who speaks of a "magneto-hydrodynamical resonance" in one or more ionospheric layers. However, up till now only the summary of his paper has come to our knowledge.

A vibration of the ionosphere would explain the great area over which the pulsation is recorded with almost constant amplitude. The difference between day and night pulsations could perhaps be associated with the existence of the E- and F_2-layers, and the difference in main periods (45 sec and 110 sec respectively) may possibly be ascribed to the different thicknesses of these layers (about 50 km and 200 km respectively). It is a pity that so few magnetic observatories are equipped with quick-run recorders (only one outside of Europe), which prevents a complete investigation of this interesting phenomenon. It would also be worth while to look for variations of the height and (or) critical frequencies of the ionosphere, which possibly correspond to the geoelectromagnetic pulsations.*

VOL. 6 1955

It is not possible to construct a complete theory for the time being, and theoretically one can only investigate the properties of some arbitrarily chosen electromagnetic field in the neighbourhood of the earth, hoping that it will not differ too much from the actually existing field.

The most simple case is that of a plane electromagnetic wave reflected by a plane surface (Fig. 5a); the amplitude A of the reflected wave is according to FRESNEL'S formula: $A = -1 + B$, where $B = \dfrac{2 \cos \alpha_0}{\cos \alpha_0 + p \cos \alpha_1}$ and p is the index of refraction, or $p = \sqrt{\varepsilon - 2i\sigma T}$ (assuming $\mu = 1$).

The value of σT is for the very long periods involved (10 to 100 seconds) great in comparison with ε, even in the case of the most insulating material. For instance: as the conductivity of consolidated rock is about 10^6 e.s.u., the value of σT is at least 10^7; in the case of a silver mirror the conductivity is $6 \cdot 10^{17}$ e.s.u. and the period of visual light is $2 \cdot 10^{-14}$ sec, hence $\sigma T = 10^4$. This means that the earth is reflecting the pulsating electromagnetic field like a very good mirror with an extremely great index of refraction $p = e^{-\pi i/4} \sqrt{2\sigma T}$.

Consequently the amplitude of the reflected wave is in first approximation equal to that of the incident wave; the resulting field is a standing wave with the following amplitude-ratios:

$H_x : H_z : E_y = 2 \cos \alpha_0 \cdot \cos (k_0 z \cos \alpha_0) : 2 \sin \alpha_0 \cdot \sin (k_0 z \cos \alpha_0) : 2 \sin (k_0 z \cos \alpha_0)$

where $k_0 = \omega/c$. The first nodal plane is the reflecting surface; in this plane H_z and E_y are equal to zero, whereas H_x reaches at $z = 0$ its maximum value $2 \cos \alpha_0$.

* HARANG observed in 1939 fluctuations of the reflection height during a giant pulsation.

In the neighbourhood of a point where one of the components of the field vanishes, this first approximation no longer suffices; in second approximation a small progressive reflected wave with amplitude B has to be considered, where $B \approx 2p^{-1} \cos \alpha_0$. In the plane $z = 0$ the amplitudes of E_y and H_z are $2p^{-1} \cos \alpha_0$ and $2p^{-1} \cos \alpha_0 \sin \alpha_0$ respectively, whereas H_x retains the value $2 \cos \alpha_0$; the amplitude ratios at the earth's surface are

$$H_x : H_z : E_y = 1 : p^{-1} \sin \alpha_0 : p^{-1},$$

showing the remarkable phase difference of $\pi/4$ between E_y and H_x.

The refracted field is at $z = 0$ equal to the total field in the vacuum; it decreases exponentially with the depth according to $e^{-ipk_0 z}$ or $e^{-(1+i)z/z_0}$, with $z_0 =$ the

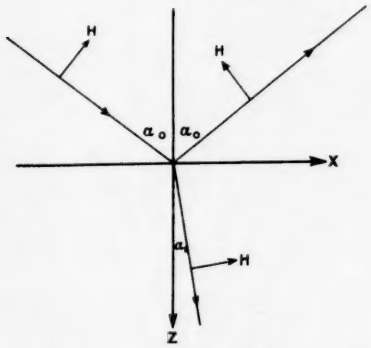

Fig. 5a. Schematic representation of a plane-wave system.

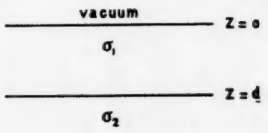

Fig. 5b.

depth of penetration $c(2\pi\sigma\omega)^{-\frac{1}{2}}$. This quantity z_0 is also of some importance to the vacuum field: the phase difference between E_y and H_x, which is at $z = 0$ equal to that between the main part of the reflected wave and the secondary part, diminishes with growing distance to the plane $z = 0$ and becomes negligible at a height where the amplitude of the standing wave is markedly greater than p^{-1}, that is at a height equal to a few times z_0. To a certain extent we may say that the consequences of the fact that the earth is not quite an ideal conductor are appreciable at a distance of a few times z_0 at both sides of the reflecting surface.

The wave inside the earth also contributes to the field outside if the earth is stratified (Fig. 5b), and if, moreover, the depth d of the layer is not much greater than z_0. In these circumstances the vertically travelling refracted wave ($\cos \alpha_1 \approx 0$) will reach the surface of discontinuity at $z = d$, and will after reflection in this point reappear at the surface with the not too great amplitude decrease e^{-2d/z_0} and a phase retardation $= 2d/z_0$. During this process the amplitude is also changed by a factor $K = \dfrac{\sqrt{\sigma_1} - \sqrt{\sigma_2}}{\sqrt{\sigma_1} + \sqrt{\sigma_2}}$, which is the FRESNEL reflection coefficient for vertical incidence at $z = d$, and by the factor $4p^{-1} \cos \alpha_0$, caused by two refractions at $z = 0$. The amplitude of this wave at its point of emergence is

therefore equal to $4p^{-1} \cos \alpha_0 . Ke^{-2d/z_0}$. The total field built up by the waves which have one or more times traversed the layer has the amplitude

$$4p^{-1} \cos \alpha_0 \{(Ke^{-2(1+i)d/z_0}) + (Ke^{-2(1+i)d/z_0})^2 + \ldots\},$$

or $\frac{2 \cos \alpha_0}{p} \cdot \frac{2Ke^{-2(1+i)d/z_0}}{1 - Ke^{-2(1+i)d/z_0}}$. Adding this amplitude to that of the directly at $z = 0$ reflected wave we find that in the case of a monostratified earth the coefficient B has to be multiplied by $\frac{1 + Ke^{-2(1+i)d/z_0}}{1 - Ke^{-2(1+i)d/z_0}}$. As the horizontal component of the magnetic field remains $2 \cos \alpha_0$ at $z = 0$, quite independently from the constitution of the reflecting earth, the amplitude ratios are now:

$$\frac{E_y}{H_x} = \frac{e^{i\pi/4}}{\sqrt{2\sigma_1 T}} \frac{1 + Ke^{-2(1+i)d/z_0}}{1 - Ke^{-2(1+i)d/z_0}} \text{ and } \frac{H_z}{H_x} = \sin \alpha_0 \cdot \frac{E_y}{H_x} \qquad (1)$$

These formulae have been derived in a somewhat different way by KATO and KIKUCHI (1950) and by CAGNIARD (1953).

When comparing these results with the observational data it is immediately clear that there is a serious discrepancy; according to the calculations H_z/H_x has to be smaller then E_y/H_x but, as is shown in Figs. 3 and 4, H_z and H_x are at various stations of the same order of magnitude, whereas E_y/H_x is of the order 10^{-6}.

VOL. 6 1955

In the above calculations the radius of the earth was supposed to be infinitely large, which is not admissible as the wavelength of the pulsations is at least $3 . 10^6$ km; it is therefore not superfluous to examine an electromagnetic field in the vicinity of a sphere.

On account of the enormous value of the index of refraction the quantity z_0 (depth of penetration or wavelength) is small in comparison with the radius; it follows that the influence of the stratification of the earth is adequately represented by the correction factor obtained in the case of a plane earth, and this means that we have to consider only a homogeneous sphere.

The Maxwell equations are for vibrations with the time factor $e^{i\omega t}$

$$\text{curl } E = -ik_0 H, \quad \text{curl } H = i \frac{k^2}{k_0} E, \quad \text{div } E = 0, \quad \text{div } H = 0$$

with $k = pk_0$; elimination of E yields curl curl $H = k^2 H$. Henceforward we use spherical coordinates r, ϑ, φ.

By means of the following identity, which is valid for an arbitrary vector V:

$$r \text{ curl}_r \text{ curl } V = -\Delta(rV_r) + \text{div } V + \frac{\partial}{\partial r}(r \text{ div } V), \qquad (2)$$

we reduce the equation $\text{curl}_r \text{ curl } H = k^2 H_r$ to the more simple one

$$(\Delta + k^2)(rH_r) = 0 \qquad (3)$$

From the two remaining equations:

$$\text{curl}_\vartheta \text{ curl } H = k^2 H_\vartheta \quad \text{and} \quad \text{curl}_\varphi \text{ curl } H = k^2 H_\varphi$$

it is easy to derive $\text{curl}_r \text{ curl curl } H = k^2 \text{ curl}_r H$, which by applying the above identity can be reduced to

$$(\Delta + k^2)(r \text{ curl}_r H) = 0 \tag{4}$$

The two equations (3) and (4) lead immediately to a division of the electromagnetic field into two parts; firstly, a part in which $\text{curl}_r H$ (and E_r) is zero (the "magnetic solution" of the field equations), and, secondly, a field where H_r vanishes (the "electric solution"). As we are mainly interested in a field with a vertical component H_r, we shall only deal with the first solution; moreover, the electric solution is quite analogous to the magnetic one.

Introducing a vector potential A, the magnetic solution is characterized by the requirement $\text{curl}_r \text{ curl } A = 0$, and this equation is according to the vector-identity (2) satisfied by $A_r = 0$ and $\text{div } A = 0$. Apparently A too can be derived from a vector potential Q (the Hertzian vector), which is in this case radially directed; it follows that $H_r = \text{curl}_r \text{ curl } Q$, or, after some reduction, $H_r = -\frac{\Delta'}{r^2} Q$, where $\Delta' = \frac{1}{\sin\vartheta}\frac{\partial}{\partial\vartheta}\left(\sin\vartheta \frac{\partial}{\partial\vartheta}\right) + \frac{1}{\sin^2\vartheta}\frac{\partial^2}{\partial\varphi^2}$. Substitution into (3) yields $(\Delta + k^2)Q/r = 0$.

With $Q = \frac{rN}{k_0}$ we finally obtain the general form of the magnetic solution:

$$H = \text{curl curl}\frac{rN}{k_0}\,;\; H_r = -\frac{\Delta' N}{k_0 r}, \quad H_\vartheta = \frac{1}{k_0 r}\frac{\partial^2 rN}{\partial r\,\partial\vartheta}, \quad H_\varphi = \frac{1}{k_0 r \sin\vartheta}\frac{\partial^2 rN}{\partial r\,\partial\varphi}$$

$$E = -i\frac{k_0}{k^2}\text{curl } H\,;\; E_r = 0, \qquad E_\vartheta = -\frac{i}{\sin\vartheta}\frac{\partial N}{\partial\varphi}, \quad E_\varphi = i\frac{\partial N}{\partial\vartheta}$$

N has to satisfy $(\Delta + k^2)N = 0$.

The solution in which the coordinates appear separately is of the form

$$N = \frac{H_{n+\frac{1}{2}}(kr)}{\sqrt{kr}} S_n(\vartheta, \varphi)$$

where H is a cylindrical function and S_n a spherical harmonic. We now introduce the functions $\zeta_n(x)$ and $\eta_n(x)$ which are defined according to Heine as:

$$\zeta_n(x) = \sqrt{\frac{\pi}{2x}}\, H^{(1)}_{n+\frac{1}{2}}(x) \quad \text{and} \quad \eta_n(x) = \sqrt{\frac{\pi}{2x}}\, H^{(2)}_{n+\frac{1}{2}}(x)$$

where $H^{(1)}$ and $H^{(2)}$ are Hankel functions of the first and second kind.

As these functions are for large values of x approximated by an exponential function:

$$H^{(1)}_{n+\frac{1}{2}}(x) \sim \sqrt{\frac{2}{\pi x}}\, e^{\pm i\left(x - \frac{n+1}{2}\pi\right)},$$

we may interpret $\zeta_n(kr) \,.\, S_n(\vartheta, \varphi) \,.\, e^{i\omega t}$ and $\eta_n(kr) \,.\, S_n(\vartheta, \varphi) \,.\, e^{i\omega t}$ respectively as waves travelling towards or away from the centre $r = 0$ (Fig. 6).

In the case of a perfectly reflecting sphere $r = a$ (reflection coefficient $= -1$) the Hertzian function N outside this sphere must be of the form

$$N = \left\{\frac{\zeta_n(k_0 r)}{\zeta_n(k_0 a)} - \frac{\eta_n(k_0 r)}{\eta_n(k_0 a)}\right\} S_n(\vartheta, \varphi);$$

it follows that

$$\frac{1}{k_0 r}\frac{\partial r N}{\partial r} = -\frac{n}{k_0 r} N + \left\{\frac{\zeta_{n-1}(k_0 r)}{\zeta_n(k_0 a)} - \frac{\eta_{n-1}(k_0 r)}{\eta_n(k_0 a)}\right\} S_n(\vartheta, \varphi).$$

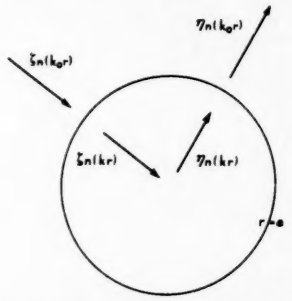

Fig. 6. Spherical electromagnetic waves inside and outside the earth.

At the surface of the sphere N and consequently H_r and E are equal to zero, whereas H_ϑ and H_φ reach at $r = a$ their maximum value, which is equal to $\dfrac{2i}{(k_0 r)^2 \zeta_n(k_0 a)\eta_n(k_0 a)}$ multiplied by $\dfrac{\partial S}{\partial \vartheta}$ (in the formula for H_ϑ), and by $\dfrac{1}{\sin\vartheta}\dfrac{\partial S}{\partial \varphi}$ (for H_φ).

This standing wave system is still a first approximation if the sphere is not quite a perfect mirror. In that case the field outside the sphere is determined by

$$N = \left\{\frac{\zeta_n(k_0 r)}{\zeta_n(k_0 a)} - A\frac{\eta_n(k_0 r)}{\eta_n(k_0 a)}\right\} S_n(\vartheta, \varphi);$$

inside the sphere the Hertzian function has to be of the form

$$N = B\frac{\zeta_n(kr) + \eta_n(kr)}{\zeta_n(ka) + \eta_n(ka)} S_n(\vartheta,\varphi),$$

as the function has to remain finite in the centre $r = 0$. The continuity of E_ϑ (or E_φ) requires the continuity of N; hence $B = 1 - A$. Again the continuity of H_ϑ (or H_φ) leads to the equation

$$\overline{\zeta_n(k_0 a)} - A\overline{\eta_n(k_0 a)} = B\,\overline{\zeta_n(ka) + \eta_n(ka)}$$

where we have used the notation $\overline{f(x)} \equiv \dfrac{1}{f(x)}\dfrac{dx\, f(x)}{dx}$. The solution is

$$A = \frac{\overline{\zeta_n(ka) + \eta_n(ka)} - \overline{\zeta_n(k_0 a)}}{\overline{\zeta_n(ka) + \eta_n(ka)} - \overline{\eta_n(k_0 a)}}.$$

VOL. 6 1955

This quantity A is not the spherical equivalent of FRESNEL's reflection coefficient; the reflected wave is here composed of the directly reflected wave at $r = a$ and of waves which, after being refracted into the sphere, emerge again in the vacuum by a second refraction. The directly reflected wave is easily separated from the rest, since its amplitude must be independent from the wave $\eta_n(kr)$; we obtain

$$A = \frac{\overline{\zeta_n(ka)} - \overline{\zeta_n(k_0a)}}{\overline{\zeta_n(ka)} - \overline{\eta_n(k_0a)}} - \frac{\overline{\zeta_n(k_0a)} - \overline{\eta_n(k_0a)}}{\overline{\zeta_n(ka)} - \overline{\eta_n(k_0a)}} \cdot \frac{\overline{\eta_n(ka)} - \overline{\zeta_n(ka)}}{\overline{\eta_n(k_0a)} - \overline{\zeta_n(ka)}} \cdot \frac{\eta_n(ka)}{\zeta_n(ka)} \cdot \frac{1}{1 + \frac{\eta_n(ka)}{\zeta_n(ka)} \cdot \frac{\overline{\eta_n(ka)} - \overline{\zeta_n(ka)}}{\overline{\zeta_n(ka)} - \overline{\eta_n(k_0a)}}}$$

Indicating the vacuum by the index 0 and the material of the sphere by 1, we denote the coefficients of internal and external reflection by R_{00} and R_{11} respectively and the coefficients of refraction by R_{01} and R_{10}; then:

$$R_{00} = -\frac{\overline{\zeta_n(k_0a)} - \overline{\zeta_n(ka)}}{\overline{\eta_n(k_0a)} - \overline{\zeta_n(ka)}}, \quad R_{11} = -\frac{\overline{\eta_n(ka)} - \overline{\eta_n(k_0a)}}{\overline{\zeta_n(ka)} - \overline{\eta_n(k_0a)}},$$

$$R_{01} = \frac{\overline{\zeta_n(k_0a)} - \overline{\eta_n(k_0a)}}{\overline{\zeta_n(ka)} - \overline{\eta_n(k_0a)}}, \quad R_{10} = \frac{\overline{\eta_n(ka)} - \overline{\zeta_n(ka)}}{\overline{\eta_n(k_0a)} - \overline{\zeta_n(ka)}}$$

and

$$-A = R_{00} + R_{01} \cdot R_{10} \cdot \frac{\eta_n(ka)}{\zeta_n(ka)} \sum_{m=0}^{\infty} \left\{ R_{11} \frac{\eta_n(ka)}{\zeta_n(ka)} \right\}^m.$$

The interpretation of this expression is obvious: the first term is the directly reflected wave, and the rest represents waves which have suffered m internal reflections. This rest may be neglected: as the depth of penetration is small compared with the radius, the amplitudes of these waves, which have to cover the distance $2a$ before they can emerge, is exceedingly small. The exponential decrease of these waves is in the formula expressed by the phase factor $\eta_n(ka)/\zeta_n(ka)$, which is for great values of $|\, ka \,|$ equal to $(-1)^{n+1}\, e^{-2ika}$.

The amplitude of the reflected wave is R_{00} or $-1 + R_{01}$; the field outside the sphere consists therefore of a standing wave and a reflected wave

$$R_{01} \cdot \frac{\eta_n(k_0r)}{\eta_n(k_0a)} S_n(\vartheta, \varphi).$$

Finally we reduce the expression for R_{01} to

$$R_{01} = \frac{2i}{k_0a \,.\, \zeta_n(k_0a) \,.\, \eta_n(k_0a)} \cdot \frac{1}{\overline{\zeta_n(ka)} - \overline{\eta_n(k_0a)}};$$

the amplitude ratios at $r = a$ are therefore:

$$\frac{E_\varphi}{H_\vartheta} = i \frac{k_0a}{\overline{\zeta_n(ka)} - \overline{\eta_n(k_0a)}} \text{ and } \frac{H_r}{E_\varphi} = -i \frac{n}{k_0a} \cdot \frac{(n+1)S_n}{\partial S_n / \partial \vartheta}.$$

The ratio between the vertical component of the magnetic field and the horizontal component of the electric field H_r/E_φ, which in the case of a plane wave reflected by a plane earth appeared to be equal to sin α_0, is here equal to n/k_0a (the factor containing the function S_n is of the order 1 and will therefore be neglected). These two results are generally quite different from each other; in fact the only case in which n/k_0a may be interpreted as the sine of the angle of incidence occurs if both n and k_0a are very great and $k_0a > n$. In these circumstances the spherical waves closely resemble plane waves.

However, in actual conditions k_0a is rather small, as $(k_0a)^{-1}$ is equal to $7.5T$, which is at least of the order 10^2; hence the ratio H_r/E_φ is much greater than the value sin α_0 of the corresponding ratio H_z/E_y. Observations show that at some stations this ratio is of the order 10^5 or 10^6, and this means that n should be at least of the order 10^3. Such a high order of the spherical harmonic S_n is, however, out of the question, as in that case the amplitude of the pulsation would vary very strongly with a variation of the latitude; observations indicate only a slow and monotonous decrease of the field with decreasing latitude.

It appears to be impossible to explain the observed great values of H_r/H_ϕ by means of a single wave. Up till now we have dealt only with the magnetic solution, as we were interested in the ratio H_r/H_ϕ, but, if we have to consider more complicated wave systems, the electric solution too must be used. It may be possible to construct a system that agrees with the observed value of H_r/H_ϕ; as we have already observed, it is not possible to extend this theory without knowledge about the generation of the pulsations. Moreover, it is uncertain whether the theory obtains for points not far away from horizontal discontinuities; as the stations which use quick-run recording are all rather close to the border of a continent, the observational data are in this respect too insufficient.

VOL. 6 1955

In contrast to H_r/E_φ the ratio E_φ/H_ϕ is for small values of k_0a not very different from E_y/H_x; in first approximation $E_\varphi/H_\phi = (p + n/ik_0a)^{-1}$, and as $p \gg n/k_0a$ if n is not too great, this is about equal to the value p^{-1} we have found for E_y/H_x in the case of a plane earth. In so far as this ratio is concerned we may neglect the sphericity of the earth.

So in the case of a monostratified earth E_y/H_x is given by (1); it follows that the ratio between the two amplitudes is

$$\left|\frac{E_y}{H_x}\right| = \frac{1}{\sqrt{2\sigma_1 T}}\left(\frac{1 + 2Ke^{-q}\cos q + K^2e^{-2q}}{1 - 2Ke^{-q}\cos q + K^2e^{-2q}}\right)^{\frac{1}{2}} \tag{5}$$

and that the phase difference is $\frac{\pi}{4} - \varphi$ where

$$\varphi = \tan^{-1}\frac{2Ke^{-q}\sin q}{1 - K^2e^{-2q}} \tag{6}$$

The deviation φ of the phase-difference from the value $\pi/4$ which is valid for a homogeneous earth is equal to zero if the layer disappears ($q = 0$); with increasing value of $q(= 2d/z_0)$ this deviation increases too, but, as it has to vanish again for

very large values of the depth of the layer ($q = \infty$), it reaches a maximum value φ_0. This maximum appears at $q = q_0$, where q_0 satisfies

$$\frac{\partial \varphi}{\partial q} = 0 \qquad \text{or} \qquad \tan q = \frac{1 - K^2 e^{-2q}}{1 + K^2 e^{-2q}}$$

The value of φ_0 appears to be $\tan^{-1} \sqrt{\cos 2q_0}$.

In Fig. 7 q_0 has been drawn against $\log \sigma_1/\sigma_2$; in the same diagram the phase-difference $45° - \varphi_0$ is shown as a function of q_0.

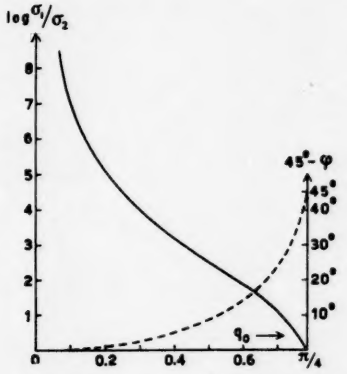

Fig. 7. Minimum value (dotted line) of the phase-difference as a function of the depth of the layer measured in wavelengths; the full-drawn curve represents the corresponding ratio σ_1/σ_2.

The determination of this minimum may be of some practical use; if φ_0 and the period at which the minimum occurs are known, the curves of Fig. 7 yield the values of σ_1/σ_2 and q_0. Consequently the depth of the layer and the conductivity of the material below it are found if the conductivity of the layer is known. This quantity is easily obtained by measuring $|E_y/H_x|$ and substitution into (5).

The formulas (5) and (6) have been checked by measurements at the magnetic observatory Wi. Figure 8 shows a sample of magnetic and electric records at normal paper speed. The record of the potential difference between two iron electrodes put into the ground 1 km apart in E–W direction follows the magnetic H-record very closely. The ratio $|E_y/H_x|$ was measured for bay disturbances of quasi-harmonic form with very long periods: the results are shown in Fig. 11. Accurate measurements of the phase-difference between E_y and H_x are not possible on account of the irregular form of the variations.

For values of T smaller than one minute the micropulsations were used. Figure 9 shows part of a Wi quick-run record (horizontal component); the scale value of the original is about 1 γ/mm and the paper speed 6 mm/minute. The time-marks are obtained by a clock which short-circuits during one second for every minute a resistance through which the recording lamp is fed; this causes sharp points in the magnetic record. The time-marks are free from any parallax, which enables the maxima and the minima of the pulsations to be read with an

accuracy of one second. A quick-run geoelectric record was obtained by means of a fast Brown recorder; a sample of this record is shown in Fig. 10: it corresponds to the framed part of the magnetic record (Fig. 9). Measurements were made of the amplitude ratio $|E_y/H_x|$, as well as of the phase-differences. The latter turn out to be very small at the observatory Wi. As can be read from Fig. 11, the phase-difference is only a few degrees for the prevailing periods of 40 and 50 seconds, which means a time-lag of no more than 0·5 second between E_y and H_x.

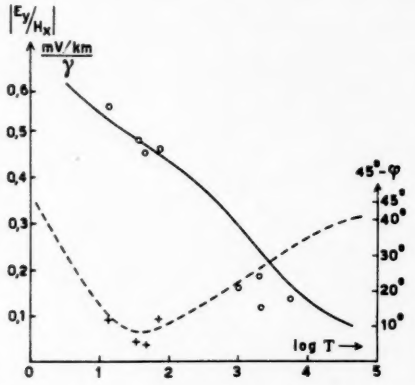

Fig. 11. Phase-differences $(45° - \varphi)$ between electric and magnetic variations (crosses) and amplitude ratios $|E_y/H_x|$ (circles) recorded at Witteveen.

It was necessary to take into account the retardations by the instruments in order to obtain a high accuracy. For the magnetic variometer this retardation is given by a formula, well known from seismometry

$$\vartheta = \tan^{-1} \frac{2\kappa\omega}{\omega_0^2 - \omega^2}$$

The damping coefficient κ of the H-variometer used was 0·04, and the own-circular frequency ω_0 was 2·4 sec^{-1}. For all frequencies involved ($T > 10$ sec) the time-lag between the magnetic variation and the movement of the variometer was quite negligible. The electric record is retarded by the Brown recorder, which is not infinitely fast; the retardation was checked by applying potential variations of various periods. It turned out to lie between 1 and 2 seconds for the periods of the recorded pulsations. The results for Witteveen are drawn in Fig. 11. The circles represent mean values of the amplitude-ratio $|E_y/H_x|$ for a great number of pulsations and bays; the phase-differences (crosses) were read from records of pulsations exclusively. The best fit was obtained with curves calculated from the following values: $\sigma_1 = 0{\cdot}02\ \Omega^{-1}\text{cm}^{-1}$, $\sigma_2 = 10^{-4}\ \Omega^{-1}\text{cm}^{-1}$, $d = 600$ m; the dotted curve represents the phase-difference and the full-drawn curve the amplitude-ratio. The used values do not agree with the conductivity as known from geological side; however, the calculation for a multi-layered earth using the geological data for Witteveen did not yield a better agreement than the mono-stratified earth. We hope that future measurements will clear up this discrepancy.

VOL. 6 1955

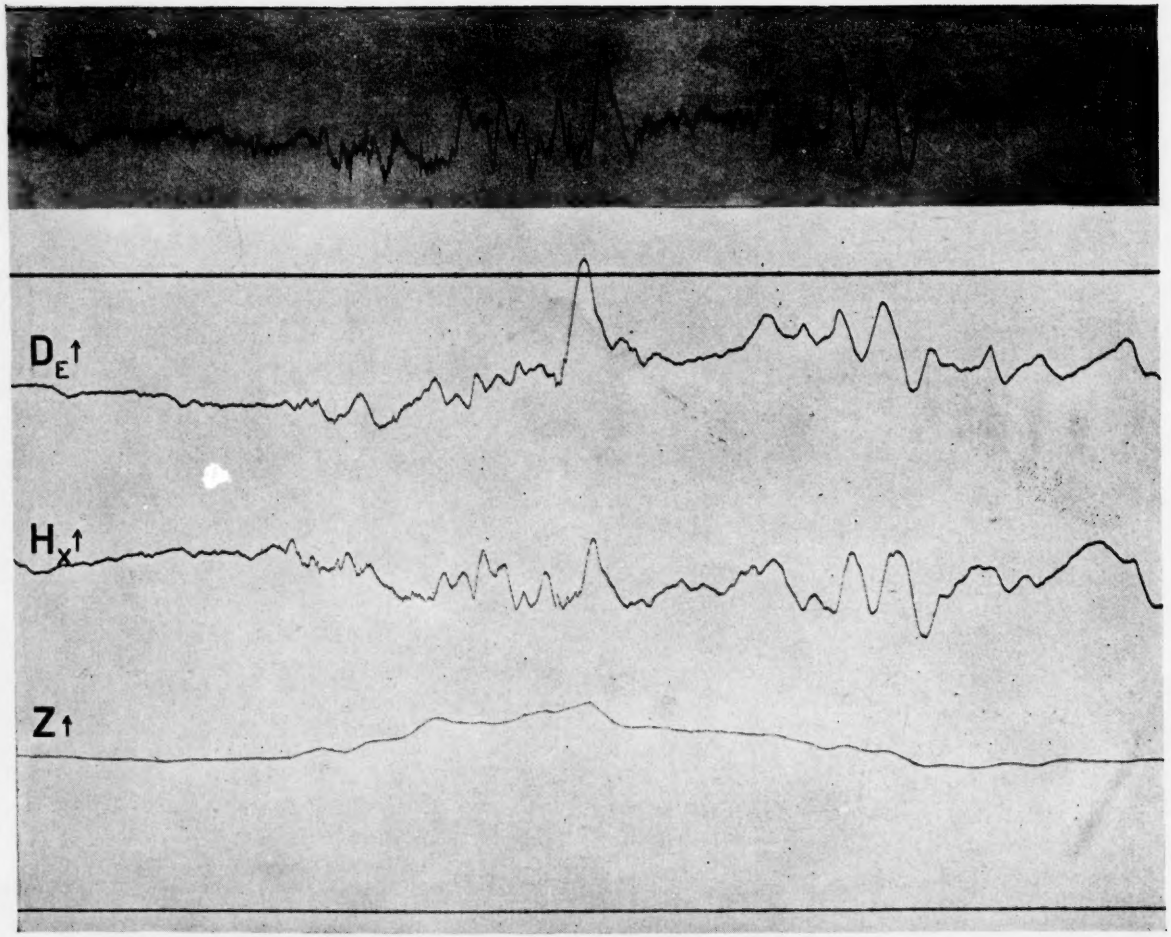

Fig. 8. Magnetic field (D, H, and Z) and electric field (east–west) recorded at the observatory Witteveen.

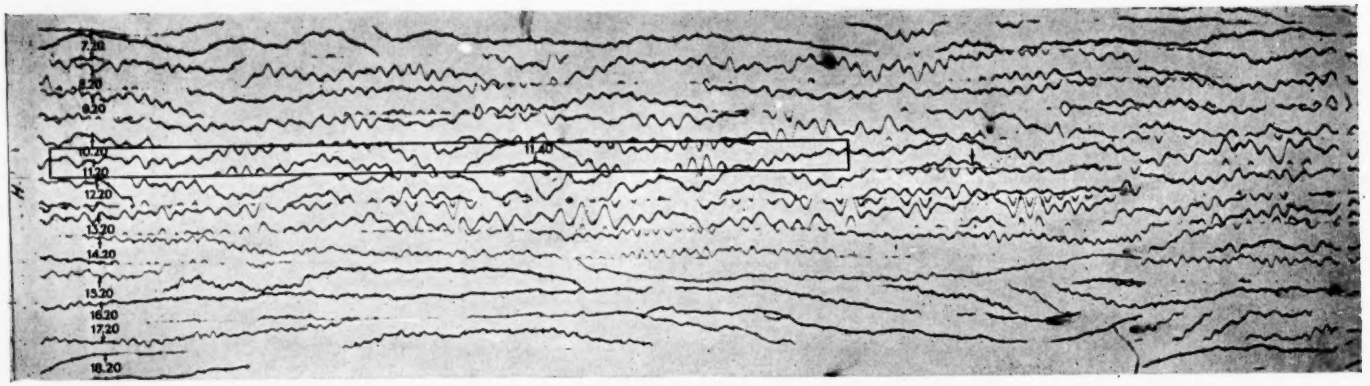

Fig. 9. Quick-run magnetogram (horizontal component) recorded on January 21, 1954, at Witteveen.

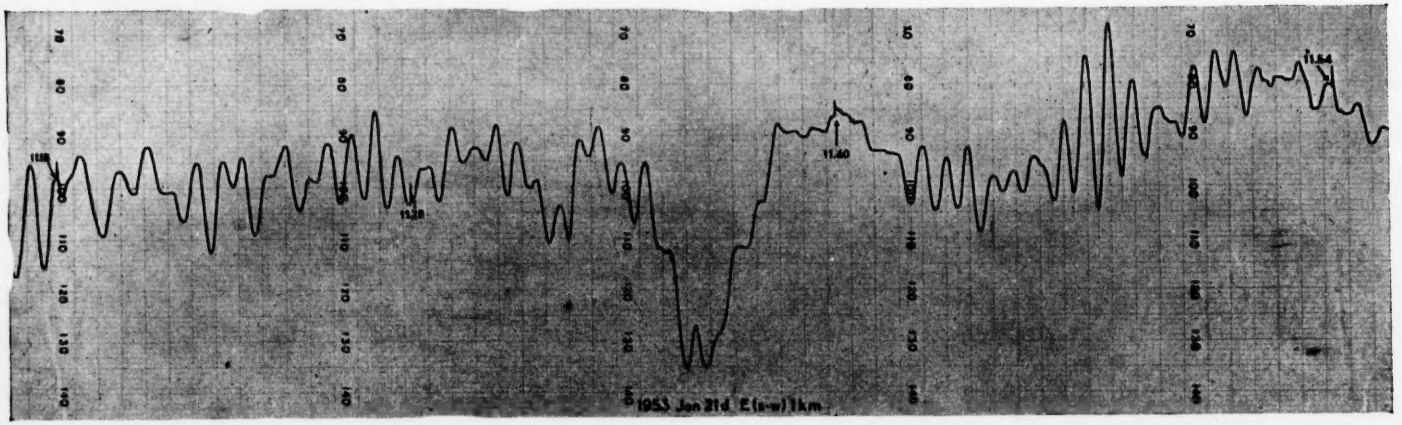

Fig. 10. Geoelectric record (east–west, distance between the electrodes 1 km), corresponding to the framed part of Fig. 9.

VOL. 6
1955

Acknowledgments—The following geomagnetic observatories kindly supplied us with magnetograms of the investigated disturbances: Tr, So, Co, Do, Le, Lo, Si, RS, Es, Me, Wn, Ab, Ma, Fü, Gt, CF, Na, Ag, Eb, Ci, IK, Tl, Ch, SM, SF, Ka, Ks, Tu, He, Ta, Ho, Te, SJ, MB, Ba, El, Bi, Va, Wa, Hr, To, Am, MI, and HI.

Mr. D. VAN SABBEN, scientific collaborator in charge of the observatory Witteveen, co-operated in producing geomagnetic and geoelectric records.

We thankfully refer to the initial discussions on this subject with Tr. A. H. DE VOOGT (Netherlands PTT).

REFERENCES

BARTELS, J., and VELDKAMP, J.	1950–1952	IATME Bulletins No 12e–g, Geomagnetic Indices K and C
BEAUFILS, Y.	1950	C. R. Acad. Sci. Paris **230,** 2108
	1953	Ann. Géoph. **8,** 100
BILLAUD, G.	1953	Trav. Inst. Météor. Algérie, fasc. **9,** 12
CASTET, J.	1953	*ibid.*, fasc. **9,** 50
CAGNIARD, L.	1953	Geophysics **18,** 605
CHAPMAN, S., and BARTELS, J.	1940	Geomagnetism (Oxford, Clarendon Press)
DE VOOGT, A. H.	1954	J. Atmosph. Terr. Phys. **5,** 108
GRENET, G.	1953	Trav. Inst. Météor. Algérie, fasc. **9,** 54
HARANG, L.	1939	Terr. Mag. **44,** 17
HOLMBERG, E. R. R.	1953	Mon. Not. Roy. Astron. Soc., Geophys. Suppl. **6,** 467
KATO, Y., and KIKUCHI, T.	1950	Tohoku Univ. Sci. Reports, Serie 5, Geophysics **2,** 138 and 142
SCHLUMBERGER, M., and KUNETZ, G.	1948	Trans. Oslo Meeting UGGT, 518
YEARBOOK, B1941	1941	Royal Neth. Meteor. Inst., de Bilt, 23

Journal of Atmospheric and Terrestrial Physics, 1955, Vol. 6, pp. 46 to 49. Pergamon Press Ltd., London

Vertical distribution of atmospheric ozone at Longyearbyen, Spitzbergen (78° N)

S. H. H. Larsen
Auroral Observatory, Tromsø

ABSTRACT

Results of the determination of the vertical distribution of atmospheric ozone at Spitzbergen (78° N) are presented and compared with the Tromsø-distribution (70° N).

Observations on atmospheric ozone were started with a Dobson Spectrophotometer in September 1950 at Longyearbyen, Spitzbergen. Several series of Umkehr-observations for determination of the vertical distribution were obtained. The calculations have been performed according to method *A*, developed in the paper by Götz, Meetham, and Dobson. In method *A* the atmosphere is divided into 5 sections, viz.:

0–5 km, 5–20 km, 20–35 km, 35–50 km, and 50–65 km.

The content of ozone in the lowest section is assumed to be about 5 per cent of the total amount (as given by measurements of low ozone). It is further assumed that practically no ozone is present above 50 km.

The densities of the air used at different heights are as follows:—

Table I

Height in km	0	10	20	30	40	50	60
Densities of the air in g/cm^3 10^{-6}	1296·00	370·00	73·60	19·00	3·98	0·85	0·18

The densities up to 20 km are taken from the paper of Tønsberg and Langlo on ozone observations at Tromsø (70° N). Above 20 km the densities are those of Chapman and Milne. The observations consist of measuring the ratio of the energies of the wavelength 3110 Å and 3300 Å. The coefficients of scattering are assumed to be about equal to those at Tromsø, i.e., for

$$\lambda = 3110 \qquad \beta = 0{\cdot}48$$
$$\lambda' = 3300 \qquad \beta' = 0{\cdot}37$$

The vertical distributions are calculated from three Umkehr-curves, one individual and two average curves with following details:

Table II

Total amount of ozone	*Number of Umkehr-curves*	*Date*	*Zenith distance of sun at noon*	*Year*
0·190 cm	1	6/9	71·5	1950
0·205 cm	4	25/9–28/9	79·0	1950
0·335 cm	3	5/4– 7/4	71·5	1951

VOL. 6 1955

Table III contains the result of the calculation and gives the total ozone content for each section, and the content per km height in the different sections, calculated on the assumption of uniform distribution within each section.

Table III

Sections	0·190 *cm* O_3		0·205 *cm* O_3		0·335 *cm* O_3	
	cm O_3	O_3/*km*	*cm* O_3	O_3/*km*	*cm* O_3	O_3/*km*
65–50 km	0	0	0	0	0	0
50–35 km	0·010	0·0007	0·008	0·0005	0·019	0·0013
35–20 km	0·126	0·0084	0·133	0·0089	0·182	0·0121
20– 5 km	0·044	0·0029	0·054	0·0036	0·117	0·0078
5– 0 km	0·010	0·0020	0·010	0·0020	0·017	0·0034
Height of centre of gravity	23·4 km		22·9 km		21·9 km	

Compared with the Tromsø-distribution (TØNSBERG and LANGLO) one can say that the picture is much the same. This is evident from Fig. 1, where one Tromsø-

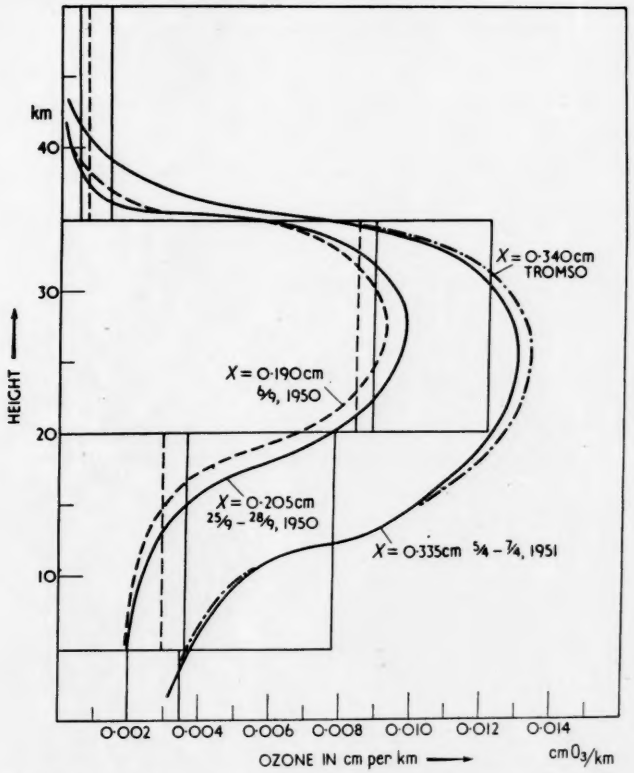

Fig. 1. Block diagram of the vertical distribution of ozone at Spitzbergen (78° N) corresponding to different ozone amounts X. The smoothed curves are drawn in such a way that the ozone content in each section has been kept equal to that in the corresponding block.

distribution is also shown. Reading off the smoothed curves we obtain the ozone content per km at all heights, and are able to calculate the ratio: volume of ozone to air which is determined by the formula $R = 10^{-5} X_h \, {}^{\rho_0}/_{\rho_h}$, where X_h is the ozone content per km at the height h. The two series of results are given in Table IV, and the latter is shown on the Fig. 2.

Table IV

Heights in km	0·190 *cm* O_3		0·205 *cm* O_3		0·335 *cm* O_3	
	O_3/km	$R.10^6$	O_3/km	$R.10^6$	O_3/km	$R.10^6$
45	0·0001	0·71	0·0001	0·36	0·0002	1·42
40	0·0005	1·63	0·0003	0·65	0·0013	4·23
35	0·0058	8·81	0·0060	9·12	0·0082	12·46
30	0·0090	6·10	0·0095	6·45	0·0123	8·39
25	0·0089	3·13	0·0093	3·27	0·0130	4·57
20	0·0067	1·18	0·0077	1·36	0·0121	2·13
15	0·0030	0·23	0·0037	0·28	0·0103	0·80
10	0·0021	0·07	0·0023	0·08	0·0053	0·19
5	0·0020	0·04	0·0020	0·04	0·0038	0·07
0	0·0020	0·02	0·0020	0·02	0·0026	0·03

R = Ozone/air by volume

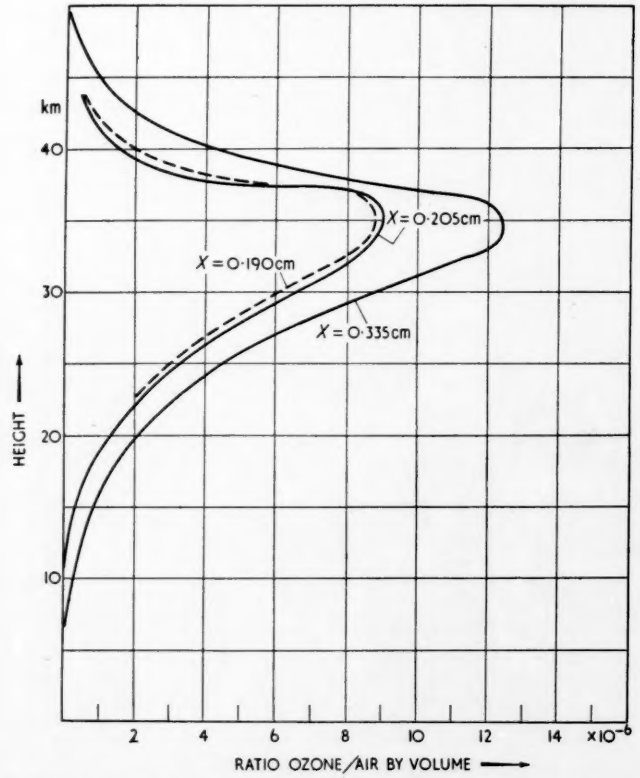

Fig. 2. The ratio ozone/air by volume at Spitzbergen corresponding to different amount of ozone.

, VOL. 6 1955

As at Tromsø we have the important feature that, while a layer of comparatively high ozone content lies between 25 and 30 km for different total ozone amounts, the increase of ozone content for the higher ozone amounts occurs mainly between 10 and 25 km.

The difference in the total amount of ozone corresponding to the single-day curve ($O_3 = 0{\cdot}190$ cm) and that for the mean three-day curve ($O_3 = 0{\cdot}205$ cm) is not very great; a small difference in the calculated height of the centre of gravity is found, however. We mention it because it is our experience that the measured values, after the passing of the "Umkehr-point," vary considerably from day to day. If such variations are real they would indicate a change in the amount of ozone in the highest levels and hence would have an effect on the height of the centre of gravity. In any case they show that observations of the zenith sky light cannot be used to give an accurate value of the total ozone when the sun is very low.

References

Chapman, S., and Milne, E. A.	1920	Quart. J. Roy. Met. Soc. **46**, 196.
Götz, F. W. P., Meetham, A. R., and Dobson, G. M. B.	1934	Proc. Roy. Soc. **145**, 416
Tønsberg, E., and Langlo, K.	1944	Geofys. Pub. **13**, 12

4 (20 pp.)

Journal of Atmospheric and Terrestrial Physics, 1955, Vol. 6, pp. 50 to 56. Pergamon Press Ltd., London

The autocorrelogram of randomly fading waves

R. B. Banerji
Ionosphere Research Laboratory, The Pennsylvania State University,
State College, Pennsylvania

(*Received* 1 *June* 1954)

ABSTRACT

The power spectrum returned by a completely rough ionosphere having a random motion superposed on a steady drift is deduced. The autocorrelograms of fading patterns corresponding to power spectra returned by the two extreme cases of this spectrum, i.e., pure drift and pure turbulence, are compared and the possibility of statistically distinguishing between them discussed. On the basis of a test of significance of autocorrelograms it is shown that a fading pattern need not contain more than 250 independent points to make a distinction between two possible types of autocorrelograms.

The effect of antenna polar diagrams on the autocorrelograms is also discussed qualitatively.

1. Introduction

The purpose of the present paper is to investigate the possibility of determining the velocity of drift and turbulence of an irregular ionosphere by studying the autocorrelogram of a fading wave at a single point. The basic principle of the method is based on the fact that doppler shifts introduced into the radio waves scattered at different points from an irregular ionosphere endow the wave with a characteristic power spectrum whose form is determined by the magnitude and direction of the velocity as well as the radiation patterns of the transmitting and receiving antennae and the angular spectrum of the returned wave.

We deduce, in Section 2, the power spectrum that would be returned from a completely rough ionosphere (one with an angular spectrum determined by Lambert's Law) having superposed steady and random motion, when the transmitting and receiving antennae have omnidirectional characteristics. The power spectrum deduced has been compared to the spectrum obtained for a turbulent ionosphere by Ratcliffe (1948) and that corresponding to a drifting ionosphere by the author in a previous work (Banerji, 1953).

Since the autocorrelograms corresponding to the three power spectra are very similar, we discuss in Section 3 the possibility of statistically distinguishing between the autocorrelograms corresponding to the two extreme cases of turbulent and drifting motion. It is shown, on the basis of a test of significance developed by the author, that no more than 250 independent points on the fading pattern are necessary to reduce the statistical fluctuations of autocorrelograms to distinguish between the two cases.

2. The Power Spectrum from a Steadily Drifting Ionosphere with Superposed Random Motion

The power spectrum from a completely rough ionosphere, when the irregularities are undergoing either a purely random or a steadily drifting motion has been deduced before. In this section we deduce the power spectrum when the motion consists of a superposition of random and steady components.

We assume, as in the previous work, a plane ionosphere at a height h above

VOL. 6 1955

the observer, and having a uniform distribution of scatterers. The coefficient of back scatter is the same for all scatterers. We also assume, as before, that the antennae are omnidirectional. The drift is v_1 along the negative X direction. The random motion, as in RATCLIFFE'S work, is omnidirectional and has a standard deviation v_0.

The doppler shift produced at a point (θ, ϕ) by scatterers having a random velocity v along the line of sight, superposed on the drift, is given by

$$f - f_0 = \frac{2f_0 v}{c} + \frac{2f_0 v_1}{c} \sin\theta \cos\phi \tag{1}$$

The power scattered depends, as indicated in the previous paper, on the solid angle and, in addition, on the probability that the random part of the velocity lies between v and $v + dv$. Assuming that the distribution of this velocity is normal, i.e.,

$$\frac{1}{v_0\sqrt{2\pi}}\, e^{-\frac{v^2}{2v_0^2}} \tag{2}$$

we have the expression for the power radiated as

$$W''(f)\, d\theta\, d\phi\, dv = \frac{Ah^2}{v_0\sqrt{2\pi}}\, e^{-\frac{c^2}{8v_0^2 f_0^2}\left\{f - f_0 - \frac{2f_0 v_1}{c}\sin\theta\cos\phi\right\}^2} \sin\theta\cos\theta\, d\theta\, d\phi\, dv \tag{3}$$

on expressing v in equation (2) in terms of frequency and the co-ordinates, and inserting the expression for the solid angle.

Since the same frequency can be returned from all points with different probability, the total power radiated in the range f to $f + df$ may be obtained as follows:

We transform co-ordinates according to the scheme:

$$\left.\begin{aligned} f &= f_0 + \frac{2f_0 v}{c} + \frac{2f_0 v_1}{c}\sin\theta\cos\phi \\ \theta &= \theta \\ \phi &= \phi \end{aligned}\right\} \tag{4}$$

reducing the expression for the power to

$$W''(f)\, d\theta\, d\phi\, df = \frac{Ah^2 c}{2\sqrt{2\pi} f_0 v_0}\, e^{-\frac{c^2}{8f_0^2 v_0^2}\left\{f - f_0 - \frac{2f_0 v_1}{c}\sin\theta\cos\phi\right\}^2} \sin\theta\cos\theta\, d\theta\, d\phi\, df \tag{5}$$

We can now integrate over θ and ϕ, i.e., over the whole plane, limiting ourselves to the frequency range f to $f + df$, to obtain the total power scattered in this frequency range. Integration over θ yields:

$$W(f)\, df = \frac{Ah^2 c\, df}{2\sqrt{2\pi} f_0 v_0 K^2} \int_0^{\pi} \frac{d\phi}{\cos^2\phi} \left[e^{-x^2} - e^{-(x - K\cos\phi)^2}\left\{1 - 2Kx\sin^2\phi\cos\phi\right\}\right] \tag{6}$$

where

$$x = \frac{f - f_0}{f_0} \cdot \frac{c}{2\sqrt{2} v_0}; \qquad K = \frac{v_1}{\sqrt{2} v_0}$$

This integral can be shown to reduce to RATCLIFFE's and our previous expression, respectively, in the extreme cases where $v_1 = 0$ and $v_0 = 0$. In the general case, however, the integral can only be evaluated approximately. This has been done by dividing the range of integration ($\phi = 0$ to $\phi = \pi$) into six equal parts and approximating the function by the straight lines joining the values at the end of the intervals. The expression for the power then reduces to

$$W(f) = \frac{\sqrt{\pi}Ah^2c}{12\sqrt{2}f_0v_0K^2}\left[\left\{\frac{35}{3} + 2K^2\left(\tfrac{1}{2} + x^2\right)\right\}e^{-x^2} - e^{-(x^2+K^2)}\cosh 2Kx\right.$$
$$- 8e^{-\left(x^2+\frac{K^2}{4}\right)}\left\{\cosh Kx - \tfrac{3}{4}Kx\sinh Kx\right\}$$
$$\left. - \frac{8}{3}e^{-\left(x^2+\frac{3K^2}{4}\right)}\left\{\cosh\sqrt{3}Kx - \frac{\sqrt{3}}{4}Kx\sinh\sqrt{3}Kx\right\}\right] \quad (7)$$

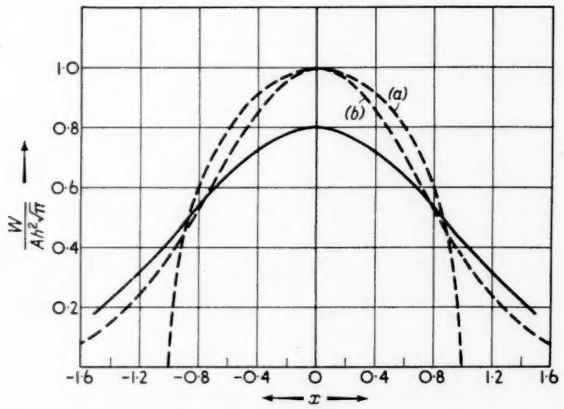

Fig. 1. The deduced power spectrum compared with those corresponding to drifting (a) and turbulent (b) ionosphere.

In Fig. 1 is shown the value of $\dfrac{W}{Ah^2\sqrt{\pi}}$ as a function of x (which is proportional to the ratio of frequency shift and the random component) for $K = 1$ (i.e., $v_1 = \sqrt{2}v_0$). The same quantity is plotted for $v_1 = 0$, shown dotted, as well as the most similar plot for the case when $v_0 = 0$.

It will be noted that the shape of the power spectrum for the intermediate case is very similar to the case of random motion with a larger r.m.s. velocity. For values of K much greater than 1, i.e., for drifts which are much larger than the turbulent velocities, the spectrum approaches that due to drift and, consequently, the difference between the two cases remains small. We will consider, in the next section, whether it is possible, in view of the statistical fluctuation of autocorrelograms derived from finite fading data, to distinguish between the autocorrelograms corresponding to the extreme cases of this spectrum, i.e., pure drift and purely turbulent motion.

VOL. 6 1955

3. The Shape of the Extreme Autocorrelograms: Possibility of Distinction

The shapes of the autocorrelograms corresponding to the extreme cases of random and drifting motion can be deduced as follows:

(i) *Turbulent motion*

The power spectrum $W_1(f)$ is given by

$$W_1(f) = A_1 e^{-\frac{c^2(f-f_0)^2}{8f_0^2v_0^2}} \tag{8}$$

where A is a constant, c the velocity of light, f_0 the midband frequency, and v_0 the r.m.s. random velocity.

The autocorrelogram with lag τ, denoted by $\rho(\tau)$, of the amplitude of the wave is then the cosine Fourier transform of this spectrum, i.e.,

$$\rho_1(\tau) \equiv \frac{\overline{R(t)R(t+\tau)} - \overline{R(t)}^2}{\overline{\{R(t)\}^2} - \overline{R(t)}^2} = \frac{\int_0^\infty A_1 e^{-\frac{c^2(f-f_0)^2}{8f_0^2v_0^2}} \cos 2\pi(f-f_0)\tau \, df}{\int_0^\infty A_1 e^{-\frac{c^2(f-f_0)^2}{8f_0^2v_0^2}} \, df}$$

By replacing $\cos 2\pi(f-f_0)\tau$ by $e^{2\pi i(f-f_0)\tau}$ and integrating over the real axis, we have

$$\rho_1(\tau) = e^{-\frac{8f_0^2v_0^2\pi^2\tau^2}{c^2}} \tag{9}$$

To facilitate later comparison, we will write equation (9) as a power series, yielding

$$\rho_1(\tau) = 1 - \frac{8f_0^2v_0^2\pi^2\tau^2}{c^2} + \frac{32f_0^4v_0^4\pi^4\tau^4}{c^4} - \dots \tag{9a}$$

(ii) *Drifting motion*

The power spectrum is given by

$$W_2(f) = \frac{A_2}{f_0v_1}\sqrt{1 - \frac{c^2(f-f_0)^2}{4f_0^2v_1^2}} \tag{10}$$

v_1 being the velocity of drift. Hence the autocorrelogram, in the same manner, is found to be given by

$$\rho_2(\tau) = \frac{J_1\left(\frac{4\pi f_0 v_1 \tau}{c}\right)}{\frac{2\pi f_0 v_1 \tau}{c}} \tag{11}$$

where J_1 is the Bessel function of the first order. This, again on expansion into Taylor's series, yields

$$\rho_2(\tau) = 1 - \frac{2f_0^2v_1^2\pi^2\tau^2}{c^2} + \frac{4f_0^4v_1^4\pi^4\tau^4}{c^4} - \dots \tag{11a}$$

It will be noticed that the two autocorrelograms are similar for small values of τ. A drift velocity $v_1 = 2v_0$ would give rise to the same autocorrelogram as a random

velocity v_0, for small values of the lag τ. This is clearly seen in Fig. 2 where $\rho_1(\tau)$ and $\rho_2(\tau)$ have been plotted against $\frac{2f_0v_0\pi}{c}\tau$ and $\frac{f_0v_0\pi}{c}\tau$ respectively.

If, therefore, an autocorrelogram from an experimental fading pattern is to be compared with the above two theoretical models, with a view to deciding

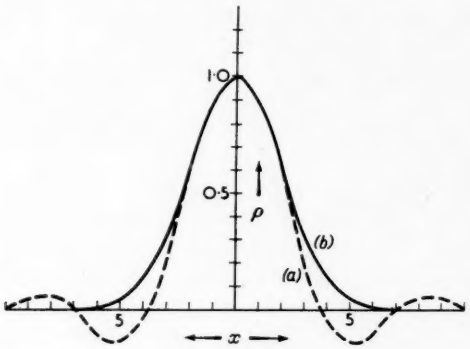

Fig. 2. (a) Autocorrelogram for a drifting ionosphere.
(b) Autocorrelogram for a turbulent ionosphere.

whether the motion of the irregularities is random or drifting, the autocorrelograms must be accurately evaluated at the "tails", i.e., for large values of the lag τ. Unfortunately, however, it is at the "tails" that an autocorrelogram is subject to the greatest inaccuracy; as has been pointed out by KENDALL (1946). This

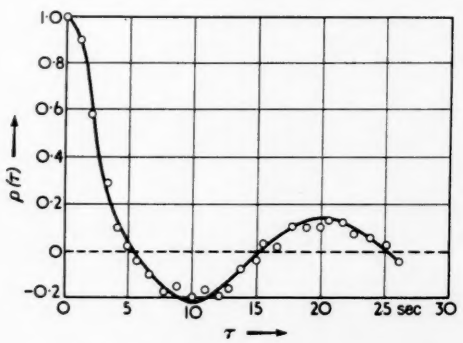

Fig. 3. Autocorrelogram obtained by MCNICOL.

fact has led ionospheric physicists to consider experimentally obtained autocorrelograms with suspicion. For example, MCNICOL (1949) obtained an autocorrelogram for the fading of short waves which is shown in Fig. 3. He was of the opinion that the oscillations in the autocorrelogram were spurious and were due to the kind of fluctuations obtained by KENDALL. On the other hand, the smooth nature of the oscillations obtained by him, and also its similarity to the theoretical

VOL. 6 1955

model in Fig. 2(a), tempts one to believe in the reality of these oscillations. To decide on this matter, as well as to gauge the possibility of distinguishing between the two autocorrelograms shown in Fig. 2, we must enquire into the cause of the inaccuracy in the evaluation of the "tails" of autocorrelograms.

Autocorrelograms obtained from finite time series, under certain restrictive conditions, have been studied by BARTLETT (1946) in some detail. He has shown that the dispersion of experimentally obtained autocorrelations is not dependent on the individual value of the autocorrelations but on the whole autocorrelogram. Thus, spurious oscillations are introduced at the "tail" when the value of the dispersion is greater than the value of the autocorrelogram itself. This can only be reduced by a suitable increase in the size of the sample, to which the dispersion is inversely proportional.

In the light of the above conclusion of BARTLETT'S we can suspect an oscillating autocorrelogram to be spurious only when the dispersion of the individual points about the mean curve is greater than the ordinate of the mean curve. This does not seem to be the case in MCNICOL'S curve, the dispersion appearing to be very low, and does not support the view that the oscillations of the mean curve are spurious.

It is also clear from the above discussion that an increase in the length of the sample is capable of reducing the statistical dispersion of the experimentally obtained autocorrelograms sufficiently to make a distinction between the two theoretical curves shown in Fig. 2 possible. The number of points on the fading pattern required for the necessary reduction of the dispersion can be found in terms of a test of significance developed by the author (1954). In the following we shall use the results of this work.

Let us initially assume that an autocorrelogram has been obtained having the shape shown in Fig. 2(a), corresponding to drift. It is our purpose to test whether this could have been obtained by random fluctuations from an autocorrelogram like Fig. 2(b), corresponding to random motion. For this we calculate, on the basis of a theoretical autocorrelogram like Fig. 2(b) and a sample of N points on the fading pattern, the probability of obtaining an autocorrelogram having the shape like Fig. 2(a) due to statistical fluctuations. It can be shown, in this case, that if x_p ($p = 1, 2, \ldots 6$) be the deviation of the experimentally obtained autocorrelogram from the theoretical one at 6 points then we must have

$$\frac{N}{4}\sum_{p=1}^{6} x_p^2 + \frac{N}{2}\sum_{q=1}^{6}\sum_{r=1}^{6} x_r x_q > 11 \qquad q \neq r$$

if the experimental autocorrelogram is to be considered significantly different from the theoretical one.

If the experimentally obtained autocorrelogram corresponds to Fig. 2(a), then by choosing six equally spaced points between 0 and 5 we have for the above inequality

$$0{\cdot}05N > 11$$

i.e.,

$$N > 220$$

Hence, if from a fading pattern containing more than 220 points we compute an

autocorrelogram having the shape of Fig. 2(a), we may say that it is highly improbable that it is due to fluctuations from an autocorrelogram like Fig. 2(b). Thus, a sample of this size can distinguish significantly between the two extreme types of autocorrelograms. For distinction from the intermediate cases, however, larger samples would be necessary.

4. CONCLUSION

It appears from the above discussion that, provided fading data for an adequate interval are available, it is possible to measure the drift velocity of ionospheric irregularities when present by the study of the autocorrelogram of the fading pattern at a single point instead of from several spaced points. It is also possible to recognize purely random velocities, when present, and measure their magnitude. In the case of superposition of random and drift motions, however, fading data for a very long interval of time would be necessary to make the measurement even theoretically possible.

In an actual application of this technique it will, usually, not suffice to use the autocorrelograms of Section 3, which are based on the assumption of omnidirectional antennae and a completely rough ionosphere. The power spectra must be deduced in accordance with the radiation pattern of the antennae and the relative positions of the receivers. In our experiments on winds in Pennsylvania State University, the three spaced receivers have loop antennae which are parallel to one another. The plane of two receiver antennae have almost the same disposition with respect to the transmitter-receiver line while the third is oriented differently with respect to this line. It has been observed that, for certain directions of drift in the ionosphere, the autocorrelograms of the first two receivers are significantly different from that at the third, the sense and magnitude of the difference depending on the direction of the wind. The quantitative theory of this phenomenon is at present being developed and will be published elsewhere.

Acknowledgments—The theoretical part of this work was carried out in the Institute of Radio Physics and Electronics, Calcutta, under Dr. S. K. MITRA, with financial subsistence from the Ministry of Education, Government of India.

The experimental work is being sponsored by the Geophysics Research Division of the Air Force Cambridge Research Center, Air Research and Development Command, under contract AF19(122)–44.

REFERENCES

BANERJI, R. B.	1953	Proc. Phys. Soc. B. **66**, 105
BANERJI, R. B.	1954	Scientific Report No. 59, Ionosphere Research Lab., The Pennsylvania State Univ.
BARTLETT, M.	1946	J. Roy. Stat. Soc. **8**, 27
KENDALL, M. G.	1946	"Contributions to the Study of Oscillating Time Series" (Camb. Univ. Press)
MCNICOL, R. W. E.	1949	Proc. Inst. Elect. Eng. (Part III) **96**, 366
RATCLIFFE, J. A.	1948	Nature **162**, 366

VOL. 6 1955

Journal of Atmospheric and Terrestrial Physics, 1955, Vol. 6, pp. 57 to 60. Pergamon Press Ltd., London

Measurements of the specific intensities of the auroral green line at College, Alaska

EDWARD V. ASHBURN
Geophysical Institute, University of Alaska
and Michelson Laboratory, U.S. Naval Ordnance Test Station,
Inyokern, China Lake, California

(*Received* 23 *June* 1954)

ABSTRACT

The specific intensities of the brightest part of the aurorae at College, Alaska, were found to range up to at least $3{\cdot}8 \times 10^{-5}$ ergs/cm²-sec-sq. degree for the 5577Å line. This is approximately seventy-five times the intensity of the zenith night-sky with no moonlight. The frequency distribution of the intensities of the brighter aurorae are given. Data are also presented which indicate that the intensity of the aurorae increases with increasing zenith distance toward the magnetic north.

INTRODUCTION

Aurorae frequently change both position and intensity too rapidly for the changes to be precisely measured by photographic techniques. A recording photoelectric photometer that had a relatively high resolution in its field of view and high speed of response would yield new information on the rapid changes of the aurorae. At the suggestion of C. T. ELVEY of the Geophysical Institute, College, Alaska, the author measured the intensities of the aurorae with such a photoelectric photometer. This paper presents a summary of some of the results that were obtained.

MEASUREMENT OF THE RADIANT ENERGY FROM THE AURORAE

A modified St. Amand (ST. AMAND, 1953) night-sky photoelectric recording photometer was used to measure the specific intensity of the aurorae. The modifications of the St. Amand photometer were: (1) the field of view of the telescope was changed to a rectangle whose one-half intensity width on the vertical was 0·3° (full width 0·6°) and whose horizontal width was approximately 5°; (2) the speed of the altitude movement on the alt-azimuth mount was increased to 5° per second; (3) the time-constant of the amplifier was changed so that a Brush Development Co. recording oscillograph could be used to follow changes up to 80 cycles per second. The paper of the recorder could be run at a speed of 5, 25, or 125 mm per second. A Baird interference filter was used in combination with a corning filter to isolate a band (half intensity width 150 Å) centred on the 5577 auroral green line. The photometer telescope was directed along the magnetic meridian. The measurements were made from the roof of the Geophysical Institute Building at College, Alaska.

Measurements of the specific intensity of the aurorae were made only during the brighter displays. The most usual routine was to move the telescope from the horizon at the magnetic north to the zenith and then reverse the motor so that the telescope returned to the horizon along the magnetic meridian. This programme could be repeated at approximately each forty-five seconds. The intensity distribution across a homogeneous arc could be measured within a period of approximately two seconds of time. Fig. 1 illustrates some of the records obtained.

The photometer was calibrated in absolute units by comparison with the daytime sky. The computed values for the day-sky were taken from SEKERA (1952) and SEKERA and ASHBURN (1953) after corrections for ozone absorption were estimated. The absolute calibration is estimated to be good to within $\pm$ 25 per cent. It is doubtful if calibrations using stars would be better than this, chiefly because of the variable sensitivity at different places in the field of view of the photometer.

RESULTS

The radiant energy reaching the photometer from an auroral display is a function of, among other things, the extinction coefficient. For the purposes of this discussion the extinction coefficient was taken as 0·20. The Rayleigh extinction

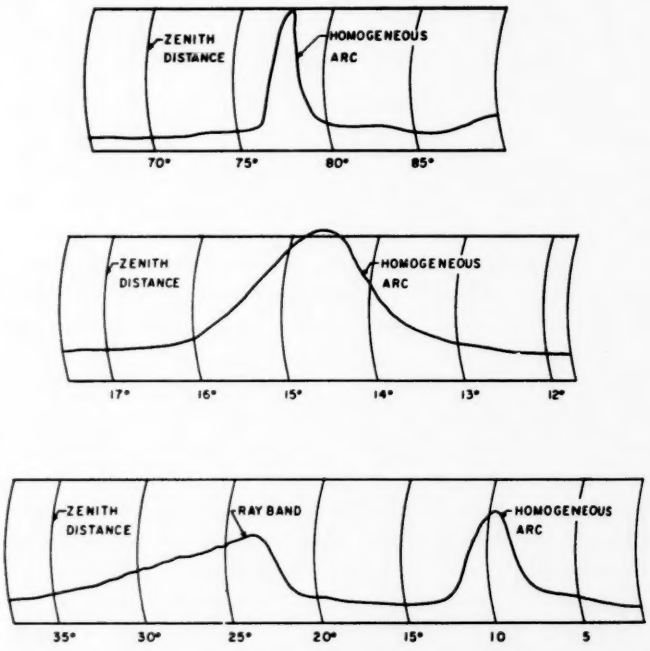

Fig. 1. Photometric records of the aurorae.

coefficient for 5577 Å is 0·092, which leaves 0·108 for ozone absorption and haze. The air at College was exceptionally clear except for ice fog in the lowlands south of the Geophysical Institute Building.

In order that a comparison may be made of the specific intensities of the aurorae that appear at different zenith distances, the observed intensities were corrected for extinction. The peak intensities were used for each arc, band, etc., when a reasonable estimate of the background radiation could be made. A total of 301 of the measurements were thought to be useful for comparative purposes. In each of these cases the peak intensity (corrected for extinction) was $6{\cdot}0 \times 10^{-6}$ ergs/cm^2-sec-sq. degree or greater. The frequency distribution of the intensities is given in Table 1.

VOL. 6 1955

The zenith night-sky background on a moonless night was found to be 5×10^{-7} in the units of Table 1. The intensities of some of the brighter aurorae were not measured, since the brighter aurorae move and change intensity rapidly and it is difficult to change the gain of the amplifier rapidly enough to keep the recorder pen on scale. If the extinction coefficient that was used is too low, the corrections that were applied to the measured readings are too low and the actual specific intensities are higher.

The intensity of the light received at the photometer from aurorae at different zenith distances may also vary due to different geometric paths through the

Table 1. *Frequency distribution of auroral intensities*

Specific intensity ergs/cm²-sec-sq. degree	*Number of observations*
6 to 8 $\times 10^{-6}$	116
8 to 10 $\times 10^{-6}$	93
1·0 to 1·2 $\times 10^{-5}$	51
1·2 to 1·4 $\times 10^{-5}$	13
1·4 to 1·6 $\times 10^{-5}$	11
1·6 to 1·8 $\times 10^{-5}$	6
1·8 to 2·0 $\times 10^{-5}$	3
2·0 to 2·2 $\times 10^{-5}$	0
2·2 to 2·4 $\times 10^{-5}$	3
2·4 to 2·6 $\times 10^{-5}$	1
2·6 to 2·8 $\times 10^{-5}$	0
2·8 to 3·0 $\times 10^{-5}$	0
3·0 to 3·2 $\times 10^{-5}$	1
3·2 to 3·4 $\times 10^{-5}$	2
3·4 to 3·6 $\times 10^{-5}$	0
3·6 to 3·8 $\times 10^{-5}$	1

aurorae and to different amounts of light emitted per unit volume along the line of view. These two effects cannot be separated by observations at a single station. Their combined effects are illustrated in Table 2. Here the average intensities, corrected for extinction, for all maximum intensities greater than 6×10^{-6} ergs/cm²-sec-sq. degree for various zenith distances along the magnetic meridian toward the north are given.

The number of observations given in Table 2 is relatively small and the observations were taken over a relatively short time period (seven nights) during a year of little auroral activity, but the data presented suggests that the intensity increases with zenith distance. Correction factors corresponding to extinction coefficients of 0·15 and 0·25 were tried with the same general results. This indicates that uncertainty in the extinction coefficient is not responsible for the major feature of Table 2. The effects of the extinction coefficient varying from night to night was not ascertained.

Table 2. Intensities as function of zenith distance

Zenith distance	*Average corrected intensity (all cases above $6{\cdot}0 \times 10^{-6}$) ergs/cm²-sec-sq. degree Å*	*Number of observations*
85°	12×10^{-5}	35
84°	$9{\cdot}0 \times 10^{-5}$	30
83°	$9{\cdot}2 \times 10^{-5}$	4
82°	$9{\cdot}1 \times 10^{-5}$	27
81°	$9{\cdot}0 \times 10^{-5}$	35
80°	$7{\cdot}9 \times 10^{-5}$	41
79°	$7{\cdot}8 \times 10^{-5}$	25
78°	$8{\cdot}5 \times 10^{-5}$	32
77°	$8{\cdot}6 \times 10^{-5}$	14
76°	$8{\cdot}7 \times 10^{-5}$	12
75°	$8{\cdot}4 \times 10^{-5}$	5
74°	$8{\cdot}3 \times 10^{-5}$	9
73°	$8{\cdot}1 \times 10^{-5}$	5
72°	$7{\cdot}8 \times 10^{-5}$	3
70°	$7{\cdot}5 \times 10^{-5}$	5
0°	$6{\cdot}1 \times 10^{-5}$	2

VOL. 6 1955

CONCLUSION

The frequency distribution and the absolute magnitudes of the specific intensities of the brighter aurorae at College, Alaska, are approximately as indicated in Table 1. The specific intensities of the aurorae increase with increasing zenith distance toward the magnetic north as indicated in Table 2.

REFERENCES

SEKERA, Z. (1952) *Tables Relating to Rayleigh Scattering of Light in the Atmosphere*, University of California at Los Angeles, Department of Meteorology, Sci. Report No. 3.

SEKERA, Z., and ASHBURN, E. V. (1953) *Tables Relating to Rayleigh Scattering of Light in the Atmosphere*, U.S. Naval Ordnance Test Station, Inyokern, NavOrd Report No. 2061.

ST. AMAND, Pierre (1953) "A Possible Relation Between the Night Airglow and the Ionosphere," Doctoral Thesis, California Institute of Technology, Pasadena, California.

RESEARCH NOTES

Intensity measurements of the second positive band system of nitrogen in high-latitude aurorae

The intensity distribution in the nitrogen band systems in the aurorae plays an important role in discussions on the temperature of the upper atmosphere and on the excitation mechanisms operative (BATES, 1949). Extensive series of intensity measurements of the nitrogen bands in high-latitude aurorae have been carried out by VEGARD and his collaborators (1932, 1951) and by PETRIE and SMALL (1952). In all these measurements there are systematic deviations from the expected intensity distribution, the intensity being too low in the ultraviolet region (BATES, 1949). The source of these deviations is still unknown. SEATON (1954) shows that it cannot be due to self-absorption in the atmosphere, and that the deviations from the expected distribution can be expressed by a function $f(\lambda)$, which is continuous and the same for all systems.

In this paper some new measurements of the near-ultraviolet bands of the second positive band system of nitrogen (N_2, $C^3\Pi_u \rightarrow B^3\Pi_g$) are reported. These measurements have been carried out in a way specially designed to avoid serious systematic errors.

A two-prism spectrograph earlier described by VEGARD (1933) was used. The transmission of this spectrograph is fairly good down to 3400 Å. The zenith distance was held constant at 60° during the exposures, thus minimizing errors due to extinction. The spectrograph was mounted on a vertical axis, and was always directed towards the strongest parts of the aurora with the zenith distance mentioned, all forms included. The aurora was focused on the slit, before which was placed a step filter. The illumination along the slit was thus not always constant, and the auroral spectrum could not be used for drawing the H–D curves. In order to ensure accurate intensity measurements, the spectrum of a nitrogen discharge lamp was exposed on each plate through the same step filter, but focused on the collimator lens. Laboratory experiments showed that the difference in the exposure time of the auroral spectrum and that of the lamp (4–6 hours and 5 minutes) gave negligible errors.

The intensity distribution in the second positive band system, as emitted from the nitrogen lamp, was measured earlier in the laboratory and has been given in another paper (OMHOLT, 1954). The auroral spectrum was measured by a direct comparison between the bands in the two spectrograms. As the spectrograph had no heating system, the spectrum was not always well focused during cold nights. For this reason, and because the rotational temperature is possibly different in the two light-sources, the intensity was measured by integrating over each band.

Seven spectra were obtained, two of which were sufficiently exposed for good intensity measurements. The results of these measurements are presented in Table 1, columns 4 and 5. For comparison is given the intensity distribution in the nitrogen lamp (column 3). The auroral spectrum No. 1 was exposed six hours during three nights from February 23 to 26, 1954. Spectrum 2 was exposed four hours during two nights from February 28 to March 2, 1954.

The intensities of the bands (0–1) and (1–2) are possibly too great because of overlapping by the bands (1–0)(3582 Å), (2–1)(3564 Å), and (3–2)(3549 Å) of the first negative band system of nitrogen. These bands are much stronger in the aurorae than in the discharge

Table 1. *Intensity distribution in the second positive band system of nitrogen* (N_2, $C^3\Pi_u \rightarrow B^3\Pi_g$) *in high-latitude aurorae*

λ	v'–v''	*Disch. lamp*	*Auroral spectra*		Petrie and Small	Vegard
			No. 1	*No.* 2		
4059	0–3	2·18	2·0	2·0	2·0	2·0
3998	1–4	2·78	2·9	3·0	2·3	2·2
3946	2–5	1·37	2·1	2·2		
3805	0–2	9·8	9·8	7·1	5·0	2·9
3755	1–3	7·1	7·5	5·1	4·0	2·5
3710	2–4	1·88	3·1	2·2	1·4	1·4
3577	0–1	30	45	37	15·1	5·8
3537	1–2	10·1	13	11	6·7	2·9

lamp. The intensities of the (0–1) and (1–2) bands of the second positive system should therefore not be trusted.

The intensities of the (0–2), (1–3), and (2–4) bands in spectrum 2 (column 5) are too low, as they are in the older measurements given in columns 6 and 7 in Table 1.

For comparison the intensities of the (0–0)(3914 Å), (0–1)(4278 Å), and (0–2)(4709 Å) bands of the first negative band system of nitrogen were measured. The resolution of the spectrograph was not good enough to make further intensity measurements in this band system. The results are given in Table 2.

Table 2. *Intensity distribution between the three strongest bands of the first negative band system of nitrogen* (N_2^+, $B^2\Sigma_u^+ \rightarrow X^2\Sigma_g^+$)

λ	v'–v''	*Disch. lamp*	*Auroral spectra*		Bates
			No. 1	*No.* 2	
3914	0–0	41	46	46	38
4278	0–1	10·0	8·9	9·9	10·3
4709	0–2	1·51	1·45	1·33	1·60

For comparison is given, in column 3, Table 2, the intensities found in the spectrum of the discharge lamp. (These were measured at the same time as those of the second positive system, though not published.) In Table 2, column 6, are given the values published by Bates (1949), based on theoretical as well as laboratory data.

For these bands the intensities measured in the aurora are too high at shorter wavelengths. It seems justified to accept all these deviations as purely experimental errors. They are possibly due to the necessary difference in the illumination of the spectrograph for the two light-sources. The aurora was focused on the slit to give highest possible light-flux through the lenses. The nitrogen lamp was, however, focused on the collimator lens to ensure even illumination of the step-filter. In this case the lenses and prisms were not filled with light.

VOL. 6 1955

The relative population rate $g(v')$ of the upper vibrational levels for a band system can be calculated from the relative intensities of any two bands (v_1', v_x'') and (v_2', v_y'') by the standard formula:

$$(1) \qquad \frac{g(v_1')}{g(v_2')} = \frac{I(v_1',v_x'')\nu(v_2',v_y'')^4 p(v_2',v_y'') \sum_{v''} p(v_1',v'')\nu(v_1',v'')^3}{I(v_2',v''_y)\nu(v_1',v_x'')^4 p(v_1',v_x'') \sum_{v''} p(v_2',v'')\nu(v_2',v'')^3}$$

$I(v',v'')$ is the band intensity, $\nu(v',v'')$ the frequency of the band, and $p(v',v'')$ the Franck-Condon factor.

The $g(v')$s are derived for the $C^3\Pi_u$ state of N_2 in the atmosphere during auroral displays from the relative intensities given in Table 1, columns 4 and 5. Only intensities within any one sequence are used, and the (0–1) and (1–2) bands are neglected. The values of $p(v',v'')$ are taken from an earlier paper (OMHOLT, 1954, Table 2). The results are given in Table 3.

Table 3. *The relative population rates of the vibrational levels of the* $N_2C^3\Pi_u$ *state in the aurorae deduced from the intensities given in Table* 1, *columns* 4 *and* 5

λ	v'–v''	$g(v')$ *Sp. No.* 1	$g(v')$ *Sp. No.* 2
4059	0–3	1·00	1·00
3998	1–4	0·59	0·61
3946	2–5	0·34	0·35
3805	0–2	1·00	1·00
3755	1–3	0·55	0·51
3710	2–4	0·33	0·32

The mean relative values of the g's given in Table 3 are 1·00, 0·56, and 0·33. This result confirms the values of $g(v')$ estimated in an earlier paper (OMHOLT, 1954) (1·00, 0·6, and 0·35), in which it was shown that this population can hardly be explained by supposing that only electrons take part in the excitation process of the second positive band system of nitrogen in high-latitude aurorae.

Acknowledgments—The author wishes to express his thanks to the Norwegian Research Council for Science and the Humanities for financial support. He is also greatly indebted to Professor VEGARD, to the Physical Institute of Oslo University, and to the Central Institute of Industrial Research for use of instruments.

A. OMHOLT

The Auroral Observatory,
Tromsö, Norway.

REFERENCES

BATES, D. R.	1949	*Proc. Roy. Soc.* **A196,** 217
OMHOLT, A.	1954	*J. Atmosph. Terr. Phys.* **5,** 63
PETRIE, W., and SMALL, R.	1952	*J. Geophys. Res.* **57,** 51
SEATON, M. J.	1954	*J. Atmosph. Terr. Phys.* **4,** 285
VEGARD, L.	1932	*Geofys. Publ.* **9,** No. 11
VEGARD, L.	1933	*Geofys. Publ.* **10,** No. 4
VEGARD, L., and KVIFTE, G.	1951	*Geofys. Publ.* **18,** No. 3

Vibrational temperatures from second positive bands*

(*Received* 9 *August* 1954)

ABSTRACT

The measurement of relative intensities and the derivation from them of vibrational temperature in the second positive band system of N_2 are discussed. It is concluded that measurements may be confined to the $\Delta v = 2$ sequence in the near-ultraviolet. A rather large number of measurements made with a photoelectric spectrometer are shown to lead to a vibrational temperature between zero and 1000°K; it is inherently impossible to distinguish any temperature in this range. The vibrational temperature therefore does not disagree with the kinetic temperature. Measurements by some other workers are briefly discussed.

Introduction

In a recent note, Omholt (1954) has deduced a vibrational temperature of around 5000°K for the second positive system of nitrogen in the aurora. He used some old intensities by Vegard and a set of transition probabilities measured by himself. The vibrational temperature was then found by comparison with the calculations of Bates (1949). We wish to discuss:

(1) Some other measurements and calculations of relative transition probabilities;

(2) Some intensity measurements which we have made on aurora; and

(3) The interpretation of the results. It is shown that temperatures in the range 0–1000°K cannot be distinguished and that most of the observations give a temperature in this range.

Relative Transition Probabilities

An extensive set of these has been calculated by Jarmain and Nicholls (1954). Intensity measurements were made in the laboratory by Tawde and Patankar (1943); these are not subject to the criticisms made by Omholt of the earlier measurements. The relative transition probabilities (or Franck-Condon factors) derived from them agree very well with those of Omholt and those of Jarmain and Nicholls. We prefer to use the last, since they cover the largest range.

Intensity Measurements on Aurora

These measurements are not easy because of the difficulty of allowing correctly for atmospheric extinction (Seaton, 1954). It is best to compare only bands in the same sequence, since they are very close together in wavelength; this was pointed out by Omholt. The results derived from the $\Delta v = 2$ sequence should be the most reliable, since the bands in it are not very different in intensity.

We have made some measurements on this sequence with a photoelectric scanning spectrometer (Hunten, 1953). With this instrument the sensitivity may be increased by decreasing the range of wavelength observed; we took advantage of this by scanning from 3650 to 3850 Å. Spectra were taken at the rate of six per minute with a spectral slit-width of 10 Å. The peak intensity rather than the area of each band was measured. This of course saves a great deal of labour, but it can also be justified by the following arguments.

The structure of this group of bands was studied on some microphotometer tracings of auroral spectrograms kindly shown to us by Dr. A. Vallance Jones. All three are of very similar shape, with a strong narrow peak on the long-wavelength side and a tail on the short-wavelength side. It appears that with 10 Å resolution the peak intensity will represent the total intensity quite well. In any case, since the three bands have nearly the same shape, the relative intensities will be very good. The area itself is very difficult to

* The research reported in this paper has been sponsored by the Geophysics Research Directorate of the Air Force Cambridge Research Center, Air Research and Development Command, under Contract AF 19(122)-152.

VOL. 6 1955

measure, since the bands appear on our traces to overlap slightly, and also since there is sometimes appreciable interference from the (1,11) and (2,12) bands of the Vegard-Kaplan system (3684 and 3768 Å). The (1,11) band is not resolved from the (2,4) second positive band and may greatly increase its apparent area; in some cases it even increases the peak height, but not as much.

An effort was made to check the correspondence between areas and heights. Three good spectra showing no signs of Vegard-Kaplan bands were selected from the night of September 28, 1952, and measured by both methods. The agreement between the two methods was rather poor, but the differences appeared entirely random. The averages for all three spectra agreed as well as would be expected, within 3 per cent of the intensity of the (0,2) band.

The effects of atmospheric extinction and spectrometer sensitivity on the wavelength response were evaluated by means of a preliminary series of spectra covering all the observable bands of the system. Intensities of bands from the same vibrational level were compared with the theoretical relative transition probabilities, and a curve of relative sensitivity vs. wavelength drawn. Since this was flat in the region of interest, it was assumed that no corrections were necessary as long as the zenith-distance of the aurora (and thus the atmospheric extinction) did not differ much from that used for the preliminary run.

In all cases several spectra were added together to reduce errors from intensity variations of the aurora and from detector noise. Results for four nights of observation are shown in Table 1 as the intensity ratio (0,2)3805 : (1,3)3755 : (2,4)3710. The numbers of spectra averaged are also given. The same ratio taken from the papers of PETRIE and SMALL (1952) and of OMHOLT (1954) are included.

Table 1. *Intensity ratios* (0,2) : (1,3) : (2,4) *for* $N_2 2PG$ *as measured on aurora, and corresponding vibrational temperatures*

Date	*No. spectra*	*Intensity ratio*	*Vibrational temperature*
April 29, 1952	36	100 : 82 : 28	0–1000°K
May 11, 1952	35	100 : 78·5 : 23	0–1000°K
May 17, 1952	78	100 : 77 : 23	0–1000°K
Sept. 28, 1952	126	100 : 84 : 27	0–1000°K
Petrie-Small	28	100 : 79 : 27	0–1000°K
Omholt-Vegard		100 : 85 : 50	6000°K ?

INTERPRETATION OF RESULTS AND CONCLUSIONS

The intensity ratio may be interpreted in terms of a vibrational temperature by means of Table 31 in a well-known paper by BATES (1949). This gives the relative population rates of the first three vibrational levels of the excited state as a function of temperature, assuming that these are excited by electron impact from the ground state. Since we are interested in only one sequence of bands, it is convenient to calculate a modified table which gives the relative intensities in this sequence directly. This has been done by means of BATES' equation (10) or OMHOLT'S equation (1), and the results are given in Table 2. The factors converting relative population rates to relative intensities are 1·33 for the (1,3) band and 1·08 for the (2,4) band. Values for 0°K were calculated directly from the transition probabilities in BATES' Table 25.

Table 2. Intensity ratios as in Table 1, but calculated by BATES *as a function of vibrational temperature*

T°K	0	500	1000	2000	4000	6000	8000
$I(0,2)$	100	100	100	100	100	100	100
$I(1,3)$	80	80	77	74	80	88	94
$I(2,4)$	25	25	26	30	38	46	52

Two things should be noted about this table:

(1) As pointed out by BATES, the accuracy of the figures is not high because of the nature of the exciting transition.

(2) The relative intensity of the (1,3) band, which can be measured most accurately, hardly changes at all from zero to 4000°. The relative intensity of the (2,4) band changes more rapidly, but certainly cannot distinguish any temperature in the range zero to 1000°. Thus any observed intensity ratio in the neighbourhood of 100 : 79 : 25 indicates a temperature between zero and 1000°K, and can be taken as consistent with the expected temperature of around 300°K. It may be seen in Table 1 that our results and those of PETRIE and SMALL are all in this neighbourhood, whereas those of VEGARD as quoted by OMHOLT yield a much higher temperature. As OMHOLT points out, the photometry leading to this last result was probably none too accurate; and it is not unlikely that the (1,11) Vegard-Kaplan band contributed materially to the intensity for the (2,4) band. It may therefore be concluded that the vibrational temperature of the second positive system is not in disagreement with the kinetic temperature, but cannot be measured with any accuracy.

The temperature of "less than 500°K" found by PETRIE and SMALL is easily shown to be in error. They calculated the population rates by taking the intensities of all observable bands, rather than just the $\Delta v = 2$ sequence. Using a preliminary set of relative transition probabilities by NICHOLLS, they found relative population rates of 100, 47, and 16. In terms of the relative intensities used here, this corresponds to 100 : 63 : 17. This does not agree with any ratio in Table 2; but PETRIE and SMALL apparently assumed that the theoretical population rates for 0°K would be 100 : 0 : 0. With this assumption, their conclusion immediately follows.

D. M. HUNTEN and G. G. SHEPHERD

University of Saskatchewan,
Saskatoon, Canada

REFERENCES

BATES, D. R.	1949	*Proc. Roy. Soc.* **A196,** 217
HUNTEN, D. M.	1953	*Canad. J. Phys.* **31,** 681
JARMAIN, W. R., and NICHOLLS, R. W.	1954	*Canad. J. Phys.* **32,** 201
OMHOLT, A.	1954	*J. Atmosph. Terr. Phys.* **5,** 63
PETRIE, W., and SMALL, R.	1952	*J. Geophys. Res.* **57,** 51
SEATON, M. J.	1954	*J. Atmosph. Terr. Phys.* **4,** 285
TAWDE, N. R., and PATANKAR, V. S.	1943	*Proc. Phys. Soc.* **55,** 396

VOL. 6 1955

The altitudes of the luminous layers in the Earth's atmosphere

(*Received 5 July* 1954)

BATES and DALGARNO (1953) have given a critical survey of the published results of the determinations of the heights from which the night airglow originates. They presented strong arguments against the heights that have been deduced by most observers from photometric data. It is the purpose of this note to point out that the observations support the arguments of BATES and DALGARNO.

The ratio of the airglow at a zenith distance, z, to the intensity of the airglow at the zenith is a function of, among other things, the atmospheric extinction coefficient and the height of the emitting layer. BATES and DALGARNO (1953) have given a table in which the importance of the extinction coefficient is clearly indicated.

The observers who have deduced heights of the airglow layer far in excess of those indicated probable by BATES and DALGARNO (1953) have not used a measured extinction coefficient. The usual method has been to assume Rayleigh scattering and ozone absorption as the only significant contributors to the extinction coefficient. Observations of the extinction coefficient are given in Table 1 below.

Table 1. *The extinction coefficient (reduced to sea level) for* 5577 Å *for selected stations as interpolated from published measurements*

Mt. Wilson (*Ref.* 3)	*Table Mt.* (*Ref.* 1) *Mean of* 39 *clearest days* 1940–1950	*Table Mt.* (*Ref.* 2) *Hazy day*	*Jena* (*Ref.* 4) *Best day of* 18 *observations*
0·177*	0·143	0·276	0·28

(1) ABBOT *et al.*, 1952.
(2) ALDRICH; personal communication.
(3) STEBBINS and WHITFORD, 1944.
(4) WEMPE, 1944.

* Commonly but erroneously used as 0·125 in the literature.

These figures are all significantly higher than the Rayleigh +ozone coefficient (approximately 0·12). If the observed values of the extinction coefficient are used in the usual method of deducing the heights of the airglow layer, the heights are found to agree with those claimed by BATES and DALGARNO (1953).

The data presented in Table 1 are for 5577 Å. Comparable data are available for the other wavelengths of interest. In every case the observed extinction coefficients are significantly greater than those that have been assumed by those who have computed the heights of the airglow layers. The difference between the observed extinction coefficients and the Rayleigh value is produced principally by the scattering of light by haze particles.

In the computation of the height of the night airglow layers from the photometric data the extinction coefficient enters into the equation in two places. The first is associated with the direct extinction of the airglow. The second is associated with the scattered light. All the published discussions of the scattered light are based entirely on isotropic or Rayleigh scattering. Observations of the day-sky can be used effectively to determine the effect of scattering without the uncertainty introduced by an unknown reflection function of the ground, non-Rayleigh scattering, and the assumption of a flat earth.

EDWARD V. ASHBURN

Michelson Laboratory,
U.S. Naval Ordnance Test Station, Inyokern,
China Lake, California.

References

Abbot, C. G., Aldrich, L. B., and Hoover, W. H. (1952) *Annals of the Astrophysical Observatory of the Smithsonian Institution*, Vol. 7.

Aldrich, L. B.; personal communication.

Bates, D. R., and Dalgarno, A. (1953) *J. Atmosph. Terr. Phys.* **4**, 112–123.

Stebbins, J., and Whitford, A. E. (1944) *Ap. J.* **98**, 20.

Wempe, J. (1944) *Mitteilungen des Astrophysikalischen Observatoriums, Potsdam*, No. 21.

Book review

Thunderstorm Electricity. Edited by Horace R. Byers, University of Chicago Press, 1953. 344 pages. 45s.

In 1950 a conference was held at Chicago on the subject of "Thunderstorm Electricity," attended mainly by American workers on the subject. The volume under review consists mainly of the papers presented at the conference, in some cases revised and brought up to date. In addition, there are a few articles by authors from outside America who did not participate in the conference. The book therefore lacks the coherence one would expect in a textbook on the subject, though this has been somewhat overcome by the arrangement of the chapters to start with basic knowledge on atmospheric electricity, thunderstorm dynamics, cloud physics, and charge generation, followed by chapters dealing more closely with thunderstorm electricity and finishing with the effects of lightning on aircraft and on power lines.

The chapters themselves are very uneven in their content; some, for example Chapter III by Koenigsfeld, consists of accounts of new work, very interesting and valuable, but, one would have thought, better published in a journal than in a volume such as this; other chapters, such as Chapter VIII by Ross Gunn, are mainly summaries of work previously published by the author, summaries which are valuable because the work had not previously been put together. In a few chapters, for example Chapter II by Israel, there is a general summary and systemization of the branch of the subject, and in some, for example Chapter XIV by Norinder, a historical survey followed by an account of recent work.

The lengths of the chapters are also very uneven, and it may be remarked that the longest, Chapter V by Weickmann, occupying 73 pages out of 344, has only two and a half pages on actual electrical phenomena, though it forms a valuable account of the precipitation in thunder-clouds; and another long Chapter VII by Loeb, is concerned with a general discussion of charge generation processes, only some of which could operate in thunder-clouds. This indicates perhaps a lack of balance between background knowledge and the actual problems of thunderstorm electricity.

For those whose work is directly concerned with thunderstorm electricity, the book is an essential, and even the well-informed on the subject will find much that is new and of interest. For those whose interest in the subject is less close, many chapters will provide accounts of recent work and much stimulus of thought. The present reviewer finds it difficult to pick out any one chapter he has found of more interest than the others, but has found something of value in every one.

It is a pity that it was not found possible to include an index and that there is no cross-referencing from one chapter to another. The volume is attractively produced, and the large numbers of diagrams and plates are very clear.

J. A. Chalmers.

VOL. 6 1955

Journal of Atmospheric and Terrestrial Physics, 1955, Vol. 6, pp. 69 to 87. Pergamon Press Ltd., London

La nomenclature ionospherique et les conventions pour le dépouillement

K. Bibl, R. Busch, K. Rawer, et K. Suchy
du Service de Prévision Ionosphérique Militaire

(*Received* 8 *May* 1954)

ABSTRACT

A proposal is made for the classification of the ionospheric layers according to their thickness. Transitorial phenomena are not to be classified amongst the normal layers; the corresponding layers are always thin.

The fundamental notions in use with ionospheric records are defined more exactly, the role of the ionosonde is also defined. In order to define the term "critical frequency" in such a way that it can also be applied to thin layers, account is taken of the intensity of the different echoes. The phenomenon of "partial reflection" cannot be neglected. It is necessary to distinguish between characteristics which are directly readable and those which are found by extrapolation.

Proposals are also made for more generally applicable definitions of the "descriptive letters."

0. Introduction

0.1. *Les conventions existantes*

La plupart des informations concernant l'ionosphère sont obtenues à l'aide des ionogrammes. Après avoir defini certaines caractéristiques fondamentales pour l'interprétation des phénomènes physiques de l'ionosphère, on pourra exprimer ces informations numériquement.

Malheureusement les caractéristiques proposées varient d'un auteur à l'autre, et de nombreuses modifications ont été proposées succesivement.

Depuis 1946 le CCIR et l'URSI ont essayé d'établir un catalogue international. Ce catalogue constitue un amalgame des conventions déjà existantes communes à plusieures services ou adoptées par une majorité. Parmi ces règles, certaines sont plus ou moins arbitraires, surtout en ce qui concerne l'emploi des lettres descriptives.

Au cours de ses travaux statistiques effectués par mécanographie, Gallet (1950) en a demandé un emploi plus rationnel.

0.2. *Importances des conventions*

Depuis la réunion de l'URSI en 1950 à Zürich, le SPIM s'est efforcé de constituer un système plus logique et plus pratique pour résoudre l'ensembles des problèmes.

Il est certain que les conventions déterminent finalement l'importance des caractéristiques mesurées et leur utilité pour déduire une information physique. Aussi la discussion des détails présente—t'elle un travail nécessaire et utile qui intéresse les recherches et les applications. Une définition mal adaptée peut conduire à des conclusions fausses. Un phénomène intéressant peut échapper à l'observation, si les conventions ne le prévoient pas, (p.e. si le phénomène en question possède des désignations différentes).

0.3. *Critiques*

Nous pouvons faire trois critiques à la nomenclature internationale actuelle:

1. La distinction des différentes couches n'est pas suffisamment précisée.

2. Les notions fondamentales utilisées (p.e. "fréquence critique") ne sont pas définies.

3. L'emploi des lettres et des différentes conventions est lourd et n'est pas rationnel, la plupart des "prescriptions" n'étant adaptées qu' à un nombre restreint de caractéristiques et de cas.

1. Classification des Régions et des Couches

1.1. *Classification des régions*

Les enregistrements de jour semblent montrer régulièrement l'existence d'un minimum d'ionisation entre 150 et 200 km. Ce fair est marqué sur l'ionogramme par la présence d'une discontinuité des hauteurs virtuelles. L'altitude de ce minimum nous permet de distinguer la région F (supérieure) et la région E (inférieure). Durant la nuit l'ionisation dans la région E est souvent très faible. L'état de nos connaissances ne nous permet pas encore de savoir, si l'introduction d'une région D, inférieure à E, est justifiée par un minimum d'ionisation. Nous désignerons toujours par "région" un certain intervalle de hauteur où peuvent se produire différents phénomènes.

1.2. *Classification des couches*

Dans une "région" peuvent se trouver plusieurs "couches." La plupart du temps ces couches sont caracterisées par un maximum d'ionisation ("peak" dans la nomenclature de Chapman, 1950). Il existe des couches plus ou moins épaisses dont les qualités de réflexion peuvent être assez différentes (voir § 2). La classification peut être basée sur différents critères:

(a) sur l'épaisseur (absolue, ou relative c.à.d. pas rapport à "l'échelle de hauteur" au niveau de la couche)

(b) sur l'altitude

(c) sur le caractère de la réflexion

(d) sur la régularité ou l'irregularité de l'apparition

(e) sur l'origine de l'ionisation.

Si l'origine des différentes couches était bien connue, la dernière methode serait très intéressante. En réalité les quatre premiers critères sont appliqués simultanément. On a donc une *classification phénomènologique*. Le danger de cette méthode est évident: il est possible que des phénomènes ayant une origine très différente soient confondus et, d'autre part, qu'un phénomène unique mais variable dans le temps soit classé différemment suivant l'état de son évolution. Malheureusement, dans l'état actuel de nos connaissances une classification suivant l'origine des couches ne peut pas être envisagée.

Dans ces conditions, nous ne croyons pas pouvoir obtenir une méthode simple et automatique pour la classification. Chaque couche doit être considérée séparément. On essayera de trouver des critères qui tout en permettant d'éliminer les phénomènes transitoires sont aptes à saisir une unité physique commune. Il est évident qu'un certain doigté est nécessaire. Le resultat doit toujours être verifié par l'expérience.

Le cas de la couche dite E, couche principale de la région E, a déjà été discute

VOL. 6 1955

(BIBL, 1951). BIBL est arrivé à une définition qui s'est révelée intéressante; en l'appliquant on obtient une plus faible dispersion des valeurs mésurées pour la caractéristique f^0E. Une corrélation remarquable entre les perturbations ionosphériques à debut brusque (PIDB) et l'ionisation de la couche E a été ainsi obtenue.

1.3. *Difficultés*

Les difficultés qui apparaissent lors de la classification sont dûes à deux causes principales.

(a) Des phénomènes transitoires (BIBL, 1952) peuvent temporairement déformer les traces des échos dans l'ionogramme*. En général on a tendance à éliminer ces phénomènes lors du dépouillement normal. Mais, pour y parvenir, il faut d'abord savoir les reconnaitre.

(b) Il peut exister une fusion partielle entre deux couches. C'est p.e. le cas des couches F_1 et F_2. Les définitions appliquées d'habitude pour ce cas mériteraient une discussion plus détaillée. L'interprétation physique des caractéristiques trouvées pour la couche F_1 peut être très délicate.

En observant l'ionogramme, on peut distinguer assez bien les couches suivant leur épaisseur. La partie inférieure au maximum d'ionisation ("increase," suivant l'expression de CHAPMAN) est observée directement. Le "decrease" ne peut être observé que par des méthodes indirectes.

1.4. *Couches épaisses et minces*

L'épaisseur absolue d'une couche est intéressante pour les phénomènes de réflexion (Annexe I). D'autre part l'épaisseur relative d'une couche, par rapport à "l'échelle de hauteur" (scale height) au niveau de la région en question peut nous donner une indication relative à l'origine de la couche. Nous avions proposé (BIBL, 1953) de préciser la distinction entre une couche "normale" et une couche "anormale" suivant ce critère c.à.d. par l'introduction d'une "*épaisseur critique.*" Pour ne pas créer de confusion nous parlerons maintenant de couches "epaisses" (= normales) et "minces" (= anormales).

La valeur de l'épaisseur critique est bien entendu variable avec l'altitude. A la base de la région E elle est de l'ordre de 15 km. Avec l'échelle de hauteur la valeur critique croît si l'altitude augmente de sorte qu'elle atteint environ 30 km au niveau supérieur de la région E. Dans la région F elle varie entre 40 et 60 km environ. Avec cette définition les couches se présentant parfois au cours du développement des phénomènes transitoires sont toujours "minces." Aussi les couches dites "sporadiques" sont minces; leur épaisseur est souvent inférieure à la limite donnée par la précision de la lecture des hauteurs virtuelles; nous dirons de ces couches qu'elles sont "très minces" (d'ailleurs le nom "sporadique" ne semble pas très heureux).

1.5. *Region F*

Dans la région F nous avons surtout deux couches "epaisses" qui sont, classées par ordre d'altitudes décroissantes F_2 et F_1. F_1 est presque toujours une "stratification," ne possédant aucun "peak." En zône tropicale il existe parfois entre

* On peut même avoir dans ce cas des rayons qui ont été réfléchis en direction oblique qui ne se prêtent pas à l'interprétation habituelle.

F_2 et F_1 une autre stratification que nous avons dénommée "$F_{1,5}$" (Delobeau *et al.*, 1950; Delobeau, 1952) tandis que d'autres l'ont appelée "lunar layer" (McNish, 1950).

Toutes les autres stratifications se manifestant dans la région F se sont révélées comme transitoires grâce à l'observation cinématographique (Bibl, 1953). Il en existe deux types caractéristiques:

(a) La stratification "F_0," relativement fréquente (Bibl, 1950), située au dessous de F_1, qui est en général d'épaisseur faible et peut être classée comme "mince." Son altitude est peu différente de celle de F_1. Dans ce cas, la trace des échos admet une courbure continue la "fréquence critique" est inférieure à f^0F_1.

(b) Une autre stratification correspondant à une couche "très mince" (au moins du coté inférieur) qui se produit assez souvent dans les régions tropicales. Cette stratification peut changer considerablement l'aspect de l'ionogramme sa hauteur minima varie plus que celle de F_0, sa fréquence critique peut être supérieure à f^0F_1. Nous proposons de classer les deux sortes de phénomènes sous le nom de "couche T" (transitoire).

1.6. *Région E*

Whale (1950) ainsi que Bibl (1953) ont montré que ces stratifications transitoires se forment dans la région F et descendent rapidement en quelques minutes au niveau de la région E. Des observations antérieures ont été publiées par Appleton, Naismith, et Ingram (1939), Munro (1950). Les couches correspondantes sont toujours minces: E_{2s} (ou même E_s). Nous avons l'impression que les couches E_2 doivent aussi être classées parmi ces phénomènes transitoires. Pour éviter un confusion avec la nomenclature de l'URSI qui distingue E_2 et E_{2s} nous utilisons pour ces deux formes de couches transitoires la désignation de "couche I" (intermédaire).

En tout cas dans la région E seule la couche dite E peut être considérée comme épaisse. Quant à E_s, il serait peut-être intéressant de distinguer (McNicol et Gipps, 1951) les types transitoires arrivant des régions élévées du type beaucoup plus fréquent de couche mince se formant à altitude constante. Cette dernière est très souvent transparente ou semi-transparente.

2. Définitions des Fréquences Caractéristiques

2.1. *Définitions générales*

Pour obtenir une définition adéquate il nous a paru nécessaire de considérer d'abord quelques détails concernant les enregistrements. L'observation d'un écho ionosphérique n'est possible que si l'intensité du champ à la réception est supérieure à la valeur minimum imposée par la sensibilité du récepteur. Or, s'il existe une forte variation de la qualité de réflexion de l'ionosphère avec la fréquence, la puissance émise et la sensibilité du récepteur en dépendent aussi.

Les conditions de réception des échos en provenance d'une couche épaisse sont indiquées sur la Fig. 1a. Nous avons tracé la courbe du décrément δ d'affaiblissement de l'intensité de l'écho en fonction de la fréquence, les deux courbes épaisses correspondent à un écho E et à un écho F (voir l'annexe I). On retrouve sur les fréquences basses l'absorption non sélective dûe à la couche D, influence diminuant

VOL. 6 1955

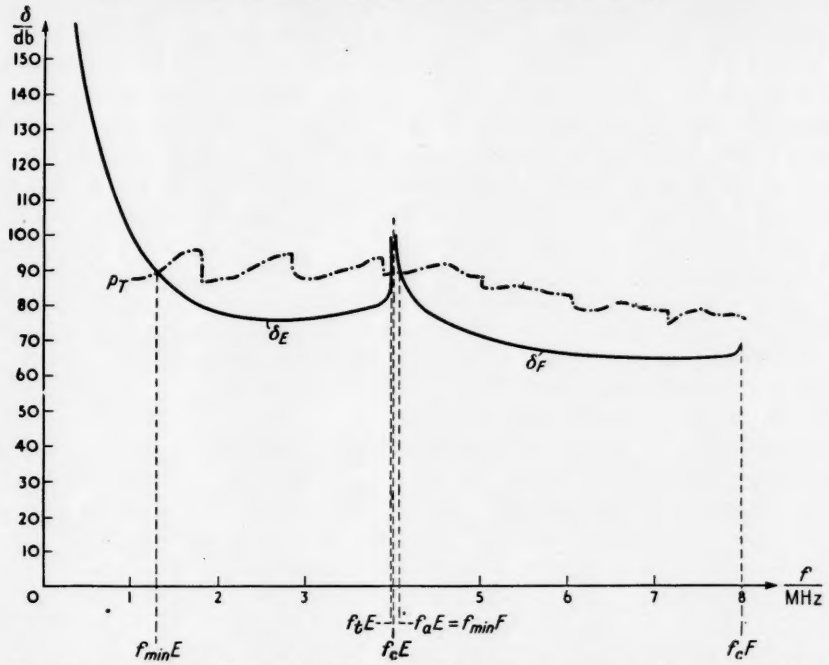

Fig. 1a. Variation du "décrement total" δ_E pour l'écho en provenance de la couche E et δ_F pour celui de la région F (Résultat obtenu à l'aide des Figs. 3, 4, et 5, avec $f_L = 1$ MHz).
Variation of the "total decrements" δ_E and δ_F.

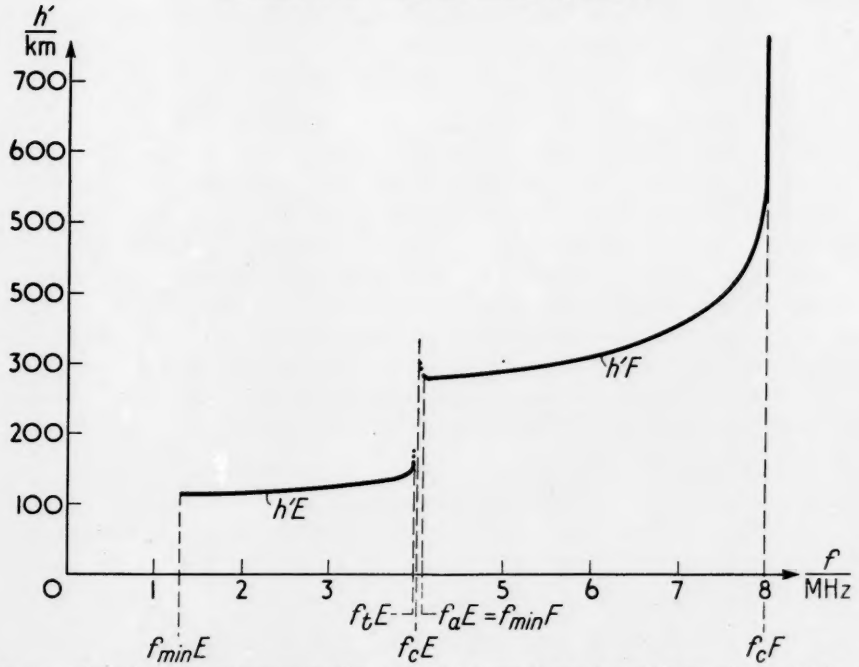

Fig. 1b. Variation des hauteurs virtuelles $h'E$ et $h'F$ (pour le cas du modèle utilisé pour la Fig. 3).
Variation of the virtual heights $h'E$ and $h'F$.

rapidement avec l'augmentation de la fréquence. Ensuite, apparaît une absorption sélective dûe à la couche E nettement mise en évidence près de la discontinuité de la trace des échos. Enfin, comme la couche E devient presque complètement transparente pour les fréquences supérieures à cette discontinuité, le décrement δ_E tend alors vers l'infini.

D'autre part en raison de l'occultation, pour les fréquences inférieures, δ_F décroit à partir d'une valeur infinie. Sa valeur est relativement faible pour les fréquences supérieures à la discontinuité.

Nous faisons figurer la courbe p_T donnant le "pouvoir transmissif"* qui est le maximum admissible de δ, compte tenu des conditions techniques de l'ionosonde (courbe en trait interrompu). Les traces des échos observables sont representées à la Fig. 1b. Nous voyons figurer un point d'errêt à l'intersection entre les courbes continues et interrompues de la Fig. 1a. On a donc à l'extrémité d'une trace $\delta_E = p_T$ ou $\delta_F = p_T$. Ainsi sont déterminées:

1. La *fréquence minimum* $f_{\min}$ d'une couche: C'est la fréquence la plus basse pour laquelle peut se produire un écho provenant de la couche considérée.

2. La *fréquence d'occultation* f_a d'une couche: C'est la fréquence la plus basse pour laquelle la couche considérée commence à devenir transparente pour des échos provenant éventuellement des couches supérieures.

3. La *fréquence critique* f_c d'une couche: C'est la fréquence la plus élevée pour laquelle la couche est aussi réfléchissante que transparente (on la détermine pratiquement en comparant l'amplitude des échos en provenance de la couche, par rapport à celles provenant éventuellement des couches supérieures).

4. La "*top-frequency*" f_t d'une couche: C'est la fréquence la plus élevée pour laquelle peut se produire un écho provenant de la couche considérée.

La lecture des caractéristiques $f_{\min}$, f_a, et f_t est immédiate, la condition est $\delta = p_T$. Ces caractéristiques ne sont pas indépendantes de la sensibilité de l'ionosonde.

Par contre f_c suivant notre définition ne dépend pas des données techniques. Cette caractéristique peut aussi être obtenue à l'aide des ionogrammes, pourvu que les différentes amplitudes soient reproduites fidèlement (voir l'annexe II). Dans la plupart des cas, f_c est obtenue par extrapolation. Pour une couche épaisse on obtient f_c avec une exactitude en général suffisante par extrapolation des traces des échos; cette extrapolation peut aussi être effectuée dans l'autre sens sur la trace correspondant à la couche supérieure en altitude (h' tend vers l'infini—ou au moins vers des valeurs très élevées) (Rawer, 1939, 1942). Dans ce cas les caractéristiques f_a, f_c, et f_t sont très peu différentes; on lit f_c entre f_a et f_t, ou par extrapolation au dessus de f_a (parfois on doit même effectuer l'extrapolation sur la trace correspondant à une couche supérieure).

2.2. *Couches très minces*

Le cas d'une couche très mince (ou semitransparente) est représenté dans les Figs. 2a et 2b. Dans ce cas le degré de transparence varie plus lentement avec la fréquence que pour une couche épaisse. f_a et f_t sont nettement différentes (Rawer, 1939, 1942).

* Voir "Instruction SPIM—A," édition janvier 1954.

VOL. 6 1955

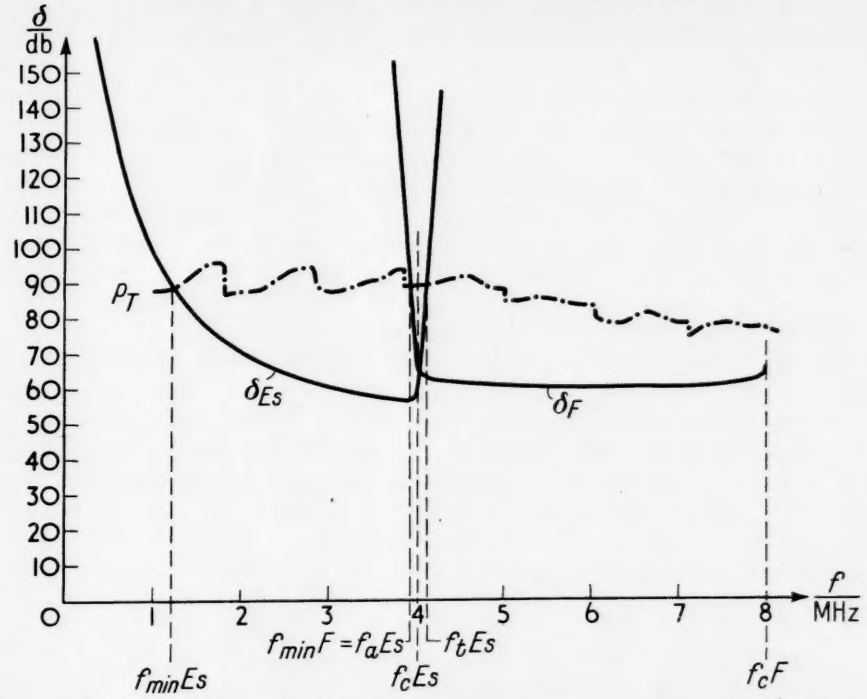

Fig. 2a. Variation du "décrement total" δ_{E_s} pour l'écho en provenance de la couche E_s et δ_F pour celui de la région F (Résultat obtenu à l'aide des Figs. 3, 4, et 6, avec $f_L = 1$ MHz).
Variation of the "total decrements" δ_{E_s} and δ_F.

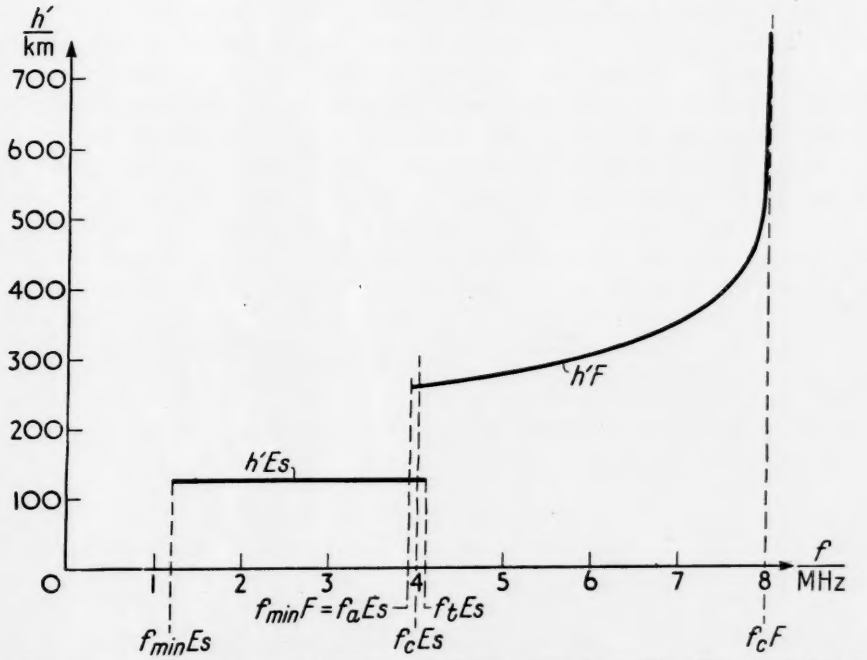

Fig. 2b. Variation des hauteurs virtuelles $h'E_s$ et $h'F$ (pour le cas du modèle utilisé pour la Fig. 3).
Variation of the virtual heights $h'E_s$ and $h'F$.

On écrit pour abréger fE au lieu de f_cE; d'autre part on écrit en général fE_s au lieu de f_tE_s. Ainsi la signification des symboles n'est plus la même pour les couches épaisses et les couches minces. Etant donné que dans ce cas la fréquence critique f_c ne peut pas être obtenue à partir de l'ionogramme, il y a peu de chance pour qu'il y ait confusion. Néanmoins une désignation plus exacte est nécessaire si l'on effectue des comparaisons d'amplitudes (Rawer, 1939). Toutefois il est bon de retenir que la lecture directe des ionogrammes ne peut pas donner une fréquence critique mais seulement une "top frequency" dans le cas d'une couche très mince; les resultats dépendent donc des caractéristiques techniques.

2.3. *Composantes magnéto-ioniques*

Nos définitions sont applicables séparément à chacune des composantes magnéto-ioniques (on écrit $f^0_{\min}$, $f^x_{\min}$, f^0_a, f^x_a, etc.). Pour les couches minces la distinction entre f^0_t et f^x_t est parfois difficile, on y parvient grâce aux méthodes suivantes:

(a) On cherche f^0_a. En raison de $f_a < f_t$ (Fig. 2b) on a: $f^0_a + \Delta f < f^x_t$ ($\Delta f \approx \frac{1}{2} . f_H$ est l'écart entre les deux composantes magnéto-ioniques). Soit f_t la valeur lue dans l'ionogramme; si $f_t < f^0_a + \Delta f$ on a f^0_t. Si non, il peut s'agir de f^x_t. Dans ce cas on procède comme suit.

(b) On cherche $f^x_{\min}$ pour la couche suivante par ordre d'altitude croissante. Si $f_t > f^x_{\min}$ on peut supposer qu'il s'agit de f^x_t. Si $f_t < f^x_{\min}$ c'est f^0_t.

2.4. *Comparaison avec l'usage actuel*

La fréquence critique de la composante ordinaire est considérée en général comme la fréquence de plasma f_e maximum, à l'intérieur de la couche. Or, les f_e ne peuvent pas être mesurées directement par une ionosonde. Par contre, f_c est définie à partir des décrements mesurés. Dans le cas d'une couche épaisse f^0_c est pratiquement égale à la fréquence de plasma f_e maximum.

La "top-frequency" f_t d'une couche mince n'est définie sans équivoque que si l'on fait intervenir les deux composantes magnéto-ioniques. C'est un usage très répandu actuellement de ne pas tenir compte des deux composantes. On lit parfoir f^0_t parfois f^x_t suivant l'importance de l'absorption. En raison de la variation de l'absorption dans le temps, la statistique observée des fE_s est souvent incorrecte (les "trous" visibles dans les champs de dispersion ne sont pas réels mais seulement apparents en raison de l'absorption différente des deux rayons). Nous avons d'ailleurs pu constater que la distinction ne fait pas trop de difficultés, même pour E_s, à condition que les enregistrements soient de bonne qualité (annexe II).

Enfin la fréquence d'occultation f_a est caractéristique pour la couche qui détermine l'occultation; la definition actuelle f_b l'introduit comme caractéristique dépendant encore d'une couche occultée. (Nous obtenons f_bE_s comme maximum de $f^0_aE_s$ et de f^0I.)

Nous donnons en annexe III une proposition pour les caractéristiques dont la lecture régulière nous semble intéressante.

3. La Hauteur Virtuelle

La définition de la "hauteur virtuelle minimum" d'une couche présente moins de difficulté. En général on lit $h' = h'_{\min}$ sur le minimum relatif de la trace, c'est

VOL. 6 1955

à dire pour $\frac{dh'}{df} = 0$. Cette condition n'est satisfaite, que s'il existe une couche d'altitude inférieure à la couche considéree. Seulement une couche inférieure peut introduire un effet de retard dont l'importance diminue si la fréquence augmente. Par contre pour une seule couche réflectrice simple (non stratifiée), la hauteur virtuelle augmente toujours avec la fréquence. Le minimum résulte de la combinaison de ces deux effets. La fréquence relative à ce minimum d'altitude ne semble avoir aucune importance physique.

S'il n'y a pas de couche inférieure, il n'existe pas de hauteur minimum répondant à la définition donnée ci-dessus. La valeur du minimum absolu dépend dans ce cas d'influences plus ou moins accidentelles. Nous distinguons les cas "*S*" (limitation par d'autres émissions, p.e. une bande radio), "*E*" (limitation par la plus basse fréquence du sondeur) et "*B*" (limitation par la fréquence minimum dûe à l'absorption non-déviative, voir annexe I). A cause de la faiblesse du retard introduit par la couche E_s et son caractère sporadique le cas d'une occultation (symbole "*A*") ne se distingue pas très bien d'un brouillage extérieur.

On a donc tendance à considérer comme "cas normal" le cas "*B*" de jour et le cas "*E*" de nuit. Les valeurs médianes mensuelles doivent correspondre à ces cas, la présence d'une autre cause ("*S*," "*A*") est considérée comme anormale, elle ne compte donc pas pour la statistique.

Etant donné que la hauteur des stratifications "*T*" our "*I*" varie constamment et d'une manière rapide, elle n'est pas notée et nous ne lisons que la fréquence critique correspondante. Par contre la déformation d'une trace correspondant à une couche normale dûe à une stratification transitoire est considérée comme un effet de perturbation. Par conséquent pour la lecture des hauteurs $h'F_1$ et $h'F_2$ il nous semble préférable d'extrapoler dans le sens du cas non perturbé.

La hauteur virtuelle $h'F_2$ ne correspond guère à une altitude bien définie. Le retard du signal dans la couche F_1 est important il est fort difficile de tirer de $h'F_2$ seule une conclusion concernant une hauteur vraie. Sans condamner $h'F_2$ nous préférons noter normalement $h'F$, la hauteur minimum de la région F et nous indiquons $h'F_2$ seulement dans le cas où F_1 est présente.

Une proposition pour les caractéristiques dont la lecture régulière nous semble intéressante, est donnée en annexe III.

4. L'Emploi des Lettres

Il se produit assez souvent qu'une caractéristique ne peut pas être lue avec l'exactitude voulue à cause d'anomalies quelconques. Il y en a beaucoup qui sont d'origine ionosphérique, p.e. l'absorption et l'occultation. Dans ces cas on a intérêt à utiliser les valeur numériques même si leur poids est faible (Gallet, 1950). Pour éliminer dans la mesure du possible l'influence de telles anomalies à condition qu'elles n'aient rien à voir avec la caractéristique en question; on fait une extrapolation dans le sens des conditions normales. La raison pour laquelle on a du extrapoler est intéressante, elle peut même posséder un certain poids statistique. C'est pourquoi elle doit toujours être indiquée par une lettre descriptive. D'habitude on met une lettre isolée si la caractéristique ne peut pas être lue. Cet usage

ne doit pas diminuer davantage l'information déduite de l'ionogramme (p.e. dans un cas d'occultation complète on écrira "A" pour f^0F_2, et l'on utilisera une valeur numérique avec le signe $>$ pour f_aE_s. Autrement une valeur importante de f_aE_s ne pouvait entrer en ligne de compte).

Par contre nous ne voulons pas utiliser des lettres à seule fin de donner une information supplémentaire ne possédant rien de commun avec la caractéristique en question. (Pour cette raison la lettre "K" a été supprimée.)

L'existence d'une extrapolation est déjà indiquée par la présence d'une lettre descriptive. Le degré de l'extrapolation ou, mieux, l'incertitude de la valeur obtenue, est précisée par des parenthèses ou des signes $>$ et $<$. Nous appliquons les règles suivantes dépendant de l'erreur possible qui est indiquée en %:

Erreur possible	*Indication*	*Exemple*
inférieure à 2%	nombre accompagné seulement d'une lettre	$2{\cdot}85^S$
entre 2 et 5%	nombre en parenthèses accompagnée d'une lettre	$(2{\cdot}85)^S$
entre 5 et 20%	nombre avec lettre descriptive et signe $>$ ou $<$	$<2{\cdot}85^S$
supérieure à 20%	seulement la lettre	S

Il existe des caractéristiques variant peu où l'emploir des signes $>$ et $<$ est sans intérêt. Dans ces cas on met la lettre seule à partir d'une erreur de 5 per cent environ. D'autre part on peut avoir intérêt à utiliser les signes $>$ et $<$ pour une incertitude supérieure à 20 per cent, notamment si la statistique peut en être nettement influencée.

Dans la nomenclature actuelle on distingue des lettres "descriptives" et "principales." Nous avons l'impression que cette distinction n'est pas très utile. Les conventions actuelles utilisent des significations trop spécialisées pour la plupart des lettres. Nous croyons avoir trouvé une "formule" permettant un emploi rationnel et beaucoup plus général des lettres en discant "La mesure a été influencée ou empèchée par . . . (suit la raison)." Parmi les raisons possibles, on a tout intérêt à mettre bien en évidence les effets d'origine ionosphérique; d'autre part la signification des lettres devrait être suffisamment générale, une lettre ne doit pas être applicable seulement pour un cas ou une caractêristique speciale. Par contre il n'y a aucun intérêt de préciser davantage si une information a été derdue pour une raison indépendante de l'état ed l'ionosphère. Nous appliquerons ponc la seule lettre "C" pour tous ces cas.

Dans le cadre du catalogue international actuel notre nouvelle rédaction (voir l'annexe IV) semble satisfaire à ces conditions.

VOL. 6 1955

Annexe I

L'Intensité des Echos

I.1. *Le décrement total*

Nous sommes d'avis que l'on doit faire entrer en ligne de compte l'amplitude des échos pour la définition des caractéristiques. D'où il résulte que le récepteur doit être en mesure de donner des renseignements précis sur l'amplitude des échos (voir l'annexe II).

Soir F_0 la "force cymomotrice" du sondeur en direction zénithale, E_r le champ à la réception. Le "décrement total" est exprimé en décibels par comparaison à une distance de référence D_0 (d'habitude = 1 km).

$$\frac{\delta}{\text{db}} = 20 \log_{10} \left(\frac{F_0}{D_0 \cdot E_r} \right) \tag{1}$$

contient les différentes influences réagissant sur l'amplitude du signal; nous distinguons

(1) δ_g le décrement de dilution du rayonnement;

(2) δ_a le décrement dû à l'absorption dans une couche, absorption soit déviative, soit non déviative. La derniére ($\delta_{a\ D}$) a la couche D pour cause. Une absorption déviative importante est causée par la couche E.

(3) δ_p le décrement dû à une pénétration partielle, δ_r le décrement dû à une réflexion partielle.

Nous ne discutons ici que les échos simples utilisés d'habitude pour la lecture des caractéristiques. Dans le cas des échos multiples il faut que l'on tienne compte aussi du pouvoir réflecteur du sol.

I.2. *Le décrement de dilution*

Le décrement géometrique a été calculé par Rawer (1948, 1950), qui obtient en incidence verticale, pour une couche parabolique:

$$\frac{\delta_g}{\text{db}} = 20 \log_{10} \left(\frac{r_0}{r_0 + h_m} \right) + 20 \log_{10} \left(\frac{2h'}{D_0} - \frac{2r_0}{r_0 + h_m} \cdot \frac{Y_m^2}{r_1 D_0} \cdot \frac{f}{f_c} \left[\log_e \left| \frac{f_c + f}{f_c - f} \right| - 2 \frac{f}{f_c} \right] \right) \tag{2}$$

r_0 étant le rayon terrestre, Y_m la demi-épaisseur de la couche, r_1 son rayon de courbure, h_m son altitude à la base, h' la hauteur effective de réflexion (c.à.d. la hauteur virtuelle):

$$h' = h_m + \frac{1}{2} \frac{r_0}{r_0 + h_m} \cdot Y_m \cdot \frac{f}{f_c} \log_e \frac{f_c + f}{f_c - f}$$

Si r_0 et $r_1 \gg h_m$ et Y_m on a sensiblement:

$$\frac{\delta_g}{\text{db}} = 20 \log_{10} \left(\frac{2h'}{D_0} \right). \tag{2a}$$

h' est une fonction monotone de la fréquenc donc δ_g augmente avec cette dernière. Notre formule correspondant à l'optique géométrique n'est plus valable pour la fréquence critique. Par l'optique physique (Rawer, 1939, 1942) on obtient une valeur finie de la hauteur effective. Ainsi l'augmentation totale de δ_g reste limitée; elle ne dépasse jamais 5 db pour la couche E, et 12 db pour la couche F_2 (Fig. 3).

Le cas où r_1 est nettement inférieur a r_0 existe assez souvent (Rawer, 1951) c.a.d. la surface inférieure des couches à un aspect ondulé. Suivant le signe de r_1 on a focalisation ou défocalisation. Ces effets variables dans le temps sont varfois gênants.

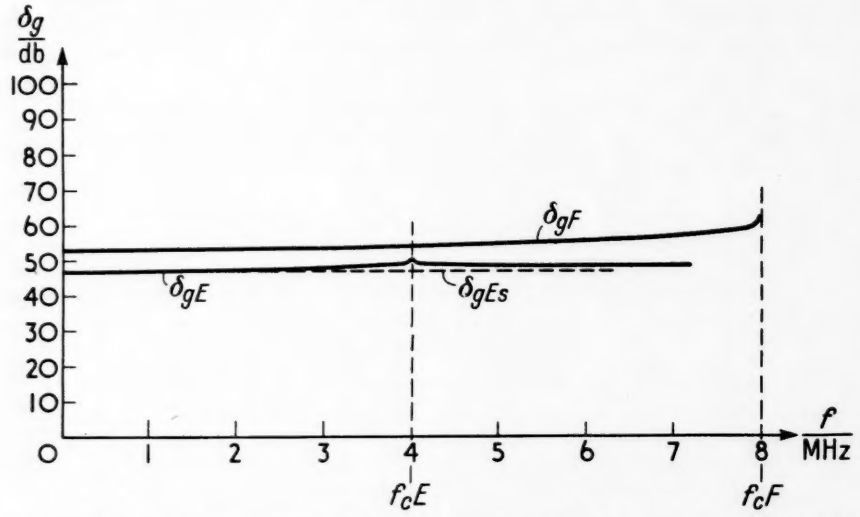

Fig. 3. Variation du décrement de dilution du rayonnement δ_g ($D_0 = 1$ km, h' a été calculé suivant des modèles paraboliques des couches E et F avec les demi-épaisseurs $Y_m = 15$ et 100 km, les hauteurs vraies h_M (du centre de la couche) de 125 et 330 km. Les valeurs maxima de h' à la fréquence critique ont été obtenues à l'aide de l'optique physique par la formule de Rawer (1939, 1942); les couches paraboliques ont été approximées par la formule d'Epstein (Rawer, 1939, 1942).

Variation of the decrement of dilution δ_g ($D_0 = 1$ km; h' is obtained from parabolic models with $Y_m = 15$ and 100 km, $h_M = 125$ and 330 km. The values of h' for the critical frequencies have been deduced from Rawer's formulae, using an "Epstein-layer" (Rawer, 1939, 1942)).

I.3. *Le décrement de l'absorption*

Pour l'absorption non-déviative dans la couche D, Booker (1935) a montré que l'approximation quasi-longitudinale est justifiée:

$$\frac{\delta_{aD}}{\text{db}} = 20\,\frac{\log_{10} e}{c}\cdot\frac{1}{(f \pm f_L)^2}\int \nu \cdot f_e^{\,2} \cdot dh \qquad (3)$$

L'intégration est effectuée entre la limite inférieure et supérieure de la couche D (f_L composante longitudinale du vecteur correspondant à la gyrofréquence, c vitesse de la lumière dans le vide, ν nombre de chocs, f_e "fréquence de plasma" dûe à la présence d'électrons libres). Le signe supérieur est valable pour le rayon ordinaire, l'autre signe pour l'extraordinaire. On a une *diminution* rapide de δ_{aD} si la fréquence augmente (Fig. 4).

Quant à l'absorption déviative, on admet l'approximation quasi-transversale de Booker (Bibl et Rawer, 1951):

$$\frac{\delta^0{}_a}{\text{db}} = 20\,\frac{\log_{10} e}{c}\cdot\frac{1}{f^2}\int \frac{\nu \cdot f_e^{\,2}}{\mu}\,\text{d}h \qquad (4)$$

(composante ordinaire) μ indice de refraction sans tenir compte de l'influence du

VOL. 6 1955

champ magnétique terrestre. L'intégration est à effectués le long du chemin parcouru *une fois* par le rayon à l'intérieur de la couche (c.a.d. dans le cas de réflexion: depuis la limite inférieure de la couche jusqu'au point de reflexion *et retour*; dans le cas de pénétration: *une fois* eutre les limites inférieure et

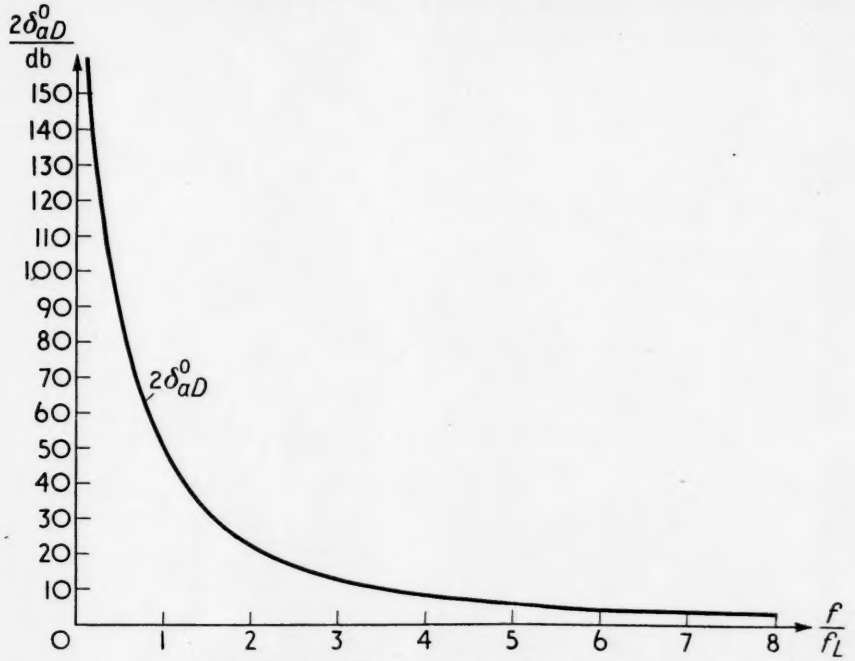

Fig. 4. Variation du décrement de l'absorption δ^0_{aD} dûe à la couche D pour le rayon ordinaire (Booker, 1935) ($\delta^0_{aD} = 100$ db pour $f = 0$).
Variation of the absorption decrement δ^0_{aD} for the ordinary ray (Booker, 1935).

supérieure de la couche). Le cas d'une couche parabolique avec variation exponentielle du nombre de chocs a été traité par Argence, Mayot, et Rawer (1950) (voir Fig. 5).

La branche de gauche de la courbe en trait plein correspond au cas de réflexion sur la couche (pour $f < f_c$) et la branche de droite au cas de transmission (pour $f > f_c$).* Dans le premier cas δ_a *augmente* avec la fréquence, dans le deuxième cas il *diminue*, l'absorption est "sélective." Les formules ci-dessus ne sont applicables que pour des couches épaisses et des fréquences de sondage bien supérieures à la gyrofréquence.

Le cas des couches minces a été traité par Rawer (1939, 1942) à l'aide de l'optique physique. L'absorption est moins sélective que pour une couche épaisse. Le décrement d'absorption est obtenu ici de manière indirecte à l'aide du calcul de la réflexion partielle (voir I.4); on fait la différence entre le resultat obtenu avec le nombre de chocs ν et avec $\nu = 0$.

* Remarque: Dans le cas de transmission, on devra compter deux fois l'absorption à cause du trajet aller et retour après réflexion sur une couche supérieure.

I.4. *Les décrements de la pénétration partielle et de la réflexion partielle*
Les décrements δ_p et δ_r, ont été obtenus par l'emploi de l'optique physique par Rawer (1939, 1942). Ils sont plus importants pour les couches minces. Même pour les couches ionosphériques les plus minces, dans le cas des fréquences supérieures à la gyrofréquence, il n'y a qu'une gamme assez restreinte où le

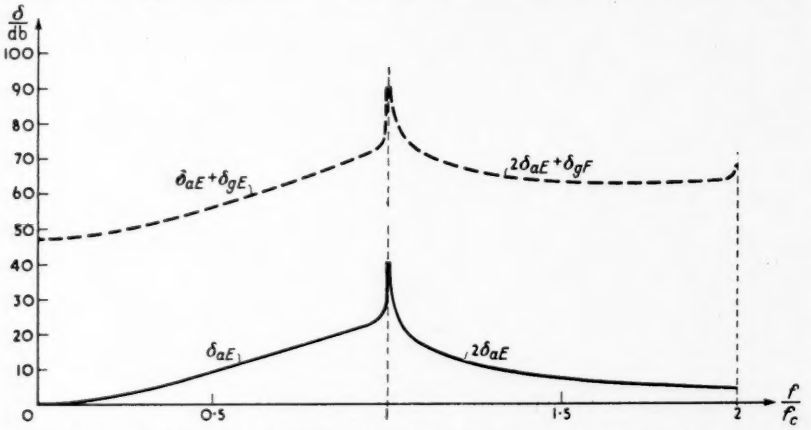

Fig. 5. Variation du décrement de l'absorption δ_{aE}, dûe à la couche E, pour le rayon ordinaire (Argence *et al.*, 1950). ($\nu_M \cdot Y_m/c = 0{\cdot}575$, ν_M est le nombre de chocs au centre de la couche.)
Variation of the absorption decrement δ_{aE} for the ordinary ray (Argence *et al.*, 1950).

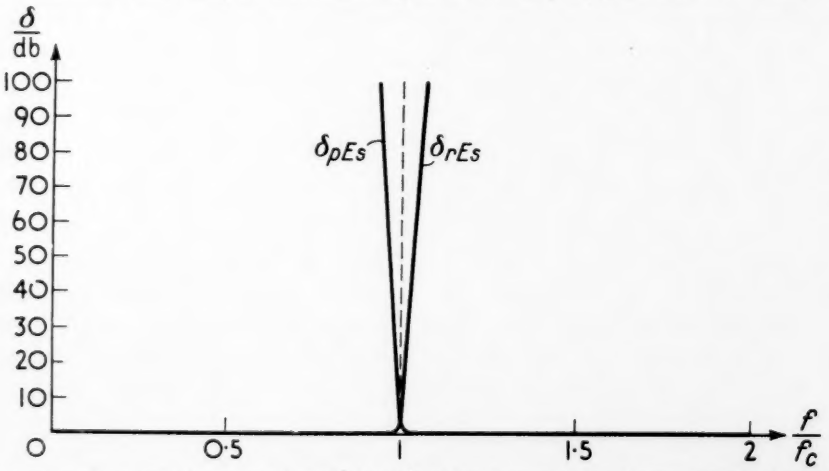

Fig. 6. Variation des décrements δ_r et δ_p dûe à la réflexion partielle. (Obtenu à partir des calculs de Rawer (1939, 1942) pour une couche de forme "Epstein" avec $S_0 = 50$; ceci correspond pour $f_c = 4$ MHz à une demi-épaisseur de $Y_m = 0{\cdot}75$ km dans le cas d'une couche parabolique.)
Variation of the decrements of partial reflexion δ_r and δ_p (Rawer, 1939, 1942). (Epstein-layer approximating a parabolic one with $Y_m = 0{\cdot}75$ km, $f_c = 4$ MHz.)

réflexion partielle est intéressante (Fig. 6). Cette gamme est centrée sur f_c de la couche. Pour une couche d'épaisseur normale le phénomène ne se produit que sur cette fréquence.

Examinons quelques exemples qui sont très fréquents:

VOL. 6 1955

Deux couches épaisses, à savoir E et F

Le "décrement total" a pour expression pour l'écho en provenance de la couche E:

$$\delta_E = \delta_{gE} + 2\delta_{aD} + \delta_{aE} + \delta_{rE} \tag{5}$$

et pour l'écho de F:

$$\delta_F = \delta_{gF} + 2\delta_{aD} + 2\delta_{aE} + 2\delta_{pE} + \delta_{aF} + \delta_{rF} \tag{6}$$

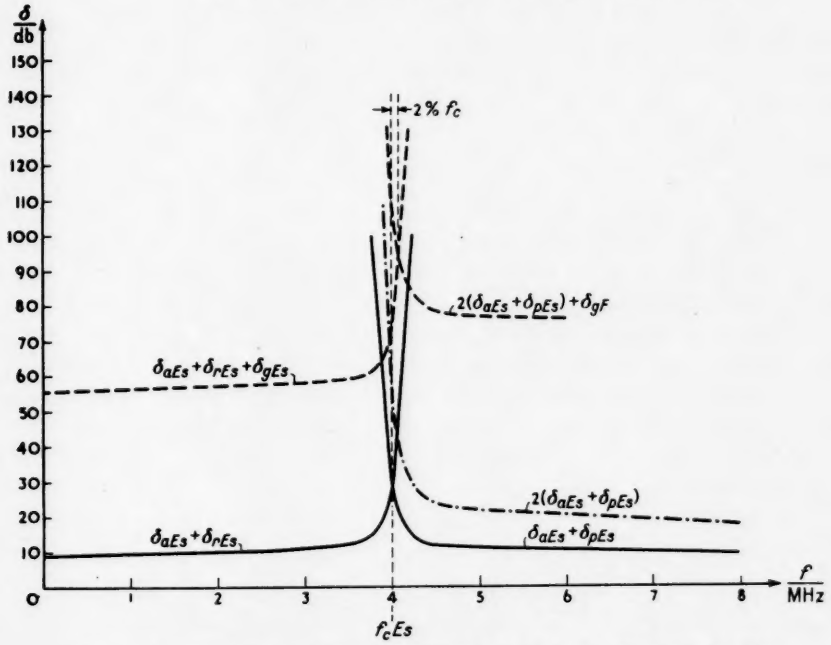

Fig. 7. Composition des différents décrements pour le cas d'une couche mince (Fig. 6 et Fig. 3—voir le texte).
Composition of the different decrements for a thin layer.

Les décrements δ_p et δ_r sont faibles pour des couches épaisses, l'absorption en F est minimum; on a sensiblement (Bibl et Rawer, 1950).

$$\delta_E \approx \delta_{gE} + 2\delta_{aD} + \delta_{aE} \tag{5a}$$

$$\delta_F \approx \delta_{gF} + 2\delta_{aD} + 2\delta_{aE}, \tag{6a}$$

sauf au voisinage immédiat de f_cE (voir la Fig. 1a). Sur cette fréquence, l'affaiblissement est élevé, mais fini (Rawer, 1939, 1942), contrairement au résultat donné par l'expression approchée généralement admise pour l'absorption (voir la Fig. 3).

Une couche mince au dessous d'une couche épaisse, à savoir E_s et F

On trouve

$$\delta_{E_s} = \delta_{gE_s} + 2\delta_{aD} + \delta_{aE_s} + \delta_{rE_s} \tag{7}$$

et

$$\delta_F = \delta_{gF} + 2\delta_{aD} + 2\delta_{aE_s} + 2\delta_{pE_s} + \delta_{aF} + \delta_{rF} \tag{8}$$

(voir la Fig. 7).

L'absorption en F est faible a cause du petit nombre de chocs; l'absorption en E_s est aussi négligeable a cause de la faible epaisseur de cette couche. δ_r est petite pour la F épaisse.

On a donc sensiblement:

$$\delta_{E_s} \approx \delta_{gE_s} + 2\delta_{aD} + \delta_{rE_s} \tag{7a}$$

$$\delta_F \approx \delta_{gF} + 2\delta_{aD} + 2\delta_{pE_s},$$

voir la Fig. 2a.

Notre définition de la fréquence critique nous conduit a la condition $\delta_r = \delta_p$. Si nous considérons p.e. le cas de la couche E_s, nous pouvons négliger δ_{aF} ainsi que δ_{rF} nous ne considérons pas δ_{aD}; ce terme s'élimine lorsque l'on fait la différence des décréments δ_{E_s} et δ_F. De l'optique physique (Rawer, 1939, 1942) on peut déduire d'abord les valeurs de δ_{rE_s} et δ_{pE_s} (Fig. 6) ensuite de $(\delta_{rE_s} + \delta_{aE_s})$ et $(\delta_{pE_s} + \delta_{aE_s})$ (voir la Fig. 7). L'intersection des courbes correspondantes donne également la fréquence critique vraie. On ne peut pas étendre ces remarques pour l'écho en provenance de F, étant donné qu'il traverse la couche E_s à l'aller et au retour. Nous avons donc dans ce cas 2 . $(\delta_{pE_s} + \delta_{aE_s})$ (voir Fig. 7). Enfin nous devons ajouter la différence des décréments géométriques (Fig. 3) pour obtenir le rapport des échos observés. Les dernières corrections décalent l'intersection des couches vers les fréquences plus élevées. Le décalage est d'autant plus faible que la couche est épaisse et l'absorption faible. L'exemple de la Fig. 7 correspond à une couche mince, où l'effet est plus important. Pour les couches épaisses le décalage est négligeable (voir la Fig. 5).

VOL. 6 1955

Annexe II

L'Influence des Caractéristiques Techniques des Sondeurs

Les renseignements que l'on peut obtenir dépendent beaucoup des caractéristiques des appareils. De la Fig. 2a on déduit comme condition nécessaire pour un dépouillement optimum que le "pouvoir transmissif" p_T ne varie pas trop avec la fréquence. Etant donné que p_T dépend de la puissance émise, ainsi que de la sensibilité du récepteur, cette condition intéresse l'ensemble du sondeur, les antennes comprises.

La précision des définitions que nous avons proposées repose sur l'analyse du décrement total δ en fonction de la fréquence. Or pour que l'on puisse juger la variation du décrement (fonction seulement des données ionosphériques), il faut que la variation des données techniques soit très faible dans la gamme considérée (p.e. au voisinage d'une fréquence critique).

L'étude de la variation de l'intensité est seulement possible si le récepteur permet de distinguer différentes amplitudes. Nous demandons donc des précisions supplémentaires sur l'intensité des échos. L'efficacité des ionogrammes dépend beaucoup de cette qualité. Un enregistrement ne donnant que des noirs et des blancs est peu utile, même s'il-paraît correct. Il est nécessaire d'obtenir un enregistrement dans lequel le noircissement puisse permettre d'évaluer l'intensité de l'écho. Nous demandons donc des enregistrements ayant entre le noir et le blanc des teintes grises intermédiaires donnant ainsi beaucoup plus d'information.

Or la gamme de la variation de l'intensité est considerable. On doit prévoir une variation de 60 db et l'on a intérêt à avoir une échelle d'intensité linéaire, graduée

en decrement et non en amplitude. Nous sommes ainsi amenes à prevoir un recepteur a courbe de sensibilite logarithmique dont la gamme de reproduction soit au moins de 60 db.

Un tel amplificateur M.F. (a double conversion) a ete realise par BIBL (1951). Il fait appel a un controle automatique du volume sur un seul etage avec une constante de temps negligeable. D'autre part, il a introduit dans la plupart des etages comme contre-reaction une resistance dans la cathode qui n'est pas shuntee par une capacite. De cette facon il arrive à une reproduction des signaux qui n'introduit aucune hysterisis. La tension de sortie du recepteur est donc uniquement fonction de l'amplitude H.F. instantanee à l'entrée. Cette qualite est très precieuse.

Pour eviter toute distorsion et pour faciliter l'etalonnage nous avons presque supprime l'amplification basse frequence. Elle ne pourrait etre admise que si une gamme basse frequence de 30 kHz comprenant la frequence zero etait transmise (amplificateur de courant continu). Nous utilisons un seul etage basse frequence qui permet de superposer les marques de hauteur aux signaux recu. Le couplage n'est ni capacitif ni inductif, mais direct. La sortie du recepteur est connectee directement au Wehnelt, sans qu'il y ait une capacite de couplage, de facon a éviter une distorsion des signaux ("differenciation") et surtout pour garder la non-ambiguite dans la reproduction des echos. Cette qualite est tres utile si l'on veut estimer la valeur de l'absorption ionospherique, p.e. pour la mesure de $f_{\min}$. S'il y a un couplage par une capacité on élimine apparemment une partie des émetteurs parasites mais on ne pourra plus distinguer un effet de brouillage d'un veritable effet d'absorption. Il arrive qu' un effet de brouillage soit attribue à une forte absorption. Ainsi les bandes noires qui apparaissent dans nos enregistrements sur les frequences des émissions radio, nous donnent plus d'information qu' on ne pourrait en obtenir si elles etaient éliminées. Ces principes de construction qui ne sont pas encore admis dans la plupart des réalisations nous semblent de grande importance. Leur application ne facilite pas seulement la lecture des caracteristiques, mais aussi l'interpretation des traces d'echos. Ceci est surtout important pour le cas des echos des couches sporadiques comme E_s; ces traces, qui apparaissent souvent interrompues dans un recepteur lineaire, se revelent continues dans le recepteur décrit.

Annexe III

CARACTÉRISTIQUES IONOSPHERIQUES

f^0F_2, f^0F_1, f^0E — Frequence critique du rayon ordinaire respectivement pour les couches F_2, F_1, E.

$f^0F_{1,5}$ — Frequence critique pour le rayon ordinaire de la stratification non-transitoire trouvee eventuellement entre les couches F_1 et F_2.

f^0E_s, f^xE_s — "Top frequency" du rayon ordinaire et extraordinaire pour une *trace continue* de la couche E_s.

fE_s — "Top frequency" de la couche E_s.

f_aE_s — Frequence d'occultation du rayon ordinaire de la couche E_s.

f^0T — Frequence critique du rayon ordinaire pour une stratification transitoire situee dans la region F.

f^0I Fréquence critique du rayon ordinaire pour une couche transitoire non transparente située entre les régions E et F.

$f_{\min}F$ Fréquence minimum du rayon ordinaire de la *région F* (c'est par définition la plus haute des valeurs f_aE_s, $f^0{}_aE \approx f^0E$ et $f^0{}_aI \approx f^0I$).

$f_{\min}$ Fréquence minimum des échos.

$h'F_2$, $h'F_1$, $h'E$ Hauteur virtuelle minimum de la trace correspondante au rayon ordinaire respectivement pour les couches F_2, F_1, E.

$h'F$ Hauteur virtuelle minimum de la trace correspondante au rayon ordinaire de la *région F* (c'est par définition la plus petite des valeurs $h'F_1$ et $h'F_2$).

$h'F_{1,5}$ Hauteur virtuelle minimum de la trace correspondante au rayon ordinaire de la stratification $F_{1,5}$.

$h'E_s$ Hauteur virtuelle minimum de la trace donnant f^0E_s.

---

h_pXX—Hauteur virtuelle du rayon ordinaire de la couche XX pour une fréquence égale à 0·834 . f^0XX.

XX–3000 MUF—Fréquence dite maximum utilisable pour une transmission à 3000 km par la couche XX; cette fréquence est obtenue par application de la courbe normalisée de transmission pour la distance de 3000 km à la trace du rayon ordinaire pour la couche XX.

$(M3000)XX$— Facteur de transmission de la couche XX, par définition, c'est le rapport $\dfrac{XX\text{–}3000\ MUF}{f^0XX}$.

XX–3000 MUF_p—Fréquence dite maximum utilisable pour une transmission à 3000 km par la couche XX; cette fréquence est obtenue par application du modèle parabolique à la trace du rayon ordinaire pour la couche XX.

$(M3000)_pXX$— Facteur de transmission de la couche XX par définition

$$\frac{XX\text{–}3000\ MUF_p}{f^0XX},$$

obtenue par application du modèle parabolique.

Annexe IV

Symboles Descriptifs

A Mesure influencée ou empêchée par suite de la présence d'une couche inférieure mince ou très mince.

B Mesure influencée ou empêchée par absorption au voisinage de la fréquence minimum des échos.

C Mesure influencée ou empêchée par un défaut quelconque d'origine non-ionosphérique.

D Mesure influencée ou empêchée par la limite supérieure normale de la gamme de fréquence de l'ionosonde.

E Mesure influencée ou empêchée par la limite inférieure normale de la gamme de fréquence le l'ionosonde.

F Mesure influencée ou empêchée par la présence des échos diffus.

G Mesure influencée ou empêchée par l'existence d'une couche épaisse inférieure.

VOL. 6 1955

H Mesure influencée ou empêchée par la présence d'une stratification.
J Caractéristique du rayon ordinaire déduite de la caractéristique mesurée sur le rayon extraordinaire et vice versa.
L Mesure influencée ou empêchée par le manque de variation nette dans les traces d'échos.
O Mesure relative au rayon ordinaire.
R Mesure influencée ou empêchée par l'absorption au voisinage d'une fréquence critique.
S Mesure influencée ou empêchée par suite de brouillage ou de parasites atmosphériques.
V Mesure effectuée sur une trace d'écho en forme de fourche au voisinage de la fréquence critique.
X Mesure relative au rayon extraordinaire.
Y Mesure effectuée sur une trace présentant plusieures interruptions.
Z Troisième composante magneto-ionique observée.

Utilisation des symboles descriptifs

La plupart des symboles est utilisé soit pour *remplacer* soit pour qualifier une valeur numérique; toutefois les symboles suivants ne sont utilisés que pour qualifier une valeur numérique: *J*, *O*, *V*, *X*, *Y*, *Z*.

Acknowledgments—Nous tenons à remercier MM. E. Argence et P. Halley qui nous ont bien aidé à la rédaction de ce texte.

References

Appleton, E. V., Naismith, R., and Ingram, L. J.	1939	Proc. Phys. Soc. A **51,** 81
Argence, E., Mayot, M., and Rawer, K.	1950	Ann. de Géophys. **6,** 242–285
Bibl, K.	1950	SPIM–R9
	1951	Ann. de Géophys. **7,** 265–267 (voir aussi l'article précedent de E. Harnischmacher)
	1952	C. R. Acad. Sci. (Paris) **235,** 734–736
	1953	Z. Geophysik. 136–141
Bibl, K., and Rawer, K.	1951	J. Atmosph. Terr. Phys. **2,** 51–65
Booker, H. G.	1935	Proc. Roy. Soc. A **150,** 267
Chapman, S.	1950	J. Geophys. Res. **55,** 398
Delobeau, F.	1952	C.R. Acad. Sci. (Paris) **235,** 1673–1675
Delobeau, F., Harnischmacher, E., and Oboril, F.	1950	Revue Scientif. **88,** 21–26
Gallet, R.	1950	SPIM–R13, 4–7
Munro, G. H.	1950	Proc. Roy. Soc. A **202,** 208
McNicol, and Gipps	1951	J. Geophys. Res. **56,** 17–31
McNish, A. G.	1950	Proc. Conf. Ionospheric Physics II
Rawer, K.	1939	Ann. d. Phys. **35,** 385–416
	1942	Ann. d. Phys. **42,** 294–296
	1948	Revue Scientif. **86,** 481–485, 585–600
	1949	Nature **163,** 528
	1950	Nature **166,** 316
	1951	J. Atmosph. Terr. Phys. **2,** 38–50
Whale, H. A.	1950	J. Atmosph. Terr. Phys. **1,** 233–243

Journal of Atmospheric and Terrestrial Physics, 1955, Vol. 6, pp. 88 to 90. Pergamon Press Ltd., London

Solar electrodynamics*

J. W. DUNGEY
Ionosphere Research Laboratory, The Pennsylvania State University†

(*Received* 2 *May* 1954)

ABSTRACT

It is suggested that confusion in Solar electrodynamics arises from the use of causal relationships borrowed from laboratory electrodynamics. A concept of "causality" is introduced which depends on the fundamental equations used, so that the causal relationships must be changed when approximations are made. This concept is used to discuss the reduction in conductivity by a magnetic field and the effect of a polarization electric field.

The fundamental basis of Solar electrodynamics has been the subject of some confusion and controversy, particularly in connection with the "reduction of conductivity" of an ionized gas by a magnetic field (SCHLUTER, 1951). In his recent survey, COWLING (p. 538, 1953) has pointed out that there is agreement about the fundamental equations, but, since most of the problems presented by the Sun are too complicated for a mathematical treatment, there is still a possibility of confusion in the qualitative conclusions drawn from the equations. It is here suggested that confusion still exists and arises from the use of causal relationships borrowed from laboratory electrodynamics.

VOL. 6 1955

In a gas of low density a strong magnetic field "reduces the conductivity" by a large factor; this occurs in the Solar atmosphere above a sunspot and in the atmospheres of Babcock's magnetic variable stars. It is tempting to conclude that the current density can have only a very small component perpendicular to the field. This conclusion follows directly, however, only when the electric field is given and, in another connection, COWLING (p. 589, 1953) points out that the Ohm's law equation must actually be used to calculate the electric field. This question, "Which equation determines which variable?" suggests the concept of "causality" to be explained here; with this concept the "causal" relationships will be found to depend on the approximations made, and it is therefore not surprising that they can differ from those of laboratory electrodynamics.

The fundamental equations include (COWLING, p. 538, 1953)

$$\partial \boldsymbol{H}/\partial t = -c \operatorname{curl} \boldsymbol{E} \tag{1}$$

$$\partial \boldsymbol{E}/\partial t = c \operatorname{curl} \boldsymbol{H} - 4\pi \boldsymbol{j} \tag{2}$$

$$\frac{m}{ne^2}\frac{\partial \boldsymbol{j}}{\partial t} = \boldsymbol{E} + \boldsymbol{u} \wedge \boldsymbol{H}/c - \boldsymbol{j}/\sigma - \boldsymbol{j} \wedge \boldsymbol{H}/nec + \text{other terms} \tag{3}$$

where $\boldsymbol{u}$ is the bulk velocity of the gas, n the electron density, m the electron mass, and σ the conductivity in the absence of a magnetic field. The term involving $\boldsymbol{j} \wedge \boldsymbol{H}$ in (3) represents the "reduction in conductivity," and may also be called "the Hall electric field." The time derivatives in (2) and (3) are neglected in Solar

* The research reported in this note has been supported by the National Science Foundation under Grant G450 and, in part, by the Geophysics Research Division of the Air Force Cambridge Research Center, under Contract AF19(122)-44.

† Now at the Cavendish Laboratory, Cambridge, England.

electrodynamics. Suppose now that initial values of all the variables are given, and it is desired to compute their values a short time later; in Solar electrodynamics the initial values must of course satisfy (2) and (3) with the time derivatives omitted. In programming the computation, one would find that the value of each variable is obtained from a particular equation and it would be necessary to work out which. Those equations which contain time-derivatives must determine the time-derivatives, and the remaining equations then determine the remaining variables in a unique way which is easily worked out. Now we can obtain a sensible scheme of "causal relationships" by saying that each variable is "caused" by the effects represented in the equation determining it; it should be emphasized that this scheme can be used for qualitative discussions, which may be regarded as "qualitative integrations" of the fundamental equations. As COWLING (p. 589, 1953) has remarked, in Solar electrodynamics (2) determines $\boldsymbol{j}$ and (3) determines $\boldsymbol{E}$, although, if the time-derivatives had been included, their roles would have been reversed.

We may now return to the question of the reduction of the conductivity by a magnetic field. Since (3) is used to determine $\boldsymbol{E}$, the immediate effect is the additional electric field, but this affects $\boldsymbol{j}$ via (1) and (2). Using these, an expression for $\partial \boldsymbol{j}/\partial t$ is obtained involving curl curl [terms on the right-hand side of (3)]. If $\boldsymbol{j}/\sigma$ were the only term involved, it is well known that a diffusion equation would result representing the decay of the current. The Hall field has a different character, however, and is not so easy to describe in a general way; usually it tends to make the direction of $\boldsymbol{j}$ rotate, so that it may be regarded as a "sideways effect" rather than a "back effect." Furthermore, it is possible with a reasonable magnetic field for the Hall field to be irrotational without vanishing. The conclusion that $\boldsymbol{j} \wedge \boldsymbol{H}$ is small does not therefore necessarily follow from a large "reduction in conductivity." On the other hand, $\boldsymbol{j} \wedge \boldsymbol{H}/c$ is also the expression for the magnetic force density and, when the magnetic pressure exceeds both the pressure and kinetic energy density of the gas, mechanical considerations may require $\boldsymbol{j} \wedge \boldsymbol{H}$ to be small. To avoid confusion, however, it must be emphasized that these considerations are distinct from the "reduction in conductivity."

A similar source of confusion is "polarization," which is synonymous with space charge. It is generally agreed that the charge density ρ is small (so that the electrostatic force density $\rho \boldsymbol{E}$ is negligible), and ρ appears only in the equation

$$\operatorname{div} \boldsymbol{E} = 4\pi\rho \tag{4}$$

Clearly (4) must be used to determine ρ, so that, in contrast to laboratory electrodynamics, ρ does not "cause" $\boldsymbol{E}$. Consequently there is no need to discuss space charge, and a "polarization electric field" may be regarded as any irrotational field. COWLING (p. 544, 1953) discusses the possibility of the induced field $\boldsymbol{u} \wedge \boldsymbol{H}/c$ being exactly balanced by a polarization field, but this reduces simply to the condition that $\boldsymbol{u} \wedge \boldsymbol{H}$ be irrotational, and it is well known that this can be expressed by saying that the magnetic field is unchanged when the lines of force move with the velocity $\boldsymbol{u}$. COWLING concludes that, because of polarization, a mass of conducting gas may be able to pass across the lines of force, but this cannot be correct, because $\boldsymbol{u} \wedge \cdot \boldsymbol{H}$ is obviously not irrotational. In fact, for the

purposes of Solar electrodynamics, it would be sufficient to use only the curl of equation (3), and it is then seen that a polarization field is always irrelevant.

It is clear that the causal relationships will need modification for particular problems, when further approximations are made. An important example is provided by quasi-equilibrium problems in which all time-derivatives are neglected. Such a problem is of course not specified by initial values, but by boundary conditions. Then (1) requires that $\boldsymbol{E}$ be irrotational but no longer determines $\boldsymbol{H}$; the curl of (3) and the other remaining equations do not contain $\boldsymbol{E}$ and so determine the other variables; $\boldsymbol{E}$ may then be obtained from (3), but is of no direct interest. This scheme may be applied to the problems of steady rotation and of tidal oscillations in the ionosphere.

REFERENCES

COWLING, T. G.	1953	*The Sun* (University of Chicago Press)
SCHLUTER, A.	1950	*Z. Naturforsch.* **5a**, 72
	1951	*Z. Naturforsch.* **6a**, 73

VOL. 6 1955

Journal of Atmospheric and Terrestrial Physics, 1955, Vol. 6, pp. 91 to 112. Pergamon Press Ltd., London

Ionospheric behaviour at Khartoum during the eclipse of 25th February 1952

C. M. MINNIS
D.S.I.R. Radio Research Station, Slough, Bucks

(*Received* 24 *June* 1954)

ABSTRACT

Automatic $h'f$ records were made at intervals of four-and-a-quarter minutes during the eclipse and at quarter-hour intervals on ten control days. The behaviour of both E- and F_1-layers can be explained in terms of Chapman layers having constant effective recombination coefficients ($\alpha'_E = 1{\cdot}5 \times 10^{-8}$ cm^3 s^{-1}, $\alpha'_{F_1} = 8 \times 10^{-9}$ cm^3 s^{-1}), and assuming a non-uniform distribution of the sources of ionizing radiation on the sun's disc. It has been possible to derive the positions and relative intensities of these sources from the E-layer data, and they appear to be related to the location of sources of intense green coronal radiation.

The F_2-layer response to the eclipse is consistent with the assumption of two component layers: a lower one, corresponding to the normal post-sunrise F_2-layer, which is sensitive to changes in solar radiation and has a high α', and an upper one which is a later development of the lower layer but which is insensitive to solar radiation and has a small α'. Changes in the absorption in D-layer confirm the asymmetrical distribution of sources of ionizing radiation. Although fEs showed a very deep minimum about an hour after totality, there is nothing to suggest that this was an eclipse effect, nor is there any evidence for a corpuscular eclipse in F_2-layer about two hours before the optical eclipse.

INTRODUCTION

The measurements described in this account were made during February and March 1952, in accommodation kindly placed at the disposal of the Department of Scientific and Industrial Research by the University College of Khartoum (latitude 15°35′ N, longitude 32°35′ E). At a height of 100 km (E-region) the eclipse was total for about three minutes, while at 250 km (F-region) the maximum obscuration of the sun's disc was about 97 per cent. The times of the various phases of the eclipse are given in Table 1.

Table 1. *Duration of eclipse at Khartoum*

Height (*km*)	*Beginning* (*LMT*)	*Middle* (*LMT*)	*End* (*LMT*)
100	0944	1110–1113 (100%)	1239
250	0944	1112 (97%)	1241

LMT (30°E) = UT + 2*h*. Noon was at 1203 LMT.

A conventional automatic ionospheric $h'f$ recorder (CLARKE and SHEARMAN, 1953) was used for all the measurements. This equipment covered the range 0·65–15·4 Mc/s in four-and-a-quarter minutes; the frequency range from 15·4 to 25 Mc/s was not required. The virtual height-scale was set to have a maximum range of 1,000 km. Terminated delta aerials were used both for transmission and reception; they had a base-length of 75 m and the apex was 24 m high.

CONTROL DATA

Hourly recordings of $h'f$ traces were commenced on 7 February and continued as part of the eclipse programme until 31 March; since then, the operation of the recorder has been continued by Professor N. F. ASTBURY of the University College. During the period 20 February to 1 March, records were made at intervals of fifteen minutes each day from 0600 to 1800 LMT. On the day of the eclipse the recorder was allowed to run continuously from 0600 to 1800 LMT, and this permitted a complete $h'f$ trace to be recorded every four-and-a-quarter minutes. Except for a few days after first being put into operation, the recorder gave no serious trouble, and only a few records were lost in spite of difficult climatic conditions.

E-LAYER: THEORETICAL BASIS

The numerical analysis of the changes which took place in f_0E during the eclipse is based on the assumption that the balance between the generation and loss of electrons can be represented by a relation of the form—

$$\frac{dN_e}{dt} = Aq_0 \cos\chi - \alpha' N_e^2 \qquad (1)$$

where A = fraction of sun's disc unobscured,

N_e = electron density,

q_0 = rate of generation of electrons,

χ = solar zenith angle,

α' = a recombination coefficient.

Some justification for the use of such a relation is necessary because, although (1) implies that electron density varies as $\cos^{\frac{1}{2}}\chi$ and critical frequency as $\cos^{\frac{1}{4}}\chi$, during the day at Khartoum it was found that the median values of f_0E during the control period indicated that the critical frequency varied as $\cos^{\frac{1}{4}}\chi$ approximately. Such a variation is of course known to occur at other locations.

A similar relation was found to be valid for the control period at Bangui, and this has been attributed by ESTRABAUD (1953) to the loss of electrons by attachment to neutral atoms to form negative ions. The relation proposed by ESTRABAUD to replace (1) is—

$$\frac{dN_e}{dt} = Aq_0 \cos\chi - \alpha_e N_e^2 - \beta N_e \qquad (2)$$

where α_e = electron recombination coefficient,

β = electron attachment coefficient.

If the existence of negative ions is assumed, it is necessary to take into account several other collision processes, discussed by BATES and MASSEY (1946), which

VOL. 6 1955

may be involved in the generation and loss of negative ions. When this is done, it can be shown that the rate of change of electron density is given by—

$$\frac{dN_e}{dt} = \frac{Aq_0 \cos\chi}{1+\lambda} - (\alpha_e + \lambda\alpha_i)N_e^2 - \frac{N_e}{1+\lambda}\frac{d\lambda}{dt} \qquad (3)$$

where α_i = negative ion recombination coefficient,

$\lambda = N_-/N_e$,

N_- = negative ion density.

Hence β in (2) must correspond to $\frac{1}{1+\lambda}\frac{d\lambda}{dt}$ in (3). It is unlikely that λ is large during the day (BATES and MASSEY, 1951) or that it can change rapidly except possibly near sunrise and sunset; consequently it is probable that β in (2) and $\frac{1}{1+\lambda}\frac{d\lambda}{dt}$ in (3) are small enough to warrant the neglect of the third terms in these equations.

The effective recombination coefficient in E-layer is known to be approximately 10^{-8} cm^3 s^{-1}, but it has long been difficult to account for such a high value. This is because it is assumed in (3) that $\lambda < 1$ and α_e is the radiative recombination coefficient of O_2^+, which is usually assumed to be the active ion in E-layer. The difficulty appears to have been resolved by BIONDI and BROWN (1949), who have measured the dissociative recombination coefficient of He_2^+ and found it to be about 10^{-8} cm^3 s^{-1}; similar measurements in oxygen have yielded an even greater value, but there is still some doubt as to the identity of the ion involved. However, the possibility that the dissociative recombination coefficient of O_2^+ may be quite large provides a possible explanation of the high values of α' observed in E-layer without the undesirable necessity of assuming a large negative ion concentration.

The full implications of a high rate of dissociative recombination in E-layer have been considered by GERJUOY and BIONDI (1953), and the relation which emerges from their discussion is—

$$\frac{dN_e}{dt} = \frac{Aq_0 \cos\chi}{1+\lambda} - \left(\alpha_e + \frac{\lambda'}{1+\lambda}\alpha_d + \lambda\alpha_i\right)N_e^2 - \frac{N_e}{1+\lambda}\frac{d\lambda}{dt} \qquad (4)$$

where α_d = dissociative recombination coefficient,

λ = ratio of densities of O_2 ions and free electrons.

This relation is identical with (3) except for the term in α_d. If the usual assumptions are made that during the day $\lambda \ll 1$ and $d\lambda/dt \ll 1$, and if $\alpha_e \ll \alpha_d \gg \alpha_i$, (4) reduces to the simple form first considered (1)—

$$\frac{dN_e}{dt} = \frac{Aq_0 \cos\chi}{1+\lambda} - \lambda'\alpha_d N_e^2 \qquad (5)$$

It is probable that $\lambda' \simeq 1$ and consequently, if the dissociative recombination hypothesis is correct, the value of α' measured in E-layer should eventually be

found to agree fairly closely with the value measured in the laboratory at E-layer temperature for whatever ion is effective in E-layer.

Since the consideration of processes other than radiative recombination does not alter the form of the basic electron balance equation, some other explanation must be sought to account for the observed departure of the relation between N and cos χ from that implied by (5). It is usually assumed that q_0 and α' are independent of χ; if, on the other hand, there is a diurnal change in the temperature of E-region they will no longer be constant. A change in temperature (T) would affect α' directly and, by causing a change in scale-height, would also affect q_0. If it is assumed that $\alpha' = \alpha_0 T^r$ and $q_0 = q_{00} H_0/H$, it can be shown that if the observed diurnal change in electron density is represented by $N \propto \cos^n \chi$, the diurnal change in scale-height which is necessary to account for the index n is given by—

$$H = H_0 \cos^{\frac{1-2n}{1+r}} \chi$$

An alternative explanation for the observed relation between N and cos χ has been given by NICOLET and BOSSY (1949), who assume that the scale-height is a function of height. It can then be shown that, with certain simplifying assumptions, if $dH/dz = \beta$, it follows that $q \propto \cos^{1+\beta} \chi$, and $N \propto \cos^{\frac{1+\beta}{2}} \chi$; hence the observed relation between N and cos χ would imply that β is positive, although to obtain a numerical value it would be necessary to have further information on the nature of the recombination process.

The virtual height-scale on the usual $h'f$ records is not sufficiently great to allow accurate measurements to be made of the thickness of E-layer which might decide which of these hypotheses is correct. For our present purpose the main consideration is that either is capable of accounting for the observed variation in N without the need for adding third terms to (1) or (5).

As has already been explained, the diurnal variation of f_0E at Khartoum is given approximately by $f \propto \cos^{\frac{1}{3}} \chi$. In fact, the exponent is not exactly 1/3, but is a function of χ; by using the quarter-hourly median values for the control period, it has been found that f can be represented by—

$$\log f = 0{\cdot}556 + 0{\cdot}330 \log \cos \chi + 0{\cdot}06 (\log \cos \chi)^2 \qquad (6)$$

There are, however, small day to day departures from this relation, and on the day of the eclipse between 0630 and 1300 LMT the observed values of f, omitting those measured during the eclipse itself, can be represented by—

$$\log f = 0{\cdot}556 + 0{\cdot}249 \log \cos \chi - 0{\cdot}114 (\log \cos \chi)^2 - 0{\cdot}065 (\log \cos \chi)^3 \qquad (7)$$

The addition of the cubic term in (7) is necessary to represent satisfactorily a rise in f_0E to a level about 3 per cent above the median value, which lasted from about 0700 LMT until the beginning of the eclipse at 0944 LMT. From (7), the relation between f and cos χ which would presumably have been valid in the absence of the eclipse can be deduced, and it is found that during the eclipse period ($\log \cos \chi \lessdot -0{\cdot}1$) the relation is very close to $f \propto \cos^{\frac{1}{3}} \chi$. It is not known whether the difference between (6) and (7) reflects a real change in the intensity

VOL. 6 1955

of the ionizing radiation or some change in the structure of the layer. However, for the purpose of isolating effects due to the eclipse from those due to diurnal and other effects, it seems logical to reject the relation given by the median values and to assume that had there been no eclipse the relation would have been $f \propto \cos^{\frac{1}{4}} \chi$ and consequently $q \propto \sec \chi$.

From the discussion given above it is concluded that—

(a) there is no need to add an electron attachment term to (5) to explain the observed median relation: $f \propto \cos^{\frac{1}{4}} \chi$,

(b) during the eclipse period, the relation which would have been valid had there been no eclipse, is $f \propto \cos^{\frac{1}{4}} \chi$. This implies that $q \propto \sec \chi$,

(c) in view of (a) and (b), (5) may be used to represent both the changes in E-layer due to the eclipse and also the simultaneous diurnal changes in χ.

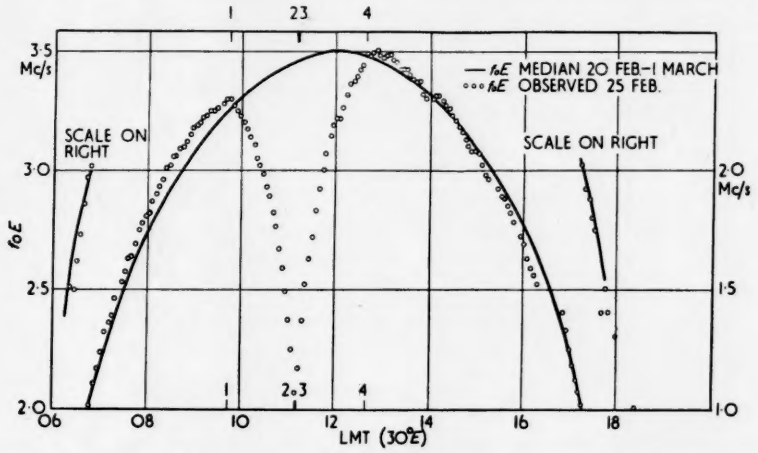

Fig. 1. Observed values of critical frequency of E-layer for control period and on 25th February

E-Layer: Results of Measurements

The E-layer critical frequency during the eclipse remained for most of the time within the open part of the frequency scale (0·02 Mc/s^{-1} mm^{-1}) and, since the cusps were usually well defined, f_0E has been estimated to the nearest 0·01 Mc/s^{-1}. The accurate measurement of the critical frequencies which has been possible on most of the records has made the measurements of rate of change of electron density much more reliable than they might otherwise have been.

Fig. 1 illustrates the changes in f_0E on eclipse day and the median curve for the ten control days represented by (6). Fig. 2 shows in more detail how f_0E varied during the optical eclipse; it also shows the changes which were expected to occur assuming that the ionizing radiation was emitted with equal intensity from all parts of the disc and that the layer behaved as a Chapman layer. It is obvious that there are serious discrepancies between the calculated and observed curves—

(a) the fall in f_0E at the beginning of the eclipse is much too rapid,

(b) the minimum value of f_0E, although not observed, must have occurred

within about 30 sec after third contact, suggesting a very high recombination coefficient,

(c) in spite of (b), the minimum observed value of f_0E is about what would have been expected for $\alpha' \simeq 0{\cdot}8 \times 10^{-8}$ cm^3 s^{-1}, but for this value of α' the time lag of the minimum after third contact ought to have been about six minutes,

(d) in spite of having risen very rapidly soon after third contact, the subsequent increase in f_0E is slower than expected, except for a rather abrupt rise near the end of the eclipse.

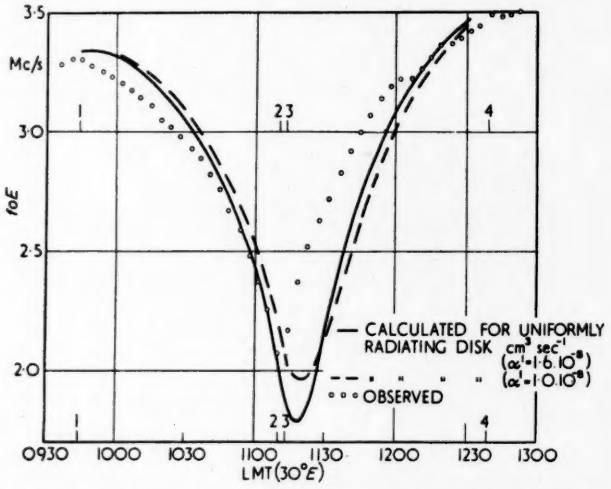

Fig. 2. Comparison between observed values of E-layer critical frequency and values calculated assuming uniformly radiating disc.

It is clear that no conceivable change in α' during the eclipse can account for these discrepancies. On the other hand they can, at least qualitatively, be explained by postulating the existence of a strong source of ionizing radiation near the west limb of the sun. The occultation of such a source soon after first contact could account for the rapid fall in f_0E between 0944 and 1040 LMT, while its reappearance just after totality could explain the unexpectedly high values of f_0E found just after third contact. A smaller source of radiation near the east limb could easily give rise to the sudden increase in f_0E just before the end of the eclipse.

It seems reasonable, therefore, that the unexpected nature of the response of E-layer to the eclipse should be attributed to a very pronounced non-uniformity in the distribution of the sources of ionizing radiation on the sun's disc. In general, it would not be possible to determine this distribution unambiguously using only the ionospheric data, but during this eclipse the distribution was such that quite an accurate reconstruction of the positions and relative intensities of the sources is possible.

As discussed earlier, for E-layer during the eclipse we may write—

$$\frac{dN_e}{dt} = Aq_0 \cos \chi - \alpha' N_e^2 \qquad (1)$$

VOL. 6 1955

and therefore—

$$\frac{Aq_0}{\alpha'} = \left(\frac{1}{\alpha'}\frac{dN_e}{dt} + N_e^2\right)\sec\chi = J \tag{8}$$

But $q_0 = \Phi na$

where Φ = flux density of ionizing radiation,

n = density of neutral particles,

a = ionizing cross-section of neutral particles.

Hence, if it is assumed that $na/\alpha' =$ constant, the changes in J, as defined in (8), will be proportional only to the changes in the intensity of the incident radiation which were directly due to the eclipse and will not be affected by the normal diurnal intensity changes.

Before (8) can be used with the experimental values of N_e and dN_e/dt it is necessary to know α'. The last measured value of f_0E occurs about a half-minute before second contact, but the curves of f_0E and dN_e/dt have been extrapolated to give estimated values at the instant of second contact, which are: $f_0E = 2{\cdot}05 \pm 0{\cdot}03$ Mc/s and $dN_e/dt = 41 \pm 1$ cm^{-3} s^{-1}. Assuming that $A = 0$ at second contact, we have from (1)

$$\alpha' = \frac{\dfrac{dN_e}{dt}}{N_e^2} = 1{\cdot}51 \pm 0{\cdot}12 \times 10^{-8}\ \text{cm}^3\ \text{s}^{-1} \tag{9}$$

The limits quoted are believed to represent the maximum experimental error incurred in measuring and extrapolating dN_e/dt and N_e. If A was 0·01 at second contact, it would be necessary to add $0{\cdot}12 \times 10^{-8}$ cm^3 s^{-1} to the value given.

Using the value for α' just found, and substituting the measured values for the other parameters, the values of J shown in Fig. 3 were obtained. The most striking feature is the sudden rise in J to nearly a third of its normal value just after third contact; since this occurred within 45 sec after third contact, it is concluded that it must have been due to the uncovering of a narrow source of ionizing radiation on the west limb of width not more than 0·009 solar diameters. To obtain some information on its extent in heliographic position angle, the behaviour of J between first and second contacts must be examined. It is then found that the observed changes can be explained by postulating the existence of a thin source on the west limb (Kh1, Fig. 3) extending from 240° to 320° and having an intensity 25 per cent of the total, and a small spot of intensity 3 per cent (Kh3) at 320°. The intensity of the uniform disc radiation is found to be 64 per cent of the total, and it is also necessary, to obtain the best fit with the experimental data and to account for the sharp rise near fourth contact, to assume the existence of a source of intensity 8 per cent near the east limb at 68° (Kh2). Owing to the small intensity of Kh2, and also for geometrical reasons, it is not possible to define its position very accurately. The computed changes in J which result from the adoption of the intensity distribution just mentioned are shown, together with the measured values, in Fig. 3. The closeness of fit of the experimental points with calculated curve is very satisfactory, except near 1150, when

a change in layer structure similar to one which occurred at 1400 (Fig. 1) appears to have occurred.

To obtain some independent evidence of the reality of the sources just described, data on f_0E obtained by PIGGOTT (1952) at Ibadan during partial eclipse have been subjected to a similar analysis. The measured values of J, shown in

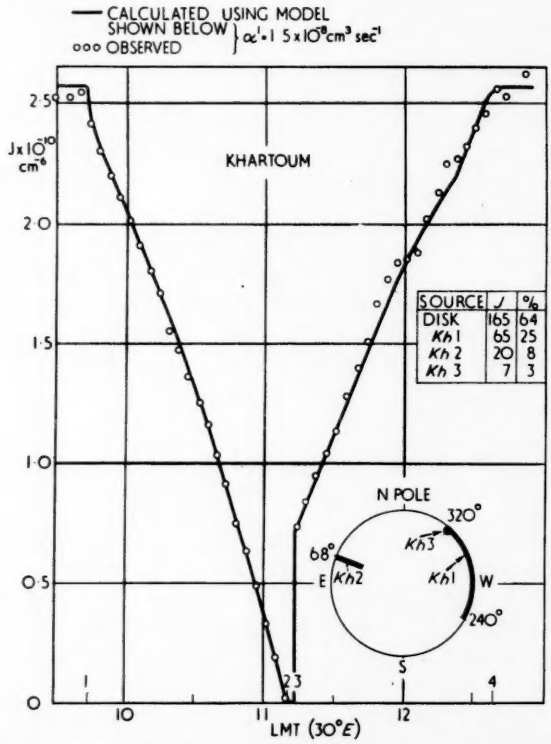

Fig. 3. Changes in intensity of E-layer ionizing radiation during eclipse (Khartoum).

Fig. 4, passed through a minimum about fifteen minutes before the expected time; this supports qualitatively the hypothesis, based on the Khartoum data, of the existence of an intense source near the west limb. Since the eclipse was partial at Ibadan, it is not possible to confirm that this source was confined to a narrow strip on the limb. If, however, this assumption is accepted, it follows that the intensity of the source was 25 per cent of the total intensity, and its extent 240°–295°, which is in good agreement with the conclusions reached using the Khartoum data. The difference in the extent might possibly be real, since there is a time difference of about two hours between the two sets of measurements, but, since the measurement of slope is important in both cases, and since the eclipse at Ibadan began soon after sunrise, it would be unwise to insist on the difference being significant. The locations and intensities of the sources necessary to account for the Ibadan results are given in Fig. 4. The changes in J calculated using this model are also shown and are seen to agree well with the measured values of J.

VOL. 6 1955

The value of α' used in computing J at Ibadan was chosen because it resulted in similar values for J before and after the eclipse and in self-consistency in the changes in J during the eclipse; other evidence also suggests that the value used is approximately correct, but since dN_e/dt was small at Ibadan for most of the time, the value of α' is not very critical.

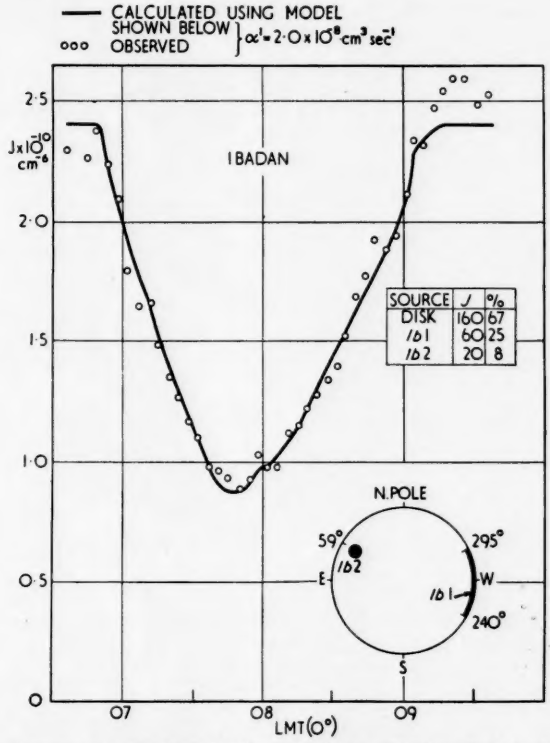

Fig. 4. Changes in intensity of E-layer ionizing radiation during eclipse (Ibadan).

It is satisfactory to find that, on the whole, the similarity between the locations and intensities of sources deduced from the two independent sets of data is quite marked. An additional connection between the Khartoum and Ibadan data depends on the fact that at 0753 UT at Khartoum, and at 0701 UT at Ibadan, the moon was in the same apparent position relative to the sun. The corresponding values of J/J_0 are 0·87 at Khartoum and 0·84 at Ibadan, where J/J_0 is the ratio of the observed value of J to the value before first contact a few minutes earlier. The agreement between the two values of J/J_0 provides additional confirmation of the validity of J as a measure of radiation intensity for E-layer. If the intensity had been proportional to the exposed area of the disc, the value of J/J_0 would have been 0·95.

Since there are good grounds for assuming that the observed changes in f_0E were due to a very asymmetrical distribution of ionizing radiation superposed on a uniformly radiating disc, it is interesting to consider the sources deduced from the ionospheric data in the light of astronomical evidence as to solar activity at

the same time. Astronomical data from a number of sources have been examined, and it is evident that, apart from two active areas near the limbs, the activity over the disc was at a low level. TROTTER and ROBERTS (1952a) consider that, in terms of flare occurrences, the region on the west limb was the more active of the two.

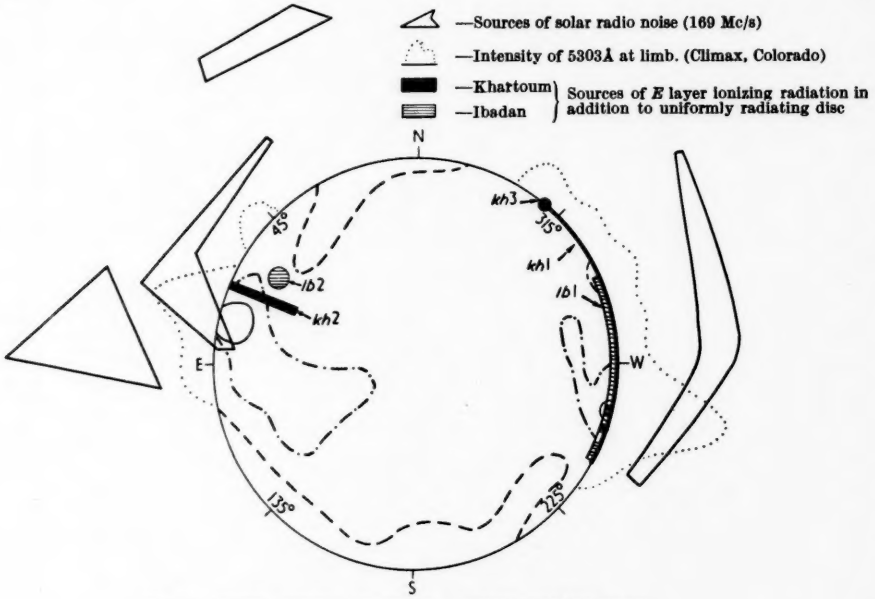

Fig. 5. THE SUN'S DISC 25TH FEBRUARY 1952
Coronal Intensity Contours (5303 Å, Pic du Midi):
——— 82 units
— · — 40 units
– – – 14 units

The visible disc phenomenon which appears to correspond most closely to the distribution of sources deduced from the ionospheric data is the intensity distribution of the coronal line at 5303 Å. This is shown in Fig. 5, in which the contours are based on measurements made at Pic du Midi and kindly made available by M. D'AZAMBUJA; the limb intensities for the same line are those measured at Climax (TROTTER and ROBERTS, 1952b). The fairly uniform intensity of the 5303 Å line over the disc is in accordance with the ionospheric model, while the similarity in position of the ionospheric active areas with the distribution of intensity of 5303 Å measured at the limbs is remarkably close.

The positions of the ionospheric bright areas seem to be related also to those of solar sources of radio noise on 169 Mc/s (Fig. 5) reported by COUTREZ, KOECKELENBERGH, and POURBAIX (1953), but the radio sources are not confined to the disc itself, as appears to be the case for the sources of *E*-layer radiation. A few radio sources found on the disc by COUTREZ and his associates (not shown in Fig. 5) do not appear to correspond to any sources of *E*-layer radiation which are distinguishable from the uniform contribution of the disc.

In the present state of knowledge of the origin of the solar corona and of solar

VOL. 6 1955

radio noise, and of the identity of the *E*-layer ionizing radiation, it is not possible to say precisely what the common factor may be.

It is interesting to note that if the intensity and maximum width of the west-limb source as deduced from the Khartoum data are accepted, it follows that the intrinsic "brightness" if this region must have been at least thirty times that of the uniform disc radiation. It has been suggested by ATHAY, EVANS, and ROBERTS (1953) that the most likely explanation for such a source is a solar flare, but several considerations lead to the conclusion that only a part of the radiation attributed to the west-limb source could be due to a flare.

The large extent of the source in heliographic latitude suggests that although it may have included a flare, it would be difficult to regard the whole of it as a flare. In addition, judging by the ionospheric data, the brightness appears to have been uniformly distributed except for a small spot at 320° (Kh3, Fig. 5), the intensity of which is only about one-tenth that of the whole source.

A comparison of the intensity of the source as determined both at Khartoum and Ibadan shows that within the limits of experimental error the same value was found at both places. The difference in time between some of the relevant measurements was as much as two-and-a-half hours, and it seems unlikely that a flare could have remained at the same intensity level for so long.

Finally, had the west-limb source owed its origin entirely to a flare, the intensity of the *E*-layer ionizing radiation during the eclipse would have been 35–40 per cent above the levels of the preceding and following days. Estimates of the day-to-day changes in intensity have been made using the hourly values of f_0E, corrected for differences in zenith angle, between 0800 and 1600 LMT daily at Khartoum. The resulting index number (Table 2) may be regarded as proportional to the mean intensity of the *E*-layer ionizing radiation each day during the interval mentioned. An intensity of 1·00 is equivalent to the mean intensity

Table 2. Mean intensity of E-layer ionizing radiation (0600–1400 *UT*) (*arbitrary units*)

1952	*Int.*	1952	*Int.*	1952	*Int.*
Feb. 15	1·04	Feb. 22	(1·08)	Feb. 29	0·97
16	0·95	23	1·04	Mar. 1	1·04
17	1·02	24	0·98	2	0·94
18	1·02	*25*	*1·04*	3	(0·95)
19	1·02	26	0·98	4	0·96
20	1·05	27	0·96	5	1·01
21	1·03	28	0·91	6	0·97

at local noon (1000 UT) during the period 7th February–14th March which corresponds to $q_0 = 258\alpha'\ 10^8\ \mathrm{cm^{-3}\ s^{-1}}$. The conclusion to be drawn from Table 2 is that there was a gradual fall in intensity of about 17 per cent during the period February 22–February 28, except on the day of the eclipse when the mean intensity was only about 6 per cent higher than on the preceding and following

days. If, instead of taking the mean intensity for the interval 0600–1400 UT on February 25, the values of f_0E for periods just before and just after the eclipse itself are used, the intensity indices become—

Feb. 25, 0500–0700 UT: 1·11; 1045–1130 UT: 1·06.

Assuming that the short-term changes in f_0E can legitimately be interpreted in this way, which is perhaps doubtful, the maximum difference between the intensity during the eclipse itself and that for the preceding and following days becomes 13 per cent; thus at the most only about half of the intensity of the west-limb source could be attributed to a short-lived source of ionizing radiation.

A further point of interest is the possibility that the uniformly distributed radiation from the disc is a permanent feature throughout the solar cycle and that it corresponds to the minimum possible level of solar activity. Assuming this to be so, then during the eclipse the ratio of the observed total intensity to the minimum possible intensity was 1·56; but the total intensity during the eclipse was about 10 per cent above the monthly median level and, if it is assumed that the day-to-day fluctuations arise from changes in the non-uniform component only, the ratio for the month becomes 1·40. According to ALLEN (1948), the intensity I_R of the E-layer ionizing radiation for a twelve-month mean sunspot number $\overline{R}$ is given by—

$$I_R = I_0(1 + 0{\cdot}0097\overline{R})$$

For February 1952, $\overline{R} = 43$, and hence $I_R = 1{\cdot}42I_0$, which agrees with the ratio referred to above.

The value of α' deduced from the behaviour of f_0E at Khartoum is $1{\cdot}5 \times 10^{-8}$ cm^3 s^{-1}, and using (1) near noon when $dN_e/dt = 0$, it can be shown that $q_0/\alpha = 258 \times 10^8$ cm^{-6}. Combining these two figures, we obtain $q_0 = 387$ cm^{-3} s^{-1}. It has been suggested by PIDDINGTON (1951) that in E-layer the effective recombination coefficient is about ten times greater than the value usually assumed; if, for example, it is assumed that $\alpha' = 10^{-7}$ cm^3 s^{-1}, then for Khartoum we have $q_0 \simeq 2{,}600$ cm^{-3} s^{-1}, which is about seven times the value obtained above. It is possible, however, to use the eclipse data to give an estimate of q_0 which is independent of α'.

(1) may be rewritten—

$$\frac{dN_e}{dt} = q_0 AD \cos\chi + q' - \alpha' N_e^2 \qquad (10)$$

where D = fraction of the total radiation emitted uniformly from the disc,

q' = electron production due to sources other than uniform disc radiation.

During the eclipse it is possible to select times before and after totality when the electron densities are equal. Assuming that α' is constant, from (10) we have—

$$\left(\frac{dN_e}{dt}\right)_2 - \left(\frac{dN_e}{dt}\right)_1 = q_0 D(A_2 \cos\chi_2 - A_1 \cos\chi_1) + q_2' - q_1'$$

or

$$y = q_0 Dx + q_2' - q_1'$$

VOL. 6 1955

Differentiating with respect to $(A_2 \cos \chi_2 - A_1 \cos \chi_1)$, we have

$$\frac{dy}{dx} = q_0 D + \frac{dq_2'}{dx} - \frac{dq_1'}{dx}$$

If the terms dq'/dx were zero it would be possible to use the slope to give a unique value for $q_0 D$. Unfortunately for the 1952 eclipse, the distribution of the isolated sources of ionizing radiation is such that the terms in dq'/dx are never zero simultaneously except for a very brief period. There are, however, two intervals during which $\sum dq'/dx$ is constant but opposite in sign and where consequently dy/dx is substantially constant. It follows that although the magnitude of $q_0 D$ cannot be given uniquely, it is possible to give limiting values. A similar procedure can be adopted by choosing times when $N_1^2 \sec \chi_1 = N_2^2 \sec \chi_2$, and this also leads to limiting values for $q_0 D$. Both sets of limits are quoted in Table 3. It is not possible

Table 3. *Limiting values of* q_0

Condition	$q_0 D (cm^{-3} s^{-1})$	
	Lower	*Upper*
$N_1 = N_2$	190	960
$N_1^2 \sec \chi = N_2^2 \sec \chi$	330	1000

to proceed to a closer estimate of q_0 without making assumptions about the magnitude of α', but, even if the actual value of q_0 was near the upper limit, which is very unlikely, it would be difficult to accept a value for α' greater than about 5×10^{-8} cm^3 s^{-1}.

This method of obtaining q_0 is not capable of giving accurate results, because the expression $(A_2 \cos \chi_2 - A_1 \cos \chi_1)$ is the difference between two quantities which are almost equal; its main virtue is that the information it provides about q_0 does not depend on an assumed value for α'.

D-Layer

No special arrangements were made to measure the absorption in *D*-layer, but the minimum frequency ($f_{\min}$) on which reflections could be seen on the $h'f$ traces were recorded and found to follow the usual diurnal variation. During the eclipse at about 1117 LMT ($\cos \chi = 0{\cdot}88$), $f_{\min}$ had fallen to a value corresponding to $\cos \chi = 0{\cdot}2$ (approx.) when the sun is unobscured; this implies a fall in $N_e \nu$ to about a quarter of its normal value. The observed time-lag in the minimum value of $f_{\min}$ after third contact was about four minutes, which is very much shorter than would be expected. The short delay could be taken to imply the existence of a strong source of *D*-layer ionizing radiation near the west limb of the sun and hence some connection between the ionizing radiations responsible for the *D*- and *E*-layers.

E_s-LAYER

For the day of the eclipse, the fourteen values of fE_s measured in a sixty-minute period have been used to compute median values at intervals of thirty minutes; these are shown in Fig. 6 with the median values, determined in the usual way, for the ten control days. Although on the eclipse day fE_s fell from a high level at 0830 to a very low level at 1230 and subsequently recovered, there is no obvious reason at present for suggesting that these changes were due to the eclipse.

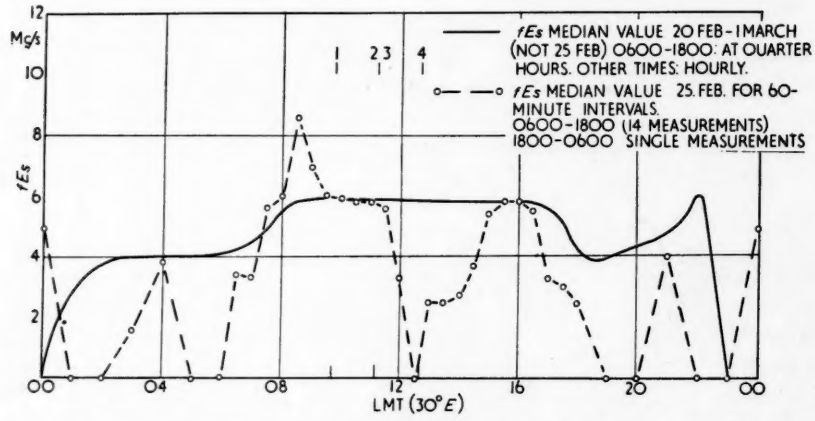

Fig. 6. Observed values of critical frequency of E_s-layer for control period and on 25th February.

F-LAYER

The structure of the F-layer at Khartoum during the control period was not unusual in any way; the peak of the F_2-layer which was at about 350 km during the day, was approximately parabolic in shape, and there was an F_1-ledge extending from about 150 to 180 km. During the control period the F_1-layer never gave rise to a sharp cusp on the $h'f$ records; its presence could be deduced only from the small additional retardation which occurred near 4 Mc/s between 0900 and 1600 LMT. Although under such conditions it is not possible to quote precise values of f_0F_1, the frequency of the point of inflexion in virtual height due to the F_1-ledge was measured. These frequencies will be referred to as f_0F_1, but it should be understood that in general a maximum in the value of the electron density is not implied; the median values of these frequencies and also those of f_0F_2 are shown in Fig. 7.

F_1-layer

It is possible to estimate the effective recombination coefficient in F_1-layer by using the same method as for E-layer (9). A measurement of f_0F_1 was made ten seconds before second contact, at which it is assumed the intensity of the ionizing radiation fell to zero. The extrapolated values are $f_0F_1 = 2{\cdot}60 \pm 0{\cdot}015$ Mc/s and $dN_e/dt = 59 \pm 6\text{s}^{-1}$, and hence $\alpha' = (8{\cdot}2 \pm 1) \times 10^{-9}$ cm^3 s^{-1}.

VOL. 6 1955

The changes in f_0F_1 which would have occurred during the eclipse of a uniformly radiating disc have been calculated for $\alpha' = 8 \times 10^{-9}$ cm^3 s^{-1}, assuming that the loss of electrons is due to an effective recombination process. The large discrepancies between the observed points and the calculated curve (Fig. 8) resemble

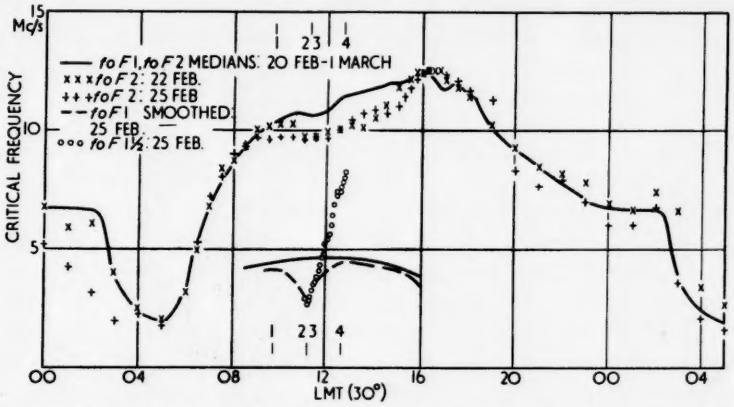

Fig. 7. Observed values of critical frequencies of layers in F-region for control period and on 22nd and 25th February.

those described for E-layer (Fig. 2), and it seems reasonable to suppose that, to a first approximation, the distribution and intensities of the sources of E- and F_1-layer ionizing radiation are similar. A recalculation of f_0F_1 has therefore been

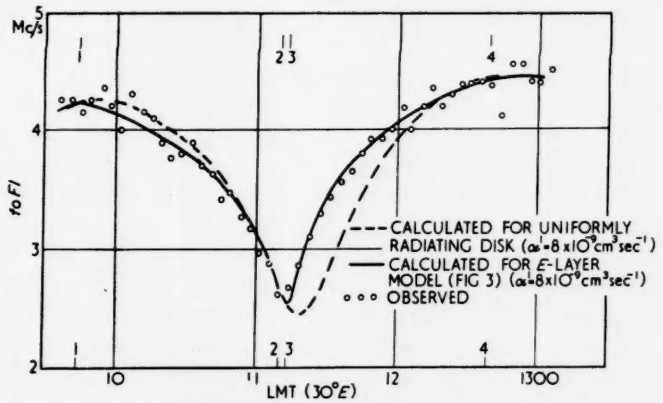

Fig. 8. Comparison between observed and calculated values of F_1-layer critical frequency during eclipse.

made on this assumption, making use of the distribution already deduced from the Khartoum data for E-layer. The resulting curve agrees quite closely with the observed points (Fig. 8), and it must be concluded that the locations of the radiation sources for the two layers are the same and that the relative intensities of corresponding sources are the same.

The value of α' deduced above is somewhat higher than that usually taken to

apply in F_1-layer, and it seemed important to determine the height to which the measurements refer. This was done using the curves of electron density as a function of true height described later, and it is found that the appropriate height is about 170 km. This is not a precise measurement, because it is necessary to interpolate the electron density between about 200 km and E-layer peak; further, it is not usually possible to "see" the F_1-layer peak or to say just where the F_1- and F_2-layers join.

F_2-layer

On the day of the eclipse, the early morning values of f_0F_2 were low, but they recovered by 0600 LMT and remained close to the median value until 0900 LMT (Fig. 7). Between 0900 and 1530, including the duration of the eclipse, f_0F_2 was well below the median value; this might well be taken to be an eclipse effect, but further investigation does not confirm this possibility. The trend of f_0F_2 on 25th February was remarkably similar to that on 22nd February, when there was no eclipse (Fig. 7), and it is, in any case, likely that f_0F_2 was depressed on 25th February by the effects of the magnetic disturbance which began on 23rd February. Consequently it is concluded that there was no significant eclipse effect in f_0F_2.

Although any eclipse effects which may have occurred near the peak of F_2-layer were indistinguishable from normal day-to-day fluctuations, those which took place at lower levels between F_1- and F_2-layers were unmistakable. From 1000 onwards during the eclipse, the appearance of the $h'f$ traces, as compared with the control days, became very abnormal; at first this was due to the fact that much more of the F_1-ledge was exposed than was usual during the control period, but after totality it was evident that a new ledge, which will be referred to as $F_{1\frac{1}{2}}$, had formed between the F_1- and F_2-layers. For about forty-five minutes the $F_1/F_{1\frac{1}{2}}$ combination gave a fairly sharp cusp, but after the bifurcation the cusps of both layers degenerated into the more usual rounded maxima. While f_0F_1 gradually returned to its normal value, $f_0F_{1\frac{1}{2}}$ increased very rapidly, at the same time producing less and less retardation, until just before 1300, when it merged into the F_2-layer and could no longer be distinguished even as a ledge (Fig. 7).

The development and decay of the $F_{1\frac{1}{2}}$-layer can be seen in the $h'f$ curves reproduced in Fig. 9 from which the extraordinary-wave components have been omitted. It is difficult to visualize the physical changes which occurred in F-layer merely be describing them in terms of critical frequencies and virtual heights. To obtain a clearer picture of the nature of these changes, it was considered desirable to calculate the distribution of electron density as a function of true height. The effort required to do this accurately would have been prohibitive, but it was thought worthwhile to use a less precise method which would still give sufficiently reliable results to justify the effort involved.

The method employed was that described by KELSO (1952), in which the true height for a given electron density is found by measuring the virtual heights at ten related frequencies. Although this method is not strictly applicable to a layer below which there is another layer having an electron density maximum, gross errors were avoided by plotting the $h'f$ curves on a logarithmic frequency scale and

, VOL. 6 1955

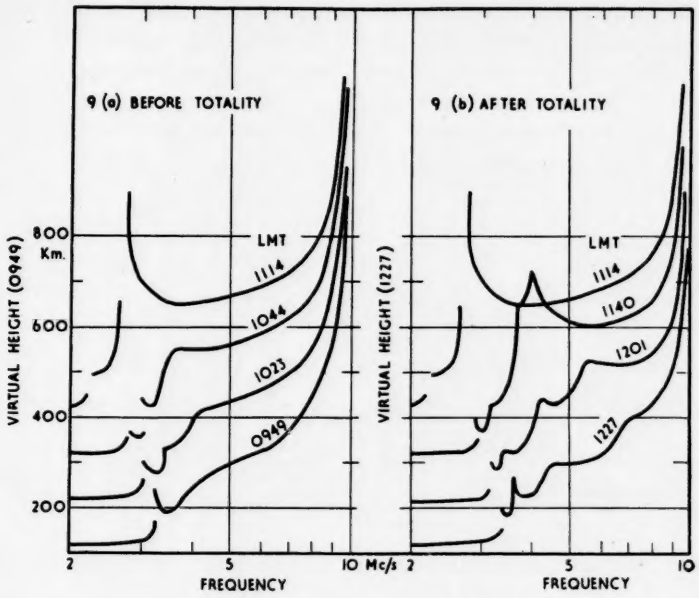

Fig. 9. Typical $h'f$ curves during eclipse.

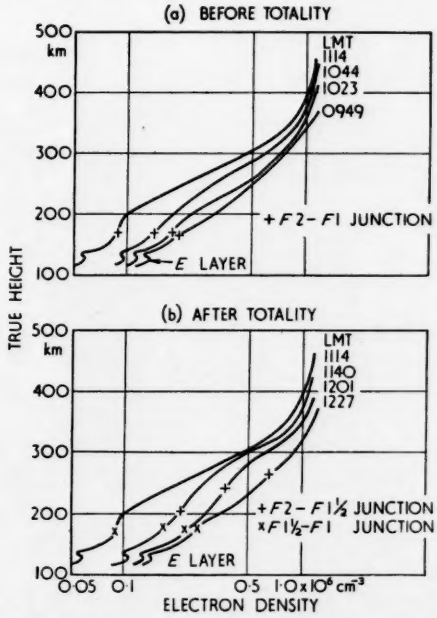

Fig. 10. Electron density distributions corresponding to curves shown in Fig. 9.

using a slider technique which allowed the sampling frequencies to be chosen so that none of them coincided with the E- or F_1-layer discontinuities.

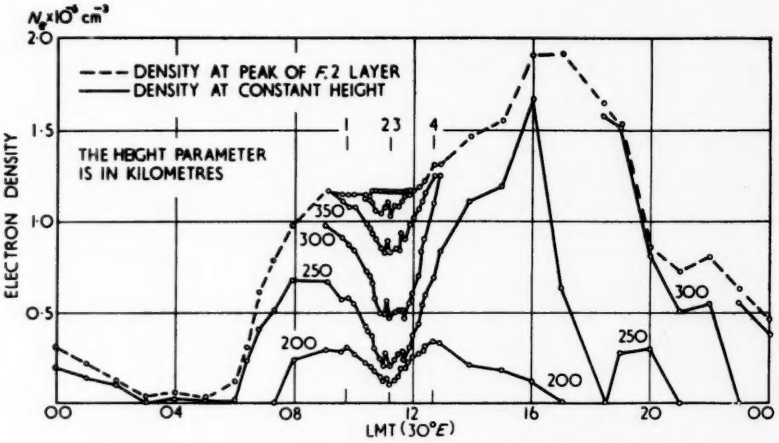

Fig. 11. Changes in electron density at constant true height on 25th February.

The electron density distributions corresponding to the $h'f$ curves in Fig. 9 are shown in Fig. 10. Although it is difficult to calculate the density below about 200 km using KELSO's method, approximate values have been obtained by other

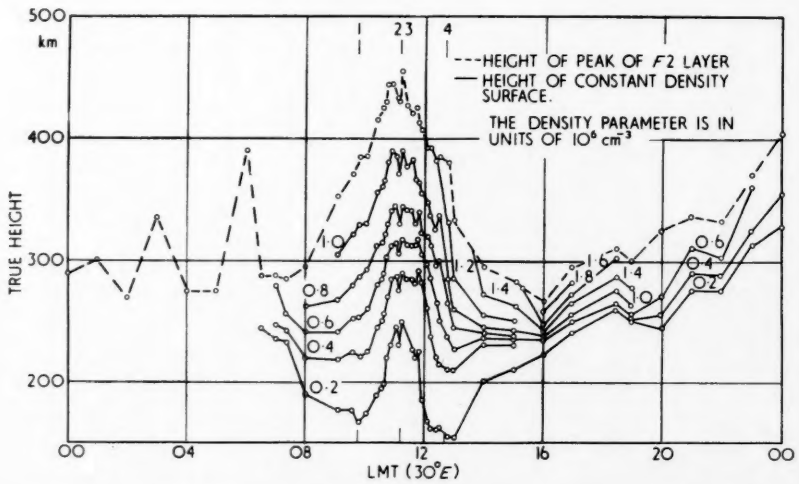

Fig. 12. Changes in true height of constant electron-density surfaces on 25th February.

means to fill the gap between E-layer and the bottom of F_2-layer. It is evident from Fig. 10 that, although there was practically no change in density at the peak of the F_2-layer, as the eclipse progressed there was a marked fall in density at

, VOL. 6 1955

lower levels. These changes are more easily seen in Fig. 11, in which density has been plotted as a function of true height; alternatively it is possible to plot the

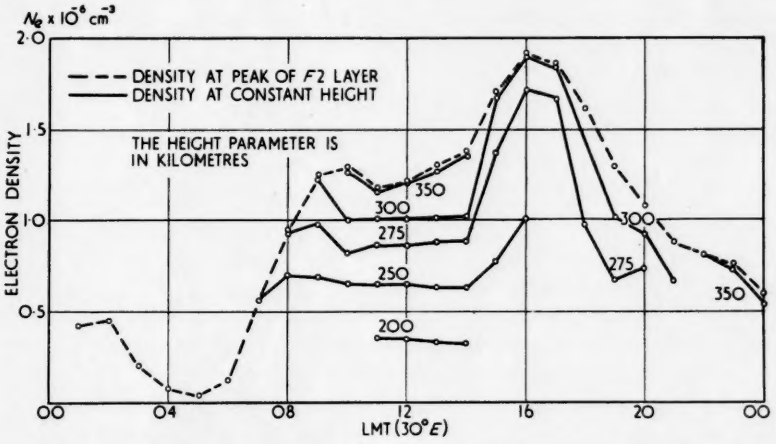

Fig. 13. Changes in electron density at constant true height on 22nd February.

change in true height for a number of values of density as in Fig. 12. The families of curves in Figs. 11 and 12 may be compared with the corresponding ones for 22nd February (Figs. 13 and 14), during which the changes in f_0F_2 closely resembled

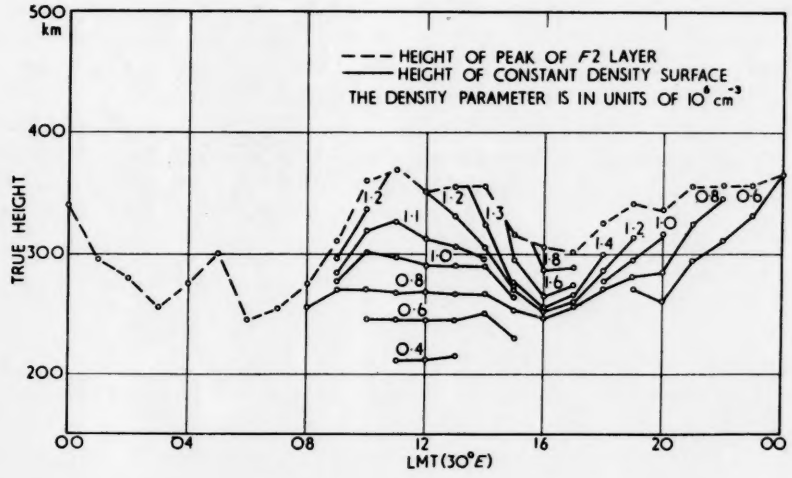

Fig. 14. Changes in true height of constant electron-density surfaces on 22nd February.

those on 25th February; the pronounced density minimum on 25th February is clearly due to the eclipse.

It is not possible to account in detail for the changes which occurred in F_2-layer

during the eclipse. However, there appears to be a similarity between the behaviour of the post-sunrise F_2-layer on a normal day and that of the $F_{1\frac{1}{2}}$-layer after totality during the eclipse. In both cases, the layer appears to form first at about 200 km; subsequently its peak rises rapidly both in true height and electron density. During this period the layer behaves as if it were controlled by the incident radiation intensity and as if α' were fairly high; the evidence for this is that when an eclipse begins while the layer is still developing, its critical frequency stops increasing and finally falls: such behaviour has been reported by LEDIG *et al.* (1946), ESTRABAUD (1952), and PIGGOTT (1952).

When the developing layer attains a height of about 300–350 km, its density and height stop increasing. It also ceases to be sensitive to further increases in incident radiation intensity and, presumably on account of the low α' at this height, decays very slowly when the radiation is removed. The initial growth stage and the later stable regime will be referred to respectively as States I and II.

The observed changes in F-layer above 200 km at Khartoum appear to be explicable in terms of this model of the development of F_2-layer. When the eclipse began, State II had already been reached and the absence of any change in f_0F_2 which could be attributed to the eclipse is, therefore, accounted for. On the other hand, the rapid fall in electron density at the lower levels during the first half of the eclipse is interpreted as being due to the solar control which is normal during State I, which also explains the creation of the $F_{1\frac{1}{2}}$-layer after totality. The development of $F_{1\frac{1}{2}}$-layer is very like that of the post-sunrise F_2-layer, Figs. 7 and 10, and its eventual submergence in the already existing F_2-layer represents the transition from State I to State II.

It is evident that, if an eclipse begins before State II has been reached, the normal stable day-time value of f_0F_2 will not have been reached. After the maximum phase of the eclipse, the development of a new post-sunrise or $F_{1\frac{1}{2}}$-layer will commence but, owing to the decrease in $\cos\chi$ since sunrise, it must soon attain a maximum electron density exceeding that of the post-sunrise layer formed earlier. This appears to account for the occultation of the "old F_2-layer" by a "new F_2-layer" which has been noticed by the authors just mentioned.

It may be asked why the electron production at low levels, which is assumed to exist both before and after totality, does not give rise to a distinct layer until the appearance of the $F_{1\frac{1}{2}}$-layer after totality. It must be remembered that the very pronounced alterations in the shape of the $h'f$ curves in Fig. 9b are due to points of inflexion in the distribution of density with height; these can be seen in Fig. 10b, but, although they have obvious effects on the group retardation, they do not imply any very drastic rearrangement of the electron distribution, as can be seen by comparing Figs. 10a and 10b. It is suggested, therefore, that the point of inflexion which is present after totality is the junction between the newly-formed $F_{1\frac{1}{2}}$-layer advancing upwards and the F_2-layer already in existence higher up. During the corresponding post-sunrise period, the very low density in the night-time F_2-layer soon results in its being occulted by the newly-formed post-sunrise F_2-layer. During the first half of the eclipse, the vertical gradient in α' could prevent the peak of the $F_{1\frac{1}{2}}$-layer from being uncovered.

VOL. 6 1955

The presence of a lower ledge in F_2-layer at Khartoum is also detectable on days besides the eclipse day, notably 24th and 27th February, and the problem requires further investigation.

Acknowledgments—The author wishes to acknowledge the assistance of Professor N. F. ASTBURY of University College, Khartoum, and his staff for their valuable co-operation during the installation of the equipment and during the eclipse; Mr. C. CLARKE, to whose credit the high quality of the $h'f$-records is due; and Mrs. V. BRAMLEY for assistance during much of the computing work.

The work described above was carried out as part of the programme of the Radio Research Board. This paper is published by permission of the Director of Radio Research of the Department of Scientific and Industrial Research.

REFERENCES

ALLEN, C. W. 1948 Critical frequencies, sunspots and the sun's ultraviolet-radiation. *Terr. Mag.* **53,** 433–448

ATHAY, R. G., EVANS, J. W., and ROBERTS, W. O. 1953 The active region on the West Solar Limb during the eclipse of 1952, February 25. *Observatory* **73,** 244–245

BATES, D. R., and MASSEY, H. S. W. 1946 The basic reactions in the upper atmosphere. *Proc. Roy Soc.* **A187,** 261–296

1951 The negative ion concentrations in the lower atmosphere. *J. Atmosph. Terr. Phys.* **2,** 1–13

BIONDI, M. A., and BROWN, S. C. 1949 Measurement of electron-ion recombination. *Phys. Rev.* **76,** 1697–1700

CLARKE, C., and SHEARMAN, E. D. R. 1953 Automatic ionospheric height recorder. *Wireless Engr.* **30,** 211–222

COUTREZ, R., KOECKELENBERGH, A., and POURBAIX, E. 1953 Observations radioastronomiques de l'éclipse solaire du 25 février 1952. *Commun. Obs. Belg.*, No. 60, 3–21

ESTRABAUD, S. 1952 Effets de l'éclipse solaire du 25 février 1952 sur la région ionosphérique F_2 en Afrique Equatoriale. *C.R. Acad. Sci. Paris* **235,** 1521–1523

1953 Influence de l'éclipse solaire du 25 février 1952 sur la région E en Afrique Equatoriale. *C.R. Acad. Sci. Paris* **236,** 833–835

GERJUOY, E., and BIONDI, M. A. 1953 Dissociative recombination in the E layer. *J. Geophys. Res.* **58,** 295–303

KELSO, J. M. 1952 A procedure for the determination of the vertical distribution of the electron density in the ionosphère. *J. Geophys. Res.* **57,** 357–367

LEDIG, P. G., JONES, M. W., GIESECKE, A. A., and CHERNOSKY, E. J. 1946 Effects on the ionosphere at Huancayo of the Solar Eclipse 25th January 1944. *Terr. Mag.* **51,** 411–418

NICOLET, M., and BOSSY, L. 1949 Sur l'absorption des ondes courtes dans l'ionosphère. *Ann. Geophys.* **5,** 275–292

PIDDINGTON, J. H.	1951	The modes of formation of the ionospheric layers. *J. Geophys. Res.* **56,** 409–429
PIGGOTT, W. R.	1952	Ionospheric measurements at Ibadan during the eclipse of the sun, 25th February 1952. Proc. Mixed Commission on the Ionosphere, August, 1952, 42–50
TROTTER, D. D., and ROBERTS, W. O.	1952a	Quarterly solar activity summary 1.1.52-31.3.52. High Altitude Observatory, Colorado, Report No. HAO-NBS 10
	1952b	Solar activity at time of eclipse 25th February 1952. High Altitude Observatory, Colorado, Report No. HAO-NBS 11

VOL. 6 1955

Journal of Atmospheric and Terrestrial Physics, 1955, Vol. 6, pp. 113 to 116. Pergamon Press Ltd., London

Sporadic *E* propagation

N. C. GERSON
Geophysics Research Directorate, AF Cambridge Research Center,
Air Research and Development Command, Cambridge, Mass.

(*Received* 26 *July* 1954)

ABSTRACT .
Studies of sporadic *E* clouds indicate that the modal station separation at time of radio contact was 1,490 km, 2,800 km, and about 4,200 km for single, double- and triple-hop communication. Large E_s clouds having an effective diameter of about 925 km were found to be fairly prevalent.

A study of sporadic *E* propagation over North America was made during the three-year period 1949–1952. In this time-interval, radio amateurs operating in the 2- and 6-metre band assisted in forming a co-operative network which reported the occurrence of any unusual long-range communication. In most instances the long paths arose from the presence of sporadic *E*. The technique, which is relatively simple, has already been described. Most of the data were obtained during summer.

This note presents the results obtained when an analysis was made of the station separation at the time of radio contact. Fig. 1 displays the number of cases as ordinate versus the distance between stations (at the time abnormal communication was established) as abscissa. In preparing the graph, over 12,500 instances of propagation at 50 Mc/sec were utilized. All propagation attributable to auroral interaction and most instances of non-E_s reflection were eliminated from the tabulation. However, it is possible that in some cases (less than two per cent) F_2-layer or tropospheric propagation were included in the results. When data were plotted separately for each month (number of cases versus distance) a curve similar to that shown was obtained. Thus, it may be assumed that the curve portrayed in Fig. 1 is typical and that no appreciable departures are encountered during the course of the year.

From the diagram it is quite apparent that the most common station separation at the time of E_s propagation was about 1,500 km. In 80 per cent of the cases the station separation ranged between 1,060 and 1,920 km, and in 60 per cent of the radio contacts, the distance between sites was in the range 1,220–1,780 km. The greatest station separation reported in North America was 4,900 km; at 50 Mc/sec this radio contact probably required three ionospheric reflections (triple-hop communication). The shortest station separation attributed to E_s propagation was about 400 km. The equivalent vertical-incidence cut-off frequency for 50 Mc/sec propagation over a distance of 400 km is about 23 Mc/sec, corresponding to an equivalent electron density of $7 \times 10^6/\text{cm}^3$. Such conditions were observed very infrequently.

Using the data provided by the tabulation, an attempt was made to differentiate those instances of abnormal propagation arising from single, double, and triple reflections from E_s areas. A tentative breakdown for the former types of E_s propagation is displayed in Fig. 1. Three categories are shown, which together

synthesize the total number of cases: (a) single hop (single cloud); (b) double hop (single cloud); and (c) double hop (two clouds).

For E_s located at an altitude of 110 km, single-hop reflection at 50 Mc/sec may occur for paths of 600–2,200 km, while double-hop reflections would presumably double this range interval. It may be expected that the most common station separation at time of radio contact by E_s would be the average of the range involved; i.e., 1,400 km, 2,800 km, and 4,200 km, respectively, for one,

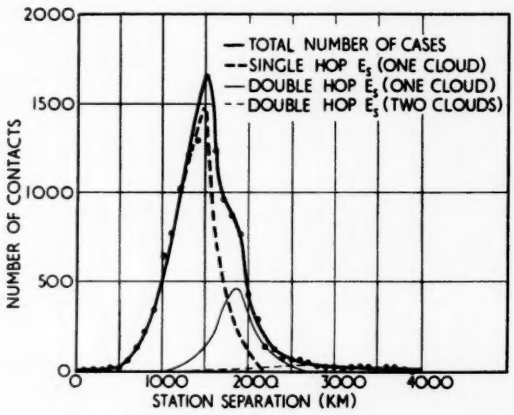

Fig. 1.

two, or three reflections. For the first two cases, the values deduced from Fig. 1 are 1,490 km and 2,800 km, respectively. An indication of the probability of occurrence of single-cloud E_s may be obtained from the ratio of the ordinates at these distances: $40/1{,}470 = 0{\cdot}027$. This ratio is a measure of P^2/P, where P is the occurrence probability of a single isolated E_s area. The value may be compared with the probability found during June 1950; the average probability for sporadic E to occur over the central portion of the U.S. was 0·032. The two values are in good agreement.

Propagation at 50 Mc/sec attributed to (a) single hop and (b) double hop are depicted in Fig. 1 for one and two E_s clouds, respectively. However, this breakdown does not synthesize the total number versus distance graph obtained from the data. When the above cases are subtracted from the total, a residual is found which has its most common station separation at 1,850 km. Several considerations led to the conclusion that the residue probably involves double hop propagation (by means of sporadic E) but from a *single* E_s cloud rather than two. Thus, the residue has been identified on the diagram as "double-hop E_s, one cloud". The ratio of the maxima of the residual and single hop curves is 0·34, indicating that conditions favouring the latter are about three times as prevalent as those favouring the former.

Several possibilities for explaining the existence of the residue suggest themselves. Because of the station separation found, it seems fairly definite that double hop propagation is involved. If two distinct E_s clouds were required, the

, VOL. 6 1955

occurrence probability would be given by the ratio 0·34 determined above. Such a probability, however, is excessively high and is difficult to justify especially since by actual count, E_s capable of allowing communication at 50 Mc/sec occurs less than 3 per cent of the time over any given site. A second possibility considers the existence of large sporadic E clouds whose size allows double hop propagation. With the latter assumption both single and double hop reflections are possible from the same cloud. If both large and small clouds existed, the maximum of the residual curve would be materially less than that of the "single hop" curve, but would exceed that of the "double hop, two-cloud" curve. It is believed that the large-cloud hypothesis clarifies the residual curve found in Fig. 1.

Some estimates of the size of the large E_s clouds may be made. At the time radio contact was established, the distance between stations was mainly in the interval 1,200–2,500 km. For double hop propagation, the cloud size should be about half this value; i.e., 600–1,250 km with a mean of 925 km. This mean, incidentally, is identical with the modal value.

Preliminary studies have indicated that some large sporadic E areas over North America may be elliptical in shape, with their major axes oriented in the North–South direction. Full utilization of the maximum propagation distance possible in the N–S direction, however, has not been taken because most of the radio amateurs were located south of 50°N latitude. Under these circumstances it is felt that the E_s cloud size as used above refers to the length of a section having an East–West component through the cloud.

It might be mentioned that at a frequency of 50 Mc/sec the smallest station separation reported was 90 km. In less than fifty reports, radio contacts were made at distances from 200–550 km. When the distance between sender and receiver was less than 400 km, the contact was tentatively considered to arise from super-refractive or ducting conditions in the troposphere.

It would be extremely interesting to undertake an analysis of 50 Mc/sec propagation conditions in other continental regions. The greatest station separation possible in the present investigation was about 5,000 km. Contacts over this distance could be reported by only a limited number of stations. For these sender-receiver pairs to contact each other, the sporadic E areas must exist in specific locations over the continent—a condition difficult to realize. On North America the orientation of stations separated by distances exceeding 6,000 km would be mainly N–S, but the sparsity of northern observers prohibited the implementation of such a network. However, 50 Mc/sec communication over distances of 6,000–7,000 km should not be unrealistic.

In the present study there was greater possibility for an east–west orientation in the direction between station pairs; however, maximum station separations in other directions should be determined. For example, radio contacts at 50 Mc/sec between North and South America have shown that station separations of about 9,600 km are quite possible, although somewhat uncommon. Undoubtedly, this distance was spanned because of F_2-layer propagation. In any event, investigation of E_s propagation should be undertaken between Europe–Africa, New Zealand–Australia, over the oceans, etc., where station separations with east–west orientations to distances of 5,000–6,000 km can be readily obtained. Studies of

this type will determine whether the average propagation distances using E_s may exceed significantly those found in a limited region of North America.

Another interesting aspect to be studied is transatlantic propagation at television frequencies during the summer, when intense sporadic E is most prevalent. At 50 Mc/sec, F_2-layer propagation between South American and South African stations on one hand and Europe and North America on the other hand requires much more intensive examination.

VOL. 6 1955

Journal of Atmospheric and Terrestrial Physics, 1955, Vol. 6, pp. 117 to 123. Pergamon Press Ltd. ,London

Horizontal movements of ionization in the equatorial *F*-region

B. W. Osborne
University of Malaya, Singapore

(*Received* 1 *June* 1954)

ABSTRACT

The velocities of horizontal movements of ionization in the *F*-region of the ionosphere at Singapore have been measured using the spaced-aerial technique. The results obtained from September 1953 to April 1954 demonstrate the existence of a regular semi-diurnal variation of sinusoidal form and of amplitude about 50 m/sec in the E–W component at the equinoxes. During the presence of thick layer structure in the mornings of the December solstice, the movements were irregular and showed frequent reversals in direction. No relation between ionization movements and virtual height was found.

Between sunset and midnight the movements were to the east, in contrast to the westerly drift of ionization at higher latitudes.

No regular N–S movements were observed.

1. Introduction

As no measurements of movements of ionization had been made near the equator it was decided to apply the spaced aerial technique in order to measure the horizontal velocity of the ionized particles in the *F*-region over Singapore. The results obtained from September 1953 to April 1954 inclusive will be described in this paper. The measurements were made at the position 1° 19′ N, 103° 49′ E, between the geographic and magnetic equators.

The method used is that in which the amplitude of a signal reflected from the ionosphere is simultaneously recorded at three spaced receiving points situated at the corners of a right-angled triangle. An irregular ionospheric layer produces a diffraction pattern on the ground (Booker, Ratcliffe, and Shinn, 1950) and this diffraction pattern moves over the ground with twice the velocity of the irregularities in the layer (Pawsey, 1935). On the occasions when the fading records obtained at the three receiving points are similar but displaced in time, measurement of the time-lags between pairs of aerials allows the determination of the velocity of the diffraction pattern over the ground (Briggs, Phillips, and Shinn, 1950) and thus of the irregularities in the ionospheric layer.

This method has been developed and used by workers at Cambridge and elsewhere (e.g., Phillips, 1952).

The results of previous measurements of movements of ionization at comparatively high latitudes have been discussed by Briggs and Spencer (1954), who on the basis of the available information came to the following conclusions with respect to the *F*-region:

(a) That by day the E–W component is consistently towards the east, with no seasonal changes (though Bramley, 1953, had observed a reversal in the direction of the E–W component in England at 1520 L.M.T.);

(b) That the N–S component is towards the north in summer and towards the south in winter in the northern hemisphere (and in the opposite directions in the southern hemisphere);

(c) That at night the N–S movements are small, and the E–W component is

towards the west except for occasional reversals after midnight during periods of magnetic disturbance (MAXWELL and LITTLE, 1952; HEWISH, 1952), and

(d) That whereas in the *E*-region there is a 12-hourly rotation in the direction of movement which is probably associated with solar semi-diurnal tidal oscillations in the atmosphere, in the *F*-region the variations have a predominant period of 24 hours.

Thus it appears from BRIGGS and SPENCER'S conclusions that in temperate latitudes the movements of the *F*-region are due more to thermal than to tidal forces.

Though WILKES (1952) has pointed out that the dynamical theory of atmospheric movements applicable at heights below 100 km has no relevance to oscillations in the *F*-region, BAKER and MARTYN (1953) have shown that the polarization field of the *E*-region will cause motion of both neutral and ionized particles in the *F*-region.

MARTYN (1953) has shown that E–W drifts of *F*-region ionization cannot be due to E–W winds, for the ionized particles cannot easily be moved transverse to the earth's magnetic field, but has suggested that E–W movements of ionization in the *F*-region may be due to N–S fields which are produced by the tidal movements of ionization in the *E*-region.

The absence of semi-diurnal movements of ionization in the *F*-region at high latitudes where large semi-diurnal movements are present in the *E*-region (BRIGGS and SPENCER, 1954) indicates that electro-dynamical interaction between the *E*- and *F*-regions is not a major factor in determining movements of *F*-region ionization at those latitudes.

VOL. 6 1955

2. EXPERIMENTAL ARRANGEMENTS

In order to measure movements of ionization by the spaced aerial method, it is necessary to use a frequency high enough not only to penetrate the *E*-region but to prevent any *E*-region irregularities from affecting the ground diffraction pattern attributed to the *F*-region. At the same time the operating frequency must be lower than f_0F_2, the ordinary ray critical frequency of the F_2 region. As values of f_0F_2 as low as 7 Mc/sec were to be expected at Singapore during daylight hours in the December solstice at sunspot minimum, it was decided to use a frequency of about 6 Mc/sec. The use of this frequency made it possible to obtain measurements from 0700 to about 2200 L.M.T.

The spaced aerials each consisted of a single turn screened loop of area about 1·5 sq metre, tuned with appropriate damping to cover the frequency range 5·8–6·8 Mc/sec. These loops and the aperiodic transmitting aerial were erected in the magnetic N–S plane, so as to reduce the amplitude of the extraordinary component of the reflected wave in relation to the ordinary component, and thus to eliminate complications due to fading between the two components of the downcoming wave.

The spacing between pairs of loops in the N–S and E–W directions was chosen to be approximately equal to one wavelength.

The loops were transformer-coupled to 100-ohm transmission lines which ran to an electronic three-way switch unit. This switch was synchronized with the

transmitted pulses so that successive pulses and echoes were accepted from each of the three loops in turn. The amplitudes of the echoes (reflected from a selected range of virtual height) at each of the three loops were simultaneously displayed, and photographed on moving film.

3. Results

Preliminary tests were made during July and August 1953, and regular measurements were obtained from September 1953 to April 1954 inclusive. During this period over 700 records each of about five minutes duration were obtained, though only 35% of these yielded measurable time delays.

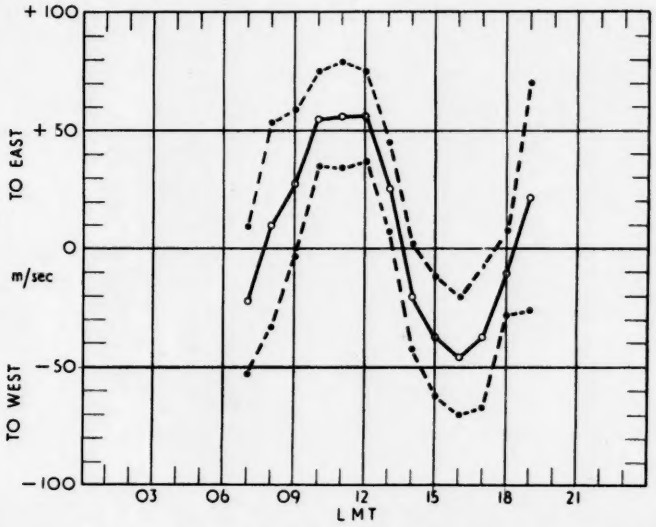

Fig. 1. Diurnal variation of E-W drift velocity in the *F*-region at Singapore during the period September–October 1953. The spacing between the broken lines is equal to twice the standard deviation.

During this programme it was seldom possible to obtain measurements of the N–S velocity component, even when the fading pattern was of a suitable form and the E–W component was measurable. The few N–S values obtained varied widely from day to day, and it was impossible to determine any significant diurnal or seasonal variations. However, the few N–S movements measured indicated a tendency for movements towards the south between 0900 and 1500 L.M.T.

It is therefore supposed that the electron wind system in the *F*-region above Singapore is predominantly E–W, though several years' measurements may be required before this can be established.

The movements of ionization in the E–W direction above Singapore showed regular diurnal and seasonal variations, which will now be described.

The results obtained during the periods September–October 1953, November 1953–February 1954, and March–April 1954 were grouped together. In order to

obtain a smoothed curve of the diurnal variation of the E–W component during each of these periods, the following procedure was adopted. For any hour t_0, all measured values obtained at times between $(t_0 - 1)$ and $(t_0 + 1)$ hours were grouped together, and the median value of this group was taken as the velocity at time t_0. The process was repeated for all hours of the day.

The diurnal variations of the median values so obtained for the periods September–October 1953, November 1953–February 1954, and March–April 1954 are shown in Figs. 1, 2, and 3 respectively, where positive values correspond to movements towards the east.

The standard deviations corresponding to the points shown on these figures

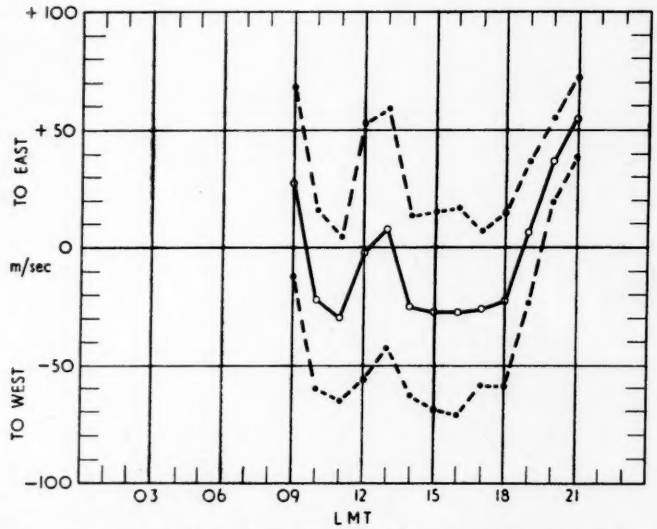

Fig. 2. Diurnal variation of E-W drift velocity in the *F*-region at Singapore during the period November 1953–February 1954. The spacing between the broken lines is equal to twice the standard deviation.

were calculated on the basis of the normal error law, and are shown by means of the broken lines. The spacing between the two broken lines at any hour is equal to twice the standard deviation at that hour.

It is evident from Fig. 1 that during the equinoctial period September–October 1953 the E–W movements varied sinusoidally during the day, with a period of approximately 12 hours and maximum amplitude 50 m/sec, directed towards the east between 0730 and 1330, and towards the west between 1330 and 1830. Every individual measurement obtained between 1000 and 1300 showed the existence of a movement to the east, and every one between 1400 and 1800 showed a movement to the west. This regularity was in marked contrast to the results of daytime *F*-region measurements at higher latitudes. It will be observed that at the times of maximum velocity the standard deviation was appreciably smaller than the median value.

The regular semi-diurnal pattern obtained at the equinox was not present at

VOL. 6 1955

the solstice. Fig. 2 shows that during the December solstice the median value of the E–W component during the morning hours was reversed in direction, the standard deviation being larger than the median hourly values. Thus at the solstice some disturbing influence was present before noon, though later in the day the diurnal variation of the E–W component was similar to that at the equinox. At night up to 2200 the movements were towards the east, the corresponding standard deviations being small. This is the opposite direction to *F*-region movements at the same time at high latitudes.

The *F*-region structure at Singapore during the morning hours of the December solstice is marked by the appearance of high level ledges of ionization within a

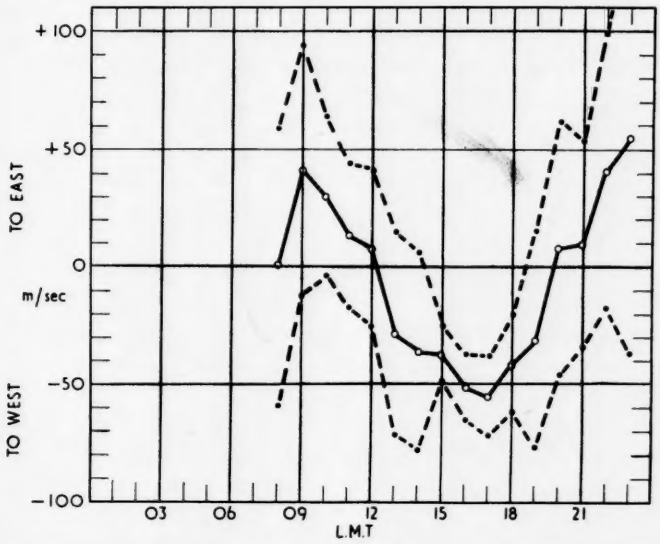

Fig. 3. Diurnal variation of E-W drift velocity in the *F*-region at Singapore during the period March–April 1954. The spacing between the broken lines is equal to twice the standard deviation.

very thick layer, with associated changes in the number of electrons below the height of maximum ionization density as the ledges of ionization move upwards (OSBORNE, 1951, 1952, 1953). This behaviour thus appears to be associated with irregularities in the E–W ionization drift velocity.

Whereas at the equinoxes all measurements were made on echoes reflected from virtual heights of between 300 and 400 km, during the morning hours of the December solstice the virtual heights of the echoes used for the measurements ranged from 450 to 650 km. Unfortunately it was not possible to determine the real heights to which the measured movements referred, as the deviative attenuation in the thick *F*-region was appreciable and the observed irregularities may have been present at any height within the lower part of the region.

No correlation between the virtual height and the velocity of movement was found.

The E–W movements of ionization at Singapore during the equinoctial period March–April 1954 are shown in Fig. 3, where it is evident that the dominant period is once again 12 hours and that the anomalous effects characteristic of the morning hours of the December solstice are absent. Comparison with Fig. 1 shows that though the amplitudes of the semi-diurnal variations at the two equinoxes are similar, the curve for March–April 1954 appears to be displaced downwards, indicating that during daylight hours the mean wind was towards the west, in contrast to the symmetrical variation of Fig. 1. It will also be noticed that during the period March–April 1954 the standard deviations were much higher in the mornings than in the afternoons.

4. CONCLUSIONS

It is concluded that regular semi-diurnal variations of the E–W movements of ionization within the *F*-region above Singapore are present at the equinoxes. The amplitude is approximately 50 m/sec, and the movements are towards the east during the mornings and between sunset and midnight, and towards the west during the afternoons.

It is supposed that the semi-diurnal movements of ionization in the equatorial *F*-region are caused by electric fields originating in the *E*-region and showing the solar semi-diurnal tidal variations characteristic of that region. Comparison of simultaneous measurements of *E*- and *F*-region movements of ionization near the equator would therefore be of interest. This has not yet been possible at Singapore. An attempt was made to measure *E*-region movements by using sporadic *E* echoes at a frequency of about 6 Mc/sec, but the occurrence of sporadic *E* was too infrequent for the results to be of use.

The cause of the disturbing influence in the equatorial *F*-region above Singapore during the mornings of the December solstice is not yet known. It is apparent that the disturbances in the layer structure at this time are associated with irregularities in the horizontal ionization drift velocity.

Acknowledgments—The author wishes to thank Mr. J. A. RATCLIFFE and Dr. B. H. BRIGGS, of the Cavendish Laboratory, Cambridge, for their most helpful co-operation and encouragement. He is indebted to the Director of Radio Research, D.S.I.R., and the staff of the D.S.I.R. Radio Research Sub-Station at the University of Malaya, for the loan of some equipment and for ready access to ionospheric data.

The work described was carried out in the Physics Department of the University of Malaya, and the author wishes to thank Mr. C. G. WEBB, the head of the department, for his co-operation.

The loan of a mast by the Telecommunications Department, Malaya, is gratefully acknowledged.

REFERENCES

BAKER, W. G., and MARTYN, D. F. 1953 Phil. Trans. Roy. Soc. A **246**, 281

BOOKER, H. G., RATCLIFFE, J. A., and SHINN, D. H. 1950 Phil. Trans. Roy. Soc. A **242**, 579

BRAMLEY, E. N. 1953 Proc. Roy. Soc. A **220**, 39

BRIGGS, B. H., PHILLIPS, F. J., and SHINN, D. H. 1950 Proc. Phys. Soc. B **53**, 106

VOL. 6 1955

Briggs, B. H., and Spencer, M.	1954	Reports on Prog. Phys. **17**, 245
Hewish, A.	1952	Proc. Roy. Soc. A **214**, 494
Martyn, D. F.	1953	Phil. Trans. Roy. Soc. A **246**, 306
Maxwell, A., and Little, C. G.	1952	Nature (Lond.) **68**, 746
Osborne, B. W.	1951	J. Atmosph. Terr. Phys. **2**, 66
	1952	J. Atmosph. Terr. Phys. **3**, 58
	1953	J. Atmosph. Terr. Phys. **4**, 82
Pawsey, J. L.	1935	Proc. Camb. Phil. Soc. **31**, 125
Phillips, G. J.	1952	J. Atmosph. Terr. Phys. **2**, 141
Wilkes, M. V.	1952	Q. J. Roy. Met. Soc. **78**, 321

L.
55

Journal of Atmospheric and Terrestrial Physics, 1955, Vol. 6, pp. 124 to 128. Pergamon Press Ltd., London

An apparatus for recording time-delays between radio fading characteristics

G. J. PHILLIPS

(*Received* 23 *June* 1954)

ABSTRACT

Details are given of a simple apparatus designed to record time-delays between the characteristics of the fading of a radio signal as received at two spaced aerials.

1. GENERAL PRINCIPLES

One method (PHILLIPS, 1952) for the study of ionospheric movements makes use of the time displacement between fading curves recorded from spaced receiving aerials. Fig. 1(a) shows a pair of fading curves of the type used, and the time-delays between the minima are indicated by the arrows. This paper describes an apparatus with which a direct record of these time-delays can be made.

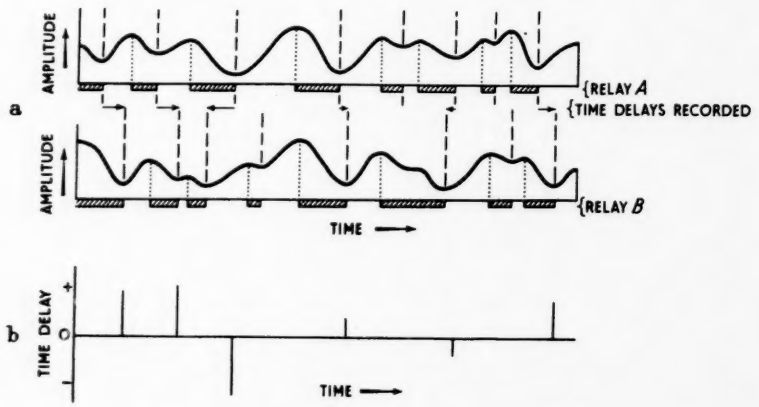

Fig. 1. (a) Fading curves, (b) Response of recorder set to operate on minima.

The principle of the method can be understood by considering its application to the records of Fig. 1(a). Whenever the two amplitudes pass in succession through minimum values a condenser is given a charge proportional to the time between the occurrences of the two minima. It is then discharged through a centre-zero pen recorder, being connected to it with a polarity which depends on the sense of the time-delay. The record corresponding to Fig. 1(a) would thus have the form shown in Fig. 1(b). Here the occurrence of a "spike" indicates that both amplitudes have passed through minimum values, the direction of the spike indicates which signal first fell to a minimum, and the length of the spike is a measure of the appropriate time interval.

Records of the new type may be made in place of records of actual fading as in Fig. 1(a). The paper can be run through the recorder considerably more slowly

VOL. 6 1955

without loss of accuracy in the time measurement, and statistics of the time-delays can be extracted more easily. The new method of recording is therefore more convenient, and is particularly useful for continuous recording over long periods. Fig. 2 shows an actual record taken on 16th October 1950 from two aerials spaced 120 m in a N–S direction and receiving a signal on 2·4 Mc/s reflected vertically from the E-layer.

In a record of this kind it is seen that there are considerable differences between successive deflections, due to the imperfect correlation between the input waveforms. The mean of the deflections (with due regard to sign) over a period of

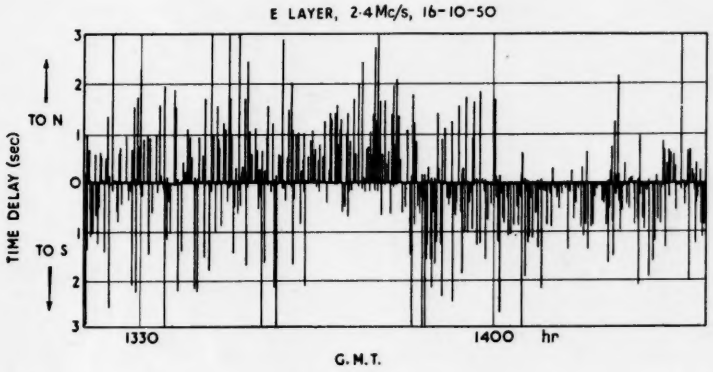

Fig. 2. Sample recording.

ten minutes or more nevertheless often differs significantly from zero, and the time corresponding to this mean deflection may be taken as the best estimate of a significant time-delay over the corresponding period.

2. Circuit Details

The working of the circuit may be considered in four parts, as illustrated in Fig. 3:

(a) Production of an "on/off" waveform in each channel.
(b) Relay responding to the magnitude of the time difference.
(c) Relays responding to the sense of the time difference.
(d) Charging of a condenser, and discharge through the recorder.

The first part of the circuit, shown in Fig. 3(a), is designed to accept a d.c. input varying in proportion to the amplitude of the signal from one aerial. Fluctuations which are too rapid to be genuine fading are first smoothed out, and relay coil X is made to operate only when the input is increasing; this in turn causes coil A to operate only when the input is decreasing. An identical circuit to that of Fig. 3(a) is associated with the second input, and operates relay B similarly, i.e., when the second input is decreasing. The operation of relays A and B which would correspond to the upper and lower curves of Fig. 1(a) is shown immediately beneath each curve.

The circuit achieves this result as follows. The valve V_2 has no grid-leak; thus whenever the input voltage is rising, the grid potential rises until limited at

-1 volt by one of the diodes V_1. When the input is falling, the grid potential falls until limited by the other diode at -3 volts. Since the range of variation of the input is kept relatively large (at least 30 volts), the grid voltage has a substantially "square" waveform between the limits of -1 and -3 volts, and the associated variations of anode current produce the required on/off action of the contact of relay X.

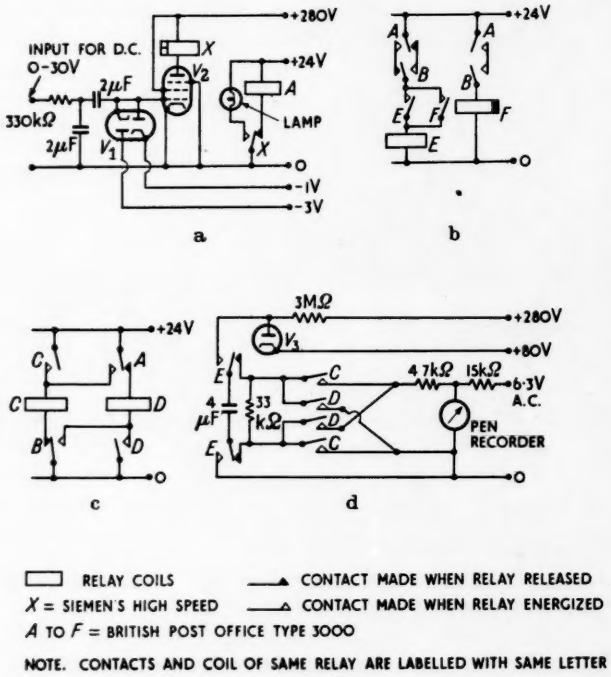

Fig. 3. Circuits of recorder.

The part shown in Fig. 3(b) is sensitive to any time difference between the release of relays A and B. (These operate the contacts marked with the appropriate letter.) It is seen that relay E is energized for a period during which relays A and B are "different"—i.e., when only one is operating—but that it will not operate in this manner unless, just previously, relays A and B were energized simultaneously. This restriction is ensured by relay F, which is arranged to have a slightly delayed release action.

The part in Fig. 3(c) responds to the time sequence of the release of relays A and B. Thus, relay C will operate if A is energized and B is not, and will remain operating if this condition is followed by the release of A, leaving both A and B de-energized. However, relay D, and not relay C, is left operating if the same final condition is approached through relay B releasing *after* relay A.

Finally, Fig. 3(d) shows how the parts of the circuit so far considered are made to control the recorder. A condenser is slowly charged for the length of time during

VOL. 6 1955

which E operates, and is then discharged through the recorder, provided that either relay C or relay D remains energized.

Consideration of the complete circuit shows that

(i) the condenser will not be charged and then discharged through the recorder unless the condition in which both A and B are energized is followed by the condition in which both A and B are released (see Fig. 1).

(ii) the condenser is charged (by a substantially constant current up to the limiting charge imposed by the diode) for the time interval between the releasing of A and of B.

(iii) the polarity with which the charge is applied to the recorder depends on the order in which A and B are released.

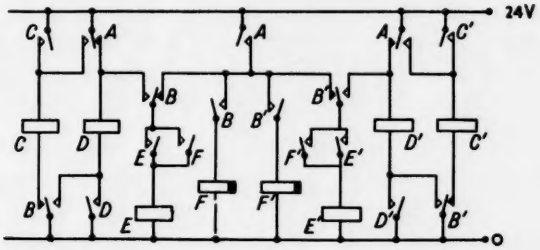

Fig. 4. Circuit used in 3-channel system.

In the first model constructed, a deflection to the edge of the recorder chart was made to correspond to about plus or minus 5 seconds; but to avoid undue jolting of the pen, the deflection was limited just short of full scale by means of diode V_3 in Fig. 3(d).

Certain practical points concerning the complete apparatus may be noted.

(i) It was found beneficial to run the heater of diode V_1 below nominal rating. This reduced leakage via the first cathode, and increased the diode impedance for small back-voltages.

(ii) The recorder may be made to time maxima of the input waveform instead of minima by interchanging make and break contacts either on relays such as X or on relays A and B. To obtain delay-times based on maxima and minima simultaneously, however, duplication of most of the recorder control circuits would be required.

(iii) At the slow recording speed used it was found that the accuracy with which the recorder returned to zero after deflection was limited somewhat by friction of the pen. It was improved by passing a small alternating current through the recorder as shown in Fig. 3(d).

(iv) Since the recorder was used ballistically, some steady form of damping was desirable. Magnetic damping proved to be the most satisfactory type to use.

(v) Strictly speaking, the switching of relay A or B does not occur exactly *at* a maximum or minimum, but when a change of amplitude of about 1 volt *following* a maximum or minimum has occurred. Some "back-lash" effect of this kind is practically essential to reduce spurious responses in the presence of small fluctuations due to noise, etc. For unattended operation over a long period it is also

desirable to use a very slowly-acting automatic gain-control arrangement to keep the mean input levels at 10 to 15 volts, otherwise trouble from overloading in the receiver may arise.

(vi) When circuits of the type described are used to record two time-delays between input pairs having a common channel, some economy of components can be made by using three (instead of four) circuits of the type shown in Fig. 3(a), followed by the circuit of Fig. 4, and finally two circuits of the type in Fig. 3(d).

3. CONCLUSION

The arrangement described can record time-delays in the range 0·1 to 5 seconds, and has an instrumental accuracy of about 0·1 second. It has been used at the Cavendish Laboratory, Cambridge, since October 1950, in a series of experiments on ionospheric movements which was started as part of a programme of radio research supported by a grant from the Department of Scientific and Industrial Research.

REFERENCE

PHILLIPS, G. J. 1952 *J. Atmosph. Terr. Phys.* **2**, 141

, VOL. 6 1955

Journal of Atmospheric and Terrestrial Physics, 1955, Vol. 6, pp. 129 to 132. Pergamon Press Ltd., London

The geomagnetic post-perturbation effect

R. P. Waldo Lewis
Meteorological Office, Edinburgh

(*Received* 22 *June* 1954)

ABSTRACT

The belief that during magnetically quiet periods following disturbance the horizontal force H continues to increase for a very long time is shown to be ill-founded. A tentative estimate is made of the actual duration of the recovery of H to its undisturbed level.

It is often stated that during periods of magnetic quiet following disturbance the horizontal magnetic field (H) continues to increase for a very long time at a virtually constant rate (Chapman and Bartels, 1940). Describing the course of a magnetic storm, Martyn (1951) says that there is "finally a slow recovery, which may take days, weeks, or even months." McNish (1936) has given a diagram purporting to show that at Watheroo H increases uniformly during quiet spells over periods of up to fourteen days at a rate of 4γ/day.

It seems desirable to investigate the evidence for these statements.

It is undoubtedly true that on occasions H does continue to increase for a long time after a magnetic storm. Chapman and Bartels (1940) give a diagram due to Schmidt (1953), consisting of a plot of monthly means of force components at Potsdam for seven years, and say that it shows "the long continuance of the increase, when the conditions are suitably quiet." Schmidt himself argues that full recovery would take years. However, if such plots of monthly or daily mean H are compared with the corresponding plots of the international C figure, it becomes clear that long-continued increases of H are associated not with long quiet periods but with a steady decrease in the average level of activity. For the six-monthly period July–December 1947 the correlation coefficient between daily mean H at Eskdalemuir and C was $-0{\cdot}65$. On taking five-day block means, the correlation was increased to $-0{\cdot}80$. This period included some long-continued increases.

We now consider McNish's paper. His diagram is based upon the selection of groups of two or more quiet days. Each day was assigned a number representing the interval of time elapsing since the last international D day. The differences between the mean daily values of H for each group of quiet days was then obtained, and the sums derived of the differences between correspondingly numbered means for all the groups. The sums were then divided by the number of differences entering into each. The result, which is that the mean difference between successive days is almost constant, is regarded by McNish as demonstrating a steady rise of H for at least a fortnight after a disturbed day.

In fact, however, the result merely shows up the non-cyclic change (NCC) on quiet days that are on average immediately preceded by days of moderate or small, though still appreciable, disturbance. An exception is formed by the very beginning of the series; this immediately succeeds a D day and would be expected to show a larger NCC: according to McNish's diagram, the mean of the first two differences is $5{\cdot}5\,\gamma$, and of the succeeding twelve, $3{\cdot}3\,\gamma$. For comparison with McNish's result, a similar selection of days from an independent

period (1940–5) was made, and applied to daily mean values of H at Lerwick. The mean of the first two differences was 3·3 γ, and of the succeeding six, 2·1 γ. (The smaller overall value of the differences is due to the higher geomagnetic latitude of Lerwick.)

It thus seems that there is no valid evidence that free recovery of H (i.e., recovery unaffected by continued particle disturbance) from its depressed value during a storm continues for long periods.

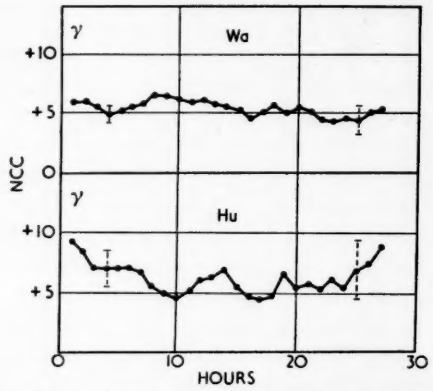

Fig. 1. Progress of 24-hour noncyclic changes in horizontal force at Watheroo and Huancayo during quiet periods Kp $\leqslant$ 1+.

VOL. 6 1955

The storm-time depression of H is usually considered to be due to an extra-terrestrial ring-current produced by solar particle radiation; the decay of this current is manifested in the post-perturbation rise of H, which may therefore be expected to have an exponential dependence on time. (This shows that the linear rise suggested by MCNISH is a priori unlikely.) Published curves showing the storm-time variation of H do indeed seem to show exponential decay, but they are irregular and are complicated by the long continuance of above-average disturbance, so that estimation of the time-constant is not possible.

An obvious way of determining the time-constant is to find the average variation of H force during an extended period of great quietness. To this end 105 periods of not less than thirty-hours duration were chosen from the years 1940–47 such that the international planetary index Kp was never greater than 1+. These periods were not long, and only forty-five lasted for more than forty-eight hours. The progress of horizontal force during these intervals could then be found by writing down the consecutive 24-hour NCC's that were wholly included in each quiet interval. (The use of a 24-hour NCC is necessary to eliminate the effect of diurnal variation.) Two stations, Watheroo (Wa) and Huancayo (Hu), were investigated. The results are shown in the figure. Standard errors (S.E.'s) of selected plotted points are indicated.

Unfortunately, the S.E.'s are too great for any estimate to be made of the time-constant: any departure of the NCC from constancy with time is not demonstrable. (The much greater SE of the curve for Hu is indicative of the large fluctuations of the Q-day variation that occur there.)

Another possible method can be developed from results given in a previous paper (LEWIS and MCINTOSH, 1953). In this paper the average effect on various parameters of a day of peak magnetic Kp disturbance was investigated. At Eskdalemuir the peak disturbance produces a delayed and asymmetrical trough in H-force; the latter part of this lies well on an exponential curve which we may assume indicates slow recovery to a level appropriate to the moderate and approximately constant disturbance that precedes and follows the isolated peak (Figs. 1a and 1b, *loc. cit.*). If H decays as $10^{-t/\tau}$, where t is time, then $\tau = 1{\cdot}7$ days, i.e., the depression of H is reduced to 0·1 of its value in 1·7 days.

Another tentative estimate of τ may be made by measuring the lag between the turning points of the disturbance and H-force curves, and using the following rather crude argument:

Suppose that a constant level of range disturbance R produces a constant depression of H-force, and that if the disturbance is removed, H recovers to its undisturbed value exponentially. If Δ is the departure of horizontal force from the quiet value, an equation satisfying the above conditions is

$$\frac{\partial \Delta}{\partial t} + \frac{1}{\tau_1}\Delta = \frac{1}{\tau_1} f(R) \tag{1}$$

$$\therefore \qquad \Delta = \frac{1}{\tau_1} e^{-t/\tau_1} \int_{-\infty}^{t} f(R)\, dt \tag{2}$$

The sizes of the trough and peak in H relative to the peak and trough in R, leads us to assume that

$$f(R) \equiv kR$$

where k is a constant.

$$\therefore \qquad \Delta = \frac{k}{\tau_1} e^{-t/\tau_1} \int_{-\infty}^{t} R\, dt \tag{3}$$

For an isolated peak disturbance, centred at $t = 0$,

$$R = R_0 \cos\left(\frac{\pi t}{2T}\right) \qquad -T < t < +T$$

$$= 0 \qquad t < -T, \quad t > +T$$

whence

$$\Delta = \text{const. } e^{-t/\tau_1}\left(1 + \sin\frac{\pi t}{2T}\right) \tag{4}$$

R is a maximum at $t = 0$. Δ is a minimum at $t = t'$, where $\left(\frac{\partial \Delta}{\partial t}\right)_{t=t'} = 0$. This gives, using (4),

$$\tau_1 = \frac{2T}{\pi} \frac{1 + \sin\left(\frac{\pi t'}{2T}\right)}{\cos\left(\frac{\pi t'}{2T}\right)}.$$

Referring to the published figure, we see that plausible values of $2T$ and t' are forty-eight hours and twelve hours respectively.

Hence $$\tau_1 = 0{\cdot}90 \text{ day}$$

or $$\tau = \frac{0{\cdot}90}{\log_{10} e} = 2{\cdot}1 \text{ days}$$

a result of the same order as that obtained above.

There thus seems to be some reason for thinking that the time-constant of decay of the delayed depression of horizontal force due to magnetic disturbance (i.e., the time in which the depression diminishes to 10 per cent of its initial value) is about two days. (This delayed depression is most marked near the equator and is masked in and near the auroral zone by a different and simultaneous effect.)

This result is not inconsistent with the variations of NCC in very quiet periods considered above, because of the large errors apparent in the latter.

Long-continued increases in H-force that occur in practice are due simply to a slow change from high magnetic activity to low magnetic activity.

This note is published by permission of the Director, Meteorological Office.

References

Chapman, S., and Bartels, J.	1940	*Geomagnetism* (O.U.P.), p. 292
Martyn, D. F.	1951	*Proceedings of the Second Meeting of the Mixed Commission on the Ionosphere*, p. 49
McNish, A. G.	1936	*Transactions of Edinburgh meeting of the I.U.G.G. Association of terrestrial magnetism and electricity*, p. 270
Lewis, R. P. W., and McIntosh, D. H.	1953	*J. Atmosph. Terr. Phys.* **4**, 44
Schmidt, A.	1925	*Z. Geophys.* **1**, 3

VOL. 6 1955

Journal of Atmospheric and Terrestrial Physics, 1955, Vol. 6, pp. 133 to 140. Pergamon Press Ltd., London

The diffusion of ionized meteor trails in the upper atmosphere

J. S. GREENHOW and E. L. NEUFELD
Jodrell Bank Experimental Station, University of Manchester

(*Received* 18 *August* 1954)

ABSTRACT

The variations with height of the durations of radio echoes from ionized meteor trails are discussed. At wavelengths of 8·27 m and 4·35 m echo duration decreases approximately exponentially between altitudes of 80 and 100 km, in the manner predicted by diffusion theory. The diffusion coefficient between these heights varies between 10^4 and 10^5 cm²/sec. These figures are very close to the theoretical estimates of diffusion coefficient, calculated from the rocket panel values of upper atmosphere air densities.

1. INTRODUCTION

Radio echoes from meteor trails have been observed over a wide band of wavelengths from 100 m to 1·4 m. Consideration of the wavelength dependence of echo duration shows that diffusion processes are mainly responsible for the dispersal of the ionized matter. Factors such as the loss of electrons by recombination and attachment are unlikely to affect the durations of the majority of echoes observed at wavelengths less than 10 m (GREENHOW, 1952; KAISER and GREENHOW, 1953). Echo duration should thus be closely related to the altitude of a meteor trail. Hitherto no direct height-duration measurements have been made, although average values of diffusion coefficient relating to the mean heights of groups of shower meteors have been determined (GREENHOW, 1952; CLOSS, CLEGG, and KAISER, 1953). The variation of diffusion coefficient and echo duration with height forms the subject of the present paper.

2. TECHNIQUE

The method used for height measurements was the split beam technique described by CLEGG and DAVIDSON (1950) and EVANS (1954). In the present experiments the transmitter operated at a wavelength of 8·27 m with a peak power of 50 kW and pulse repetition frequency of 600 + 150 c/s (every fourth pulse is doubled to remove range ambiguities). The transmitting aerial consisted of a horizontal half-wave dipole and reflector at a height of $\lambda/2$ above the ground. Two receiving aerials similar in construction to the transmitting aerial were used. These were at heights of $\lambda/2$ and $\lambda/4$ above a good reflecting surface. Ground reflections cause differences in the polar diagrams of the two aerials, and the ratio of the echo amplitudes received by each gives the elevation of the reflecting point. The ratio-elevation relation is given in Fig. 1. An error in ratio of 5 per cent (an approximate value for a ten-times receiver noise echo, lasting 0·05 sec) leads to an error in elevation of 1·2°. Ranges can be measured to within $\pm 1{\cdot}5$ km; thus for a trail at an elevation of 45° the error in height is $\pm 2{\cdot}5$ km.

For duration and elevation measurements the receiver outputs were displayed as vertical deflections on two cathode-ray tubes. The horizontal deflections on these tubes were time bases triggered by the first echo pulse of predetermined amplitude to be received from an ionized trail. One time base had a duration of

0·07 sec, and enabled very short duration echoes to be observed accurately, since successive echo pulses separated by 1·2 milli-sec could be resolved. The other time base had a duration of 0·3 sec. This was long enough to include the half-amplitude decay times of 95 per cent of all meteor echoes. Echo range was recorded on a third cathode-ray tube. Each time an echo triggered the apparatus the display was automatically photographed, the film then winding on in preparation for the next echo.

In addition to the height-duration observations made at a wavelength of 8·27 m, a number of 4·35 m meteor height measurements obtained in the course of another experiment (EVANS, 1954) have also been analyzed for height-duration correlations.

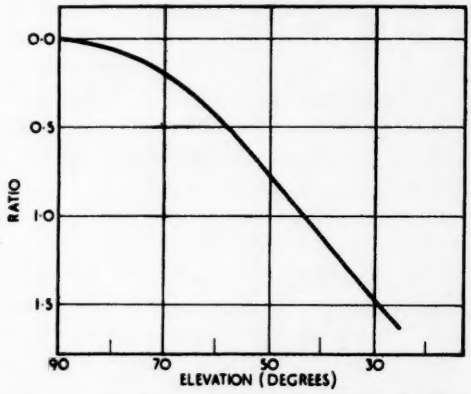

Fig. 1. Ratio of echo amplitude received by an aerial at a height of $\lambda/2$, to that received by an aerial at a height of $\lambda/4$, as a function of elevation of the reflecting point.

VOL. 6 1955

3. SELECTION OF ECHOES IN HEIGHT-DURATION ANALYSIS

(a) *Low electron density trails*

The ionized trails can be divided into two main groups, in which the linear electron density α is greater or less than approximately 10^{12} electrons/cm (GREENHOW, 1952; KAISER and CLOSS, 1952). For low-density trails with $\alpha < 10^{12}$ electrons/cm HERLOFSON (1948) has shown that the echo amplitude decays in the manner

$$A = A_0 \exp(-16\pi^2 Dt/\lambda^2) \qquad (1)$$

Where A_0 is the initial amplitude and A the amplitude after time t. The decay constant $T_L = \lambda^2/16\pi^2 D$, which defines the duration to $1/e$ of the initial amplitude, depends only upon the wavelength and diffusion coefficient. Thus at a given λ and D the echoes from all "low-density trails" decay with the same time constant (Fig. 2).

Examples of echoes from such trails are shown in Fig. 3(a) to (e). These are characterized by a rapid initial rise in echo strength, followed by small amplitude fluctuations due to diffraction effects during the formation of the trail (DAVIES and ELLYETT, 1949). The maximum echo amplitude coincides with the first maximum of the diffraction pattern. Beyond this point the echoes decay exponentially with the decay constant T_L.

Eq. 1. was derived on the assumption that a meteor trail is formed instantaneously. In practice this is not so, since a meteor has a finite velocity V, generally in the range 15–70 km/sec. If the time taken for the meteor to travel through the first Fresnel zone is large compared with the decay constant T_L, then the wavelets scattered from small elements of trail at the beginning of the zone will have already decayed to $1/e$ of their initial values before the formation of the zone is complete.

Thus when $$VT_L \leq 2\,(R\lambda/2)^{\frac{1}{2}} \qquad (2)$$

the maximum theoretical echo amplitude is never attained (KAISER, 1953), and

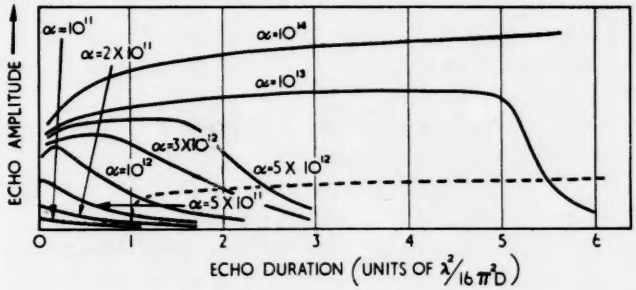

Fig. 2. Theoretical echo forms as a function of electron line density α (after KAISER). The broken line indicates the duration to $1/e$ of the maximum amplitude.
Abscissa: Time after trail formation, in units of $\lambda^2/16\pi^2 D$. Ordinate: Relative amplitude.

appreciable departures from the simple decay predicted by Eq. 1 may be expected. [$(R\lambda/2)^{\frac{1}{2}}$ is the radius of the first Fresnel zone.] As $T_L \propto \lambda^2/D$ this condition is reached first at shorter wavelengths and greater heights.

Only echoes showing exponential amplitude decays are used in the analysis. Smooth curves are drawn through the small diffraction fluctuations, and the decay times $T_{\frac{1}{2}}$ to one-half the maximum amplitude are measured. ($T_{\frac{1}{2}} = \log_e 2 \,.\, T_L$.)

(b) *High electron density trails*

When $\alpha > 10^{12}$ electrons/cm the volume electron density in a trail may exceed the critical density N_c at large-trail radii. These "high-density trails" behave as totally reflecting cylinders, and an echo is received as long as the electron density is greater than N_c (GREENHOW, 1952). For this reason the echo duration T_H depends upon α, in addition to varying with λ and D. These echoes may also show the rapid initial rise in amplitude, followed by diffraction fluctuations. Instead of decaying exponentially, however, the amplitudes remain fairly constant for some time and then rapidly fall to zero (Fig. 2). Most echoes of this type have durations $\gg 0{\cdot}3$ sec at $\lambda = 8{\cdot}27$ m, and cannot be completely recorded on the slow-time base (Fig. 3(h)). Fig. 4 is the plot of an echo obtained using an earlier continuously moving film recorder. The deep amplitude fluctuations which begin after 1 sec are due to distortion of the initially linear trail by irregular high atmosphere winds, causing deviations from the theoretical model (GREENHOW, 1950, 1952).

Echoes from trails near the transition region between the "low" and "high" electron density groups are illustrated in Fig. 3(f) and (g). These echoes show the

flattening in the amplitude envelopes associated with over-critically dense trails, while still retaining appreciable exponential tails. Echoes of the type discussed in Sect. 3(b) have been excluded from the following analysis, as their durations do not vary with height in any simple manner.

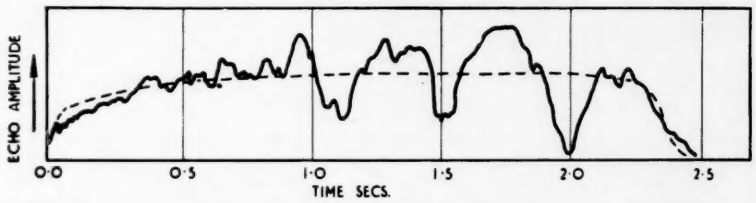

Fig. 4. Plot of an echo from a "high-density" trail observed at a wavelength of 8·27 m. The theoretical amplitude envelope for $\alpha = 2 \times 10^{13}$ electrons/cm and $D = 4 \times 10^4$ cm²/sec is shown for comparison.

4. Experimental Results

(a) *Wavelength of* 8·27 *m*

Combined height-duration measurements were carried out on a number of occasions during November 1953. The half-amplitude duration distribution of the 268 measurable "decay"-type echoes obtained during 10 hrs observation is given in Fig. 5(a). The most probable duration is 0·05 sec, 50 per cent lying between 0·03 and 0·08 sec. Only 5 per cent of the echoes have durations greater than 0·2 sec, and the shortest observed duration was 0·005 sec. The echoes have been divided into a number of duration groups. The mean heights and height spreads of the echoes in each group are given in Table 1.

VOL. 6 1955

Table 1. *Results of height-duration experiment at a wavelength of* 8·27 *m*

Half amplitude duration (sec)	*Mean height (km)*	*Number of echoes*	*Height spread (km)*
0·009	108·8	8	±5·5
0·015	105·6	24	±6·0
0·025	98·8	54	±5·1
0·040	97·0	70	±3·9
0·065	92·1	46	±5·0
0·107	89·4	35	±4·2
0·177	87·2	23	±3·8
0·294	84·5	8	±4·4
			Mean spread ±4·8 km

The experimental height-log duration relation is illustrated in Fig. 6, and a smooth curve AB has been drawn through the points. The half-amplitude durations at a wavelength of 8·27 m vary from 0·3 to 0·01 sec between heights of 85 and 107 km. Fig. 6 shows that echo decay time decreases approximately exponentially with height, the duration falling by a factor $1/e$ every 6·5 km. If diffusion is responsible for the dispersal of the ionized matter, then the duration

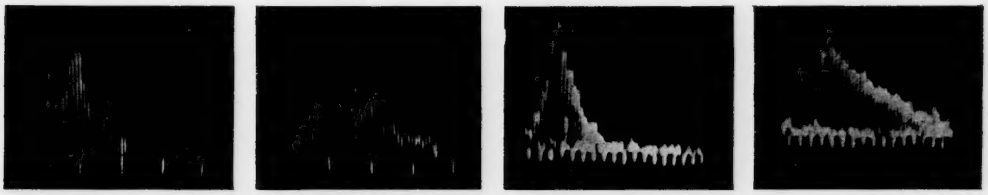

(a) $T\frac{1}{2}$ = 0·008 secs
P.R.F. = 600 c/s

(b) $T\frac{1}{2}$ = 0·02 secs
P.R.F. = 600 c/s

(c) $T\frac{1}{2}$ = 0·04 secs
P.R.F. = 150 c/s

(d) $T\frac{1}{2}$ = 0·12 secs
P.R.F. = 150 c/s

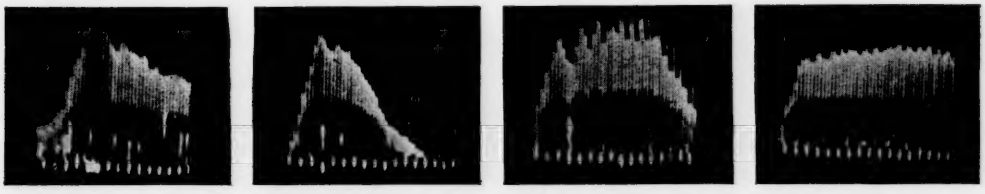

(e) $T\frac{1}{2}$ = 0·25 secs
P.R.F. = 150 c/s

(f) $\alpha \sim 2 \times 10^{12}$ electrons/cm
P.R.F. = 150 c/s

(g) $\alpha \sim 7 \times 10^{12}$ electrons/cm
P.R.F. = 150 c/s

(h) $\alpha > 10^{13}$ electrons/cm
P.R.F. = 150 c/s

Fig. 3. Observed echo forms at a wavelength of 8·27 m. (a) to (e) are echoes from low density trails; (f) to (h) are echoes from trails with $\alpha > 10^{12}$ electrons/cm. 50c/s bright up pulses mark the base of the receiver noise.

, VOL.
6
1955

$\propto 1/D \propto$ pressure; hence the echo duration should fall by $1/e$ in a scale height H. The value $H = 6{\cdot}5$ km is in good agreement with the average scale height between 80 and 100 km. Although H is proportional to the atmospheric temperature θ, as D varies only as $\theta^{\frac{1}{2}}$, the variation in temperature between 80 and 100 km is insufficient to give a measurable variation in the slope of the log duration-height curve. The slope of the curve does decrease above a height of 100 km, as illustrated by the departure from the broken line in Fig. 6. This is due to the effect of finite meteor velocity (Sect. 3(a)), and will be discussed later.

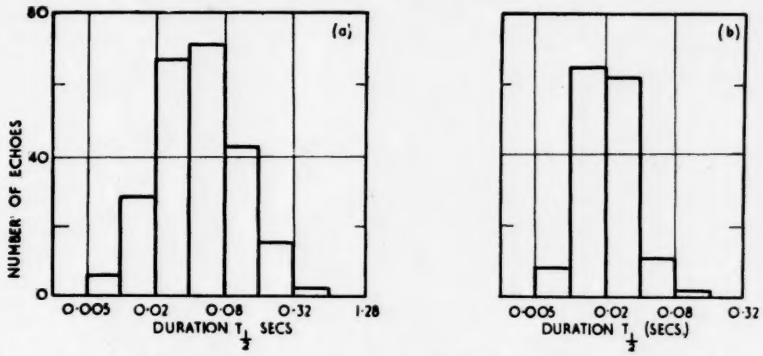

Fig. 5. Distributions of half-amplitude decay times of echoes used in height-duration analysis. (a) $\lambda = 8{\cdot}27$ m. (b) $\lambda = 4{\cdot}35$ m.

(b) *Wavelength of* 4·35 m.

A number of film records obtained by EVANS (1954) during height observations at a wavelength of 4·35 m have been analyzed for height-duration correlations. The 147 measurable decay echoes recorded over the period January to July 1952 have been treated in the same way as the 8·27 m observations (Table 2, Fig. 5(b)). The log duration-height relation is shown by the curve CD in Fig. 6. The decay times, of course, are much shorter than those for echoes at similar heights observed at the longer wavelength. The slope of the curve, however, is the same as that for $\lambda = 8{\cdot}27$ m up to a height of 95 km, giving a similar value for the scale height. Above 95 km there is an appreciable reduction in slope, as there was for $\lambda = 8{\cdot}27$ m above 100 km. This is shown by the departure of CD from the broken line, and as

Table 2. Height-duration measurements at a wavelength of 4·35 *m*

Half amplitude duration (sec)	*Mean height (km)*	*Number of echoes*	*Height spread (km)*
0·010	102·0	23	±4·1
0·016	97·0	42	±3·9
0·022	93·2	47	±3·8
0·033	90·5	22	±4·2
0·051	87·5	13	±4·3
			Mean spread ±4·1 km

before it is due to finite meteor velocity effects which become appreciable at lower heights on the shorter wavelength.

5. VARIATION OF DIFFUSION COEFFICIENT WITH HEIGHT

(a) *From observed echo durations*

The duration-height relations shown in Fig. 6 are applicable only to echoes observed on wavelengths of 8·27 or 4·35 m. A curve of more general application can be obtained by converting the decay times in Fig. 6 to the corresponding diffusion coefficients, using Eq. 1. For the idealized case of a meteor with infinite velocity, the curves of diffusion coefficient vs. height would then coincide for observations at all wavelengths.

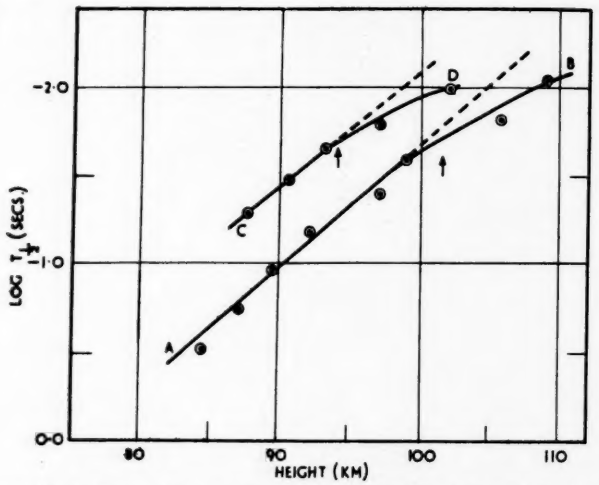

Fig. 6. Half-amplitude decay time $T_{\frac{1}{2}}$ vs. height, for echoes observed at $\lambda = 8{\cdot}27$ m (AB), and $\lambda = 4{\cdot}35$ m (CD). The arrows indicate the heights at which the condition given by Eq. 2 is reached.

The diffusion coefficients derived from the decay times of AB and CD, Fig. 6, are given in Fig. 7(a). Up to a height of 95 km the curves for 8·27 and 4·35 m are almost parallel, but displaced by approximately 1·5 km in height. This difference is probably caused by a systematic error in one or other of the two height-finding equipments. Elevations are measured using the calculated aerial polar diagrams, and a deviation in either polar diagram of only a half degree would produce a height error of 1·5 km for an echo at an elevation of 30°. In view of this factor, the agreement between the heights measured at wavelengths of 8·27 and 4·35 m is good.

At a height of 95 km the slope of the 4·35 m diffusion coefficient-height curve begins to fall below that of the 8·27 m curve. Adopting a value $D = 5 \times 10^4$ cm^2/sec for the 95 km level, the condition given by Eq. 2 is satisfied for a meteor at a range of 150 km, travelling with a velocity of 40 km/sec. Thus the concept of an instantaneously formed trail begins to break down in the 95 km region for a wavelength of 4·35 m. The apparent values of D measured from the decays of echoes above this height are therefore below the true values. The discrepancy amounts to approximately 30 per cent at a height of 97·5 km.

VOL. 6 1955

Because of the variation of the decay constant T_L with wavelength, the condition given by Eq. 2 is not reached at $\lambda = 8{\cdot}27$ m until a height of 100 km, where once more the apparent values of D begin to deviate from the true values. The discrepancy is approximately 30 per cent at a height of 102·5 km.

The adopted curve of diffusion coefficient vs. height is given in Fig. 7(b). The heights measured by the two equipments have been normalized, those at $\lambda = 8{\cdot}27$ m being reduced by approximately 0·75 km and those at $\lambda = 4{\cdot}35$ m increased by 0·75 km.

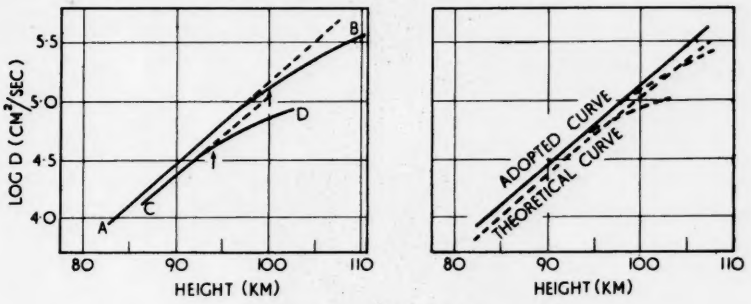

Fig. 7. Diffusion coefficient as a function of height.
(a) From observed echo durations at $\lambda = 8{\cdot}27$ m (AB), and $\lambda = 4{\cdot}35$ m (CD).
(b) Adopted values (continuous curve). The broken curve shows the calculated values of diffusion coefficient.

(b) *Theoretical variation of diffusion coefficient with height.*

The above experimental results may be compared with the theoretical values of diffusion coefficient in the following manner. An expression for D taking account of the electrostatic forces between the electrons and positive ions has been derived by KAISER (1953):

$$D = \frac{8}{3}\lambda_i \left(\frac{2k\theta}{\pi\mu}\right)^{\frac{1}{2}} \text{cm}^2/\text{sec} \qquad (3)$$

where λ_i is the ion mean free path, k Boltzmann's constant, θ the temperature, and μ the mean mass of a diffusing particle. Substituting JEAN'S formula for the mean free path in Eq. 3 gives

$$D = \frac{3{\cdot}5}{\pi n {\sigma_i}^2} \left(\frac{k\theta}{\pi\mu}\right)^{\frac{1}{2}} \text{cm}^2/\text{sec} \qquad (4)$$

Eq. 4 thus gives a direct relation between atmospheric particle density n and the rate of diffusion of meteor ionization, in terms of known or measurable quantities. The chief uncertainty in (4) is σ_i, the collision diameter for ionized meteor atoms and air molecules. No measurements for collisions between heavy meteor ions (Fe^+, Ca^+, Si^+, Mg^+, etc.), and air molecules (N_2, O_2), have been made, but experiments involving collisions between the ionized alkali metals (K^+, Na^+) and N_2 and O_2 molecules indicate that σ_i is of the order of $9{\cdot}2 \times 10^{-8}$ cm (RAMSAUER and BEECK, 1928). The theoretical variation of diffusion coefficient with height, obtained using Eq. (4) and the rocket panel air densities (1952), is shown for comparison with the experimental curve of Fig. 7(b). There is good agreement between the two curves.

6. ESTIMATION OF METEOR HEIGHTS FROM ECHO DURATIONS

The direct radio echo measurement of the heights of meteor trails requires accurately calibrated apparatus, employing multiple receiving aerials and carefully prepared reflecting surfaces. For some purposes an approximate estimate of meteor height is all that is required (GREENHOW, 1954), and this may be obtained for trails with $\alpha < 10^{12}$ electrons/cm from the echo decay time, using the experimentally observed variation of diffusion coefficient with height (Eq. 1).

Tables 1 and 2 show that the spread in heights for echoes of a given duration group is appreciable. The experimental error in each individual 8·27 m height determination is $\pm 2{\cdot}5$ km, and in each 4·35 m height measurement $\pm 1{\cdot}2$ km. A further $\pm 2{\cdot}0$ km is introduced because of the finite width of each duration group, and $\pm 1{\cdot}5$ km through the uncertainty in estimating the decay time of an echo. The error in estimating the height of an individual reflecting point from the echo duration is thus approximately $\pm 3{\cdot}0$ km. The residual error, which is due to a true spread of 1·5 : 1 in the decay times of echoes observed at a given height, may be caused by plasma resonance effects discussed by HERLOFSON (1948), and KAISER and CLOSS (1952). Echoes showing marked peaks which could be interpreted as reasonance phenomena, however, are excluded from the analysis as they do not satisfy the criteria given in Sect. 3(a).

A further cause of possible deviations from simple diffusion theory is the presence of the earth's magnetic field. This could reduce the rate of diffusion of electrons in a direction perpendicular to the lines of force. Because of collision frequency considerations, the earth's field is unlikely to influence echo durations at heights below 100 km (KAISER, 1953).

Acknowledgments—The work described in this paper was carried out at the Jodrell Bank Experimental Station, University of Manchester, under the direction of Professor A. C. B. LOVELL. The authors wish to thank Mr. S. EVANS for the use of his 8·27 m receiving aerials, and his valuable advice on height-finding techniques. They are also indebted to him for permission to analyze many of his 4·35 m height records for duration measurements. The Department of Scientific and Industrial Research have contributed to the cost of this experimental work, and one of the authors (J. S. G.) is in receipt of a D.S.I.R. Senior Research Award.

REFERENCES

CLEGG, J. A., and DAVIDSON, I. A.	1950	Phil. Mag. **41**, 77
CLOSS, R. L., CLEGG, J. A., and KAISER, T. R.	1953	Phil. Mag. **44**, 313
DAVIES, J. G., and ELLYETT, C. D.	1949	Phil. Mag. **40**, 614
EVANS, S.	1954	Mon. Not. Roy. Ast. Soc. (In press)
GREENHOW, J. S.	1950	Phil. Mag. **41**, 682
	1952	Proc. Phys. Soc. B**65**, 169
	1954	Phil. Mag. **45**, 471
HERLOFSON, N.	1948	Phys. Soc. Rep. Prog. Phys. **11**, 444
KAISER, T. R.	1953	Phil. Mag. Supp. **2**, 495
KAISER, T. R., and CLOSS, R. L.	1952	Phil. Mag. **43**, 1
KAISER, T. R., and GREENHOW, J. S.	1953	Proc. Phys. Soc. **B66**, 150
RAMSAUER, C., and BEECK, O.	1928	Ann. Physik. **87**, 1
Rocket Panel	1952	Phys. Rev. **88**, 1027

VOL. 6 1955

Journal of Atmospheric and Terrestrial Physics, 1955, Vol. 6, pp. 141 to 148. Pergamon Press Ltd., London

An ionospheric attenuation equivalence theorem

SIR EDWARD APPLETON* and W. J. G. BEYNON†

(*Received* 30 *September* 1954)

ABSTRACT

The phenomenon of radio-wave attenuation by way of ionospheric partial reflections and scattering is examined theoretically, and an equivalence theorem, relating oblique incidence to vertical-incidence phenomena, is derived. For radio frequencies well in excess of the equivalent critical frequency of the medium this may be written

$$\left[\rho\right]_{i_0}^{f} = \lambda \left[\rho\right]_{0}^{f\cos i_0}$$

where ρ is the fractional attenuation, f is the frequency, and i_0 the angle of incidence in the oblique-incidence case. Where the radio-wave electric vector is at right angles to the plane of propagation, λ is unity; when the electric vector lies in the plane of propagation, λ is equal to the usual obliquity factor $\cos 2i_0$.

1. INTRODUCTION

In a previous communication (APPLETON *et al.*, 1948) we have drawn attention to some experimental evidence indicating that scattering by sporadic *E*-layer clouds could, on occasion, be an important source of attenuation under conditions of practical radio communication. It thus appears that, in attempting to account for the variation of signal intensity with distance in cases of transmission by way of oblique incidence on the ionosphere, we must take into account three types of attenuation, namely—

(a) spatial attenuation;

(b) collisional electron-friction attenuation; and

(c) attenuation due to partial reflection or to scattering by ionospheric irregularities.

In previous studies of this subject only two of these three types of attenuation, namely (a) and (b), had been taken into account. In this communication we comment, in a general way, on all three types and draw attention to a new ionospheric attenuation theorem relating to (c).

2. SPATIAL ATTENUATION

In the absence of any deviation of an emitted beam of radio waves the signal intensity, of course, varies inversely as the distance. But, in the case where reflection by the ionosphere involves the travel of waves along a considerable curved path within the refracting layer, no such simple rule applies.

It is, however, possible to estimate the spatial attenuation in such cases, using the general theory we have previously given for ionospheric refraction at oblique incidence by a thick layer surrounding a curved earth (APPLETON and BEYNON, 1940; APPLETON and BEYNON, 1947). Knowing the ionospheric layer parameters, it is possible to express the range of transmission D in terms of α, the angle between

* The University, Edinburgh
† Department of Physics, University College of Swansea

the initial emergent beam at the sender and the vertical. If, now, we introduce an effective distance of transmission r', we have shown that

$$r' = \sqrt{\frac{R \sin \frac{D}{R} \cdot \frac{dD}{d\alpha}}{\tan \alpha}} \tag{1}$$

where R is the radius of the earth.

Here r' is the quantity to be introduced into the free-space transmission formula

$$E = \frac{7\sqrt{GW}}{r'} \tag{2}$$

to give the correct signal strength in the case of ionospheric refraction.

It will therefore be seen that the spatial attenuation of the ionospheric ray does not, in general, vary in a simple manner with the value of the range D. It will also be noted that (1) indicates two conditions under which marked focusing occurs. When $dD/d\alpha$ is zero, as it is under M.U.F. conditions, r' is zero and the signal infinite. We also see that, for radiation starting out tangential to the earth, tan α is infinite and the signal, again, infinite also. Of course the signal in such cases does not, in practice, actually assume infinite values, for it is under just such focusing conditions that a ray-treatment breaks down and must be replaced by a wave-treatment, as we have previously pointed out in our experimental study of M.U.F. conditions (APPLETON and BEYNON, 1947).

VOL. 6 1955

It is easy to transform (1) so that it relates to the case of a plane earth. For short distances sin (D/R) is equal to D/R, and we have

$$r' = \sqrt{\frac{D \frac{dD}{d\alpha}}{\tan \alpha}} \tag{3}$$

For sharp boundary conditions this becomes, as it should,

$$r' = \frac{2h}{\cos \alpha} \tag{4}$$

where h is the height of the ionosphere.

3. ATTENUATION DUE TO "ELECTRON COLLISIONAL FRICTION"

This type of attenuation has been fully studied in many previous papers. It is only necessary to note here that, for the magneto-ionic ordinary ray, we have, approximately,

$$-\log \rho = \frac{\nu}{2c}(P' - P) \tag{5}$$

where ρ is the effective reflection coefficient of the ionosphere, ν is the electron collisional frequency, P' the group path, P the phase path, and c the velocity

of light in free space. Both P and P' can be calculated from the parabolic-layer theory we have previously given. When we can neglect the influence of the earth's magnetic field, a convenient formula, relating oblique-incidence absorption to vertical-incidence absorption, is due to MARTYN (1935), namely

$$\left[\log \rho\right]_{i_0}^{f} = \cos i_0 \left[\log \rho\right]_0^{f \cos i_0} \tag{6}$$

Here i_0 is the angle of incidence of the oblique ray on the ionosphere. The quantity $f \cos i_0$ is termed the "equivalent vertical-incidence frequency."

It is important to note that MARTYN'S theorem is based on the assumption of a plane ionosphere.

4. Attenuation due to Partial Reflection or to Scattering by Ionospheric Irregularities

We originally identified the existence of this type of attenuation in the course of some oblique-incidence experimental studies when it was found impossible to account for the results in terms of MARTYN'S theorem. By comparing oblique-incidence attenuation on a frequency f with vertical-incidence attenuation on the equivalent frequency $f \cos i_0$ it was found that the relation (6) was not obeyed. The oblique-incidence absorption was always larger than that predicted from a knowledge of the vertical-incidence absorption on the equivalent frequency. Instead, we found that our results fitted better the following relation

$$\left[\log \rho\right]_{i_0}^{f} = \left[\log \rho\right]_0^{f \cos i_0} \tag{7}$$

At the same time we proved, from a subsidiary experiment, that our measurements related to conditions of substantial sporadic E scattering. The frequencies used at oblique-incidence were also only slightly in excess of the theoretical oblique-incidence penetration frequency for the normal E-layer.

We have also found that this discrepancy between oblique and normal absorption is apparent not only in short-distance transmission, but often also occurs in very long-distance transmission paths (BEYNON, 1954).

We now wish to point out that there is considerable theoretical support for the relation (7) which we found in the first instance empirically. We consider some theoretical aspects of the problem in the following paragraphs.

5. An Ionospheric Attenuation Equivalence Theorem

It is well known that the intensity and distribution of sporadic E ionization varies considerably both in time and space. In its less dense form this type of ionization can be regarded as a large number of cloudlets of comparatively small dimension. At other times, under so-called "blanketing" conditions (the "intense E" condition first identified by APPLETON and NAISMITH (1935), we may have extensive sheets of ionization of small thickness but of high density. In the latter circumstances it would seem appropriate to apply the theoretical analysis valid for reflection at a sharp boundary, whereas in the former case it is more appropriate to examine the problem from the point of view of scattering by ionospheric irregularities.

(a) *Partial reflection at a sharp boundary*

We consider first the case of reflection of waves from a sharp boundary at which the refractive index changes suddenly from unity to $(1 - \Delta\mu)$, where $\Delta\mu$ is small compared with unity. Part of the radiation is assumed to be reflected at the sharp boundary, the remainder being transmitted (Fig. 1). From the usual Fresnel equations it can then be shown that the reflection coefficient ρ, for the two specified polarization states are given by

$$\rho_\perp = \left(\frac{\cos i_0 - \sqrt{\cos^2 i_0 - 2\Delta\mu}}{\cos i_0 + \sqrt{\cos^2 i_0 - 2\Delta\mu}}\right) \quad \text{(electric vector perpendicular to the plane of incidence)} \tag{8}$$

and

$$\rho_\parallel = \left(\frac{\sqrt{\cos^2 i_0 - 2\Delta\mu} - \cos i_0(1 - 2\Delta\mu)}{\sqrt{\cos^2 i_0 - 2\Delta\mu} + \cos i_0(1 - 2\Delta\mu)}\right) \quad \text{(electric vector in the plane of incidence)} \tag{9}$$

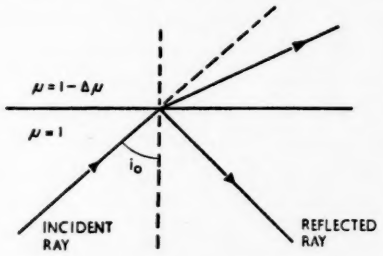

Fig. 1

With a little rearrangement, and bearing in mind that $(1 - \Delta\mu)$ is equal to $\left(1 - \frac{f_c^2}{2f^2}\right)$, where f_c is the critical penetration frequency of the medium, these expressions may be written in the form

$$\rho_\perp = \frac{x' - \sqrt{(x')^2 - 1}}{x' + \sqrt{(x')^2 - 1}} \tag{10}$$

and

$$\rho_\parallel = \frac{x' - \sqrt{(x')^2 - 1} - \sin^2 i_0/\sqrt{(x')^2 - 1}}{x' + \sqrt{(x')^2 - 1} + \sin^2 i_0/\sqrt{(x')^2 - 1}} \tag{11}$$

respectively. In these expressions $x' = x \cos i_0 = \frac{f \cos i_0}{f_c}$, where f is the signal frequency and f_c, as stated, the normal incidence penetration frequency of the layer. For normal incidence $i_0 = 0$, and equations (10) and (11) each reduce to

$$\rho = \frac{x - \sqrt{x^2 - 1}}{x + \sqrt{x^2 - 1}} \tag{12}$$

Comparing equations (10) and (12), the equivalence theorem

$$\left[\rho\right]_{i_0}^{x} = \left[\rho\right]_0^{x'} \quad \text{or} \quad \left[\rho\right]_{i_0}^{f} = \left[\rho\right]_0^{f \cos i_0} \tag{13}$$

VOL. 6 1955

is evident. But we see that the same theorem does not apply to the case of the electric vector polarized in the plane of incidence.

The relationship between the two types of polarization becomes relatively simple, however, if we take the case of $x' \gg 1$, which corresponds to practical conditions in which the equivalent vertical-incidence frequency employed is large compared with the natural critical frequency of the medium. In such a case equation (10) becomes $\rho_\perp = \dfrac{1}{4x'^2}$ whereas (11) becomes $\rho_\parallel = \dfrac{1}{4x'^2}[1 - 2\sin^2 i_0] = \dfrac{\cos 2i_0}{4x'^2}$. It will be noted that $\rho_\perp > \rho_\parallel$; also that $\rho_\parallel$ vanishes at the polarizing angle $i_0 = 45°$. For our purpose it is convenient to regard ρ as a positive quantity, the ratio of the reflected to the incident amplitude; it is the magnitude of the Fresnel coefficient, which may itself be a negative quantity.

Thus for $x' \gg 1$ our two equivalence theorems become

$$\left[\log \rho_\perp\right]_{i_0}^{f} = \left[\log \rho_\perp\right]_{0}^{f\cos i_0} \tag{14}$$

and

$$\left[\log \rho_\parallel\right]_{i_0}^{f} = \left[\log \rho_\parallel\right]_{0}^{f\cos i_0} + \log|\cos 2i_0| \tag{15}$$

It is easy to see that, in this case of high radio frequencies, the term $(\cos 2i_0)$, in the case of the electric vector in the plane of incidence, is merely the obliquity factor relating the direction of the reflected electric vector to that of the incident electric vector.

(b) *Case of a stratified layer without sharp boundary*

An alternative proof of the equivalence theorem (14), for the case of the electric vector at right angles to the plane of propagation, has been indicated to us by Dr. H. Bremmer, and we are indebted to him for permission to quote it here. In this case we can picture the ionization in a stratified layer varying quite arbitrarily with height. Neglecting the earth's magnetic field and electron collisional effects, we have

$$f_c^2 = \frac{e^2}{\pi m} N(z)$$

where

$$\mu^2 = 1 - \frac{f_c^2}{f^2}$$

as representing the distribution of N, and μ, with vertical height z. In this case the wave equation for the Hertzian vector is

$$\Delta\Pi + \frac{4\pi^2 f^2}{c^2}\mu^2(z)\Pi = 0 \tag{16}$$

We obtain the complete solution for a plane wave arriving from the homogeneous space below the ionosphere with an angle of incidence i_0, by putting

$$\Pi(x, y, z) = e^{j\frac{2\pi f}{c}\sin i_0 x}\, g(z) \tag{17}$$

It should be emphasized that this solution comprises the upward wave, as well as the downward one; it should satisfy the boundary condition that there is no downward wave at large z.

Substitution of (17) into (16) yields

$$\frac{d^2g}{dz^2} + \frac{4\pi^2 f^2}{c^2}(\mu^2(z) - \sin^2 i_0)\, g = 0 \tag{18}$$

or

$$\frac{d^2g}{dz^2} + \frac{4\pi^2}{c^2}(f^2 \cos^2 i_0 - f_c^2)\, g = 0 \tag{19}$$

Now the boundary condition at infinity is independent of the only parameter ($f \cos i_0$) that occurs in the problem. Therefore $g(z)$, too, is uniquely determined by ($f \cos i_0$).

In its turn, the reflection coefficient is completely determined by $g(z)$, since, for large negative z, $g(z)$ can be split into two parts which are to be interpreted, after multiplication by the exponential function in (17), as the rising part and the down-going part of the wave. Therefore, the reflection coefficient, being the ratio of these two parts, also merely depends on $g(z)$, that is (for the given electronic distribution) on the parameter $f \cos i_0$. We thus have

$$\left[\log \rho\right]_{i_0}^{f} = F(f \cos i_0)$$

The above general treatment refers, as stated, only to the case of the electric vector at right angles to the plane of propagation. We are, however, indebted to Dr. P. M. DAVIDSON and Dr. H. BREMMER for showing us that, also in this case of a continuous N distribution, the equation (15) above is valid when the electric vector lies in the plane of propagation and the radio frequency is sufficiently high.

(c) *Scattering by a spherical ionized cloud*

We now consider a case where the ionization has spherical symmetry. Referring to Fig. 2, where the centre of the cloud is situated at O in a symmetrical position relative to the sender S and the receiver R, and the linear dimensions of the cloud are very small compared with OR, we restrict ourselves, for the moment, to the case of the electric vector at right angles to the plane of propagation. If E_i is the incident electric intensity at O, due to the sender S, and E_r is the corresponding quantity in the scattered radiation at R, it is easy to show that

$$\frac{E_r}{E_i} = \frac{L}{r} \tag{20}$$

where r is the distance from O to R, and L is the scattering factor of the cloud. Note that L has the dimensions of a length, and for a single electron is equal to e^2/mc^2, the so-called "radius of the electron."

Let us now assume that, in the cloud, $N(r)\,dr$ is the number of electrons

VOL. 6 1955

between radius r and $(r + dr)$. Then using the familiar results of X-ray atomic-scattering theory, we can show that

$$L = \frac{e^2}{mc^2} \int_0^\infty \frac{N(r) \sin \left(\frac{4\pi r}{\lambda} . \sin \frac{\phi}{2} \right) dr}{\frac{4\pi r}{\lambda} . \sin \frac{\phi}{2}} \tag{21}$$

where ϕ is the angle of scattering and λ is the wavelength (which is assumed unaltered in the medium).

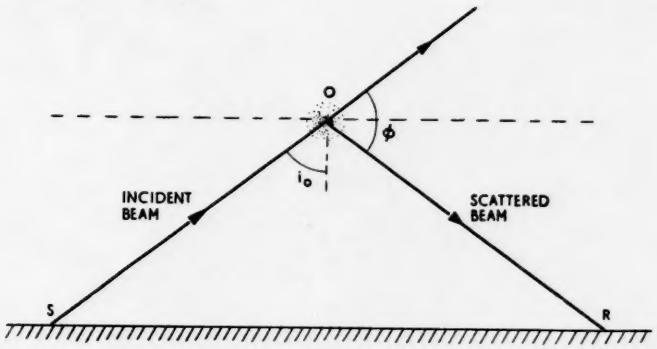

Fig. 2.

In the case of the scattering of radio waves by an electron cloud, as in Fig. 2, we note that $i_0 = (\pi - \phi)/2$, so that L is unchanged if $(\cos i_0/\lambda)$ is kept constant. Moreover, this property does not depend on the spherical symmetry of the cloud. A general integral expression for L, valid when the cloud has any shape and density, has the same property. We thus arrive at the same basis as before for the ionospheric equivalence theorem. Also we may note that in the case of the electric vector in the plane of propagation we must include the obliquity factor $\cos \phi$, which is equal to $|\cos 2i_0|$.

It may not be superfluous to add that we do not know of any comparable treatment of scattering by a cloud of spherical symmetry under conditions where the electron density, at some level, exceeds the critical penetration value, and we wish to commend this problem for examination to our mathematical colleagues. The case of a cylindrical cloud of corresponding character might also merit similar mathematical treatment.

Acknowledgments—We wish to express our warm appreciation of the generous help we have received by way of discussions with Dr. H. Bremmer (of Philips Research Laboratories, Eindhoven) and with Dr. P. M. Davidson (of the University College of Swansea).

The work was carried out as part of the programme of the Radio Research Board of the Department of Scientific and Industrial Research.

References

Appleton, E. V., and **Beynon**, W. J. G.	1940	*Proc. Phys. Soc.* **52**, 518
	1947	*Proc. Phys. Soc.* **59**, 58
Appleton, E. V., Beynon, W. J. G., and Piggott, W. R.	1948	*Nature* **161**, 967, June 19
Appleton, E. V., and Naismith, R.	1935	*Proc. Roy. Soc.* A **150**, 685
Beynon, W. J. G.	1954	*Proc. Inst. Elect. Engrs.* **101**, Part III, 15
Martyn, D. F.	1935	*Proc. Phys. Soc.* **47**, 323

VOL. 6 1955

Journal of Atmospheric and Terrestrial Physics, 1955. Vol. 6, pp. 149 to 159. Pergamon Press Ltd., London

Point discharge currents from a captive balloon

J. Alan Chalmers
Senior Lecturer in Physics

and W. W. Mapleson*
Durham Colleges in the University of Durham

(*Received* 5 *July* 1954)

ABSTRACT

Measurements are described of the point discharge current, I, from a point attached to a captive balloon, and these have been correlated with the height, h, the potential gradient at the ground, F, and the wind-speed, W. An approximate theoretical formula is developed, giving $I = K(Fh)^{q-1}W^{3-q}$. The observational results check the validity of certain aspects of this formula within a limited range of the parameters, with q about 2·77 and K about 0·02 (or 0·015 after estimating a correction for systematic error in F) when I is measured in μA, Fh in kV, and W in km/hr. Measurements for an eight-point discharger show that this gives in all about half the current from a single point under similar conditions.

1. Introduction

Point discharge from exposed points plays an important part in the transfer of electricity between clouds and earth during stormy weather, but it has not been certain on what parameters the magnitude of this current depends. Detailed investigations with natural points or with artificial points of similar height, which give point discharge only in stormy weather, are hampered because point discharge is infrequent and is confined almost entirely to occasions when other conditions, e.g., the electric potential gradient, are varying widely and rapidly.

Laboratory investigations of point discharge are not generally applicable to problems of atmospheric point discharge, because of the vast difference in linear scale; it is not possible to make a scale model, since one cannot scale down the movements of the ions which, by the production of space charge, play an important part.

Natural point discharge in the atmosphere can, however, occur in fine weather, with reasonably steady conditions, if a point is raised to a sufficient height. Among the pioneers of atmospheric electricity, possibly Lemonnier (1752) with a pole, and certainly de Romas (1753) with a kite, obtained point discharge in fine weather. More recently, Rangs (1942) with a kite and Davis and Standring (1947) and Wichmann (1951) with captive balloons, have measured discharge currents in fine weather.

Simpson and Scrase (1937) and Simpson and Robinson (1940) have made use of point-discharge currents through points attached to a free balloon to estimate potential gradients below, in, and above clouds. In default of other data, they used the relation between point-discharge current and potential gradient found for a point situated similarly to other discharging points. If a formula can be established for a point which is situated well away from other points, this would be better applicable to the free-balloon results.

* Now at the Department of Anaesthetics, Welsh National School of Medicine, Cardiff.

The present work is concerned with a study of the influence of various parameters upon the current from a point attached to a captive balloon.

2. Parameters

The point-discharge current through an earth-connected point may depend upon:

(a) the potential that would exist at the position of the point, in the absence of the point,

(b) the wind-speed and, possibly, its direction,

(c) the nature of the point,

and, possibly,

(d) other properties of the atmosphere such as conductivity or pressure.

Of these, (d) was neglected, as being likely to have little effect, and (c) was eliminated in most of the measurements by using similar points, but one set of measurements was made with an eight-point discharger; (b) was measured as described later. (a) could not be determined directly, but measurements were made of:

(e) the electric potential gradient at the ground, and

(f) the height of the point.

In the absence of natural space-charge in the atmosphere below the point, the product of these two parameters gives (a); it is believed that natural space-charge may be responsible for many of the inconsistencies in the results.

The parameters (b) and (e) are not under control, so it was necessary to rely upon chance to get a full range of values. The wind-speed was limited to values of less than 25 km/hr, otherwise the angle of the cable supporting the balloon was too great and there was danger of fouling trees or buildings. In regard to (f), four cable-lengths were chosen; 50 m, 100 m, 150 m, and 200 m; fewer would have been insufficient to give a definite relation with height, and more might not have allowed a full range of variation of (b) and (e).

3. Previous Measurements

Most of the previous measurements relating point-discharge current and potential gradient have been made, using a point in an approximately similar situation to neighbouring points. Whipple and Scrase (1936) found the relation:

$$I = a(F^2 - M^2) \tag{1}$$

where I is the point-discharge current, F the potential gradient at the ground near by, and a and M are constants. This was verified by Chiplonkar (1940) and Hutchinson (1951), though the latter found "humps" which he explained as due to the effects of other dischargers, lower than his point.

Rangs (1942) made measurements with a kite, but did not separate results for different heights. Davis and Standring (1947) measured currents from a captive kite-balloon and found a general increase of current with height, with wind-speed, and with the potential gradient at the ground, but gave no comprehensive

VOL. 6 1955

formula; their heights were considerably greater than those used in the present work.

4. The Balloon and Point

The discharge point was supported by a captive, nominally spherical, rubber balloon having two necks and filled to a diameter of about 2 m, which was tethered by a whipcord of about 1·5 mm diameter. The point consisted of about 40 cm of 12-gauge copper wire, with a piece of 0·25 mm diameter platinum wire soldered on to project about 2 mm beyond the end of the copper wire. It was clamped to the upper neck of the balloon and connected to earth (through the recording galvanometer) by 26-gauge copper wire.

For some observations, the single discharging point was replaced by a group of eight points, each of which was essentially similar to the single point. The copper wires were grouped together at the base and bent so that the tips of seven of them formed an approximately regular heptagon, of side 15 cm, with the eighth tip at the centre.

5. Measurements

Continuous photographic recording was used to measure the point-discharge current and also the potential gradient on the same record. Simultaneously, visual observations were made of the cable angle and the cable direction; definite lengths of cable were used, and so the balloon height could be determined from the cable angle, correcting for the curvature of the cable.

The point-discharge current was measured directly by a galvanometer critically damped; two sensitivities were available: 1·0 cm/μA and 0·3 cm/μA.

The potential gradient was measured at the earth's surface at a distance of 50 m from the base of the cable, in a direction as closely as possible to windward, using a "Field Mill" which is being described separately (Mapleson and Whitlock, 1954); four sites for the mill were fixed, and the one most suitable according to the wind direction was used for each recording. The mill was calibrated in each position by reference to the potential on a stretched wire with fuse.

Wind-speed was determined from the cable angle, a separate calibration having been made (Mapleson, 1954); owing to different shapes of balloon, the actual wind-speeds may have been in error by up to about 15 per cent.

The records were measured to give average values over half-minute periods. Each recording lasted about an hour, but in suitable conditions a fresh recording was started immediately one ended.

Calculations on the lines of those of Davis and Standring (1947) showed that the induced charge on the cable would have negligible effect on the potential gradient at 50 m to windward, but that a small effect might be expected from the space charge liberated by the point discharge, especially for large currents and light winds. However, on the occasions when the balloon burst during the recording, thereby terminating the point discharge, there was no appreciable change in the potential gradient, so that it can be concluded that measurement of the potential gradient at 50 m to windward gives a reliable value of the undisturbed potential gradient. The absence of any effect when the balloon bursts shows that any charge on the balloon itself is small.

6. Observational Data

After eliminating all those periods for which the records were, for any reason, unsatisfactory, there remained for analysis 1,620 half-minute periods, divided, according to the length of cable used, into 430 at 50 m, 360 at 100 m, 350 at 150 m, and 320 at 200 m, together with 160 at 50 m with the eight-point discharger. For each cable length, there was a considerable range of values of field and of wind-speed.

Inspection of the results showed that, as was expected, the point-discharge current generally increases with increase of potential gradient, increase of height, and increase of wind-speed. But the results for a cable length of 200 m did not show the regularity of the other observations and clearly could not be subjected to analysis; the main reason for the irregularity shown must be that natural space charge between the balloon and the ground has sufficient effect in this case to destroy any regularity, whereas for lower heights the effect is less. The irregularity for the 200 m results is caused by the fact that winds are steadier at 200 m than at lower heights. Therefore results for any one range of wind-speed at 200 m tended to come from a single hour's observations, when the natural space charge is relatively constant; for lower cable lengths, results for one range of wind-speed were derived from several separate hours' observations with different amounts of natural space charge, and thus an averaging process gives greater apparent regularity. With reluctance, the 200 m results were eliminated from further consideration.

As various ways were possible for further analysis, theory was invoked to suggest the most suitable approach.

VOL. 6 1955

7. Theoretical Discussion

Point discharge occurs when the field strength in the neighbourhood of the point is large enough to give ionization by collision. Ions of one sign then enter the point, while the ions of opposite sign travel away from the point and form a space charge which tends to reduce the field strength near the point.

When the processes are studied in detail, it is found that the discharge, at any rate when the point is negative, consists of pulses, of approximately the same quantity of charge, but of frequency dependent on the potential gradient (Trichel, 1938).

But if we consider just the average condition over a time long compared with the repetition period of the pulses, then, with a steady field, there is set up a stationary state which can be discussed without considering the details of the production of the ions. The potential difference between the point and a region well above it is determined by the external conditions and also depends on the space charge of the ions; but the space charge is related to the current, and there is only one value of the current which will fit any given conditions. Chalmers (1952) has discussed this in more detail and has applied the ideas to the derivation of a formula for the point-discharge current from one of a series of points in rectangular array, obtaining a formula similar to that of Whipple and Scrase (1936). Here the same ideas have to be applied to the case of an isolated point.

At a considerable height above a discharging point, the lines of force are

vertical, and if we follow these downwards, we can divide them into those which end on the point or on ions liberated by point discharge, and those which end on the earth. This divides the volume of air above the point into what we can call the "point region" and the "earth region." In this and what follows, we are neglecting natural space charge in the atmosphere and assume that, in the absence of the balloon and point, the potential gradient remains uniform up to all heights considered. In the absence of wind and of diffusion, the upward-moving ions from the point would follow the lines of force and so would remain within the point region. Near the point, the ionic velocity in the field is large compared with wind or diffusion velocities and the ions do remain within the point region, but well away from the point the ionic velocity in the field is much smaller and wind moves the ions out of the point region. We can obtain an approximate result by assuming that the ions remain in the point region so long as the ionic velocity is greater than the wind velocity and that the ions are completely dispersed when the ionic velocity is less than the wind velocity; a gradual transition is thus replaced, in our approximate treatment, by a sudden change of conditions.

For the conditions when the ions remain in the point region, CHALMERS (1952) assumed the vertical component of the potential gradient to be uniform across each cross-section of the point region. He then obtained (converting into MKS units)

$$(Xs)^2 - (X_0 s_0)^2 = \frac{2I}{w\varepsilon_0}(v - v_0) \tag{2}$$

where I is the total current from the point, X the potential gradient where the cross-section of the point region is s, v the volume of the point region from the point to this level, X_0 the limiting potential gradient for ionization by collision, s_0 the cross-section of the point region where $X = X_0$, and v_0 the volume of the point region from the point to this level. w is the mobility of the ions, and ε_0 is the "permittivity of free space" or "electric space constant."

Unless X or I is small, the terms in s_0 and v_0 in (2) can be neglected compared with the other terms.

If we can now assume that the point region has a shape given by $s = kx^q$, where s is the cross-sectional area at a height x above the point, which is itself at a height h above the ground, then (2) gives:

$$X^2 = \frac{2I}{w\varepsilon_0 k(q+1)x^{q-1}} \tag{3}$$

If V is the potential difference between the point and the level x,

$$V = \int_0^x X\,dx = \left[\frac{2I}{w\varepsilon_0(q+1)k}\right]^{\frac{1}{2}} \frac{2}{(3-q)}\, x^{(3-q)/2}$$

and

$$V/X = \frac{2}{(3-q)}\, x \tag{4}$$

If W is the wind velocity, then our assumption is that the ions remain within the point region up to the level where $wX = W$; let $x = p$ at this level.

Now let us assume that, at $x = p$, the potential is uniform both inside and outside the point region; this must then be $F(h + p)$, so that, from (4)

$$\frac{F(h+p)}{W/w} = \frac{2p}{(3-q)}$$

from which, if wF is considered small compared with W, as is true in the conditions for which the formula is required:

$$p = \frac{(3-q)hwF}{2W}$$

Substituting these results in (3),

$$I = \frac{k}{2^q}(q+1)(3-q)^{q-1}\,\varepsilon_0 w^{q-2} W^{3-q}(Fh)^{q-1} \tag{5}$$

If, instead of assuming that, at $x = p$, the potentials are the same inside and outside the point region, we consider that the point region still obeys the law $s = kx^q$ above $x = p$, though there is no space charge inside it, and we go on to $x = g$, at which height we assume that both potential gradients and potentials are the same inside and outside the point region, we get:

$$I = \frac{k(q-1)^{q-1}(3-q)^{q-1}}{2(q+1)^{q-2}}\,\varepsilon_0 w^{q-2} W^{3-q}(Fh)^{q-1} \tag{6}$$

(5) and (6) can be put in the form:

$$I = KW^{3-q}(Fh)^{q-1} \tag{7}$$

From the form of (5) and (6), it is clear that q must lie between 1 and 3, but it does not appear possible to find, theoretically, the values of q or k.

Although it is clear that there will be no point discharge at all if the product (Fh), which we can call the "voltage," is too low, it does not seem possible to derive a modified form of (7) to include a constant corresponding to "M" in (1). The present formula (7) is only approximately true, and the assumptions made show that it cannot be accurate for low voltages; for higher voltages, any terms such as "M" would be of little importance.

8. Tests of Theoretical Formula

The observational results are not sufficiently extensive or complete (because of the unavoidable effect of natural space charge) to permit a rigorous test of the theoretical formula (7), though certain aspects of it are susceptible to checking.

Firstly, a check of whether the point-discharge current depends simply on the voltage at the point (Fh) or on the potential gradient and height independently, may be made by plotting average values of I against Fh for various small ranges of wind-speed. In most of the graphs obtained (of which Fig. 1 is an example) the points lie more or less on a single curve when cable lengths of 100 m and 150 m are considered; as already mentioned, results for 200 m show irregularities and must be rejected. Results for a cable-length of 50 m are consistently low, but can be brought into line if 10 m is subtracted from the measured height. The need for

VOL. 6 1955

this is explained in terms of the effect of surrounding trees and buildings, which will be to make equipotentials, particularly near the ground, higher over the balloon site than over clear level ground near by; then the effective height for a cable-length of 50 m is less than the true height. The equipotentials level out at a greater height, so that a similar correction for effective height does not operate at 100 m or higher. The theoretical result that I depends on Fh is verified for 100 m and 150 m, and this is used to correct h for the 50-m results.

Secondly, we see that (7) may be written:

$$I = K(Fh)^{\alpha}W^{\beta} \tag{8}$$

where $\alpha + \beta$ is found by theory to be 2.

Taking the general form (8), the observational results can be used to find the "best" values of α and β; logarithms were taken of both sides and a partial regression analysis performed. For the observational results, those for the 200 m

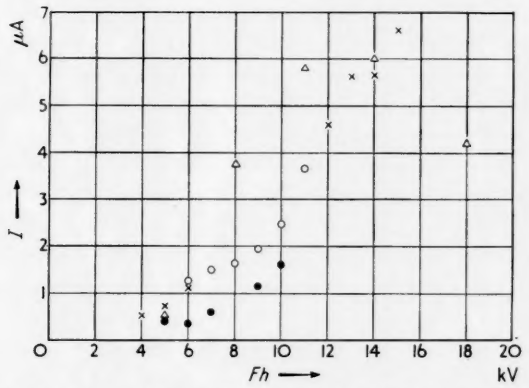

Fig. 1. Means of observed values of I plotted against uncorrected values of Fh for W = 13·5 to 14·5 km/hr and for different cable lengths.
• 50 m × 150 m
o 100 m △ 200 m

cable were rejected and those for the 50 m cable corrected as described. Since the theoretical formula does not hold for low voltages, low currents, or low wind-speeds, all voltages less than 3 kV, currents less than 0·2 μA, and wind-speeds less than 2 km/hr were rejected.

This gave:

$$\alpha = 1{\cdot}79 \pm 0{\cdot}04$$
$$\beta = 0{\cdot}24 \pm 0{\cdot}03$$
$$\alpha + \beta = 2{\cdot}03 \pm 0{\cdot}05$$

where the errors represent the standard deviations. Thus when values of α and β are determined independently so as to get the "best" fit of equation (8) to the observations, the deviation of $\alpha + \beta$ from the theoretical value of 2 is only 0·6 of the standard deviation, a result which lends encouraging support to the theory.

9. Analysis of Results

The preceding analysis cannot give a value for K, so (7) was used. By taking logarithms and using the method of least squares, the following values were obtained:

$$q = 2{\cdot}77 \pm 0{\cdot}02$$
$$K = 0{\cdot}021 \pm 0{\cdot}0004$$

where errors represent standard deviations and I is measured in μA, Fh in kV, and W in km/hr.

The final formula is then

$$I = 0{\cdot}021 W^{0{\cdot}23}(Fh)^{1{\cdot}77} \tag{9}$$

It should be pointed out, however, that the stretched wire (to which measurements of F are referred) was rather poorly exposed, and consequently the value of K should be decreased, perhaps to 0·015, if F is measured at a "good" site. Then a "rounded off" formula might be:

$$I = 0{\cdot}015 W^{1/4}(Fh)^{7/4} \tag{10}$$

Figs. 2 and 3 show graphs of I against (Fh) for various values of W, and I against W for various values of (Fh), the lines representing equation (9). The agreement is seen to be reasonably good, except for high values of (Fh); the observations giving these high values were all obtained with the 150 m cable and it may be that natural space charge is here showing an effect similar to that for the 200 m cable.

VOL. 6 1955

10. Results for the Eight-Point Discharger

These results were analyzed in the same way as those for the single point, and equation (7) was then fitted, giving:

$$q = 2{\cdot}83 \pm 0{\cdot}02$$
$$K = 0{\cdot}011 \pm 0{\cdot}0002$$

where the errors again represent standard deviations and the units are as before.

The difference between the values of q for the single point and the eight points is $0{\cdot}06 \pm 0{\cdot}03$, which is not significant. On the other hand, K for the eight points is only about half its value for the single point.

Thus Chiplonkar's (1940) results for multiple points are confirmed and Belin's (1948) results of laboratory calibration are shown not to be applicable in the atmosphere.

The results here presented prompt the speculation that q is the same for different points and that k, and so K, may depend on the nature of the point.

11. Application to Alti-Electrograph

The alti-electrograph (Simpson snd Scrase, 1937; Simpson and Robinson, 1940) consists of a balloon carrying a group of four points just below it, and a single point 20 m lower down. For the purpose of comparison with the present results, we shall consider the four, rather well spaced, points to be equivalent to a single point, so that the recording apparatus in the balloon will be at the potential of the air half-way between the dischargers. Then the conditions are somewhat similar to

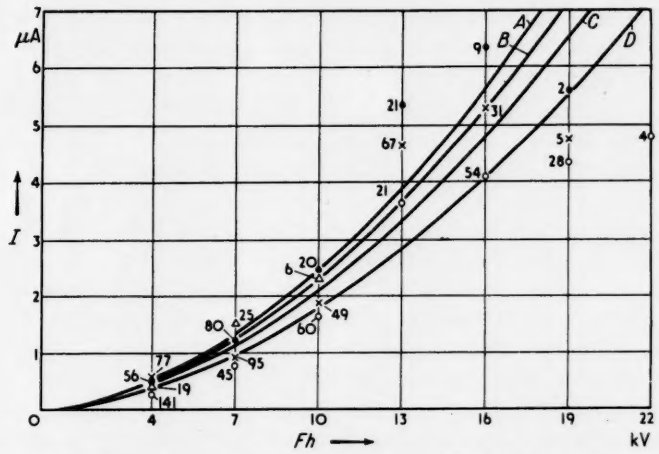

Fig. 2. The points represent means of observed values of I for different ranges of Fh and W. The lines are calculated from $I = 0{\cdot}021(Fh)^{1{\cdot}77}W^{0{\cdot}33}$.

A for $W = 20$ km/hr
B for $W = 15$ km/hr
C for $W = 10$ km/hr
D for $W = 5$ km/hr

Points represent: △ $W = 18$–22 km/hr
• $W = 13$–17 km/hr
× $W = 8$–12 km/hr
o $W = 3$–7 km/hr

The figures beside the points indicate the number of observations used for each point.

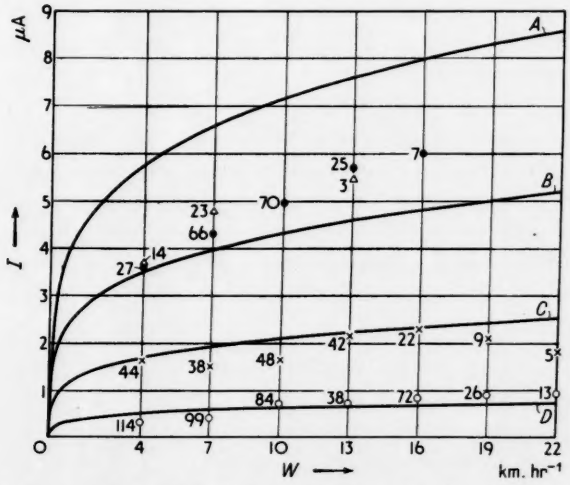

Fig. 3. The points represent means of observed values of I for different ranges of W and of $Fh = V$ The curves are calculated according to the same formula as in Fig. 2.

A for $V = 20$ kV
B for $V = 15$ kV
C for $V = 10$ kV
D for $V = 5$ kV

△ for $V = 18$–22 kV
• for $V = 13$–17 kV
× for $V = 8$–12 kV
o for $V = 3$–7 kV

The figures beside the points indicate the number of observations used for each point.

those of the present measurements with $h = 10$ m. It certainly appears closer to the truth to compare the alti-electrograph with the present measurements than with the measurements of Whipple and Scrase (1936), whose point was one of a number more or less similarly situated. In both cases, a wide extrapolation is required, since the present measurements extended only to 7 μA and those of Whipple and Scrase only to 5 μA, while the alti-electrograph gave currents of 300 μA.

To apply equation (10) it is necessary to know the wind velocity; the alti-electrograph balloon, being free, experienced no horizontal wind, but it rose at a rate of 5 m/sec (18 km/hr); clearly it is not quite correct to use this value in place of the horizontal wind of (10), yet it can be seen that this value for W fits well for the upper points with the idea of the space charge remaining in the point volume while $wX > W$ and not for lower values of X.

Simpson and Scrase (1937) used the Whipple-Scrase formula, obtaining the constant by measurements of current and potential gradient at the start of ascents, and, apart from a correction for pressure, obtained:

$$I = 0{\cdot}030\ F^2$$

Using (10), the result is

$$I = 0{\cdot}031\ F^{7/4}$$

Comparing the values of F for $I = 300$ μA, assuming the formulae to hold with wide extrapolation, the present work gives 190 V/cm as compared with 100 V/cm from the earlier results. The application of the present results therefore does little to resolve the discrepancy between potential gradients as measured by the alti-electrograph and the much higher potential gradients predicted (e.g., by Whipple and Scrase (1936)).

VOL. 6 1955

12. Conclusion

The results of the present observations show that the formula (10), derived theoretically as an approximation, holds fairly well up to the limits of voltage and wind-speed that were available. To investigate whether the same formula is applicable for higher values, it would be necessary to support the point in some way that can still be used in higher winds and more stormy conditions; a kite-balloon would be one possibility, or a mast of sufficient height.

Acknowledgments—The authors wish to thank: The Council of the Durham Colleges for—(1) A research studentship for one of us (W. W. M.) for two years, (2) a year of sabbatical leave for one of us (J. A. C.) which has allowed the progress of the work to be uninterrupted by other duties, and (3) grants from their Research Fund for the purchase of various items of equipment; The Academic Board of King's College, Newcastle, for the award of the British Association Studentship to one of us (W. W. M.) for one year; The Meteorological Office for additional equipment; The Ministry of Civil Aviation for permission to fly the balloon; The Mathematics Department of the Durham Colleges and the Department of Medical Statistics of the Institute of Preventive Medicine, Cardiff, for the use of calculating machines; Dr. E. Lewis-Faning of the Welsh National School of Medicine for general statistical advice.

References

Belin, R. E.	1948	*Proc. Phys. Soc.* **60,** 381
Chalmers, J. A.	1952	*J. Atmosph. Terr. Phys.* **2,** 292
Chiplonkar, M. W.	1940	*Proc. Ind. Acad. Sci.* **12A,** 50
Davis, R., and Standring, W. G.	1947	*Proc. Roy. Soc.* **A191,** 304
Hutchinson, W. C. A.	1951	*Quart. J. Roy. Met. Soc.* **77,** 627
Lemonnier, L. G.	1752	*Mem. de l'Acad. des Sci.* **2,** 233
Mapleson, W. W.	1954	*Quart. J. Roy. Met. Soc.* **80,** 449
Mapleson, W. W., and Whitlock, W. S.	1954	Not yet published
Rangs, —	1942	*Z.W.B.* Nr. 699 (Min. Supp. ref. IIB/6022)
de Romas, J.	1753	*Mem. à l'Acad. de Bordeaux*
Simpson, Sir G. C., and Robinson, G. D.	1940	*Proc. Roy. Soc.* **A177,** 281
Simpson, Sir G. C., and Scrase, F. J.	1937	*ibid.* **161,** 309
Trichel, G. W.	1938	*Phys. Rev.* **54,** 1078
Whipple, F. J. W., and Scrase, F. J.	1936	*Met. Off. Geophys. Mem.* **68**
Wichmann, H.	1951	*Arch. f. Met. Geoph. Biokl.* **A3,** 290

Journal of Atmospheric and Terrestrial Physics, 1955, Vol. 6, pp. 160 to 170. Pergamon Press Ltd., London

Studies on the sunrise effect in regions *E* and *F*

S. S. Baral
Institute of Radio Physics and Electronics, University of Calcutta

(*Received July* 1954)

ABSTRACT

The characteristics of an ionospheric layer are known to undergo variations during sunrise in the layer (sunrise-effect). The sunrise-effect begins not when the solar rays first strike the layer, but later. This delay phenomenon in the "sunrise-effect" has been studied for the *E*- and *F*-regions of the ionosphere at Calcutta during the period January 1947 to June 1952. It is shown that the observed delay times can be explained as due to the difference between the night-time and daytime heights of an ionospheric layer. The early-morning rays which strike the night side of the ionospheric layer and increase its ionization, must pass above the daytime height of the layer, in order that the active wavelengths do not get absorbed by the thickness of the air through which the rays pass. The measured daytime height of the layer (after the occurrence of the sunrise-effect) agrees reasonably well with the height grazing which the solar rays strike the nighttime height of the layer at the time of commencement of the sunrise-effect.

1. Introduction

The ionospheric characteristics—the maximum ionization and the equivalent height of a layer—are known to vary during the early morning sunrise in the layer. The variations begin not when the solar rays first strike the layer, but later. Sufficient experimental study of this phenomenon (known generally as the "sunrise-effect") does not appear to have been made, though evidently the study is expected to yield useful information regarding the physical conditions of the ionospheric layer concerned.

In the present paper an account will first be given of the observations that have been made at Calcutta during the years 1947–1952 on the delay in the occurrence of the sunrise-effect in the *E*- and *F*-regions of the ionosphere. A possible explanation of the delay in the occurrence of the effect will then be discussed.

2. Observations on the Sunrise Effect

The observations were made twice a week from January 1947 to December 1949, and thereafter once a week up to June 1952. The observations consisted in the measurement of the critical frequency ($f°$) and the height of maximum ionization (h_m) of regions *E* and *F*, commencing at least one hour before sunrise at 250-km height and continuing the same till the "sunrise-effect" had occurred in both the regions (the measurements were made at intervals varying from two to four minutes). The time at which the separation of the single *F*-region into the two F_1- and F_2-regions commenced was also noted. Fluctuations of *F*-region height and the frequent occurrence of sunrise-time sporadic *E*, necessitated the collection of a large amount of data before any attempt at their interpretation could be made. Some typical examples of the early-morning variations of $f°$ and h_m of regions *E* and *F* are given in Figs. 1 and 2. The mean intervals between the time of sunrise and the time of the commencement of the "sunrise-effect" in the different regions in different months of the years 1947–1952 are given n Tables 1, 2, and 3.

VOL. 6 1955

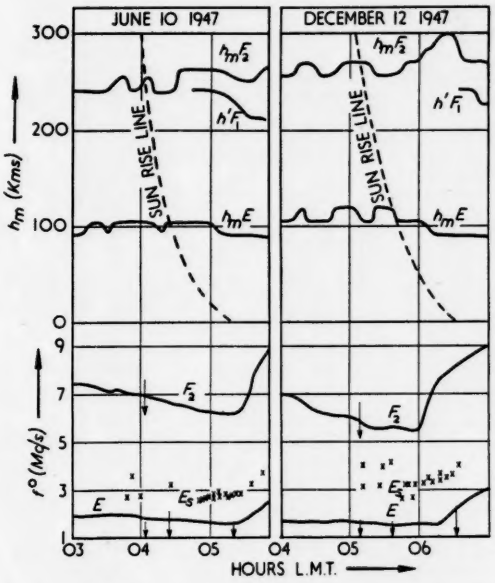

Fig. 1. Example of "sunrise-effect" observations in regions E and F on a summer day and on a winter day in 1947.

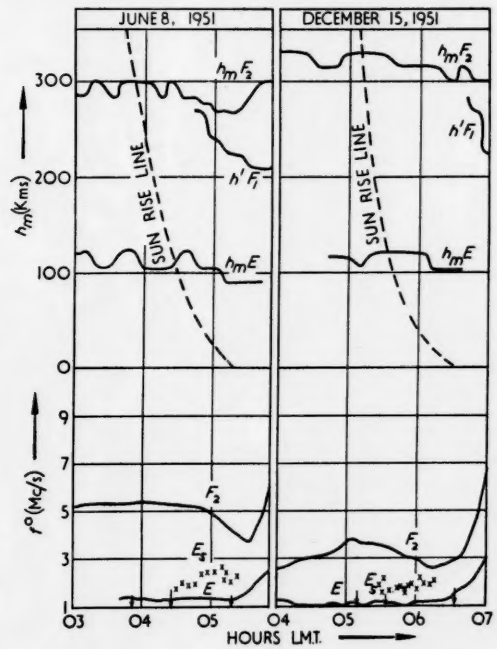

Fig. 2. Example of "sunrise-effect" observations in regions E and F on a summer day and on a winter day in 1951.

E-region

It will be seen from Table 1 that the sunrise-effect in the normal *E*-region ionization occurs after a delay of about forty to fifty minutes from the time of

Table 1. *Mean interval (in minutes) between time of sunrise and time of sunrise-effect in the E-region*

Months \ Years	1947	1948	1949	1950	1951	1952
January	43	45	46	40	44	42
February	46	42	47	45	48	45
March	48	46	50	48	50	46
April	48	48	50	42	52	42
May	42	43	42	46	46	43
June	45	46	49	46	48	40
July	50	48	52	48	46	—
August	45	48	52	48	44	—
September	42	45	46	45	45	—
October	40	42	45	50	44	—
November	42	44	42	50	43	—
December	46	48	46	44	42	—

sunrise in the region. Calculations show that this delay corresponds very nearly to the time when the rays fall on the region after grazing a height of about 100 km above the surface of the earth. No definite seasonal variation of the delay is

Table 2. *Mean interval (in minutes) between time of sunrise and time of sunrise-effect in the F-region*

Months \ Years	1947	1948	1949	1950	1951	1952
January	70	65	64	60	58	62
February	70	65	67	60	60	64
March	72	68	69	65	60	65
April	72	72	74	68	62	62
May	74	80	75	72	74	73
June	82	84	80	78	83	82
July	85	82	80	73	75	—
August	82	84	78	65	70	—
September	80	75	70	68	70	—
October	80	80	65	68	62	—
November	75	70	68	72	58	—
December	67	68	60	62	60	—

observed in Table 1. It is to be mentioned that the occurrence of the sunrise-effect was always found to be associated with an abrupt fall in the height of maximum ionization of the layer.

, VOL. 6 1955

"Sunrise-time" E_s

It has often been found that about thirty minutes after sunrise at the height of the E-layer, weak E_s reflections appear over an appreciable range of frequencies. This type of E_s is of almost regular occurrence at low latitude (BARAL, 1952) and has been termed "sunrise-time" E_s. During our early-morning observations we detected them in more than 60 per cent of the total observations (Table 4). The time of occurrence of sunrise-time E_s, measured from the time of E-region sunrise, undergoes a seasonal variation. In summer it corresponds to the time when the solar rays fall on the region grazing a height of about 50 km; in winter it corresponds to the time when the rays fall on the region grazing a height of about 30 km.

Table 3. Mean interval (in minutes) between time of sunrise in F-region and time of splitting of the region into F_1 and F_2

Months \ *Years*	1947	1948	1949	1950	1951	1952
January	78	70	68	72	70	70
February	74	70	82	72	68	76
March	70	72	75	70	68	78
April	70	70	78	64	70	75
May	65	74	72	70	72	72
June	72	72	74	72	72	72
July	70	70	72	68	64	—
August	70	72	70	62	64	—
September	78	78	75	60	78	—
October	78	85	72	78	78	—
November	82	80	75	80	75	—
December	75	80	70	80	70	—

F-region

It will be seen from Table 2 that the delay in the sunrise-effect in region F, as measured from the time of sunrise in the region, is more than an hour. The delay increases from winter to summer. It was also noted that the delay in the occurrence of the sunrise-effect in the winter months is smaller during years of low solar activity than during years of high solar activity. No such difference was noticed in the summer months.

It will be seen from Tables 2 and 3 that splitting of the combined F-layer into F_1 and F_2 begins *before* the occurrence of sunrise-effect in the region in summer but *after* it in winter.

It was often found that the night-time decay of the electron density of the region is accentuated instead of being checked when the ground tangent ray falls on the region in the early hours of the morning.

Absorption

Absorption of both the E- and F-region echoes begins at least half an hour before the occurrence of the sunrise-effect in the E-region. No detailed study of absorption has, however, been made.

Complete disappearance of ionospheric reflections in the early morning, as has recently been reported from Kodaikanal (BHARGAVA, 1952), was not observed during our early-morning studies of the ionosphere.

Table 4. *Frequency of occurrence of "sunrise-time" E_s*

	1947	1948	1949	1950	1951	1952	*Total*
Total number of observations	86	90	92	50	52	20	390
Number of cases when E_s occurred after sunrise in E-region height but before sunrise effect	50	48	60	25	27	10	220
Number of cases when E_s was already present before sunrise in the E-region	25	32	20	10	12	5	104
Number of cases when E_s was not observed in the interval between E-region sunrise and E-region sunrise-effect	9	10	12	10	5	5	51
Number of cases when E_s could not be interpreted properly	2	nil	nil	5	8	nil	15

Height variations

In this connection it should be remarked that the height of maximum ionization of the E-region, as measured by our apparatus, was very nearly constant till the time of sunrise-effect; that of the F-region, however, varied widely, and the time of sunrise in the layer was obtained from the point of intersection of the two curves, sunrise-time *versus* height and the time *versus* height of maximum ionization (Figs. 1 and 2). The height of maximum ionization of the F-region was found to increase in summer and to decrease in winter, following the incidence of solar rays in the early morning.

3. DISCUSSION OF THE OBSERVATIONAL RESULTS

The results of the above observations made at Calcutta may be compared with those of similar observations made earlier at Calcutta and also at other places.

GHOSH at Calcutta found (M.Sc. thesis, Calcutta University, 1938) that the hour of sunrise-effect in the E-region corresponds to the time when the solar rays are incident on the region grazing the ozonosphere. Unfortunately, no distinction

VOL. 6 1955

between normal and sporadic *E* was made. The time of sunrise-effect in the *F*-region was found to be farthest removed from the time of sunrise in the region in summer.

According to observations at Slough (APPLETON and NAISMITH, 1935) sunrise-effect in both *E*- and *F*-regions occurs prior to ground sunrise in all seasons.

According to observations at Washington during the period May–June, 1949 (WELLS, 1949), sunrise-effect in the *F*-region was found to occur after ground sunrise.

The occurrence of sunrise-effect in the region of maximum ionization of a layer may be compared with that in a region below the maximum. This has been made by several investigators working on frequencies appreciably below the critical frequency.

Vertical incidence observations with 325 kc/s waves at Stanford, California, have shown that the intensity of reflection tended to increase at the time when solar rays tangent to ground struck the region concerned. Observations with 100 kc/s showed that the *E*-region height drops appreciably at the time of ground sunrise. *F*-region sunrise-effect occurs when solar rays strike the region grazing a height greater than about 200 km.

Vertical incidence observations with 150 kc/s at Pennsylvania (LINDQUIST, 1952) showed that sunrise-effect on *E*-region height occurs when the solar rays strike the region grazing a height of about 100 km.

Oblique incidence observations with 300 kc/s (WATTS, 1952) showed that the sunrise-effect on the height of reflection starts when the rays are incident on the region grazing the ozonosphere.

Oblique incidence observations with 16 kc/s (BROWN and PETRIE, 1954) showed that the sunrise-effect occurs about one hour before ground sunrise.

Reception of short-wave radio signals (BANERJEE and SINGH, 1949) has shown that sunrise-effect in *F*-region occurs after ground sunrise.

From the above it appears that the occurrence of the sunrise-effect at the lower part of an ionospheric region precedes the sunrise-effect at the height of maximum ionization of the region. This is particularly the case for region *E*.

4. Possible Origin of the Sunrise-effect Delay

According to CHAPMAN'S theory (1931) the early morning increase in ionization of a layer at *E*-region height and concentric with the earth will begin when the solar rays strike the layer from 2°–5° below the horizon. The interval between the time of this increase and time of ground sunrise will show a seasonal variation which will be smaller for low than high latitudes.

Two other theories have also been proposed to account for the delay in the occurrence of sunrise-effect in an ionospheric region measured from the time of sunrise in the region. The first (MITRA, 1948) is based upon the phenomenon of filtering of solar ultraviolet radiation by atmospheric ozone. According to this theory, the time of *E*-region sunrise-effect is expected to undergo a seasonal variation with the seasonal variation of ozone distribution. The theory, however, as shown below, does not explain the time of occurrence of normal *E*-region sunrise-effect, although it explains the time of occurrence of sunrise-time sporadic

8–(12 pp)

E. The sunrise ionization, according to this theory, is due to the detachment of electrons from negative ions of oxygen. But the presence of negative ions in sufficient number for the purpose is questionable (BATES and MASSEY, 1951).

The second theory (LINDQUIST, 1952) is based upon the phenomenon of absorption of the effective solar radiation which ionizes O_2. According to this theory, however, the time of sunrise-effect measured from the time of sunrise in the *E*-region is not expected to undergo a seasonal variation.

Thus, neither of the above theories can explain fully the results of observations on the sunrise-effect delay. Further, these theories attempt to explain the sunrise-effect observations in region *E* only.

In what follows, we shall consider a process which appears to explain satisfactorily the sunrise-effect in both *E*- and *F*-regions.

We first note that in order that the ionization of any layer may be increased by the action of the solar rays, the active rays striking the region must not be significantly absorbed by the mass of air through which they have to pass. It therefore follows that the oblique solar rays in the morning, in order that they may ionize the active particles in an ionospheric region on the nightside, must pass at least above the height of the dayside maximum of the region.

Now, it is known that the height of an ionospheric layer in daytime is different from that in night-time. This means that if we draw a great circle dividing the nightside from the dayside, then the ionospheric level across the great circle in the region concerned will not be horizontal (Fig. 3), but will slope east or west according as the daytime height is lower or higher than the night-time height. If, therefore, the night-time height is greater than the daytime height, the delay in the sunrise-effect will be such that the effect will occur before ground sunrise, but after sunrise in the region, the delay being determined by the difference between the daytime and night-time heights of the layer. If, on the other hand, the daytime height is greater than the night-time height, the sunrise-effect in the region will occur after ground sunrise.

VOL. 6 1955

To check the above hypothesis, the night-time height of maximum ionization h_m (night) of a layer and the time of the commencement of the sunrise-effect (t_s) in the layer were noted. Hence, the height Z, grazing which the sun's rays strike the height h_m (night) at the time t_s, was calculated from the formula

$$Z = a \frac{h_m \text{ (night)} - d}{a + d}$$

where d is the height at which the sun rises at the time of sunrise-effect, and a is the radius of the earth. It is clear that according to the above hypothesis, the calculated height Z should correspond roughly with the measured daytime h_m of the layer in question after sunrise.

In Tables 5 and 6 are given the measured values of h_m (night), t_s, h_m (day), and the calculated height Z of the *E*- and *F*-regions on a number of days during the period June 1947 to June 1952.

It will be seen from the tables that Z, the calculated height grazing which the solar rays fall on the region at the time of commencement of the sunrise-effect, is approximately equal to the value of h_m (day), the height of maximum ionization

of the layer after the sunrise-effect. When h_m (day) is greater than h_m (night), as often happened in summer for the F-region, sunrise-effect occurred in the region after ground sunrise.

It may thus be concluded that the solar rays in the early morning begin to increase the ionization of an ionospheric layer only when the rays have passed above the region of maximum ionization of the same layer on the dayside. In other words, the tilt of the layer across the sunrise line determines the time of the sunrise effect. It may be mentioned in this connection that BUREAU (1942)

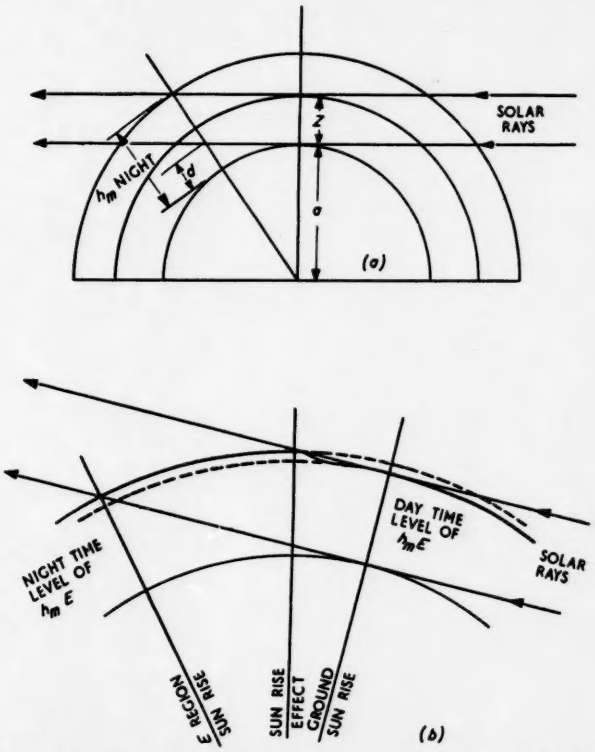

Fig. 3(a). Solar rays striking h_m on the nightside grazing a height Z.

Fig. 3(b). Solar rays striking the nightside of a tilted (west–east) ionospheric layer (height less on the dayside than on the nightside) grazing the daytime h_m.

in his studies on the sunrise-effect on the intensity of distant atmospherics, has offered a similar explanation for the characteristic variations in the intensity of the early-morning atmospherics, namely, that the effect is caused by the existence of a west to east inclination of the E-region level near the sunrise line.

It is to be noted that according to the process discussed above, the time of commencement of the sunrise-effect in an ionospheric layer is expected to undergo a seasonal variation parallel with the seasonal variation of daytime h_m of the layer. However, no definite seasonal variations in the time of E-layer sunrise-effect was observed during our measurements. This may be due to the fact that the

seasonal variation in the height of the E-layer is small. Unlike the h_m of the region E, that of the F-region undergoes large seasonal variation, and a definite seasonal variation in the time of the sunrise-effect was observed in this case. Since the F-region height varies also with the solar cycle, a solar-cycle variation

Table 5. Values of h_m (night), t_s, Z, and h_m (day) for the E-region

Date	*Measured night-time h_m before sunrise-effect* km	*Time of the commencement of the sunrise-effect measured from the time of sunrise at night-time height h_m* min	*Calculated height 'Z' of the layer grazing which the solar rays strike the night-time h_m (measured) at the time of sunrise-effect* km	*Measured daytime h_m after sunrise-effect* km
10. 6.47	120	45	108	105
24. 6.47	105	45	100	90
30. 6.47	120	43	105	105
6.12.47	105	43	105	105
16.12.47	90	47	105	105
9. 6.48	105	42	90	90
24. 6.48	105	45	100	90
7.12.48	90	42	90	90
14.12.48	105	40	88	90
24.12.48	120	48	100	105
16. 6.49	120	50	110	105
24. 6.49	120	48	108	105
7.12.49	105	45	95	90
21.12.49	105	48	100	105
7. 6.50	120	46	108	105
22. 6.50	120	47	109	105
8.12.50	105	42	90	90
14.12.50	105	44	92	90
9. 6.51	105	45	100	90
23. 6.51	120	40	103	105
4.12.51	120	40	104	90
27.12.51	120	38	100	90
14. 6.52	120	38	98	90
25. 6.52	105	44	98	90

in the time of sunrise-effect is also to be expected. Table 2 clearly shows the existence of such a variation.

The "tilt" hypothesis cannot, however, explain the formation of sunrise-time E_s. It has already been mentioned that although sunrise increase in normal E ionization occurs about forty to fifty minutes after sunrise in the region, sunrise-time E_s appears about ten to fifteen minutes earlier. One may suppose that the sunrise-time E_s is formed as a result of detachment of electrons from negative ions

VOL. 6 1955

Table 6. Values of h_m (night), t_s, Z, and h_m (day) for the F-region

Date	*Measured night-time h_m before sunrise effect* km	*Time of sunrise-effect measured from the time of sunrise at night-time height h_m before sunrise-effect* min	*Calculated height 'Z' of the layer grazing which the solar rays strike the night-time h_m (measured) at the time of sunrise-effect* km	*Measured day-time h_m after sunrise-effect* km
10. 6.47	360	84	—	390
24. 6.47	450	82	415	420
30. 6.47	375	76	360	360
6.12.47	390	68	360	360
16.12.47	360	61	340	330
26.12.47	390	59	335	330
4. 6.48	450	95	—	480
9. 6.48	420	82	400	405
24. 6.48	390	92	—	420
7.12.48	390	66	365	360
14.12.48	420	64	358	360
24.12.48	360	60	325	330
17. 6.49	360	82	—	390
24. 6.49	420	75	386	390
7.12.49	330	58	302	300
13.12.49	330	57	300	300
21.12.49	360	60	325	330
7. 6.50	285	80	—	330
14. 6.50	285	82	—	360
22. 6.50	330	70	305	300
8.12.50	270	58	248	240
14.12.50	285	60	270	270
27.12.50	300	62	276	270
2. 6.51	360	86	—	390
9. 6.51	300	84	—	330
23. 6.51	315	75	302	300
4.12.51	330	58	307	300
18.12.51	360	57	320	305
27.12.51	360	61	330	330
7. 6.52	330	62	310	300
14. 6.52	330	88	—	360
25. 6.52	315	65	296	300

Sunrise-effect occurred after ground sunrise on days marked (—) in column 4.

of oxygen by solar rays which have grazed the top of the ozonosphere. This is because both in summer and in winter, the time of occurrence of E_s very nearly corresponds to the time when solar rays fall on the *E*-region grazing the top of the ozonosphere. But, as has been said earlier, the presence of negative ions in sufficient numbers in the region is questionable.

The tendency of the F-region height to increase in summer after the occurrence of the sunrise effect in the region can be attributed to solar tidal effects. Analysis of the ionospheric data for solar tides has shown that at the latitude of Calcutta, the solar tidal drift in the early morning hours is upward in summer and downward in winter (MITRA, 1950). The tendency of the layer to move upwards in the early morning in summer helps in the rapid bifurcation of the layer; the tendency to move downwards in winter retards the same. This is also verified by the experimental results stated above regarding the time at which the bifurcation starts in the F-layer. In summer the bifurcation occurs even before the occurrence of F-region sunrise-effect; formation of the F_1-region at this hour is, however, difficult to explain on the basis of our existing knowledge.

Acknowledgment—The work forms part of the programme of the Radio Research Committee of the Council of Scientific and Industrial Research, Government of India.

The author is indebted to Professor S. K. MITRA for helpful discussions and advice during the progress of the work and to the Council for financial assistance.

REFERENCES

APPLETON, E. V., and NAISMITH, R.	1935	*Proc. Roy. Soc.* **150,** 685
BANERJEE, S. S., and SINGH, R. N.	1949	*Nature (Lond.)* **164,** 925
BARAL, S. S.	1952	*J. Sci. Ind. Res. (India)* 11A, 290
BATES, D. R., and MASSEY, H. S. W.	1951	*J. Atmosph. Terr. Phys.* **2,** 1
BHARGAVA, B. N.	1952	*Nature (Lond.)* **170,** 983
BROWN, S. B., and PETRIE, W.	1954	*Canad. J. Phys.* **32,** 90
BUREAU, R.	1942	*Notes Préliminaires du L.N.R.*, No. 36, 41
CHAPMAN, S.	1931	*Proc. Phys. Soc.* **43,** 483
LINDQUIST, R.	1952	*J. Geophys. Res.* **57,** 439
MITRA, A. P.	1950	*Ind. J. Phys.* **24,** 387
MITRA, S. K.	1948	*Upper Atmosphere* (First edition) R.A.S.B., p. 320
WATTS, J. M.	1952	*J. Geophys. Res.* **57,** 487
WELLS, H. W.	1949	*J. Geophys. Res.* **54,** 277

VOL. 6 1955

RESEARCH NOTE

Collisional deactivation and the night airglow

(*Received* 5 *January* 1955)

In the region near the 100-km level the mean number of oxygen molecules dissociated by photo-action is of the order of $10^{12}/cm^2$ column sec. This must also be the mean number of associations that take place. Molecules in the $X^3\Sigma_g^-$ ground state and the $a^1\Delta_g$, $b^1\Sigma_g^+$, $^1\Sigma_u^-$, $^3\Delta_u$, and $A^3\Sigma_u^+$ excited states should be formed, since the atoms may approach each other along the appropriate potential surfaces. Allowing for the possibility that the ground state may be favoured to a certain extent, it might therefore be predicted that the band systems originating from the excited states mentioned would be emitted with photon intensities of perhaps some 10^{10} to $10^{11}/cm^2$ column sec. However, most of these systems have in fact not been detected in the spectrum of the night airglow (cf. Chamberlain and Meinel, 1954); and though the Herzberg system is prominent, its photon intensity (integrated from λ3100 to λ3900) has been found by Barbier (1954) to be only $1{\cdot}5 \times 10^8/cm^2$ column sec. Molecular oxygen thus seems to radiate much less strongly than might at first be expected (Bates, 1954).

To remove the discrepancy, it is natural to seek to invoke collisional deactivation, but it is improbable that the mechanisms usually considered could suppress the emission by as large a factor as is apparently required. Deactivation through the transfer of the electronic energy to another system may be ignored, since this does not prevent emission. For the deactivation to be effective it is necessary for the electronic energy to be converted into kinetic energy. *Direct* conversion (involving as it does an electronic transition) does not occur readily in collisions between heavy particles* (Massey, 1949). When the amount of energy concerned is as much as several e volts, the chance of such conversion in a thermal encounter could scarcely be very much greater than 10^{-6}, which value would correspond to a rate coefficient of 3×10^{-16} cm^3/sec for deactivation (cf. Massey and Burhop, 1952). If the rate coefficient were as low as this, a metastable oxygen molecule in the region near the 100-km level (where the particle concentration is $2 \times 10^{13}/cm^3$) would have a life towards deactivation of approximately 200 sec, so that unless the life towards radiation is longer than is judged likely from the absorption measurements of Herzberg (1952, 1953), pronounced suppression of the emission would not be anticipated.

There is, however, another deactivation mechanism to which it is desired to call attention, namely the *indirect* conversion of electronic into kinetic energy through atom-atom interchange. To take a specific example, a free oxygen atom may displace one of the atoms comprising an oxygen molecule in a state α to form an oxygen molecule in a lower state β, thus

$$O(^3P) + O_2(\alpha) \rightarrow O_2(\beta) + O(^3P).$$

The process is essentially an ordinary chemical one. Its rate coefficient may be expressed in the standard Arrhenius form. The controlling parameters, that is the steric hindrance factor and more especially the activation energy (which is a decreasing function of the vibrational and rotational quantum numbers), are not easy to estimate in any particular case, but it can be said that a rate coefficient as high as about 10^{-10} cm^3/sec is not excluded

* It is clear from the work of Seaton (1954) that deactivation by electron collision is unimportant in the present connection.

or even unduly exceptional. In view of the small binding energies of $O_2(^1\Sigma_u^-, {}^3\Delta_u$, and $A^3\Sigma_u^+$), and of the fact that association tends to populate high vibrational and rotational levels, it would not be surprising if atom-atom interchange, resulting in deactivation, occurs rapidly. Hence a considerable fraction of the excited molecules may not radiate. Deactivation of $N_2(A^3\Sigma_u^+)$ by atom-atom interchange is another process which may be of interest in aeronomy. A laboratory study of the various possibilities presented is of course needed before an assured conclusion can be drawn.

Acknowledgments—Thanks are due to Dr. J. W. CHAMBERLAIN for stimulating correspondence.

Department of Applied Mathematics,
The Queen's University of Belfast.

D. R. BATES.

REFERENCES

BARBIER, D.	1954	*Ann. d'Astrophys.* **17,** 9
BATES, D. R.	1954	*The Earth as a Planet* (ed. G. P. KUIPER) (Chicago University Press)
CHAMBERLAIN, J. W., and MEINEL, A. B.	1954	*The Earth as a Planet* (ed. G. P. KUIPER) (Chicago University Press)
HERZBERG, G.	1952	*Canad. J. Phys.* **30,** 185
	1953	*Canad. J. Phys.* **31,** 657
MASSEY, H. S. W.	1949	*Reports on Progress in Physics* **12,** 248
MASSEY, H. S. W., and BURHOP, E. H. S.	1952	*Electronic and Ionic Impact Phenomena* (Oxford, Clarendon Press).
SEATON, M. J.	1954	*J. Atmosph. and Terr. Phys.* **4,** 295

VOL. 6 1955

ERRATUM

It is regretted that an error occurs in the paper by N. C. BARFORD, G. DAVIS, A. J. HERTZ, R. M. TENNENT, and D. A. TIDMAN on "High-altitude free balloon flying" which appears on page 219 of volume 5 (1954).

In the two diagrams figures 4 and 5, the time scale is shown as a line representing 10 minutes duration of level flight. The line should represent 20 minutes.

Journal of Atmospheric and Terrestrial Physics, 1955, Vol. 6, pp. 173 to 175 Pergamon Press Ltd., London

Indices of geomagnetic activity

of the Observatories ABINGER (*Ab*), ESKDALEMUIR (*Es*), and LERWICK (*Le*)

September to December 1954

The figures given on pages 173 to 175 represent the K-indices for three-hour intervals, beginning with 00–03 hrs for the first and ending with 21–24 hrs for the eighth figure.

September, 1954

Day	*Ab* *Range for* $K = 9 : 500\gamma$			*Es* *Range for* $K = 9 : 750\gamma$			*Le* *Range for* $K = 9 : 1000\gamma$			*Day*
	K-Indices		*Sum*	*K-Indices*		*Sum*	*K-Indices*		*Sum*	
1	3333	4445	29	2223	4355	26	2222	4456	27	1
2	4333	2334	25	5333	1323	23	6432	1333	25	2
3	2224	4455	28	2223	4444	25	3122	3445	24	3
4	3333	3523	25	3223	3413	21	5222	3412	21	4
5	3223	3232	20	3223	3222	19	3222	2221	16	5
6	3222	2463	24	2222	2463	23	2121	2464	22	6
7	2333	3444	26	2333	2343	23	3322	2343	22	7
8	3212	3342	20	3212	3331	18	3211	2231	15	8
9	2332	4424	24	2332	3323	21	1332	3223	19	9
10	2323	3323	21	2222	3222	17	2212	2213	15	10
11	2233	3423	22	2223	2323	19	2222	2323	18	11
12	1023	2223	15	0112	2223	13	1011	2223	12	12
13	2122	2225	18	2012	2115	14	1111	1115	12	13
14	3543	4425	30	3433	4324	26	5542	4325	30	14
15	2233	3323	21	3233	3323	22	3223	3323	21	15
16	4433	4333	27	4323	4333	25	4323	3233	23	16
17	4322	2233	21	4212	1133	17	4221	0133	16	17
18	4233	2334	24	4232	1334	22	4222	1334	21	18
19	2231	2233	18	2221	2233	17	2121	2233	16	19
20	3333	4664	32	3332	4564	30	3332	4775	34	20
21	3333	3553	28	3333	3553	28	4333	3543	28	21
22	3223	3332	21	2122	4332	19	2212	3231	16	22
23	2233	2221	17	1022	3221	13	1022	2121	11	23
24	2222	2324	19	2101	1334	15	1111	1324	14	24
25	3232	3353	24	2232	3353	23	2232	2353	22	25
26	3222	3232	19	2222	3232	18	2122	2231	15	26
27	2222	2444	22	1212	2344	19	1112	2343	17	27
28	5322	3323	23	5322	3212	20	4323	3213	21	28
29	4323	3555	30	4323	2555	29	4322	3555	29	29
30	2333	3344	25	2323	2244	22	2333	2344	24	30

K-indices

October, 1954

Day	*Ab* Range for $K = 9 : 500\gamma$		Sum	*Es* Range for $K = 9 : 750\gamma$		Sum	*Le* Range for $K = 9 : 1000\gamma$		Sum	Day
	K-Indices			*K-Indices*			*K-Indices*			
1	4444	3543	31	3444	3533	29	4544	2643	32	1
2	3322	3124	20	3320	2024	16	2321	2125	18	2
3	4433	3335	28	4432	3335	27	4433	2346	29	3
4	5333	2433	26	5323	2423	24	7422	2333	26	4
5	1222	2343	19	1211	1343	16	1111	1243	14	5
6	3333	4523	26	1332	4523	23	3322	3523	23	6
7	2223	3422	20	1223	2322	17	1112	3311	13	7
8	3222	4334	23	2221	3323	18	2211	3234	18	8
9	2232	1112	14	2121	0002	8	3212	1102	12	9
10	2211	2221	13	1111	1021	8	2221	1021	11	10
11	2222	2110	12	2221	1000	8	2221	1110	10	11
12	0021	1110	6	0000	0000	0	0000	1001	2	12
13	0022	1223	12	0001	1112	6	0001	1112	6	13
14	3123	1243	19	2002	1243	14	2102	1143	14	14
15	2222	2211	14	1111	1101	7	1111	1101	7	15
16	2122	2332	17	1010	2332	12	2011	2332	14	16
17	2212	3134	18	2212	1234	17	2111	0124	12	17
18	4434	5523	30	4434	5523	30	4333	4533	28	18
19	3234	4433	26	2224	4433	24	3223	3432	22	19
20	3233	3223	21	3232	2232	19	3333	2223	21	20
21	2222	2131	15	1012	2231	12	2011	1121	9	21
22	0222	2333	17	0012	2333	14	1122	2344	19	22
23	3333	3444	27	3233	3444	26	3233	3355	27	23
24	4543	3653	33	4443	3554	32	5544	4764	39	24
25	4433	3332	25	4323	3221	20	5532	3321	24	25
26	2232	2343	21	2222	2333	19	2222	2233	18	26
27	1234	4421	21	1234	3411	19	1123	3321	16	27
28	3222	2322	18	2211	1212	12	2112	1212	12	28
29	1123	2223	16	0013	2013	10	0012	1103	8	29
30	3432	3234	24	3411	3134	20	3421	2134	20	30
31	2233	3344	24	2222	3344	22	2122	2444	21	31

November, 1954

1	3332	4455	29	3322	3454	26	2322	3454	25	1
2	5433	4343	29	5322	3343	25	6332	3243	26	2
3	4332	3443	26	3322	2332	20	3321	2432	20	3
4	1223	2312	16	1002	2212	10	1112	1311	11	4
5	3232	2221	17	3132	2120	14	3222	1121	14	5
6	3222	2343	21	3211	1343	18	3221	1243	18	6
7	3111	1111	10	3111	1001	8	3011	0101	7	7
8	2122	2232	16	2111	1132	12	2111	1132	12	8
9	1222	1331	15	0110	1221	8	0101	1211	7	9
10	2112	1111	10	2000	0001	3	2010	0001	4	10
11	1112	2232	14	0111	2131	10	0101	1131	8	11
12	2323	3133	20	1322	2122	15	1312	2122	14	12
13	2122	2222	15	1111	1122	10	1111	0112	8	13
14	2221	1223	15	2110	1223	12	2110	1223	12	14
15	2111	2121	11	2000	0000	2	2000	0010	3	15

, VOL. 6 1955

November, 1954 (*contd.*)

Day	*Ab* Range for $K = 9 : 500\gamma$		Sum	*Es* Range for $K = 9 : 750\gamma$		Sum	*Le* Range for $K = 9 : 1000\gamma$		Sum	Day
	K-Indices			*K-Indices*			*K-Indices*			
16	1112	1111	9	1000	0000	1	1000	0000	1	16
17	1122	2101	10	0011	1001	4	0010	1001	3	17
18	1112	3333	17	1001	2222	10	1101	2211	9	18
19	1322	2333	19	1322	1333	18	2311	0233	15	19
20	2232	4432	22	2232	3332	20	2232	3421	19	20
21	2222	3223	18	2122	2113	14	2122	2103	13	21
22	2232	1122	15	2230	0022	11	2121	0022	10	22
23	1222	2543	21	1212	1442	17	1111	1543	17	23
24	1222	2331	16	1211	1230	11	1111	1231	11	24
25	1222	2123	15	0112	2013	10	0111	1103	8	25
26	2122	2233	17	2011	2222	12	2111	1112	10	26
27	2222	1231	15	2222	1330	15	2111	1230	11	27
28	1012	2123	12	1002	2113	10	1001	1113	8	28
29	1012	4433	18	1002	3333	15	1012	3323	15	29
30	3421	2333	21	3421	1333	20	3331	1333	20	30

December, 1954

1	3221	1222	15	3121	0111	10	3111	1112	11	1
2	2211	2213	14	1101	1203	9	2111	1213	12	2
3	3122	1122	14	3010	0111	7	2011	0122	9	3
4	0112	2131	11	0002	2110	6	0001	1021	5	4
5	1121	1332	14	1000	1322	9	1110	1222	10	5
6	1221	1122	12	1111	1012	8	1111	1022	9	6
7	2121	2234	17	2120	2233	15	2110	1233	13	7
8	1211	1112	10	1110	1001	5	1210	1001	6	8
9	2212	2121	13	2112	2010	9	1111	2011	8	9
10	1011	1121	8	0001	1011	4	1011	0011	5	10
11	1012	2111	9	1001	1100	4	1001	1000	3	11
12	0121	1333	14	0021	1233	12	0011	1233	11	12
13	3212	2142	17	3110	0033	11	3101	1122	11	13
14	2211	1211	11	2100	0000	3	1100	1001	4	14
15	1111	1000	5	0000	0000	0	1001	0001	3	15
16	1212	2111	11	0000	0000	0	0001	0000	1	16
17	2244	3323	23	1233	2323	19	1133	2313	17	17
18	4313	3124	21	4312	2124	19	4322	2113	18	18
19	2122	3332	18	1111	3222	13	1111	2122	11	19
20	1222	3224	18	1212	3224	17	1212	2114	14	20
21	2112	2122	13	2002	1112	9	1011	1111	7	21
22	3212	2121	14	3001	1110	7	3111	1121	11	22
23	0111	1221	9	1111	1201	8	0111	0111	6	23
24	1122	3111	12	0001	2011	5	1111	2011	8	24
25	2012	3221	13	2010	2222	11	1001	2222	10	25
26	1112	3122	13	1101	2122	10	1101	2001	6	26
27	4312	5224	23	4212	4214	20	4211	4214	19	27
28	3312	2321	17	3202	1221	13	3211	1211	12	28
29	1123	3221	15	1012	2211	10	1111	2121	10	29
30	1113	3113	14	1112	2103	11	0012	2002	7	30
31	2213	3221	16	2102	2210	10	1102	1110	7	31

Book review

HOMER E. NEWELL, Jr.: **High Altitude Rocket Research.** Pp. 298 + xiv. Academic Press Inc., New York. $7.50.

THE appearance of the first book on the use of rockets for studying the properties of the high atmosphere of the earth is an important event. It shows how far this work has now progressed and what useful and often unexpected results it can provide. There is no doubt that there is a very big future in the use of rocket vehicles for geophysical and astronomical research. Altitudes of over 200 kilometres have already been reached, and it is already possible to observe the solar spectrum free from terrestrial atmospheric absorption. Plans for use of satellite vehicles are now being actively discussed, and there is growing interest in scientific circles, not only because of the value of the scientific information which can be obtained, but also because of the scope afforded for ingenuity in design of experiments which must be carried out within the vehicle during flight and from which the data obtained must be signalled to ground through a telemetering system.

The full fascination of the subject is manifest from Dr. NEWELL's book. He has been associated with the work of the U.S. Rocket Research Panel from its earliest days and has known frustration as well as elation in abundant measure.

After an introductory chapter in which the general features of the upper atmosphere are described and a summary account given of the rockets and firing facilities available in the U.S.A., the next two chapters are concerned with the technique of rocket experiment. Chapter II discusses the difficulties involved in utilizing a rocket as a very mobile (and not often controllable) and very confined physics laboratory. The recovery of the data measured in situ by the apparatus within the rocket is the concern of Chapter III. This is an art of great importance. It is simpler to devise methods of measurement so that the observed data can be telemetered to ground, but the problem of physical recovery after flight has also been successfully tackled.

The remaining seven chapters describe the methods used and the results obtained in studying different physical properties and phenomena, namely Pressures, Densities and Temperatures, Winds, Solar Radiation, Composition, Ionosphere and Earth's Magnetic Field, Cosmic Rays and High Altitude Photography. Some of the most interesting observations described in Chapter VI are those of the solar emission in the soft X-ray region and in the far ultraviolet. The possibilities opened in research in the electrical properties of the high atmosphere are clearly very great, and the main results, after an encouraging beginning, are still to come. Remarkable ingenuity is displayed in the methods used to study pressure, density, and temperature, as indeed in all the technique.

The book is written in an easy and pleasant style with adequate but not overwhelming detail. It is well illustrated and is attractively set out. The physicist or engineer attracted by the title should be rewarded by an interesting account which should give him a good idea of the highlights, while at the same time the upper-atmospheric specialist should find the book a very useful and stimulating summary of the present position.

H. S. W. MASSEY

VOL. 6 1955

Journal of Atmospheric and Terrestrial Physics, 1955, Vol. 6, pp. 177 to 188. Pergamon Press Ltd., London

Some geomagnetic effects in the equatorial F_2-region

N. J. SKINNER and R. W. WRIGHT
University College, Ibadan, Nigeria

(*Received* 6 *June* 1954)

ABSTRACT

The diurnal variations of the values of many ionospheric parameters obtained at Ibadan, Nigeria, close to the magnetic equator, are investigated on magnetically quiet days and on magnetically disturbed days. It is found that the midday minimum of the maximum concentration of ionization N_m in the F_2 layer disappears as the days become more disturbed. On quiet days there is very little scatter of values of N_m, but on disturbed days this is much increased. Furthermore, both N_m and the total ion content, n, of a column of unit cross-section below the height of maximum ionization are greater at all times of the day on disturbed days than they are on quiet days.

The perturbation of the quiet-day variation introduced on disturbed days, S_D, has not only a diurnal (twenty-four hours) component, but also a semidiurnal component.

Whilst there is general agreement in the behaviour of the results described here and the theory of ionospheric disturbances proposed by MARTYN (1953), our data imply that the phases of the motions differ appreciably from those suggested by MARTYN.

1. INTRODUCTION

It is well known that the earth's magnetic activity exerts an influence on the ionospheric parameters f_0F_2 and $h'F_2$ over a wide range of latitudes. APPLETON, NAISMITH, and INGRAM (1937) established a close correlation between the noon and midnight critical frequencies in the F_2-layer (f_0F_2) and the magnetic activity at places of high latitude. For the Polar Year 1932–33 they obtained a correlation coefficient of $-0{\cdot}34$ (for Tromso) and $-0{\cdot}40$ (for Slough) between f_0F_2 at noon and the daily magnetic activity. In addition, they noted the presence of a seasonal variation in the relation between magnetic and ionospheric disturbances which has recently been confirmed by APPLETON and PIGGOTT (1952). A rather different technique was used by BERKNER and SEATON (1940), who considered the correlation between the mean electron density throughout the day and magnetic activity for the stations Watheroo and Huancayo. The temperate station gave results agreeing in general with APPLETON *et al.*, but it was found that for the equatorial station the correlation was reversed in sign and f_0F_2 increased during magnetically disturbed periods.

More recently MARTYN (1953) has investigated in a more systematic manner how the diurnal variations of f_0F_2 and the virtual height $h'F_2$ may be affected by magnetic activity. He considered the three moderate latitude stations, Watheroo, Washington, and Canberra, and found that the mean level of f_0F_2 was depressed during magnetic disturbance in the summer and at the equinoxes, but that there was a very much smaller effect in winter, f_0F_2 actually being slightly raised for Canberra and Watheroo.

We have examined below the difference between the magnetically quiet and disturbed day variations of the maximum ion concentration N_m (proportional to $(f_0F_2)^2$) for the equatorial station Ibadan (lat. 7° 26′ N, long. 3° 54′ E, magnetic lat. about $2\frac{1}{2}$° S). The difference is so marked that we have extended the analysis to include most of the other ionospheric parameters connected with the F_2-layer. Explanations are suggested which seem to explain many of our experimental results.

2. Treatment of Data

The results of ionospheric records obtained at Ibadan in 1952 have been utilized. The days have been divided into three groups according to the sums of the geomagnetic planetary three-hour-range indices Kp. Table 1 shows how the division was made and gives the percentage number of days in each group.

Table 1

Magnetic activity	*Symbol*	*Kp*	*Percentage number of days in each group*	*Mean sunspot number*
Quiet	Q	0–15 inc.	23	34·4
Medium	M	16–30 inc.	52	33·8
Disturbed	D	$\geqslant 31$	25	34·8

For each ionospheric characteristic considered, the average quiet (Q) day variation has been plotted on the same axes as the average disturbed (D) day variation. In some cases, the diurnal variation has also been evaluated for M days.

For the evaluation of N_m, not all the available data were used, because we were particularly interested in comparing its behaviour to that of $y_m \cdot N_m$, (which is proportional to n, the total ion content in a column of unit cross-section below the height of maximum ionization in the F_2-layer). Accordingly, only values of N_m obtained on hours for which y_m (the semi-thickness of the F_2-layer) had been measured, were used. This had little effect on the shape of the mean N_m curve, except that at night, when it is often impossible to measure y_m, there are few values of f_0F_2 and the averages are somewhat more erratic.

There are some obvious objections to the above method of analysis. It will be seen that we have taken the magnetic activity of the whole day as governing the ionospheric state throughout the day. This will be discussed further in the next section. Also, it is well known that there is a correlation between sunspot numbers, magnetic activity, and ionization in the ionosphere. It might be suggested that D days and Q days represent days of high and low sunspot activity respectively. Table 1, however, shows that there is a negligible difference between the mean sunspot number for Q, M, and D days in 1952.

3. The Maximum Concentration of Electrons N_m

The maximum concentration of electrons in the F_2-layer, N_m, is proportional to the square of the critical frequency. When f_0F_2 is measured in Mc/s

$$N_m = 1{\cdot}24 \times 10^4 \times (f_0F_2)^2$$

The behaviour of N_m is more relevant to the layer processes than f_0F_2, so we have accordingly considered N_m (expressed in terms of $(f_0F_2)^2$ in $(\mathrm{Mc/s})^2$) in detail, rather than the critical frequency. Fig. 1 shows the diurnal variations of N_m on D and Q days. The differences between the two groups are very great. This is very important in radio communications, especially as about half of all days fall definitely into these extreme groups with about equal numbers in each. Fig. 2,

VOL. 6 1955

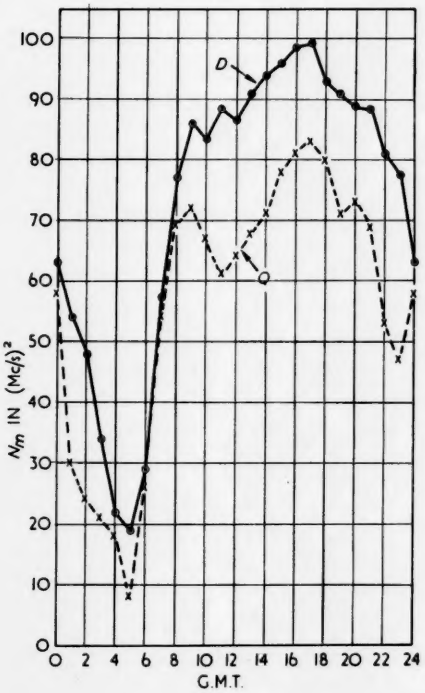

Fig. 1

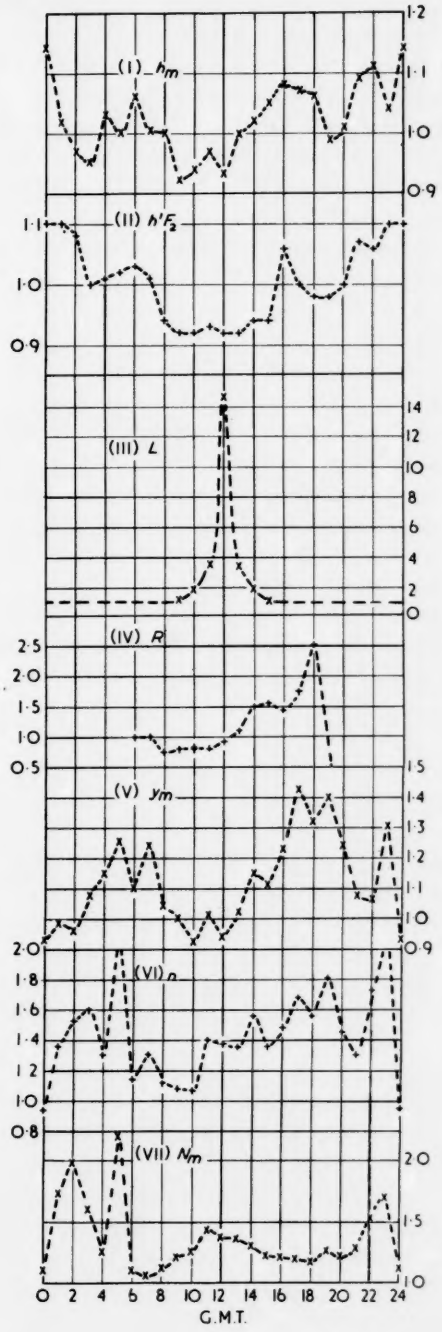

Fig. 2

Curve VII, shows the ratio D/Q of the hourly values of N_m on D and Q days. The increase of about 40 per cent during the daytime on disturbed days is in the opposite direction to that which is encountered in temperate latitudes. Although the large peak at 0500 hr occurs at the local time showing maximum ratio at higher latitudes, the shape of the $N_m(D)/N_m(Q)$ curve suggests that the peak may not be reliable. In practice this is the most difficult time of the day at Ibadan to measure N_m, and the number of observations is therefore abnormally small.

In view of the practical importance of this parameter, a more detailed investigation has been made into its behaviour. The days have been redivided into smaller

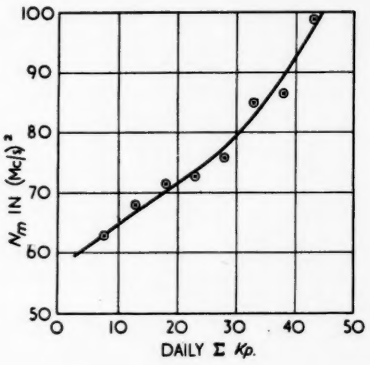

Fig. 3

groups, with daily total Kp figure of 0–10, 11–15, 16–20, 21–25, 26–30, 31–35, 36–40, and those greater than, or equal to, 41. Whilst the number of days in each group is made rather small, the trend of the change as the day becomes more disturbed is very marked, though crossovers do occur. The complete figure is not reproduced here, but in Fig. 3 the mean value of N_m between the hours of 1000 and 1400 inclusively are plotted for each of these groups of days against the mean daily Kp figure of the group. The monotonic increase which is obtained is all the more striking when it is considered that data at all seasons have been included. An analysis into seasons has been made, but the overall diurnal variations of the Q and the D days are little changed and discussion of this point is deferred until a later date. The most marked fact about the change in the diurnal variation as the days become more and more disturbed is the manner in which the midday minimum of ionization on Q days gradually disappears and on very disturbed days is replaced by a pronounced maximum. It would be interesting to know whether the geomagnetic anomaly of a minimum of noon f_0F_2 at other stations along the magnetic equator is also removed by a similar consideration of very disturbed days alone.

The distribution of the values of f_0F_2 is shown in Fig. 4, where the number of times a value of f_0F_2 is obtained in a small range of values is plotted against the median value of the range. Curves are given showing (1) all days. (2) quiet days. and (3) disturbed days. Again it must be realized that all seasons are included in these curves. The width of the distribution curve for quiet days may be almost completely explained by the variation which must occur throughout the year due

VOL. 6 1955

to seasonal changes. Disturbed day values are very much more scattered, but about a much higher median value.

It is mentioned above that we have used the daily Kp figure to characterize the whole day from 0000 hr to 2400 hr. A more exact analysis would seem to involve using the Kp figure for the twenty-four hours preceding the hour in question. The probable effects of such a treatment have been considered in two ways. Firstly, we

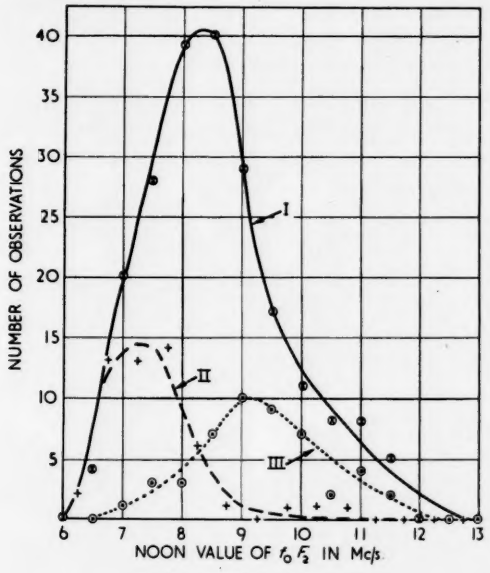

Fig. 4

have investigated the diurnal behaviour of N_m on the days which follow D days, and the days which follow Q days, called briefly $D + 1$ and $Q + 1$ days. It is to be expected that the $D + 1$ days would resemble the D days since appreciable magnetic activity usually lasts for periods longer than twenty-four hours. In fact, the average Kp figure for a D day is 36·9, whilst for a $D + 1$ day it is 31.5. There is no significant deviation between $D + 1$ and D days or $Q + 1$ and Q days. Secondly, the correlation coefficient has been worked out not only between the noon values of $(f_0F_2)^2$ and the daily Kp figure, r_1, but also between the noon values of $(f_0F_2)^2$ and the Kp figures for the period 0600–1200 hr on the day in question, r_2. It is found that $r_1 = +0{\cdot}43$, and $r_2 = +0{\cdot}44$, both values being obtained from 274 pairs of values. The difference is hardly significant. From both the above considerations it will be seen that the method of classifying the day does not lead to any marked differences in the results obtained.

Martyn in his discussion of the behaviour of the ionosphere during periods of magnetic activity has studied the behaviour of f_0F_2 and $h'F_2$ as a function of storm time. At Ibadan during 1952 we have records for only seven storms classified severe or moderately severe, the majority of which commenced around midnight. However, even with so few storms the variation of f_0F_2 with storm time is marked. Upon removal of the normal quiet-day variations it is found that f_0F_2 is given a

pronounced decrease at the beginning of an ionospheric storm for a period of about ten hours. After this, f_0F_2 rises above normal, as would be expected in a period of disturbed days. This is the opposite of MARTYN's general results obtained when discussing temperate stations, as is to be expected. It must be remembered, that not much reliance should be placed upon the results from only seven storms, and a further analysis is desirable.

4. OTHER IONOSPHERIC PARAMETERS

(a) *The semi-thickness of the F_2-layer — ym*

Fig. 5 shows the average Q and D diurnal variations for y_m. The values of y_m have been deduced for the most part by APPLETON and BEYNON's method. However, when an individual hourly record showed that a non-parabolic type of

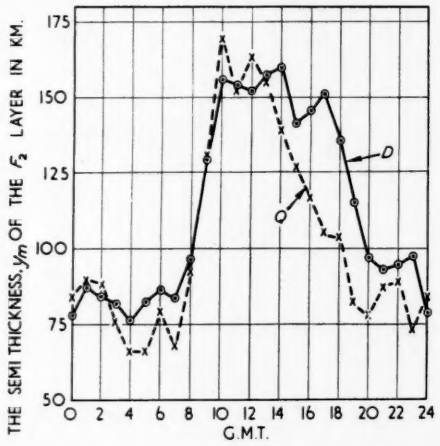

Fig. 5

electron distribution existed in the F_2-region, an equivalent semi-thickness T_{eq}. was evaluated instead, using techniques evolved by RATCLIFFE (1951). This expedient was frequently resorted to during the daylight hours 0800–1200, 1500–1800. It is seen in Fig. 5 that there is a general tendency for $y_m(Q)$ to exceed $y_m(D)$ for the morning hours 0900–1300, whereas in the afternoon from 1300 onwards $y_m(D)$ is markedly greater than $y_m(Q)$. In Fig. 2, Curve V, the ratio of y_m on D days to that on Q days is plotted for each hour of the day. There is seen to be quite a pronounced semi-diurnal oscillation.

(b) *Total ion content in unit column below h_m — n*

RATCLIFFE (1951) has described a quick method of analyzing $h'f$ records whereby n, the total ion content of a column of unit cross-section below the height of maximum ionization in the F_2-layer, can be obtained. The authors (1954) found that for Ibadan, the mean diurnal variation of n was of a much more regular nature than that for N_m. In particular, consideration of n largely removed the characteristic midday "equatorial bite-out" that is present throughout the year in the daily variations of N_m.

VOL. 6 1955

The value of n is related to N_m by the expression

$$n = 2/3\ y_m N_m$$

so that one would expect from our individual graphs for y_m and N_m that n would be larger on D days than Q days. Fig. 6 shows the mean diurnal variation of n_Q

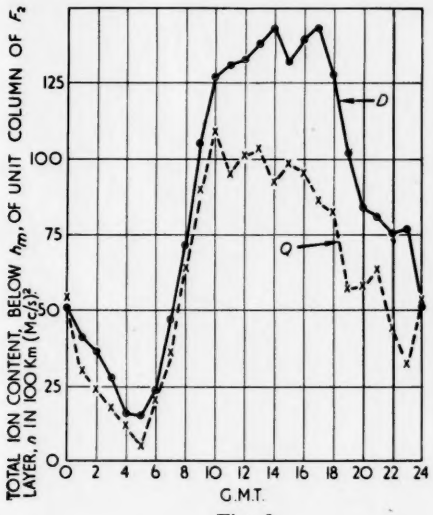

Fig. 6

and n_D (in units of km(Mc/s)²) and it is seen that n_D is greater than n_Q for every hour. In Fig. 2, Curve VI, the variation of the ratio n_D/n_Q is illustrated.

(c) *Percentage ridge occurrence—R*

Ridges and thick-layer phenomena in the F_2-region are found to occur almost every day at Ibadan and have been the subject of an earlier communication

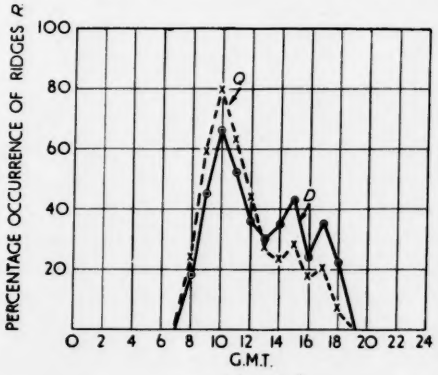

Fig. 7

(Skinner, Brown, and Wright, 1954). The variation of the percentage probability of ridge occurrence R with time of day showed a pronounced maximum at 1000 hr followed by a dip at 1300 hr. There were usually one or more peaks in the

afternoon, but ridges were not so pronounced then as in the morning periods. Fig. 7 shows the mean diurnal variation of R_Q and R_D, and it is clear that there is a greater probability (about 14 per cent) of ridge occurrence at 1000 hr on quiet days than on disturbed days. However, afternoon ridges appear to be more frequent on disturbed days.

Fig. 2, Curve IV, shows the diurnal R_D/R_Q variation, which is seen to consist of a negative phase followed by a positive phase.

(d) *Virtual height of the F_2-layer — $h'F_2$*

Previous workers have found that for temperate- and high-latitude stations, the virtual height of the F_2-layer $h'F_2$ was increased during magnetically disturbed periods. In agreement with the general tendency for correlation of the opposite sign in equatorial regions, we find that $h'F_2$ tends to be decreased during magnetic disturbance for the daylight hours when the F_2-layer is separated from the

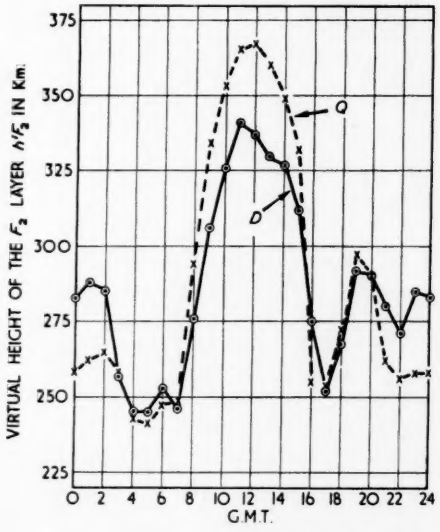

Fig. 8

F_1 (Fig. 8). This tendency has been found to persist at all seasons of the year. Fig. 2, Curve II, shows the ratio of the values of $h'F_2$ on D days to those on Q days. It is interesting to notice that the near-unity ratio between 1500 hr and 2000 hr strongly supports the authors' suggestion that the sunset maximum of $h'F_2$ observed at Ibadan is largely accounted for by difficulties of reduction at that time.

A short analysis has been effected for variations during storms, as is mentioned above. With the limited data available it is still possible to observe that there is an initial increase of $h'F_2$ at the beginning of a storm, lasting about fifteen hours, followed by an overall decrease. However, since $h'F_2$ seems larger during the night on D days, this can be linked with the fact that most of the storms used began at midnight. Much more data are required, but it is felt that a more

VOL. 6 1955

reliable parameter than $h'F_2$ should be used (such as h_m), since $h'F_2$ is capable of no single simple meaning.

(e) *Bifurcation of the F-layer — L*

The symbol L is internationally used in routine reduction of ionospheric records instead of numerical values of f_0F_1 and $h'F_2$ when there is no clear maximum of ionization density in the F_1-layer. The percentage occurrence of L thus presents a convenient method of assessing the degree of bifurcation of the F-layer at any hour, and it has been examined to see whether it is subject to geomagnetic control (Fig. 9). It is found that there is a consistently greater probability of L occurrence during magnetic disturbance, i.e., during disturbed periods the degree of bifurcation is smaller. Fig. 2, Curve III, shows the ratio of the percentage occurrence of L on disturbed and quiet days. At temperate latitudes this effect is reversed, bifurcation being greatest in disturbed periods.

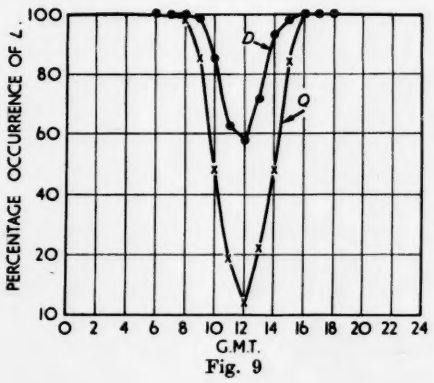

Fig. 9

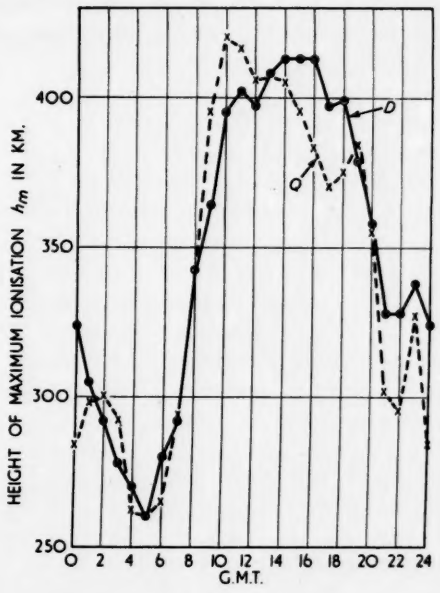

Fig 10.

(f) *The height of maximum ionization — h_m*

Values of h_m were reduced by APPLETON and BEYNON's method whenever a parabolic distribution of electron density existed. Values of h_m were also calculated for non-parabolic distributions, provided that the deviation from parabolism was slight. The average diurnal variations of $h_m(D)$ and $h_m(Q)$ are shown in Fig. 10. The general shapes are seen to be similar to those for y_m and R with a "cross over" at 1300 hr. The morning increase of $h_m(Q)$ above $h_m(D)$ may be accentuated by the fact that more ridges occur on quiet days than on disturbed, so that values of h_m will appear to be larger, due to group retardation in the ridges. Fig. 2, Curve I, shows the ratio of values of h_m obtained on disturbed days and quiet days.

5. DISCUSSION

MARTYN (1953) has developed a theory, according to which all ionospheric disturbance variations are due to the effect of an electrostatic field which is developed in the auroral zone. This field spreads over the earth through the ionosphere in such a way as to produce the current responsible for the disturbed days diurnal magnetic variation, and the combined effect of the current and the earth's magnetic field is to produce a vertical ionic drift velocity which perturbs the normal quiet-day (S_Q) variations of the ionospheric parameters. MARTYN computed the disturbance daily variations (S_D) of the characteristics f_0F_2 and $h'F_2$ by subtracting, for each month, the average daily variation for the five International magnetically quiet days from its average daily variation on the five International magnetically disturbed days, and found a strong diurnal (24-hour) harmonic present in the S_D (f_0F_2) and $S_D(h'F_2)$ variations for stations of moderately low latitude. The D/Q variations shown in Fig. 2 [which represent $(S_D + S_Q)/S_Q$] should give the shape of the S_D variations, and it is seen that whereas $h'F_2$ shows a strong diurnal component for Ibadan, the y_m and N_m curves have marked semi-diurnal harmonics in addition.

The quiet-day variation S_Q of the parameter is considered by MARTYN's theory (1947) to be due to solar semi-diurnal tides in the ionosphere which produce vertical ionic drifts. Unfortunately, the phases of these S_Q motions cannot as yet be said to be definitely known, particularly close to the magnetic equator, and this complicates the present discussion. However, it is fairly simple to discuss the relative phases of the effects of the two motions S_Q and S_D. One of the effects of the quiet-day tidal variation, S_Q, at low latitudes is to assist the separation of the F_2-layer from the F_1. Fig. 9 shows that at Ibadan bifurcation is less marked on disturbed days. It would follow that the S_D and S_Q fields are in opposition during the daylight period at least. Confirmation of this is afforded by consideration of the following experimental evidence:

(1) $h'F_2$ is lower on disturbed days, indicating that the F_1-F_2-layer separation is less (the F_1-layer is relatively unaffected by magnetic disturbances).

(2) Both h_m and y_m are increased in the morning and reduced in the afternoon by the S_Q movements on quiet days. On disturbed days the rate of increase in the mornings and the rate of decrease in the afternoons are both less than on quiet days.

(3) The probability of morning-ridge occurrence is decreased on disturbed days. Ridges are obviously a dynamic phenomenon, and thus fewer ridges indicate less motion. The afternoon anomaly of R_D greater than R_Q is more difficult to explain. However, ridges are far less pronounced in the afternoon, being mainly "thick layers." On disturbed days with little bifurcation the whole F-layer is not far removed from one thick layer, so that little motion will be required to produce the occurrence of R. (It is seen from (2) above that the layer is already thicker in the afternoons of disturbed days.)

(4) Evidence of the N_m variation depends upon the absolute phases of S_Q, and will be discussed later.

The night-time situation is complicated by several factors. It seems likely that the S_D variation has a fairly large semi-diurnal, as well as diurnal, component. The latter could reinforce the S_Q semi-diurnal motions over a period of about twelve hours at night, and still oppose them during the day. There is slight

, VOL. 6 1955

experimental evidence for this, as examination of the curves will show. There might also be a change in the phase-lag between the field variations and the resulting ionospheric effects from night to day. In addition, the considerable differences of height of the layer between night and day may result in different velocity gradients, so that in all it is difficult to draw any unique set of conclusions from the night-time results.

The question of the absolute phases of the S_Q and S_D motions may now be considered. MARTYN (1948), from an analysis of a wide range of stations, has suggested that there may be a phase-lag of from $\pi/2$ to π between maximum drift motion and the maximum resulting effect on the ionospheric parameters. In order to simplify the discussion we shall consider first the phases of the effects produced by the motions. MARTYN has suggested that the maximum effect of the upwards ionic drift will occur at 1200 hr, in the region of the equator. This will produce a maximum value of N_m at noon. Hence, in order to explain the increased values of N_m on D days, the motion must be increased. This contradicts the evidence so far discussed, and, moreover, such a phase does not explain the midday minimum of N_m. Some additional effect is therefore required to explain this midday minimum, and if this effect is opposed by the S_D motions, or not present on D days, the difficulty is overcome. Such an additional mechanism has, in effect, been suggested by MCNISH and GAUTIER (1949), depending upon the large values of dH/dt at the equator before and after noon. A vertical ionic motion downwards just before noon and upwards soon after noon is produced. At first glance this would seem to account for the absence of the "bite-out" on disturbed days, since dH/dt would not change so smoothly as on quiet days, and so no continuous motion would be set up. Consideration of the S_Q and S_D magnetic variations for an equatorial station (Huancayo—BARTELS and JOHNSTON, 1939) would seem to indicate that the perturbation of dH/dt on disturbed days is not sufficient to justify this explanation. Nevertheless, this choice of phase satisfactorily explains the experimental facts, provided that some such additional mechanism is postulated. The variations of n may be accounted for by considering that on Q days the morning upward motion carries a considerable proportion of ionization above h_m.

We consider, however, that changing the phase of the S_Q variation better explains the experimental facts. A tide whose phase is such that the maximum effect of the downward velocity occurs at noon will explain the following points:

(1) There is a midday minimum of N_m which disappears when S_D opposes S_Q.

(2) h_m and $h'F_2$ increase to a maximum at noon on Q days (provided that an appropriate velocity gradient is assumed).

(3) There is a maximum of y_m at noon on Q days.

(4) h_m, y_m, and $h'F_2$ are smaller before noon on D days than on Q days and larger after noon.

(5) n is larger on D days than on Q days. (This is because on Q days, when the downward motion to regions of high α is larger, there is a greater loss of ions by recombination. This effect may be partly cancelled out by the downward motion bringing a greater proportion of ionization below the maximum.)

(6) The behaviour of R and L is explained in the same way as for the alternative choice of phase.

The phases of the actual motions of the ions will depend upon the phase-lag between the ionic velocity and the effects considered. If MARTYN is correct and the phase-lag in the F_2-layer is π, then his analysis indicates that the maximum downward motion at the equator should occur at noon. We suggest instead a maximum upward velocity at noon with the same phase-lag. If the phase-lag is $\pi/2$ then these suggestions are $\uparrow$ 1500 hr and $\downarrow$ 0900 hr, respectively.

We would suggest that either of the above theories would explain the experimental results obtained at Ibadan. It must be remembered that this station is very close to the magnetic equator, and effects which are of secondary importance in higher magnetic latitudes may here become predominant. It would be instructive to analyze results from stations slightly farther from the equator, especially those in the intermediate zone where N_m is neither increased nor decreased during magnetic disturbance. Seasonal effects would then become significant in determining phases.

The authors would like to acknowledge the constant encouragement of Professor N. S. ALEXANDER and the very helpful advice given by Mr. W. R. PIGGOTT, of the Radio Research Station, Slough.

REFERENCES

APPLETON, E. V., and BEYNON, W. J. G.	1940	*Proc. Phys. Soc.* **52,** 518
APPLETON, E. V., NAISMITH, R., and INGRAM, L. J.	1937	*Phil. Trans. Roy. Soc.* **A236,** 19
APPLETON, E. V., and PIGGOT, W. R.	1952	*J. Atmosph. Terr. Phys.* **2,** 236
BARTELS, J., and JOHNSTON, H. F.	1939	*Terr. Mag. & Atmos. Elec.* **44,** 455
BERKNER, L. V., and SEATON, S. L.	1940	*Terr. Mag. & Atmos. Elec.* **45,** 419
MARTYN, D. F.	1947	*Proc. Roy. Soc.* **A189,** 241
MARTYN, D. F.	1948	*Proc. Roy. Soc.* **A194,** 445
MARTYN, D. F.	1953	*Proc. Roy. Soc.* **A218,** 1
MCNISH, A. G., and GAUTIER, T. N.	1949	*J. Geophys. Res.* **54,** 181
RATCLIFFE, J. A.	1951	*J. Geophys. Res.* **56,** 463
SKINNER, N. J., BROWN, R. W., and WRIGHT, R. W.	1954	*J. Atmosph. Terr. Phys.* **5,** 92
SKINNER, N. J., and WRIGHT, R. W.	1954	*J. Atmosph. Terr. Phys.* **5,** 290

, VOL. 6 1955

Journal of Atmospheric and Terrestrial Physics, 1955, Vol. 6, pp. 189 to 197. Pergamon Press Ltd., London

On a new method of determining the height of the nightglow

PIERRE ST. AMAND,[1] HELEN B. PETTIT,[2] F. E. ROACH,[3] and D. R. WILLIAMS
U.S. Naval Ordnance Test Station, Inyokern, China Lake, California

(*Received* 11 *August* 1954)

ABSTRACT

A new method of determining the height of the nightglow by triangulation is described. A height between 80 and 100 km is indicated for the λ5577 [OI] radiation.

INTRODUCTION

Measurement of the height of the nightglow is difficult because of the dim and amorphous nature of the phenomenon. The lack of a discernible aurora-like structure precludes the ready application of the techniques [1] used to measure the height of the aurora polaris. The usual method of estimating the height is that of VAN RHIJN. This depends on several assumptions and choices as to the proper values of coefficients of atmospheric extinction and scattering [2].

An independent method seems to be needed, and a new technique involving a statistical triangulation is described and examples of the application are given.

THEORY

Assume that two nightglow observatories on the surface of the earth, separated by a distance comparable to the height of the nightglow, record the intensity of the emission as a function of time and zenith distance in the vertical plane containing the stations. Assume further that the nightglow changes, both in space and in time.

If both stations observe the same point in the luminous region, both should indicate similar changes in intensity with time. Geometric enhancements will of course mask the similarity. If, however, the intersection of the two lines of sight is not in the luminous region, the changes during the night should be different.

OBSERVATIONS

Such observations were made of the intensity of the 5577 [OI] nightglow emission between Cactus Peak and Palomar Mountain, California, on 10–11 and 11–12 August 1950. The instruments used had a one-degree vertical and ten-degree horizontal field of view. The distance between the stations is 317 km.

Fig. 1, drawn to scale, displays the various heights of intersection associated with combinations of zenith distances for the two stations. Fig. 2 shows the time variations for a concordant and a discordant intersection.

(1) Fulbright Scholar to France 1954–1955, now at Inst. d'Astrophysique, Paris, France.
(2) Now at High Altitude Observatory, Sunspot, New Mexico.
(3) Now at the Central Radio Propagation Laboratory, National Bureau of Standards, Boulder, Colorado.

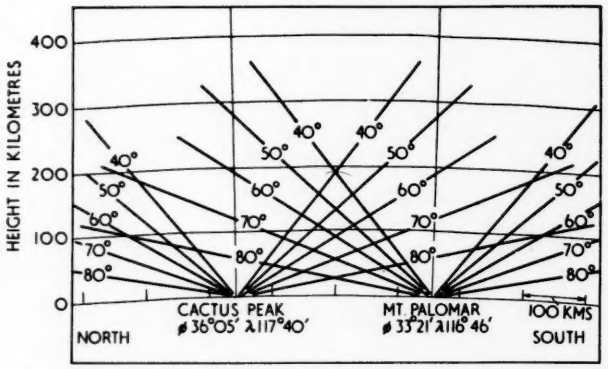

Fig. 1. Scale drawing of the lines of sight and intersections used in the triangulation.

VOL. 6 1955

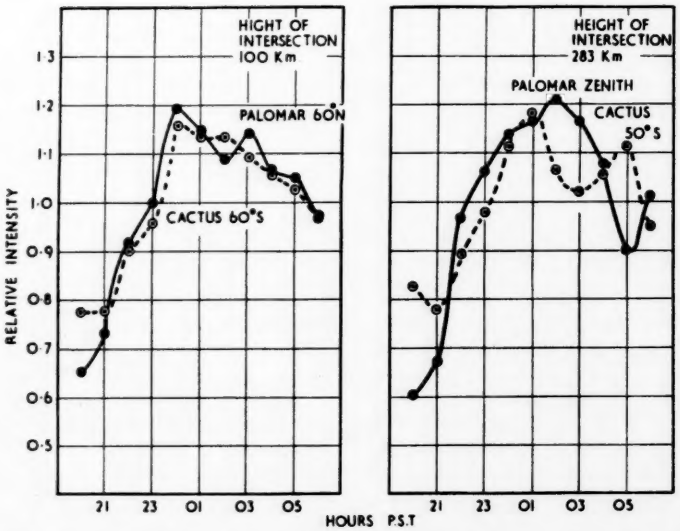

Fig. 2. The diurnal variation of the nightglow (5577 [OI]) as seen from Cactus Peak and from Mount Palomar at two different combinations of zenith distance, one of which shows a greater similarity of form than the other; 10–11 August 1950.

Table 1. *Relative values of nightglow intensity*

10–11 August 1950 — Cactus Peak, California

Time (*PST*)	80N	70N	60N	50N	40N	0	40S	50S	60S	70S	80S
20·5	0·562	0·502	0·553	0·707	0·638	0·585	0·759	0·830	0·781	0·672	0·680
21	0·632	0·693	0·665	0·626	0·596	0·602	0·804	0·779	0·778	0·765	0·723
21·5	0·743	0·829	0·808	0·895	0·851	0·808	0·982	0·901	0·900	0·934	1·045
22	0·893	1·040	0·951	1·123	1·021	1·137	1·071	0·979	0·960	1·014	0·992
22·5	1·023	1·213	1·187	1·179	1·277	1·104	1·116	1·116	1·158	1·082	1·071
23	1·329	1·178	1·087	1·064	0·979	1·187	1·161	1·183	1·135	1·161	1·224
23·5	1·292	1·091	1·097	1·024	0·979	1·254	1·027	1·065	1·135	1·161	1·232
0	1·157	1·215	1·174	1·042	1·191	0·992	0·982	1·022	1·095	1·134	1·134
0·5	1·085	0·995	1·016	1·002	0·979	1·132	1·116	1·057	1·059	1·120	0·977
1	1·130	1·082	1·156	1·175	1·319	1·053	1·116	1·116	1·032	0·973	0·932
1·5	1·154	1·161	1·305	1·164	1·149	1·148	0·893	0·952	0·970	0·984	0·987

10–11 August 1950 — Palomar Mountain, California

Time (*PST*)	80N	70N	60N	50N	40N	0	40S	50S	60S	70S	80S
20·5	0·569	0·633	0·652	0·667	0·690	0·609	0·751	0·731	0·702	0·839	0·891
21	0·711	0·759	0·730	0·772	0·730	0·675	0·790	0·782	0·819	0·827	0·870
21·5	0·877	0·944	0·923	0·867	0·960	0·969	1·186	1·173	1·150	1·026	0·874
22	1·059	1·022	0·996	0·991	1·075	1·065	1·107	1·081	1·076	1·069	1·036
22·5	1·154	1·121	1·194	1·302	1·155	1·141	0·988	1·020	1·097	1·168	1·160
23	1·130	1·199	1·147	1·112	1·115	1·167	1·225	1·258	1·255	1·310	1·270
23·5	1·096	1·042	1·087	1·143	1·075	1·212	1·225	1·122	1·185	1·161	1·185
0	1·031	1·038	1·139	1·051	1·040	1·167	1·146	1·187	1·117	0·960	0·934
0·5	1·047	1·083	1·103	1·137	1·230	1·081	0·830	0·816	0·831	0·856	0·862
1	1·067	1·093	1·053	0·985	1·000	0·903	0·790	0·894	0·878	0·823	0·959
1·5	1·256	1·062	0·975	0·972	0·925	1·015	0·949	0·938	0·889	0·965	0·961

Treatment

In order to estimate the degree of concordance or discordance, the values of intensity relative to the mean for the whole night for each zenith distance at each station were plotted against time to permit interpolation. This reduces effects due to geometric brightening. The data are shown in Table 1.

Differences were then formed between simultaneous values for all possible intersections. The sums of the squares of the difference, divided by the number of observations, were calculated for each intersection in Table 2. In Fig. 3 these sums are plotted as a function of the height of the intersection.

Table 2. Cactus Peak—Palomar

$$\frac{1}{n}\sum d^2$$

Height	*Combination*	1950 10–11 *Aug.*	*Means*	1950 11–12 *Aug.*	*Means*
28	P80N C80S	16·86	16·9	19·0	19·0
39	P70N C80S P80N C70S	9·62 10·67	10·1	18·9 13·2	16·0
45	P60N C80S P80N C60S	11·37 13·57	12·4	30·8 13·1	22·0
49	P50N C80S P80N C50S	13·05 16·36	14·7	25·0 16·7	20·8
52	P80N C40S P40N C80S	18·6 12·6	15·6	25·9 19·2	22·6
57	P70N C70S	3·7	3·7	13·7	13·7
60	P80N C Z P Z C80S	6·75 3·68	5·2	9·0 7·3	8·2
71	P60N C70S P70N C60S	2·46 5·29	3·9	23·8 6·9	15·4
75	P40S C80S P80N C40S	8·4 16·1	8·4	9·6 25·9	17·8
82	P50N C70S P70N C50S	5·79 5·21	5·5	18·5 9·9	14·2

VOL. 6 1955

Table 2 (continued)

$\frac{1}{n}\sum d^2$

Height	*Combination*	1950 10–11 *Aug.*	*Means*	1950 11–12 *Aug.*	*Means*
84	P80N C50N P50S C80S	5·70 8·35	7·0	11·8 18·5	15·2
90	P40N C70S P70N C40S	4·18 5·20	4·7	12·8 13·0	12·9
92	P60N C60S	2·62	2·6	13·8	13·8
101	P60S C80S P80N C60N	5·98 4·86	5·4	18·5 12·7	15·6
110	P50N C60S P60N C50S	4·24 5·73	4·9	11·2 17·8	14·5
122	P70N C Z P Z C70S	10·69 2·77	6·7	30·5 8·7	19·6
125	P60N C40S P40N C60S	6·5 5·88	6·2	21·1 7·5	14·3
135	P50N C50S	8·95	8·9	18·1	18·1
159	P50N C40S P40N C50S	9·8 7·76	8·8	18·1 10·6	14·4
174	P80N C70N P70S C80S	4·97 17·79	11·4	17·0 20·0	18·5

Table 2 (continued)

$\frac{I}{n}\sum d^2$

Height	*Combination*	1950 10–11 *Aug.*	*Means*	1950 11–12 *Aug.*	*Means*
183	P40S C70S P70N C40N	19·5 18·6	19·0	14·3 23·5	18·9
191	P40N C40S	5·5	4·3	12·6	12·6
193	P60N C Z P Z C60S	13·09 7·96	10·5	44·9 12·1	28·5
245	P70N C50N P50S C70S	7·40 16·70	12·0	18·9 14·7	16·8
280	P50N C Z P Z C50S	14·2 15·01	14·6	46·1 11·7	28·9
400	P40N C Z P Z C40S	14·4 15·4	14·9	39·5 16·3	27·9
425	P40S C60S P60N C40N	24·0 17·3	20·6	21·5 36·4	29·0

These values of $\frac{1}{n}\sum d^2$ should by our reasoning be a minimum when the intersections fall in the emitting region. This minimum appears to be somewhere between 75 and 105 km. The minimum is broad and no doubt includes a range greater than the thickness of the nightglow layers. We do not wish to overinterpret our results, and so will not conclude a thickness for the layer, nor will we attach too great a significance to any of the details of the structure. However, the small minimum below 75 km may be due to OH radiations entering the photometers as a contaminant.

A similar treatment using correlation coefficients was employed. The results appear in Fig. 4. Here the data have undergone an additional manipulation.

VOL. 6 1955

When the raw data were used, the coefficients were all near unity. An average curve for the diurnal variation was then determined and subtracted from the curves for each zenith distance. The differences were then correlated. As can be seen, the form of the distribution as a function of height is similar to that obtained by the method of least differences in Fig. 3.

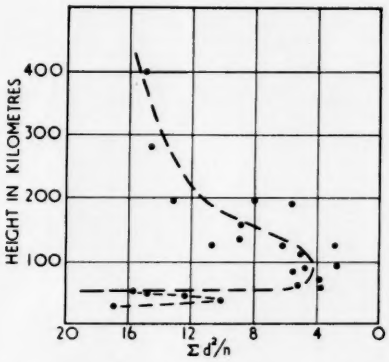

Fig. 3. The differences in diurnal variation as a function of the height of intersection of various lines of sight between Cactus Peak and Mount Palomar, 10–11 August 1950.

The secondary maxima near 75 km is still present and a third at 180 km is also indicated; this may perhaps be due to production of 5577 in the region where, we presume, 6300 is produced, perhaps by dissociative recombination of O_2^+ with electrons followed by radiation.

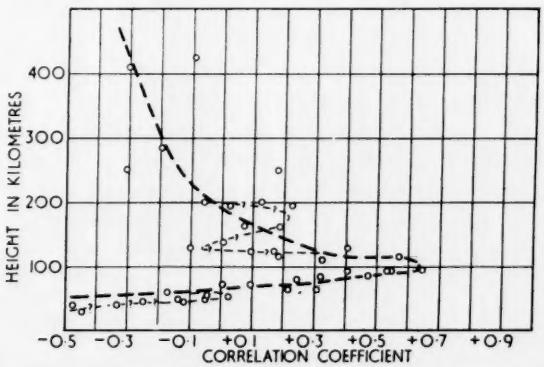

Fig. 4. Correlation of small differences in the diurnal variations as seen from Cactus Peak and Palomar Mountain as a function of the height of intersection of various lines of sight, 10–11 August 1950.

This technique should yield the height of that part of the layer which changes most, and this may or may not correspond to the region of maximum intensity.

Data from Cactus Peak and from Sacramento Peak, New Mexico, for the night of 9–10 August 1953 were treated by the method of least differences to form Fig. 5. Here the distance, 1,160 km, was too great to permit an investigation of

the region below 100 km, and although the values of $\frac{1}{n}\sum d^2$ are decreasing towards the lower heights, a minimum is not observed. The photometer used in these observations had a roughly circular field of view five degrees in diameter.

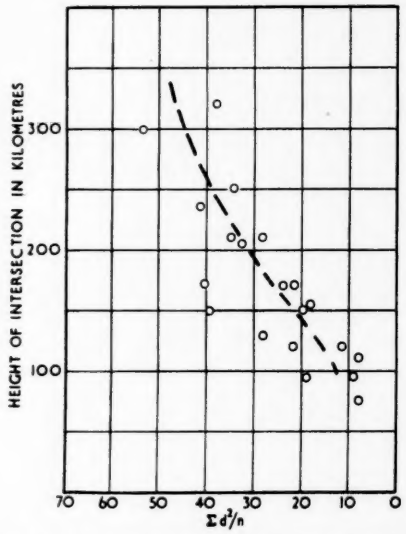

Fig. 5. The differences in the diurnal variation between Sacramento Peak, New Mexico, and Cactus Peak, California, as a function of the height of intersection of various lines of sight, 9–10 August 1953.

VOL. 6 1955

CONCLUSIONS

It appears from these scanty results that the portion of the 5577 nightglow layer which is variable in space and time may be lower than that given by the van Rhijn technique for the region as a whole, when theoretical values of extinction, $\tau_1 = 0{\cdot}125$, and scattering $\tau_2 = 0{\cdot}125$, coefficients are used, but agree well with such calculations based upon observed values of the extinction coefficient $\tau_1 = 0{\cdot}15$ atmosphere and Rayleigh values $\tau_2 = 0{\cdot}092$ of scattering coefficient. Table 3 gives comparative heights obtained by the methods.

Table 3

Dates 1950	*Heights, km.*		
	Statistical triangulation	*Van Rhijn technique*	
		$\tau_1 = \tau_2 = 0{\cdot}125$	$\tau_1 = 0{\cdot}15 \quad \tau_2 = 0{\cdot}092$
10–11 August	100 ± 10	200 ± 20	93 ± 15
11–12 August	80 ± 15	200 ± 20	93 ± 15

It is felt that this triangulation method deserves a further trial, because the reduced heights do not depend upon assumptions as to extinction and scattering. The scattered light from the rest of the sky will tend to generalize the minimum of $\frac{1}{n}\sum d^2$, but should not change the height at which these minima occur. Repeated observation from a number of stations might eventually reveal the true heights of the emitting regions.

Acknowledgment—The authors wish to express their gratitude to Dr. I. S. BOWEN and the staff of the Palomar Observatory, for permission to observe at Palomar Mountain, and for their hospitality. Mr. E. V. ASHBURN's assistance in observing at Cactus Peak is also appreciated. This work was supported in part by a research grant from the Office of Naval Research, Project NR–082–045.

REFERENCES

[1] HARANG, L. 1951 *The Aurorae*, John Wiley and Sons

[2] BARBIER, D., DUFAY, J., and WILLIAMS DONALD 1951 *Ann. Astrophys.*, Tome 14, fasc 4, Oct–Dec.

Journal of Atmospheric and Terrestrial Physics, 1955, Vol. 6, pp. 198 to 214. Pergamon Press Ltd., London

Radio reflections from aurorae—II

K. BULLOUGH and T. R. KAISER
Jodrell Bank Experimental Station, University of Manchester

(*Received* 12 *October* 1954)

ABSTRACT

Auroral echoes recorded on a meteor survey apparatus at Jodrell Bank between June 1949 and December 1953 are discussed. It is inferred that the reflecting regions, in general, follow parallels of geomagnetic latitude. The diurnal variation in echo frequency exhibits a well defined minimum between 2100 h and 2200 h U.T. and there is a complete absence of echoes between about 0600 h and 1300 h. The evening sequence (1300 h–2100 h) is marked by diffuse echoes and systematic westward motions of the reflecting regions, while the echoes in the morning sequence (2200 h–0600 h) have pronounced discrete structure and systematic eastward motions. The mean velocity of the reflecting regions changes from 600 m sec^{-1} westwards at 1500 h to 600 m sec^{-1} eastwards at 0500 h and is zero at about 2100 h (i.e., coincident with the minimum in echo frequency).

1. INTRODUCTION

In a recent paper (BULLOUGH and KAISER, 1954, henceforth referred to as I) results were given of some radio echoes from aurorae obtained during 1953 with an equipment employing an aerial system, rotating about a vertical axis, with a low elevation beam. The echoes were interpreted as originating from a reflecting region extending along an arc following approximately a parallel of geomagnetic latitude several degrees to the north of the observing site at Jodrell Bank (geomagnetic latitude 56°). It was concluded that the hypothesis of specular reflection from auroral features following the direction of the terrestrial magnetic field was inconsistent with the observations, and that the reflecting structure was probably composed of blobs of over-critically dense ionization (electron density $> 6{\cdot}7 \times 10^7$ cm^{-3}), distributed along the arc at a height in the vicinity of 120 km. Echoes at about 1800* on October 15, 1953, contained structures exhibiting approaching velocities in the NE and receding in the NW which were interpreted as relatively intense reflecting centres and regions moving from east to west along the arc with velocities of the order of 1 km sec^{-1}.

Auroral echoes have also been observed at Jodrell Bank on a continuous survey meteor apparatus (Meteor Radiant Equipment, ASPINALL *et al.*, 1951) on thirty-six occasions since June 1949, and this paper presents an analysis of these echoes made especially in the light of the above deductions concerning the nature of the reflecting regions. Auroral observations made with the radiant equipment have previously been reported by ASPINALL and HAWKINS (1950) and HAWKINS (1954), who have given brief details of the equipment which has operated throughout on a wavelength of approximately 4 m, and has a low elevation (8·5°) beam of azimuthal width (to half-amplitude) $\pm 5°$ directed 68° W of N (i.e., about 50° W of the geomagnetic meridan). A second similar aerial beam is directed towards the SW, and observations are, in fact, made alternately on the two for the purpose of determining the radiants of meteor showers. No aurorae have been observed on this

* Universal Time is quoted throughout.

VOL. 6 1955

aerial. The half-amplitude beam limits of the NW aerial are shown, projected on to a plane tangent to the earth at Jodrell Bank, in Fig. 1. The equipment radiates pairs of pulses, separated by one-third of a millisecond with a recurrence rate of 150 sec^{-1}.

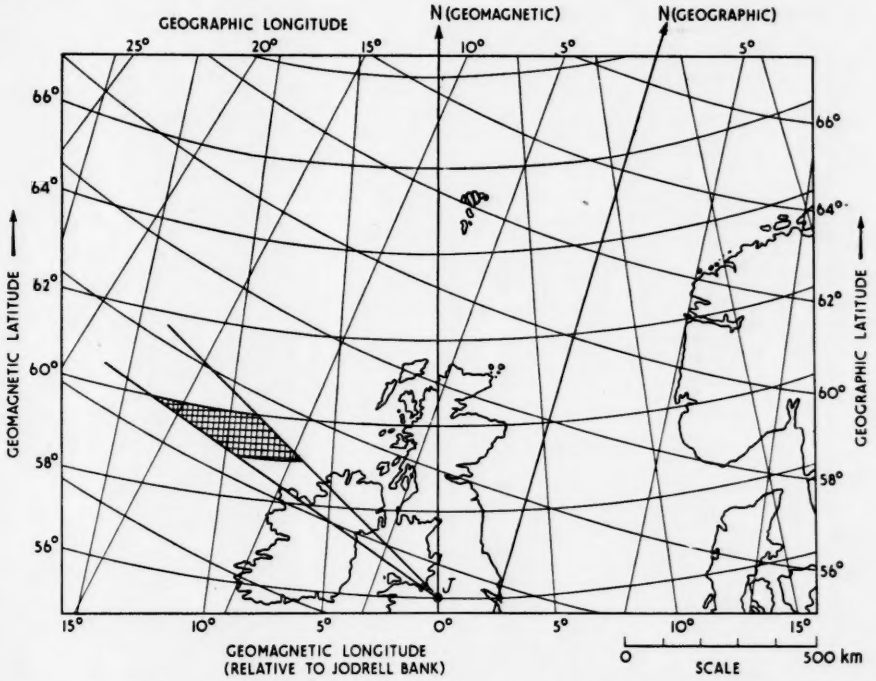

Fig. 1. Limits of the radiant equipment aerial beam projected onto a plane tangent to the earth at Jodrell Bank. The hatched region is that in which the majority of the echoes originated (see § 4).

2. Characteristics of the Echoes

A representative group of auroral echoes is shown in Fig. 2. They may be diffuse (extended in range with no noticeable fine structure) and apparently stationary as in Fig. 2(a); diffuse, but showing movements in range (Fig. 2(b)); or they may exhibit, often coexisting with diffuse echoes, a discrete structure which also may have pronounced movements in range (Fig. 2(c)). The duration of individual echoes may vary from less than a minute to an hour or more, and on occasions echoes were intermittently visible for many hours. An interesting case is the echo sequence extending from 2215 to 0630 on August 19/20, 1950. Discrete structure was present until 0240, when it rapidly multiplied, the individual discrete echoes coalescing into an intense continuum extending in range from 400 to 1000 km, which persisted until 0430, when it broke up again into a multiplicity of resolvable discrete echoes.

If the reflecting regions follow the geometry deduced in I, the radiant equipment echoes can be interpreted as follows. A stationary diffuse echo as in Fig. 2(a) would probably consist of a distribution of unresolved blobs of ionization extending through

the aerial beam, the range limits corresponding to the intersections of the limits of the beam with the arc. In this case any motion along the arc would be undetected. A moving diffuse echo (Fig. 2(b)) would be a similar distribution occupying a length

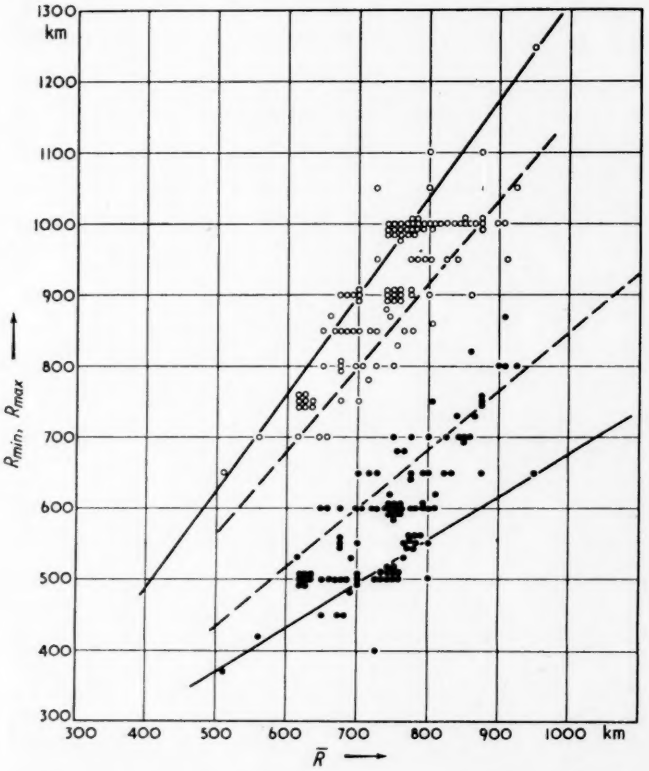

Fig. 3. Maximum range, ○, and minimum range, ●, as a function of their mean, $\bar{R}$. The values predicted on the assumption of an auroral arc (following a parallel of geomagnetic latitude) are indicated by the broken and full lines which correspond to the limits of the aerial beam between, respectively, half-amplitude points and zeros.

of the arc less than that intercepted by the aerial beam and moving through the beam towards the east or west. The discrete echoes likewise would be situated and move on the arc, consisting either of large single blobs or localized aggregates with an extent in range which is small compared with that corresponding to the separation between the pulse pairs (50 km).

Strong support for the above view follows from the analysis of the maximum and minimum echo ranges, R_{max} and R_{min}, shown in Fig. 3. We have plotted the values of R_{max} and R_{min} obtained during individual hourly intervals against their mean ($\bar{R}$). The values to be expected on the hypothesis of a reflecting arc following a parallel of geomagnetic latitude are also given. The broken lines correspond to the half-amplitude beam limits and the full lines to the total azimuthal width between zeros ($\pm 9°$) of the main aerial beam.

, VOL. 6 1955

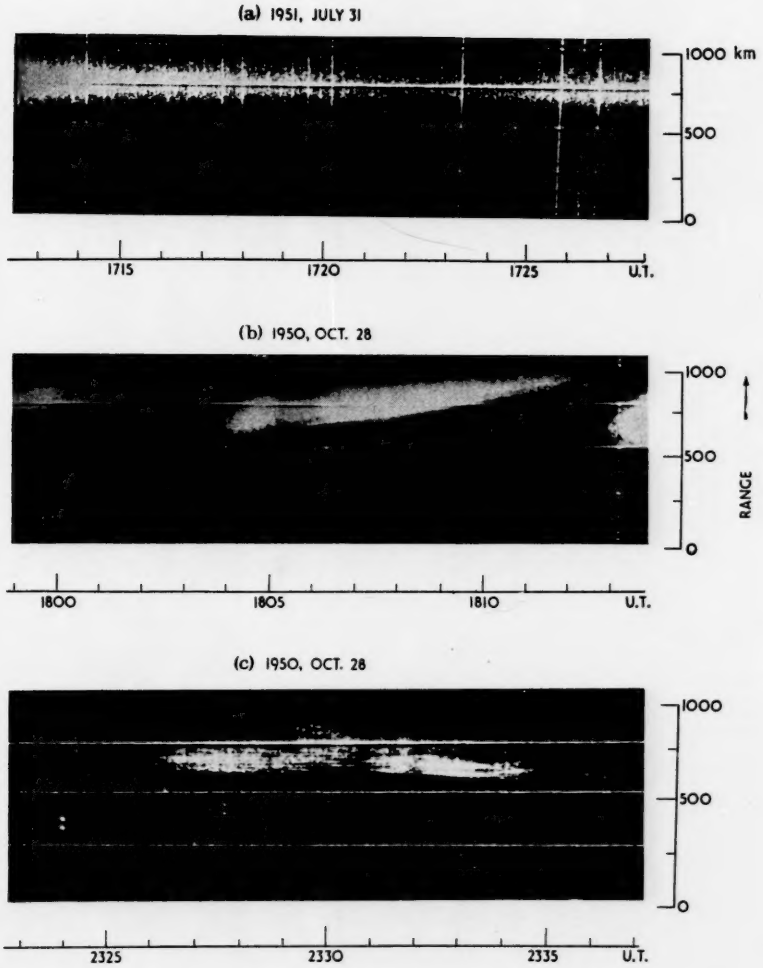

Fig. 2. Typical radio echoes. (The bright short duration echoes at 2323·8 and 2326·6 in (2c) are due to meteors.)

VOL.
6
1955

3. Frequency of Occurrence of Auroral Echoes

A table of the dates and hours of occurrence of auroral echoes on the radiant equipment is given in Fig. 4. The equipment functioned only intermittently in 1949, but has been operated continuously (except for brief servicing intervals) during 1950–51–52–53, and, of course, during the present year, which is not included

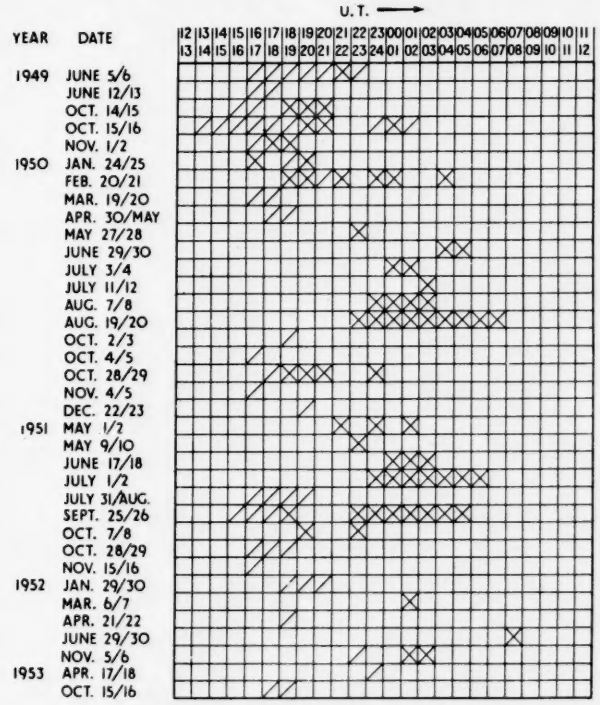

Fig. 4. Hours of occurrence of auroral echoes.
⊠–Auroral echo observed in specified interval.
⊠–Auroral echo with discrete structure.

in the analysis. On only one of the occasions during 1953 (Oct 15) were simultaneous echoes received on the rotating aerial and radiant equipments. On May 15/16 (see paper I) the reflecting region probably scarcely extended at all into the radiant aerial beam, while the lack of echoes with the rotating aerial on April 18 may be due to a difference in equipment sensitivities, since the radiant echoes were weak. On March 9 weak echoes were observed with the rotating aerial at 0443, but were not detected on the radiant equipment. The following analysis refers only to echoes obtained on the radiant equipment.

Figs. 5(a) and (b) give respectively the number of days (taking a day as commencing at 1200) and hourly intervals during 1950–53 in which auroral echoes were observed. The marked fall in activity since 1950 corresponds to the decline in solar activity during the period. The echo frequency is continuing at a low level during 1954.

The diurnal frequency variation is as shown in Fig. 6. The most striking features are the maxima at approximately 1800 and 0100 separated by a well-defined minimum between 2100 and 2200, and the lack of discrete echoes during the evening hours (these features have been previously pointed out by HAWKINS, 1954).

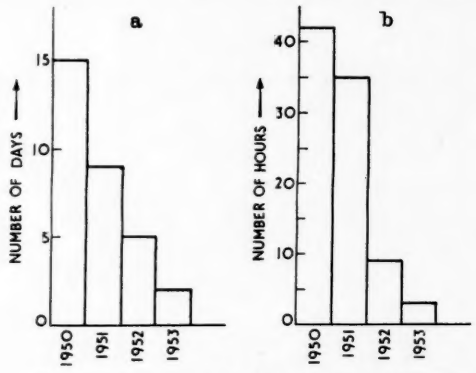

Fig. 5. Frequency of auroral echoes, 1950–53.
(a) Number of days.
(b) Number of hourly intervals.

Discrete echo structure was present during 90 per cent of the hourly intervals in which echoes were observed after 2200, but during only 25 per cent before 2100. The diurnal variation is directly apparent from Fig. 4. It is clear that a sequence of echoes commencing in the early evening in general ceases before 2100, while

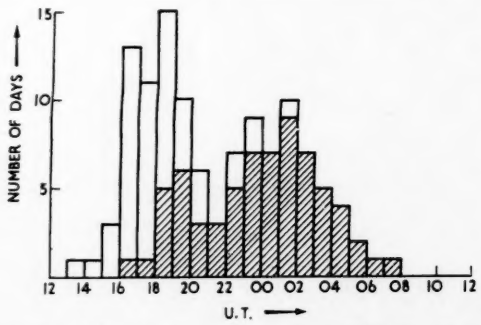

Fig. 6. Diurnal variation in auroral frequency, 1949–53. The shaded portion indicates the occasions on which discrete echo structure was evident.

sequences extending into the morning hours commence after 2200. On several occasions echoes were observed in the evening and in the morning of the same day with a gap at about 2100–2200. An example is the occasion of September 25/26, 1951, which shows well the difference in character of the two echo sequences (few discrete echoes in the evening sequence).

Figs. 7(a) and 7(b) show respectively the number of days and of hourly intervals in which echoes were observed for each month of the year. In Figs. 8(a) and (b)

VOL. 6 1955

the data is divided between the two groups of echoes (evening and morning). The main significant feature is the large autumnal equinoctial peak in the evening echoes. The morning echoes show a summer maximum; however, this is scarcely significant in view of the small number of occurrences.

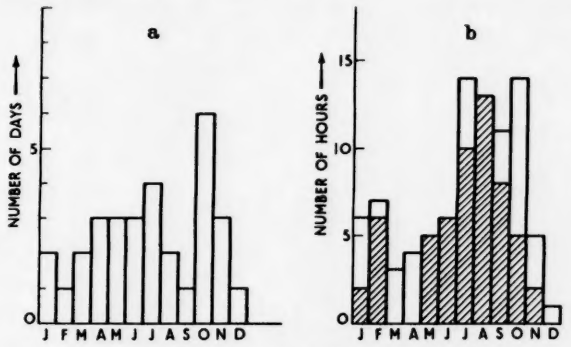

Fig. 7. Annual variation in auroral frequency, 1950–53.
(a) Number of days.
(b) Number of hourly intervals (the shaded portion refers to discrete echoes).

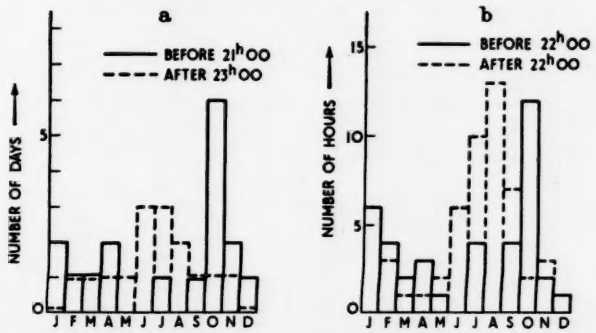

Fig. 8. Annual variation in auroral frequency (1950–53) shown separately for the two echo sequences.

4. Location of the Reflecting Regions

The mean ranges (see above for definition) were determined for hourly intervals and are distributed as in Figs. 9(a) and 9(b). The corresponding values of the latitudes of the reflecting regions (on the assumption that they follow parallels of geomagnetic latitude) are distributed as in Figs. 10(a) and 10(b). It will be seen that a majority of echoes originated between geomagnetic latitudes 59° and 60° (i.e., in the hatched region in Fig. 1) with a maximum at 59·7°. The morning echoes on the average show somewhat greater ranges, and hence correspond to a reflecting region at more northerly latitudes than for the evening echoes. This feature is apparent on the occasion September 25/26, 1951, when the mean evening latitude was 59·4°, receding to 60·0° during the echo sequence commencing at 2205. During any single echo sequence the standard deviation of a single hourly estimate of the

geomagnetic latitude is about 0·2°, thus the latitude remains constant, probably to within the experimental errors. The values of the mean latitude during the various echo sequences (treating September 25/26, 1951, as two separate sequences) are distributed as indicated by the broken lines in Fig. 10(a).

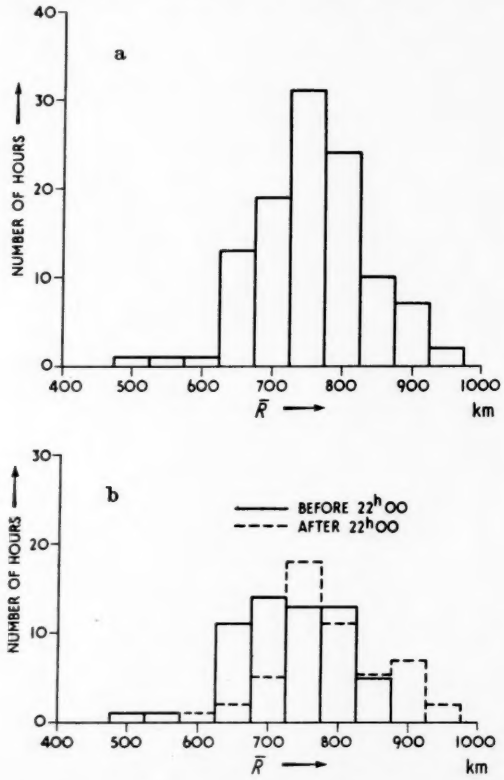

Fig. 9. Distribution of mean echo ranges, 1949–53 (based on hourly intervals).

5. Correlation with Visual Aurorae

The radio echo occurrences are arranged according to Carrington's synodic series of solar rotations in Fig. 11, and may be compared with the occasions on which aurorae were observed visually in Great Britain from locations in and to the south of geomagnetic latitude 56° during the years 1950–53 (solar rotations 1289–1340).* Radio echoes were observed on thirty-one occasions during 1950–53, and aurorae were visible south of latitude 56° and 55° on forty-three and twenty-two occasions, respectively, the number of coincidences with the radio observations being, respectively, thirteen and ten.

Table 1 gives the available visual data for the dates on which echoes were obtained. It shows that the estimated geomagnetic latitude of the reflecting region

* The visual data are drawn from reports by Paton appearing in The Observatory and the *J. Brit. Ast. Assoc.*

VOL. 6 1955

was, on the average, some 4° (i.e., ~500 km) north of the southernmost reported visual observations, and within 0·6° of the latitudes at which aurorae were visible in the zenith.

An interesting occasion, when an aurora was visible from Jodrell Bank, was September 25/26, 1951. According to LITTLE and MAXWELL (1952), a stable auroral

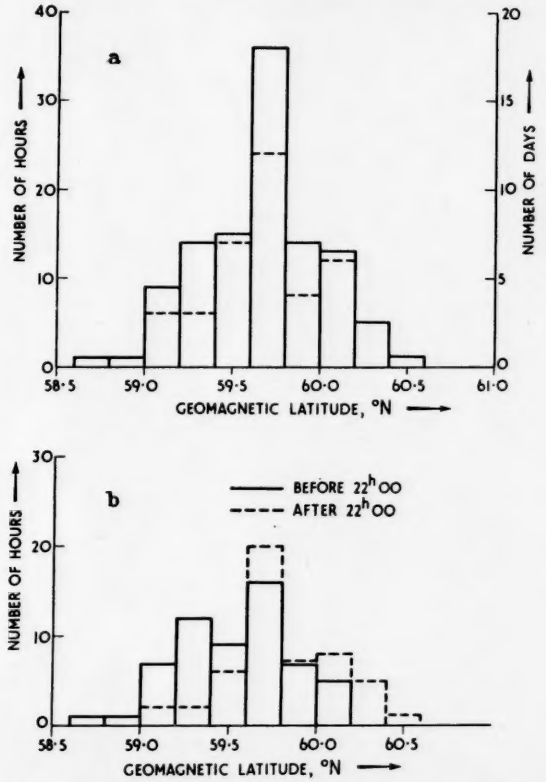

Fig. 10. Latitude distributions of aurorae observed on the radiant equipment (1949–53). The full lines in (a) give the latitude evaluated for individual hourly intervals, and the broken lines the average for individual days (on September 25/26, 1951, 1500–1900 and 2200–0500 are included separately).

arc broke up at 2130* into a series of pulsating rays and diffuse patches, the flaming aurora then observed being the brightest recorded in Britain for twenty years. This change in the auroral structure actually occurred in the no-echo period (1840–2155) separating the diffuse echo and discrete echo sequences.

6. Correlation with Magnetic Activity

As expected, there is a fair correlation between terrestrial magnetic activity measured at Eskdalemuir (geomagnetic latitude 58·5°) and the radio echo observations. This is shown by Fig. 12, which includes all occasions on which echoes were

* Dr. MAXWELL has informed us privately that the time was incorrectly quoted as 2030 in the paper referred to.

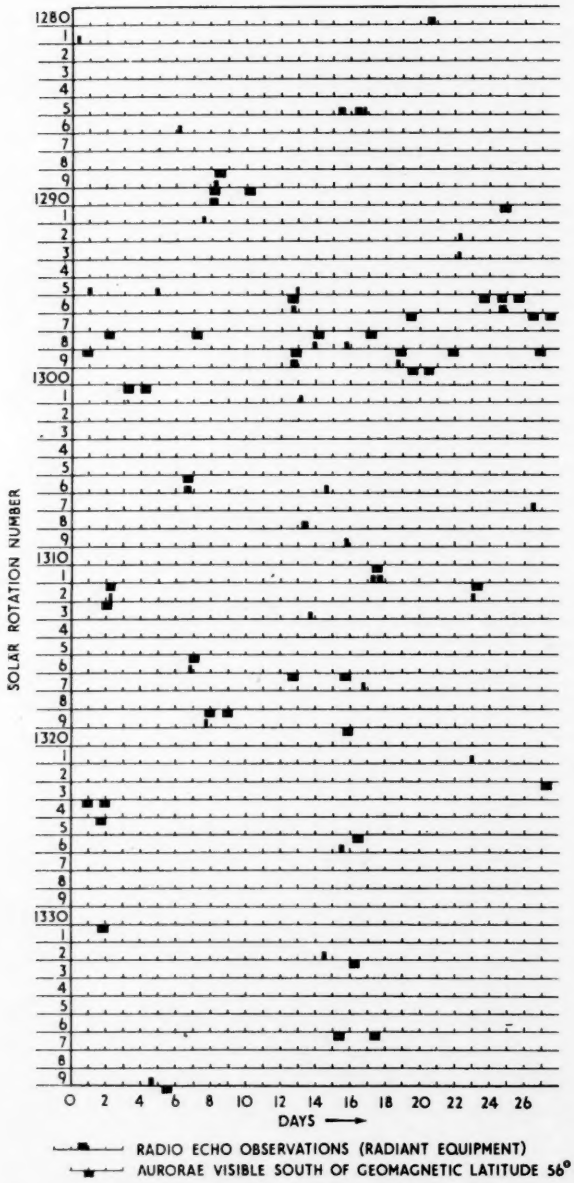

Fig. 11. Radio echo and visual auroral observations arranged according to CARRINGTON's synodic series of solar rotations (the visual data commence at rotation number 1289).

VOL. 6 1955

Table 1.* *Visual-radio echo correlations*

Year	*Day*	*Time (U.T.)*	λ_R	λ_1	λ_2	$\lambda_R - \lambda_1$	$\lambda_R - \lambda_2$
		hour					
1950	Jan. 24/25	16–17, 18–20	59·5°	53°	—	6·5°	—
	Feb. 20/21	18–22, 23–01, 03–04	59·6	52	—	7·6	—
	Mar. 19/20	16–18	59·2	61	—	1·8	—
	April 30/May 1	17–19	59·9	No Visual		—	—
	May 27/28	22–23	59·1	No Visual		—	—
	June 29/30	03–05	60·1	No Visual		—	—
	July 3/4	00–02	59·8	No Visual		—	—
	July 11/12	02–03	59·8	No Visual		—	—
	Aug. 7/8	23–03	60·1	55	—	5·1	—
	Aug. 19/20	22–07	59·7	52	—	7·7	—
	Oct. 2/3	18–19	60·1	56	—	4·1	—
	Oct. 4/5	16–17	59·8	No Visual		—	—
	Oct. 28/29	17–21, 23–24	59·5	56	—	3·5	—
	Nov. 4/5	16–17	59·8	56	—	3·8	—
	Dec. 22/23	19–20	—	61	—	—	—
1951	May 1/2	21–22, 23–24, 01–02	59·8	55	—	4·8	—
	May 9/10	22–23	60·2	57	60	3·2	0·2
	June 17/18	00–03	59·7	No Visual		—	—
	July 1/2	23–06	59·9	No Visual		—	—
	July 31/Aug 1	16–20	59·7	No Visual		—	—
	Sept. 25/26	15–19, 22–05	59·4, 60·0	53	58	6·4, 7·0	1·4, 2·0
	Oct. 7/8	19–20, 22–23	60·1	54	57	6·1	3·1
	Oct. 28/29	16–19	59·5	54	57	5·5	2·5
	Nov. 15/16	16–17	59·8	No Visual		—	–
1952	Jan. 29/30	18–21	60·1	54	63	6·1	−2·9
	Mar. 6/7	01–02	—	60	—	—	—
	April 21/22	18–19	59·8	54	61	5·8	−1·2
	June 29/30	07–08	59·7	No Visual		—	—
	Nov. 5/6	22–23, 01–03	59·9	60	—	−0·1	—
1953	April 17/18	23–24	59·5	No Visual		—	—
	Oct. 15/16	17–19	59·6	61	—	−1·4	—
				Mean		+4·3	+0·6

λ_R = Mean geomagnetic latitude, radio echo observations.
λ_1 = Southernmost visual aurora.
λ_2 = Aurora observed (visually) in zenith.

* NOTE: The lack of data on 1950 December 22/23 and 1952 May 6/7, is due to the fact that the original records for these dates were not available.

obtained and on which the magnetic K-index was >7. Fig. 13 shows the diurnal variation in the occurrence of $K > 7$ with the radio echo data indicated, for comparison, by the broken line. The minimum in echo frequency at 2100–2200 is obscured by the grouping into three-hour intervals.

Auroral echoes were observed on twelve out of twenty days during 1950–53 on which $K > 7$.

On September 25/26, 1951, a magnetogram taken by MAXWELL at Jodrell Bank shows a quiet period between 1850 and 2130, separating periods of intense magnetic fluctuations. This interval falls within the no-echo period (1840–2155).

7. Auroral Motions

Individual echo features exhibiting movements in range with speeds of the order of 1 km sec^{-1} have been reported by Aspinall and Hawkins (1950) and by Hawkins (1954), who states that the directions are random. This is indeed far from the case, as is clear from the scatter diagram of radial velocities as a function of time of day

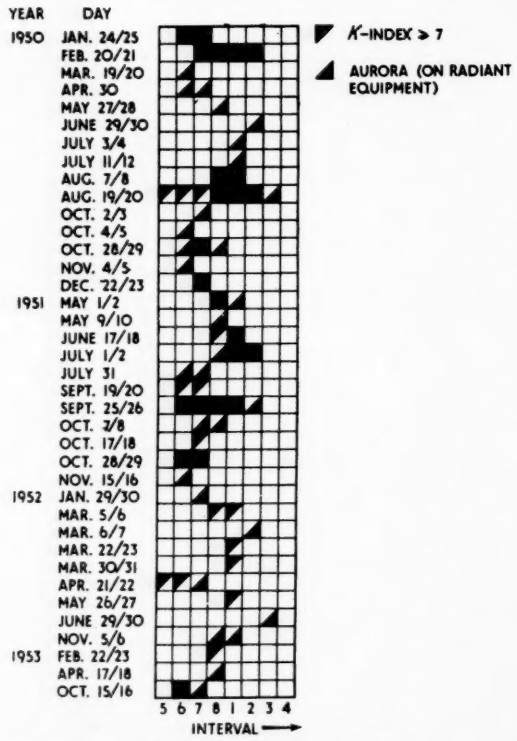

Fig. 12. Correlation between auroral echoes and magnetic activity (at Eskdalemuir).

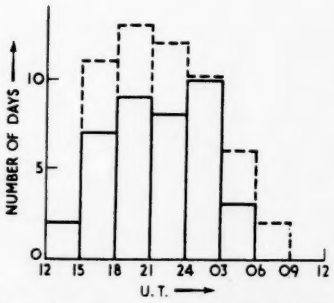

Fig. 13. Diurnal frequency distributions:
- - - - - auroral echoes (3-hourly intervals).
——— magnetic K-index (Eskdalemuir) > 7.

given in Fig. 14. The points correspond to velocities measured on individual auroral features, circles for moving diffuse echoes and dots for discrete. Figs. 15 and 16 show, respectively, the hourly mean velocities for each occasion and the overall mean. It is clear that there is a marked diurnal variation from 500 m sec^{-1} receding at 1800 to 500 m sec^{-1} approaching at 0600, the reversal occurring between 2100 and 2200, i.e., coincident with the minimum frequency of occurrence of echoes (see § 3). We interpret these results as representing a true motion along the arc changing from about 600 m sec^{-1} westwards at 1800 to 600 m sec^{-1} eastwards at 0600.

It is interesting to note the extent to which individual echo sequences follow the above trend (as shown in Fig. 15). Only four outstanding exceptions were observed. On February 20/21, 1950, a single discrete feature at 1830 gave a

VOL. 6 1955

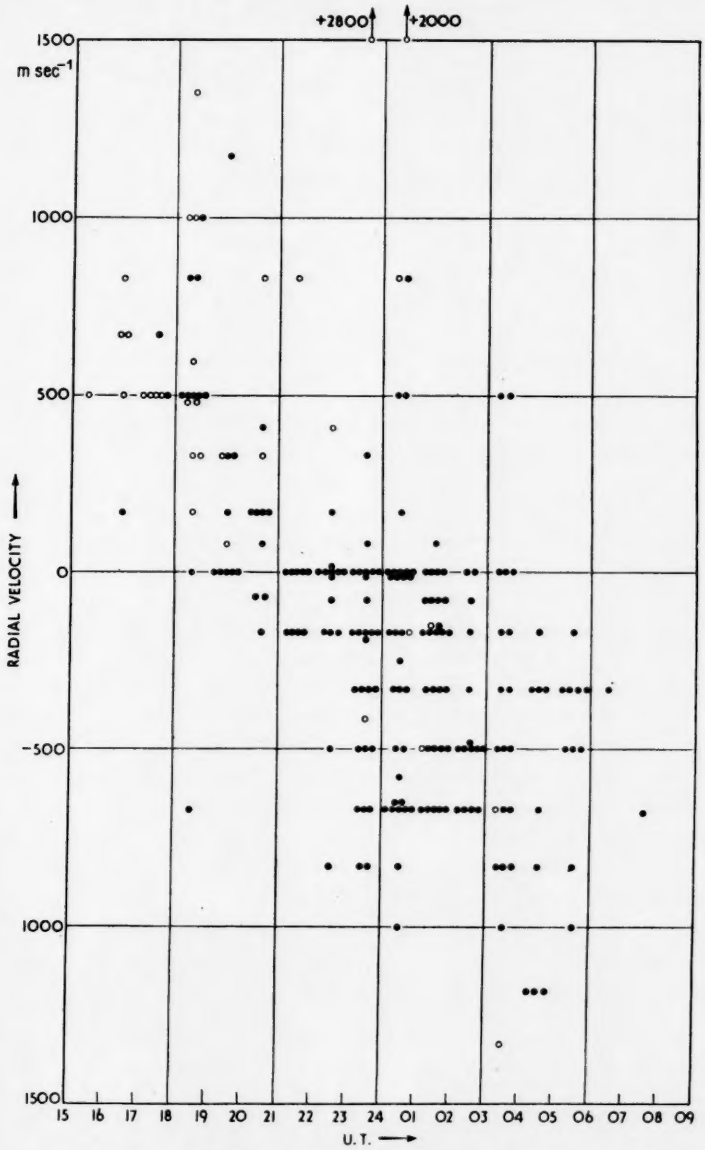

Fig. 14. Auroral apparent radial velocities measured from individual echo features (1949–53).
○—from moving diffuse echoes.
●—from discrete echoes.

velocity of -670 m sec^{-1} (approaching) compared with a mean for 1800–1900 of $+180$ m sec^{-1} (receding) (Fig. 17(a)). In actual fact the particular discrete feature was not well defined and this result is doubtful. On this same day, however, the motion, which had been consistently approaching since 2321, suddenly changed at 0336 to 500 m sec^{-1} receding and reverted to an approaching motion at 0344

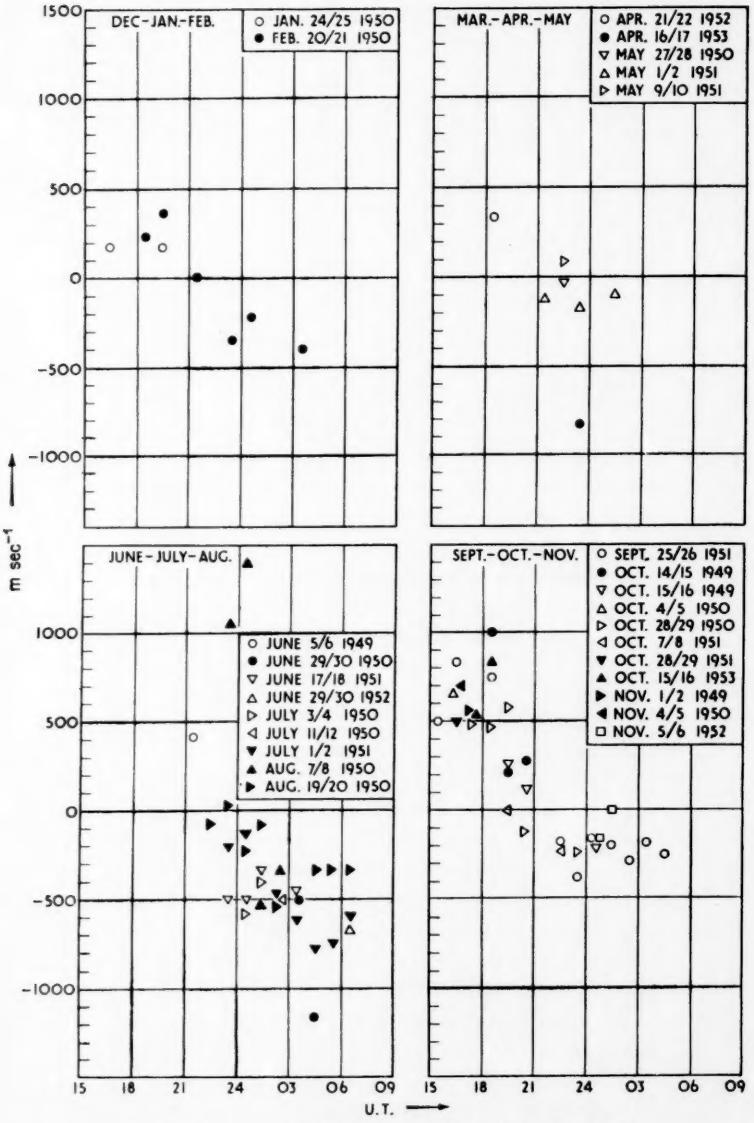

Fig. 15. Hourly mean radial velocities, 1949–53.

(Fig. 17(b)). Similarly on July 1/2, 1951, at 0055 (Fig. 17(d)) the motion temporarily changed from an approaching velocity of about 500 m sec^{-1} to a receding one of the same magnitude. It should be noted that with the exception of the second reversal on July 1/2, 1951 (not shown in Fig. 17(d)), the echoes faded out before the change in direction of motion. On August 7/8, 1950 (Fig. 17(c)), echoes observed between 2312 and 0028 contained features with receding velocities ranging from zero*

* It is possible that the discrete feature with zero velocity is a long duration meteor echo.

, VOL. 6 1955

to 2,800 m sec^{-1}; there was a gap between 0028 and 0115, after which the motion was as usual at this time, i.e., approaching with velocities ranging from 300–600 m sec^{-1}.

On several occasions rather interesting sequences of moving diffuse echoes were observed. For instance on October 15/16, 1953, (see I) it appeared that several extended reflecting regions spaced by several hundred km moved in succession

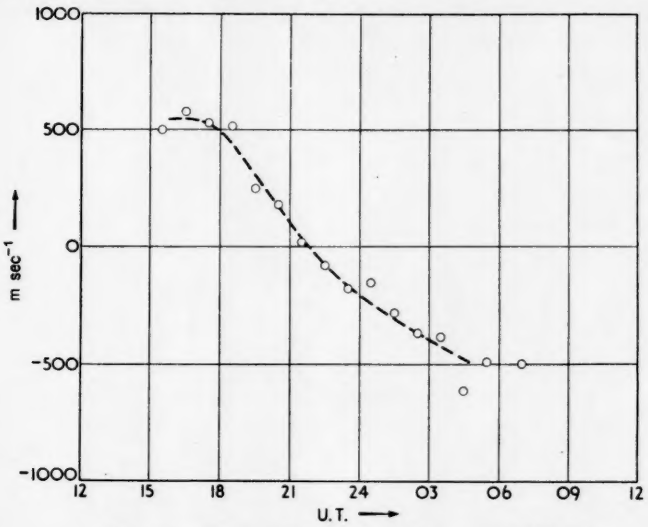

Fig. 16. Mean radial velocity (all aurorae, 1949–53).

through the aerial beam. On October 28/29, 1950, between 1752 and 1849 (see Fig. 2(b)), and on October 28, 1951, no less than seven moving diffuse echoes with receding velocities of 500 m sec^{-1} were observed in succession. Those on October 28/29, 1950, were separated in time by intervals of approximately 11 min, and hence the spatial separations must have been about 400 km. It was as if a wave motion were being propagated along the arc, regions near the maxima (of some 100 km or more in linear extent) containing over-critically dense blobs. If all seven regions existed simultaneously they would have extended some 3,000 km along an arc at geomagnetic latitude 59·5°, i.e., more than one-tenth of the circumference of this parallel.

Discussion

The analysis of the maximum and minimum ranges observed with the radiant equipment supports the idea that in general the region in which the radio echoes originate lies approximately along a parallel of geomagnetic latitude, as was deduced in I from the observations during 1953 with the rotating aerial equipment.

On this assumption, the distribution in latitude of the reflecting regions has been estimated (§ 4). The fall in frequency for geomagnetic latitudes $> 60°$ is to be expected, since, assuming a height of 120 km, the elevation of the reflecting region will be well below the maximum of the aerial beam and falling rapidly with increasing latitude. The close correlation with visual aurorae observed in and south of

geomagnetic latitudes 55–56° suggests that the decrease in frequency of radio echoes for latitudes below 59·7° probably represents a real decrease in auroral occurrence.

Perhaps the most important new information reported here is that concerning the diurnal variation of the motion of intense reflecting centres (discrete echoes) and regions (moving diffuse echoes), which is obviously closely linked to the diurnal

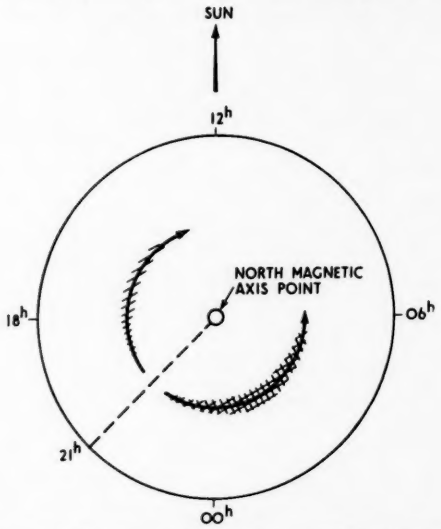

Fig. 18. Schematic diagram of the synoptic distribution of the aurorae.
The arrows indicate the directions of the apparent motions.
//////////—region giving diffuse echoes.
×××××—region giving discrete echoes.

variation in the frequency and character of the radio echoes. The results are in agreement with photographic observations made in the U.S.A. by Meinel and Schulte (1953), who found the auroral motions to be westward in the evening and eastward in the morning, with speeds between 500 and 1,300 m sec^{-1} The reversal in direction of motion and the minimum in echo frequency occur between 2100 and 2200, whereas magnetic midnight at the location of the aurorae occurs shortly after 2300 (see Hawkins, 1954). The relative absence of discrete echo structure before 2100 indicates a change in character of the reflecting regions at about this time. It may be that this is simply a change in scale of the blobs of ionization, those in the evening being generally too small to give detectable discrete echoes. Diurnal frequency distributions of radio echoes from aurorae observed at Saskatoon (Canada) have been given by Currie *et al.* (1953). These show no marked minimum; however, it is possible that it is obscured owing to the high echo rate enjoyed by these workers (just as happens when the Jodrell Bank echoes are grouped into three-hourly intervals). The synoptic distribution of the aurorae deduced from the diurnal effects is indicated schematically in Fig. 18.

Motions similar to the above have been deduced by Maxwell and Dagg (1954) from observations of radio-star scintillations originating in the auroral zone. They find a partial reversal in wind direction at 2100, in agreement with the above,

VOL. 6 1955

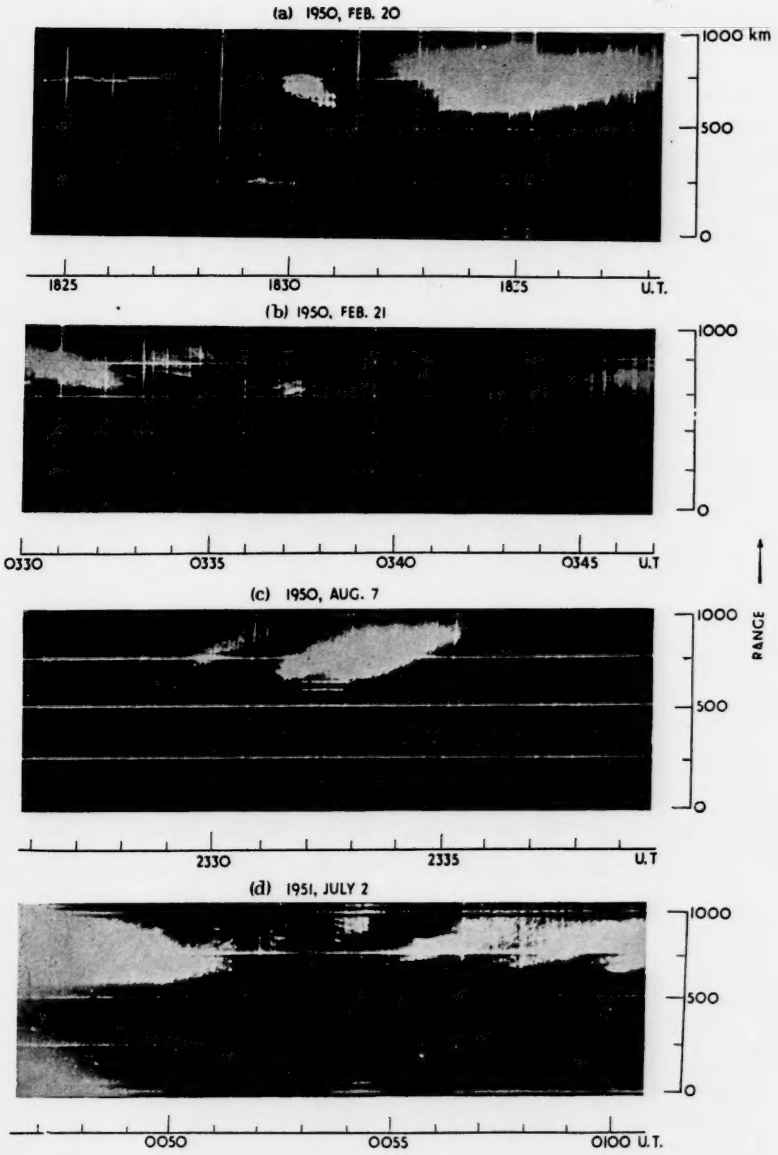

Fig. 17. Echoes exhibiting anomalous behaviour.

VOL.
6
1955

whereas on other occasions the reversal occurs several hours later. The scintillation phenomena, however, are normally interpreted as occurring in the *F*-region. LITTLE and MAXWELL (1952), have reported scintillations observed on a wavelength of 4 *m* during the aurorae of September 25/26 and October 28, 1951. On the former occasion the rapid fluctuations in the radio-star intensity commenced at 2140, which was approximately coincident with the recommencement of intense magnetic activity (see § 6) but was earlier than the onset of the discrete (approaching) radio echoes (2155). They reported no outstanding scintillations during the evening diffuse echo sequence, although the radio echo equipment detected receding velocities of the order of 1 km sec^{-1}. This may be a further result of a difference in the scale of the reflecting irregularities between the two echo sequences. On October 28, the above authors reported a diminution in the intensity of the radio emission extending over several minutes at about 1940. On this occasion the radio echoes ceased at about 1815, which might suggest that both the radio emission diminution and the absence of radio echoes at 1940 arose from a real absorption of the radio waves, perhaps due to an abnormally high level of ionization in the *D*-region.

The auroral velocities on occasions are greatly in excess of the velocity of sound in the *E*-region, and yet meteor trails observed to the north of Jodrell Bank during auroral activity exhibit normal *E*-region wind velocities ($\sim$50 m sec^{-1}). Hence it is unlikely that the auroral motions are due to winds (mass motion), but are probably the apparent effect of a redistribution of ionization.

A fair correlation is found between the radio echoes, the occurrence of visual aurorae, and magnetic activity. In this latter respect and in relation to the apparent motions, some observations made by SANGSTER (1910) are of interest. He states: "On the occasion of a brilliant display of aurora, some apparent rotatory movements in the position of the corona suggested to the author the possible existence of similar changes of direction of the total magnetic force during the disturbance." From an analysis of magnetic records for the years 1900–1907 SANGSTER found, in fact, that the magnetic vector at Greenwich tended to rotate in an anticlockwise direction before, and a clockwise direction after, midnight.*

ACKNOWLEDGMENTS

The authors are indebted to those colleagues, past and present, who have participated in the auroral observations made during the period covered by this paper, in particular to Mr. A. ASPINALL, Dr. G. S. HAWKINS, and Mr. T. DAVIDSON. We wish to thank Dr. A. MAXWELL for discussions on the relation between these results and his radio-star scintillation observations, and Dr. J. S. GREENHOW and Mr. E. L. NEUFELD for the information concerning their measurements of the motions of meteor trails during auroral activity.

This work was supported by a grant from the Department of Scientific and Industrial Research, and one of us (T. R. K.) is indebted to Messrs. Imperial Chemical Industries Limited for the award of a Research Fellowship, during the tenure of which this work was carried out.

* A further study has shown a close correlation between the echo characteristics and frequency with the distribution of positive and negative magnetic bays. Fig. 18 resembles closely the idealized atmospheric electric current distribution of CHAPMAN (1935) if allowance is made for the asymmetry of the geomagnetic field (VESTINE, 1938).

References

Aspinall, A., Clegg, J. A., and Hawkins, G. S.	1951	*Phil. Mag.* **42,** 504
Aspinall, A., and Hawkins, G.S.	1950	*J. Brit. Ast. Ass.* **60,** 130
Bullough, K., and Kaiser, T. R.	1954	*J. Atmosph. Terr. Phys.* **5,** 189
Chapman, S.	1935	*Terr. Mag.* **40,** 344
Currie, B. W., Forsyth, P. A., and Vawter, F. E.	1953	*J. Geophys. Res.* **58,** 179
Hawkins, G. S.	1954	U.G.G.I. Assoc. of Terr. Mag. and Elec., Transactions of Brussels Meeting, 1951, p.229
Little, C. G. and Maxwell, A.	1952	*J. Atmosph. Terr. Phys.* **2,** 356
Maxwell, A., and Dagg, M.	1954	*Phil. Mag.* **45,** 551
Meinel, A. B., and Schulte, D. H.	1953	*Ap. J.* **117,** 454
Sangster, R. B.	1910	*Proc. Roy. Soc.* **A84,** 85
Vestine, E. H.	1938	*Terr. Mag.* **43,** 261

, VOL.
6
1955

Journal of Atmospheric and Terrestrial Physics, 1955, Vol. 6, pp. 215 to 226. Pergamon Press, Ltd. London

The significance of a nonterrestrial magnetic field in neutral stream theories of the aurora

B. C. LANDSEER-JONES

(*Received* 1 *November* 1954)

ABSTRACT

The possibility that the existence of a nonterrestrial magnetic field in a neutral stream of ions, travelling from the sun with a speed of 10^8 cm/sec, would remove a serious difficulty in the way of explaining aurorae by means of the stream when there is no such field, is examined. The analysis, which is intended to be exhaustive, leads to a process satisfactory for this purpose and needing a field in the same direction as the earth's and of a strength not less than 10^{-7} gauss, although other considerations make 10^{-5} gauss preferable. Other processes considered, requiring field strengths of at least 10^{-4} gauss, are rejected as implying great magnetic storms throughout every auroral display.

It is also shown that a stream which is flowing uniformly in a magnetic field can never move out into field-free space.

INTRODUCTION

The difficulty found in detecting streams of particles travelling from the sun to the earth sets a limit to their density. The corresponding free-paths of the particles are then so great that the effect of collisions is negligible, at least throughout the part of the stream which is affected by the earth's magnetic field. Consequently, the equations of motion need contain no purely dynamical terms other than those of inertia.

The remaining terms include, as well as forces due to the relative motion of the charged particles and the magnetic field, a purely electric force given by the space-charge which may occur in the stream. It has been shown (LANDSEER-JONES, 1952) that the difference between the densities of unlike charges needed to give an electric force comparable with the other terms is a small fraction of the probable total density. This fact allowed the neutral stream to be treated as two streams of ions of opposite signs flowing independently except for having equal densities at every point.

A serious hindrance to the developing of a theory of the aurora on this basis is a condition found to limit the width of a stream moving through a given magnetic field. The difficulty it raises is due to the quantity of flux of the earth's dipole field which particles must pass through to reach the auroral zones, and to the speed of about 10^8 cm/sec adopted for the stream. The problem of penetrating this flux has been dealt with by STØRMER and, later, by ALFVÉN. It was ignored by MARTYN (1951) in setting up his ring current, for which it is assumed that the particles can not only penetrate the flux but also acquire considerable energy, which appears later as potential energy in a radial electric field.

A theory is also unsatisfactory which implies that all aurorae are accompanied by worldwide magnetic storms. In fact, intense aurorae often appear while there is only local magnetic activity or, sometimes, none at all (VEGARD, 1916).

The difficulty due to the magnetic flux springs, in this case, from the use of FERRARO'S conservation of vorticity theorem, which holds because of the initial conditions of uniform flow and zero magnetic field assumed. While the condition

of uniform flow cannot be relaxed significantly without assuming a particular velocity distribution, which would also give rise to a magnetic field, the existence of only a magnetic field far from the earth seems to have nothing inherent against it. The consequences of assuming such a field will here be considered.

1. The Fluid Properties of Magnetic Flux

In treating the motion of two streams of particles as that of fluids in a magnetic field, it is often convenient to think of magnetic flux as a third fluid which also has a velocity in some fixed co-ordinate system: the relative velocities of the flux and particle fluids then determine the electromagnetic forces. A difficulty in three-dimensional space is that flux has extension in only the two dimensions at right angles to the magnetic vector. This may be overcome by considering only the velocities in a surface, which can always be a stream surface for one type of particle.

If Λ is a unit vector normal to the surface, the flux density at each point is defined to be $\Lambda \,.\, H$. It may be positive or negative. The rate of increase of flux in a region σ of the surface bounded by the closed curve, s, is $\dfrac{\partial}{\partial t}\int_\sigma H \,.\, \Lambda \, d\sigma$. If flux can be treated as a fluid, this must be balanced by a flow into the region across the boundary. Suppose, therefore, that a velocity of flow can be defined as a vector, U, always lying in the surface ($U \,.\, \Lambda = 0$). Then the density of flow is $H \,.\, \Lambda U$, so that $\dfrac{\partial}{\partial t}\int_\sigma H \,.\, \Lambda \, d\sigma = \int_s H \,.\, \Lambda U \,.\, \Lambda_\Lambda \, dS$, dS being an element of length of s. The integrand for the curve may be rewritten, since $\Lambda \,.\, U = 0$, $\Lambda \,.\, dS = 0$ by definition,

$$H \,.\, \Lambda U \,.\, \Lambda_\Lambda \, dS = H \,.\, \Lambda U_\Lambda \, \Lambda \,.\, dS = (H \,.\, \Lambda U_\Lambda \Lambda - H \,.\, U_\Lambda \Lambda\Lambda) \,.\, dS$$
$$= -H_\Lambda \Lambda_\Lambda U_\Lambda \Lambda \,.\, dS = U_\Lambda H \,.\, dS$$

By Stokes's theorem, the integral over the surface σ is $\int_s \dfrac{\partial A}{\partial t} \,.\, dS$. Comparing the expressions for the rate of increase of flux shows that U will be a velocity, satisfying an equation of continuity, if it is defined by $U_\Lambda H = \partial A/\partial t$, $U \,.\, \Lambda = 0$. Any magnetic field may be considered due to a system of currents, the dipole field being the limiting case of a ring shrinking to a point as the current becomes infinite. The field at R due to an element of current dI at R' is $dH = dI_\Lambda (R - R')/|R - R'|^3$. The integral of this expression over a plane vanishes, and therefore the flux through the plane for any finite current-system is zero. Since $\nabla \,.\, H = 0$, the same is true for any surface of which the points are given by projection of those of a plane along the field H. The flux in such a surface is conserved and a change in the system of currents alters only its distribution. During the change it moves with the flow density $H \,.\, \Lambda U$, which is continuous except at singularities of $\partial A/\partial t$. The velocity U has discontinuities at all points at which $H \,.\, \Lambda = 0$, at which it changes sign. As the surface may be chosen to consist of streamlines of the velocity field V for particles, U and V are directly comparable.

VOL. 6 1955

2. Initial Conditions and the Possibility of Gyrational Motion

The characteristics of the stream far from the earth are those discussed earlier (Landseer-Jones, 1952) except there is now a magnetic field H_0, supposed uniform over a region large in comparison with that where the earth's dipole field is of equal or greater strength. The uniform velocity of charged particles of both signs is again V_0. This now needs an electric field E_0 to balance the Lorentz force $V_{0\Lambda}H_0/c$, which may consist of two terms $(\nabla\phi)_0$ and $\frac{1}{c}\frac{\partial A_0}{\partial t}$. The second represents a movement of flux in the direction of V_0.

As well as the kinetic energy of its translational motion $mV_0^2/2$, each ion may now have an energy $mW_0^2/2$, where W_0 is the velocity of gyration about a centre moving with velocity V_0. At any time W_0 is taken to be distributed at random over the particles so that the gyration cannot contribute to the current or set up space-charge in the stream. This does not mean that it has no magnetic effect, as each gyrating ion has a dipole moment $mw_0^2/2h_0$. If μ is the mean moment for all ions and n_0 their number-density, they give a field of strength $4\pi n_0\mu$, which must be small compared with h_0 for the stream to be stable. Nevertheless, the present case is quite different from one in which particles in streamline motion were to begin to gyrate. As the velocities of gyration would then be in phase for the particles in each small region of space, they would set up currents and a large space-charge, approaching infinity at the end of the first quarter revolution.

Alfvén (1950a) has developed a method of dealing with the motion of gyrating particles in a varying magnetic field on condition that (a) the variation in the field is small along the radius of gyration, and (b) that any change in the translational motion is small compared with the gyrational acceleration, so that the gyration can be considered in an inertial frame. His equations will now be derived in a more general way and extended to include a variable electric field, so that gyrational and nongyrational motion can be handled, as far as possible, together.

3. Alfvén's Theory of Gyrational Motion

The position of a charged particle of mass m and charge ε is described by a vector R to the centre of gyration and a vector P from this centre to the particle. Its velocity is then $U = V + W$ where $V = \dot{R}$ and $W = \dot{P}$. If H, E are the magnetic and electric fields at R, those at the particle are $H + P \,.\, \nabla H$, $E + P \,.\, \nabla E$. The equation of motion of the particle is then

$$m\frac{d}{dt}(V + W) = \frac{\varepsilon}{c}(V + W)_\Lambda(H + P \,.\, \nabla H) + \varepsilon(E + P \,.\, \nabla E) \qquad (1)$$

which may also be written

$$m(V \,.\, \nabla V + W \,.\, \nabla W + V \,.\, \nabla W) = \frac{\varepsilon}{c}(V_\Lambda H + W_\Lambda P \,.\, \nabla H + W_\Lambda H + V_\Lambda P \,.\, \nabla H) + \varepsilon(E + P \,.\, \nabla E) \qquad (2)$$

The notation $V \,.\, \nabla V$ must not be taken to imply a velocity field, and terms of

this form are defined only on the path of the single particle. There is no term $W \cdot \nabla V$, because a change in V occurs only when the centre of gyration moves.

The condition (b) of the last section gives for the gyration

$$W \cdot \nabla W = \frac{\varepsilon}{mc} W_\Lambda H.$$

When (a) also holds, an approximate solution of this equation is

$$W = \frac{\varepsilon}{mc} P_\Lambda H \tag{3}$$

Of the remaining terms in (2), some are wholly periodic and others aperiodic, while one is mixed. Equating the aperiodic terms

$$mV \cdot \nabla V = \frac{\varepsilon}{c}(V_\Lambda H - \overline{P \cdot (\nabla H)_\Lambda W}) + \varepsilon E \tag{4}$$

where the bar denotes taking the mean for one revolution, thus separating the aperiodic part. This mean may be found by substituting the solution for W of equation (3) and writing the term in the form $\frac{\varepsilon}{mc}(\nabla H) : \overline{(PHP - PPH)}$ where : denotes scalar multiplication between the first two vectors in each tensor. If an orthogonal triad of unit vectors (I, J, K) is then chosen, moving with velocity V and with K along the axis of gyration, the components of P have the form $(p \cos \phi(t),\ p \sin \phi(t),\ 0)$, $\phi(t)$ being the azimuth of the particle in its plane of gyration. Taking the mean values for one revolution, the only nonvanishing components of the tensor are those containing $\cos^2 \phi$ and $\sin^2 \phi$, each contributing $p^2/2$. The mean of the term is $\frac{\varepsilon}{2mc} p^2(IHI + JHJ - IIH - JJH) : \nabla H$. Since H is along K and the magnitude of P is given by equation (3) to be $p^2 = \frac{m^2c^2w^2}{\varepsilon^2 h^2}$, this may be rewritten

$$\frac{\varepsilon p^2}{2mc}(IHI + JHJ + KHK - IIH - JJH - KKH) : \nabla H = -\frac{mw^2c}{2h\varepsilon} \nabla h$$

The equation of motion for V is then

$$mV \cdot \nabla V = \frac{\varepsilon}{c} V_\Lambda H - \frac{mw^2}{2h} \nabla h + \varepsilon E \tag{5}$$

The variation of w along the path of the particle is determined by an equation given by multiplying equation (2) by W and equating the aperiodic terms

$$V \cdot (\nabla W) \cdot W = \frac{\varepsilon}{mc} \overline{V_\Lambda P \cdot (\nabla H) \cdot W} + \frac{\varepsilon}{m} \overline{P \cdot (\nabla E) \cdot W}$$

The means can be found in the same way as before, giving

$$V \cdot \nabla w^2 = V \cdot \frac{w^2}{h} \nabla h + \varepsilon \frac{pw}{m} \left| \nabla_\Lambda E \right|$$

VOL. 6 1955

and therefore

$$V \cdot \nabla \left(\frac{w^2}{h}\right) = \frac{cw^2}{h^2} \left| \nabla_\Lambda E \right| = \frac{w^2}{h^2} \frac{\partial h}{\partial t} \tag{6}$$

This equation expresses the fact that the energy lost or gained by the translational motion through the term $\frac{mw^2}{2h} \nabla h$ is balanced by a change in the gyrational energy. The coefficient $\mu = \frac{mw^2}{2h}$ is constant, according to equation (6), on condition that E is a gradient field.

4. Energy and Width of a Stream of Ions in a Magnetic Field

The general equation of conservation of vorticity in a stream of ions where there are no collisions was found to be (Landseer-Jones, 1952)

$$\frac{dQ}{dt} = Q \cdot \nabla V - Q \nabla \cdot V \tag{7}$$

where Q is defined by $Q = \nabla_\Lambda V + \frac{\varepsilon}{mc} H$. If at some time $Q = 0$, a singular solution of this equation gives Ferraro's theorem, $Q = 0$ throughout the stream.

It will be assumed hereafter in this section that the nongradient part of E is negligible compared with the term $\frac{1}{c} V_\Lambda H$. The quantity μ is then constant, and the equation of motion for the stream, including the possibility of gyration, is

$$m \frac{dV}{dt} = \frac{\varepsilon}{c} V_\Lambda H - \mu \nabla h + \varepsilon E \tag{8}$$

This is the same as for nongyrating particles, except for the gradient $\mu \nabla h$. As this term vanishes under multiplication by ∇_Λ, equation (7) holds for both nongyrating particles or for their centres of gyration if they gyrate, E being restricted in the way proposed above.

It follows equally from equation (7) that if in the stream initially $Q \neq 0$, then this relation also holds throughout. As the velocity field is initially uniform, $Q_0 = H_0$. At all other points, where the magnetic field is H, either of two relations holds:

(a) $H \cdot H_0 > 0$. Then $Q_0 \cdot H_0 > 0$, so that $Q \cdot H_0 > 0$, i.e., $H_0 \cdot \nabla_\Lambda V + \frac{\varepsilon}{mc} H \cdot H_0 > 0$. If $H_0 \cdot \nabla_\Lambda V < 0$ the magnitude $\left|\nabla_\Lambda V\right|$ is restricted by $\left|H_0 \cdot \nabla_\Lambda V\right| < \left|\frac{\varepsilon}{mc} H \cdot H_0\right|$.

(b) $H \cdot H_0 < 0$. As before, $Q \cdot H_0 > 0$.

Therefore, both $H_0 \cdot \nabla_\Lambda V > 0$ and $\left|H_0 \cdot \nabla_\Lambda V\right| > \left|\frac{\varepsilon}{mc} H \cdot H_0\right|$.

As the object in assuming $H_0 \neq 0$ is to avoid the large values of $\nabla_\Lambda V$ demanded by $Q = 0$, it is essential that (a) should also be assumed, because (b) leads to even greater $\nabla_\Lambda V$.

The regions now of interest are those where $\nabla_\Lambda V \ll \frac{\varepsilon}{mc} H$. (If this condition holds throughout the stream, equation (7) becomes $\frac{dH}{dt} = H \cdot \nabla V - H \nabla \cdot V$. If also the field V is symmetrical for reflection in a plane at right angles to H, in this plane $V \cdot H = 0$ and $H \cdot \nabla V = 0$, so that $\frac{dH}{dt} = -H \cdot \nabla V$ or $\frac{1}{h}\frac{dh}{dt} = -\nabla \cdot V$. Comparing this with the equation of continuity, $\frac{1}{n}\frac{dn}{dt} = -\nabla \cdot V$, both are satisfied if $h = n \times$ const. This relation is independent of mass and charge, and so might hold for both components of a neutral stream moving in, for instance, the equatorial plane of a magnetic dipole.)

Equation (7) may be written in the alternative forms:

$$\frac{\partial Q}{\partial t} = \nabla_\Lambda V_\Lambda Q, \qquad \nabla_\Lambda \left(V_\Lambda Q - \frac{\partial V}{\partial t} - \frac{\varepsilon}{mc}\frac{\partial A}{\partial t} \right) = 0,$$

$$V_\Lambda Q - \frac{\partial V}{\partial t} - \frac{\varepsilon}{mc}\frac{\partial A}{\partial t} = \nabla \psi \tag{9}$$

where ψ is some scalar. Over any considerable time $\partial V/\partial t$ is negligible compared with $\frac{\varepsilon}{mc} V_\Lambda H$, because of the small value of m for ions. The part of $\frac{\varepsilon}{mc}\frac{\partial A}{\partial t}$ which cannot be absorbed in $\nabla\psi$ has already been assumed negligible.

If S_0 is the initial distance between two surfaces $\psi =$ const., near enough for V and H to be taken constant between them, and S is the distance where the field is H and where $\nabla_\Lambda V \ll \frac{\varepsilon}{mc} H$

$$\frac{s}{s_0} = \left| \frac{V_{0\Lambda} H_0}{V_\Lambda H} \right| = \frac{v_0 h_0}{vh \sin\theta} \tag{10}$$

In a neutral stream there are streams of ions of both signs, each satisfying equation (10), so that

$$\frac{s_1}{s_0} = \frac{v_0 h_0}{v_1 h \sin\theta_1} \qquad \frac{s_2}{s_0} = \frac{v_0 h_0}{v_2 h \sin\theta_2}$$

If the positive and negative ions at any point were initially moving in the field H_0 at a distance δ apart, and with the gyrational energies $\frac{m_1 w_{10}^2}{2}$, $\frac{m_2 w_{20}^2}{2}$, their total energies are related by

$$m_1 v_1^2 + m_2 v_2^2 = (m_1 + m_2) v_0^2 \pm 2\delta \frac{\varepsilon v_0}{c} h_0 - (m_1 w_{10}^2 + m_2 w_{20}^2)\left(\frac{h}{h_0} - 1\right)$$

VOL. 6 1955

The relations $v_1 \ll v_0$ and $v_2 \ll v_0$ can only both be true if either

(i) $\left| 2\delta \frac{\varepsilon v_0}{c} h_0 - (m_1 + m_2)v_0^2 \right| \ll (m_1 + m_2)v_0^2$

(ii) $\left| \left(\frac{h}{h_0} - 1\right)(m_1 w_{10}^2 + m_2 w_{20}^2) - (m_1 + m_2)v_0^2 \right| \ll (m_1 + m_2)v_0^2$

(iii) $\left| 2\delta \frac{\varepsilon v_0}{c} h_0 - \left(\frac{h}{h_0} - 1\right)(m_1 w_{10}^2 + m_2 w_{20}^2) - (m_1 + m_2)v_0^2 \right|$

$$\ll (m_1 + m_2)v_0^2, 2\delta \frac{\varepsilon v_0}{c} h_0 \gg (m_1 + m_2)v_0^2$$

Otherwise either $v_1 \geqslant v_0$ or $v_2 \geqslant 0$, and from equation (10)

(iv) Either $\frac{s_1}{s_0} \leqslant \frac{h_0}{h \sin \theta_1}$ or $\frac{s_2}{s_0} \leqslant \frac{h_0}{h \sin \theta_2}$

In each of the first three cases, ions of both signs lose translational energy, in (i) to potential energy in the electric field, and in (ii) to energy of gyration. In (iii) the chief transfer of energy for a pair of ions is from potential energy to gyrational energy, needing a greater value of δ than in (i). Although (i) and (ii) are not mutually exclusive, either one or the other is enough to exclude (iv).

5. The Influence of the Stream on the Earth's Magnetic Field

As the dimensions of the stream are always taken to be large compared with those of a region where it is affected by the earth's magnetic field, there is, when considering the flow in this region, nothing against assuming that the stream stretches on all sides to infinity. It will then fill the whole of space except for a hollow round the dipole. Any plane intersecting this hollow will be a simply-connected surface in the stream, and Stokes's theorem may be applied to any region enclosed by a contour in it. Such a plane is the equatorial plane of the dipole or one parallel to it, this family containing all currents in the stream.

In the case when $H_0 = 0$, so that $Q_1 = 0$, $Q_2 = 0$, let σ be any circle in such a plane with its centre at the dipole, or at the intersection of its continuation with the plane, and radius r_0. Integrating Q_1 and Q_2, by means of Stokes's theorem, over the region $r > r_0$ and σ, it is seen that the current round σ, given by the integral of $V_1 - V_2$, is always directed so as to increase the flux in the region $r < r_0$. It follows that, when $H_0 = 0$ the stream is always diamagnetic and will move the earth's magnetic flux in such a way as to increase the field strength at the surface of the earth. When $H_0 \neq 0$, the same argument applies in case (b) of Section 4. In case (a) it no longer holds, and the effect of currents in the stream may be to decrease the field at the surface of the earth.

In the theory of Section 4 it was assumed that the nongradient part of $\partial A/\partial t$ was negligible. In the actual stream, this term would correspond to movement of the earth's magnetic flux in a frame fixed to the earth. According to Chapman and Ferraro's theory, this movement is greatest during great magnetic storms, when all the flux outside a circle of radius about 10α in the equatorial plane is

compressed by the stream within it. If this view is correct, most of the flux to be penetrated by particles to reach the auroral zones lies in the neighbourhood of this circle during magnetic storms, as well as in the unperturbed dipole field. It is therefore the value of $\partial A/\partial t$ near this circle which is of interest in applying the results of Section 4.

If α is the radius of the earth and β its magnetic moment, the flux moved across the circle s of radius 10α during a great magnetic storm is $2\pi\beta/10\alpha$. Stokes's theorem gives

$$\int \frac{\partial H}{\partial t} \cdot d\Sigma = \int \frac{\partial A}{\partial t} \cdot dS, \qquad \frac{2\pi\beta}{10\alpha t} = 2\pi \cdot 10\alpha \left| \overline{\partial A/\partial t} \right|$$

where $\overline{\partial A/\partial t}$ is the mean magnitude of $\partial A/\partial t$ round the circle during the time t. As an aurora may last for 10^4 sec, the mean speed of the flux during this time is 10^5 cm/sec. During relatively undisturbed magnetic conditions it will be small compared with this, so that, if the speed of the particles in this region is greater than 10^5 cm/sec, the nongradient part of $\partial A/\partial t$ will be negligible for most of the time of an auroral display.

6. The Magnitude of the Field H_0

It will be assumed in this section that the strength of the total magnetic field near the earth is given, when disturbances at the surface are small, by $h = h_0 + \beta/r^3$. The stream is supposed, then, to flow uniformly except inside a sphere of radius r_0, where $\beta/r_0^3 = h_0$.

If m_1, m_2 are taken to be the masses of protons and electrons and $v_0 = 10^8$cm/sec, the values of h_0 required by the conditions (i) to (iv) of Section 4 can be estimated.

(i) As ions of unlike signs must converge from a distance δ apart, $\delta \leqslant r_0$, r_0 being defined above. The condition can then be written, since $m_1 \gg m_2$,

$$2\delta \frac{\varepsilon v_0}{c} h_0 = m_1 v_0^2 \quad \text{or} \quad m_1 v_0^2 \leqslant 2 \frac{r_0 \varepsilon v_0}{c} h_0 \quad \text{and} \quad r_0 \leqslant \left(\frac{2\varepsilon\beta}{m_1 v_0 c} \right)^{1/2}$$

The least value of h_0, corresponding to this greatest r_0, is $\sim 10^{-7}$ gauss.

The convergence implies a difference in the velocities of the two streams of ions, the lighter electrons moving nearly along the equipotential surfaces of the electric field and the protons moving across them against the field. The resultant current, it may be noticed, is in the opposite sense to that in ALFVÉN's drift theory. The magnetic effect of this current may be roughly estimated.

If $\bar{v}$ is the mean speed with which the stream approaches the dipole, the mean current density will be $\overline{nv} \dfrac{\varepsilon\delta}{r_0}$. The dimensions of the current system are $\sim r_0$, so that the mean field on its boundary is $\bar{h} \sim \dfrac{4\pi \overline{nv} \varepsilon\delta}{c}$, or, since $\overline{nv} \sim n_0 v_0$, $\varepsilon\delta = \dfrac{m_1 v_0 c}{2h_0}$, $\bar{h} \sim \dfrac{4\pi m_1 n_0}{2h_0} v_0^2$. As the magnetic effect of the current must be small, $\bar{h} < 10^{-4}$ gauss. Taking m_1 for protons and $v_0 = 10^8$ cm/sec gives $\dfrac{n_0}{h_0} < 10^3$. The minimum

VOL. 6 1955

h_0 found above (10^{-7} gauss) then limits the initial number-density of ions to 10^{-4}/cc.

(ii) In cases here of interest, $h \gg h_0$, so the condition may be written $\frac{h}{h_0}(m_1 w_{10}^2 + m_2 w_{20}^2) = (m_1 + m_2)v_0^2$. When $\phi_1 - \phi_{10} = \frac{m_1 m_2}{m_1 + m_2}\left(1 - \frac{h}{h_0}\right)(w_{10}^2 - w_{20}^2)$ the translational energy of both ions may be lowered while $V_1 = V_2$ and no current flows, $\phi_1 - \phi_{10}$ being the change in potential energy along the path of each ion pair. However, the magnetic field due to the gyration is $4\pi \frac{m_1 n_0}{2h_0} w_{10}^2$ (assuming $m_1 w_{10}^2 \gg m_2 w_{20}^2$) which, for stability, must be less than h_0, giving $\frac{n_0}{h_0} < 10^3$, as for (i).

(iii) This condition clearly requires a greater minimum value of $h_0\delta$, and therefore of h_0, than (i). Both ions have to gain gyrational energy by crossing the surfaces of electric potential, causing a current in the opposite sense from in (i). ALFVÉN's (1950b) drift theory is a case to which this condition can be applied, as it needs the assumptions $m_1 w_{10}^2 \gg m_1 v_0^2$ and $m_2 w_{20}^2 \gg m_2 v_0^2$ in the stream near the earth. A comparison with the evaluation of h_0 in (i) above gives here $h_0 \sim 10^{-4}$ gauss, showing ALFVÉN's value of 10^{-6} gauss for a solar magnetic field to be significantly too small. This conclusion can be verified from one of ALFVÉN's results. In his notation, the nearest approach of a stream to the earth is $0{\cdot}74L$, where $L = \left(\frac{\mu M}{\varepsilon E}\right)^{1/4}$, M being the magnetic moment of the earth and E a constant electric field, denoted here by $e_0 = \frac{v_0 h_0}{c}$. The assumption $w_{10}^2 \sim 10 v_0^2$ for protons then leads to $L = \left(\frac{m_1 10 v_0 c}{2h_0^2 \varepsilon}\right)^{1/4} = 100\alpha$, so that the positive ions cannot penetrate to a distance 10α required. In fact, ALFVÉN did not make this assumption specifically for positive ions, but only for electrons. Although in this way the difficulty of a too-small h_0 for the positive ions was avoided, the drift theory no longer applies to them; they cannot then be taken to move with the same density as the electrons, and the field E will not be constant.

(iv) The width (i.e., the dimension in the direction $V_A H$) of that part of the stream flowing in a field of strength $\sim 10^{-4}$ gauss to reach a distance 10α from the earth cannot be less than 5α. In all but a small part of this region, $\sin\theta_1$ and $\sin\theta_2 \sim 1$. Setting $s_1 = s_2 = s$, the width of either ion stream which may converge into this region is initially s_0 and, as before for δ, $s_0 \leqslant r_0$. The condition then becomes $\frac{s}{r_0} \leqslant \frac{h_0}{h}$, needing an initial field $h_0 \sim 10^{-4}$ gauss.

It appears that both (iii) and (iv) require a field h_0 which would be observed as a large magnetic disturbance at the surface of the earth, and that neither, therefore, is a satisfactory basis for a general theory of the aurora.

The minimum field strength for (i) is the conveniently low value of 10^{-7} gauss, but the greatest allowed density in this case, as also for (ii), is only 10^{-4} ions/cc. The energy radiated during an auroral display is usually taken to be about 10^{-1} ergs/sq. cm column. This column, produced along the magnetic field to a

distance 10α from the earth, will there have a cross-section 10^3 sq. cm. It will there intersect the stream for about 5α of its length, and the time for which the stream flows through all such columns will be $10\alpha/v$. If, during this time it loses 1/100th of its ions, each with energy $\frac{\varepsilon vh}{c}$. 10α after acceleration to the auroral zones, the total energy supplied for excitation will be $10^3 \cdot \frac{\varepsilon v^2}{c} hn10^9$ ergs/sq. cm/sec. Since $nv = n_0v_0$ and $vh = v_0h_0$, this gives $10^8n_0h_0$, which must be greater than 10^{-1}, so that $n_0h_0 > 10^{-9}$. Together with $n_0/h_0 < 10^3$, this requires $h_0 \sim 10^{-5}$ gauss.

The highest energy which any ion can be given by acceleration down a line of force to the earth is the potential difference across the stream, $\frac{\varepsilon v_0 h_0}{c}$. 10α e.s.u., or $5 \times 10^9 h_0$ eV. If electrons must penetrate the atmosphere down to 100 km by virtue of an energy of over 10^4 eV, h_0 must on this account also be as great as 10^{-5} gauss.

7. The Origin of the Field H_0

The lowest strength for a nonterrestrial magnetic field considered in the last section was 10^{-7} gauss. This is only one-tenth of the value used by ALFVÉN, and might still be due to a solar dipole, taking into account later measurements of the sun's general field. Nevertheless, a field as strong as 10^{-5} gauss seemed to be more satisfactory. This would most likely be due to flux carried by the stream, a possibility allowed for in Section 2.

, VOL. 6 1955

The transport of a magnetic field in this way has been suggested by ALFVÉN (1950c) and also by HOYLE (1949), who based a theory of aurorae on it. This theory requires h_0 to be as great as 10^{-4} gauss, and differs from every case so far considered in having H_0 opposed to the earth's field. Although $\nabla_\Lambda V$ is then governed by the relation (b) of Section 4, the resultant field H in this particular case will be small in the neighbourhood of some circle $r = 10\alpha$, to allow the stream to approach. However, the field strength, h_0, is too great for aurorae under all conditions to be explained.

The question of whether the stream can in fact carry out flux from a magnetic region of the sun belongs properly to a discussion of the process of emission, when forces not included in equation (8) will be active. Nevertheless, a theorem concerning the later behaviour of such a flux-bearing stream follows from equation (9).

Equation (9) for both streams of ions gives

$$V_{1\Lambda}Q_1 - \frac{\varepsilon}{m_1 c}\frac{\partial A}{\partial t} = \nabla\psi_1, \qquad V_{2\Lambda}Q_2 + \frac{\varepsilon}{m_2 c}\frac{\partial A}{\partial t} = \nabla\psi_2$$

Suppose that on a surface, o, through the stream the flow is uniform ($V_1 = V_2 = V_0$), the magnetic field is H_0 and the vector distance between two neighbouring surfaces $\psi_1 = $ const. and $\psi_2 = $ const. for each ion stream, here the same, is S_0. If on another surface, p, $H = 0$ and the vectors between the same ψ-surfaces are S_1 and S_2, where $S_1 \cdot S_2 > 0$, then

$$\frac{\varepsilon}{m_1 c}(V_0 - U_0)_\Lambda H_0 = (\nabla\psi_1)_0 \qquad V_{1\Lambda}\nabla_\Lambda V_1 = (\nabla\psi_1)_p$$

$$-\frac{\varepsilon}{m_2 c}(V_0 - U_0)_\Lambda H_0 = (\nabla\psi_2)_0, \qquad V_{2\Lambda}\nabla_\Lambda V_2 = (\nabla\psi_2)_p \quad (11)$$

U_0 being the flux velocity corresponding to $\partial A/\partial t$.

As there is no field H on p, $V_1 = V_2 = V$, so when $U_0 \neq V_0$ equation (11) gives

$$S_1 \cdot V_\Lambda \nabla V_1 = \delta\psi_1 = S_0 \cdot (V_0 - U_0)_\Lambda H_0 \frac{\varepsilon}{m_1 c}.$$

$$S_2 \cdot V_\Lambda \nabla_\Lambda V_2 = \delta\psi_2 = -S_0 \cdot (V_0 - U_0)_\Lambda H_0 \frac{\varepsilon}{m_2 c}. \quad (12)$$

Defining two nonvanishing functions γ_1, γ_2 by $V_\Lambda\nabla_\Lambda V_1 = \gamma_1 S_1$, $V_\Lambda\nabla_\Lambda V_2 = \gamma_2 S_2$, equation (12) leads to $m_1\gamma_1 S_1^2 + m_2\gamma_2 S_2^2 = 0$, implying $\gamma_1\gamma_2 < 0$. Since $S_1 \cdot S_2 > 0$ by definition, $(V_\Lambda\nabla_\Lambda V_1) \cdot (V_\Lambda\nabla_\Lambda V_2) = \gamma_1\gamma_2 S_1 \cdot S_2 < 0$, and since $(V_\Lambda\nabla_\Lambda V_1) \cdot (V_\Lambda\nabla_\Lambda V_2) = -V \cdot (\nabla_\Lambda V_1)V \cdot (\nabla_\Lambda V_2) + V^2(\nabla_\Lambda V_1) \cdot (\nabla_\Lambda V_2)$, it follows that $\nabla_\Lambda V_1 \neq \nabla_\Lambda V_2$.

This result is inconsistent with $H = 0$ ($V_1 = V_2$) over p. The alternatives allowed by equation (12) are (i) $U_0 = V_0$, or (ii) $\nabla_\Lambda V_1 = 0 = \nabla_\Lambda V_2$. If (i) holds, the flux at every point where the velocity fields are uniform moves with the velocity of the stream. The flow cannot become significantly nonuniform ($Q_1 = 0 = Q_2$), because Q_1 and $Q_2 \neq 0$ on o, so that the stream cannot in this case escape from the magnetic field. The condition (ii) requires $s_1, s_2 \to \infty$, and the stream to become infinitely wide as the magnetic field approaches zero.

It follows that a stream which is flowing uniformly in a magnetic field must always remain in a magnetic field. This implies that such a stream from the sun, unless the total magnetic flux which it bears away is zero, must return to the sun.

8. The Alternative to a Field H_0

Clearly, if the stream can be given an initial speed of about 10^{10} km/sec, or the product of the masses $m_1 m_2$ increased by a factor 10^4, the present need for a nonterrestrial magnetic field does not arise. Otherwise, if the usual speed and masses are retained, there seems to be only one alternative to it. It is to suppose that the stream in which $Q_1 = Q_2 = 0$, on entering the earth's magnetic field, splits into layers between surfaces containing V_1, V_2, and H. There will then be no simply-connected planes in the stream like those in Section 5, but each layer will be diamagnetic and the flux from it displaced into the space between it and its neighbours, these spaces being closed and a current circulating about them. The stream could thus penetrate the flux necessary to reach the auroral zones while disturbing the dipole field only locally. The splitting also holds out hope of explaining the radial structure of some aurorae.

Note: Vectors are denoted by capital letters and their magnitudes by the same small letter.

REFERENCES

ALFVEN, H.	1950a	*Cosmical Electrodynamics*, Oxford University Press, Chap. 2
	1950b	*ibid.* Chap. 6
	1950c	*ibid.* Chap. 7
HOYLE, F.	1949	*Some Recent Researches in Solar Physics*, Cambridge University Press, Chap. 6
LANDSEER-JONES, B. C.	1952	*J. Atmosph. Terr. Phys.* **3,** 41
MARTYN, D. F.	1951	*Nature*, London **167,** 92
VEGARD, L.	1916	*Ann. Phys.* **50,** 853

, VOL.
6
1955

Book reviews

Astronomical Photoelectric Photometry. Edited by FRANK BRADSHAW WOOD. Publication for the American Association for the Advancement of Science, 1515 Mass. Avenue, N.W., Washington 5, D.C. pp. VII + 141. $3.75.

This slim volume contains eight papers presented at a symposium, held in Philadelphia in December 1951, as part of the activity of the astronomy section. The discussion was limited to problems of instrumentation and techniques, and likewise the papers are confined to these aspects. The main papers deal with the use of d.c. techniques in photoelectric photometry of the stars (A. P. LINNELL), with a.c. techniques and sources of error in the same applications (J. S. HALL), with pulse-counting techniques (W. BLITZSTEIN), with pulse-counting steller photometers (R. O. REDMAN and G. C. YATES), and with the use of servomechanisms (TH. WALRAVEN). Finally, A. E. WHITFORD concludes with a critical summary and comparison of several techniques, paying particular attention to the limits of sensitivity and attainable precision.

The volume is naturally one which aims at satisfying some of the needs of astronomers in a field of technique which proves of increasing value. Nevertheless it is possible that many other workers will find material of real value. It is obvious that the contributors have produced instruments of high sensitivity and precision, and they write from a sure personal knowledge of their subject. For this reason all who are closely concerned with the refined applications of photomultipliers can learn from their discussion of their methods.

There is, as is perhaps to be expected, clear evidence of the individual outlook of the different authors. Thus the discussion on d.c. techniques carries a very lengthy reference list (575 in all), while that on a.c. techniques is followed by the modest total of 21 references. Such very obvious differences detract from the uniformity of the volume as a whole and make it difficult for the reviewer to assign it a place in the general body of the literature. The volume can be warmly recommended to those directly concerned with photometry of stars. All concerned with detailed applications of photomultipliers will find it useful reading.

S. C. CURRAN

Rocket Exploration of the Upper Atmosphere. Edited by R. L. F. BOYD and M. J. SEATON. pp. 376. Pergamon Press Ltd., London. 75s.

In August 1953, a conference with the title "Rocket Exploration of the Upper Atmosphere," organized jointly by the United States Upper Atmosphere Rocket Research Panel and the Gassiot Committee of the Royal Society, was held at Oxford. The main topic of the conference was the work which has been carried on in the U.S.A. since the war and, thanks to the excellent co-operation of the American Panel, who sent some twenty delegates, the subject was covered in the most comprehensive manner. Pergamon Press have now published all the papers and the main contributions to the discussion as a supplement to *J. Atmosph. Terr. Phys.*, in an attractively presented volume.

The rapid development of the rocket in Germany during the war, placed at the disposal of the atmospheric physicists the means for extending direct measurements on the upper air, from the balloon ceiling 40 km to unlimited altitudes. In the United States this new research tool was speedily exploited, initially with captured V2 rockets which were capable of carrying about a ton of payload to a maximum altitude of nearly 200 km. Sixty-nine of these rockets were fired during the years 1946–1951, more than two-thirds of them attaining heights greater than 80 km. The V2 has now been superseded by the Viking and Aerobee rockets, the former being about half the size of the V2 but with a substantially higher ceiling, while the latter is a much smaller rocket of half-ton gross weight and a maximum altitude of 130 km. Since these missiles are extremely expensive (the Viking costs about $450,000 and the Aerobee $25,000), there has, naturally, been some incentive to use cheaper rockets. A paper by VAN ALLEN and GOTTLIEB describes one very promising method of doing this. They outline a technique in which

relatively inexpensive solid propellant rockets are lifted initially to some 50,000 ft by means of ballons and launched from that altitude. Much of the performance loss arising from atmospheric resistance is avoided in this way and altitudes up to 100 km have been reached with cheap solid rockets.

The studies described in *Rocket Exploration of the Upper Atmosphere* can be divided roughly into three categories, namely; (i) the measurement of common physical properties and chemical constitution of the air; (ii) investigations of radiations from the sun and primary cosmic radiations, which are not observable at sea-level; (iii) observation of phenomena induced in the atmosphere by the incoming radiations, e.g., the ionosphere.

The various papers, which discuss the measurement of the physical properties of the upper air, indicate clearly the great difficulties that are encountered in making measurements from a rocket. The high velocity of the rocket produces a considerable modification of the atmospheric properties in the immediate vicinity of the vehicle, so that the ambient properties have to be deduced, often by devious means. Thus, direct measurement of ambient temperature is prevented by the existence of high stagnation temperatures around the rocket, and consequently, this quantity must be deduced from measurements of the local sonic velocity, or, alternatively, from the observed pressure and density. In either case, reduction of the data requires that assumptions be made regarding the constitution of the air. Measurement of pressure and density, also, are made difficult by the effects of the rocket's motion through the air and by outgassing from the material of the vehicle.

Similar difficulties are encountered in the determination of the chemical constitution of the atmosphere. Members of the University of Michigan and Prof. PANETH'S team at Durham have analyzed the helium, neon, argon, and nitrogen of the upper atmosphere from samples collected in special bottles carried in rockets and opened and sealed during the flight, in an attempt to detect diffusive separation. The results, at the time of the conference, had established that no separation occurs up to heights of 60 km, but little confidence was felt concerning the validity of results obtained in the more rarified air at greater altitudes. Data obtained by a N.R.L. group with a rocket-borne mass spectrometer, between 96 and 137 km, which failed to show any change in the ratio of argon to N_2, were considered to be invalidated, because the sampled air was contaminated by gas carried with the rocket.

VOL. 6 1955

Many of the investigations reported, however, appear to stand upon a much firmer footing, for example, spectrometer data on the ultraviolet radiation of the sun. Knowledge of the solar spectrum has been extended down to 2,000 Å, using spectrometers carried in rockets, and information obtained about the ozone distribution in the air. Observations made with photon-counters on the intensities of soft solar X-rays and extreme ultraviolet radiation are also reported. The intensity of the X-radiation appears to be sufficient and its height of absorption correct, to account for the *E*-layer ionization.

Both radio techniques and rocket measurements using the Langmuir probe method, in attempts to study the structure of the ionosphere, are described. In his discussion of these investigations, D. R. BATES throws considerable doubts upon the very high negative-ion density ($10^8/cm^3$) which have been measured in the *D*-layer, and implies that this must be in error. Such doubts emphasize the extremely tentative nature of many of the results so far obtained with rockets and accentuate the need for extending the work on a much wider scale.

A short paper by S. F. SINGER directs our attentions to the future scientific uses of the rocket. He points out that, in the near future, it will be possible to fire rockets into more or less permanent orbits around the earth and that such rockets carrying suitable recording instruments would be invaluable in the study of primary cosmic radiations and the radiations from the sun. Although a satellite rocket would be extremely expensive, the long period over which it would continue to record and transmit data would make it much more economical than the Viking rocket, which has a working lifetime of only seven to eight minutes.

Not all of the papers presented at the Oxford Conference and reproduced in this book are devoted to the use of rockets in upper air investigations. Several of the many other techniques that are employed to determine the behaviour and phenomena of the high atmosphere are also described, thereby giving a fairly complete picture of the whole field of atmospheric research rather than a restricted view of one aspect of the work.

It is inevitable that a collection of papers by many authors should lack the continuity of a work by a single writer. The style and lucidity of the contributors vary considerably and there is a certain amount of repetition. However, it must be remembered that this is a collection of reports on a particular field of research, and as such it is most comprehensive. The only major omission, in the opinion of the reviewer, is the lack of any detailed description of the rocket vehicles used in this research, particularly the Viking and Aerobee. The printing and reproduction of illustrations are of a high quality and the book is a credit to its editors and publishers. It can be strongly recommended to anyone who has an interest in upper atmosphere research or the possible non-military uses of the rocket.

L. R. SHEPHERD

The Sun (Volume 1 of **The Solar System**). University of Chicago Press/Cambridge University Press. $15 / 94s.

THIS volume is the first of four dealing with the members of the Solar System. Dr. GERARD P. KUIPER is the editor of the series. "The Sun" comprises nine chapters, and these are written, on a research level, by authors distinguished as prominent investigators.

Chapter 1, by Dr. LEO GOLDBERG, is regarded by the editor as introductory. It gives a brief history of solar research and a very valuable outline of the problems that arise. An outline of this kind is difficult to write, and Dr. Goldberg must have taken considerable pains before he achieved the excellent result printed. Chapter 2, by Professor BENGT STRÖMGREN, deals with "The Sun as a Star." It gives an account of current theory of the internal constitution of stars, with special reference to the sun. Professor Strömgren then passes on to a discussion of various models that have been worked out, and concludes his chapter with sections dealing with effects of accretion and of loss of mass by corpuscular radiation and with the evolution of the sun.

Chapter 3, entitled "The Photosphere," is by Professor M. MINNAERT. It deals with the escape of radiation through the outer layers of the sun, and includes accounts of the theory of the outflow of continuous radiation and of the theory of the formation of Fraunhofer lines. These two subjects taken together comprise what may be termed the basic solar physics as developed during the first half of the twentieth century, and Professor Minnaert must have been hard put to it to compress his material into a chapter of ninety pages. The result is a very valuable exposition. It is doubtless inevitable that the difficult task of compression should have produced some minor blemishes. The symbolism is not always consistent, the symbol t being sometimes used for optical depth and sometimes for mass depth. On page 113 a factor 2 is omitted from formula (25). There is one blemish which is rather more than minor; on page 114 the ROSSELAND mean absorption coefficient is wrongly defined, and the definition of the CHANDRASEKHAR mean does not make it clear that the weighting flux is the flux in the equivalent grey atmosphere. No mention is made of the fact that the ROSSELAND and CHANDRASEKHAR means are both approximations to the correct mean. The correct mean is actually printed on page 114 as the Chandrasekhar mean; it suffers from the disadvantage that it cannot be calculated rigorously until the problem has been solved and the net outward monochromatic fluxes of radiation are known. It can therefore only be found by successive approximation.

Professor Minnaert's exposition of the theory of Fraunhofer lines calls for special comment. It is a very valuable contribution made by a distinguished research worker in this field.

Chapter 4, by Dr. CHARLOTTE E. MOORE, deals with "The Identification of Solar Lines," a subject which probably appears easy to those who have not been actively involved in it. It is valuable to have this account, which fairly and squarely sets forth the difficulties and the problems.

In Chapter 5, Professor H. C. VAN DE HULST deals with "The Chromosphere and Corona." This is a subject for which, in the present state of knowledge, a balanced treatment requires an

impartial and critical survey of the available observational material and of the various theories which have been advanced. The editor is to be congratulated on his choice of an author who has presented the data and problems in an admirable way. For the chromosphere the outstanding problems are connected with its heating and support. Professor van de Hulst comments (page 253) that "the aspects that have been worked out theoretically . . . fail to explain the observations" and that "the one thing about which the observations leave us no doubt (the existence of the flamelike spicules) is not quite understood theoretically." As regards the heating of the corona (page 313), three diverging points of view are under discussion; (*a*) the heating is from the inside, by the motions of the chromospheric spicules; (*b*) the heating is from the outside, by accretion; and (*c*) the heating is by electric currents set up by electric fields. Having satisfied the requirements of impartiality, Professor van de Hulst allows himself to indicate his preference for (*a*). He considers (page 314) that compressional waves arising from the granulation region of the photosphere may degenerate into rising masses of gas (spicules) whose energy is dissipated into thermal energy. He had previously (page 254) inclined to the view that this mechanism might convey heat to the chromosphere.

In Chapter 6, Professor K. O. KIEPENHEUER gives a comprehensive account of solar activity. This chapter comprises 144 pages and is packed with well-arranged information. It is followed by Chapter 7, in which Dr. J. L. PAWSEY and Mr. S. F. SMERD give an equally comprehensive account of our present knowledge of solar radio emission. This subject is now just twelve years old; it has been a very active twelve years, and the chapter sets forth the considerable observational data that has now accumulated. The authors precede this account by giving an outline of that part of the theory of the generation and propagation of radio waves which is relevant to the sun. They conclude their chapter with a discussion of further theoretical considerations, necessarily somewhat controversial at the present stage of development of the subject, relating to the mechanism of origin.

Chapter 8, by Professor T. G. COWLING, is entitled "Solar Electrodynamics." As the author himself indicates, a more apt title would be "Solar Hydromagnetics," that is, the hydrodynamics of solar material in the presence of a magnetic field. The subject matter includes discussions of solar rotation, the origin of solar magnetic fields, sunspots and the solar cycle, and electromagnetic theories of flares. Hydromagnetics is a new subject and a fascinating one, but, as Professor Cowling remarks, "it is also one in which the probability of being led astray by seductive theories is very high." The reviewer has formed the opinion that Professor Cowling does not respond easily to attempts at seduction, and that contact with this subject has merely made him critical, although fair-minded. He sets out to do justice to all the rival opinions, but he does not hesitate to criticize. It is interesting to note that he comes down heavily against discharge theories of solar flares. He certainly seems successfully to have demolished existing discharge theories, of which he gives a fair and detached account, reserving his criticism for a separate section.

In Chapter 9 accounts are given of various empirical problems and the equipment in connection therewith. Several authors have contributed. The chapter opens with a section by Professor C. W. ALLEN dealing with the measurement of the solar constant. Other articles follow, and they include descriptions of the most recent equipment. Perhaps many readers will regard Dr. R. TOUSEY's account of "Solar Work at High Altitudes from Rockets" as a high-light in this chapter. We are in a stage of rapid development in the technique of this new research weapon, and the author has found it necessary to give a kind of stop-press addendum which includes a plate displaying the emission Lyman-alpha line of hydrogen (1216A) of the solar spectrum photographed from an "Aerobee" rocket on December 12, 1952. But it is somewhat invidious to select one section from this excellent chapter for special comment. There are many highlights; considerations of space prevent the reviewer from saying any more.

It is wellnigh impossible to give an adequate review of a volume as comprehensive as this. The present reviewer certainly cannot. He wishes, however, to say, as emphatically as he can, that no astrophysical research worker or student can afford to be without this book. The lists of references given form a valuable addition to a valuable volume. It only remains to say the volume is excellently printed and illustrated.

W. M. H. GREAVES

VOL. 6 1955

An Atlas of Typical Expansion Chamber Photographs. GENTNER, W., MAIER-LEIBNITZ, H., and BOTHE, W., X + 199 pp., with 194 plates. Pergamon Press Ltd., London, 1954. £5 5s.

This handsome volume is in effect volume 2 of a new edition of a one-volume work by the same authors published (in German) under the same title in Berlin in 1940. It is not described as such, nor was *Cloud Chamber Photographs of the Cosmic Radiation* by Rochester and Wilson, published by Pergamon Press two years ago, officially described as volume 1 of the new edition, but there is no doubt that their readers will accept these two publications as close companions, if not as parts of the same work (a third related publication, *Atlas of Emulsion Method Photographs*, is promised in due course). The independence allowed to the two groups of authors is reflected in the fact that 18 of the 194 plates in the work now under review appeared as illustrations in the companion work reviewed in this journal two years ago (*J. Atmosph. Terr. Phys.* **3**, 226, 1953). An overlap of 10 to 15 per cent in the matter of illustration is not inconsiderable (the volumes are priced almost exactly in proportion to the numbers of plates which they contain), but to have avoided it would obviously have required a degree of formal collaboration at an early stage which the publishers apparently did not wish to impose on their authors. And, in any case, how ingracious it is of a reviewer to cavil at being presented anew with reproductions of some of these superb photographs!

As before, many of the photographs are described as "unpublished" (that is, not previously used to illustrate papers in the regular scientific journals)—and the varied provenence of these unpublished photographs is a tribute alike to the universality of application of the Wilson method and to the very real support which the authors have had from their colleagues throughout the world. For the first time the attribution of certain photographs is anonymous—seven are attributed to "Radiation Laboratory, Berkeley, Cal." That these photographs were taken in the neighbourhood of the 187-inch cyclotron is perhaps sufficient reason why they are amongst the most impressive and breath-taking in the whole collection. For sheer impressiveness, however, the present reviewer is inclined to award the palm to the unpublished photograph by C. P. LEAVITT showing in clear view the whole sequence $\pi \rightarrow \mu \rightarrow e$ in a chamber containing helium at 200 atmospheres pressure and in a field of 9000 gauss.

It was a feature of the 1940 *Atlas*, extended in the volume by ROCHESTER and WILSON, that explanatory photographs were provided directing the reader's attention to the important features of each photograph and providing a brief exposition of the fundamentals of particle physics, and of the way in which the Wilson method has enriched the content of that branch of science. That feature has been continued in the present volume, and the explanatory photographs have now been printed in English, German, and French versions. This is possibly a concession to "the general reader": clearly it is—or should be—a luxury for the professional researcher. The authors acknowledge the help of Drs. PIATIER and PEYROU, who provided the translations from German into French. No similar acknowledgment is made in respect of translations from German into English, and it is to be presumed that this was the authors' own responsibility. Generally speaking, the English version reads easily and smoothly, but there are instances of wrong, or infelicitous, or vague translations here and there (e.g., on pp. 10, 80, 146), and in all three versions (p. 106) the neutron is incorrectly described as having "atomic number unity." On page 136 the English version contains the un-English abbreviation "resp." even when this does not occur in the German! When strict literality of translation does not obtain, the French version usually scores, in matter of precision, over the other two.

Finally, the twenty-four diagrams distributed throughout the book should be mentioned. These represent an extension and distribution of the experimental data presented graphically in the section entitled "General results relative to the different types of radiation" included in the introductory matter of the 1940 *Atlas*. They provide in a condensed form a very useful background of ascertained fact against which the interpretation of the photographs is the better appreciated. It is only unfortunate that mistakes in lettering or legend represent minor blemishes in so many of them (e.g., in diagrams 14, 15, 16, 20, and 24)—and the tri-lingual nature of the publication has resulted, rather amusingly, in mixed abbreviations in the legend of diagram 1. At some stage in the compilation of the volume (see table of contents) it is evident that the original diagram 18 was omitted: it does not appear in the published volume, in which diagrams 19 to 25 of the table of contents are numbered 18 to 24 in the text.

It is clear, then, that criticisms in matters of detail can be made against the new *Atlas*—as indeed they can be made with more or less justification against any publication, if the reviewer is not prepared to curb his pedantry now and again—but they do not amount to very much. Anyone who is able to possess this volume will certainly delight in it perennially; no serious student of physics will pass it over on the shelves of his departmental library; from the date of its publication it must surely have established itself in a position of its own amongst the standard reference books of science. And, entirely appropriately, it includes as a frontispiece a reproduction of JAMES GUNN's portrait of "C. T. R."—Professor CHARLES THOMSON REES WILSON, C.H., F.R.S., Nobel laureate, who at the age of 85 is still active, and in his native modesty still open to be persuaded by his friends that the method of experimenting which he devised nearly sixty years ago has contributed greatly to the advancement of human knowledge.

N. FEATHER

VOL. 6 1955

Journal of Atmospheric and Terrestrial Physics, 1955, Vol. 6, pp. 233 to 242. Pergamon Press Ltd., London

Conductivity measurements in the stratosphere

C. G. STERGIS, S. C. CORONITI, and A. NAZAREK
Geophysics Research Directorate, Air Force Cambridge Research Center,
Air Research and Development Command

and

D. E. KOTAS, D. W. SEYMOUR, and J. V. WERME
Minneapolis-Honeywell Regulator Co., Philadelphia, Pennsylvania

(*Received* 16 *July* 1954)

ABSTRACT

The electrical conductivity of the atmosphere from ground up to 100,000 ft was measured during a series of five balloon flights made in 1953. The tests indicate that the conductivity of the atmosphere increases monotonically up to the maximum height at which measurements were made. The variation of conductivity with altitude follows closely the variation expected from cosmic-ray intensity data. On none of the flights was there a clear indication that the conductivity diminishes in the region of 65,000 ft above sea-level as obtained during the Explorer II flight in 1935. We conclude that the phenomenon observed on Explorer II is not a universal one.

1. INTRODUCTION

Prior to 1953 the only measurements, to our knowledge, that were made of the electrical conductivity of the stratosphere were those obtained by GISH and SHERMAN (1936) during the famous flight of the balloon Explorer II in November 1935. On this flight, the conductivity was found to increase with height until an elevation of 62,000 ft was reached. The conductivity then began to diminish and continued doing so up to 72,000 ft, the maximum elevation attained by the balloon.

This diminution in conductivity could not be explained by GISH and SHERMAN in a completely satisfactory manner. Their best hypothesis was that the diminution was due to the presence of Aitken nuclei in this region of the stratosphere. But this hypothesis raised even more questions. Why are such large particles found in this region of the stratosphere? Are they formed there somehow or do they originate at the surface of the earth and ascend to this region? If the former is so, what are the agents responsible for the formation of nuclei? If the latter, what is the mechanism by which nuclei are transported to this region of the stratosphere? And why should this region be favoured with the accumulation of nuclei? Is this low conductivity region limited between 62,000 and 72,000 ft or does it extend higher into the stratosphere? Also, since only one flight was made, the question is immediately raised as to whether the effect observed on Explorer II is a universal phenomenon or just an isolated case.

This matter lay dormant until 1951, when HOLZER and SAXON (1952) raised some of the above questions in their theoretical paper on the current distribution in the vicinity of thunderstorms. And then in 1953 MCDONALD (1953) attempted to account for the presence of nuclei in the lower regions of the stratosphere. He examined the hypothesis that thunderstorm updrafts carry nuclei from the lower levels of the troposphere, where nuclei are plentiful, through the troposphere, and inject them into the lower regions of the stratosphere. He concluded that this

hypothesis is incapable of explaining the conductivity observations that had been made up to that time.

In an effort to answer some of the questions raised by the Explorer II flight and to extend the measurements of the conductivity of the atmosphere up to 100,000 ft, this investigation was undertaken.

2. Experimental Method

The instrument used for measuring the conductivity of the atmosphere is a modified Gerdien-type chamber which has been described previously.* It consists essentially of two concentric cylinders across which a given voltage is applied. Air passing through this chamber gives up a fraction of its electric charge to the inner electrode which is connected to a d.c. electrometer-amplifier. This in turn drives a standard radiosonde transmitter operating at 1,680 megacycles per sec. The signals from this transmitter are received at the ground and automatically recorded. The following parameters are periodically telemetered: conductivity, temperature, pressure, and certain reference signals for an indication of the reliability of the instrument.

The conductivity chamber is transported into the stratosphere by means of a single plastic balloon or by a cluster of rubber balloons, the average rate of ascent being approximately 1,000 ft/min. At the end of a predetermined time-interval, this interval being long enough to permit the balloon to reach maximum altitude, the balloon is cut down automatically. The instrument then descends by parachute at a rate which is approximately 7,000 ft/min at the beginning of the descent and about 2,000 ft/min at the end of the descent.

To minimize the electrostatic effects of the balloon and parachute on the instrument, the conductivity chamber is suspended several hundred feet below the balloon on the ascent and the same distance below the parachute on the descent.

3. Experimental Results

All the flights were made during the daylight hours at Holloman Air Development Center, Alamogordo, New Mexico. Out of a total of eight flights, five were successful. These occurred on 16 July, 21, 27, 28, and 30 October, 1953. The maximum heights attained during these flights were 68,000, 72,000, 82,000, 90,000, and 100,000 ft, respectively. Since the variation of conductivity with altitude during all these flights was essentially the same, we shall restrict the discussion to the last two flights, the ones which attained altitudes of 90,000 and 100,000 ft, respectively. We shall refer to these as flights No. 4 and No. 5.

On flight No. 4 the conductivity chamber was carried aloft by an 80-ft plastic balloon. Fig. 1 shows the altitude of the chamber as a function of time. This information is necessary in determining whether the air-flow through the chamber is sufficient for proper operation. On this figure, the altitude values were calculated from the telemetered pressure readings by means of the Rocket Panel data of 1952.

It is observed that the instrument was carried aloft at a fairly constant ascent rate of approximately 1,000 ft/min up to an altitude of about 70,000 ft. The ascent

* Coroniti, S. C., *et al.*, submitted to the *Rev. Sci. Instrum.*

VOL. 6 1955

rate then began to decrease gradually until an altitude of 87,000 ft was reached, at which time the balloon practically ceased rising. Then for about an hour the balloon floated at almost constant altitude. At a predetermined time the conductivity chamber was separated from the balloon and descended by parachute.

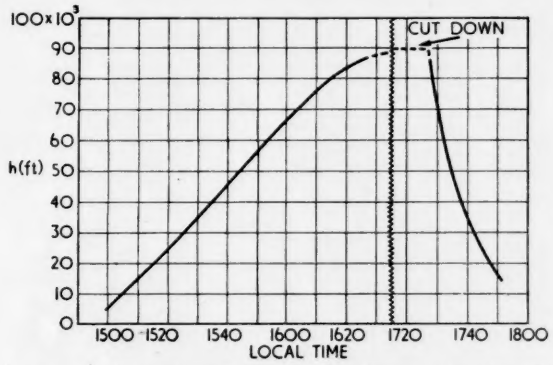

Fig. 1. Altitude of conductivity chamber as a function of time.

It is observed that the initial descent rate was approximately 7,000 ft/min. The descent rate gradually diminished to a value of about 2,000 ft/min at the lower levels of the atmosphere.

Fig. 2 shows the temperature that was measured as a function of height on flight No. 4 for both ascent and descent. It is observed that the temperature minimum

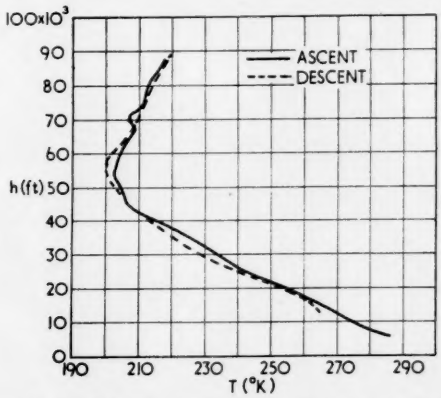

Fig. 2. Temperature of the atmosphere as a function of altitude. The solid line represents the ascent data and the dashed line the descent data.

occurs at about 55,000 ft above sea level and has a value of approximately 200°K. This temperature distribution is used in the calculation of the expected conductivity values in the atmosphere as well as in the indication of the height of the tropopause on this particular day. This latter information is of use in the consideration of problems such as the probable distribution of Aitken nuclei in the atmosphere.

The values of conductivity measured on the ascent of flight No. 4 are shown in

Fig. 3. It is observed that, in general, the conductivity increases with altitude but that considerable variations exist. These variations become very pronounced at the higher altitudes. So much so, in fact, that it is impossible to say whether there exist in the stratosphere any regions having abnormal values of conductivity. We shall reserve until later the question of whether these fluctuations are due to

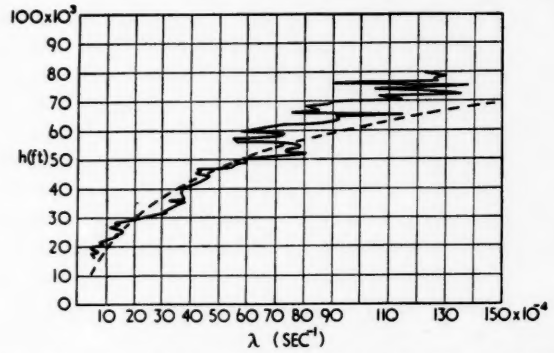

Fig. 3. Negative conductivity of the atmosphere as a function of altitude for flight No. 4. The solid line represents the ascent data and the dashed line the theoretical curve.

real phenomena in the atmosphere or to instrumental difficulties. For now we shall merely present the data as recorded.

Fig. 4 shows the values of conductivity measured on the descent of flight No. 4. It is observed that the descent data are markedly different from the ascent data. On the descent there is practically no fluctuation in the conductivity values. In

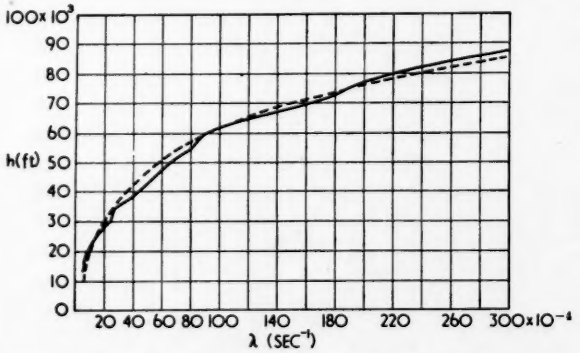

Fig. 4. Negative conductivity of the atmosphere as a function of altitude for flight No. 4. The solid line represents the descent data and the dashed line the theoretical curve.

fact, the descent curve is so smooth that any regions of abnormally low conductivity would have been detected easily. None were.

The question immediately arises as to why there should be such a great difference between the ascent and descent data. We shall attempt to answer this presently, but first let us present the experimental results obtained on the next flight.

VOL. 6 1955

On flight No. 5 the measured temperature as a function of altitude and the altitude of the balloon as a function of time were very similar to those obtained on flight No. 4, and so will not be presented here. Figs. 5 and 6 show the measured conductivity values for ascent and descent on flight No. 5. It is observed that the characteristics exhibited by these curves are very similar to those exhibited on

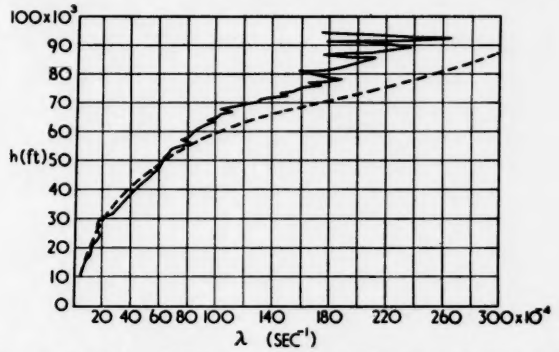

Fig. 5. Positive conductivity of the atmosphere as a function of altitude for flight No. 5. The solid line represents the ascent data and the dashed line the theoretical curve.

flight No. 4 and shown in Figs. 3 and 4. In fact, these same characteristics were found on all of the successful flights.

We may summarize the results of the measured values of conductivity thus: (1) In general, the value of conductivity increases with altitude. (2) The values of conductivity on the ascent show a considerable amount of fluctuation, this

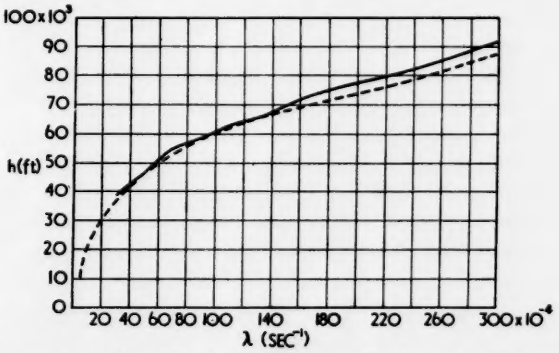

Fig. 6. Positive conductivity of the atmosphere as a function of altitude for flight No. 5. The solid line represents the descent data and the dashed line the theoretical curve.

fluctuation being quite small at the lower elevations but becoming very pronounced at the higher altitudes. (3) The values of conductivity on the descent show practically no fluctuation. (4) The descent data show that the value of conductivity increases monotonically with increasing altitude. There is no indication whatsoever of the presence of regions of abnormally low values of conductivity in the region of the atmosphere investigated.

4. Theoretical Calculations

In this section we shall calculate the values of conductivity as a function of altitude to be expected from cosmic-ray intensity data. The equation governing the time rate of change of atmospheric ions is given by

$$\frac{dn}{dt} = q - \alpha n^2 - \beta N n \tag{1}$$

where n represents the concentration of small positive or negative ions (ions/cc), q the rate of production of ions (ion-pairs/cc-sec), α the recombination coefficient between small ions, N the concentration of Aitken nuclei, charged and uncharged, and β the combination coefficient between nuclei and small ions. Thus, the αn^2 and $\beta N n$ terms represent the destruction of small ions due to combination with small ions and Aitken nuclei, respectively.

If ionic equilibrium exists and no nuclei are present in the region of the atmosphere under consideration, then

$$q = \alpha n^2. \tag{2}$$

The conductivity of the atmosphere is given by

$$\lambda = nek \tag{3}$$

where λ represents the conductivity, e the unit electrical charge, and k the mobility of the small ions. From these equations we immediately obtain

$$\lambda = \sqrt{\frac{q}{\alpha}}ek. \tag{4}$$

Thus, the conductivity of the atmosphere, assuming ionic equilibrium and the absence of nuclei, may be calculated from a knowledge of q, α, and k.

The rate of production of ions, q, was obtained from Millikan's (1938) cosmic-ray intensity data obtained at San Antonio, Texas, in 1938. Now cosmic-ray intensities at Texas in 1938 may not be the same as those at New Mexico in 1953, but nothing better was available. Millikan's data are expressed in terms of ion-pairs/cc-sec at a pressure of 76 cm Hg and 20°C. To reduce these to the values to be expected for our measured temperatures and pressures, we made use of the relation that the ionization intensity is directly proportional to the density of the gas.

The mobility, k, as a function of altitude was calculated using a value of $1{\cdot}3\ \frac{\text{cm/sec}}{\text{volt/cm}}$ as the mobility at 273°K and 76 cm Hg (this value having been measured by several investigators) and the relation that the mobility of the ions is inversely proportional to the density of the gas.

The recombination coefficient, α, was calculated using the Thomson theory of volume recombination (Loeb, 1939). According to this theory

$$\alpha = 1{\cdot}75 \times 10^{-5}\left(\frac{273}{T}\right)^{3/2}\left(\frac{1}{M}\right)^{1/2} f(x) \tag{5}$$

VOL. 6 1955

where T represents the absolute temperature, M the molecular weight of the ions in question, and $f(x)$ the probability that recombination will occur after the ions have approached to a certain critical distance where active attraction sets in. The probability function $f(x)$ is given by

$$f(x) = 1 - \frac{4}{x^2}[1 - e^{-x}(x + 1)]^2 \tag{6}$$

where the independent variable x is given by

$$x = 0{\cdot}81 \left(\frac{273}{T}\right)^2 \left(\frac{p}{760}\right) \frac{L_A}{L} \tag{7}$$

and where p represents the pressure in mm Hg, and L_A/L is the ratio of the mean free path of a molecule to that of an ion at normal temperature and pressure. This ratio is approximately 3 for air.

The probability function $f(x)$ has been calculated for values of x from 0·03 to 2·5, this range of values being sufficient for the altitude range from ground to 100,000 ft. The values obtained are tabulated in the Appendix.

The molecular weight of the ions is also unknown. This may be found by inserting a measured value of α in equation (5). The value of α at 20°C and 760 mm Hg has been reported by quite a few investigators to be $1{\cdot}6 \times 10^{-6}$ cc/sec. Using this value in equation (5) we obtain

$$\alpha = 1{\cdot}93 \times 10^{-6} \left(\frac{273}{T}\right)^{3/2} f(x) \tag{8}$$

as the relation for the recombination coefficient which was used in these calculations.

Having determined q, k, and α as a function of altitude, the values of conductivity as a function of altitude were calculated by means of equation (4). The results of the calculations for flights Nos. 4 and 5 are shown in Figs. 3, 4, 5, and 6. These theoretical curves, we should emphasize, are the curves to be expected if cosmic-rays are the only source of ions and no Aitken nuclei are present in the atmosphere. Aitken nuclei, if present in sufficient concentration, would cause a diminution in the values of conductivity from those calculated.

5. Discussion of Results

Examination of the experimental and theoretical ascent curves given in Figs. 3 and 5 shows that at the lower regions of the atmosphere the measured values of conductivity exhibit a moderate amount of fluctuation and follow approximately the theoretical values. In the higher regions of the atmosphere however, the fluctuations in the measured values become very pronounced and the average value of the measured conductivity is definitely less than the theoretical value.

The descent curves given in Figs. 4 and 6, however, give an entirely different picture. In this case, not only do the measured values of conductivity follow very closely the theoretical values, but there is practically no fluctuation in the measured values throughout the entire region investigated.

The question immediately arises as to why there should be such a difference in

the ascent and descent results. Are the fluctuations observed on the ascent indicative of conductivity fluctuations in the atmosphere or is the effect instrumental? We have no definitive answers to these questions, but shall mention some probable causes for the results obtained.

First, from the fact that practically no fluctuations are present on the descent, we conclude that the ascent fluctuations are instrumental and not indicative of conductivity fluctuations in the atmosphere. One may argue that the instrument

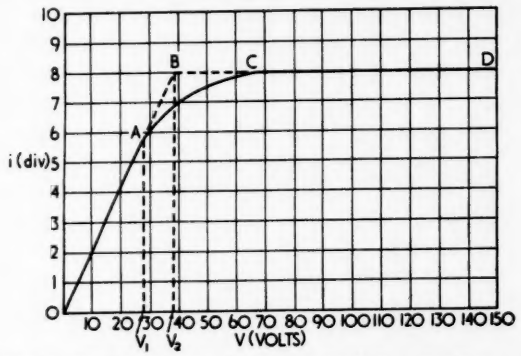

Fig. 7. Current-voltage characteristics of the conductivity chamber. *OACD* represents the experimental curve and *OABCD* the theoretical curve.

descended so fast that any conductivity fluctuations that may have been present in the atmosphere were automatically averaged out. However, when the rate of descent and the response of the instrument are taken into account it appears very unlikely that this is so.

As to the possible reasons why fluctuations are present on the ascent and not on the descent, we may cite the following. The electrostatic charge on the balloon may very well have affected the instrument on the ascent. This effect would, of course, be absent on the descent by parachute. That balloons charge up has been known for a long time, but the order of magnitude of this charge is completely unknown, as far as we are aware. We did try to minimize this effect by suspending the instrument several hundred feet below the balloon, but interference from the balloon cannot be ruled out.

Another factor which varies between ascent and descent is the rate at which air flows through the conductivity chamber. From Fig. 1 it is noticed that the descent rate is much greater than the ascent rate. What possible effect might this have on the conductivity readings? Fig. 7 shows the current-voltage characteristics of a conductivity chamber of the type used on these flights. The curve *OACD* is the experimental curve obtained under laboratory-controlled conditions, whereas *OABCD* is the theoretical curve for this type of chamber. If the chamber is operated on the linear portion of the curve *OB*, then theoretically if the applied voltage across the chamber is less than V_2 the conductivity measured should be independent of the speed of the air through the chamber. Experimentally, however, we find that the applied voltage should be below V_1 in order for the chamber to be operating on the linear portion of the curve. In the case shown on Fig. 7, V_1 is about 26 per cent lower than V_2. Under other laboratory conditions.

VOL. 6 1955

V_1 was found to be from 20 to 50 per cent lower than V_2. Thus to be sure that the conductivity chamber is operating properly, the applied voltage should be at least 50 per cent lower than the calculated voltage V_2.

On the descent of the chamber where the air speed was relatively high, we feel certain that the chamber was operating on the linear portion of the characteristic curve where the conductivity measured is independent of the air speed. On the ascent, however, the operating voltage was not too much lower than V_2. Changes in air speed would, therefore, affect the measured values of conductivity. And the speed of the air through the chamber is far from constant. Observation of the balloon as it ascends indicates that its motion is quite irregular. Such conditions, of course, are ideal for obtaining fluctuations in the conductivity values. This possible explanation also fits the fact that the mean value of the measured conductivity is less than the calculated value, for a low value of air speed means a low value of conductivity.

We may thus state that the conductivity values obtained on the descent are much more reliable than those obtained on the ascent.

6. Conclusions

Assuming the descent data shown in Figs. 4 and 6 to be fairly reliable, we may make the following conclusions:

(1) The conductivity of the atmosphere increases monotonically with height from ground up to 100,000 ft above sea-level.

(2) The measured values of conductivity agree very well with the calculated values based on cosmic-ray intensity data.

(3) No indication was obtained of a diminution in conductivity at 65,000 ft above sea-level, as observed on the Explorer II flight. This means that during the periods of our flights no Aitken nuclei were detected in this region of the stratosphere. This does not mean that nuclei are never present in the stratosphere. All we can say from our limited number of flights is that the presence of nuclei in the stratosphere is not a universal phenomenon.

Acknowledgments—We are grateful to the members of the balloon unit at Holloman Air Development Center, Alamogordo, New Mexico, for successfully launching the balloons used in this investigation.

References

Bowen, I. S., Millikan, R. A., and Neher, H. V.	1938	*Phys. Rev.* **53,** 856
Gish, O. H., and Sherman, K. L.	1936	The National Geographic Society-U.S. Army Air Corps Stratosphere Flight of 1935 in the Balloon Explorer II, Nat. Geo. Soc., Stratosphere Series, No. 2, p. 94, Washington
Holzer, R. E., and Saxon, D. S.	1952	*J. Geophys. Res.* **57,** 207
Loeb, L. B.	1939	*Fundamental Processes of Electrical Discharge in Gases* (John Wiley and Sons, New York), p. 112
McDonald, J. E.	1953	*Trans. Amer. Geophys. Un.* **34,** 529

Appendix

Probability function $f(x)$

x	0	1	2	3	4	5	6	7	8	9
0·03	0·03916	0·04044	0·04172	0·04299	0·04426	0·04553	0·04680	0·04806	0·04933	0·05059
0·04	0·05185	0·05311	0·05437	0·05562	0·05688	0·05813	0·05938	0·06063	0·06187	0·06312
0·05	0·06436	0·06560	0·06684	0·06808	0·06932	0·07055	0·07179	0·07302	0·07425	0·07547
0·06	0·07670	0·07792	0·07914	0·08037	0·08158	0·08280	0·08402	0·08523	0·08644	0·08765
0·07	0·08886	0·09007	0·09127	0·09248	0·09368	0·09488	0·09608	0·09727	0·09847	0·09966
0·08	0·1009	0·1020	0·1032	0·1044	0·1056	0·1068	0·1080	0·1091	0·1103	0·1115
0·09	0·1127	0·1139	0·1150	0·1162	0·1174	0·1185	0·1197	0·1209	0·1220	0·1232
0·1	0·1243	0·1358	0·1472	0·1583	0·1694	0·1802	0·1910	0·2015	0·2119	0·2222
0·2	0·2324	0·2423	0·2522	0·2619	0·2715	0·2809	0·2903	0·2994	0·3085	0·3175
0·3	0·3263	0·3350	0·3435	0·3520	0·3603	0·3686	0·3767	0·3847	0·3926	0·4004
0·4	0·4080	0·4156	0·4231	0·4304	0·4377	0·4449	0·4519	0·4589	0·4658	0·4726
0·5	0·4793	0·4859	0·4924	0·4988	0·5051	0·5114	0·5175	0·5236	0·5296	0·5355
0·6	0·5414	0·5471	0·5528	0·5584	0·5639	0·5694	0·5748	0·5801	0·5853	0·5905
0·7	0·5956	0·6006	0·6056	0·6105	0·6153	0·6201	0·6248	0·6294	0·6340	0·6385
0·8	0·6430	0·6474	0·6517	0·6560	0·6602	0·6644	0·6685	0·6726	0·6766	0·6805
0·9	0·6844	0·6883	0·6921	0·6958	0·6995	0·7032	0·7068	0·7103	0·7138	0·7173
1·0	0·7207	0·7241	0·7274	0·7307	0·7339	0·7371	0·7403	0·7434	0·7465	0·7495
1·1	0·7525	0·7555	0·7584	0·7613	0·7641	0·7669	0·7697	0·7724	0·7751	0·7778
1·2	0·7804	0·7830	0·7856	0·7881	0·7906	0·7931	0·7955	0·7979	0·8003	0·8027
1·3	0·8050	0·8072	0·8095	0·8117	0·8139	0·8161	0·8182	0·8203	0·8224	0·8245
1·4	0·8265	0·8285	0·8305	0·8325	0·8344	0·8363	0·8382	0·8401	0·8419	0·8437
1·5	0·8455	0·8473	0·8490	0·8508	0·8525	0·8541	0·8558	0·8574	0·8591	0·8607
1·6	0·8623	0·8638	0·8654	0·8669	0·8684	0·8699	0·8713	0·8728	0·8742	0·8756
1·7	0·8770	0·8784	0·8796	0·8811	0·8824	0·8837	0·8850	0·8863	0·8876	0·8888
1·8	0·8901	0·8913	0·8925	0·8937	0·8948	0·8960	0·8971	0·8983	0·8994	0·9005
1·9	0·9016	0·9027	0·9037	0·9048	0·9058	0·9068	0·9079	0·9089	0·9098	0·9108
2·0	0·9118	0·9127	0·9137	0·9146	0·9154	0·9165	0·9174	0·9182	0·9191	0·9200
2·1	0·9208	0·9217	0·9225	0·9233	0·9242	0·9250	0·9258	0·9266	0·9273	0·9281
2·2	0·9289	0·9296	0·9304	0·9311	0·9318	0·9325	0·9332	0·9339	0·9346	0·9353
2·3	0·9360	0·9367	0·9373	0·9380	0·9386	0·9393	0·9399	0·9405	0·9411	0·9417
2·4	0·9423	0·9429	0·9435	0·9441	0·9447	0·9452	0·9458	0·9464	0·9469	0·9475

, VOL. 6 1955

Journal of Atmospheric and Terrestrial Physics, 1955, Vol. 6, pp. 243 to 249. Pergamon Press Ltd., London

L'influence du cycle solaire sur le facteur de transmission $(M3000)F_2$

E. THEISSEN
Ingénieur au Service de Prévision Ionosphérique Militaire

(*Received* 15 *July* 1954)

ABSTRACT

The influence of the solar cycle on the height of the F_2-layer, as characterized by the "transmission factor," depends not only on the geophysical co-ordinates but also on the hour and on the season. The time of day is most important, especially near the equator. There is a maximum in the afternoon. It cannot be justified to use noon or midnight values as representative of day and night.

La facteur de transmission $(M3000)F_2$ est déterminé par un grand nombre de stations ionosphériques suivant la méthode de N. SMITH (1937, 1938). On applique un jeu de "courbes de transmission" à l'ionogramme et l'on obtient ainsi le rapport

$$\frac{F_2 - 3000\text{-}MUF}{f_0F_2} = (M3000)F_2 = M \qquad (1)$$

La méthode de SMITH est rigoureuse si la courbure de l'ionosphère et l'influence du champ magnétique terrestre sont négligées. Une autre méthode pour déterminer un tel facteur est dûe à APPLETON et BEYNON (1940, 1947). Ces auteurs ont utilisé une couche parabolique; dans ce cas on peut tenir compte de la courbure de l'ionosphère (FÖRSTERLING et LASSEN, 1931). La deuxième méthode met directement en évidence l'influence prépondérante de la hauteur h du centre de la couche. Il existe également une influence moins importante de son épaisseur et de sa forme réelle. Néanmoins la relation $M(h)$ est suffisament bien définie; elle a une forme hyperbolique permettant l'approximation linéaire:

$$M = M_0 - \alpha \cdot h \qquad (2)$$

Ainsi l'observation de la variation de M permet d'établir une méthode assez simple pour suivre en première approximation les variations de h, hauteur du centre de la couche.

On sait que les hauteurs des différentes couches ionosphériques sont plus ou moins dépendantes de l'activité solaire (GALLET*; THEISSEN, 1953). C'est surtout le cas de la couche F_2 (BURKARD, 1950; THEISSEN, 1950). Durant la période du maximum du cycle solaire les hauteurs des couches E, F_1 et surtout F_2 sont supérieures à celles observées durant la période du minimum. BURKARD et EYFRIG (1950) ont pu constater une relation presque linéaire entre les moyennes glissantes (sur 12 mois) du nombre relatif des taches solaires R et celles de la hauteur h:

$$\bar{h} = h_0 + \beta \cdot \bar{R} \qquad (3)$$

Cette relation a été obtenue avec les observations de midi seulement. Il y a, bien entendu, encore une influence saisonnière sur les valeurs de h_0 et β.

* Communication privée (influence sur la couche E)

Des relations (2) et (3) suit une variation de M avec l'activité solaire caractérisée par R. En première approximation on peut écrire:

$$\overline{M} = \tilde{M} - \gamma \cdot \bar{R} \tag{4a}$$

où $\tilde{M}$ correspond au minimum du cycle.

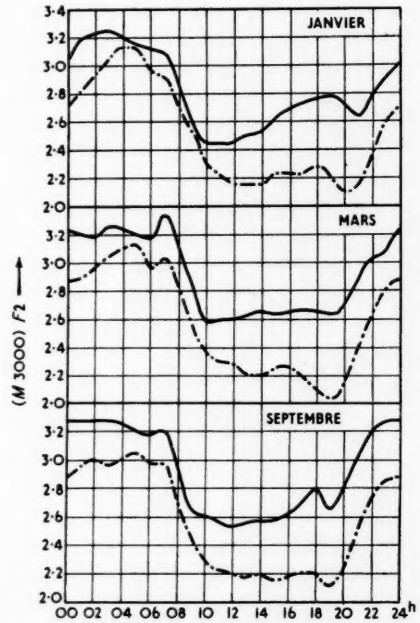

Fig. 1. Comparaison du facteur de transmission $(M3000)F_2$ en fonction de l'heure pour différentes valeurs de l'activité solaire. Huancayo (12·0° S; 75·3° W). (a) Janvier; (b) Mars; (c) Septembre.
Trait plein: Minimum d'activité solaire.
Trait pointillé: Maximum d'activité solaire.

Fig. 1. Comparison of transmission-factor $(M3000)F_2$ in function of day-time for different values of solar activity. Huancayo (12·0° S; 75·3° W). (a) January; (b) March; (c) September.
Full line: Minimum of solar activity.
Broken line: Maximum of solar activity.

Pour arriver d'ici à la valeur mensuelle il faut multiplier $\overline{M}$ par "l'effet saisonnier," $f(\tau)$, où τ est la saison:

$$M(\tau) = \overline{M} \cdot f(\tau) \tag{4b}$$

Or EYFRIG (1951) a établi directement ces relations; il a examiné pour beaucoup de stations les valeurs de M obtenues dans les années 1944–1947 à midi et à minuit. Il apparait alors que les paramètres $\tilde{M}$, γ, et f sont fonction des coordonnées de la station. En général ces paramètres sont nettement différents pour midi et pour minuit; l'influence de l'activité solaire γ, est toujours plus grande à midi qu'à minuit.

Ces résultats peuvent faire supposer que les valeurs obtenues pour minuit

VOL. 6 1955

(ou midi) sont caractéristiques de la nuit (ou de la journée). En réalité les paramètres dépendent de l'heure (comme exemple voir Fig. 1). Ce fait nous conduit à écrire plus précisément:

$$M(t, \tau; \bar{R}) = [\tilde{M}(t) - \gamma(t) \cdot \bar{R}] \cdot f(t; \tau) \tag{5}$$

Pour l'activité nulle nous avons:

$$\bar{R} = 0: \; M_0(t; \tau) = M(t) \cdot f(t; \tau)$$

Posons encore

$$\delta(t; \tau) = \gamma(t) \cdot f(t; \tau)$$

nous avons

$$M(t; \tau; \bar{R}) = M_0(t; \tau) - \delta(t; \tau) \cdot \bar{R} \tag{6}$$

Nos paramètres M_0 et δ sont donc fonction de deux variables. (EYFRIG ne les avait déterminés que pour $t = 00$ h et $t = 12$ h). Or il nous a paru intéressant de les connaitre en fonction des deux variables t et τ. Pour parvenir à ce résultat nous avons besoin d'une série d'observations de plusieures années. Nous avons choisi un certain nombre de stations dont on possède un ensemble d'au moins 8 années d'observations de M (suivant la méthode de SMITH, voir le tableau 1).

Tableau 1. *Stations et temps sur lesquels nous avons fait les recherches*

	Station	*Latitude*	*Longitude*	*Données utilisées*
a	Huancayo	12·0° S	75·3° W	II. 1944–XI. 1953
b	Brisbane	27·5° S	153·0° E	VII. 1944–VI. 1953
c	Canberra	35·3° S	149·0° E	VIII. 1944–VII. 1953
d	Washington	39·0° N	77·5° W	III. 1944–XII. 1953
e	San Juan	18·4° N	66·1° E	III. 1944–II. 1953
f	Freiburg	48·1° N	7·8° E	III. 1948–XII. 1953
g	Trinidad	10·6° N	61·2° W	III. 1944–VI. 1951

Pour chacune de ces stations nous avons d'abord dessiné trois cartes auxiliaires de la valeur moyenne de M pour plusieurs années, en fonction de t et de τ (exemple voir Fig. 2), à savoir:

1—$\bar{\bar{M}}$ pour toutes les années d'observation (en général 1944 à 1953).

2—$\bar{M}_{max}$ pour les années de forte activité solaire (juillet 1946 à juin 1950).

3—$\bar{M}_{min}$ pour les années de faible activité solaire (1944 à 1946, 1951 à 1953).

Le calcul de la moyenne a été effectué point par point pour les 288 combinaisons de t (heure) et de τ (mois). En principe l'activité solaire moyenne peut différer d'un mois à l'autre, soit d'une ligne à l'autre de la carte. En réalité elle est sensiblement constante pour chacune des trois cartes vue le nombre d'années d'observation. (Les valeurs $\bar{\bar{R}}$, $\bar{R}_{max}$, $\bar{R}_{min}$ ne sont pas les mêmes pour toutes les stations considérées en raison des périodes d'observation légèrement différentes.)

La présentation des données numériques a plusieurs avantages:

— les inexactitudes existant dans les observations mêmes et d'autres variations non-systématiques sont éliminées,

— par contre les variations systématiques, même celles de moindre importance, se présentent nettement (voir p.e. Huancayo, la variation vers 06 h du matin en été).

Sur les cartes de M l'influence de l'heure et de la saison est très visible. Il en résulte que cette influence est plus complexe qu'elle n'apparait au premier abord (exemple voir Fig. 2). Les valeurs de midi et de minuit ne sont point du tout représentatives pour le jour et la nuit.

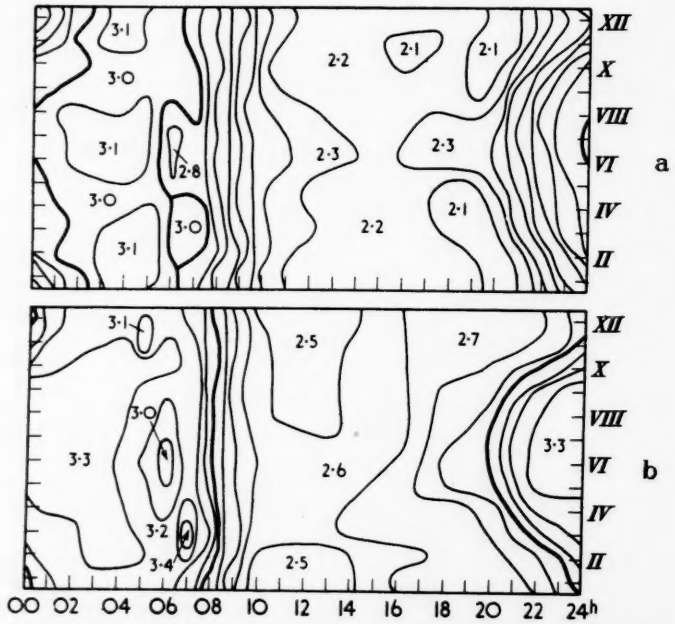

Fig. 2. Facteur de transmission $(M3000)F_2$ en fonction de l'heure et de la saison pour différentes valeurs de l'activité solaire. Huancayo (12·0° S; 75·3° W).
(a) pour $\bar{R}_{max} \approx 130$; (b) pour $\bar{R}_{min} \approx 40$.

Fig. 2. Transmission-factor $(M3000)F_2$ in function of day-time and season for different values of solar activity. Huancayo (12·0° S; 75·3° W).
(a) $\bar{R}_{max} \approx 130$; (b) $\bar{R}_{min} \approx 40$.

De ces cartes nous pouvons obtenir les paramètres M_0 et δ de l'éq. (6). Nous avons:

$$\delta(t;\tau) = \frac{\bar{M}_{min} - \bar{M}_{max}}{\bar{R}_{max} - \bar{R}_{min}} \tag{7}$$

et

$$M_0(t;\tau) = \bar{\bar{M}}(t,\tau) + \bar{\bar{R}} \cdot \frac{\bar{M}_{min} - \bar{M}_{max}}{\bar{R}_{max} - \bar{R}_{min}} \tag{8}$$

A l'aide de ces équations nous avons enfin obtenu deux jeux de cartes valables pour δ (Fig. 3) et pour M_0 (Fig. 4).

VOL. 6 1955

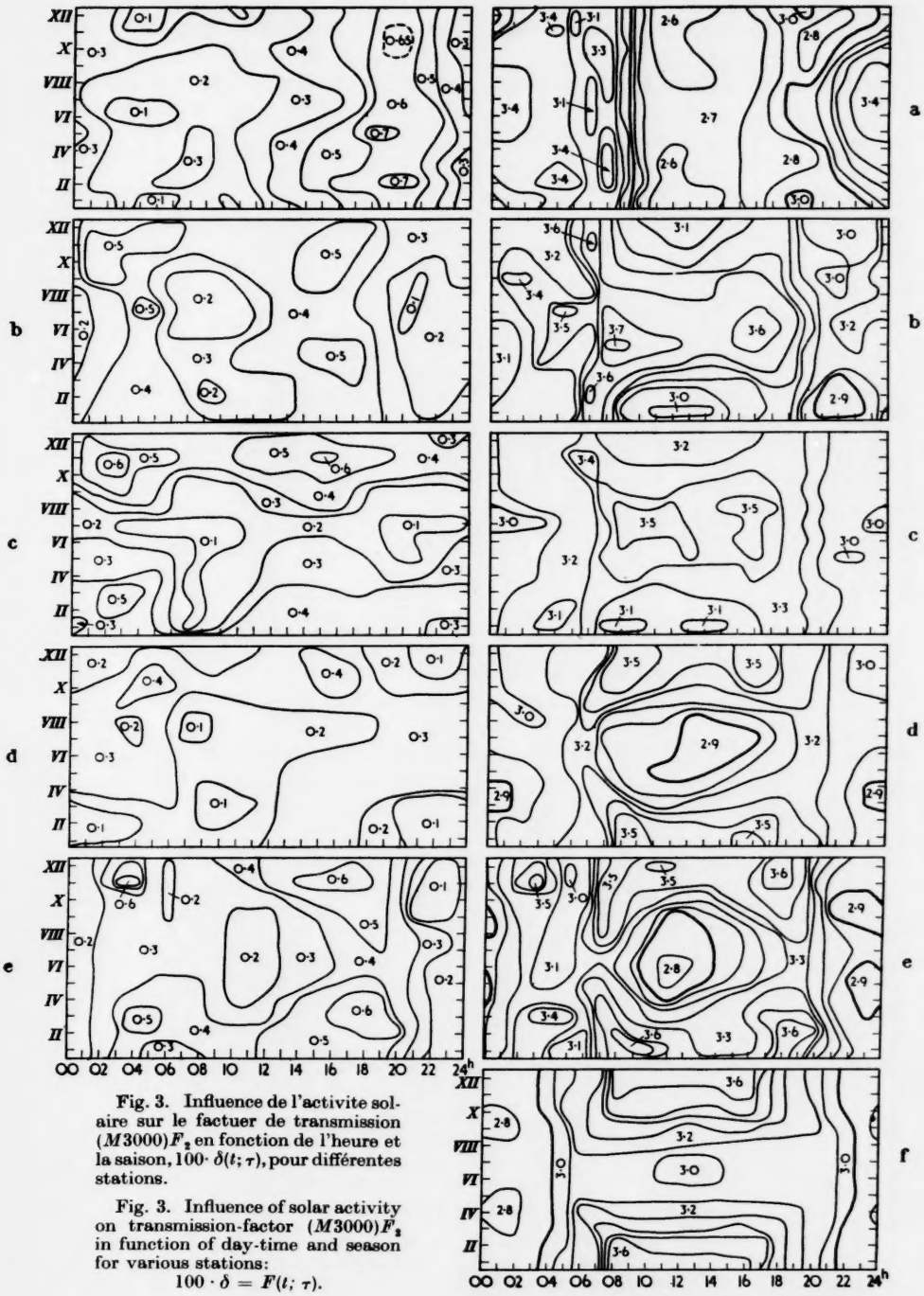

Fig. 3. Influence de l'activite solaire sur le factuer de transmission $(M3000)F_2$ en fonction de l'heure et la saison, $100 \cdot \delta(t;\tau)$, pour différentes stations.

Fig. 3. Influence of solar activity on transmission-factor $(M3000)F_2$ in function of day-time and season for various stations:

$$100 \cdot \delta = F(t;\tau).$$

Fig. 4. Facteur de transmission $(M3000)F_2$ en fonction de l'heure et de la saison, réduit sur l'activité solaire $\bar{R} = 0$, $M_0(t;\tau)$, pour différentes stations.

Fig. 4. Transmission-factor $(M3000)F_2$ in function of day-time and season, reduced to solar activity $\bar{R} = 0$ for various stations: $M_0 = F(t;\tau)$.

Les Figures 3 mettent en évidence le fait que la variation journalière de δ est la plus importante: Toutes les stations montrent une influence faible de l'activité solaire le matin; cette influence croît pendant la journée. Le maximum se situe

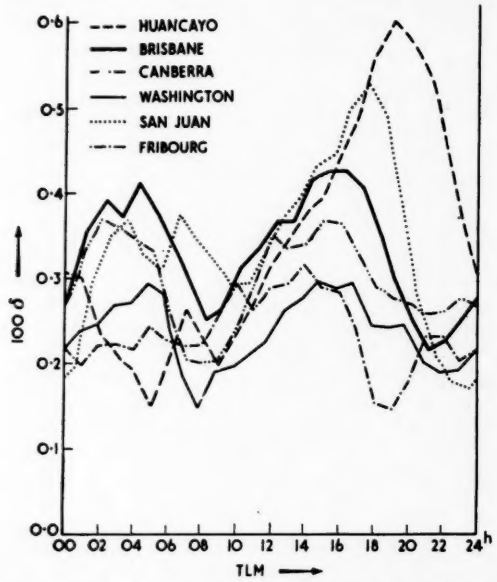

Fig. 5. Moyennes annuelles de $\delta(t)$ [comparer Fig. 3] pour différentes stations.
Fig. 5. Yearly mean of $100 \cdot \delta(t)$ for various stations [cf. Fig. 3].

entre 14 h et 20 h; il est d'autant plus fort et se produit d'autant plus tard que la station se rapproche de l'équateur. (La variation est environ 1/4 sur l'équateur et inférieur à 1/2 aux latitudes tempérées; comparer Fig. 5.) Après minuit le

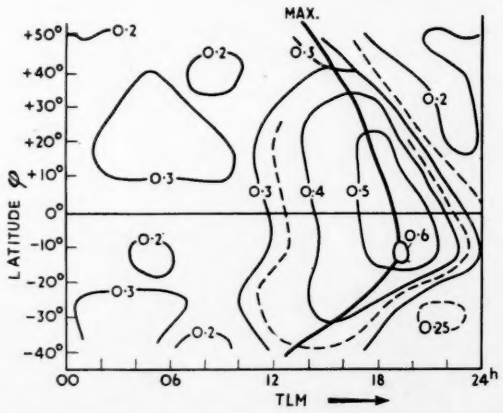

Fig. 6. Variation mondiale de la moyenne annuelle de $100 \cdot \delta(t)$ au cours de la journée. (Ces résultats ont un caractère provisoire à cause du petit nombre de stations.)
Fig. 6. World-wide variation of the yearly mean of $100 \cdot \delta(t)$ in function of day-time. (Provisional values on account of the small number of available stations.)

VOL. 6 1955

caractère de δ varie d'une facon différente avec chaque station; nos résultats ne permettent pas encore de mettre en évidence les lois de cette variation.

Les Figures 3 prouvent que les heures de midi et de minuit ne sont pas privilégiées; au contraire la variation de δ en fonction de t est très importante pour ces heures (EYFRIG *et al.*, 1950).

Les Figures 4 représentent les variations journalières et saisonnière de M, pour les cas où $\bar{R} = 0$.

Nous espérons pouvoir disposer dans quelques années d'un nombre suffisant de données afin de pouvoir examiner un réseau plus nombreux de stations. Ainsi on pourra sans doute arriver à une analyse mondiale de l'influence étudiée. Dans la Fig. 6 nous avons essayé de donner une présentation qualitative de la variation mondiale de δ.

REFERENCES

APPLETON, E. V., and BEYNON, W. J. G.	1940	*Proc. Phys. Soc.* **52,** 518
	1947	*Proc. Phys. Soc.* **59,** 58
BURKARD, O.	1950	*Geofisica pura e applicata* **16,** 63–68
BURKARD, O., and EYFRIG, R.	1950	*Geofisica pura e applicata* **16,** 123–127
EYFRIG, R.	1951	*Z. angew. Phys.* **3,** 96–103
EYFRIG, R., HARNISCHMACHER, E., and RAWER, K.	1950	*J. Geophys. Res.* **55,** 261
FÖRSTERLING, K., and LASSEN, H.	1931	*Z. techn. Phys.* **12,** 453
SMITH, N.	1937	*Nat. Bur. Stand. J. Res.* **19,** 89
	1938	*Nat. Bur. Stand. J. Res.* **20,** 683
THEISSEN, E.	1950	Paramètres de la couche F_2 d'après le modèle parabolique. Rapport SPIM-R10
	1953	*C.R. Acad. Sci.* (Paris) **237,** 1104–1106

Journal of Atmospheric and Terrestrial Physics, 1955, Vol. 6, pp. 250 to 262. Pergamon Press Ltd., London

Light-pulses from the night sky and Čerenkov radiation

Part I

W. GALBRAITH and J. V. JELLEY
Atomic Energy Research Establishment, Harwell, Berks

(*Received* 18 *August* 1954)

ABSTRACT

Further investigations have been made of the phenomenon of the light associated with cosmic-ray air-showers. The polarization and directional properties of the light have been investigated and an experiment has been done to study its colour. The results are consistent with at least some of the light being Čerenkov radiation.

1. INTRODUCTION

A considerable amount of work has been done on the Čerenkov effect (Čerenkov, 1934; FRANK and TAMM, 1937), but this work has been concerned with the Čerenkov radiation produced by the passage of charged particles through liquid and solid media, the radiation being emitted in the form of visible light having a continuous spectrum. BLACKETT (1948) pointed out that the effect should exist in gases* and suggested that there would be a contribution to the light of the night sky from the Čerenkov radiation produced by cosmic-ray particles traversing the atmosphere. The mean intensity of this contribution was calculated to be $\sim 10^{-4}$ of the total intensity, and thus would not be detectable by normal photometric methods.

In extensive air-showers there are large numbers of electrons which would produce Čerenkov radiation. These air-shower particles would be accompanied by short pulses of Čerenkov light, and the detection of such pulses by a photomultiplier appeared to be feasible. Preliminary experiments carried out at Harwell by the authors (GALBRAITH and JELLEY, 1953; JELLEY and GALBRAITH, 1953) showed the existence of light-pulses associated with extensive air-showers. In this early work, however, there had been no direct evidence that the observed pulses could be indentified with Čerenkov radiation.

In the present papers, further experiments are reported on the light-pulses and their association with air-showers. In Part I, experiments are described in which some of the properties of the radiation are investigated, and the results show that the light detected has properties consistent with Čerenkov radiation. Part II covers the relationship of the light to the associated air-showers, a series of experiments on time variations and a search for possible point sources of cosmic radiation.

To obtain a high proportion of nights of constant clarity, an expedition was made, taking a limited amount of apparatus, to the Pic du Midi Observatory (altitude 2,860 m) in France, and these experiments were done during the moonless fortnights of July-September 1953. Some limitations were imposed on the arrangement of the apparatus by the space available on the mountain, but these did not give rise to any serious disadvantages.

* Recently ASCOLI BALZANELLI and ASCOLI (1954) have detected Čerenkov radiation from the passage of fast particles through 80 cm of air and chloroform vapour at atmospheric pressure.

, VOL. 6 1955

There are at least two other processes* which might give rise to pulses of light associated with showers, namely Bremsstrahlung and recombination radiation following ionization; these will now be considered in turn and compared with Čerenkov radiation.

Bremsstrahlung

This radiation has certain features which are similar to those of Čerenkov radiation. An experiment designed to study, for example, the directional properties of the light would not in itself distinguish the two processes, because the angle of emission of Bremsstrahlung light would be comparable to that of Čerenkov radiation. For an electron of energy 10^8 eV, the mean angle of emission of Bremsstrahlung ($\theta \sim mc^2/E$) is 0·3° (compared with ~1° for Čerenkov radiation in air at N.T.P.—see Appendix). Furthermore, the Bremsstrahlung radiation, as seen by a light receiver at some distance from the core of a shower, would exhibit polarization similar to that for Čerenkov radiation, namely with the electric vector radial to the shower core. However, considering intensities, in a particular case worked out for Bremsstrahlung light in air at N.T.P. for the wavelength region 4,000–5,000 Å, the number of photons emitted per cm of track was only 6×10^{-6}, compared with 0·5 photon per cm for Čerenkov radiation. In the calculation it was assumed that the Bremsstrahlung spectral and angular distribution given by HEITLER was valid for these wavelengths and that nuclear screening was complete (HEITLER, 1949).

In the Appendix it is shown that the Čerenkov radiation detected by a light receiver at a given distance from the axis or core of a shower comes from only a small portion of the shower-track. Bremsstrahlung radiation, on the other hand, would be detected from a much larger portion of the track falling within the cone of the receiver's field-of-view. In spite of this, a calculation shows that the intensity of the light detected from Bremsstrahlung would still be small compared with Čerenkov radiation, and one is confident in neglecting any light from the former process.†

Recombination radiation

There is little information on the intensity of the radiation associated with recombination processes following ionization. A. WARD (private communication), in studying the light produced by the passage of α-particles through different gases, has found that about 150 quanta (in the wavelength region again about 4,000–5,000 Å) are emitted when a 5-MeV α-particle comes to rest in air at atmospheric pressure. Thus is this case we deduce that only about 10^{-4} of the energy lost in ionization processes appears as visible light.‡ If we can assume that this

* Estimates have also been made of the intensity of light expected from the radiation of the electrons in traversing the horizontal component of the earth's magnetic field; the magnitude of this effect is quite negligible in comparison with the other processes discussed herein.

† Nothing can at present be said about the possible contribution from double-quanta Bremsstrahlung, which might enhance the radiation intensity in the visible region.

‡ In a laboratory experiment carried out more recently by JELLEY (unpublished), Čerenkov radiation has been detected from single μ-mesons in a 600 cm air path. In this experiment it was established that the light associated with ionization was $<10^{-2}$ of that due to Čerenkov radiation, or $<4 \times 10^{-6}$ of the total energy loss by ionization.

fraction is independent of the type and energy of the particle, this corresponds to an emission of about 0·06 photon per cm of path for a relativistic particle. Since this light is emitted isotropically, it would be detected from all parts of the track of a shower within the field-of-view of the light receiver, but its intensity falls off as the square of the distance from the point of its origin. In a calculation of the intensity of recombination light on the ground from a shower, a number of assumptions have to be made which might lead to a value wrong by an order of magnitude, and one cannot immediately dismiss this source of light on the basis of such a calculation. However, recombination light would not be polarized, and an experiment was devised to detect polarization of the light which would distinguish Čerenkov radiation from it. The results of this are presented in Section 3.

An experiment to study the directional property of the light is described in Section 4, and this also serves to distinguish the two processes.

Finally, if one could study the colour of the light, this might indicate its origin. Čerenkov and Bremsstrahlung radiation both have continuous spectra, though of different forms, while recombination radiation would have a line- or band-spectrum. For the reasons set out in Section 5, an experiment to determine the colour of the light with any accuracy is inherently very difficult. The present one, described in Section 5, is crude, but the result adds some weight in support of the other two experiments of Section 3 and 4.

, VOL. 6 1955

2. DESCRIPTION OF THE APPARATUS

The light receivers

As previously described (GALBRAITH and JELLEY, *loc. cit.*), each light-receiver consisted of a parabolic mirror* and an end-window photomultiplier, mounted with its cathode surface at the focus of the mirror (see plate I). Four mirrors were used for the various light-receivers, two having a diameter of 61 cm and a focal length of 25 cm, and two a diameter of 25 cm, and a focal length of 11 cm. Two types of 11-stage photomultipliers were used, one with a 50-mm diameter cathode (E.M.I. type 6260) and the other an experimental model with a 125-mm diameter cathode. Because of the high average intensity of the light of the night sky as received on the photocathodes, it was necessary to use dynode resistors of relatively low value, and low gain in the phototubes, to prevent d.c. saturation effects.

A blackened light-screen was placed around the mirror and phototube to cut out stray light from buildings and distant lightning. With the two sizes of mirror and the different phototubes, together with metal stops of various diameters placed over the phototube cathodes it was possible to select the light-gathering power and the field of view of the receivers. Each unit was fitted with a 2·5-volt filament lamp mounted at the edge of the mirror, so that the mean light of the night sky could, if necessary, be enhanced artificially (see below).

* The mirrors were silvered on the underside of the glass; it would have proved quite impracticable to keep top-surface silvered mirrors clean in the presence of fine wind-blown dust that was often experienced, without damaging their surfaces. The results of some subsidiary experiments carried out with a photomultiplier having a quartz window, and a mirror silvered on the upper surface, showed that there would have been no marked improvement in performance if top-silvered mirrors had been used.

OL.
6
955

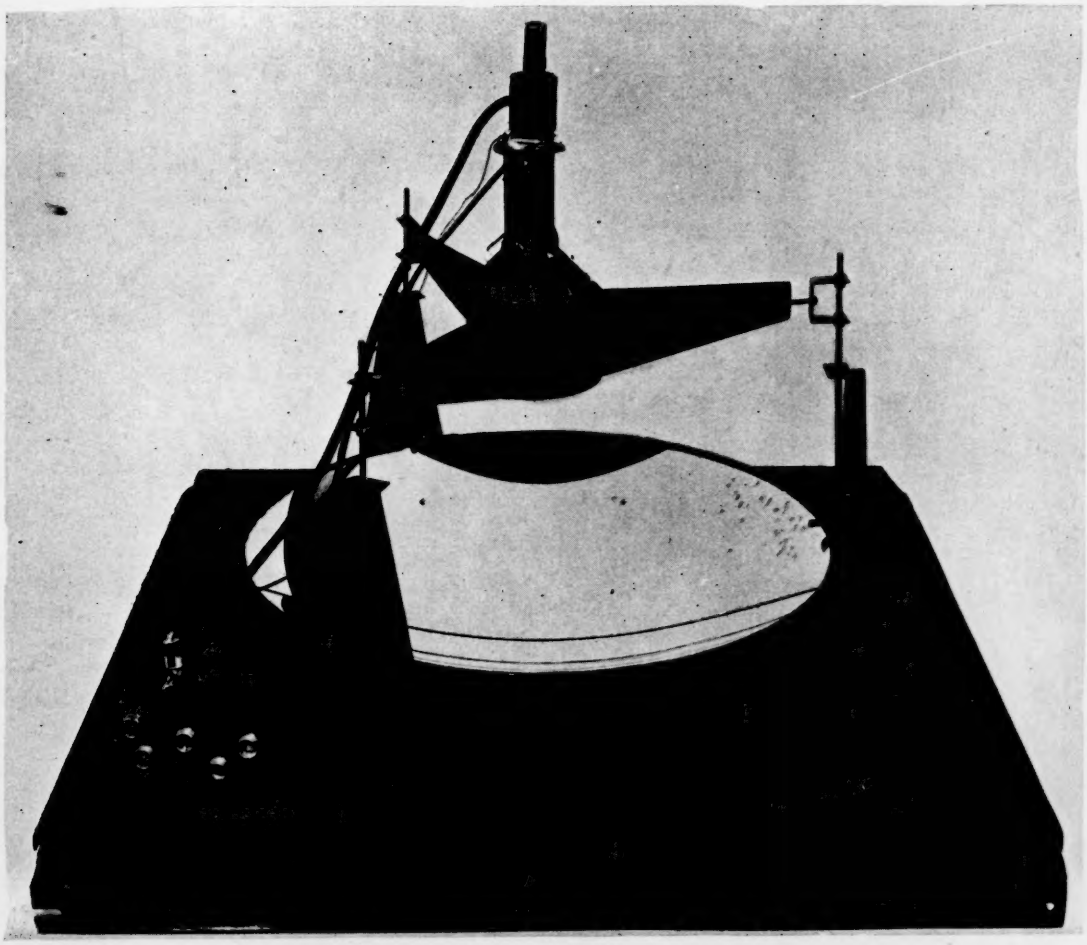

Plate I. Typical light-receiver comprising 61-cm mirror and 125-mm phototube.

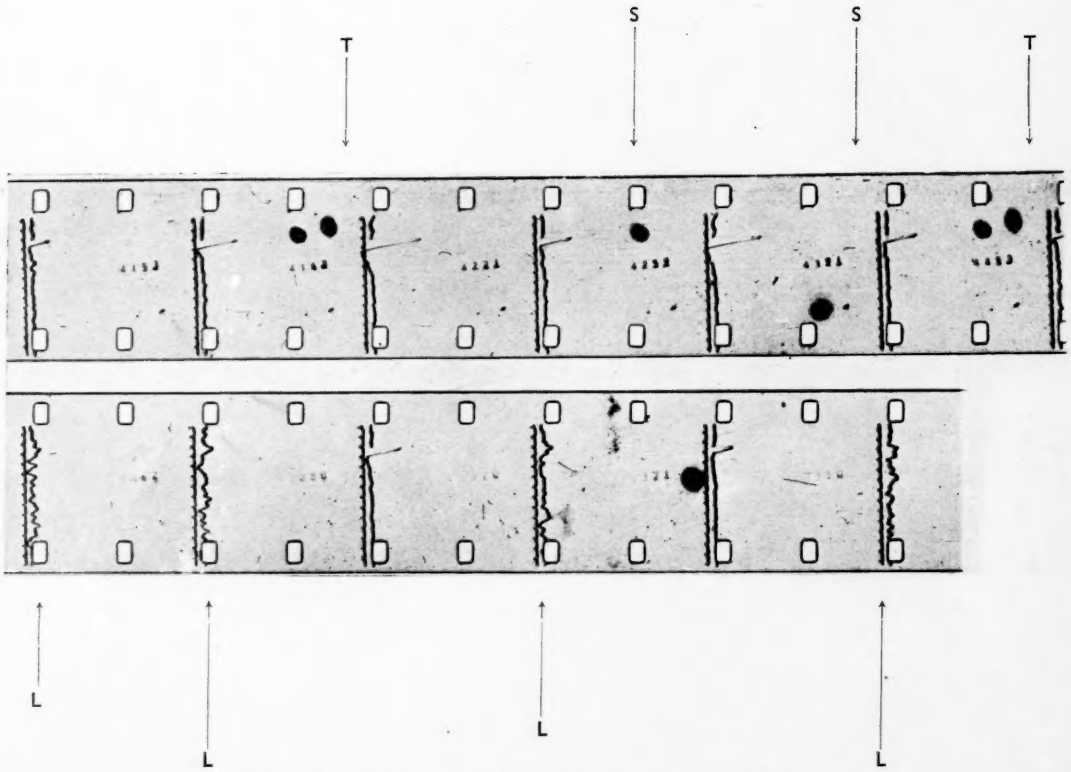

Plate II. Typical record of light-pulses on a 15-μsec time-base.
S Single counter event, *T* Two-fold counter events, *L* Recordings of lightning pulses.

VOL.
6
1955

The Geiger-counter trays

Five Geiger-counter units were used for the experiments in which the light-pulses were correlated with extensive air showers, each unit consisting of a tray containing four counters each of area 200 cm². The positions of the units relative to the light-receiver were influenced by the space available on the mountain; the arrangement used is described below for the appropriate experiment.

The electronic apparatus

The essential features of the electronic apparatus are shown in the block diagram of Fig. 1.* The light-pulses appeared as deflections on a 15μ-sec time-base of an oscilloscope, and were photographed. The camera also recorded indicator

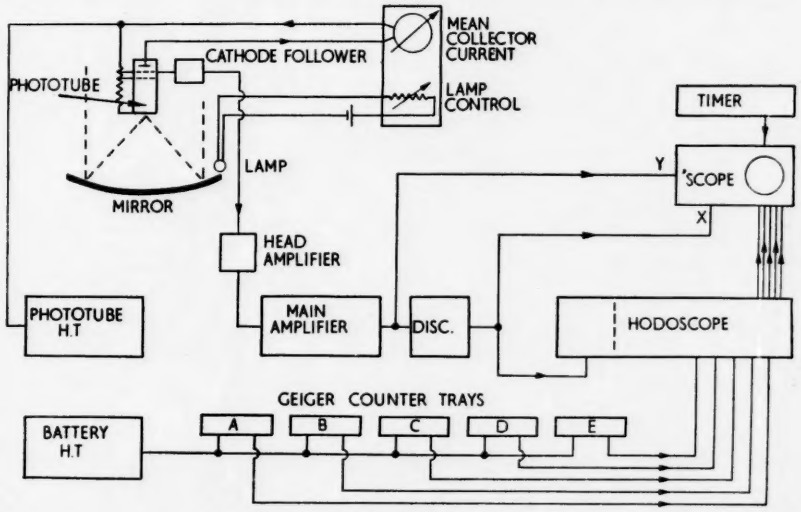

Fig. 1. Block diagram of apparatus.

lamps connected to the hodoscope. Photographs of light-pulses are shown in plate II. Pulses occasionally recorded and due to distant lightning could readily be distinguished from light-pulses, as seen in the photograph.

In all the experiments the time constants of integration and differentiation in the main pulse amplifier were set at the nominal values of 0·08 μsec.

It is necessary to describe here, for completeness, a particular technique that was used in many of the experiments. It was found that the mean current in the phototubes varied by about a factor of 2, depending on whether a light-receiver was looking at a bright region of the sky, such as the Milky Way, or at a dark region. It was known from our previous work that the integral pulse-height distributions of the light-pulses were very steep. Consequently, the counting rate of pulses at a given bias would be expected to vary as the noise varied, because the noise- and light-pulses would be additive. To overcome this difficulty, the mean

* When using two light-receivers, the amplifiers, discriminator, power supplies, and mean-current meters were duplicated.

current in the phototube, and hence the noise, was kept constant throughout an experiment by adjusting the brightness of the small lamp by the mirror. In most of the experiments, the discriminator was biased at twice noise, defining noise as the bias level at which the counting rate was ~1 count per second. It was verified, by taking bias curves, that the noise characteristics of the light from the lamp were identical with those of the light of the night sky (see Section 1 of part II).

3. POLARIZATION EXPERIMENTS

The essential features of the Čerenkov effect in air are given in the Appendix, and it is seen that the radiation has unique properties of direction of emission and

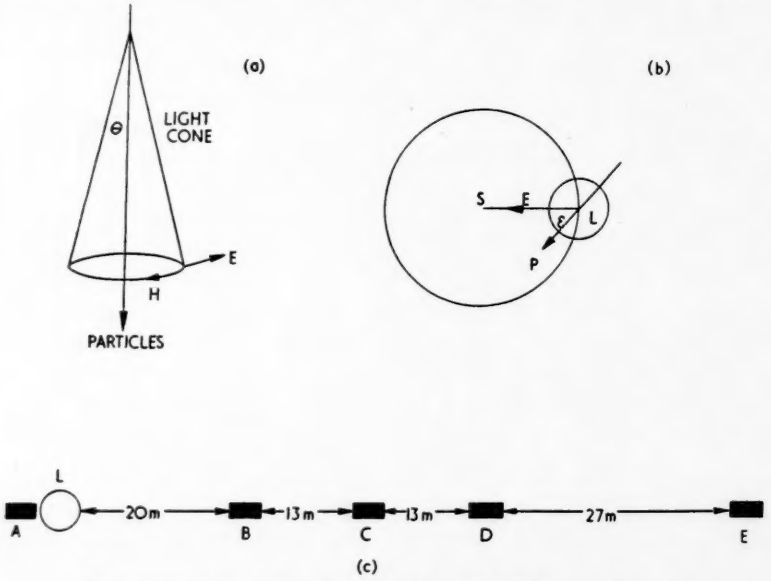

Fig. 2. Illustrating the principle of the polarization experiment.

polarization, illustrated in Fig. 2(a). There is an electric vector E perpendicular to the surface of the light cone, and a magnetic vector H tangential to the cone.

If the observed light-pulses are due at least, in part, to Čerenkov radiation, one might expect that the light would be polarized. (Bremsstrahlung radiation is assumed to be negligible—see Section 1 above.)

The principle of the experiment devised to detect polarization is shown in Fig. 2(b). Suppose the core of a vertical shower falls on the ground at the point S, and that most of the Čerenkov light is emitted from this core in which the particle density is very great. A light-receiver, with polarizer placed over the cathode of the phototube, located somewhere within the light cone at L, will then give pulses of a certain average height when the plane of polarization P of the polaroid is in the same plane as the radial vector E. If now the polarizer is rotated through 90°, no light will be received. In general, for showers falling anywhere around the receiver, the average intensity of the light-pulses will vary as $\cos^2 \epsilon$, where ϵ is the angle between the vectors, E and P.

VOL. 6 1955

In the present experiment a single 61-cm light-receiver L, with a field of view of $\pm 18°$, was situated at the end of a straight-line array of Geiger units A, B, C, D, and E (see Fig. 2(c)) at distances of 0, 20, 33, 46, and 73 metres respectively from L, each unit containing four Geiger counters of total area 800 cm^2. In this way the positions of the cores of the air-showers could be defined only very approximately along the line AE, but it was hoped that some difference would be detected in the rate of coincidences between the light-pulses and discharges of the Geiger units when the polaroid was orientated with the P vector along or at right angles to this line. More accurate positioning of the showers would have required more elaborate apparatus, which was not feasible with the portable equipment at our disposal.

KN36 Polaroid was used as the polarizing medium because it had a high extinction ratio and also a relatively good transmission over the spectral region in which the phototube was sensitive. The polaroid was placed directly in contact with the cathode of the phototube. It was shown by a subsidiary experiment, using a souce of plane polarized light and a collimator, that the plane of polarization was not rotated, or the degree of polarization reduced, by reflection of the light at the surface of the mirror.

The arrangement of the apparatus was as shown in Fig. 1, and the experiment was carried out in the following way. Recordings were taken at half-hour intervals throughout seven nights of observation; at each half-hour interval the orientation of the polaroid was changed by 90°, and the rotation was always made in the same direction to eliminate possible asymmetries in azimuth, either in the polaroid absorption or the photocathode sensitivity. The results of these experiments are summarized in Table 1; the figures in this table refer to the number of events in which a light-pulse was associated with a shower which discharged one or more of the Geiger units. Any event which increased in frequency when the vector P of the polaroid was along the line of the counters, compared with the frequency when the vector P was perpendicular, is evidence in favour of Čerenkov radiation.

From these results it is seen that, whereas the single events (with the exception of the counter tray E) and threefold events show no evidence for polarization, the double events show quite a marked effect. The ratio of the rates for the two settings of the polaroid in this case is $(3{\cdot}0 \pm 0{\cdot}5) : 1$. The slight polarization effect for the single counters discharging tray E can be completely accounted for by assuming that some of these are of the same type as the double events, and that a further counter (F), if it had existed, would have been discharged by them. It is thus necessary to explain why the twofold events show the effect of polarization, but not the single or threefold events.

The following tentative explanation is put forward but does not rest upon any certain evidence. First, it must be remembered that the single events do not necessarily correspond to small showers falling near the counter discharged, because such small showers may produce light-pulses which are too weak to be detected. In fact, there is some evidence (see appendix of Part II) that the showers producing light-pulses have energies $\gtrsim 10^{14}$ eV, and it can be shown (Whitehouse, W. J., private communication) by the type of calculation introduced by Cocconi (1946), that these showers would normally discharge two or even three trays if

they fell within 20 metres of the line AE. It is probable, therefore, that the observed coincidences with single counter trays are due to the skirts of air showers falling a considerable distance away from AE, and that no observed correlation with polaroid angle would be expected.

Table 1. *Results of polaroid experiment*

Orientation of polaroid vector	*Total number of light-pulses*	*Frequency with which counters were discharged*										
		Single units						*Multiple events*				
		A	*B*	*C*	*D*	*E*	*B* + *C* + *D* + *E*	*BC*	*CD*	*DE*	*BCD*	*CDE*
Parallel to counter line	1024	101	59	55	39	38	191	45	47	26	26	9
	Normalized to 1047 pulses	103	60	56	40	39	195	46	48	27	26	9
								121 ± 11				
Perpendicular to line	1047	108	59	55	45	26	185	19	12	9	22	10
								40 ± 6				

One now has to account for the polarization effect shown by the twofold events, and the apparent non-existence of an effect for the threefolds. The most probable shower size and the area within which these showers can fall to produce, for example, a twofold event, say BC, can be estimated assuming that all showers have a common structure and that the frequency-vs-energy spectrum of the incoming primary particles obeys a power law. By "common structure" is meant that, at a given distance from the core, the density of electrons is proportional to the total number of particles in the shower, which in turn is a function of the energy of the primary particle producing the shower. A similar estimation can be made for the threefold events BCD and CDE. In general, most of the showers producing twofold events fall closer to the line AE than those showers producing the threefold events, and from this it is reasonable to expect that, at least, the twofold events would show a polarization effect. One might then estimate the fraction of the showers producing the threefold events which fall sufficiently close to line AE and therefore would also be expected to show a polarization effect. This fraction, probably 0·1–0·2, is so small that the statistical errors in the number of threefold events observed (e.g., BCD about twenty and CDE about ten events for either

, VOL. 6 1955

orientation of the polaroid) are large enough to mask the expected polarization effect.

At different conditions in the sensitivity of the light-receiver (e.g., change of discriminator bias for the light-pulses) it might be expected that the polarization effects would show up at other shower energies. In spite of the qualitative nature of these arguments, they are put forward to point the way to a reasonable explanation of the results.

4. The Directional Property of the Light

It is known (see Appendix) that Čerenkov radiation is emitted at a small angle to the track of the particle in air, and therefore an experiment was devised to see if the light emitted by the air-showers had any marked directional properties. In this experiment, the change in coincidence rate between two light-receivers placed side by side, each of limited field of view, as the angle ψ between their optic axes varied, was measured. If it is assumed that (a) most of the light comes from particles near the core of the shower, and (b) the spread in directions of these particles due to Coulomb scattering is small, then the coincidence rate would be expected to vanish immediately the fields of view of the two receivers ceased to overlap, provided that all the light was due to Čerenkov radiation. If the light was due to Bremsstrahlung or recombination processes, the coincidence counting rate would persist for values of ψ greater than the sum of the two fields (see below).

In the present experiment, two 61-cm light-receivers were set up, with their optic axes set parallel by observing visually that the image of the star Vega fell in the centre of the fields of view defined by the stops placed over the photocathodes. At the start of the run the two receivers were pointing almost to the zenith. The output pulses of the amplifier from one receiver triggered the time-base of the oscilloscope, while the output of the amplifier from the other receiver was applied to the Y-deflection circuits of the oscilloscope. The unit connected to the Y plates was then tilted through known angles and the changes in the coincidence rate observed. The coincidence rate was expressed as the number of time-bases having light-pulses at the correct place on the time-base and of a height of greater than twice the peaks of the noise-pulses, to the total number of time-bases. Throughout the experiment the noise in each receiver was kept at a constant level by varying the intensity of the small lamps at the side of the mirrors (as described in Section 2).

A relatively wide field of view, α, of $\pm 3{\cdot}6°$ was used in an initial experiment. The results of this are shown in Fig. 3(a), in which A and B refer to the tilted and stationary receiver respectively. A second experiment of higher resolution was then carried out with α equal to $\pm 2{\cdot}2°$, and the results of this are shown in Fig. 3(b). The errors on the values of ψ are derived from an estimate of the accuracy with which it was possible to align the optic axes of the two units.

The experimental results may be compared with those expected theoretically for light which arises either from Čerenkov radiation only or from ionization processes only. This has been done, and the dotted curves in Fig. 3(b) represent these two cases.* The curve for Čerenkov light was calculated on the assumption

* The corresponding curve for Bremsstrahlung has not been calculated, but it would be expected to have a shape more like that for the Čerenkov case than that for recombination.

that the light is parallel and hence gives rise to point images (the spacing of the receivers, ~1 metre, is in general small compared with the distance of the shower core from either receiver). The second curve was based upon the assumption that the images of the shower cores were straight lines and that these lines were orientated at random. In both calculations, the Coulomb scattering of shower particles was neglected.

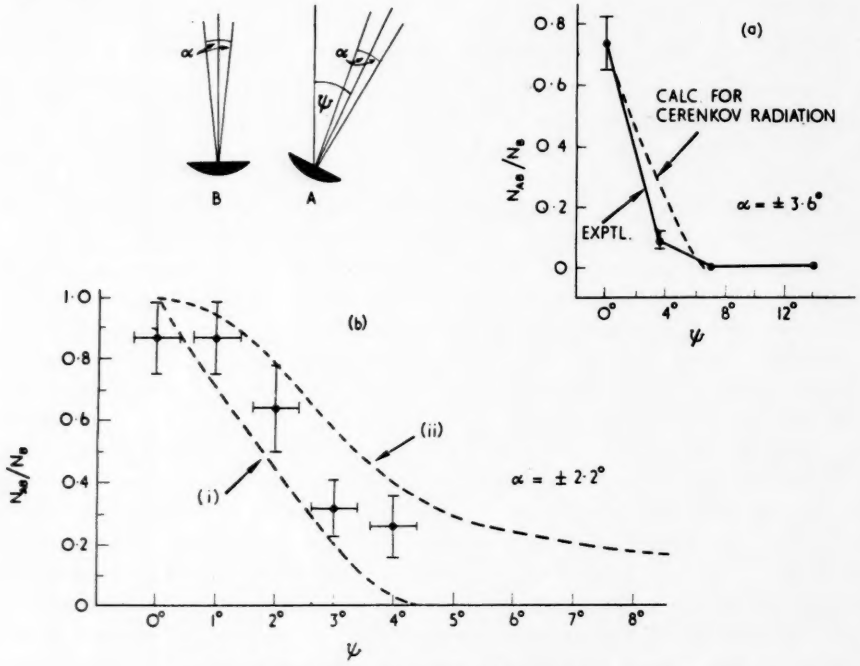

Fig. 3. Coincidence rate for two light-receivers, as function of ψ.

It is seen that the experimental "points" lie in between the two curves. Thus, although giving no direct proof for Čerenkov radiation, there is some evidence in favour of it, since the points lie consistently below the curve for ionization light. Any contribution of light from particles appreciably scattered, or other sources of spread in the images of the light-pulses on the photomultipliers, would only raise the experimental points at any given value of ψ.

It was found from a separate experiment in which two light-receivers were directed to the zenith, that the pulse amplitudes were unequal from the two units. This was largely due to the presence of the noise; the effect certainly existed in the present experiment, and would cause a flattening of the curve in Fig. 3.

5. Experiments with Colour Filters

It is impracticable to make any precise measurements on the spectrum of the light emitted by air-showers. The use of any form of spectrometer to investigate the spectrum of the radiation is prohibited because of the low light intensity. However, a crude but simple experiment may be done using wide-band colour filters, provided

VOL. 6 1955

that the transmission of the filter and the spectral response of the phototube cathode are known.

In the present experiment, two colour filters (blue, Wratten type C-5, No. 47; and green, type B-2, No. 58) were used. It was not possible to use a red filter, because the response of the phototube to this light was negligible. The light-receiver comprised the 61-cm mirror and 12·5-cm phototube, and the experiment was to place, in turn, the filters over the photocathode and to record the rate of light-pulses greater than a fixed bias set on the discriminator. In practice this bias was set at twice the level of noise-pulses from the light of the night sky when the blue filter was placed on the photo-cathode. The hodoscope was triggered from the light-pulses in order to give some indication of the size of shower producing sufficient light to be detected through the colour filter; the arrangement of Geiger-counter units was the same as that in Fig. 2(c). The light-pulses and the hodoscope lamps were photographed on the recording oscilloscope as described in Section 2.

The results of three nights observation are presented in Table 2.

Table 2. Results of colour-filter experiments

Filter	*Total counts*	*Total time (minutes)*	*Rate: counts per minute*	*Number of light-pulses associated with showers discharging 3 or more G.M. units*
Blue	208	207	1·00 ± 0·07	29
Green	160	686	0·23 ± 0·02	45

The ratio of the rate of pulses with the two filters is

$$\frac{\text{Blue rate}}{\text{Green rate}} = 4{\cdot}3 \pm 0{\cdot}4.$$

The hodoscope information shows that, in general, larger showers are detected when the green filter is used. This is to be expected, because, as seen below, the overall sensitivity of the light-receiver is more reduced by the green filter than by the blue.

A spectrophotometer was used to measure the response curves of the photo-multiplier to an equi-energy source, when covered by the two filters in turn. (Curves *a* in Fig. 4.) The ratio of the areas under the curves is R_1 (blue : green) $= 1{\cdot}85 \pm 0{\cdot}15$. It was found (Part II, Section 2) that the frequency of pulses with a height greater than H is given by a power law of the form $N\,(>H) = AH^{-\delta}$, where A is a constant. From the photographs of the pulses in this experiment, it was shown that, for the two pulse-height distributions with the filters, the constant δ was independent of the filter used, within the accuracy of the measurements, and equal to $1{\cdot}8 \pm 0{\cdot}2$.

Therefore the ratio

$$\frac{\text{Blue pulse rate}}{\text{Green pulse rate}} = (R_1 R_2)^{\delta} \qquad (1)$$

where R_2 is the ratio of the energy per unit wavelength interval, for the mean blue and green wavelengths transmitted by the filters. The Čerenkov radiation has a continuous spectrum of the form $dW/d\nu = k\nu$, where W is the energy per unit path length, ν the frequency of the light, and k is a constant if dispersion is neglected. (See Fig. 4.)* From this curve the value of R_2 is estimated to be 1·17.

Finally, by multiplying the response curves (curves *a*) by the energy distribution of the radiation, we obtain the theoretical response of the system to Čerenkov radiation, shown in the curves (*b*).

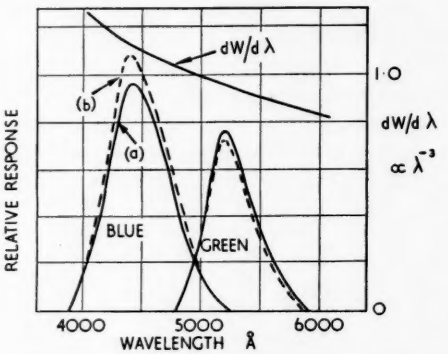

Fig. 4. Sensitivity curves for a receiver with colour filters over the photo-cathode.

Inserting the values of R_1, R_2, and δ in equation (1), we obtain for the calculated ratio of blue : green pulse-rate the value $4{\cdot}0 \pm 1{\cdot}0$, which agrees, within the errors, with the ratio of pulse-rates found in practice.

Unfortunately the method is rather insensitive to the spectral distribution of the radiation, but at least it shows that the light resembles Čerenkov radiation in that it contains more blue light than green.

6. Conclusions

The result of the experiment on the polarization of the light (Section 3) provides evidence that some, at least, of the light detected by apparatus of the type described is Čerenkov radiation. This conclusion is supported by the results of experiments on the directional properties (Section 4) and colour (Section 5) of the light. In addition, it is seen from the results in Section 4 that most of the light comes from particles having very small Coulomb scattering ($< 5°$), and it is tentatively assumed that most of the light detected arises in the cores of air-showers where the density of particles is high.

Acknowledgments—We wish to express our thanks to the following of our colleagues at A.E.R.E.: Mr. F. R. Barclay, for help in constructing and assembling the apparatus for these experiments; Dr. A. H. Gillieson, for spectro-photometric measurements; and Dr. J. B. Harding, for the design of the simple hodoscope circuit. We are grateful to Dr. T. E. Cranshaw and Mr. W. J. Whitehouse for

* In Fig. 4 the spectral distribution has been expressed in terms of the wavelength λ of the light, rather than the frequency.

VOL. 6 1955

helpful discussions on the work, and particularly to the last-named for calculations in connexion with the polarization experiment and criticism of this paper. We thank Dr. J. Rösch, Director of the Pic du Midi Observatory, and his staff for their hospitality and co-operation. Finally, we thank Dr. E. Bretscher for his continued interest in this work.

APPENDIX

Some Features of Čerenkov Radiation in the Atmosphere*

When a charged particle traverses a dielectric medium with a velocity βc greater than the phase velocity of light in the medium, Čerenkov radiation is emitted from all parts of the track, and at an angle θ with respect to the track, given by the Čerenkov relation

$$\cos\theta = \frac{1}{\beta n} \tag{2}$$

where n is the refractive index of the medium and β is the ratio of the velocity of the particle to that of light in vacuo. In the atmosphere at sea-level, $n = 1{\cdot}00029$ and the maximum value of θ (for an ultra-relativistic particle) is $1{\cdot}3°$. The threshold energy, for which $\theta = 0$, is 21 MeV for electrons. The contribution made to the light by mesons and nucleons is negligible in comparison with that made by electrons in the showers.

For a single ultra-relativistic particle traversing the atmosphere vertically, it can be shown in the following way that there is a maximum radius r_{max} to the pool of light on the ground.

Consider radiation emitted from an element, dh, of track at height h. In equation (2) put $\beta = 1$ and $n = (1 + \eta)$, where $\eta \ll 1$, then for small values of θ we find

$$\theta = (2\eta)^{1/2} \tag{3}$$

Since η is proportional to the density of air, it varies approximately exponentially with height

$$\eta = 2{\cdot}9 \times 10^{-4} e^{-h/\lambda} \tag{4}$$

where $\lambda \sim 7{\cdot}1$ km when h is measured in km. The radius of the Čerenkov cone at sea-level is $r = h\theta$, whence

$$r = (5{\cdot}8 \times 10^{-4})^{1/2}\, h e^{-h/2\lambda} \tag{5}$$

which has a maximum value when $h_{max} = 2\lambda$, i.e., when $h = 14$ km; $r_{max} = 126$ metres.

The atmospheric pressure at this height is about 140 g cm^{-2}, the value of η is about 4×10^{-5}, and the Čerenkov angle is about 9×10^{-3} radians.

The intensity I of Čerenkov radiation, falling in the annulus of radius r, can be found from the equation of Frank and Tamm (*loc. cit.*).

$$\frac{dW}{dh} = \frac{e^2}{c^2}\int_{\beta n>1}\left(1 - \frac{1}{\beta^2 n^2}\right)\omega\, d\omega \tag{6}$$

where $\dfrac{dW}{dh}$ is the energy radiated per unit path, e is the electronic charge, c the velocity of light in vacuo, and ω the angular frequency of the radiation. Neglecting dispersion, and using the same approximation as before, we have

$$\frac{dW}{dh} = 2\frac{e^2}{c^2}\eta\int_{\beta n>1}\omega\, d\omega \tag{7}$$

* We have just noticed a reference to a very recent paper on the theoretical aspects of Čerenkov radiation in the atmosphere, of interest to the present work, Goldanskii, V. I., and Zhdanov, G. B. (1954) *Zhur. Eksp. Teor. Fiz.* **26**, 4, p. 405.

Writing $I = dW/2\pi r\,dr$ and $dh = dr/\theta$, we have, from equations (3), (4), and (5):

$$I \alpha \frac{1}{r} e^{-h/h_{max}} \tag{8}$$

showing that the intensity from a single particle, travelling vertically, falls off slightly more rapidly than r^{-1} near the path of the particle.

In all experiments described, it should be noted that the effects of dispersion, refraction, and light absorption are negligible.

In the above analysis of the Čerenkov radiation in the atmosphere we have ignored multiple Coulomb scattering. In the absence of information on the energy spectrum of electrons in shower cores it is not possible to calculate the average scattering angles with any accuracy. However, it is important to realize that the angles of scattering may be comparable or even larger than the Čerenkov angle.

For instance, if we consider a vertical shower falling 10 m away from a light-receiver of aperture 60 cm, the Čerenkov light will be received from a portion of track of length 26 m at a height of 440 m. If now we assume an average electron energy of 10^8 eV, the r.m.s. angle of scatter over this same portion of track (ROSSI and GREISEN, 1941) will be $\sim 3°$, which is at least twice the Čerenkov angle.

REFERENCES

ASCOLI BALZANELLI, A., and ASCOLI, R.	1954	*Nuovo Cimento* XI, 562
BLACKETT, P. M. S.	1948	*Physical Society Gassiot Committee Report*, 34
ČERENKOV, P. A.	1934	*C.R. Acad. Sci. U.S.S.R.* **2**, 451
COCCONI, C., LOVERDO, A., and TONGIORGI, V.	1946	*Phys. Rev.* **70**, 846
FRANK, I., and TAMM, IG.	1937	*C.R. Acad. Sci. U.S.S.R.* **14**, 109
GALBRAITH, W., and JELLEY, J. V.	1953	*Nature* (London) **171**, 349
HEITLER, W.	1949	*Quantum Theory of Radiation*, Oxford University Press, 170
JELLEY, J. V., and GALBRAITH, W.	1953	*Phil. Mag.* **44**, 619
ROSSI, B., and GREISON, K.	1941	*Rev. Mod. Phys.* **13(4)**, 264

VOL. 6 1955

Journal of Atmospheric and Terrestrial Physics, 1955, Vol. 6, pp. 263 to 267. Pergamon Press Ltd., London

Radio observations of the aurora

N. C. GERSON
AF Cambridge Research Center, Air Research Development Command

(*Received* 20 *August* 1954)

ABSTRACT

A summary of observations made on the ionized aurora indicates that it occurred with greatest frequency during the equinoctial periods. The data were obtained mainly by means of radio-wave probings at 50 Mc/sec over North America.

It seems of interest to note for the record instances when aurorae were observed by radio-wave probings. During the period 1949–1951 an average of about 350 radio amateurs reported instances of long-range communication over North America (GERSON, 1951). Most of the data were obtained at a frequency of 50 Mc/sec. but a fair number of contacts at 144 Mc/sec were also reported. The average power transmitted by the amateurs was much less than 80 watts, but some employed the maximum allowed of 1 kW. Directive antennas were used on many occasions.

In their search for abnormal propagation conditions, the amateurs also reported cases where radio contact was made by means of auroral interaction. In this case the radio wave travels from the transmitter to the ionized aurora (which is not always associated with the luminous aurora) and returns to a receiver by refraction or scattering from the ionized volumes. Many instances of auroral interaction have been observed during daylight.

As is well known, radio waves returned from the aurora have several distinct peculiarities (MOORE, 1951). In most cases, the signals have a characteristic flutter typically described as "hissing," "rumbling," "garbling," etc. In some instances. the distortion of any type of signal modulation is so severe that no intelligence can be extracted from the signal. To establish radio contact under these circumstances, recourse must be made to CW. However, at other times the intensity of the reflected waves may be remarkably constant, allowing extensive use of radiotelephone. Analysis of the returned signals has indicated that they have fading rates of 50–200 cycles/sec (BOWLES, 1952). In order to obtain maximum signal intensities at the receiver site, it has been found that both transmitting and receiving antennas, if directive, should be pointed towards the ionized aurora. However, the brilliance of a visible display gives no indication of the VHF communication possibilities.

Table 1 lists the time and duration of auroral interaction observed over North America south of 50° N by the radio amateurs. The tabulation does not include several doubtful cases or instances where only one or two observers reported auroral activity for only a few minutes. The data are summarized in Fig. 1, which indicates the number of "days of occurrence" by months. In order to allow comparison with similar graphs made for visual aurora, a "day of occurrence" was considered to be the 24-hour interval beginning at 1200 noon EST. However, the graph would not be materially altered in form if the beginning of the 24-hour

Table 1. *Auroral interaction at* 50 *and* 144 *Mc/s**
(Noted by Es Observers)

Year	*Month*	*Day*	*Duration*		*Year*	*Month*	*Day*	*Duration*	
			Begin (EST)	*End (EST)*				*Begin (EST)*	*End (EST)*
1949	January	6	?	?	1949	November	2	1900	2319
		7	1945	—			12	1835	2220
		8	—	0011			19	1855	2045
		18	1952	2022					
		24	1915	2318	1950	February	20	1700	—
		25	1545	—			21	—	0101
		26	—	0008			23	1635	2209
	February	3	1910	2140		March	19	0740	1050
		4	2049	2119					
		21	1953	2315		April	1	1505	1735
							1	2130	2250
	March	6	?	?			2	1700	1800
		13	2020	2232			5	1646	2100
		21	1941	—			6	1830	1845
		22	—	0120			7	2330	2345
		22	2245	2309			23	2245	2350
							29	2140	2215
	April	7	1855	—			30	1429	1550
		8	—	0140					
		12	2320	2339		May	2	1720	2200
							4	1730	1930
	May	2	1950	2125			5	2017	2150
		3	1745	2235			27	1625	1840
		12	1910	2337			27	2115	—
		30	1715	2305			28	—	0130
							28	1006	1148
	June	4	1540	1842					
		4	2201	—		June	23	1640	2010
		5	—	0133			29	1800	—
		5	1518	1953			30	—	0052
		12	1542	2043					
						July	3	1830	2035
	August	2	2046	—			11	2044	2355
		3	—	0000			24	1737	2200
		3	2003	—					
		4	—	0105		August	7	1740	2333
							9	1705	1843
	September	7	1935	2010			18	1915	2319
		24	2130	2230			19	0630	1050
							19	1437	—
	October	6	2250	—			20	—	0048
		7	—	0045			20	0630	0700
		7	1850	2200					
		13	2040	2320					
		14	1704	2255		September	3	1732	1930
		15	1300	—			4	1750	1930
		16	—	0205			5	1700	2135
		21	1700	1825			17	1925	2200
		27	1740	2330			19	1710	1805
		28	1900(?)	?			23	1658	1725
		30	1100	1245			23	2035	2045

*NOTES

1. All doubtful observations have been omitted from the Table. The tabulation does not include cases where less than three radio contacts (involving six separate observers and made by means of reflections from the ionized aurora) were reported.

2. Separate listings on the same calendar day were made whenever no reports on the existence of an ionized aurora were received for a period of 150 minutes or longer.

VOL. 6 1955

Table 1—continued

Year	Month	Day	Duration		Year	Month	Day	Duration	
			Begin (EST)	*End (EST)*				*Begin (EST)*	*End (EST)*
1950	September	24	1600	2355	1951	April—*contd.*	5	1740	1938
		30	2207	—			6	1718	1925
							9	2023	2147
	October	1	—	0110			11	1823	2130
		2	1615	1825			12	1820	2225
		2	2200	2245			18	1755	2030
		3	2240	2350			20	1640	2012
		27	2200	2250			21	1844	—
		28	1330	1929			22	—	0003
		29	2004	2200			22	1515	1840
							24	1807	2139
	November	22	1750	1845			25	0009	0024
		24	1845	2345			25	1922	1952
	December	12	1640	1940		May	1	1537	2108
		13	1600	1955			2	1710	1948
		13	2128	2207			3	1905	2015
		14	1615	1715			9	1730	1805
		22	2000	2013			14	1845	2135
							15	1805	2125
1951	January	12	?	?			17	1648	2206
		31	2000	2109			26	1500	2230
	February	5	1730	—		June	14	1813	1855
		6	—	0022			17	1829	—
		11	2006	—			18	—	0025
		12	—	0025					
		22	1745	2246		July	1	1800	—
		23	0200	0315			2	—	0344
		23	1747	2105			2	1942	1955
		26	2033	—					
		27	—	0300		August	1	2046	2146
		27	2250	—			19	2315	2353
		28	—	0152			25	0100	0230
		28	2120	2200					
						September	11	2020	2327
	March	8	1700	2030			12	1845	1912
		8	2340	—			13	1745	1900
		9	—	0315			25	1630	—
		9	1730	—			26	—	0015
		10	—	0305			26	2110	2330
		13	1627	1925		October	16	2245	—
		14	1707	2340			17	—	0150
		22	1625	1918			25	1925	1940
		28	1758	1823			28	1400	1514
	April	2	1735	2205		November	13	1725	1830
		3	1757	2000					
		4	1825	2237		December	27	2215	2300

3. Auroral interaction was reported in the Southern Hemisphere on 10, 11, and 12 November 1950.
4. Two instances of auroral interaction were reported at 2310–2311 EST, 13 March 1951.
5. One instance of auroral interaction was reported at 2222 EST, 6 April 1951.
6. Scattered, non-verified reports on radio contacts by means of auroral propagation were received from 1830–2016 EST, 27 May 1951. However, in view of the strong Es which was present throughout this period, these reports are considered doubtful.
7. A noticeable decrease in reports of auroral interaction was reported from about 2200–2400 EST, 1 July 1951.

period were chosen differently. As would be expected, Fig. 1 is almost identical to similar curves prepared for the visual aurora.

Radar-wave probings of the aurora suffer from several limitations: they are very sensitive (a) to the aspect (or geometry) of transmitter-aurora-receiver; and (b) to the auroral forms present (CHAPMAN, 1952; CURRIE *et al.*, 1953). Generally, reflections are obtained from aurorae having rayed structure. A quiet arc, for example, may provide a weak reflection or possibly none at all. When an arc disintegrates into rays, the intensity of the reflected signal suddenly increases.

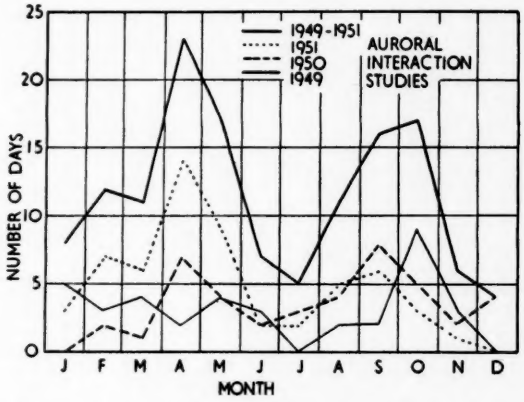

Fig. 1. Monthly variation in the occurrence of the ionized aurora.

While the restrictions imposed by geometry are severe in the one-dimensional radar case, they may be mitigated considerably when a network (two-dimensions) is utilized.

On some occasions, radio waves are reflected from the ionized aurora where no visible forms appear to be present, and vice versa. While it is possible for ionized auroral activity to exist independent of the visual aurora, it seems more probable that the accompanying visual or infrared emissions are so weak that they have not been observed. Reports indicate that the brightest aurora or the brightest portion of an aurora is not necessarily the best reflector or scatterer of radio waves. It is not known whether this condition arises because of geometry, or because the most intense ionization and excitation volumes are independent of each other.

Radio-wave probings of the aurora have some distinct advantages over visual or photographic observations. Data may be obtained irrespective of cloud or weather conditions. Some 50 Mc/sec reflections from the aurora have been observed during the afternoon, implying the existence of an ionized aurora during daylight. Unfortunately, however, present observations do not differentiate among the auroral forms present. Further, the obtainment of positive results with the essentially linear radar probings is very dependent upon the geometry at the time of observation. The latter objection may be removed if a transmitter-receiver network is utilized over a large area.

In spite of its limitation, the method provides an inexpensive tool which should be fully exploited in auroral investigations. Studies in the frequency

VOL. 6 1955

range 20–400 Mc/sec are desired, although, in general, the probability of obtaining reflections diminishes considerably as the frequency of the probing radio wave increases. A simple system would require only a receiver and directive antenna. The system would monitor existing VHF or television transmitters so located that signals would be received only when an aurora is present.

References

Bowles, K.	1952	*J. Geophys. Res.* **57,** 191
Chapman, S.	1952	*J. Atmosph. Terr. Phys.* **3,** 1
Currie, B. W., Forsyth, P. A., and Vawter, F. E.	1953	*J. Geophys. Res.* **58,** 179
Gerson, N. C.	1951a	*Nature* **167,** 804
	1951b	*Canad. J. Phys.* **29,** 251
Moore, R. K.	1951	*J. Geophys. Res.* **56,** 97

Journal of Atmospheric and Terrestrial Physics, 1955, Vol. 6, pp. 268 to 279. Pergamon Press Ltd., London

Ionospheric self-interaction of radio waves

F. H. HIBBERD
Department of Physics, The University of New England, Armidale, N.S.W., Australia

(*Received* 30 *August* 1954)

ABSTRACT

A theory is developed for the self-interaction of a modulated continuous wave in the ionosphere. In general, self-interaction will result in a reduction of modulation of a modulated wave and in the generation of harmonics of the original modulation frequency in its passage through the ionosphere. The effects should be greatest for a high-power, medium- to low-frequency wave with low modulation frequency. The magnitude of the demodulation appears to be sufficiently large to measure. It is possible to determine from it the electron collision frequency in the lower *E*-layer. Effects near the gyro-frequency have not been considered.

1. INTRODUCTION

Almost all previous investigations of ionospheric interaction have been concerned with the interaction of two waves. One wave (the disturbing wave) is such that it communicates an appreciable amount of energy to the ionospheric electrons. The disturbed region of the ionosphere is then examined by observing the effects produced on a second wave (the wanted wave) which passes through the disturbed region and there suffers some absorption. The wanted wave thus acts as a "sonde" to detect the effects produced by the disturbing wave. It will be seen that, provided the disturbing wave can be observed after its passage through the region it has disturbed, the desired information will be contained in the downcoming disturbing wave and this wave can thus take the roles of both wanted and disturbing wave. This effect has been called "self-interaction." Its existence was first predicted by V. A. BAILEY in 1935, and it is discussed very briefly by BAILEY and MARTYN (1935) and by BAILEY (1937a). The most detailed reference is in the last of these papers, and quoted in full is: "The sky-wave received from a powerful, long-waved station like Luxembourg or Droitwich appears to have its own modulation distorted in favour of the high notes, which is a distortion opposite to that occurring in the interaction of two waves. This self-distortion increases with the power and wavelength of the station, and should be greater when daytime exists at the region of ionospheric reflection than when night-time exists."

The possibility of the existence of self-interaction has been referred to since by several authors (RATCLIFFE and SHAW, 1948; SHAW, 1951) especially I. J. SHAW, but the only experimental evidence is that of M. CUTOLO (1951, 1952), who recently reported having observed self-interaction with a gyro-wave. While self-gyro-interaction is basically similar to the non-gyro case, its analysis is more complicated and requires a different approach. This problem is being studied separately and is not considered further in this paper. What follows is a detailed treatment of the self-interaction of a modulated continuous wave, excluding gyro-waves.

2. THE VARIATION OF THE ELECTRON COLLISION FREQUENCY

Throughout this paper when values of properties of electrons are mentioned these will refer to values averaged over a large number of electrons; the velocity distribution will not be considered in detail. We consider the time variation of the electron

VOL. 6 1955

collision frequency, at a point in the ionosphere, due to the passage of a modulated wave. The magnitude of the electric field at the point may be represented by $E = E_0(1 + M \cos \omega t) \cos pt$, where M is the modulation depth, ω is the modulation angular-frequency, and p is the wave angular-frequency. The following symbols are introduced:

$\bar{\nu}_0$—frequency of collision of an electron with gas molecules, in the undisturbed state; i.e., in the absence of an electric field.

ν—instantaneous value of the electron collision frequency, in the steady state, when a field is present.

$\bar{\nu}$—time-average of ν

$\bar{Q}_0$—kinetic energy of agitation of the electrons in the absence of a field.

Q—instantaneous value of the electron energy when a field is present.

$\bar{Q}$—time-average of Q.

In the absence of an electric field, the electrons in the ionosphere are continually losing and gaining energy in collisions with the gas molecules and are in dynamic equilibrium such that the net mean loss, and rate of loss, of energy by the electrons is zero. In this state the energy of agitation $\bar{Q}_0$ of the electrons is equal to that of the gas molecules. When an electric field (in this case a high-frequency field) is applied, the electrons acquire energy from the field. The increase in the electron energy increases the rate at which the electrons lose energy in collisions. In the steady state a new equilibrium is established in which the mean electron energy is greater than that of the gas molecules, and is such that the net mean rate of loss of energy by the electrons in collisions is equal to their rate of gain of energy from the field.

When the amplitude of the field is modulated at a low frequency, the energy of the electrons undergoes a periodic variation the fundamental frequency of which is equal to the modulation frequency. The absorption of energy from the field raises the average value of the electron energy from the undisturbed value $\bar{Q}_0$ to a new value $\bar{Q}$. The instantaneous electron energy Q fluctuates about $\bar{Q}$ with an amplitude that is less than $Q - \bar{Q}_0$, and that decreases with increasing frequency of modulation. Following BAILEY (1937b), we assume that, for electrons whose energies are only a few per cent greater than that of the gas molecules, the mean free path is independent of the electron energy. Then the electron collision frequency is proportional to the square root of the electron energy, and therefore the instantaneous value ν fluctuates about the new mean value $\bar{\nu}$. We proceed to calculate the amplitudes of the fluctuations of the electron energy and of the collision frequency.

If w_0 is the power communicated to an electron by an unmodulated field $E_0 \cos pt$, then the power w communicated by a modulated field $E = E_0(1 + M \cos \omega t) \cos pt$ is

$$w = w_0 (1 + M \cos \omega t)^2$$

$$= \bar{w} + 2w_0 \left(M \cos \omega t + \frac{M^2}{4} \cos 2\omega t \right)$$

where $\bar{w} = w_0 \left(1 + \frac{M^2}{2} \right)$ denotes the value of w averaged over a cycle of modulation.

When the ratio of the field to the gas pressure is small, so that $Q - \bar{Q}_0 \ll Q$, it is usually assumed that the loss of energy by an electron on collision with a gas molecule is proportional to the energy difference $Q - \bar{Q}_0$. We thus write the energy-loss per collision as $G(Q - \bar{Q}_0)$, where G is the constant of proportionality. The value of G has been determined in laboratory experiments, and the most recent measurement (CROMPTON *et al.*, 1953) for air gives $G = 0{\cdot}9 \times 10^{-3}$. The rate of loss of energy at any instant by an electron is therefore $G\nu(Q - \bar{Q}_0)$, and so, by the conservation of energy, we have

$$\frac{dQ}{dt} + G\nu(Q - \bar{Q}_0) = w$$
$$= \bar{w} + 2w_0\left(M\cos\omega t + \frac{M^2}{4}\cos 2\omega t\right) \tag{1}$$

The mean value $\bar{Q}$, about which Q fluctuates according to (1), is the value that would be maintained by an unmodulated field communicating mean power $\bar{w}$ to each electron, and so

$$G\bar{\nu}(\bar{Q} - \bar{Q}_0) = \bar{w} \tag{2}$$

Subtracting (2) from (1), and writing $\frac{d}{dt}(Q - \bar{Q})$ for $\frac{dQ}{dt}$, we get

$$\frac{d}{dt}(Q - \bar{Q}) + G\nu(Q - \bar{Q}_0) - G\bar{\nu}(\bar{Q} - \bar{Q}_0) = 2w_0\left(M\cos\omega t + \frac{M^2}{4}\cos 2\omega t\right) \tag{3}$$

Since
$$\nu^2/\bar{\nu}^2 = Q/\bar{Q}, \tag{4}$$

we may derive from (3) equations with either ν or Q as sole dependent variable, and the solutions would give ν, or Q, as a function of time. The solution of the resulting equations is not simple.

An approximate solution to (3), applicable if $\omega/2\pi$ is greater than about 200 c.p.s., can be obtained if in (3) we replace ν by $\bar{\nu}$. Equation (3) then becomes

$$\frac{d}{dt}(Q - \bar{Q}) + G\bar{\nu}(Q - \bar{Q}) = 2w_0\left(M\cos\omega t + \frac{M^2}{4}\cos 2\omega t\right)$$

and its steady-state solution is

$$Q = \bar{Q}[1 + 2m_1\cos(\omega t - \phi_1) + 2m_2\cos(2\omega t - \phi_2)] \tag{5}$$

where
$$m_1 = \frac{w_0 M}{\bar{Q}[(G\bar{\nu})^2 + \omega^2]^{1/2}},\quad m_2 = \frac{w_0 M^2}{4\bar{Q}[(G\bar{\nu})^2 + 4\omega^2]^{1/2}} \tag{6}$$

and
$$\tan\phi_1 = \omega/G\bar{\nu},\ \tan\phi_2 = 2\omega/G\bar{\nu} \tag{7}$$

From the relations (4) and (5), and the fact that m_1 and m_2 are small compared with unity, we get

$$\nu = \bar{\nu}[1 + m_1\cos(\omega t - \phi_1) + m_2\cos(2\omega t - \phi_2)] \tag{8}$$

Equation (8) gives the variation with time of the electron collision frequency at

VOL. 6 1955

a point in the ionosphere due to the passage of a modulated wave. This result is essentially that given in the original theory of wave-interaction.*

3. Ionospheric Self-demodulation of a Modulated Wave

The absorption coefficient k for a wave in an ionized medium is a function of the electron collision frequency. A powerful sinusoidally modulated wave produces the periodic variation of ν described by equation (8). Thus in general it will also produce a periodic variation of the absorption coefficient. Qualitatively we therefore expect the following to take place: When k increases with ν, then maxima in the absorption will occur in the same quadrant as maxima in the wave-envelope amplitude. The maxima of the wave will be absorbed more strongly than the minima, resulting in a partial demodulation (i.e., reduction of modulation) of the wave. The phase difference between the absorption variation and the amplitude variation will increase from zero to $\pi/2$ with increasing modulation frequency.

To examine the matter in detail we shall consider the collision frequency fluctuating about a mean value $\bar{\nu}$, and correspondingly the absorption coefficient fluctuating about a mean value $\bar{k}$. The instantaneous value of k is given by

$$k = \bar{k} + \frac{\partial k}{\partial \nu} \Delta\nu$$

where $\Delta\nu$ is the instantaneous value of the fluctuation of ν and is given by (8). That is

$$\Delta\nu = \nu - \bar{\nu} = \bar{\nu}[m_1 \cos(\omega t - \phi_1) + m_2 \cos(2\omega t - \phi_2)]$$

and therefore

$$k = \bar{k} + \frac{\partial k}{\partial \nu} \bar{\nu}[m_1 \cos(\omega t - \phi_1) + m_2 \cos(2\omega t - \phi_2)] \tag{9}$$

We consider a single ray-path of a modulated wave in the ionosphere. The amplitude of the electric vector of the wave on entering the ionosphere will be represented by $E = E_0(1 + M \cos \omega t)$. It will be attenuated by absorption by the factor $\exp\{-\eta\}$, where $\eta = \int_0^s \bar{k}\, ds$ and s is the length of the trajectory in the ionosphere. It will also be attenuated with distance by a factor such as $1/s$. So the amplitude on emergence may be represented by

$$E' = E_0(1/s)(1 + M \cos \omega t) \exp\{-\eta\} \tag{10}$$

By (9) the total absorption η becomes

$$\eta = \bar{\eta} + \int_0^s \frac{\partial k}{\partial \nu} \bar{\nu}[m_1 \cos(\omega t - \phi_1) + m_2 \cos(2\omega t - \phi_2)]\, ds$$

where $\bar{\eta} = \int_0^s \bar{k}\, ds.$

* L. G. H. Huxley (1953) has recently proposed an alternative theory of interaction based on assumptions different from those above. Further ionospheric and other experiments are obviously needed to decide between the two theories. In this paper the original theory has been adopted, but this adoption is not intended to indicate any marked preference by the author for this theory over Huxley's alternative. It would not be difficult to modify the following so as to make it conform with the alternative theory.

The attenuation factor, $\exp\{-\eta\}$, thus becomes

$$\exp\{-\eta\} = \exp\{-\bar{\eta}\} \exp\left\{-\int_0^s \frac{\partial k}{\partial \nu} \bar{\nu} m_1 \cos(\omega t - \phi_1)\, ds\right\}$$
$$\exp\left\{-\int_0^s \frac{\partial k}{\partial \nu} \bar{\nu} m_2 \cos(2\omega t - \phi_2)\, ds\right\} \qquad (11)$$

In general $\frac{\partial k}{\partial \nu}$, $\bar{\nu}$, the m's, and the ϕ's will vary along the path. The collision frequency does not decrease very rapidly with altitude. If it be assumed that the wave does not penetrate the ionosphere (lower E-layer) more than a few kilometres, or alternatively that the major part of the absorption and self-interaction occurs within a horizontal layer only a few kilometres thick, then an average value $\bar{\nu}$ may be assigned with small error to the collision frequency in this thin layer. Such an assumption makes $\bar{\nu}$ independent of s, and by (7) we see that ϕ_1 and ϕ_2 do not vary along the path. Thus equation (11) becomes

$$\exp\{-\eta\} = \exp\{-\bar{\eta}\} \exp\left\{-\int_0^s \frac{\partial k}{\partial \nu} \bar{\nu} m_1\, ds \cos(\omega t - \phi_1)\right\}$$
$$\exp\left\{-\int_0^s \frac{\partial k}{\partial \nu} \bar{\nu} m_2\, ds \cos(2\omega t - \phi_2)\right\} \qquad (12)$$

We shall now briefly examine the quantity $\int_0^s \frac{\partial k}{\partial \nu} \nu\, ds$. If the effect of the terrestrial magnetic field is neglected we may write as a reasonable approximation for most propagation conditions:

$$k = \frac{B\nu}{p^2 + \nu^2}, \text{ where } B \text{ is independent of } \nu.$$

Then
$$\frac{\partial k}{\partial \nu} = \frac{B(p^2 - \nu^2)}{(p^2 + \nu^2)^2} = \frac{k(p^2 - \nu^2)}{\nu(p^2 + \nu^2)}$$

When $p^2 \gg \nu^2$, as is commonly the case, this reduces to

$$\frac{\partial k}{\partial \nu} = \frac{k}{\nu}, \text{ giving } \frac{\partial k}{\partial \nu} \nu = k$$

and so
$$\int_0^s \frac{\partial k}{\partial \nu} \nu\, ds = \int_0^s k\, ds = \eta$$

When $p^2 \ll \nu^2$ we obtain

$$\frac{\partial k}{\partial \nu} = -\frac{k}{\nu}, \text{ giving } \frac{\partial k}{\partial \nu} \nu = -k$$

and so
$$\int_0^s \frac{\partial k}{\partial \nu} \nu\, ds = -n$$

Thus $\int_0^s \frac{\partial k}{\partial \nu} \nu\, ds$ lies between $+\eta$ and $-\eta$, passing through the value zero when $\nu = p$.

VOL. 6 1955

These conclusions will not be greatly modified by the presence of the magnetic field, except perhaps when p lies near the gyro-frequency of the electrons.

We shall be interested in observing waves after reflection in the E-layer, and the frequencies of such waves will lie in the low- to medium-frequency radio bands. For these waves the magnitude of η is of the order of unity or smaller. Further, studies of the interaction of two waves have shown that the m's (i.e., the relative amplitudes of oscillation of the electron collision frequency caused by the passage of a modulated wave) do not, in general, exceed several per cent. These two facts lead to the result

$$\int_0^s m \frac{\partial k}{\partial \nu} \bar{\nu}\, ds \ll 1 \tag{13}$$

The last two exponentials on the right-hand side of (12) may thus be expanded and terms involving powers of small quantities higher than the first may be neglected. To a first approximation the second harmonic may also be disregarded. (The inclusion of the second harmonic is dealt with in Section 7 below.) This expansion yields

$$\exp\{-\eta\} = \exp\{-\bar{\eta}\}\left[1 - \int_0^s m_1 \frac{\partial k}{\partial \nu} \bar{\nu}\, ds \cos(\omega t - \phi_1)\right] \tag{14}$$

$$= \exp\{-\bar{\eta}\}[1 - A \cos(\omega t - \phi_1)] \tag{15}$$

in which is put, for brevity, $A = \int_0^s m_1 \frac{\partial k}{\partial \nu} \bar{\nu}\, ds$ (16)

Equation (10), which gives the amplitude of the wave on emergence from the ionosphere, then becomes

$$E' = E_0'(1 + M \cos \omega t)[1 - A \cos(\omega t - \phi_1)] \tag{17}$$

where $$E_0' = E_0(1/s) \exp\{-\bar{\eta}\}.$$

On multiplying out and rearranging, (17) yields

$$E' = E_0'[1 - (MA/2) \cos \phi_1 + \{(M - A \cos \phi_1)^2 + (A \sin \phi_1)^2\}^{1/2} \cos(\omega t + \Phi_1) - (MA/2) \cos(2\omega t - \phi_1)] \tag{18}$$

where $$\tan \Phi_1 = A \sin \phi_1/(M - A \cos \phi_1).$$

Neglecting the small amount of second harmonic, (18) represents the field of a modulated wave of frequency ω with modulation depth M' given by

$$M' = [(M - A \cos \phi_1)^2 + (A \sin \phi_1)^2]^{1/2}/[1 - (MA/2) \cos \phi_1]$$

$$= M[1 - (2A/M) \cos \phi_1 + (A/M)^2]^{1/2}/[1 - (MA/2) \cos \phi_1]$$

Since $A \ll 1$, $M < 1$, and $|\cos \phi_1| \leq 1$,

$$M' \fallingdotseq M[1 - (A/M) \cos \phi_1][1 + (MA/2) \cos \phi_1|$$

$$\fallingdotseq M[1 - (A/M)(1 - M^2/2) \cos \phi_1]$$

or $$(M - M')/M = (A/M)(1 - M^2/2) \cos \phi_1 \tag{19}$$

On substituting from (16) and (6) for A and m_1, and from (7) for $\cos \phi_1$, this becomes

$$(M - M')/M = (1 - M^2/2) \frac{G\bar{\nu}}{(G\bar{\nu})^2 + \omega^2} \int_0^s (w_0/\bar{Q}) \frac{\partial k}{\partial \nu} \bar{\nu} \, ds \qquad (20)$$

This gives the factor by which the depth of modulation, of frequency ω, is reduced from M to M' by self-interaction, if one considers only the effect produced in the ionosphere by the single ray that is observed.

4. The Multiplicity of Rays

In general one does not have solely a single ray passing through an ionized region and there interacting with itself. The whole ionospheric region traversed by the

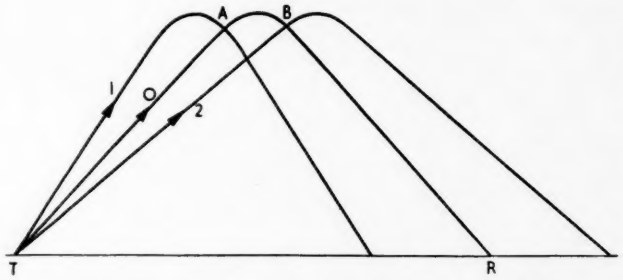

Fig. 1. The ray 0 from the transmitter T is observed at the receiver R, after reflection in the ionosphere. A portion of 0, such as AB, lies in the ionosphere, and this ionospheric region receives energy from the ray 0 and also from rays such as 1 and 2.

received ray is disturbed by a diverging beam from the transmitter, there will be magneto-ionic splitting, and there may be multiple reflections.

To discuss the effect of the diverging beam we refer to Fig 1, in which T denotes the position of the transmitter and R that of the receiver.

Suppose 0 represents the ray that is observed at the receiver R. The ionospheric region through which the ray 0 passes has its electron energy increased not only by this ray but also by those such as the "direct" ray 2 or the "reflected" ray 1. The phases of the energy-effects produced by each of these at any given point on AB will be different. Nevertheless, provided that the transit times between T and a point on AB, by any path, differ by an amount very much less than the period $2\pi/\omega$ of the modulation, the phase differences in the individual energy-effects will be negligibly small. It is obvious that under these conditions the phase of the modulation, and therefore of the energy variation, will be practically the same over the whole of the path AB. Thus we may regard the electron energy of the region about AB as undergoing a periodic variation as a whole, with the same phase at every point.

The same conclusion holds when we consider the ordinary and extraordinary components into which the wave divides on entering the ionosphere, for the relative retardation between the components in travelling a distance of the order of the length of AB is very much less than the modulation period.

VOL. 6 1955

We shall examine now the manner in which equation (20) must be modified to include the effects of all the rays. The integral $\int_0^s (w_0/\bar{Q}) \frac{\partial k}{\partial \nu} \bar{\nu}\, ds$ in equation (20) takes account of the power expended on the electrons lying along the trajectory of the observed ray, by the field of the observed ray alone. It is now seen that these electrons also receive energy from other rays that intersect this trajectory. Excluding the case of vertical incidence and assuming that there is no penetration of the layer, it can easily be seen that in a stratified layer, with a transmitter on the ground regarded as a point source, every point in the layer that is traversed by rays is traversed by two, and only two, rays from the transmitter. In Fig. 1 the ray 0 from the transmitter at T is the ray that is observed at R. Rays 1 and 2 are two of the rays within the diverging cone from T that pass through quasi-symmetrical points A and B about the apex of the trajectory of the ray 0. The field of ray 1 at A will be approximately equal to that of ray 0 at B. The field of ray 2 at B will be approximately equal to that of ray 0 at A. Similar statements hold for all pairs of corresponding points of the trajectory of the observed ray 0 that lie within the layer. The work done on electrons along the path of the ray 0, in the layer, by all of the rays is therefore approximately equal (except for effects arising from the geometrical asymmetry associated with oblique incidence) to the work that would be done by the observed ray passing from left to right plus an identical ray passing from right to left along the same path.* Thus, to take account of the effects of all of the rays within the diverging beam from the transmitter, it is necessary to multiply the right-hand side of equation (20) by a factor approximately equal to 2, and this yields

$$\frac{M - M'}{M} = (2 - M^2) \frac{G\bar{\nu}}{[(G\bar{\nu})^2 + \omega^2]} \int_0^s (w_0/\bar{Q}) \frac{\partial k}{\partial \nu} \bar{\nu}\, ds \qquad (21)$$

When multiple reflections also occur, the situation becomes far too complicated for quantitative analysis. First, interference at the receiver between two or more rays would render modulation measurements almost meaningless. Secondly, the region where the second ionospheric reflection of a twice-reflected ray occurs will also be disturbed by the direct ray from the transmitter. At this region there will be an appreciable modulation phase difference between the reflected and the direct ray. That is, the observed downcoming ray will have undergone interaction in a region which has been disturbed by a ray whose modulation is there appreciably out of phase with that of the observed ray.

Briefly, then, interpretable observations are possible only when a once-reflected sky-wave alone is received. Also it is necessary that the ground-wave be absent or that, if present, it be suppressed.

---

* Strictly, one should consider the resultant field at each point. The directions and phases of the two fields (belonging to ray 0 and to the other ray intersecting it), at a point on ray 0, will be different. But since the equivalent path differences (measured from the transmitter) between the ray 0 and the intersecting ray vary relatively rapidly as one passes along 0, the average power communicated by the resultant field may be taken as the sum of the powers that would be communicated by the individual fields acting separately.

5. Determination of the Collision Frequency

Let us suppose that observations are made successively on two similar waves modulated to the same depth M but at different modulation frequencies ω_a and ω_b respectively. We shall denote the respective resultant modulation depths by M'_a and M'_b. It is clear from equation (21) that we should then have

$$\frac{M - M'_a}{M - M'_b} = \frac{(G\bar{\nu})^2 + \omega_b^2}{(G\bar{\nu})^2 + \omega_a^2} \tag{22}$$

From this, $G\bar{\nu}$ can be obtained and, since G is known, it is possible to determine $\bar{\nu}$.

6. The Magnitude of the Effect

The magnitude of the demodulation to be expected as a result of self-interaction may be estimated by means of equation (21). Without assigning a structure to the ionospheric layer, it is not possible to evaluate the integral $\int_0^s (w_0/\bar{Q}) \frac{\partial k}{\partial \nu} \bar{\nu}\, ds$ occurring on the right-hand side of this equation. The limits within which its value must lie may, however, be determined by the use of the mean value theorem of the integral calculus, viz.:

$$\int_a^b f(x)\phi(x)\, dx = f(\xi) \int_a^b \phi(x)\, dx$$

where ξ lies between a and b. From this it follows that

$$\left[\frac{w_0}{\bar{Q}}\right]_{s=0} \int_0^s \frac{\partial k}{\partial \nu} \bar{\nu}\, ds \geq \int_0^s (w_0/\bar{Q}) \frac{\partial k}{\partial \nu} \bar{\nu}\, ds \geq \left[\frac{w_0}{\bar{Q}}\right]_{s=s} \int_0^s \frac{\partial k}{\partial \nu} \bar{\nu}\, ds$$

In particular, when $p^2 \gg \nu^2$ so that $\int_0^s \frac{\partial k}{\partial \nu} \bar{\nu}\, ds = \bar{\eta}$, we have

$$\left[\frac{w_0}{\bar{Q}}\right]_{s=0} \bar{\eta} \geq \int_0^s (w_0/\bar{Q}) \frac{\partial k}{\partial \nu} \bar{\nu}\, ds \geq \left[\frac{w_0}{\bar{Q}}\right]_{s=s} \bar{\eta} \tag{23}$$

To calculate the order of magnitude of the demodulation to be expected we shall consider a transmitter radiating 100 kW on a frequency of 500 kc/s from a vertical quarter-wave aerial over a conducting ground. Let us suppose that observations are made at a point 400 km from the transmitter. Then the peak-value E_0 of the field at the end of a radius vector of length r making an angle θ with the vertical is given by

$$E_0 = \frac{14{\cdot}04\ P^{1/2} \cos\left(\frac{\pi}{2} \cos\theta\right)}{r \sin\theta} \qquad \text{(M.K.S. units)}$$

where P is the power radiated. For the above example this yields for the field at a height of 90 km, midway between transmitter and receiver, the value

$$E_0 = 1{\cdot}77 \times 10^{-2} \text{ volts per metre.}$$

From a result deduced by Bailey (1937c) on the motion of electrons in gases

VOL. 6 1955

it may be easily shown, for $p^2 \gg \nu^2$, and p somewhat removed from the gyrofrequency, that the mean power w_0 expended on the electrons by an alternating field of amplitude E_0 is given approximately by

$$w_0 = \frac{e^2 \nu E_0^2}{2mp^2} \tag{24}$$

Taking $\nu \sim 1 \times 10^6$, we obtain for w_0, due to the transmitter postulated above, the value $w_0 = 4{\cdot}5 \times 10^{-12}$ ergs per sec. This is the value of w_0 corresponding to $s = 0$, i.e., at the point of entry of the wave in the E-layer. Also we have, approximately, that

$$[w_0]_{s=s} = [w_0]_{s=0} \exp(-2\bar{\eta}) = 0{\cdot}14\,[w_0]_{s=0}$$

since a typical value for $\bar{\eta}$ here would be unity (MARTYN, 1935). Further, if it be assumed that the electron energy is not raised far above its undisturbed value, we may take $\bar{Q}$ as approximately equal to $\bar{Q}_0$. Corresponding to a gas temperature of 200°K, $\bar{Q}_0$ may be assigned the value $4{\cdot}0 \times 10^{-14}$ ergs. Therefore by (23) the value of the integral $\int_0^s (w_0/\bar{Q}) \dfrac{\partial k}{\partial \nu} \bar{\nu}\, ds$ in equation (21) must lie between 110 $\sec^{-1}$ and 15 $\sec^{-1}$.

Let us suppose now that the transmitted wave is originally modulated at a low modulation frequency to a depth of 80 per cent, i.e., $M = 0{\cdot}80$. If we take $G\bar{\nu} \fallingdotseq 10^3$ we then find that the value of the right-hand side of (21) will lie between 0·15 and 0·02. That is, M' lies between 68 and 78 per cent. Thus the decrease in the modulation depth may be large enough to be detected and measured.

7. The Generation of Harmonics of the Modulation Frequency

In the expansion of equation (12) in Section 3, the second harmonic term was disregarded, since its amplitude is much less than that of the fundamental. We shall now include this term and see that as a result both second and third (but no other) harmonics are generated by self-interaction. (This is to be contrasted with the effect occurring in the interaction of two waves, where only the second harmonic is generated and appears in the transferred modulation.) We write equation (12) as

$$\exp\{-\eta\} = \exp\{-\bar{\eta}\} \exp\{-A_1 \cos(\omega t - \phi_1)\} \exp\{-A_2 \cos(2\omega t - \phi_2)\}, \tag{12a}$$

in which for brevity we have written

$$A_1 = \int_0^s m_1 \frac{\partial k}{\partial \nu} \bar{\nu}\, ds \quad \text{and} \quad A_2 = \int_0^s m_2 \frac{\partial k}{\partial \nu} \bar{\nu}\, ds$$

On expanding the two cosine exponential terms on the right, we get

$$\exp\{-\eta\} = \exp\{-\bar{\eta}\}[1 - A_1 \cos(\omega t - \phi_1) - A_2 \cos(2\omega t - \phi_2)]$$

wherein terms containing products, squares, and higher powers of the A's have been neglected, since both A_1 and A_2 are $\ll 1$.

The complete term, corresponding to the right-hand side of equation (17), for the resulting modulation is now

$$[1 + M \cos \omega t][1 - A_1 \cos (\omega t - \phi_1) - A_2 \cos (2\omega t - \phi_2)]$$

This is equal to

$$1 + M \cos \omega t - A_1 \cos (\omega t - \phi_1) - A_2 \cos (2\omega t - \phi_2) - MA_1 \cos \omega t \cos (\omega t - \phi_1) - MA_2 \cos \omega t \cos (2\omega t - \phi_2)$$

which becomes

$$1 + M \cos \omega t - A_1 \cos (\omega t - \phi_1) - A_2 \cos (2\omega t - \phi_2) - (MA_1/2)[\cos \phi_1 + \cos (2\omega t - \phi_1)] - (MA_2/2)[\cos (\omega t - \phi_2) + \cos (3\omega t - \phi_2)]$$

The constant part of this is

$$1 - (MA_1/2) \cos \phi_1 \tag{25}$$

The terms containing the fundamental of the modulation frequency are

$$M \cos \omega t - A_1 \cos (\omega t - \phi_1) - (MA_2/2) \cos (\omega t - \phi_2) \tag{26}$$

The terms containing the second harmonic are

$$-A_2 \cos (2\omega t - \phi_2) - (MA_1/2) \cos (2\omega t - \phi_1) \tag{27}$$

and for the third harmonic

$$-(MA_2/2) \cos (3\omega t - \phi_2). \tag{28}$$

The resulting modulation depth of the fundamental tone is calculated from the ratio of (26) to (25), which is

$$\frac{M \cos \omega t - A_1 \cos (\omega t - \phi_1) - (MA_2/2) \cos (\omega t - \phi_2)}{1 - (MA_1/2) \cos \phi_1}$$

This may obviously be written in the form $M'' \cos (\omega t - \alpha)$ if desired, giving the more accurate new modulation depth M'' that, for greater accuracy, should replace the M' of equation (19). It may, however, easily be shown that M' differs but little from M'' and for most purposes equation (19) is sufficiently accurate.

Second and third harmonic modulation tones appear with small amplitudes. These may be calculated from (27,) (28), and (25). It would probably be difficult to eliminate harmonic tones completely from the emitted modulation. If it can be established experimentally, however, that the modulation of the received wave is relatively richer in these harmonics, this would be good evidence for the occurrence of self-interaction.

VOL. 6 1955

8. Conclusions

The principal effects of self-interaction are:

(i) A relatively small demodulation of powerful modulated waves that are reflected in the E-layer. The demodulation is directly proportional to the power emitted. Within the medium- and low-frequency broadcast bands it should increase as the wave frequency decreases, except in the vicinity of $p \sim \nu$, where it will approach zero. (Since the magnetic field has been ignored, no statement can be made concerning effects at the gyro-frequency.) It decreases as the modulation frequency increases.

(ii) Second and third harmonics of the original modulation frequency are generated with small amplitude.

Acknowledgments—The author desires to thank Dr. M. Cutolo of the University of Naples for first interesting him in the study, Dr. K. Landecker of the University of Sydney for the benefit of many valuable discussions, and his colleague Mr. R. A. Smith for helpful criticism.

References

Bailey, V. A.	1935	*World Radio*, 25th Jan.
	1937a	*Wireless World*, 224–226
	1937b	*Phil. Mag.* **23**, 929–959
	1937c	*Phil. Mag.* **23**, 774–791
Bailey, V. A., and Martyn, D. F.	1935	*Wireless Engineer*, March
Cutolo, M.	1951	*Nature* **167**, 314–315
	1952	*Il Nuovo Cimento* **IX**, 687–698
Crompton, R. W., Huxley, L. G. H., and Sutton, D. J.	1953	*Proc. Roy. Soc.* **A218**, 507–519
Huxley, L. G. H.	1953	*Proc. Roy. Soc.* **A218**, 520–536
Martyn, D. F.	1935	*Proc. Phys. Soc.* **47**, 323–339
Ratcliffe, J. A., and Shaw, I. J.	1948	*Proc. Roy. Soc.* **A193**, 311–343
Shaw, I. J.	1951	*Wireless Engineer* **28**, 335–342

RESEARCH NOTES

A note on factors affecting the interpretation of observations of transient echoes from the ionosphere

(*Received* 27 *January* 1955)

It is well known that when high-powered radars are operated at frequencies of tens of megacylces, short-lived echoes are often returned from scattering centres in a region just below 100 km above the earth. The diurnal and seasonal variations in the occurrence of these echoes have been studied in some detail (APPLETON and NAISMITH, 1947; EASTWOOD and MERCER, 1948), and it has been found that the scattering centres are most likely patches of ionization caused by meteors, although a pronounced midday maximum in the rate of occurrence has not been satisfactorily explained.

We wish firstly to draw attention to the important effect of variations in the intensity of cosmic radio noise on the observed rate of occurrence of these transient echoes. EASTWOOD and MERCER showed that the echo-rate is proportional to the square root of the transmitter power, and hence the echo-rate will be proportional to the square root of the power sensitivity of the receiving equipment. This sensitivity is set by the noise level and, at frequencies in the range about 10 or 20 Mc/s to 100 Mc/s, cosmic noise usually far outweighs atmospherics and receiver noise as the most important factor controlling the sensitivity. Therefore at frequencies in this range it follows that, even if the rate of appearance of the scattering centres were constant, the echo-rate will be inversely proportional to the square root of the cosmic-noise intensity. Even with only a simple dipole receiving aerial, the cosmic-noise power changes by a factor greater than 2 in the course of a sidereal day (HERBSTREIT and JOHLER, 1948). As the directivity of the aerial is increased, the ratio of maximum to minimum noise increases, and in addition, at frequencies of about 20 Mc/s, increases in ionospheric attenuation may either increase or decrease this ratio, especially if the aerial is directed at a low angle of elevation.

In 1947 a short series of observations was made in this laboratory, using a 100-kw pulsed transmitter operating at 18·3 Mc/s in conjunction with a sensitive receiver and an aerial of moderate directivity, the aerial beam being directed vertically. The average diurnal variation of the rate of occurrence of the transient echoes observed over a period of a few weeks in April and May 1947 is shown by the full line in Fig. 1. The general shape is very similar to curves reported previously. The peak at 0500 hour agrees well with the maximum in the rate of occurrence of sporadic meteors, but the large midday peak was rather puzzling. However, for the particular receiving aerial used and for the ionospheric conditions during the experiment, it is now known (SHAIN, 1951) that the cosmic-noise power received at the earth during midday hours was only about one-tenth of the noise power received at 0600 hour. The observed echo-rates have been adjusted to allow for the cosmic-noise variations, taking 0600 hour as standard, and when plotted as crosses in Fig. 1 it is seen that the midday maximum has been eliminated. Similar corrections to the echo-rates appear to be necessary in the case of the results reported by EASTWOOD and MERCER. Care must also be taken in the determination of meteor-stream radiants by any method which involves measurements of the rate of occurrence of echoes.

It should be possible to use this effect to set either an upper or a lower limit to the height at which increased absorption occurs during sudden ionospheric disturbances. EASTWOOD and MERCER have shown that the transient echoes occur within a narrow region at a height of about 86 km. Let the echo-rate in the absence of excess absorption be n echoes per minute, and let the excess absorption be such that the intensity of radiation passing once through the absorbing region is reduced to a times its usual value. If the S.I.D. absorption occurs above the region in which the transient ionization is formed, the received echoes will

VOL. 6 1955

be unattenuated, but cosmic noise will be reduced to a times its usual intensity. The observed echo-rate will then increase to $na^{-1/2}$ echoes per minute. On the other hand, if the absorption is below the transient echo region, cosmic noise will be reduced as before, but the echo intensity will be a^2 times the unattenuated value. In this case the observed echo-rate will decrease to $na^{1/2}$ echoes per minute. It is possible that during an S.I.D. the echo-rate will be affected directly by the disturbed solar conditions, but a detailed comparison of the echo-rate and cosmic-noise intensity should show whether ionospheric absorption alone is

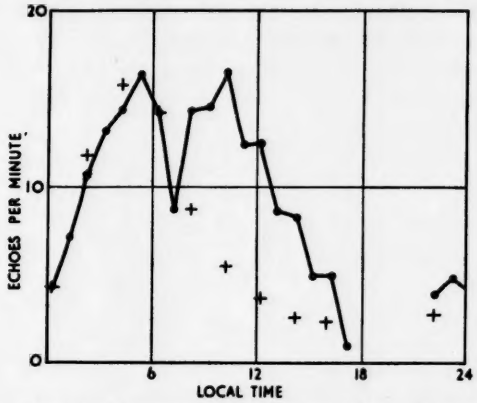

Fig. 1. Diurnal variation of rate of occurrence of transient echoes. The points connected by the full line show the rates observed. The crosses show rates which would have been observed if the cosmic-noise intensity had been constant (rate at 0600 hour taken as standard).

varying the echo-rate and, if so, whether the absorption is above or below the region in which the transient ionization occurs. There are indications from our own observations that the echo-rate increased during a few S.I.D.'s. This would imply a comparatively high absorbing region, but the observations were not sufficiently detailed to be conclusive.

The observations referred to above also drew attention to an apparent marked grouping of the echoes in time. Recently ISTED (1954) has reported the occurrence of multiple bursts, having an apparent regular time separation of the order of seconds, in records of the field strengths of distant transmitters operating in the range of frequencies 30 Mc/s to 100 Mc/s. Such apparent multiple bursts were also noticed in our own observations at 18·3 Mc/s, but it was found, by comparison with the theory of MARSDEN and BARRATT (1911), that the distribution in time of our echoes was consistent with a hypothesis that the echoes occurred at random times. The apparent grouping is due to the more frequent occurrence of short, rather than long, intervals between echoes. By a simple extension of MARSDEN and BARRATT's theory it can be shown that if the mean interval between events occurring at random is 3 seconds and the accuracy of timing $\pm 0{\cdot}1$ second, there should, on the average, be one "group" of three equally-spaced events every 1·5 minutes. It is not clear from the data given by ISTED whether or not his apparent grouping of bursts is statistically significant. A statistical analysis of the observations would be desirable, in view of his interesting suggestion with regard to the physical cause of the transient echoes.

Division of Radiophysics, C.S.I.R.O.
Sydney, Australia.

C. A. SHAIN
F. J. KERR

REFERENCES

APPLETON, E. V., and NAISMITH, R.	1947	*Proc. Phys. Soc.* **59,** 461
EASTWOOD, E., and MERCER, K. A.	1948	*Proc. Phys. Soc.* **61,** 122
HERBSTREIT, J. W., and JOHLER, J. R.	1948	*Nature* **161,** 515
ISTED, G. A.	1954	*Marconi Review* **17,** 37
MARSDEN, E., and BARRATT, T.	1911	*Proc. Phys. Soc.* **23,** 367
SHAIN, C. A.	1951	*Aust. J. Sci. Res.* **A4,** 258

Solar prominences and geomagnetic disturbance*

(*Received* 28 *December* 1954)

Identification of the hypothetical M-regions of the sun earlier postulated (BARTELS, 1932) to explain 27-day recurrent geomagnetic storms, has eluded astronomers for many years. ALLEN (1944) concluded that M-regions, which are most evident in years preceding minimum solar activity, coincide with undisturbed areas of the solar surface. BRUZEK (1952) and BELL and GLAZER (1954) showed that geomagnetic disturbances are, on the average, more severe when pronounced minima of the emission corona are three days of solar rotation, or about 40° of longitude, past central meridian of the sun. PECKER and ROBERTS (1955)

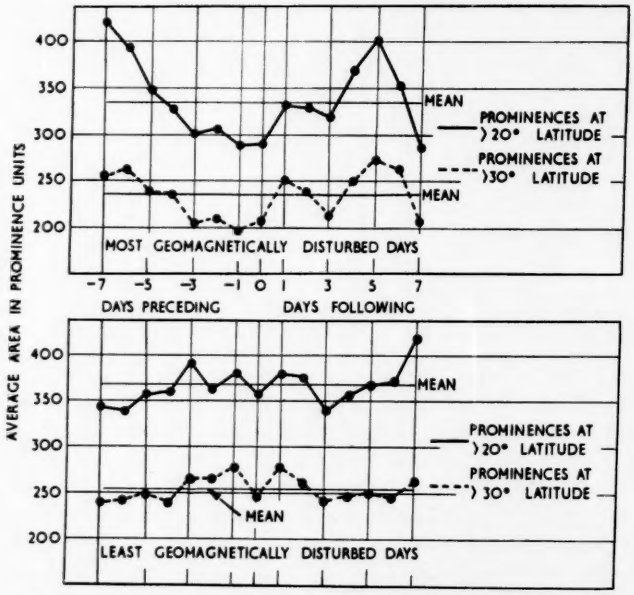

Fig. 1. Above: Course of average prominence on days preceding and following zero days representing the five most geomagnetically disturbed days in each month.
Below: Same for zero days representing the five least geomagnetically disturbed days.

suggested that solar spicules distributed over the whole solar disc shoot corpuscular streams into the solar atmosphere, and that these streams are favourably deflected towards earth, when they lie in regions of low coronal emission over undisturbed solar areas. In all of these authors' views geomagnetic disturbances result when the corpuscular streams reach earth about three days after leaving the sun.

KIEPENHEUER (1947), however, suggested the contrary hypothesis that the corpuscular source is not spicules, but rather the large quiescent prominences found at intermediate and high latitudes in years preceding solar minimum. To test KIEPENHEUER's hypothesis with material from an independent sample, we have now measured limb prominence areas

* This research was sponsored in part by the Geophysics Research Directorate of the Air Force Cambridge Research Center, Air Research and Development Command, under contract AF 19(604)-969.

† One international prominence unit corresponds to an area at the solar limb bounded by 1 second of arc of the celestial sphere in height and one degree of angle of the solar periphery in length.

VOL. 6 1955

from maps prepared and distributed by the High Altitude Observatory (TROTTER and ROBERTS, 1951–54) and compared the average prominence areas with selected days of large and small geomagnetic disturbance. KIEPENHEUER studied dark filament areas on the solar disc, rather than limb prominence areas. It seems to us, however, that the prominence areas, projected to CMP from both limbs, should reflect the effect suggested by KIEPENHEUER.

Our prominence maps have been prepared from photographic limb-prominence observations in Balmer-alpha of hydrogen made with birefringent filters of 4 Å half-width at the Upper Air Research Observatory, Sunspot, New Mexico, by Harvard College Observatory, and at Climax, Colorado, by the High Altitude Observatory. The periods covered by maps now available include May–November 1951; February–October 1953; and February–June 1954. From these maps we measured first the area in international prominence units† of all prominences in latitudes greater than 20° and then all lying in latitudes above 30°. We used only those central meridian dates for which we had prominence data from both east and west limbs. Such measures were available for 79 per cent of the days in our study. For each date we summed all prominence areas within the specified latitude zones.

We then subjected the area sums to superposed epoch analysis, using, as zero dates, as shown in Fig. 1: (a) the five most magnetically disturbed dates of each month, and (b) the five most magnetically quiet days (CRPL, 1951–54). Thus the figures show average prominence areas corresponding to the days preceding and following geomagnetically disturbed and quiet days. Mean prominence areas for the whole time-sample are also shown. Each graph contains eighty-three zero dates for each curve.

No significant trends of prominence area with respect to the magnetic disturbance dates can be discerned. The results, thus, do not confirm the finding of KIEPENHEUER (1947) for the years of low activity 1910–14 and 1920–25, which gave a maximum average disc prominence area on the fourth day preceding disturbed magnetic conditions. The upper curves of Fig. 1 show that the values for these days lie slightly below the mean. Nor do we find any trend with quiet days. We intend soon to repeat this analysis, using instead of limb prominences the projected areas of dark filaments near the solar centre. We conclude, nonetheless, that these results support the supposition that the *M*-regions must be identified with some solar feature other than the large prominences at intermediate and high solar latitudes.

WALTER ORR ROBERTS
DOROTHY E. TROTTER

High Altitude Observatory
Boulder, Colorado

REFERENCES

ALLEN, C. W.	1944	*Mon. Not. Roy. Astr. Soc.* **104,** 13
BARTELS, J.	1932	*Terr. Magn.* **37,** 1
BELL, B., and GLAZIER, H.	1954	*J. Geophys. Res.* (in press); Harvard Observatory Scientific Report No. 17
BRUZEK, A.	1952	*Z. Naturforschung* **7a,** 708
CRPL F-Series, monthly Ionospheric Data	1951–54	Issued by U.S. Department of Commerce, National Bureau of Standards, Central Radio Propagation Laboratory, Boulder, Colorado
KIEPENHEUER, K. O.	1947	*Astrophys. J.* **105,** 408
PECKER, J-C., and ROBERTS, W. O.	1955	*J. Geophys. Res.* (in press, for March)
TROTTER, D. E., and ROBERTS, W. O.	1951–54	Quarterly Summaries of Solar Activity distributed quarterly from High Altitude Observatory under sponsorship of the Central Radio Propagation Laboratory of the National Bureau of Standards

Measurements of limiting polarization of radio waves reflected from the *F*-layer

(*Received* 31 *August* 1954)

ABSTRACT

Polarization measurements have been made at Kjeller on *F*-echoes close to the critical frequency. The values for the axis ratio of the ellipse of polarization found were between 0·8 and 1·0. This is in contrast to recent measurements reported, where values of the axis ratio of 0·1 to 0·2 have often been observed.

1. Introduction

Measurements of the state of polarization of radio echoes have been made by a number of observers (Appleton and Ratcliffe, 1928; White and Ratcliffe, 1933; Green, 1932; and others). In these measurements the state of polarization of the reflected waves has always been found to be in accordance with the magneto-ionic theory. Recently, Morgan (1953) has reported that when measuring the state of polarization of *F*-echoes a discrepancy has been observed. According to Morgan, the *F*-echoes become nearly linearly polarized when the frequency approaches the critical frequency of the layer, otherwise they are more circularly polarized.

From November 1950 a number of measurements have been made at Kjeller on echoes from the *F*-layer. The purpose of these measurements was to record small variations in the axis ratio of the ellipse of polarization. Usually the measurements were made on such frequencies that the ordinary magneto-ionic and the extraordinary magneto-ionic component was separated in time; the ordinary component therefore was often considerably group-retarded. The echoes were still found to be nearly circularly polarized. In order to investigate the phenomenon reported by Morgan more closely, new measurements have been carried out at Kjeller during May 1954. The results of these measurements will be presented in this note.

VOL. 6 1955

2. Experimental Technique

The experimental procedure for the measurements was the standard system using crossed loops, separate receiving channels, and an oscillographic representation of the ellipse of polarization. The radio polarimeter is described elsewhere (Landmark, 1952). The radio polarimeter was modified in such a way as to enable that parameters determining the state of polarization could be observed continuously. The parameters chosen were the radius vector r and the argument φ of the complex polarization Q, where

$$Q = re^{j\varphi} = E_y/E_x.$$

Here E_x and E_y are the components of the electric field of the wave in geomagnetic N–S and E–W directions respectively.

A typical recording is presented in Fig. 1. This recording was obtained at Kjeller on the 19th of May from 1450 to 1452 MET. The three parameters recorded are r, $\cos\varphi$, and the amplitude A of the signal from one of the loops. In order to determine r, the MF-voltages from the two channels were fed through peak voltmeters to a mechanical voltage dividing servo system. In addition, the MF-voltages were fed through limiting circuits to a coherent phase detector giving $\cos\varphi$.

3. Observations

In May 1954 a total of ten individual tests were made at Kjeller in order to establish whether or not the effect observed by Morgan was present at the more northern station at Kjeller. In these tests the measurements were made either on different frequencies up

to the highest one reflected from the F_1- or F_2-layer, or the measurements were made on a fixed frequency over a period of time such that the critical frequency of the layer was increasing (or decreasing) through the test frequency. In all tests made, the waves were

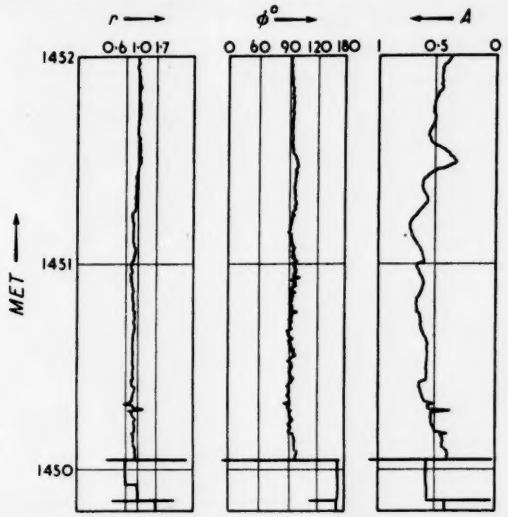

Fig. 1. Typical recording obtained at Kjeller on the 19th of May 1954.
The recorded parameters are: r, φ, and the amplitude A of the signals.

found to be nearly circularly polarized, and no correlation was found between departures from circularity and group retardation of the waves.

In Table 1 three of the tests which were made at Kjeller are presented. The values observed for $\bar{r}$ and $\bar{\varphi}$ are mean values for the periods of observation. The values for the

Table 1. *Observed state of polarization for three individual tests*

Date	*Time MET*	*Test frequency Mc/s*	*Virtual height of layer km*	$\bar{r}$	$\bar{\varphi}$	$\bar{\varepsilon}$
19th May	1440–43	3·6	280	0·85	83	0·81
	1450–53	3·8	400	0·90	94	0·87
	1510–11	4·0	600	0·85	100	0·78
24th May	0750–55	3·2	250	1·0	90	1·0
	0805–10	3·3	250	1·0	79	0·82
	0815–19	3·5	260	1·18	80	0·78
	0830–33	3·8	550	1·0	80	0·83
	0840–44	4·2	450	1·0	78	0·81
24th May	1640–50	3·6	300	0·85	80	0·78
	1655–59	3·8	350	1·0	90	1·0
	1710–13	4·0	380	1·1	85	0·87
	1730–35	4·2	450	1·0	100	0·83

axis ratio $\bar{\varepsilon}$ of the ellipse of polarization are computed from the $\bar{r}$ and $\bar{\varphi}$ values by simple geometry. In Fig. 2 are plotted the values for $\bar{\varepsilon}$ together with the routine *hf*-recordings obtained during the periods of polarization measurements.

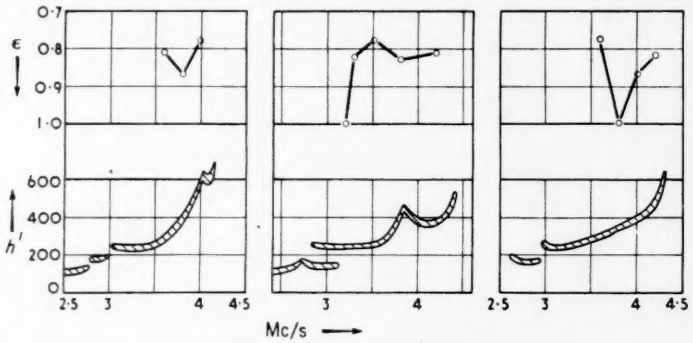

Fig. 2. Plotted observations of the limiting polarization together with *hf*-recordings obtained at Kjeller.

The conclusion to be drawn from the measurements is that no correlation is found at Kjeller between the magnitude of group retardation of the reflected echoes and the state of polarization. The observations at Kjeller give values of the axis ratio in, the range 0·8–1·0. This is not in accordance with MORGAN'S measurements. He observes often values of the axis ratio in the range 0·1–0·2.

BJORN LANDMARK

Auroral Observatory, Tromsö, and
Norwegian Defence Research Establishment, Kjeller, Oslo

VOL. 6 1955

REFERENCES

APPLETON, E. V., and RATCLIFFE, J. A.	1928	*Proc. Roy. Soc.* **117,** 576
GREEN,	1932	*Coun. Sci. Ind. Res. Bulletin* 59
LANDMARK, B.	1952	*Tellus* **4,** 319
MORGAN,	1953	Presented at an URSI meeting in Washington, April 1953
WHITE, and RATCLIFFE, J. A.	1933	*Phil. Mag.* **16,** 125

Journal of Atmospheric and Terrestrial Physics, 1955, Vol. 6. pp. 287 to 289. Pergamon Press Ltd., London

Indices of geomagnetic activity

of the Observatories ABINGER (*Ab*), ESKDALEMUIR (*Es*), and LERWICK (*Le*)

January to March 1955

The figures given on pages 287 to 289 represent the K-indices for three-hour intervals, beginning with 00–03 hrs for the first and ending with 21–24 hrs for the eighth figure.

January 1955

Day	*Ab* Range for $K = 9 : 500\gamma$		*Sum*	*Es* Range for $K = 9 : 750\gamma$		*Sum*	*Le* Range for $K = 9 : 1000\gamma$		*Sum*	*Day*
	K-Indices			*K-Indices*			*K-Indices*			
1	1222	2233	17	1011	1122	9	1111	1133	12	1
2	3122	2212	15	2111	1212	11	3011	0102	8	2
3	1112	2112	11	1011	1102	7	1011	1101	6	3
4	4312	3223	20	4211	2222	16	3211	2223	16	4
5	1111	2234	15	1000	1134	10	0010	0134	9	5
6	3322	2231	18	2211	1231	13	2211	1131	12	6
7	2222	2232	17	2111	2132	13	2111	2121	11	7
8	1011	1123	10	1011	0123	9	1010	0122	7	8
9	4132	3531	22	4132	3430	20	3132	3430	19	9
10	1122	1120	10	0011	1120	6	0011	1120	6	10
11	2212	5235	22	2111	4125	17	2101	3116	15	11
12	4222	1121	15	4111	0110	9	4211	0010	9	12
13	3223	3223	20	3223	2112	16	3212	2123	16	13
14	1212	3241	16	0011	3241	12	1111	2241	13	14
15	1011	1101	6	0000	0000	0	0001	1001	3	15
16	2113	3233	18	1112	2122	12	2112	2133	15	16
17	0334	6555	31	0223	6455	27	1222	5546	27	17
18	6542	2544	32	7542	2544	33	9642	2543	35	18
19	4454	4444	33	4454	3444	32	5564	4445	37	19
20	4321	3344	24	4221	2243	20	4321	2243	21	20
21	4211	2233	18	3110	0132	11	4110	0133	13	21
22	3121	2112	13	3110	1001	7	3110	1011	8	22
23	3222	3343	22	3222	2343	21	3221	2343	20	23
24	1111	2212	11	1101	1101	6	1100	1112	7	24
25	1111	1121	9	0001	1011	4	1010	1011	5	25
26	0112	1111	8	0001	1110	4	0000	0100	1	26
27	0023	1444	18	0002	1444	15	0011	1343	13	27
28	2222	1222	15	2211	0112	10	3211	0103	11	28
29	1112	1134	14	1001	0134	10	1011	1033	10	29
30	2202	3223	16	1101	2223	12	1101	2123	11	30
31	2122	1123	14	2111	0113	10	1101	0013	7	31

February 1955

Day	*Ab* Range for $K = 9 : 500\gamma$		Sum	*Es* Range for $K = 9 : 750\gamma$		Sum	*Le* Range for $K = 9 : 1000\gamma$		Sum	Day
	K-Indices			*K-Indices*			*K-Indices*			
1	1011	2222	11	0001	2112	7	0010	1112	6	1
2	1121	2222	13	1011	2122	10	1011	1112	8	2
3	4322	2223	20	3221	1113	14	3211	1113	13	3
4	1234	3354	25	1223	3344	22	1223	2254	21	4
5	3323	3244	24	3122	2234	19	3222	2234	20	5
6	1222	3334	20	3222	3333	20	1211	2224	15	6
7	3332	4332	23	3322	3221	18	3321	3221	17	7
8	2222	2444	22	2112	1434	18	2111	1444	18	8
9	2232	2231	17	1232	2221	15	2222	1231	15	9
10	2122	2222	15	1021	1122	10	1121	1022	10	10
11	0121	2454	19	1010	2454	17	1011	1465	19	11
12	3321	3334	22	3221	2234	19	3221	2134	18	12
13	4223	2330	19	3212	2330	16	4312	2330	18	13
14	1222	3434	21	1221	2324	17	1222	2324	18	14
15	3322	2100	13	3222	1000	10	3321	1000	10	15
16	0122	3132	14	0012	3133	13	0011	2132	10	16
17	3222	2213	17	3212	2102	13	3112	1002	10	17
18	1222	1144	17	1321	1133	15	1311	0034	13	18
19	2232	2222	17	2121	2111	11	3111	1112	11	19
20	1222	3232	17	1311	2231	14	0211	2231	12	20
21	3432	3332	23	3322	2221	17	3321	2231	17	21
22	3433	2233	23	3423	2333	23	3423	2233	22	22
23	3233	4453	27	2223	3453	24	3223	4452	25	23
24	3332	3232	21	3222	3132	18	2212	3132	16	24
25	3323	2323	21	3322	2312	18	3322	2322	19	25
26	3322	2221	17	3312	1121	14	3311	1121	13	26
27	0112	2123	12	0011	1122	8	0011	1122	8	27
28	5543	4322	28	5533	4301	24	5643	4311	27	28

March 1955

1	1111	2221	11	1112	2211	11	1111	1211	9	1
2	2122	1211	12	2122	2110	11	2121	2101	10	2
3	0222	2100	9	0112	2100	7	0111	1101	6	3
4	0102	0133	10	0102	1023	9	0011	1122	8	4
5	2221	2334	19	2212	2224	17	2111	2234	16	5
6	4232	3232	21	3222	2132	17	3321	2132	17	6
7	5332	2564	30	5332	1573	29	5322	1564	28	7
8	3232	2553	25	3222	2543	23	3221	2543	22	8
9	3232	2454	25	3221	2354	22	3222	3564	27	9
10	3333	3344	26	2233	3233	21	2223	3344	23	10
11	3233	3422	22	3233	3412	21	4222	2411	18	11
12	4432	3444	28	3432	2344	25	3322	2444	24	12
13	3232	3343	23	2222	3343	21	2222	2343	20	13
14	4222	2443	23	4212	2443	22	4212	2443	22	14
15	4333	3244	26	3333	3233	23	3433	2234	24	15

, VOL. 6 1955

March 1955 (*contd.*)

Day	*Ab* *Range for K = 9 : 500γ*			*Es* *Range for K = 9 : 750γ*			*Le* *Range for K = 9 : 1000γ*			*Day*
	K-Indices		*Sum*	*K-Indices*		*Sum*	*K-Indices*		*Sum*	
16	3312	1343	20	3312	2243	20	3311	1244	19	16
17	3243	3323	23	3133	3312	19	4133	2212	18	17
18	2232	2543	23	2122	3543	22	1122	2542	19	18
19	3221	2232	17	3112	2132	15	3111	1132	13	19
20	2112	2214	15	1112	2113	12	2111	2103	11	20
21	3121	2233	17	3012	2133	15	3111	2133	15	21
22	2234	4543	27	2123	5742	26	1123	7752	28	22
23	2122	4455	25	2011	3445	20	1011	3355	19	23
24	3323	2121	17	3323	2111	16	4322	2111	16	24
25	0022	1333	14	0011	2232	11	1011	1232	11	25
26	1233	3313	19	1133	2213	16	1132	3312	16	26
27	1124	3322	18	1113	2312	14	1113	2212	13	27
28	2122	1112	12	1111	1112	9	1011	1102	7	28
29	2221	1010	9	2111	1001	7	1000	1000	2	29
30	1023	3246	21	1013	3246	20	1003	2246	18	30
31	4454	3445	33	5553	3445	34	6554	3454	36	31

OL.
6
955

Book review

W. FLÜGGE: **Four-Place Tables of Transcendental Functions.** 136 pages. Pergamon Press Ltd., London, 1954. 25s. FRIEDRICH LÖSCH: **Siebenstellige Tafeln der elementaren transzendenten Funktionen.** 335 pages. Springer-Verlag, Berlin, Göttingen, Heidelberg, 1954.

THE first volume, by FLÜGGE, contains tables limited to four decimal places; the latter, by LÖSCH, contains tables with seven decimal places. The first is meant to be used when only slide rule precision is needed, the second when a higher accuracy is required. In practical work both accuracies have their field of application.

The first book lists the following functions: trigonometric and hyperbolic functions, exponential function and natural logarithm, the Bessel functions $J_0(x)$, $J_1(x)$, $Y_0(x)$, $Y_1(x)$, $I_0(x)$, $I_1(x)$, $K_0(x)$, $K_1(x)$, $ber(x)$, $bei(x)$, $ber'(x)$, $bei'(x)$, $ker(x)$, $kei(x)$, $ker'(x)$, $kei'(x)$, the elliptic integrals $F(x,y)$ and $E(x,y)$, the error integral $erf(x)$, the Fresnel integrals $C(x)$ and $S(x)$, the $Ci(x)$, $Si(x)$ and $Ei(x)$ functions, and finally $\Gamma(x)$.

Each chapter contains a few introductory pages of formulae concerning the relative functions. (On page 39 in the expression for $K_0(x)$ the denominator under the sum sign should contain $(m!)^2$ rather than $m!$ On page 9 the last expression on the first line should be $2\,\mathrm{Sinh}^2 x$ in place of $\mathrm{Sinh}^2 x$).

The choice of the functions is a matter of personal taste and the applications the compiler had in view. Perhaps the Legendre polynomia might, in future editions, well replace the 16 pages now devoted to the *bei* and *ber* functions.

The book is clearly printed.

The second book, by LÖSCH, lists the following functions: φ, sin x, cos x, tg x, Sinh x, Cosh x, Tangh x, ln x, e^x, e^{-x}, arc sin x, arc tg x, Arc Sinh x, Arc Cosh x, Arc Tangh x, Arc Cotgh x. Nine decimals are given for $x = 0(0{\cdot}0001)0{\cdot}1$ and seven decimals for the ranges $x = 0{\cdot}1(0{\cdot}005)3{\cdot}15$, $x = 3(0{\cdot}01)10$, and $x = 10(0{\cdot}1)20$. These tables, which form the body of the book, cover in all 319 pages. At the end of the book there are a few shorter tables of elementary functions for a larger range but also with larger steps, again in seven decimals.

The tables are printed in a very readable form and clear to the eye. They should certainly be recommended.

BALTH. VAN DER POL

, VOL. 6 1955

Journal of Atmospheric and Terrestrial Physics, 1955, Vol. 6, pp. 291 to 303. Pergamon Press Ltd., London

The effect of vertical ion transport on the night-time *E*-region*

H. R. Peiffer and A. P. Mitra
Ionosphere Research Laboratory, The Pennsylvania State University, State College, Pennsylvania

(*Received* 13 *July* 1954)

ABSTRACT

This paper considers the effect of vertical ion transport on the ionization distribution of the night-time *E*-region. The nature and magnitude of the tidal velocities and of the recombination coefficient, which enter into the calculations, are obtained from various sources, both experimental and theoretical.

It is shown that vertical ion transport is of importance in the night-time *E*-region and that this factor is capable of explaining certain heretofore anomalous experimental observations pertaining to the night-time *E*-layer.

1. Introduction

Although a great deal of work by Martyn (1947a, 1947b, 1948) and others (Chowdhury, 1951; Kirkpatrick, 1949; Mitra, 1951; and Weiss, 1952) has been done on the tidal effects occurring in the F_2-region, very little has been attempted in relation to the *E*-layer. This lack of study appears to be due to the fact that, in the *E*-region, the lifetime of an electron is short and, thus, the small oscillations in electron density due to tides in this region would be masked by the larger variations in the rate of electron production and recombination.

At night, however, when the normal solar ion production is absent, the effect of large drift velocities may be important; particularly if there is an appreciable gradient in such drifts.† Moreover, it is not necessary that the drift-producing mechanism should be tidal in nature. Any large-scale motion in the atmosphere will cause vertical ion drifts, depending on the inclination of the terrestrial magnetic field.

Major theoretical advances have been made regarding the formation, chemistry, and physics of the *E*-region in recent years, but several experimental anomalies still persist. Some of these can be explained by the application of atmospheric photochemistry and the recent ideas on the height variations of t mperature and pressure in the upper atmosphere. On the other hand, others cannot be fully explained in this manner. Of these, those which appear to show effects due to ion drifts, are:

(1) Night-time variation of the *E*-layer maximum electron density.
(2) Night-time variation of "main" reflection level at 150 kc/s.
(3) Variation of the height of the "coupling" level at night (150 kc/s).
(4) Temporary "breaking" or loss of the "main" reflection level echoes from the *E*-layer with accompanying reflection of a 150-kc/s wave from a height averaging approximately 150 km.
(5) Formation of the night-time sporadic *E*-layer.

* The research reported in this paper has been sponsored by the Geophysics Research Division of the Air Force Cambridge Research Center, Air Research and Development Command, under Contract AF19(122)-44.

† Recent observations by Whipple (1953) of meteor trails have revealed surprisingly high wind shears.

The E-region maximum electron density, N_{max}, at night shows a great change during the first few hours after sunset and then remains approximately constant for the remainder of the night. The "main" and "coupling" heights of reflection for 150 kc/s show similar variations with time. These variations can be explained for the first six or seven hours of the night by properly adjusting the recombination coefficient. However, after this time has elapsed, a mechanism such as ion transport is needed to explain the variation.

The so-called "breaking" of the E-layer occurs only at night. This phenomenon is one in which the reflection of a 150-kc/s wave from the normal height is noted until, suddenly, the reflection occurs at a much greater height, i.e., around 150 km. The new height of reflection is observed for an interval of many minutes to a few hours, and then the normal reflection from the E-layer again appears.

The night-time sporadic E-layer occurs at a height of approximately 110 km. It appears to be a very thin layer with a maximum electron density of about 10^4–$10^5/cm^3$.

All of the aforementioned anomalies of the E-layer are studied in this work, with emphasis on an attempt to determine if the observed experimental variations may be attributed to the effect of vertical ion transport.

2. Effect of Transport on Ionospheric Ionization

If one considers the ionospheric region to be a compressible fluid capable of accommodating a variable number of electrons, and if the decay of ionization up to a time, t, is represented by αN^2, then the temporal variation of electron density, for night-time conditions, may be written

$$\frac{\partial N}{\partial t} = -\alpha N^2 - \operatorname{div}[NV] \tag{1}$$

where α is the effective recombination coefficient and V is the velocity of the medium.

Now, if one confines attention to the vertical-drift velocity component in the equation of continuity (1), the above becomes

$$\frac{\partial N}{\partial t} = -\alpha N^2 + \frac{\partial (Nv)}{\partial z} \tag{2}$$

where v is the vertical ionic-drift velocity measured positively downwards, and z, the height, is measured positively upwards.

It should be noted that the vertical ion drifts may arise from local drifts or turbulence, diffusion, thermal transport, or, as we shall here consider, tidal sources.

Various solutions to the above equation have been studied. Martyn (1947a) neglected the recombination term (as well as the electron production term) in his study of F-region anomalies. This simplification allowed the continuity equation to be solved quite easily. Kirkpatrick (1949) and Weiss (1952) have considered the entire equation. The present work will also attempt the complete solution of the equation at night under the most realistic conditions, in which the effective recombination coefficient varies with height (and in some instances with time).

VOL. 6 1955

From equation (2) we obtain

$$\frac{\partial N}{\partial t} = -\alpha N^2 + N\frac{\partial v}{\partial z} + v\frac{\partial N}{\partial z} \tag{3}$$

Following WEISS (1952), we will now concentrate attention upon a given initial level, z_0, and follow the motion of electrons contained in a small "cell" as they are moved by the vertical tidal motion.

Since

$$\frac{dz}{dt} = -v$$

the above relation may be written

$$\frac{dN}{dt} = -\alpha(z)N^2 + N\frac{\partial v}{\partial z} \tag{4}$$

in which the height dependence of α is included in $\alpha(z)$.

This is recognized as a Bernoulli-type equation which can be readily solved.

If we assume the drift velocity to be of the type

$$v = v(z)\sin(\omega t + \phi),$$

where $\omega = \frac{\pi}{6}$/hr, and ϕ is a phase constant, and let

$$K = \frac{\partial v(z)}{\partial z},$$

then the solution of (4) is

$$N = \frac{\exp[-(K/\omega)\cos(\omega t + \phi)]}{\alpha\sum Y_n + \dfrac{[\exp - \{(K/\omega)\cos\phi\}]}{N_0}} \tag{5}$$

where $$\sum Y_n = t + \sum \frac{(-1)^n}{n!}\left(\frac{K}{\omega}\right)^n \int \cos^n \omega t\, dt$$

with $$n = 1, 2, 3, 4, \text{ etc.}$$

and N_0 is the initial electron density distribution at $t = 0$.

Expression (5) along with the equation

$$\frac{dz}{dt} = -v(z)\sin(\omega t + \phi)$$

allows one to solve the equation of continuity by following small cells of ionization as they move through the ionosphere.

3. Relevant Parameters

3.1. *Drift velocity*

MARTYN (1947a, 1947b) used, for his study of the E-region, velocities of the form $v = v_0 e^{-\gamma z}$ and also $v = v_0 \sin(\omega t + \sigma z)$. In his study of the E-region, KIRKPATRICK (1949) also made use of the velocity $v = v_0 \sin(\omega t + \sigma z)$, with $v_0 = 22{\cdot}5$ km/hr, and, furthermore, assumed a constant value for the recombination coefficient α, i.e., 10^{-8} cm^3/s. For the F_2-region, WEISS (1952) utilized velocities

of the type $v = v_0 \cos(\omega t + \varepsilon)$ and $v = v_0(1 + \sigma z)\cos(\omega t + \varepsilon)$, CHOWDHURY (1951) employed a velocity of the form $v = v_0 e^{-\gamma z}\cos(\omega t + \sigma z)$, and MITRA (1951) $v = v_0 e^{-\gamma z}\sin(\omega t + \sigma z)$.

The essential idea in all of these equations is to have a velocity function which is semi-diurnal in nature and with amplitude and/or phase decreasing with height. In the *E*-region, we need not consider the variation of phase with height. This permits setting $\sigma z = 0$. It may be noted that these equations, although specifically formulated for tidal drifts, may also apply, approximately, for other drifts with appropriate changes in γ and ω.

The value of the quantity $v(z)$ is not definitely known. CHAPMAN-BARTELS (1940), FEJER (1953), and MARTYN (1954) have given the magnitude of the drift velocities of the ionization in a uniform ionosphere under the influences of an electric field and/or atmospheric wind. These calculations are closely related to such studies as ionospheric conductivity and the "dynamo" currents causing the variations in the terrestrial magnetic field. The observed variation in the terrestrial magnetic field helps in estimating the orders of magnitude of such drift velocities. They may range from 1–20 km/hr, depending on the various assumptions employed. Since the problem of conductivity and "dynamo" currents, and of the atmospheric oscillations, cannot as yet be considered as satisfactorily resolved, the values obtained from such considerations are only approximate. However, the rather extended range of 1–20 km/hr should cover the probable physical situation. As we shall see later, this range includes the type of velocity required to explain some of the night-time anomalies of the *E*-region. It may also be noted that analysis for the solar semi-diurnal component in the horizontal winds in the *E*-region, as measured by the spaced receiver technique, yields amplitudes of the order of 100 km/hr (DEB, 1953; MITRA, S. K., 1952). Consequent vertical drifts due to this cause will have amplitudes in the above range.

VOL. 6 1955

In addition to vertical drifts caused by horizontal atmospheric motions we may also have vertical atmospheric winds which, in the *E*-region and below, will drag the ions and electrons along with the neutral air molecules. MANNING and others (1954) have given the approximate magnitudes of turbulent vertical wind velocities using meteor-radar experiments. It appears that such vertical winds have velocities of the order of 5 km/hr.

In view of the above, velocity amplitudes ranging from 1–10 km/hr are used in the present work. We shall only consider the drifts of semi-diurnal period, so that (as was stated previously) the velocity used is of the type

$$v = v(z)\sin(\omega t + \phi)$$

where $\omega = 30°/\text{hr}$.

In choosing the phase ϕ, use was made of the various calculations involving the "dynamo theory," and also of various semi-empirical determinations from ionospheric parameters. Although both lunar and solar semi-diurnal drifts exist, the solar semidiurnal component is larger, in the *E*-layer, than the lunar. It is therefore necessary to only consider the solar drifts. FEJER (1953) gives maximum upward drift (solar) at 04–05 hours in high latitudes and 11–13 hours at low latitudes. These results apply to the *E*-region. MARTYN (1947a, 1947b, 1948),

MITRA (1951), and WEISS (1952) have considered the oscillation in ionization and height in the F_2-region for a wide number of stations scattered over the world, and have indicated the possible values of ϕ applying at the height of this layer.

From the available material the phase was chosen for high and low latitudes such that the maximum upward velocity would occur at 0300 and 2100 hours, respectively. That is to say, $\phi = 0$ and $\phi = \pi$ for the high and the low latitudes. respectively, with $t = 0$ chosen at 1800 hours.

The first type of tidal velocity amplitude $v(z)$ to be used, which henceforth shall be called Type A, is of the form

$$v(z) = v_0 \frac{\omega^2}{\omega^2 + \nu^2}$$

where ω is the gyrofrequency,

and ν is the collision frequency.

By using the ν-model of NICOLET (1953) the velocity equation was put into a more useful form of the type

$$v(z) = v_0(1 - ce^{-pz})$$

where c and p are constants.

Secondly, a velocity distribution approximating the vertical drifts given recently by MARTYN (1954) and FEJER (1953) was used. This velocity shall be referred to as Type B, and may be written with the form:

$$v(z) = v_0\left(\frac{a}{z^2} + \frac{b}{z} + c\right)$$

and a, b, and c are constants.

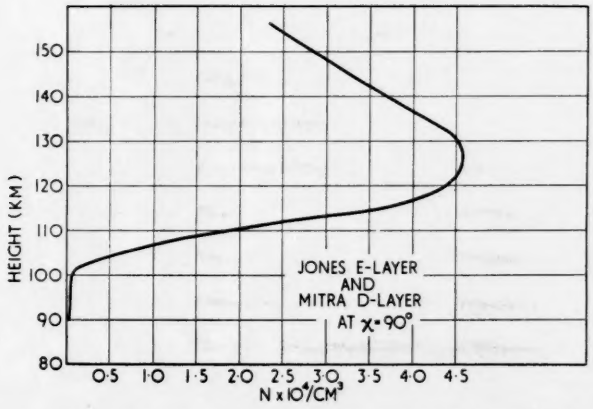

Fig. 1. JONES E-layer and MITRA D-layer at $\chi = 90°$ (evening conditions).

3.2. *Sunset ionization and night-time recombination*

The initial electron density distribution, N_0, that is needed to obtain numerical results from equation (5) was chosen to be the E-layer model for $\chi = 90°$ obtained by JONES (1953). In addition to this, a D-layer model for $\chi = 90°$ was needed. The model chosen was MITRA's (1954a). Fig. 1 shows the combined models.

The recombination model chosen was that recently proposed by MITRA (1954b) as a tentative night-time model. In addition, some use was made of the MITRA-JONES (1954) daytime recombination model. Fig. 2 shows these recombination models plotted against height.

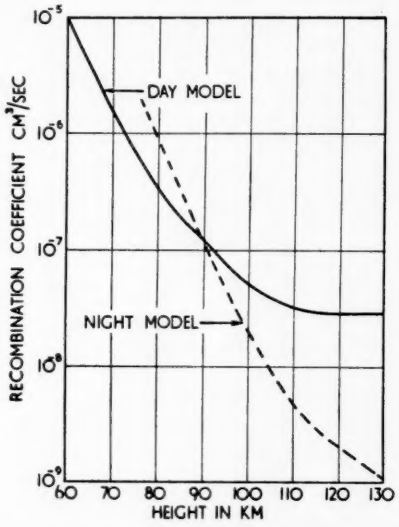

Fig. 2. Height variation of the effective recombination coefficient for average day and night conditions.

VOL. 6 1955

3.3. *Theoretical results*

Figs. 3 and 4, respectively, show the electron density distribution for Type A and type B velocities with $v_0 = 1$ km/hr and 10 km/hr, respectively. Both figures are for $\phi = \pi$ and show the distributions for various times after sunset.

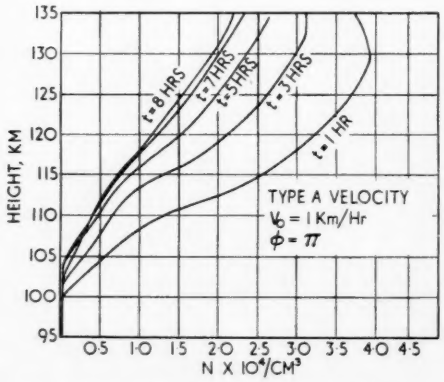

Fig. 3. Changes in the E-region electron distribution at different times of the night for Type A vertical drift with $v = 1$ km/hr and $\phi = \pi$ and for the night-time recombination model given in Fig. 2.

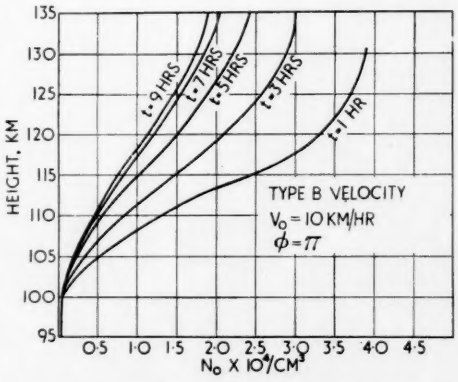

Fig. 4. Changes in the E-region electron distribution at different times of the night for the Type B vertical drift with $v = 10$ km/hr and $\phi = \pi$ and for the night-time recombination model given in Fig. 2.

4. Experimental Observations and Their Implications

An annual average of Lindquist's (1952) "main" and "coupling" heights of reflection at 150 kc/s, of night-time absorption at 150 kc/s (Benner, 1952), of Watheroo f_0E data, and a monthly average of Bracewell's (1951) 16 kc/s phase-height data are shown in Fig. 5. From this figure it is seen that around 0000 to

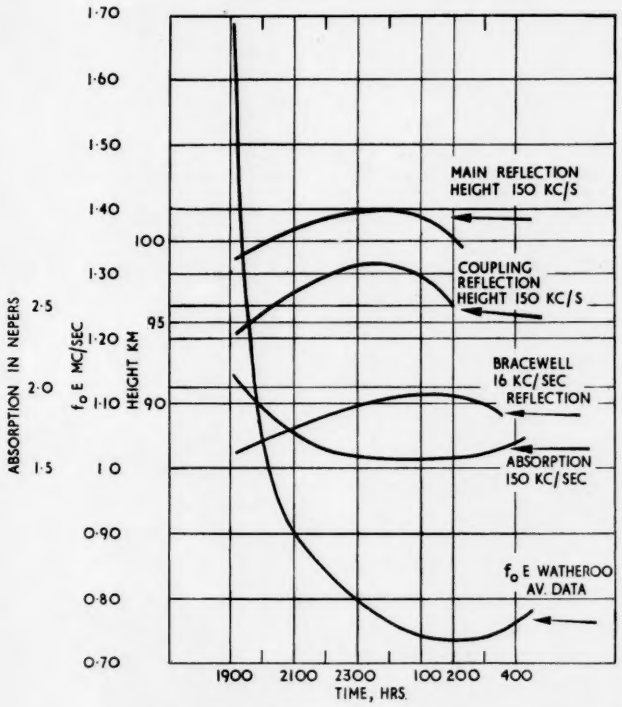

Fig. 5. Experimental variation of E-region parameters.

0200 hours the f_0E data shows an increase and the heights of reflection a decrease. These phenomena cannot be explained by recombination alone, and an explanation in terms of vertical ion transport appears desirable.

The night-time variations in the main reflection level for 150 kc/s ($N = 3000/\text{cm}^3$), as found from the electron density distribution, were plotted against time and compared with the experimental results obtained by Lindquist (1952). Fig. 6 shows this comparison. The same type of comparison was made using the height of the coupling level at 150 kc/s; i.e., $N = 267/\text{cm}^3$. Fig. 7 shows this comparison.

Data obtained from Watheroo concerning night-time f_0E were also used and compared with the theoretical results obtained in this work. It is seen in the upper part of Fig. 8 that there is very little correlation of theory with experiment when the "night"-α model given in Fig. 2 is used for the entire night. This model represents only the average value of the recombination coefficient for a ten-hour

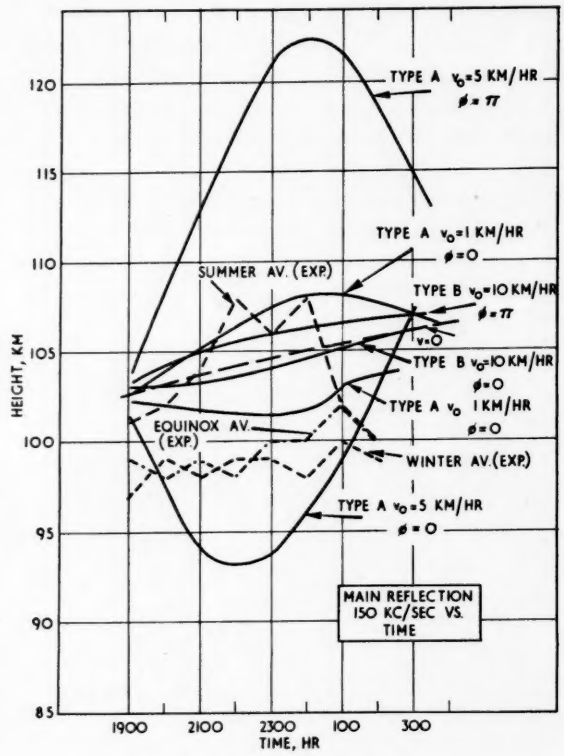

Fig. 6. Main reflection 150 kc/s vs. time.

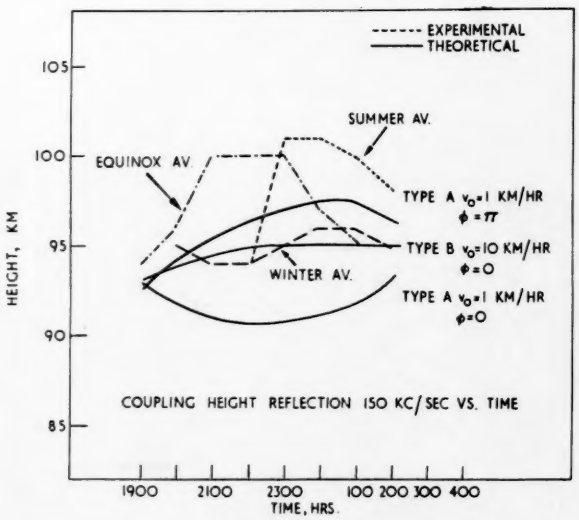

Fig. 7. Coupling height reflection 150 kc/s vs. time.

, VOL. 6 1955

night. There are indications that the effective recombination coefficient immediately after sunset is much larger than that at later hours (MITRA, 1954b). It appears that a fairly satisfactory representation of the nocturnal variation of the recombination coefficient would be obtained by using the so-called daytime model in Fig. 2 for the first two hours after sunset and the night-time recombination model for the remainder of the night. The results of using this revised recombination model are also shown in Fig. 8. The velocities used in this computation

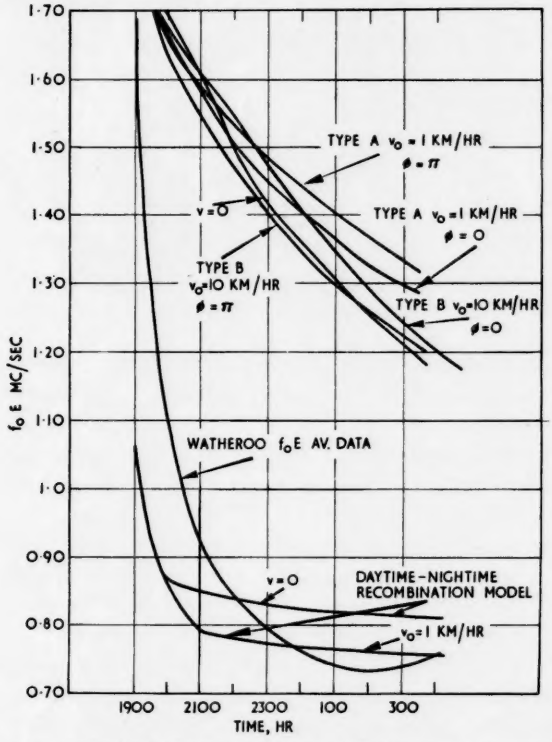

Fig. 8. Observed night-time variation of Watheroo f_0E compared with the theoretical values.

were zero and $v = v_0 \sin \omega t$ with $v_0 = 1$ km/hr. The latter velocity is an approximation for the Type A velocity in this instance. This is true in that the $N_{\max}$ of the E-layer is presumably above 100 km at all times, and the Type A velocity is constant, or nearly so, above 100 km.

Examining the experimental f_0E data closely, one notes that, near 0200 hours, long before sunrise, there is an increase of f_0E, thus suggesting a change in phase of the velocity near this time. From these data the orders of magnitude of α and of the drift velocity may be estimated as follows:

If one assumes that $t = 0$ at the change of phase of the velocity and if one chooses t_1 and t_2 such that $t_1 = -t_2$ and also that $v = v_0 e^{-\gamma z} \sin \omega t$, then, at t_1,

$$\left(\frac{dN}{dt}\right)_{t_1} = -\alpha N_1^2 - V N_1 \sin \omega t_1 \qquad (6)$$

and, at t_2,

$$\left(\frac{dN}{dt}\right)_{t_2} = -\alpha N_2^2 - VN_2 \sin \omega t_2 \tag{7}$$

if $V = \gamma v_0 e^{-\gamma z}$.

Now, since $t_1 = -t_2$, the expressions (6) and (7) become

$$\left(\frac{dN}{dt}\right)_{t_1} = -\alpha N_1 - VN_1 \sin \omega t_1 \tag{8}$$

$$\left(\frac{dN}{dt}\right)_{t_2} = -\alpha N_2^2 + VN_2 \sin \omega t_2 \tag{9}$$

Solving for α and V, one obtains

$$\alpha = -\frac{N_2\left(\frac{dN}{dt}\right)_{t_1} + N_1\left(\frac{dN}{dt}\right)_{t_2}}{N_1N_2(N_1 + N_2)} \tag{10}$$

and

$$V \sin \omega t = -\frac{N_2^2\left(\frac{dN}{dt}\right)_{t_1} - N_1^2\left(\frac{dN}{dt}\right)_{t_2}}{N_1N_2(N_1 + N_2)} \tag{11}$$

By applying these equations to the experimental data of Fig. 8 the velocity and effective recombination coefficient were estimated to be of the order of 1 km/hr and 10^{-9}–10^{-11} cm^3/s, respectively.

In order to obtain better agreement between theory and experiment, MITRAS's α model was used until 2300 hours, and from then on values of α used were those computed from Watheroo data. A velocity of the form $v = v_0 \sin(\omega t + \pi)$ with $v_0 = 1$ km/hr was also used, and, in addition, an adjustment of the parameters was made such that the annual average of the "main" and "coupling" reflection heights at 150 kc/s, of the f_0E data from Watheroo, and the monthly average of BRACEWELL's 16 kc/s phase-height results agreed at 1900 hours.

These results are shown in Fig. 9. It is readily seen that the use of a temporal varying effective recombination coefficient yields results that show a closer agreement with experimental data. The discrepancy still present can be attributed to the lack of information concerning the variation of α with time and, further, the velocity form utilized could possibly be improved upon.

Some attempt has been made to explain the "breaking" of the E-layer. This phenomenon, described previously, is shown in some of the records presented by LINDQUIST (1952). By assuming a velocity of the type $v = v_0 \sin \omega t$ and using the night-time model for recombination, we obtain, as is shown in Fig. 10, "breaking" occurring four hours after sunset if $v_0 = 20$ km/hr.

Although the "breaking" can be explained in this manner, the re-formation of the latter cannot be accounted for. Possibly the introduction of localized nocturnal ionization into the continuity equation, in conjunction with the above, would afford an explanation of this phenomenon.

One may estimate the magnitude and phase of the tidal velocity or recombination coefficient that would cause "breaking," by making use of the available 150 kc/s records. By so doing it has been found that, in order to explain "breaking"

VOL. 6 1955

six hours after sunset, a velocity of the order of 10–15 km/hr must be used. On the other hand, if recombination alone were to cause the "breaking" phenomena, the coefficient would have to be of the order of 15×10^{-9} cm^3/sec—a value much larger than seems possible at night (1954b).

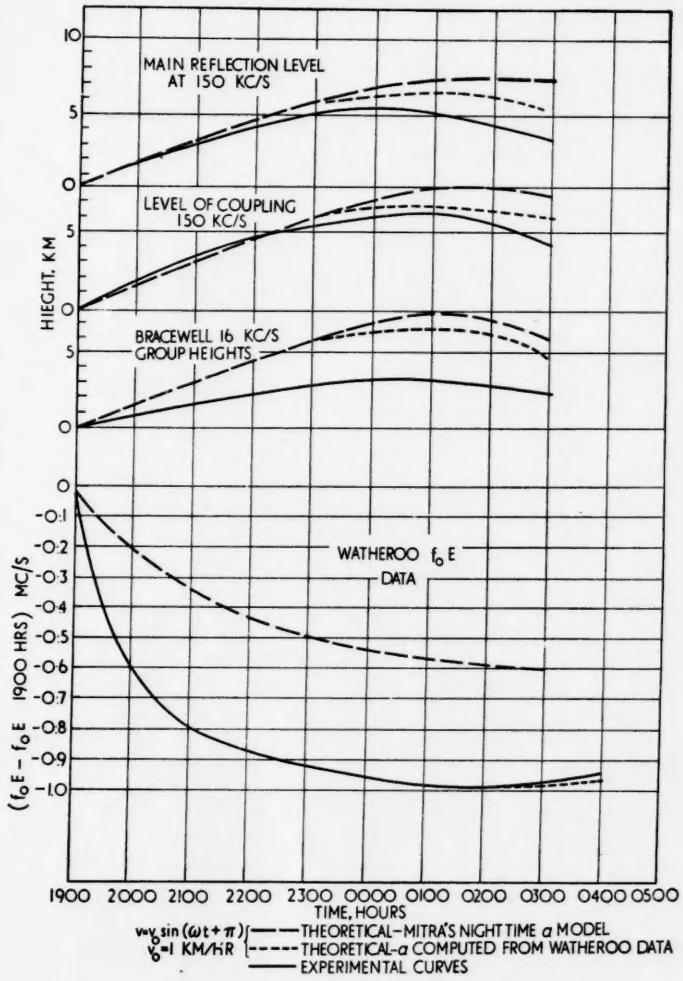
MAIN REFLECTION LEVEL AT 150 KC/S
LEVEL OF COUPLING 150 KC/S
BRACEWELL 16 KC/S GROUP HEIGHTS
HIEGHT, K M
WATHEROO f_0 E DATA
$(f_0E - f_0E$ 1900 HRS) MC/S
TIME, HOURS
$v_0 \sin(\omega t + \pi)$ v_0=1 KM/HR
THEORETICAL–MITRA'S NIGHT TIME α MODEL
THEORETICAL-α COMPUTED FROM WATHEROO DATA
EXPERIMENTAL CURVES

Fig. 9.

5. Conclusions

(1) Although the effect of vertical drift motion is not as great in the E-region as in the F-region, it is sufficient to cause appreciable changes in the observed ionospheric parameters associated with this layer. Experimental variations in various ionospheric parameters confirm such a view.

(2) Although both α and v have been used in our solution, it is very difficult to separate the effect of one from the effect of the other.

(3) The temporal variation of α is very important and must be considered in order that close agreement with experiment may be obtained.

(4) There is some error introduced in our use of α, in that a linear average of this parameter was assumed. However, it was felt that the approximation would not greatly affect the results, as our night-time recombination model is still tentative.

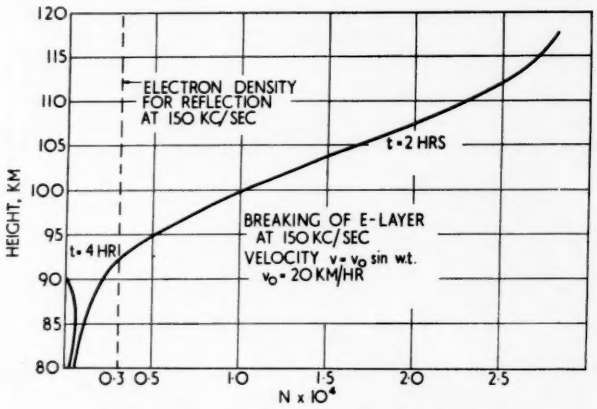

Fig. 10. Breaking of E-layer at 150 kc/s.
Velocity $v = v_0 \sin \omega t$
$v_0 = 20$ km/hr.

VOL. 6 1955

REFERENCES

BENNER, A. H.	1952	Scientific Report No. 18, Ionosphere Research Laboratory, State College, Pennsylvania
BRACEWELL, R. N., BUDDEN, K. G., RATCLIFFE, J. A., STRAKER, T. W., and WEEKES, K.	1951	*Proc. Inst. Elect. Eng.*, Part III, **98**, 221
CHAPMAN, S., and BARTELS, J.	1940	*Geomagnetism*, Vol. 1 (Clarendon Press, Oxford), 531–538
CHOWDHURY, D. C.	1951	*Ind. J. Physics* **25**, 1
DEB, S.	1953	*J. Atmosph. Terr. Phys.* **4**, 28
FEJER, J. A.	1953	*J. Atmosph. Terr. Phys.* **4**, 184
JONES, R. E.	1953	Scientific Report No. 48, Ionosphere Research Laboratory, State College, Pennsylvania
KIRKPATRICK, C. B.	1949	*Aust. J. Sci. Res.*, Series A **1**, 423
LINDQUIST, R.	1952	Scientific Report No. 38, Ionosphere Research Laboratory, State College, Pennsylvania
MARTYN, D. F.	1947a	*Proc. Roy. Soc.* A **189**, 241
MARTYN, D. F.	1947b	*Proc. Roy. Soc.* A **190**, 273
MARTYN, D. F.	1948	*Proc. Roy. Soc.* A **194**, 429
MARTYN, D. F.	1954	*Trans. Roy. Soc. London*, Ser. A, 246
MANNING, L. A., PETERSON, A. M., and VILLARD, O. G., Jr.	1954	*J. Geophys. Res.* **59**, 47
MITRA, S. K.	1952	*Upper Atmosphere*, 2nd Ed., The Asiatic Soc., Calcutta, India, 33–345

MITRA, A. P.	1951	*J. Atmosph. Terr. Phys.* **1,** 286
MITRA, A. P.	1954a	*J. Atmosph. Terr. Phys.* **5,** 28
MITRA, A. P.	1954b	In process of preparation
MITRA, A. P., and JONES, R. E.	1953	Scientific Report No. 44, Ionosphere Research Laboratory, State College, Pennsylvania.
	1954	*J. Geophys. Res.* **59,** 391
NICOLET, M.	1953	*J. Atmosph. Terr. Phys.* **3,** 200
WEISS, A. A.	1953	*J. Atmosph. Terr. Phys.* **3,** 30
WHIPPLE, F. L.	1953	"High Altitude Winds by Meteor Trail Photography," *Proc. of Conf. on Motion in the Upper Atmosphere,* 38

Journal of Atmospheric and Terrestrial Physics, 1955, Vol. 6, pp. 304 to 312. Pergamon Press Ltd., London

Light pulses from the night sky and Čerenkov radiation
Part II

J. V. JELLEY and W. GALBRAITH
Atomic Energy Research Establishment, Harwell, Berks

(*Received* 18 *August* 1954)

ABSTRACT

Further experiments on the Čerenkov radiation produced by extensive air showers in the atmosphere are described. The integral pulse-height distribution of the light pulses is found to fit closely a power law. The variation in rate of firing of a Geiger counter falls off slowly with distance from the light-receiver. Although the pulse-height distribution is a broad one, it is found that, in general, the larger light pulses are associated with the higher energy showers. The variation in pulse rate with zenith and azimuth angle of a light-receiver has been studied, and the receivers have been used for searching areas of sky for possible point sources of cosmic radiation.

1. INTRODUCTION

In Part I, experiments were described in which some of the properties of the light emitted in the atmosphere by extensive air showers were investigated. The main conclusion drawn from this work was that the light detected had properties consistent with Čerenkov radiation. In this second part, the experiments were also carried out at the Pic du Midi Observatory in France and refer in more detail to the relationship between the light pulses and the air showers. Since this is a new field of work, the experiments were very simple and were, of necessity, within the limitations of the apparatus taken.

It is not proposed to describe again in any detail the apparatus for the various experiments. A description of the equipment has already been given in Part I (Section 2).

2. THE PULSE-HEIGHT DISTRIBUTION OF THE LIGHT PULSES

The early experiment (JELLEY and GALBRAITH, 1953) in which the differential pulse-height distribution of the light pulses was measured, showed that an exponential curve could be fitted more closely than a power law, to the observed distribution. Attempts to explain the exponential distribution from elementary theory were not satisfactory. It is not proposed to discuss the theory here, but it can be shown that the frequency spectrum of pulse heights should be a power-law distribution.

Another experiment was therefore made to investigate the anomaly. The receiver used comprised a 61-cm mirror and the 12·5-cm phototube with a 7·5-cm stop, the optic axis of the receiver pointing to the zenith. The integral pulse-height distribution of the light pulses was measured using a discriminator and scaler, and, at the same time, the differential distribution was obtained by photographing the pulses on a recording oscilloscope and subsequently measuring their heights.

Fig. 1 shows a typical pulse-height distribution; it is seen that the "noise" from the general background of night-sky light falls off much more steeply than the light pulse distribution. (Also shown on this figure is a curve of artificial noise, i.e., the noise produced by the small lamp used in many of the experiments and

VOL. 6 1955

referred to earlier in Part I. The form of the distribution of noise pulses for this light is similar to that for night-sky light.)

The results of this experiment showed conclusively that the frequency distribution in height of the light pulses, detected with the existing apparatus, is a power-law distribution, the number of light pulses of height greater than H being given by the relation:

$$N(>H) \propto H^{-1\cdot6\pm0\cdot1} \tag{1}$$

The exponential form obtained in the earlier work was incorrect, and, on investigation, was found to be due to a nonlinearity in the amplifiers.

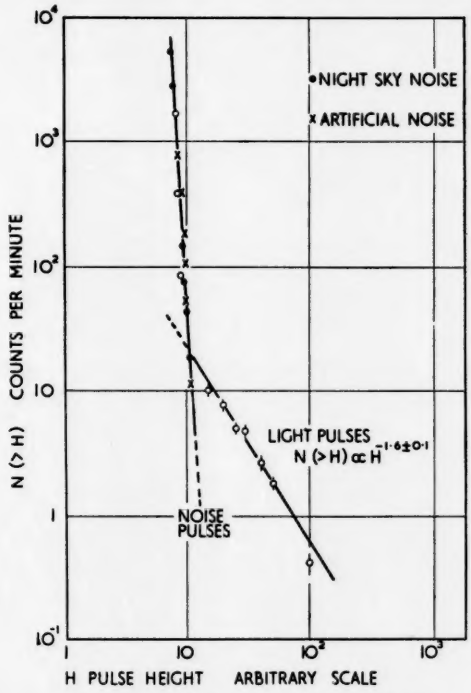

Fig. 1. Integral pulse-height distribution.

3. The Frequency of Discharge of Geiger Units with Distance from the Light-receiver

An experiment was done to investigate the frequency with which showers, producing sufficient light to be detected by a light-receiver, discharged a Geiger counter unit, as a function of the distance of that unit from the light-receiver. From considerations of the lateral spread of the showers and from an estimate of the area of ground covered by the Čerenkov light from the showers, it was not expected that the rate of discharge of the counter with distance would fall off very steeply.

In the course of the various experiments in which a single receiver was directed to the zenith and the hodoscope was triggered from the light pulses, records were

obtained from which the frequency-versus-distance curve could be derived. Two areas of Geiger unit were used (200 cm² and 800 cm²) and the maximum distance of a unit from the receiver was 110 metres. The results are shown in Fig. 2.

It is clear that the result of this experiment is at variance with earlier results obtained at Harwell (JELLEY and GALBRAITH, *loc. cit.*) in which the corresponding curve had a maximum occurring some distance from the light-receiver. It must however be realized that the conditions of the two experiments were different.*

In the present experiments, it is seen that the difference in the curves for the two counter areas is not significant, although the curve for the counters of 200 cm² area appears to fall off less steeply than that for the larger area. This might be

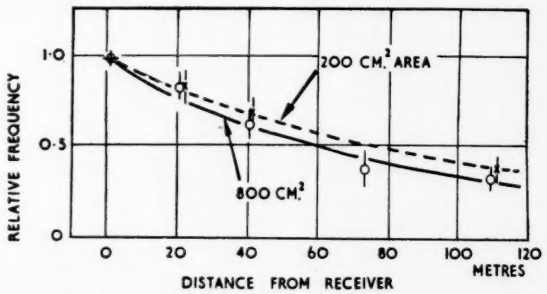

Fig. 2. Frequency of discharge of a Geiger counter unit with distance from the light-receiver.

VOL. 6 1955

expected since the small area counters are detecting, in general, the showers of higher particle density, and consequently the rate of firing with distance would fall off less steeply.

4. THE PULSE HEIGHT RELATIVE TO THE SIZE OF SHOWER

It may be assumed that, in general, the largest light pulses are produced by showers of the greatest energy. It was realized from early experiments to correlate pulse-height with the size of the shower, that a very wide spread in pulse-heights was obtained for showers discharging a specific arrangement of counters. One reason for this is the large spread in energy of showers discharging a given counter arrangement.

However, it was possible to obtain some correlation between average pulse height and shower energy, by measuring the fraction of events discharging one or more Geiger counter units as a function of the bias on the discriminator following the amplifier of the light-receiver. The units were arranged in the same manner as described for the polarization experiment (Section 3, Part I) i.e., they were placed in a straight line from the light-receiver in the east-west direction. The distances of the units A, B, C, D, and E from the receiver were 0, 20, 33, 46, and 73 metres respectively. The results are given in Table 1, from which it is seen that, in general, the larger light pulses are associated with the showers of higher particle density.

* The experiment was again done at Harwell using both the 16 Geiger counter array (JELLEY and GALBRAITH, *loc. cit.*) and the counter units used at the Pic du Midi. These later results agreed with those reported here.

Table 1. *Results of experiment to correlate light pulse height with shower energy*

Arbitrary pulse height greater than	*Fraction of events which discharged one or more Geiger units (area 200 cm²)*
15 volts	0·10 ± 0·01
50 volts	0·27 ± 0·07
100 volts	0·40 ± 0·11

5. The Variation of Light Pulse Rate with Zenith and Azimuth Angles

(i) *Zenith angle experiment*

For this experiment a receiver consisting of a 61-cm mirror and a 5-cm phototube (field of view $\pm 6°$) was used; the receiver was placed on a simple mounting, so that the direction of its optic axis could be varied in zenith and azimuth angles. The mean current in the phototube was kept constant by varying the brightness of the small lamp, as described in Part I, Section 2. The Geiger counter units were again used and gave us information about how their frequency of discharge varied with the zenith angle of the showers. The azimuth direction of the receiver was along the east-west line of the units (azimuth angle $\phi = 0$). The zenith angle ψ was varied in coarse steps and the count rate taken at each setting at a fixed bias on the discriminator.

The observed frequency of light pulses, $R(\psi)$, as a function of ψ, is shown in Fig. 3(a). It is seen that, over the range $0 < \psi < 70°$, $R(\psi)$ may be expressed as

$$R(\psi) \propto \cos^{\eta} \psi \qquad (2)$$

where η lies between 2 and 3.

During this experiment, pulse-height distributions were obtained at various zenith angles. It was found that, within the limits of the statistics, the form of these distributions was the same as in equation (1), so that the results should be independent of the discriminator bias. The decision to fix the bias throughout these experiments was therefore justified.

The results in Fig. 3(a) have not been corrected for light absorption in the atmosphere. The information available (Norton, 1950) for a correction of this type refers to stars observed from sea-level, in which the correction factor, normalized to unity at the zenith, increases to 1·2 at 50° and then, more rapidly, to 2·5 at 70°. However, in the present experiment, the sources of light are within the atmosphere and the observations are made at mountain altitudes, thus the corrections for light absorption will certainly be less than those given by Norton. In practice such corrections would raise the points for the larger values of ψ in Fig. 3(a).

The Geiger hodoscope data enable us to plot a curve of the type shown in Fig. 3(b); in this, the frequency with which Geiger counter unit A (alongside the receiver) is discharged in coincidence with the light-pulse is plotted as a function of ψ. Allowance has been made in reducing the results for a $\cos \psi$ factor, because the area

of the unit presented to a shower, at an angle, is smaller by this factor than for vertical showers. Similar curves can also be drawn for the other Geiger counter units: Fig. 3(b), however, illustrates the following point. It is seen by comparing Fig. 3(a) and (b) that the shower rate falls off more steeply with ψ than the light-pulse rate. This would be expected because of the greater absorption of the shower particles, compared with the absorption of the light, in the atmosphere. The angular distribution of the showers as measured by the Geiger units may be represented by a $\cos^n \psi$ distribution, with n about 6. It is of interest to note that the results of KRAYBILL (1954), who finds a $\cos^{5\cdot5} \psi$ distribution for showers at

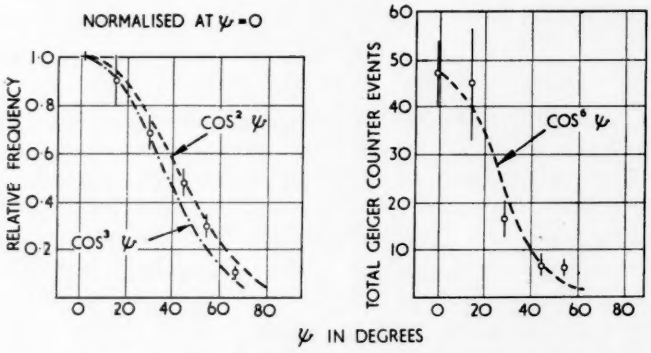

Fig. 3. (a) Pulse rate at a given bias, vs. zenith angle ψ.
(b) Discharge rate of Geiger counter unit "A" in coincidence with light-pulse, vs. ψ.

3,500 metres and a $\cos^{7\cdot5} \psi$ distribution at sea-level, are in agreement with the present experiment, if we assume that the showers detected in all these experiments are of similar energies.

(ii) *Azimuth angle experiment*

In the second part of this experiment, the light-receiver was tilted at a zenith angle of 45° and the count rate observed at azimuth angles ϕ of 0 and $\pm 90°$. It was not possible to set an azimuth angle of 180° because the observatory buildings obscured part of the field of view. No significant difference was found in the counting rates at the three azimuth angles.

6. TIME-VARIATION OF LIGHT PULSE RATE AND THE SEARCH FOR POSSIBLE POINT SOURCES OF COSMIC RADIATION

RYLE (1949), among others, suggested that the intense point sources of radio-emission might in addition be emitters of cosmic-rays. The highly directional features of the Čerenkov light-receivers (Part I, Section 4) make these instruments suitable for searching selected regions of the sky, in that they are shower detectors of considerable effective area possessing an angular resolution hitherto unattainable with simple apparatus. In view of this, a number of experiments were carried out to see if any significant variation of light pulse rate was observable when a light-receiver was directed towards particular regions of the sky. Two types of experiment were done and, throughout these, the mean phototube current was

VOL. 6 1955

kept constant during the night by adjusting the lamp, and the amplifier discriminator was set at twice noise as described before.

(i) A light-receiver (61-cm mirror, field-of-view $\pm 8{\cdot}5°$) was set up with its axis pointing to the zenith, and the counting rate was observed continuously throughout the night on four successive nights. The results for these four runs, added together, are shown in Fig. 4, in which the total counts per time interval of 20 minutes duration, are plotted against sidereal time. With this arrangement, at the latitude of the observatory, the instrument swept out a region of sky which included a portion of the Milky Way and the Cygnus source, the transit times for which are

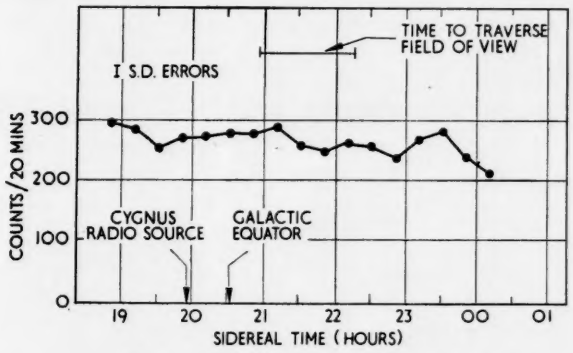

Fig. 4. Time-variations of light pulse rate.

indicated on the figure. It is evident that there is no increase outside the statistical errors in the rate of light pulses.

The results for a similar run on another night, when two 61-cm light-receivers were used each having fields of view of $\pm 2{\cdot}2°$, again showed no significant time variations. The instruments were lined-up on the star Vega and again the Cygnus radio source traversed the field of view.

(ii) A light-receiver having a mirror of 25-cm diameter and a field of view of $\pm 4{\cdot}7°$ was used on a simple mounting, and the light pulse rates compared as the unit was directed, in turn, towards or away from the following particular regions of sky: the two strong radio sources in Cassiopeia and Cygnus, and the Andromeda nebula.*

The receiver was fitted with a cross-wire finder, of field $\pm 2{\cdot}6°$, and the settings, taken from a star atlas, were estimated correct to 1°. In this experiment the runs were each of 30 min. duration, alternately on and off the selected source. Each run off a source was carried out at the same zenith angle as the immediately previous run on the source, thus obviating the changes of rate with zenith-angle discussed in Section 5. The results of these experiments are shown in Table 2(A). Again there is no evidence for any increase in rate of light pulses, and hence of the associated showers, from the three regions studied.

* The Crab nebula, another intense radio emitter, could not be studied because of the proximity of the bright planet Jupiter. Subsequently, at Harwell, this region has been studied and the results are similar to those obtained in the present experiments. For this experiment a light-receiver with a 16-in. mirror was used. This was mounted on an equatorial mounting kindly lent by Dr. BLACKWELL of the University Observatories, Cambridge.

Further results, presented in Table 2(B), from the azimuth angle experiment described in Section 5, also show that there is no significant change in rate when the receiver is directed onto or away from the plane of the Milky Way.

By calculations based upon a simplified theory (see Appendix) we believe that the light pulses detected are, in general, associated with showers of energy 10^{14} eV and greater. Recent experiments on extensive air showers (CRANSHAW and GALBRAITH, 1954) have shown that the flux of primary particles is isotropic for energies up to at least 10^{16} eV, but the existence of isotropy is established in these experiments using apparatus of wide angular resolution. Such apparatus might not detect a small anisotropy coming from a narrow solid angle against the general large background of isotropic radiation, and it was thought that the good angular resolution of the light-receiver might have shown up the presence of such an effect.

Table 2. Results of a search for possible "point" sources of cosmic radiation

All figures refer to total number of light flashes

A						*B*	
Radio source in Cygnus		*Radio source in Cassiopeia*		*Andromeda nebula*		*Galactic plane*	
2 *nights*		3 *nights*		2 *nights*		1 *night*	
On position	*Off position*	*On position*	*Off position*	*On position*	*Off position*	(*Compass points indicated*) *On*	*Off*
						29 (S)	37 (W)
37	39	71	75	67	60	30 (W)	28 (NW)
±6	±6	±8	±9	±8	±8		
						59 ± 8	65 ± 8

7. CONCLUSIONS

The following conclusions are drawn from the experiments described in this paper.

(i) The integral pulse-height distribution of the light pulses follows a power law of the form

$$N(>H) \propto H^{-1\cdot6\pm0\cdot1}$$

where $N(>H)$ is the number of pulses greater than height H.

(ii) The frequency of discharge of a Geiger counter with distance from the light-receiver falls off smoothly with this distance, being largest at the receiver.

(iii) The larger light pulses are, in general, associated with the higher energy showers, but it is not possible to say that a given height of pulse corresponds to a particular shower energy.

(iv) The rate of light pulses at an angle ψ to the vertical is of the form

$$R(\psi) \propto \cos^{\eta}\psi$$

where η lies between 2 and 3.

VOL. 6 1955

(v) The angular distribution of the showers, as measured by the frequency of discharge of a Geiger unit in coincidence with a light pulse, is given by the form $\cos^n \psi$, with n about 6.

(vi) A light-receiver was used to search regions of the sky for possible point sources of cosmic radiation. The results of such searches revealed no significant variations for the two intense radio noise sources in Cygnus and Cassiopeia, the Andromeda nebula and the Milky Way generally.

(vii) An estimate has been made of the shower energy to which the receiver is sensitive and this is approximately 10^{14} eV, or higher.

Acknowledgments—We are grateful to Mr. T. GOLD of the Royal Greenwich Observatory, Herstmonceux, for suggestions and discussions on our work. We re-express our indebtedness to all those acknowledged in Part I of this paper.

Appendix

SHOWER ENERGY DETECTED BY A LIGHT-RECEIVER

To calculate accurately the Čerenkov light intensity distribution on the ground, as functions of the distance from the core of a shower and the energy of the shower, would be a problem of

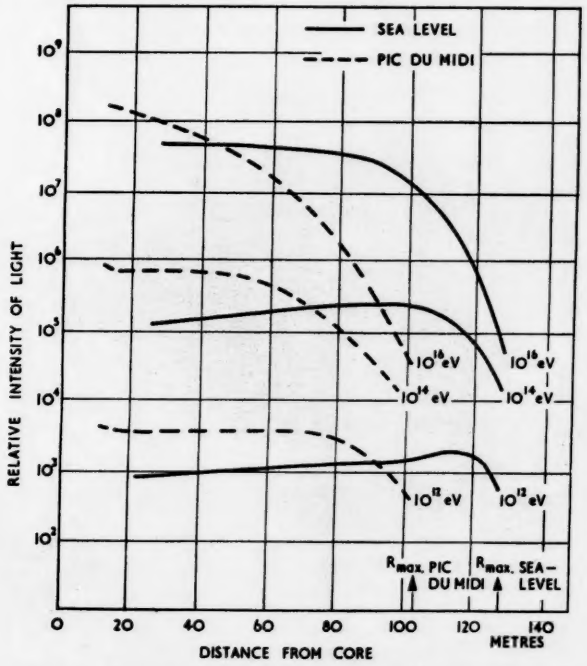

Fig. 5. The distribution, on the ground, of the intensity of Čerenkov radiation, for vertical showers of various energies.

considerable magnitude. Approximations can be made, however, in an attempt to determine the energy of the showers to which a light-receiver is sensitive.

First it is assumed that, for a light-receiver pointing to the zenith, all the showers are vertical

and that most of the light comes from the particles near the core of the shower, where the Coulomb scattering is small (see Part I, Section 4). This implies that the lateral spread of the core on the ground is very much smaller than the diameter of the pool of Čerenkov light. Secondly, the number of electrons having energies $> 10^8$ eV, for different heights in the atmosphere and for various shower energies, is given approximately by the curves produced by CRANSHAW and GALBRAITH (1953) from a modification of the photon-electron cascade theory (ROSSI and GREISEN, 1941) taking into account meson production and the nucleon cascade (MESSEL, 1951). Finally, the intensity of Čerenkov light on the ground from a single relativistic particle travelling vertically is given by the equation (8) derived in the Appendix of Part I.

With the above assumptions, the relative intensity distributions for the light flux on the ground, as a function of the distance from the core of the shower, has been worked out for particular cases. In Fig. 5 are shown curves calculated for vertical showers of various energies at sea-level and the altitude of the Pic du Midi. The change in altitude, as can be seen, makes a considerable difference to the form of the curves.

An order of magnitude estimate of the lower limit to the shower energy detected with the existing apparatus was obtained as follows. A typical light-receiver pointing to the zenith and having a field of view of $\pm 4{\cdot}7°$ gave a rate of detection of light-pulses of 32 pulses/hour at the Pic du Midi. Taking 60 metres for the radius of a circle over which the light intensity is fairly uniform (see Fig. 5), a solid angle of 0·021 steradians (from the above field of view), and the above pulse-rate as the rate of arrival of primary particles at the top of the atmosphere, it is seen that the corresponding flux for these primary particles is $4{\cdot}10^{-9}$ cm^{-2} sec^{-1} steradian^{-1}. From the vertical intensity of the primary particles given by BARRETT *et al.* (1952), the above flux corresponds to showers of energy $> 3{\cdot}10^{14}$ eV. It is emphasized that the effects of Coulomb scattering have here been ignored; this effect would increase the radius of the pool of light and raise the figure for the shower energy.

REFERENCES

BARRETT, P. H., BOLLINGER, L. M., COCCONI, G., EISENBERG, Y., and GREISEN, K.	1952	*Rev. Mod. Phys.* **24,** 133
CRANSHAW, T. E., and GALBRAITH, W.	1953	A.E.R.E. Report No. N/R 1151
	1954	*Phil. Mag.* **45,** 1109
JELLEY, J. V., and GALBRAITH, W.	1953	*Phil. Mag.* **44,** 619
KRAYBILL, H.	1954	*Phys. Rev.* **93,** 1362
MESSEL, H.	1951	*Comm. Dublin Institute for Advanced Studies*, Series A, No. 7
MOLIÈRE, G.	1945	*Cosmic Rays.* Dover Publications
NORTON, A. P.	1950	*Star Atlas and Reference Handbook*, p. 42. Gall and Inglis, London
ROSSI, B., and GREISEN, K.	1941	*Rev. Mod. Phys.* **13,** 240
RYLE, M.	1949	*Proc. Phys. Soc.* **A62,** 491

, VOL. 6 1955

Journal of Atmospheric and Terrestrial Physics, 1955, Vol. 6, pp. 313 to 321. Pergamon Press Ltd., London

The location and shape of the auroral zone

J. H. MEEK*

Radio Physics Laboratory, Defence Research Board of Canada

(*Received* 15 *September* 1954)

ABSTRACT

Variations of the earth's magnetic field have been examined, using data of the Polar Year 1932–33. It is concluded that the auroral zone takes the form of two opposing Størmer-like spirals, one due to positive-particle precipitation and the other due to negative-particle precipitation. These spirals intersect each other at a high latitude at about 10 a.m. local geomagnetic time, and at a lower latitude at about 10 p.m., and move around the earth with the sun. It is proposed that the disturbance-particle stream coming from the sun is not necessarily continuous or uniform. As it passes the earth, charged particles are ejected from it and follow Størmer trajectories into the auroral zone, resulting in the observed auroral light displays and magnetic disturbances. Some of the observed characteristics of aurora are discussed in view of this proposal.

INTRODUCTION

Variations of the earth's magnetic field and auroral displays as observed at Saskatoon show that it is not possible to explain changes observed in particular disturbances by the present theories of magnetic storms and aurorae. One reason for this is that these theories have been formulated to explain the average field variations obtained from statistical analysis of a relatively small amount of polar magnetic data. The statistical averages are not representative of the variations observed in any single disturbance.

In this paper the magnetic data for the Polar year of 1932–33 have been re-examined in an attempt to find general proposals which may be applicable to magnetic and auroral variations observed on particular days. There is insufficient data available to do this properly, but by attempting to avoid any bias toward present theories, some points have arisen which are worth presenting.

Remarks on theories of aurorae and magnetic storms

BIRKELAND (1908), as a result of his detailed analysis of magnetic disturbances, decided that both auroral light and magnetic disturbances were due to precipitation into the upper atmosphere at high latitudes, of electrons coming from the sun. This was supported by his experiments where he projected cathode rays at a magnetized sphere. STØRMER (HARANG, 1951) worked out the mathematical theory for the trajectories of electrons moving in the field of a magnetic dipole, confirming BIRKELAND'S experimental results. He then extended the theory to explain the existence of the auroral-light zone. The Birkeland-Stormer auroral zone was in the shape of a spiral, and thus differed from the closed curve found by statistical analysis of auroral-light observations.

A primary objection to the Birkeland-Stormer theory is that a stream of charged particles of one sign coming from the sun should disperse before reaching the earth. CHAPMAN and FERRARO (1933), by assuming an electrically neutral stream of particles, and ALFVÉN (1950), by assuming that the particles are

* Seconded to University of Saskatchewan, Saskatoon.

moving under the influence of a general solar magnetic field of the order of 50 gauss, indicated possible means of avoiding this difficulty. Some doubt has been expressed about the existence of a solar magnetic field and, as a result, the Chapman-Ferraro explanation is favoured at present. A secondary objection is the apparent time (about twenty-four hours) for the particles to reach the earth from a solar disturbance. Particles of this speed should not have sufficient energy to penetrate to the ionospheric levels at the latitudes where aurora is observed. The ring current, proposed by STØRMER, avoided this difficulty, although it is now believed that a ring current of the size required (twenty earth radii) would not be maintained, due to the mutual repulsion of the charged particles.

The analysis of CHAPMAN and FERRARO showed that a neutral stream of particles would become electrically polarized on passing near the earth, the magnetic field of the latter carving out a hollow in the stream. MARTYN (1950) more recently proposed that this hollow closes in behind the earth, forming a closed-ring current with a radius of about 5·5 earth radii. His estimate of the size of the ring current (also Chapman and Ferraro's size of the hollow) is based on the assumption that the sudden commencement associated with a geomagnetic storm is due to the approach of the solar stream of particles. Since SUGIURA (1953) has recently shown that the sudden commencement (SC) is a localized equatorial phenomenon, the above method of estimating the size of the ring may not be valid. SUGIURA's conclusion is supported by observations of the magnetic field at Saskatoon. If the SC is due to an effect at some distance from the earth which affects the H (horizontal) component at the equator, a variation at the same time should be observed in the Z (vertical) component at the poles. It is estimated that the accompanying variation in the Z at Saskatoon should be about three-fourths of that in H at the equator on the basis of MARTYN's ring current distance. In the past two years Saskatoon records have seldom shown any indication of variations corresponding to the general equatorial SSC as reported in *The Journal of Geophysical Research.*

The following discussion assumes that geomagnetic disturbances are due to a stream of particles ejected from the sun, that the charges separate as they become under the influence of the earth's magnetic field, and that these particles are precipitated into the atmosphere, as proposed by BIRKELAND and STØRMER. Such a process may be fitted to observed diurnal variation of magnetic and auroral disturbances better than the MARTYN and ALFVÉN proposals of charges leaking down the lines of force of the earth's magnetic field.

EXAMINATION OF POLAR YEAR 1932–33 DISTURBANCE DATA

Apart from BIRKELAND'S work, the main effort has been to produce a smoothed worldwide model of polar disturbances, which is based on statistical analyses of magnetic and auroral observations. Due to the comparatively small amount of data in existence, it appears desirable to re-examine it from the point of view of variations in separate disturbances. VESTINE (1947) has tabulated and charted hourly averages of the 1932–33 Polar-Year data in several ways. Using his values of hourly averages for the year of "disturbed days minus quiet days," a polar plot was made of the local geomagnetic time of the diurnal maximum decrease in H for all available magnetic stations north of 40°N. As is seen from

VOL. 6 1955

Fig. 1, all points but one lie along a spiral which expands in a clockwise direction. A corresponding plot of the maximum diurnal increase in H shows a spiral expanding in the opposite direction.

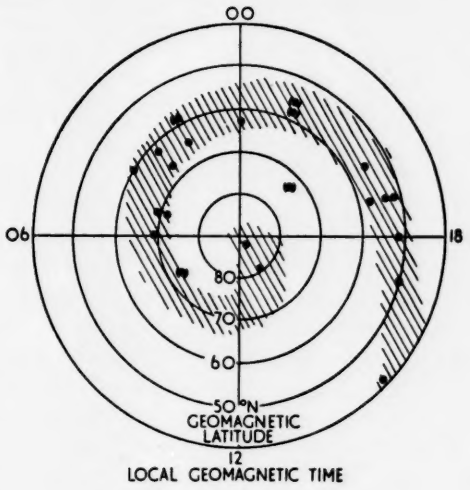

Fig. 1.

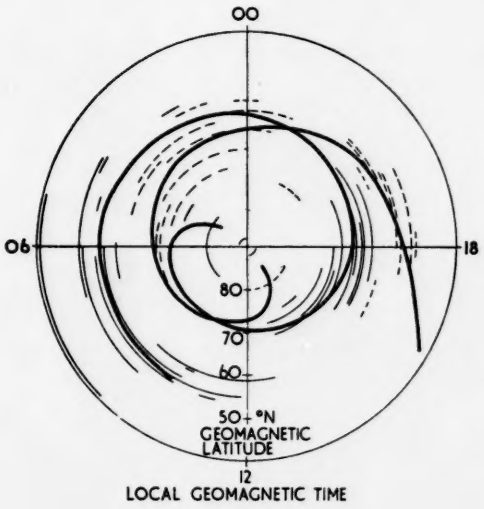

Fig. 2.

A better estimate of the shapes of the spirals was obtained by drawing arcs for each station that covered the hours of the day when the deviation of H was greater than half its diurnal positive maximum and negative diurnal minimum respectively. Fig. 2 illustrates the spirals that result from this procedure. Near the cross-over points of the spirals at about 10 a.m. and 10 p.m. local geomagnetic time,

one would not expect to observe pronounced deviations of H; magnetic stations near these latitudes have maxima displaced to either an earlier or later hour.

Contours for 50-gamma intervals of deviations of H and Z for the same group

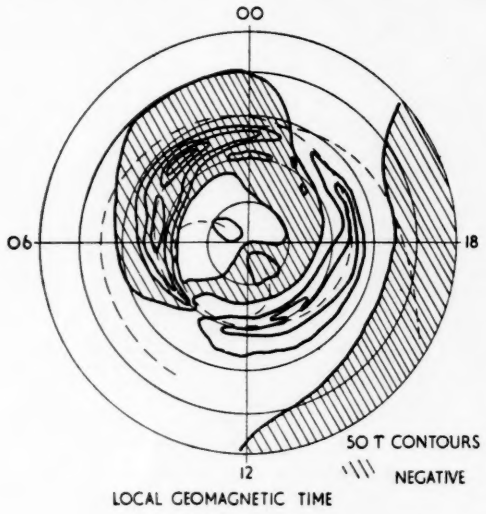

Fig. 3.

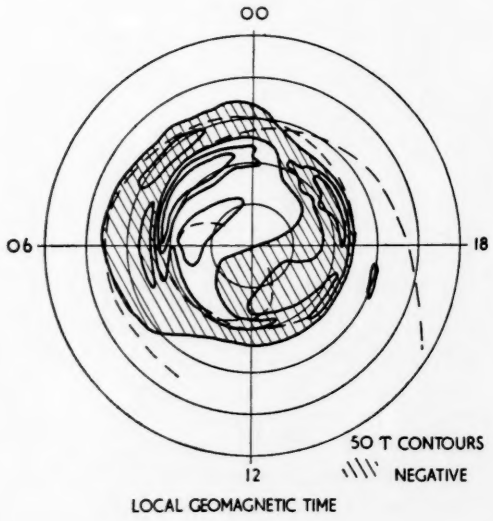

Fig. 4.

of stations are shown in Figs. 3 and 4. These are based on hourly values. The spirals from Fig. 2 are superimposed. These spirals follow the maximum ΔH curve, closely except near the cross-over points. They also follow the zero line for ΔZ, showing that the magnetic-field deviations may be the result of horizontal overhead currents. The large variations observed in declination near the auroral

VOL. 6 1955

zone during disturbances rule out the possibility of a simple, long, uniform line-current along the auroral zone. Although the spirals in Figs. 3 and 4 cannot be traced past the cross-over points, due to the rapid decrease in amplitude of the disturbance field, Figs. 1 and 2 indicate that they exist.

Discussion of the spirals

These spirals immediately bring to mind the precipitation spirals of STØRMER. It is not possible at present to show that they are actually Størmer spirals, but by making such an assumption, a number of the characteristics of auroral and magnetic disturbances can be explained.

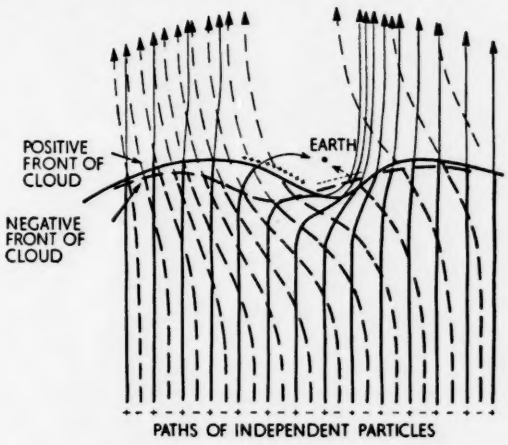

Fig. 5.

Suppose that geomagnetic disturbance is the result of a stream of particles coming from the sun, electrically neutral but not necessarily uniform. In the case of weak disturbances, the groups of particles are actually in isolated clouds, each cloud identifiable with a separate geomagnetic bay and auroral display.

On approaching the earth, a cloud, which is very much larger than the earth, will be indented as the charged particles come under the influence of the earth's magnetic field. Fig. 5 illustrates schematically (not to scale) how the individual charged particles may separate on passing the earth, leaving an excess of positive charges at the leading edge of the cloud on one side of the earth and an excess of negative charges on the other side. Some of the particles will be ejected with high energy from the main cloud toward the earth, travelling along Størmer trajectories to the ionosphere and resulting in the observed precipitation spirals. The spiral expanding clockwise will be due to the precipitation of negatively charged particles, while the spiral expanding anticlockwise to positively charged particles.

As a pure speculation, it is also suggested that the equatorial magnetic sudden commencement is due to neutral particles near the centre of the cloud travelling straight into the ionosphere at the equator. In this case there should be an equatorial SC identified with each polar bay.

The sporadic nature of particular disturbances is illustrated by Figs. 6 and 7, showing plots of the bay disturbance of April 30, 1933, and of May 1, 1933, respectively. These were the most prominent disturbances of the 1932–33 Polar Year,

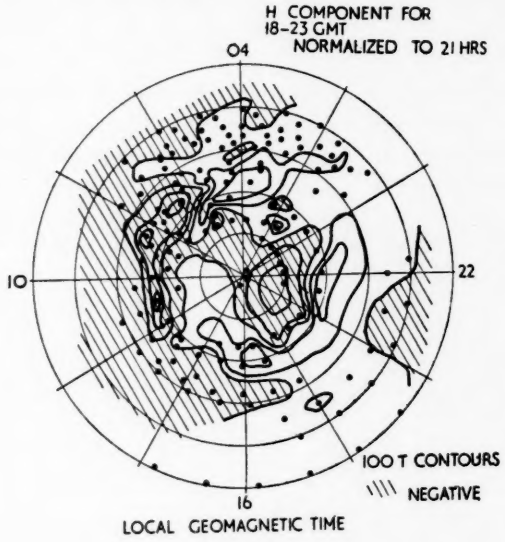

Fig. 6.

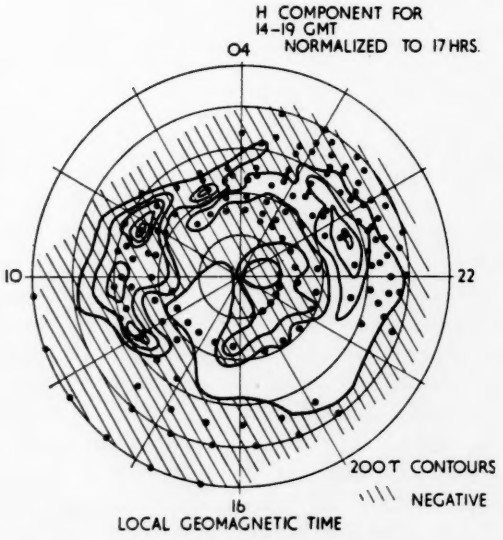

Fig. 7.

and have been investigated by a number of workers. Due to the large areal gaps in the data, it was not possible to draw useful disturbance-field contours for any one hour. Instead, hourly data for a six-hour period were used, displaced at hourly

VOL. 6 1955

intervals on the assumption that the disturbance moved around the earth with the sun. Data were normalized to the hour of maximum disturbance. This method of combining data is normally unsatisfactory, since the usual bay disturbance lasts not more than two hours. Here, the bay on April 30 lasted for about six hours, while that on May 1 lasted about eight hours. The contours for Fig. 7 are drawn at 100-gamma intervals, while those on Fig. 8 are drawn at 200-gamma intervals. The dots in these figures indicate the points where observations were available and thus indicate the areas which were filled in by rough interpolation.

The nonuniform nature of the disturbances is quite marked, and with a little imagination the spiral tracks of maximum disturbance can be seen. It should be noted that STØRMER's theory indicates that the amount of precipitation even from a uniform approaching stream varies along the spiral. If it is assumed that the stream is not necessarily uniform, the sporadic nature of magnetic disturbances is easily understood.

Comparison with auroral light observations

Although definite proof is lacking, there are substantial reasons for believing that the magnetic-disturbance deviations are due to motions of electrical charges near the base of auroral forms (isolated rays are a possible exception). Along the precipitation spirals the magnetic-disturbance vector is nearly horizontal, indicating a horizontal-line current overhead. The observed variations in azimuth of the disturbance vector show that the line current, if it exists, varies in intensity and direction. However, a simple uniform hemispheric auroral zone line current will not explain all the magnetic variations observed during particular disturbances.

The pitch of the precipitation spirals and consequently the location of the auroral-light displays is fixed by the momentum of the precipitating particles. The brilliance of the aurora is related to the numbers of particles coming in as well as to their energy. Both these may be assumed to increase during disturbed periods, accounting for the observed expansion of the auroral zone. One would also expect the disturbed region to extend farther along the spiral, since the cloud of particles from the sun is likely to be denser.

(a) *Diurnal occurrence*

The diurnal variation of aurora will depend upon the position of the observing station relative to the precipitation spirals. From a station situated well inside the spirals one would expect to have a minimum of zenithal aurora near 10 p.m., geomagnetic time. If the inside hooks of the spirals are accompanied by visible aurora, it should take place near sunrise, the arc and bands extending in directions differing greatly from east–west, as is common outside the auroral zone. For stations near the most intense parts of the spirals (65 to 68°N geomagnetic), the maximum auroral frequency should take place near the middle of the night, when aurora due to precipitations from both spirals could be seen at a single station. This is supported by statistical frequency plots, which show a maximum near 10–11 p.m. local geomagnetic time (VEGARD, 1939).

Well south of the auroral zone, visible aurora is likely to be associated with the tails of the spirals. This may explain why MEINEL and SCHULTE (1953) observed

very little aurora near midnight. Incidentally, it will also explain why their drift motions were opposite in direction to those expected from observed magnetic deviations in the main part of the auroral zone.

(b) *Diurnal movement.*

VEGARD (1939) has noted that the aurora draws south in the evening and north in the morning. This follows for auroral-zone stations, since aurora would be expected along the tails of the spirals only during more severe disturbances.

A suggestion was made by myself (1954) that the aurora may expand or extend northward on the northern side of the zone in the early evening. Following proposals in the present paper, the zone probably expands with the onset of a disturbance, but would not generally move northward.

(c) *Direction of arcs*

CURRIE and JONES (1941) note, at Chesterfield (63·3°N, 90·7°W) in 1932–33, a significant decrease in angular direction of auroral arcs towards magnetic east-west direction for a few hours after sunset and another decrease for the few hours before dawn. Other workers have not observed the latter, possibly due to most of their observations having been made during the first part of the night.

Following the proposals of this paper, the changes such as observed by CURRIE and JONES would be expected at a station just inside the maximum auroral zone.

VOL. 6 1955

(d) *Auroral spectrum.*

The anticlockwise spiral has been identified with precipitation of positively-charged particles, so that along this spiral one would expect to detect lines and bands due to positive-particle excitation. For example, at a station just south of the maximum auroral zone such as Saskatoon, one might expect to detect Hα in the northern part of an auroral display before about 11 p.m., and in the southern part after this time. The other parts of displays are more likely to be due to negative-particle excitation and would show the associated spectral features such as the N_2^+ bands.

CONCLUSION

A new version of STORMER'S theory has been presented here, resulting from direct examination of magnetic data. A part of it is pure speculation, but is a reasonable alternative for explaining auroral and magnetic disturbances. It is flexible enough to be applied to individual disturbances and to be used as a guide for detailed analysis of magnetic and auroral observations.

Recent suggestions (WULF, 1953; VESTINE, 1953) that magnetic disturbances are entirely atmospheric circulation effects have not been considered. It would be difficult to explain the presence of the above observed spirals by such theories.

Acknowledgments—This work is done as a project of the Defence Research Board of Canada. The author would like to thank Dr. B. W. CURRIE, Dr. A. VALLANCE JONES, and Dr. D. M. HUNTEN of the University of Saskatchewan for their interest in and their comments and criticisms of this paper.

References

Alfvén, H.	1950	*Cosmical Electrodynamics*, Ch. 6, Oxford.
Birkeland, Kr.	1908	*Norwegian Aurora Polaris Expedition of* 1902–1903, Christiania
Chapman, S., and Ferraro, V. C. A.	1932–33	*Terr. Magn.* **38** and **37**
Currie, B. W., and Jones, C. K.	1941	*Terr. Magn.* **46**, 269
Martyn, D. F.	1950	*U.R.S.I. Mixed Commission on Ionosphere*, p. 49, Brussels Meeting September 1950
Meek, J. H.	1954	*J. Geophys. Res.* **59**, 87
Meinel, A. B., and Schulte, D. H.	1953	*Ap. J.* **117**, No. 3
Størmer, C.	1951	Theory summarized in L. Harang, *The Aurorae*, Chapman and Hall
Sugiura, M.	1953	*J. Geophys. Res.* **58**, 560
Vegard, L.	1939	*Terrestrial Magnetism and Electricity*, Ch. XI, Ed. J. Fleming, McGraw-Hill
Vestine, E. H.	1953	*J. Geophys. Res.* **58**, 531
Vestine, E. H., Laporte, L., Lange, I., and Scott, W. E.	1947	Carnegie Institution of Washington, Pub. No. 580
Wulf, O. R.	1953	*J. Geophs. Ryes.* **58**, 539

Journal of Atmospheric and Terrestrial Physics, 1955, Vol. 6, pp. 322 to 327. Pergamon Press Ltd., London

An experimental problem in the atmospheric-electrical synopsis

The separation of conduction current and Maxwell's displacement current in measurements of the air-earth current

Paper presented to the Joint Meeting of the IATME and the Association of Meteorology of the JUGG at Rome on 18 September 1954 by

H. ISRAËL
Meteorologisches Observatorium Aachen des Deutschen Wetterdienstes

(*Received* 11 *December* 1954)

ABSTRACT

In order to separate the different influences causing the atmospheric-electrical variations, a synoptical method of research has been applied. The measurement of the air-earth current, needed in this method, is commonly disturbed by the variations of the atmospheric-electrical field which produce a displacement current in the "antenna." This difficulty can be avoided by an arrangement proposed by H. W. KASEMIR, which enables us to separate the displacement current and the conduction current. The "method of adaptation" is described. A few examples show that by employing this method all variations of the air-earth current can be measured correctly.

1. THE ROLE OF THE AIR-EARTH CURRENT IN SYNOPTICAL ATMOSPHERIC-ELECTRICAL STUDIES

As we know, the electric field of the atmosphere is caused primarily by the global thunderstorm activity and is modified by local meteorological effects which change the conductivity of the air. In order to separate these two influences, a synoptical method of research has recently been applied (ISRAËL, 1954).

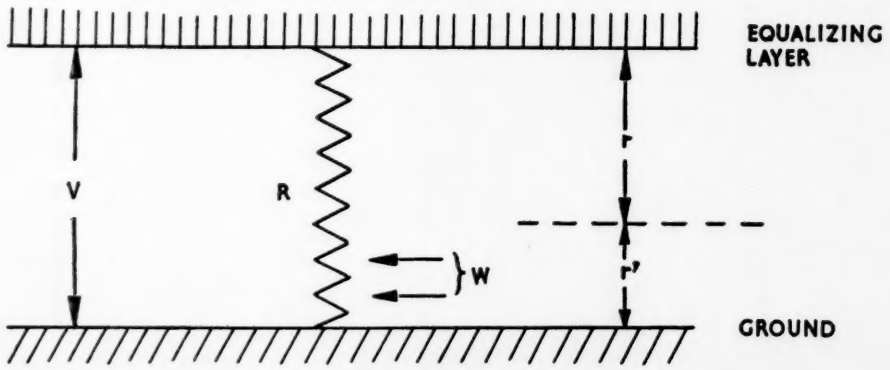

Fig. 1. The electrical conditions in the atmosphere.

The term "synoptical method" means an *expansion* of the researches as well as an *extension*—an *expansion over a network of stations, and an extension to include the study of several elements simultaneously*. In this respect combined measurements of the potential gradient E and the air-earth current i are of particular interest.

Fig. 1 represents the electrical conditions in the atmosphere. The potential gradient E, the density i of the air-earth current, the specific resistance w, and the

VOL. 6 1955

conductivities λ^+ and λ^- of the air are connected for stationary conditions by the equations:

$$i = E/w \qquad w = 1/\Lambda = 1/(\lambda^+ + \lambda^-)$$

$$i = V/R \qquad R = \int_0^\infty w(h)\, dh = (r + r')^* \tag{1}$$

$$E = w \,.\, V/R$$

Thus for stationary conditions a simultaneous measurement of two electrical elements—E and i, E and w, i and w—will give a complete picture of the atmospheric-electrical current system. It is obvious that the best combination will be the simultaneous measurement of E and i, because we can separate by this, furthermore, conduction currents and convection currents in the atmosphere. Also when the supposed stationary conditions are fulfilled not wholly it is to expect that the air-earth current will be affected to a smaller extent by local variations of the conductivity than the potential gradient—by reason of the fact that the current has the tendency to reach the same value in all heights.

2. The Measurement of the Air-earth Current

Measurements of the air-earth current are commonly disturbed by the variations of the atmospheric-electrical field: The current entering the Wilson-plate P (see Fig. 2) produces across the high-resistance R a potential drop which can be

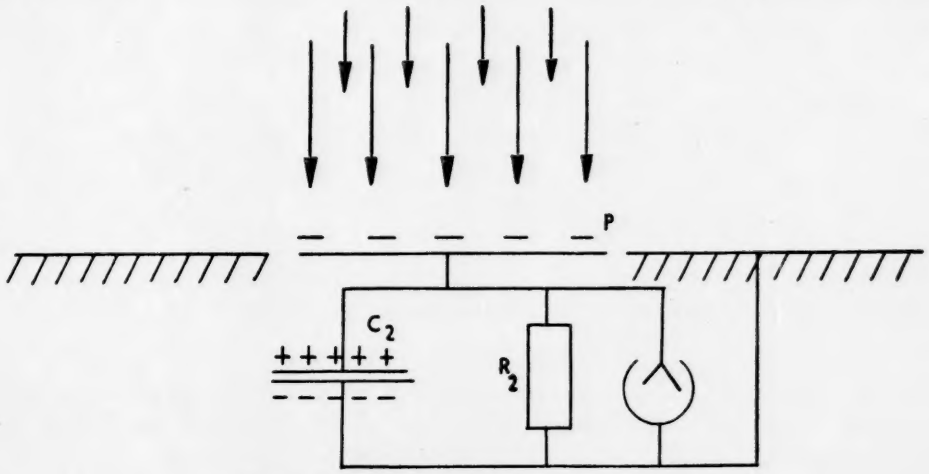

Fig. 2. Principle of measuring air-earth current.

measured. A simultaneous variation in the electric field will produce a displacement current which may be erroneously interpreted as a part of the conduction current.

Methods to avoid such an error as proposed by C. T. R. Wilson (1908), F. J.

* The division of the columnar resistance R into the two parts r and r' means, that the upper part R normally is constant whereas the lower part r' becomes variable by meteorological influences (Wait, 1952).

SCRASE (1933), and others are satisfactory for studies on time-averages of the current. For fast time-variations a method proposed by H. W. KASEMIR (1954) may be adapted to solve this difficulty in the following manner (see Fig. 2).

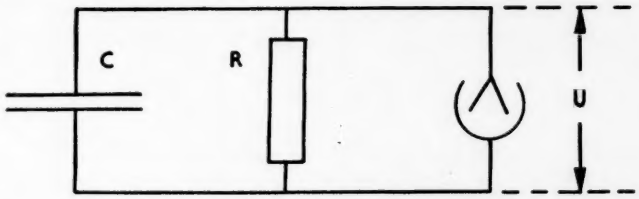

Fig. 3. Time-constant of a "C-R element."

When for constant atmospheric conductivity the electric field E varies, the current i will vary proportionally. If the values for C and R can be chosen so that the displacement current will give a voltage drop across C which is equal to the voltage drop across R caused by the conduction current, then a true measurement of conduction current will be obtained. Furthermore, we shall see now that such values for C and R which are found to fulfil our condition for one frequency, fulfil

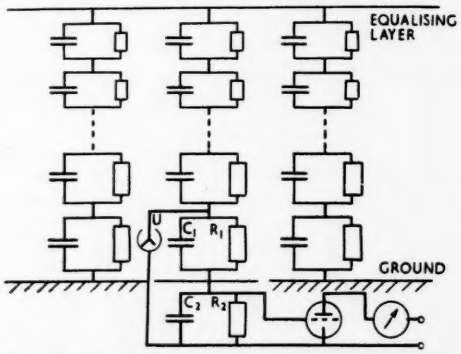

Fig. 4. Equivalent circuit of the atmospheric-electrical system.

this condition for *all* frequencies. That means, that both periodic and nonperiodic variations of the conduction current can be properly measured.

3. CALCULATION OF R AND C

If changes occur in the atmospheric-electrical system, the electric field does not immediately reach its new stationary value, but does so after a few multiples of the "relaxation time" T (6), as given by equations (2):

$$E_t - E_\infty = (E_0 - E_\infty) \,.\, e^{-t/T} \qquad (2)$$

$$T = \tfrac{1}{4}\pi\Lambda = \varepsilon/\Lambda$$

The dimensions are given by equation (2a):

$$[T] = [\varepsilon/\Lambda] = [\text{farad/cm . ohm . cm}] = [\text{farad . ohm}] = [R \,.\, C] \qquad (2a)$$

$1/\Lambda$ is the specific resistance of the air. If we identify the dielectric constant ε with the specific capacity of volume, then the process given in equation (2) corresponds to the discharge of a condenser C through a resistor R as given in Fig. 3.

VOL. 6 1955

Therefore the electrical features of the atmosphere may be demonstrated by the equivalent circuit shown in Fig. 4.

Each unit of air corresponds to a "C-R element." The value of R decreases rapidly with increasing height, while the value of C remains nearly constant for all heights.

The arrangement for measuring the field and air-earth current as given in the lower part of Fig. 4 is shown separately again in Fig. 5.

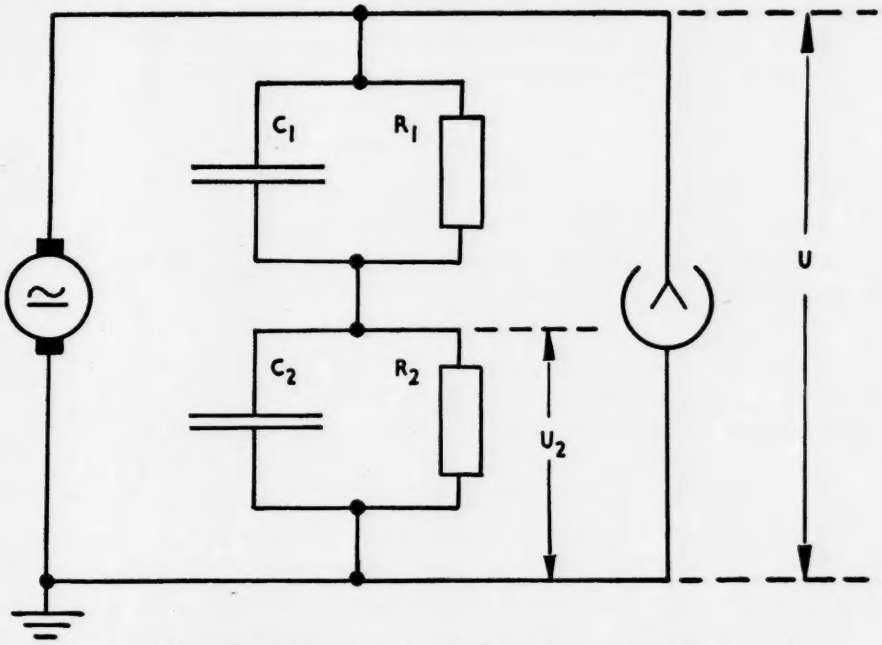

Fig. 5. Principle of measuring the field and air-earth current.

The upper RC element (R_1C_1) represents the lowest part of the atmosphere; the lower RC element (C_2, R_2) represents the measuring equipment. U is the value of the potential difference between the point in the atmosphere where the collector is situated and the ground, varying with the time. Thus by U is given a value for the electric field. On the other hand, U_2 represents the potential difference between the Wilson-plate P and the ground, giving a value for the air-earth current. The electric field E is always proportional to the air-earth current. For this reason a correct measurement of the current density i is possible only if

$$\frac{U_2}{U} = \text{const.} \tag{3}$$

The equation for this proportion is:

$$\frac{U_2}{U} = \frac{1 + j\omega R_1 C_1}{1 + \frac{R_1}{R_2} + j\omega R_1 (C_1 + C_2)} \tag{4}$$

$j = \sqrt{-1}$

ω = circular frequency of the potential U.

Equation (4) can be transformed into

$$\frac{U_2}{U} = \frac{C_1}{C_1 + C_2} + \frac{\dfrac{R_2}{R_1 + R_2} - \dfrac{C_1}{C_1 + C_2}}{1 + j\omega \dfrac{R_2}{R_1 + R_2} \dfrac{C_1 + C_2}{C_1}} R_1 C_1 \tag{5}$$

and again by the substitution

$$\frac{C_1}{C_1 + C_2} = c; \quad \frac{R_2}{R_1 + R_2} = r; \quad R_1 C_1 = T_1 \tag{6}$$

into

$$\frac{U_2}{U} = c + \frac{r - c}{1 + j\omega \dfrac{r}{c} T_1} \tag{7}$$

The value of U_2/U ceases to be complex and is independent of the frequency and always constant if

$$r = c; \text{ i.e., } T_1 = T_2. \tag{8}$$

This means that the potential U_2 of the Wilson-plate P, and with it the measured value of the density of the air-earth current i, follows all variations of the potential gradient without any phase-shift and is always proportional to it.

, VOL. 6 1955

4. THE PROCEDURE OF "ADAPTATION" ("Matching"? = "Anpassung")

We now have to consider how we can determine the values of C and R for the "adaptation" of the measuring circuit. There are several possibilities:

(a) Using the equations (2) and (8), we can calculate the values of C and R: Since the conductivity of the atmosphere in the lower layers has nearly the value $\Lambda = 2 \cdot 10^{-4}$ e.s.u., the time-constant of the measuring circuit should be nearly 400 sec.

(b) From the simultaneous records of the electric potential gradient and the air-earth current phase-differences may be inferred, which give an approximate information with regard to the adaptation which is sufficient in many cases.

(c) A more accurate information is given by the study of current changes caused for example by lightning (see Fig. 7) or by sudden field-changes produced artificially in the air surrounding the measuring antenna.

Since the time-constant of the apparatus must agree with the relaxation-time of the surrounding air, consequently the degree of "adaptation" will be changed by variations of the conductivity of the air. Calculating the values of U_2/U for diverse frequencies by equation (7), one can see that the changes of the degree of adaptation are unimportant when the variation of the conductivity is small. For researches of the hourly means or the diurnal variations of the air-earth current the normal variation of the conductivity during the day is irrelevant, whereas the record of a current variation caused by lightning, as shown in Fig. 7, claims an adaptation as correct as possible.

5. Examples

Figs. 6 and 7 give examples of records with a properly adapted measuring circuit (Kasemir, 1945).

Fig. 6 shows in detail the parallel nature of potential gradient and air-earth current curves when the equipment is properly "adapted."

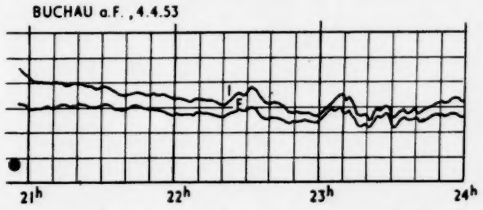

Fig. 6. Parallel curves of potential gradient and air-earth current when the apparatus is "adapted." (Buchau a.F., 4. IV. 1953.)

Fig. 7 shows a record of the air-earth current during a thunderstorm. The current changes caused by lightning are exactly the same as the well-known field changes caused by lightning and its recovery. This is evidence for the fact that *all* frequencies are reproduced correctly when the "adaptation" of the measuring equipment is correct.

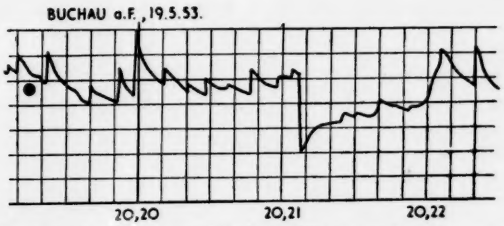

Fig. 7. Thunderstorm-record with a well-"adapted" apparatus for current-measurements. (Buchau a.F., 15. V. 1953.)

References

Benndorf H. 1925 Grundzüge einer Theorie des elektrischen Feldes der Erde. 1927 Wiener Berichte (II a) **134,** 281–315 und **136,** 175–194.

Israël H. 1954 Luftelektrische Synopsis. *Mitteilungen des Deutschen Wetterdienstes* Nr. 7 (April)

1954 Atmospheric electricity and meteorology. (Paper presented to the Conference on atmospheric electricity at Wentworth-by-the-Sea, Portsmouth, N.H. (May 19–21) (in press).

Kasemir H. W. 1954 Measurement of the air-earth current density. (Paper presented to the Conference on atmospheric electricity at Wentworth-by-the-Sea, Portsmouth, N.H. (May 19–21) (in press).

Scrase F. J. 1933 The air-earth current at Kew Observatory. *Geophys. Memoirs (London),* **7,** No. 58,

Wait G. R. 1952 Electrical resistance of a vertical column of air over Watheroo (Western Australia) and over Huancayo (Peru). *Terr. Magn.* **47,** 243–249

Wilson C. T. R. 1908 On the measurement of the atmospheric electrical potential gradient and the air-earth current. *Proc. Roy. Soc.* **A80,** 537–543

Journal of Atmospheric and Terrestrial Physics, 1955, Vol. 6, pp. 328 to 335. Pergamon Press Ltd., London

On the measurement of rotational temperature from unresolved auroral nitrogen bands*

G. G. SHEPHERD† and D. M. HUNTEN
University of Saskatchewan, Saskatoon

(*Received* 14 *September* 1954)

ABSTRACT

It is pointed out that the intensity of an unresolved profile depends not only on the intensity of the lines but also on their spacing. Neglect of the correction for spacing can give rotational temperatures too low by 40° at 250°K and 400° at 1000°K when the 3914 Å band of N_2^+ is used. 180 temperature measurements have been made on aurora, and fifteen are accompanied by measured heights. Although the observations cover too small a height-range to be conclusive, both the variation of temperature with height and the variation with type of aurora appear to agree with the generally accepted temperature gradient in the auroral region.

INTRODUCTION

The measurement of rotational temperature in the aurora is of considerable interest in the study of the upper atmosphere. VEGARD (1947, 1951) has made extensive measurements, using unresolved negative-group N_2^+ bands at 3914 Å and 4278 Å. The average temperature obtained by him is about 230°K, which agrees with the generally accepted value of kinetic temperature at 100 km, the height at which most aurora occurs. However, the same temperature was obtained from aurora at much greater heights. This is very much in disagreement with current ideas on the kinetic temperature, which is believed to increase rapidly with height above 100 km.

PETRIE (1953) obtained a spectrum of the 3914 Å band in which the peaks of the lines were resolved, but the lines not fully separated. A temperature of 500–750°K was deduced from this spectrum, which was obtained from high altitude aurora.

VALLANCE JONES *et al.* (1953) have more recently obtained auroral spectra of the 3914 Å band in which the lines are completely separated. These yield temperatures of about 300°K.

The present measurements have been carried out on the same band with a scanning spectrometer previously described (HUNTEN, 1953). This spectrometer has a 4″ × 4″ plane grating and a 1P21 photomultiplier detector cooled with dry ice. A range of about 50 Å was scanned in 10 seconds. With slit-widths such that the resolution was 2 Å, unresolved spectra could be obtained from moderately bright aurora. The short scanning time made it practical to take simultaneous double-station photographs from which the heights of the auroral forms could be measured. One of the auroral cameras was mounted on the spectrometer and adjusted so that the field of the spectrometer (about 1/4° wide and 3° high) was in the centre of the picture. Unfortunately, only fifteen heights were obtained, and the range of height was rather small. The rest of the temperatures were used by

* The research reported in this paper has been sponsored by the Geophysics Research Directorate of the Air Force Cambridge Research Center, Air Research and Development Command, under Contract AF 19 (122)–152.

† Holder of a Bursary from the National Research Council of Canada.

VOL. 6 1955

studying the variation with type of aurora. Both methods indicate that the temperature increases with height.

Resolution of the rotational lines could have been accomplished only with a large decrease in signal-to-noise ratio, resulting in greatly increased errors in intensity measurements. It is therefore more accurate, under these conditions, to measure intensities from the unresolved profiles. These profile intensities must, however, be corrected for resolution to give line intensities; this correction seems to have been neglected by previous workers.

We proceed to describe the method of correction, and its testing in the laboratory with a discharge-tube source. Some preliminary measurements on aurora are then presented, and these results and those of other workers are discussed.

Intensity Correction of Unresolved Profiles

The rotational temperatures were measured in the usual way, by plotting log (I/K') against $K'(K'+1)$ for the R branch of the band, where I is the relative line intensity and K' the rotational quantum number of the line. The temperature is found from the slope of the resulting linear plot. This method is well described by Petrie (1953).

The height of the unresolved profile at any wavelength (see Fig. 1) depends both on the line intensity and the line spacing at that wavelength. Since the spacing in the R branch varies along the band, it is apparent that a correction is necessary. It is reasonable to take the profile height as inversely proportional to the line spacing. On this basis, multiplying the profile heights along the band by factors proportional to the line spacing gives the relative line intensities. Table 1 gives the correction factors for the profile at the positions used.

Table 1. *Correction factors for profile intensities*

K'	*Correction factor*	K'	*Correction factor*
5	0·84	11	1·12
6	0·89	12	1·16
7	0·93	13	1·21
8	0·98	14	1·26
9	1·02	15	1·30
10	1·07		

The validity of the correction was checked by constructing a spectrum corresponding to a temperature of 250°K, and graphically finding the profile resulting from 2 Å resolution. The above correction was applied to it, and the temperature found to be within 3 per cent of the original 250°K.

Neglecting the correction would make temperature values too low. The error is only 40° at 250°K, but is 400° at 1000°K.

It has been pointed out by Dr. A. Vallance Jones in a private discussion that this method might not be valid for photographic spectra taken with a very narrow

slit. The resolution is then defined by the spreading of the image in the emulsion, rather than by the slit. This spreading is probably not simple enough to be described as we have done. On the other hand, if the slit is wide enough so that its image can be fully resolved by the emulsion, the correction should be applicable.

LABORATORY TEST OF THE CORRECTION

Several spectra of the 3914 Å band were obtained from the hollow-cathode discharge tube used by VALLANCE JONES and HARRISON (1955). Temperatures obtained

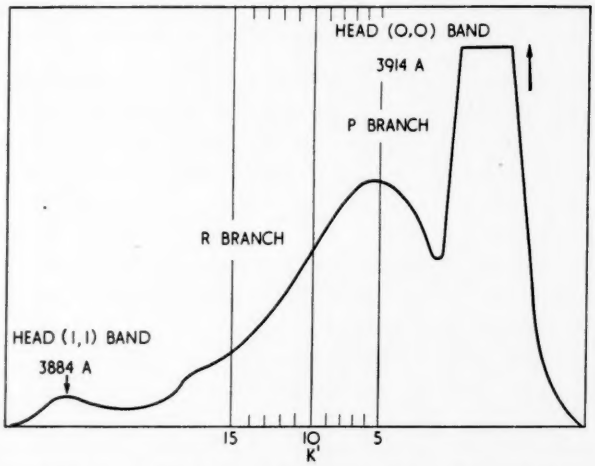

Fig. 1. Typical spectrum of the 3914 Å negative group N_2^+ band obtained from a hollow-cathode discharge tube. The P-branch intensity is greater than full scale. K' values and positions of lines in the R branch are indicated.

from these spectra were compared with values that they obtained using a spectrograph which separates all the lines. They found that as the current through the tube decreased, the rotational temperature approached room temperature. With a small current, the mean of eleven temperatures obtained with the scanning spectrometer was 20°C, very close to room temperature. This demonstrates that the method used is reliable. Fig. 1 shows a sample spectrum obtained from the discharge tube, and Fig. 2 the corresponding plot of log (I/K') against $K'(K'+1)$.

PRELIMINARY RESULTS FROM AURORAL SPECTRA

Because of the present minimum in the eleven-year sunspot cycle, only a limited number of auroral spectra have been obtained, and there is little prospect of obtaining more until the auroral activity increases. Thus, although these results may not be conclusive, it is felt that they are of sufficient interest to publish at the present time.

Examples of auroral spectra corresponding to various temperatures are given in Fig. 3. Unlike the laboratory spectrum of Fig. 1, these profiles have been smoothed by eye to reduce random noise. The plots of log (I/K') against $K'(K'+1)$ for these spectra are shown in Fig. 4. They are nearly straight, as may be seen. The

VOL. 6 1955

spectra chosen gave temperatures near the maximum and minimum obtained, with another near the mean value.

In all, 180 temperature values were obtained from six nights of observation. They vary from 150°K to 465°K, with a mean of 258°K. Although double-station

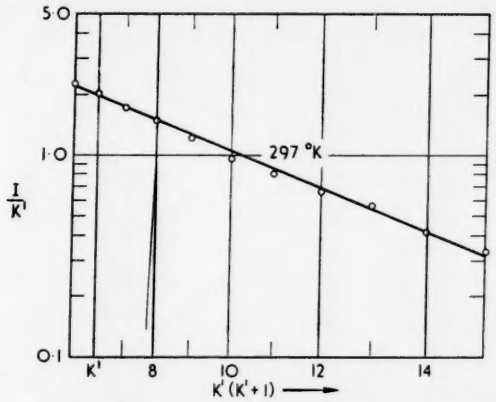

Fig. 2. Plot of log (I/K') vs. $K'(K'+1)$ for the spectrum shown in Fig. 1. The slope corresponds to a temperature of 297°K.

photographs were taken on three of these nights, only a few usable spectra have accompanying height measurements. Many spectra were too faint to be measured accurately, and many auroral forms giving good spectra were not suitable for height determinations. (To be suitable, a form must have a sharp border oriented correctly

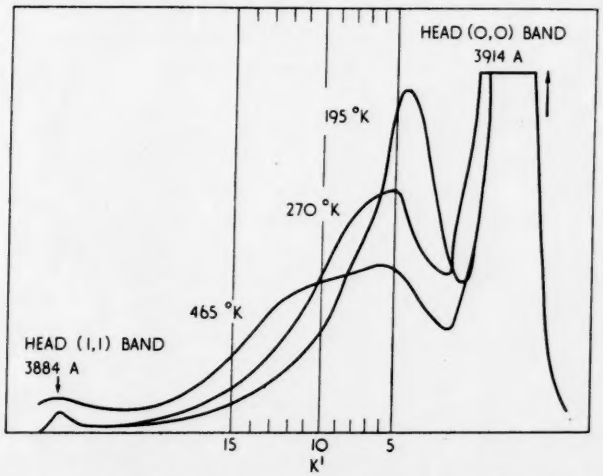

Fig. 3. Auroral spectra of the 3914 Å negative group N_2^+ band corresponding to the various temperatures indicated. The area under the R branch is normalized. (These profiles are smoothed of noise.)

with respect to the baseline.) So far only fifteen simultaneous sets of temperature and height measurements have been obtained. Fig. 5 shows a plot of the temperatures against the corresponding height. The mean temperature curve from rocket measurements (The Rocket Panel, 1952) is shown for comparison.

Our points are distributed about this curve, indicating that the kinetic and rotational temperature are roughly in agreement. A temperature gradient is suggested, but the evidence is hardly conclusive. There is, however, a striking

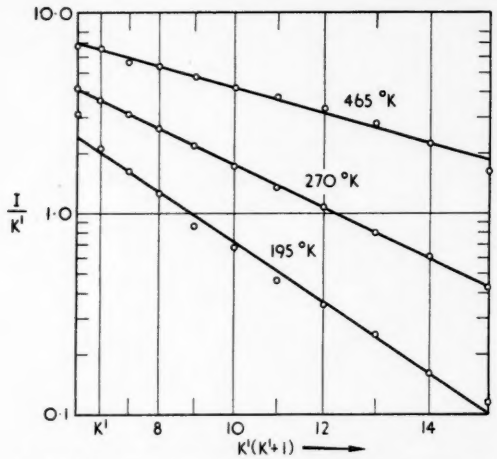

Fig. 4. Plots of log (I/K') vs. $K'(K'+1)$ for the auroral spectra in Fig. 3.

difference between these measurements and those of VEGARD, which would lie along a vertical line if plotted on this graph. According to The Rocket Panel, the true curve of temperature versus height is probably very irregular at any moment, the mean curve giving a poor representation of the actual conditions at any instant.

VOL. 6 1955

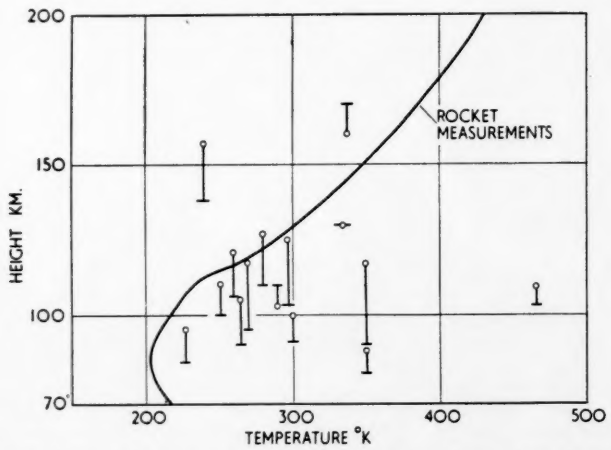

Fig. 5. Rotational temperature measurements with heights obtained by parallactic photography. Vertical lines indicate extension from measured point on auroral contour, with the bar showing the measured point and the circle the centre of the spectrometer field. The Rocket Panel curve is shown for comparison.

If this is so, our measurements may not be as inconsistent as they at first appear. Measurements from greater heights would probably settle the question, but we have so far been unable to get any.

More evidence on the variation of temperature with height is obtained from the measurement of temperature for different types of aurora. It is known that rays and draperies are usually found at the greater heights, and that forms with red lower borders (Type *B*) are usually rather low. Ordinary green arcs and bands can be expected to be in between. The aurora was thus classified into the groups shown in Table 2 (we observed no arcs), and the percentages of each group giving high, medium, and low temperatures were found. Table 2 shows that most of the rays and draperies give high temperatures, most of the Type *B* bands give low temperatures, and the homogeneous and ray bands favour the intermediate temperatures.

Table 2. Variation of temperature with auroral type.
The percentage of a type in each temperature class is given.

Auroral type	*Rays and draperies*	*Homogeneous and ray bands*	*Type B bands*
Number of observations	34	104	30
High 275–465°K	85%	26%	10%
Average 221–274°K	9%	48%	37%
Low 150–220°K	6%	26%	53%

This is strong evidence for a temperature increasing with height. Together with the temperature-height measurements, it indicates that the rotational and kinetic temperatures may be in agreement.

The accuracy of parallactic height measurements is limited by the length of the base line, and by the position of the auroral forms relative to it. The base line used here was about 34 km long, which is near the minimum useful length. The most serious error, however, enters in finding the height of the point on the aurora at which the spectrometer was directed, because there is a good deal of variation with different auroral forms on same photograph. Only the heights of well-defined borders may be measured; other points must be estimated with respect to these. This was done by assuming that the vertical extension of the aurora is along magnetic lines of force. Such a procedure may in some cases lead to considerable error.

Discussion

It is important to attempt to decide whether or not the rotational temperature should be expected to be the same as the kinetic temperature in the aurora. There are at least four possibilities to be considered:

(1) The N_2^+ ion spends enough time in the excited state to reach thermal equilibrium before radiating.

(2) The N_2^+ ion is excited from the ground state of the neutral molecule by

electron impact, leaving the total angular momentum unchanged, so that a thermal distribution will exist in the upper state.

(3) Excitation as in (2), but from the ground state of the N_2^+ ion rather than the neutral molecule.

(4) Some other type of excitation, as for example by heavy particles.

Case (1) is immediately excluded because of the long time between collisions as compared with the lifetime of the state. Cases (2) and (3) are both plausible. Case (2) is generally considered as being true, because of the larger number density of the neutral molecule, but SWINGS and MEINEL (1952) advocate case (3) because the lower excitation energy required is more consistent with the rest of the auroral spectrum. On the other hand, the relative populations of the vibrational levels giving this band system are strongly in favour of Case (2) (PETRIE and SMALL, 1953; and unpublished measurements of our own). Fortunately, since the B values of all three states are very nearly the same, it does not make much difference to the computed temperature. We have adopted case (2) for the aurora, and (3) for the laboratory discharge as being most probable. These have B values of 2·010 cm^{-1} and 1·932 cm^{-1} respectively (HERZBERG, 1950).

Case (4) would probably result in a non-thermal distribution giving non-linear plots of log (I/K') against $K'(K'+1)$, or unreasonable temperatures. Neither has been observed.

Because of the relatively small number of high temperatures obtained here, it appears that it would be difficult to obtain a high temperature when a long exposure time is used. Even when an attempt is made to include only high-altitude forms, a significant portion of the radiation received may originate from lower altitudes. This may in part be the reason why VEGARD did not detect temperature changes with height. In addition, as mentioned previously, the effect on the profile due to lack of resolution may be difficult to allow for where the resolution is determined not by the slit-widths, but by some other effect. Although PETRIE (1953) obtained a high rotational temperature from high-altitude forms, his result is somewhat uncertain (as he himself points out) because of the difficulty of correcting for the varying distance between the lines. It does, however, give evidence of a temperature gradient.

The work of VALLANCE JONES and HARRISON (1955) is in agreement with the present results. They found that the assumption of a temperature gradient was necessary in order to produce the spectra they obtained.

VOL. 6 1955

CONCLUSIONS

Fairly accurate rotational temperatures may be obtained from unresolved profiles with a scanning spectrometer, provided a suitable correction is made. The short scanning time makes it possible to obtain spectra of specific forms, whose height may be measured simultaneously by parallactic photography. Preliminary results indicate a rotational temperature increasing with height through the lower auroral region, in agreement with the generally accepted kinetic temperature. We should like to express our thanks to Dr. B. W. CURRIE, who initiated us into the art of measuring auroral heights; to Mr. R. P. PENNER, who took the second-station photographs; and to Dr. A. VALLANCE JONES, who participated in many discussions.

References

Herzberg, G.	1950	*The Spectra of Diatomic Molecules*, 2nd ed., Van Nostrand, New York, Table 39, p. 553.
Hunten, D. M.	1953	*Can. J. Phys.* **31**, 681
Petrie, W.	1953	*J. Atmosph. Terr. Phys.* **4**, 5
Petrie, W., and Small, R.	1953	*Canad. J. Phys.* **31**, 911
Rocket Panel, The	1952	*Phys. Rev.* **88**, 1027
Swings, P., and Meinel, A. B.	1952	*The Atmospheres of the Earth and Planets*, 2nd ed. (ed. G. P. Kuiper), University of Chicago Press.
Vallance Jones, A., Hunten, D. M., and Shepherd, G. G.	1953	*Astrophys. J.* **118**, 350
Vallance Jones, A., and Harrison, A. W.	1955	*J. Atmosph. Terr. Phys.* **6**, 336
Vegard, L.	1947	Report Gassiot Committee, Phys. Soc. Lond.
	1951	*The Aurorae* (L. Harang), Chapman and Hall, London, p. 83

Journal of Atmospheric and Terrestrial Physics, 1955, Vol. 6, pp. 336 to 343. Pergamon Press Ltd., London

Rotational temperatures of the auroral N_2^+ bands*

A. VALLANCE JONES and A. W. HARRISON
University of Saskatchewan, Saskatoon, Sask., Canada

(*Received* 14 *September* 1954)

ABSTRACT

A series of auroral spectra in which the 0–0 N_2^+ band is completely resolved, have been obtained at Saskatoon. Analysis of the plots of log I/K' against $K'(K'+1)$ for intensity distribution of the rotational fine structure lead to temperatures ranging from 250° to 400°K. Some of the plots exhibit a curvature which has been interpreted as arising from a variation of temperature with height through the auroral region. The conclusions reached have been tested by obtaining spectra from a laboratory source of the N_2^+ bands.

INTRODUCTION

The temperature of the upper atmosphere may be estimated in a number of different ways; one of the most easily applied methods is based upon the temperature dependence of the intensity distribution in the rotational fine structure of molecular bands emitted by the aurora and airglow. This method is certainly valid, if conditions of thermal equilibrium obtain and self-absorption of the emitted radiation is small. Since the auroral luminosity is not excited thermally but by collisions with fast primary or secondary particles, the derivation of a temperature from the rotational intensity distributions depends upon a number of special circumstances and assumptions.

It must be assumed that the auroral process does not materially disturb the condition of thermal equilibrium defined by the local kinetic temperature. This temperature may be derived from the rotational intensity distribution of emission bands for two cases.

Case (a). The lifetime of the excited molecule is long compared to the interval between collisions, so that it is likely that the excited molecules will come into thermal equilibrium with their surroundings as far as concerns rotational, translation, and vibrational energy. In this case the rotational intensity distribution provides a direct method of measuring the local temperature.

Case (b). The lifetime of the excited state is short compared to the collision interval, so that the distribution of the excited molecules among the rotational energy levels will be dependent upon the rules governing changes in rotational quantum number in the excitation process. In this case it is necessary to have or assume some special knowledge of the excitation process. This paper is concerned with an example of the second case, i.e., a permitted transition.

Of the strong permitted band systems of the aurora, only the N_2^+ First Negative system is suitable for accurate measurements of rotational intensity distribution. An estimate of the temperature may then be made if it is assumed that the excitation process is such that $\Delta J \simeq 0$. While this is undoubtedly true for excitation by electron collision, it may not be true for excitation by proton collision. However, the success of the method in practice provides the best justification for this assumption. As a consequence of this assumption the distribution of the excited molecules

* The research reported in this paper has been sponsored by the Geophysics Research Directorate of the Air Force Cambridge Research Center, Air Research and Development Command, under Contract AF 19 (122)–152.

, VOL. 6 1955

with J' will be the same as the distribution of the unexcited molecules with J''. The latter distribution depends on B'', the rotational constant of the unexcited state. In the case of the First Negative bands in the aurora, the unexcited state is taken as the N_2 molecule; it has also been suggested (SWINGS and MEINEL, 1952) that the excitation takes place directly from N_2^+ molecules in their ground state. Fortunately, in this work, it does not make much difference which of the two alternatives is chosen, since the B values for $N_2(X^1\Sigma_g^+)$ and $N_2^+(X^2\Sigma_g^+)$ differ by no more than 4 per cent.

This method of determining temperatures in auroral regions has been extensively applied by VEGARD and his collaborators. The results of this work have been summarized by HARANG (1951). PETRIE (1952) has recently published some results obtained by this method. Some preliminary results of the present investigation have already been published (VALLANCE JONES, HUNTEN, and SHEPHERD, 1953). VEGARD'S measurements were made on spectra for which the fine structure of the R branch of the N_2^+ bands was unresolved. These measurements gave a mean temperature of about 230°K, $\pm 20°$ for all types of aurora regardless of height. While this temperature is very reasonable for low-level aurora, it was most surprising that the same temperature should be obtained from high-level forms, since other methods of temperature determination indicate a rapid increase in temperature above 100 km (The Rocket Panel, 1952).

Recently, SHEPHERD and HUNTEN (1955) have employed this method, using a scanning spectrometer capable of obtaining spectra of individual auroral features in about four seconds. They obtained direct evidence for an increase of rotational temperature with height; the temperatures derived varied from 150°K to 465°K.

The present work was carried out using a new spectrograph of high dispersion built to the specifications of Dr. W. PETRIE. With this instrument the lines of the R branch of the 0–0 N_2^+ band may be completely separated and their intensity measured accurately.

EXPERIMENTAL

The high-dispersion spectrograph is essentially similar to the instrument described by PETRIE and SMALL (1952), except that the Schmidt camera has a relative aperture of $f/2{\cdot}5$ and a focal length of 22·5 in. The grating is an 8 in. × 8 in. Bausch and Lomb replica. The 0–0 N_2^+ band was photographed in the third order with a dispersion of about 7 A/mm. A 12-in. focal length quartz lens and a movable mirror were used to focus an image of the aurora upon the slit. Five plates were obtained, and the details are set out in Table 1.

During these exposures there were short periods of exposure to brilliant auroral forms and longer intermediate periods of exposure to forms and glows of lower intensity. No attempt was made at this time to differentiate between different types or altitudes of aurora.

A microphotometer tracing of the 0–0 band from Plate 2 is reproduced in Fig. 1. The intensities of the individual lines were calculated by taking advantage of the 2 : 1 intensity ratio between alternate lines. The procedure used is described as follows:

(1) A base line for zero intensity was drawn in by extending the clear plate microphotometer trace across from both sides of the band.

(2) A smooth curve was drawn through the peaks of the strong lines of the *R* branch and another curve through the peaks of the weak lines.

(3) The strongest line of the branch was assigned an intensity of 100 arbitrary units, which was plotted against the interval between the base line and the peak of this line.

(4) The corresponding point on the curve through the weak lines must have an intensity of 50. This provided a second point on the calibration curve.

Table 1

Plate number	*Date*	*Conditions of exposure*	*Temperatures derived*	
			Low K′	*High K′*
1	3–4 April 1953	Brilliant display*	330°K	330°K
2	15–16 April 1953	Diffuse Aurora	281°K	353°K
3	18–19 April 1953	Bright steady arcs and diffuse features	367°K	367°K
4	19–20 April 1953	Brilliant active display	251°K	341°K
5	6–7–8 May 1953	Brilliant active display	284°K	376°K

* Spectrograph not accurately guided on aurora for this exposure.

(5) The procedure was repeated as far as necessary and was found to give a satisfactory calibration for lines on either side of the maximum of the *R* branch. The calibration curve could be checked readily, since the 2 : 1 intensity ratio must hold for all wavelengths between the weak and strong curves.

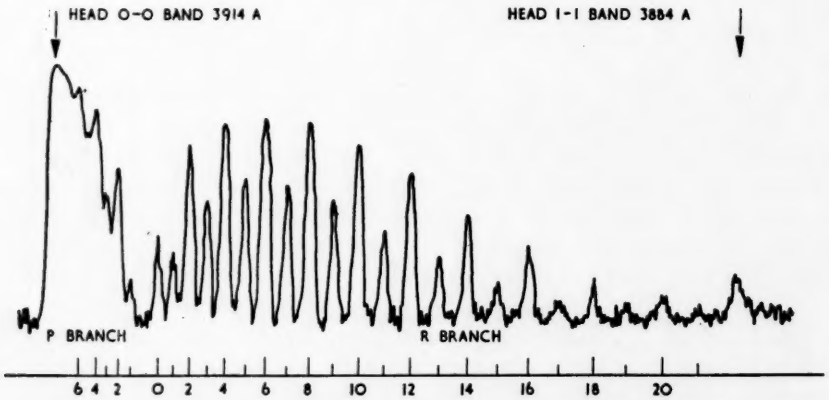

Fig. 1. Microphotometer tracing of 0–0 N_2^+ First Negative band (from Plate 2).

To determine the temperature, plots were made of log I/K' against $K'(K'+1)$. These plots are shown in Fig. 2. The interpretation of these plots will be discussed below. For at least two of the plates it is not possible to draw a single straight line through the points obtained. This effect may arise in several possible ways, of

VOL. 6 1955

which the most obvious is that the procedure used in calibrating the plates was defective.

This possibility was tested by setting up a laboratory hollow-cathode discharge tube so that spectra of N_2^+ bands could be obtained with the auroral spectrograph under the same conditions as for the auroral spectra. Calibration exposures were applied to the plates by means of a step-sector disc and a continuous source. These laboratory plates were microphotometered, and log I/K' against $K'(K' + 1)$

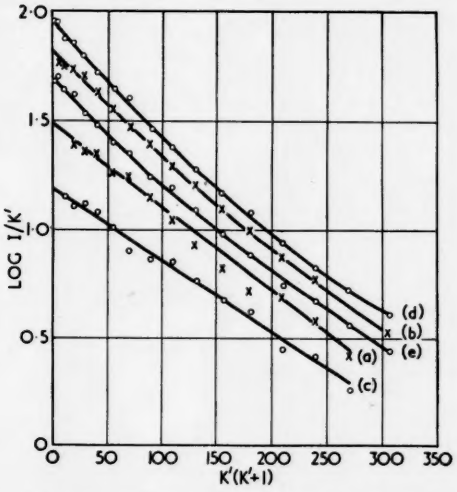

Fig. 2. Plots of log I/K' against $K'(K' + 1)$ for auroral plate.
(*a*) Plate 1, (*b*) Plate 2, (*c*) Plate 3, (*d*) Plate 4, (*e*) Plate 5.

plots were made both by the procedure used for the auroral plates and from the calibration of the plate from the step-sector exposure. In all cases straight-line plots were obtained by both procedures. In all cases the slopes of the straight lines were the same within experimental errors.

It thus appears safe to conclude that the curvature of the log I/K' against $K'(K' + 1)$ plots obtained from the auroral spectra is real.

Results

The temperatures corresponding to the slopes of the plots of Fig. 2 are listed in Table 1. Two temperatures corresponding to the initial (low K') and final (high K') slopes are listed for the curved plots.

Discussion

It is necessary to consider the reason for the curvature of the log I/K' against $K'(K' + 1)$ plots. There are three possible reasons:

(1) Self-absorption by N_2^+ molecules in ground state.

(2) Non-uniformity of temperature of regions from which the aurora is emitted.

(3) Excitation by proton collision.

SELF-ABSORPTION BY N_2^+ MOLECULES

PENNER (1954) has shown that self-absorption of radiation from sources in thermal equilibrium may produce deviations from linearity similar to those observed. According to PENNER, self-absorption effects are important unless:

$$[1 - \exp(-\tau)] \leqslant 0{\cdot}30, \quad \text{i.e.,} \quad \tau \leqslant 0{\cdot}35,$$

where τ is the optical depth of the strongest line of the band. τ may be calculated from a knowledge of the f-value of the transition and the line shape. The line shape was assumed to be controlled by Doppler broadening at a temperature of 300°K.

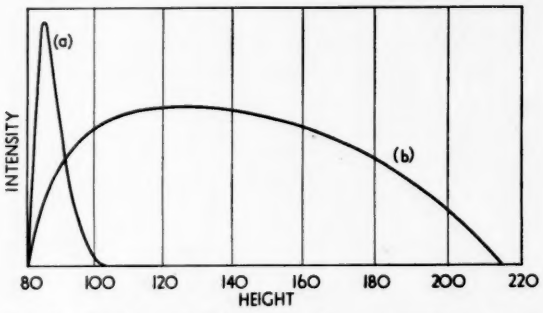

Fig. 3. Intensity distribution with height after VEGARD (1938): (*a*) arcs, (*b*) rays.

Then: $$\tau = 7 \times 10^{-14}\, nl.$$

Where l is the path length in cm.

Where n is the total concentration per cm^3 of N_2^+ ions in the ground electronic state. Self-absorption effects will therefore be unimportant unless this concentration exceeds 5×10^7 ions/cm^3 over a path of 1 km.

However, SEATON (1954) has shown that a concentration of N_2^+ ions of this order of magnitude may be approached for intense aurora, so that one cannot immediately discount self-absorption. However, SHEPHERD and HUNTEN have obtained no evidence of curvature of their $\log I/K'$ against $K'(K'+1)$ plots obtained from the records of their scanning spectrometer from intense aurora. If self-absorption were important, one would expect to observe greater departures from linearity for the plots obtained from intense aurora than for those from weaker aurora. If anything, the reverse is the case. Indeed, the results of SHEPHERD and HUNTEN may be used to place an upper limit upon the quantity of N_2^+ ions in the line of sight.

NON-UNIFORMITY OF TEMPERATURE THROUGH AURORAL REGION

A priori one might expect that a protracted exposure to aurora of different types would include radiation from features distributed in the height range 80 to 250 km or higher. Rocket data indicate a temperature variation of from 200° to 1000°K over this range.

Spectra corresponding to an inhomogeneous source of this kind may be expected to show an anomalous intensity distribution of the type observed. This may be shown as follows: Suppose that the intensity distribution with height of the aurora observed during a lengthy exposure corresponds to a mixture of features having

VOL. 6 1955

the height distribution appropriate to homogeneous arcs and to features having the distribution characteristic of rays (VEGARD, 1938) (Fig. 3). The arc-type contribution was assumed to be 1·6 times the ray-type. The resultant distribution, $I(h)$,

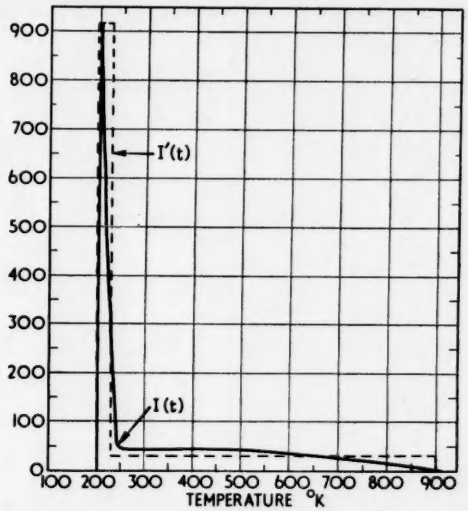

Fig. 4. Hypothetical intensity distribution with temperature. $I(t)$: Distribution derived from Fig. 3 with integrated arc intensity = 1·6 × integrated ray intensity. $I'(t)$: Rectangular approximation to $I(t)$.

was then plotted as a function of temperature, $I(t)$, using The Rocket Panel data (Fig. 4). Then a simplified rectangular distribution, $I'(t)$, was chosen to facilitate calculation of the synthetic spectrum. Finally, the intensity of each line of the R branch was calculated by integrating over the whole temperature range:

$$I_{K'} = 2K' \int_0^\infty \frac{I'(t)}{Q(t)} \cdot \exp\left[-BK'(K'+1)hc/kt\right] dt$$

where $I_{K'}$ is the intensity of the line arising from the K'th level of the upper state, i.e., $R(K'+1)$, B is the rotational constant for $N_2(X'\Sigma_g^+)$, and $Q(t)$ is the rotational partition function for N_2 at temperature t°K.

A plot of $\log I/K'$ against $K'(K'+1)$ was then made from the calculated intensities. Fig. 5 shows the curve obtained (solid line) compared with the observed points from Plate 5. Close agreement is obtained.

This agreement indicates that the observed intensity distribution could arise from aurora distributed through an atmosphere the temperature of which varies with height in a manner similar to that indicated by The Rocket Panel results.

It is not possible to reproduce the observed results unless the maximum of the low-temperature peak of the intensity distribution is lowered to about 200°K. The temperatures from the initial and final slopes in Table 1 thus correspond to rather conservative upper and lower limits for the temperature range.

Excitation by Proton Impact

Excitation of the $B^2\Sigma_u^+$ state of the N_2^+ through proton collisions would possibly lead to simultaneous changes in rotational angular momentum. It is quite conceivable

that the number of excited ions having high and low K values might be increased so that a curvature of the $\log I/K'$ against $K'(K'+1)$ plots would result. The results of HUNTEN and SHEPHERD, however, indicate that this effect is not the dominant cause of the observed curvature; it may, however, play some part.

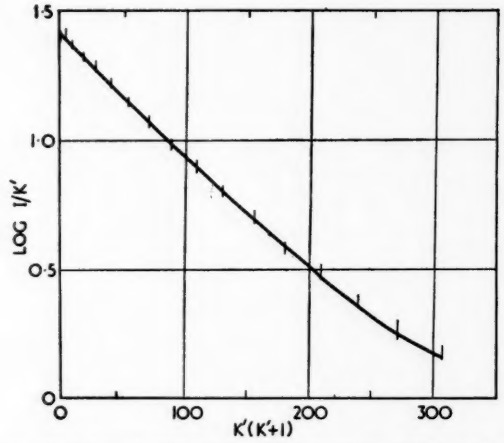

Fig. 5. Comparison of observed plot of $\log I/K'$ against $K'(K'+1)$ (vertical lines) and that calculated from hypothetical intensity distribution $I'(t)$ (solid line).

VOL. 6 1955

CONCLUSIONS

The long exposures required with the high-dispersion spectrograph render it impossible to obtain spectra from single auroral features of which the height can be measured. However, certain definite results have been established from long exposures to one or more displays.

(1) Spectra are obtained which do not have the intensity distribution to be expected from a homogeneous source at a constant temperature.

(2) Spectra of intense auroral displays indicate that the temperature in the auroral regions certainly varies from below 250°K to above 390°K. A considerable contribution from a region having a temperature as low as 200°K is necessary to reproduce the observed intensities.

These results are in harmony with expectation and with the results of SHEPHERD and HUNTEN. It would seem possible that VEGARD'S results refer to low-level aurora and that the emission from high-level forms must have been strongly diluted by the more intense radiation from 80–100 km.

PETRIE'S results, which indicated a temperature of 450–700°K, were obtained both by estimating the strongest line of the R branch, and by plotting the intensities of the lines in the usual manner. The first method is somewhat uncertain since it is extremely difficult to allow for the effect of the overlapping tails of the rotational lines when the lines are barely resolved. The second method is liable to give a temperature approaching the upper limit of the auroral temperature range, since greater weight was given to the lines with higher K values. The high figures quoted

by PETRIE are thus understandable, especially so if the spectrograph was pointed near the summit of the visible aurora.

It is a pleasure to acknowledge many valuable discussions with Dr. B. W. CURRIE and Dr. D. M. HUNTEN.

REFERENCES

HARANG, L.	1951	*The Aurorae*, John Wiley & Sons
SHEPHERD, G. G., and HUNTEN, D. M.	1955	*J. Atmosph. Terr. Phys.* **6**, 328
PENNER, S. S.	1953	*J. Chem. Phys.* **20**, 31, 507–510
PETRIE, W.	1953	*J. Atmosph. Terr. Phys.* **4**, 5–9
PETRIE, W., and SMALL, R.	1952	*Astrophys. J.* **116**, 433–441
THE ROCKET PANEL	1952	*Phys. Rev.* **88**, 1027
SEATON, M. J.	1954	*J. Atmosph. Terr. Phys.* **4**, 285
SWINGS, P., and MEINEL, A. B.	1952	*The Atmospheres of the Earth and Planets*, 2nd ed. (Ed. G. P. KUIPER), University of Chicago Press
VALLANCE JONES, A., HUNTEN, D. M., and SHEPHERD, G. G.	1953	*Astrophys. J.* **118**, 350
VEGARD, L.	1938	*Geofys. Publ.* **12**, No. 7

RESEARCH NOTE

The charge on the earth

(*Received* 31 *January* 1955)

It has been tacitly assumed by many authors, among them GISH (1949) and SCHONLAND (1953), that the total charge on the earth's surface is proportional to the product of the fair-weather surface electric field and the earth's area. It is the purpose of this note to question that assumption and to show that the magnitude of the earth's negative charge may be appreciably less than the value calculated on that basis.

In the recent exchange of research notes by CHALMERS (1953) and PARKINSON (1954), it is shown by the former that the total charge on the inner side of the ionosphere is zero. By applying GAUSS' theorem to the volume inside a surface S of constant conductivity as close to the earth as possible, the total charge on the earth plus the atmospheric space charge enclosed by S is given by

$$4\pi Q = \int_s F \,.\, ds.$$

The application of CHALMERS' method to this volume yields the conclusion that Q is zero provided that no current crosses S other than conduction current. This requires that the net space charge convection current across S must be zero. Although convection in the lower atmosphere is by no means negligible, its integrated current over the surface S may be.

By applying GAUSS' theorem to the earth's surface, the average electric field under thunderstorms which would be required for zero total charge on the earth may be computed. This is possible because the electric field beneath thunderstorms is generally opposite in direction and greater in magnitude than the fair-weather field. According to WHIPPLE and SCRASE (1936), the average total worldwide thunderstorm area is approximately 800,000 km^2. Thus, the average thunderstorm area is 0·0016 of the earth's area. Using the world-wide average value for the fair-weather field given by GISH (1951) of 130 V/m, the average field beneath thunderstorms required for zero earth's charge is 810 V/cm.

A reliable average experimental value for this quantity is not available, because the electric fields beneath thunderstorms have complex structures which have been quantitatively reported from only a few scattered areas. In a recent investigation using improved instruments, GUNN (1954) found a maximum measured surface field of only 140 V/cm. On the other hand, the critical field for breakdown in air at sea-level of approximately 4,500 V/cm given by NORINDER and SALKA (1951), together with the field values up to 1,000 V/cm measured by GISH and WAIT (1950) above thunderstorms, indicate that the computed value of 810 V/cm is within reason. This is particularly true if the relative values of conductivity above and beneath thunderstorms are considered. However, even if the average surface thunderstorm field is comparable to GUNN's typical field, the earth's negative charge is still appreciably less than the value given by GISH or SCHONLAND.

Naval Research Laboratory,
Washington, D.C.

J. F. CLARK
J. H. KRAAKEVIK

VOL. 6 1955

References

Chalmers, J. A.,	1953	*J. Atmosph. Terr. Phys.* **3,** 345
Gish, O. H.	1949	*Physics of the Earth,* VIII, 211
Gish, O. H.	1951	*Compendium of Meteorology,* 108
Gish, O. H., and Wait, G. R.	1950	*J. Geophys. Res.* **55,** 473
Gunn, R.	1954	*J. Meteor.* **11,** 131, 132
Norinder, H., and Salka, O.	1951	*Arkiv Fysik* **3,** 347–386
Parkinson, W. D.	1954	*J. Atmosph. Terr. Phys.* **5,** 106
Schonland, B. F. J.	1953	*Atmospheric Electricity,* 42
Whipple, F. J. W., and Scrase, F. J.	1936	*Meteor. Off. Geophys. Mem.* No. 68, 19

OL.
5
955

Journal of Atmospheric and Terrestrial Physics, 1955, Vol. 6, p. 346. Pergamon Press Ltd., London

Indices of geomagnetic activity

of the Observatories ABINGER (*Ab*), ESKDALEMUIR (*Es*), and LERWICK (*Le*)

April 1955

The figures given on page 346 represent the K-indices for three-hour intervals, beginning with 00–03 hrs for the first and ending with 21–24 hrs for the eighth figure.

April 1955

Day	*Ab* Range for $K = 9 : 500\gamma$			*Es* Range for $K = 9 : 750\gamma$			*Le* Range for $K = 9 : 1000\gamma$			Day
	K-Indices		*Sum*	*K-Indices*		*Sum*	*K-Indices*		*Sum*	
1	3222	2125	19	2212	2115	16	3232	2215	20	1
2	3222	4344	24	2222	3334	21	3222	3344	23	2
3	2233	3332	21	2223	3322	19	2322	3232	19	3
4	1123	3444	22	1113	3444	21	1112	2344	18	4
5	4233	4242	24	4223	4242	23	4322	3232	21	5
6	3313	3324	22	3323	3314	22	3312	3214	19	6
7	4333	3233	24	4333	3233	24	4422	2233	22	7
8	2232	2323	19	2221	2223	16	3121	1223	15	8
9	1212	0114	12	1211	1114	12	1111	1103	9	9
10	1113	3423	18	1003	3322	14	2002	3323	15	10
11	2332	2322	19	2221	3322	17	3221	2211	14	11
12	2332	3233	21	2322	3233	20	3311	2133	17	12
13	3322	2324	21	3322	2323	20	4421	2224	21	13
14	3222	2111	14	2212	3111	13	3212	2101	12	14
15	2122	3312	16	1111	3311	12	1111	2210	9	15
16	1212	2132	14	0111	2122	10	0010	2221	8	16
17	1112	2221	12	1111	2221	11	1021	2110	8	17
18	1121	2211	11	0001	2210	6	1001	1210	6	18
19	1221	2221	13	1110	1111	7	1110	1111	7	19
20	2331	2322	18	2222	2221	15	1221	2221	13	20
21	2222	3322	18	2122	3322	17	1122	3322	16	21
22	2322	2232	18	2312	1231	15	2221	1131	13	22
23	0011	2211	8	0001	2200	5	1011	1110	6	23
24	2212	4444	23	1111	4444	20	1111	4565	24	24
25	3321	3342	21	2211	2342	17	4221	2242	19	25
26	4233	2344	25	4233	2244	24	3223	2245	23	26
27	4321	2566	29	3220	1467	25	3322	1488	31	27
28	6333	3445	31	6333	3445	31	8343	3356	35	28
29	4323	3454	28	4323	3344	26	6422	4344	29	29
30	4323	2333	23	4322	2333	22	5323	2233	23	30

VOL. 6 1955

OL.
6
955